TOPICS ON

PHASE BEHAVIOR AND FLOW OF PETROLEUM RESERVOIR FLUIDS

Curtis H. Whitson

The University of Trondheim

Norwegian Institute of Technology

Departments of Petroleum and Chemical Engineering

1983

$$∓$

TOPICS ON PHASE BEHAVIOR AND FLOW
OF PETROLEUM RESERVOIR FLUIDS

Submitted by

Curtis H. Whitson

to

The University of Trondheim
Norwegian Institute of Technology
Departments of Petroleum
and Chemical Engineering

as fulfillment of
requirements for the degree
doctor of the technical sciences

August 1983

DEDICATION

To muzcats and the like ...

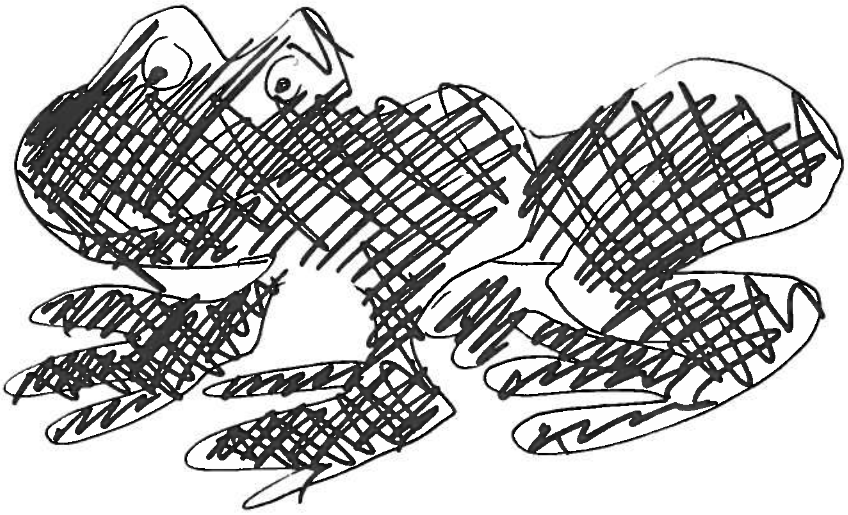

FOREWORD

This thesis gives a review of independent research performed during the period 1978 to 1983. It started in August, 1978 when i arrived in Trondheim, Norway at the Norwegian Institute of Technology (NTH). Without certain inspiration from M.B. Standing at Stanford University during my four-year undergraduate studies (1974 to 1978), the arrival at NTH would probably never have been realized.

My first professional contact in Norway was with Ø. Glasø who headed the fluids (PVT) laboratory at SINTEF (the research organization affiliated with NTH). He promptly put me to work repairing a vacuum pump, the first of numerous jobs i had while working in the PVT laboratory. Without regret, it should be noted that none of the experimental work completed during this first year was of any merit. The experience did, however, give me insight into the importance of high quality experimental data and the difficulty in its measurement. Glasø deserves special thanks for allowing me this opportunity.

Several collegues at NTH deserve credit for inspiring my work in fluid flow. Professor T. van Golf-Racht was particularly patient and allowed me to develop the engineering skills i was supposed to have learned as an undergraduate. He introduced me to the dynamics of reservoir engineering and particularly the importance of understanding fluid flow in porous media; his liberal use of Muskat's examples and approach to reservoir engineering stimulated my interest in the area of fluid flow in porous media. Most of all he let me discover reservoir engineering on my own.

After spending the first two years at NTH as a teacher's assistant and guest lecturer, i spent three years (1980 to 1983) as a research fellow for Rogaland Regional College (RDH). Funds were provided by NAVF, the Norwegian general research council. The fellowship gave me the time and freedom to develop new projects and continue those which had started in Trondheim. It also introduced me to an active experimental program in chemical analysis of petroleum fluids: the Oil and Gas Laboratory at Rogaland Research Institute (RRI), headed by Tor Austad and Olav Vikane.

Michael Golan and later (through his introduction), Mike Fetkovich and Raj Raghavan provided important insight into practical problems of flow in porous media. Discussions with these three led to several papers on the same subject (A.7 to A.9). Somewhat of an exception was the paper Two-Phase

Pressure Test Analysis, which stemmed from work my first year at RDH with coauthors Arild Bøe and Svein Skaeveland. Bøe was responsible for the theoretical developments and i performed all numerical calculations.

Throughout the three-year fellowship it was a pleasure to work with Leif Larsen at RRI. We enjoyed numerous discussions about the more theoretical aspects of pressure transient testing, a subject on which Larsen has made considerable contributions during the short period he has worked in the field.

One year spent at IKU (Continental Shelf Institute) in Trondheim (1982) provided the catalyst for my work with equation-of-state development and application. Discussions with Vilgeir Dalen and Rasmus Risnes were particularly helpful. More recently it has been my pleasure to work with Haakon Norvik on implementation of the generalized cubic equation of state proposed in this study, as well as learning about the methods of numerical solution used to solve multicomponent VLE calculations.

The following organizations have been central in providing services such as computing, travel, financial support, and access to experimental data:

- Norwegian Institute of Technology (NTH)
- Rogaland Regional College (RDH)
- Norwegian General Research Council (NAVF)
- Rogaland Research Institute (RF)
- Continental Shelf Institute (IKU)
- Norwegian Petroleum Directorate (NPD/OD)
- Norsk AGIP A/S
- Phillips Petroleum Company

Without their help the research would not have been possible.

It is a pleasure to recognize those who have made the thesis worth finishing: Grete, m & d, Pokey, grandpa, Andreas, Lucille, Barth, and Josef Faust. As far as Craig and frying pan go, yall provided the laughs when they were most welcome. Takk ska dåkke ha!

TOPICS ON PHASE BEHAVIOR AND FLOW OF PETROLEUM RESERVOIR FLUIDS

CONTENTS

DEDICATION i

FOREWORD ii

INTRODUCTION 1

SUMMARY 2

Chapter 1 6

✓ REVIEW AND DEVELOPMENT OF CUBIC EQUATIONS OF STATE

1.1 What is a Cubic Equation of State? 6
1.2 A Short Review of Cubic Equations 9
1.3 Redlich/Kwong Modifications 10
1.4 Peng/Robinson Equation 12
1.5 Usdin/McAuliffe Equation 14
1.6 Comparison of Three Cubic Equations 15
1.7 Proposed Equation-of-State Modifications 28
Nomenclature 45

Chapter 2 47

✓ CHARACTERIZING PETROLEUM FRACTIONS

2.1 Introduction to the Problem 47
2.2 Proposed Molar Distribution Model 48
2.3 Estimating Specific Gravity and Boiling Point ... 64
2.4 Traditional Critical-Property Estimation 66
2.5 Equation-of-State Critical-Property Estimation .. 68
2.6 Equation-of-State Predictions Using Proposed Critical-Property Estimation 99
Nomenclature 106

Chapter 3 107

FLOW IN POROUS MEDIA

3.1 Introduction to Fluid Flow in Porous Media 107
3.2 Corey/Burdine Relative Permeability Model 113
3.3 Constant-Rate Well Testing Under Conditions of Two-Phase, Gas-Oil Flow 121
3.4 Determining Deliverability by Multirate Testing . 125
3.5 Constant-Pressure Dimensionless Rate Solution During Depletion 128
3.6 Partial Penetration Effects on Fluid Flow 134
Nomenclature 137

REFERENCES 140

Appendix A A.1-1

PUBLISHED/UNPUBLISHED TECHNICAL PAPERS

A.1 Glasø, Ø. and Whitson, C.H.:
The Accuracy of PVT Parameters Calculated From Computer Flash Separation at Pressures Less Than 1,000 psia A.1-1

A.2 Whitson, C.H.:
Characterizing Hydrocarbon Plus Fractions A.2-1

✓ A.3 Whitson, C.H. and Torp, S.B.:
Evaluating Constant-Volume Depletion Data A.3-1

A.4 Whitson, C.H.:
Effect of Physical Properties Estimation of Equation-of-State Predictions A.4-1

A.5 Whitson, C.H.:
A Family of Cubic Equations of State A.5-1

✓ A.6 Austad, T., Hvidsten, J., Norvik, H. Whitson, C.H.:
Practical Aspects of Characterizing Petroleum Fluids A.6-1

A.7 Bøe, A., Skjaeveland, S.M., and Whitson, C.H.:
Two-Phase Pressure Test Analysis A.7-1

A.8 Whitson, C.H.:
Reservoir Well Performance and Predicting Deliverability A.8-1

A.9 Whitson, C.H.:
Discussion of Constant-Rate Decline During Depletion A.9-1

Appendix B B.1-1

EXPERIMENTAL DATA FOR SEVERAL PETROLEUM RESERVOIR FLUIDS

B.1 Hoffman/Crump/Hocott Fluids B.1-1
B.2 Standing/Katz Recombined Mixtures B.2-1
B.3 Eilerts Fluids B.3-1
B.4 Jacoby Recombined Mixtures B.4-1
B.5 Olds/Sage/Lacey Recombined Mixtures B.5-1

INTRODUCTION

this is the short and long of it - W. Shakespeare

Two subjects have been considered in this thesis. The first, phase behavior of petroleum reservoir fluids, covers cubic equations of state and characterization of petroleum fractions. The second, fluid flow in porous media, reviews a hodgepodge of new and historical ideas ranging from two-phase flow to partial penetration effects. Combined, the two subjects represent a type of dipole moment - the product of two topics with dissimilar nature of equal importance.

A good introduction should review the pertinent literature associated with the subject being discussed. This has been delegated to individual chapters. References are given at the end of the thesis but have been separated into two lists, reflecting the two general subjects of the thesis. A review of what has been done is given in the Summary section, once again separated in two.

Several papers, some published and some not, have resulted during the past five years. They should be considered on their own merit. The three chapters of the thesis do not, in general, repeat material found in the papers. Instead they provide new work, together with elaboration and criticism of the old. Mere repetition of the papers would lend the thesis to Frank Dobie's definition as a "transference of bones from one graveyard to another." Hopefully this has been avoided.

If i were to suggest a way of getting through the thesis with minimum pain and effort, it would be to first read the Summary section, then the first sections of each chapter (introductions), next to the papers, and finally the main text in Chapters 1, 2, and 3. Obviously the choice is up to you. Whether burdened with the reading or made by choice, i hope you enjoy the remainder.

Style Note:

The unorthodox practice of combining multiple authors into a combined form using slash (/) instead of hyphen (-) tries to circumvent confusion resulting from the increasing use of two surnames combined by a hyphen. Hopefully this will not detract from readability.

SUMMARY: Chapters 1 and 2

(1) It is doubtful that any cubic equation of state can accurately predict phase behavior of petroleum reservoir fluids over the full range of pressure, temperature and composition normally encountered between the outer boundary of a reservoir and the final pre-processing stage of production.

(2) The description of the heavy fractions is very important to the predictive capabilities of cubic equations of state and should be given serious consideration. However, it does not appear that even the best characterization will guarantee that cubic equations can be used as an accurate predictive tool.

(3) Having attempted to properly define the properties of individual components in a mixture, the engineer should be prepared to make adjustments based on experimental data. A practical approach should involve initial adjustment of properties for the heaviest petroleum fraction - e.g., the boiling point and molecular weight of distillation residue. If this does not result in the desired match of experimental PVT data, manipulation of petroleum-fraction critical properties or EOS constants can be tried, though not necessarily limited to the heaviest fraction.

(4) Before characterizing a petroleum reservoir fluid with an equation of state the engineer should define why the calculations are being performed. If high accuracy is required - e.g., minimum miscibility determination - experimental data should be obtained in the pressure-, temperature-, and composition range of interest. Considerable effort should be given to heptanes-plus characterization.

(5) Development in cubic equations of state should concentrate on improving volumetric predictions, and particularly liquid density estimation. Several attempts have been made in this study to improve existing equations and develop new ones with the goal of improving liquid density estimation. The first suggestion is a modification of the three-constant Usdin/McAuliffe EOS. Saturated liquid densities are fit by including a second correction factor for EOS constants; the functional form of this correction factor is simple and does not introduce additional correlating parameters. The next development is a family of cubic equations based on the four-constant Martin equation. The specification of critical compressibility and a numerical constant simplifies the general equation to almost any two-or three-constant EOS of interest. By minimizing

the absolute error of saturated liquid densities, an optimal EOS has been proposed; for compounds similar to hexane and heptane the new EOS simplifies to the PR EOS.

(6) A probabilistic model has been proposed for describing the relation between molar quantity and molecular weight of petroleum fractions - i.e., molar distribution. In the absense of distillation or chromatographic data, the model can be used to generate a molar distribution based on the average molecular weight of the petroleum-fraction mixture. If a partial analysis is available, the model can be used to extrapolate or split the heaviest fraction, having first matched data for the lighter fractions. The model has been improved by introducing the concept of cumulative normalized quantities.

(7) A method based on the Watson characterization factor is proposed for estimating petroleum-fraction specific gravities and boiling points. The necessary data include molar quantity and molecular weight of each fraction, and average specific gravity of the total petroleum-fraction mixture. The method is simple to use and can be solved explicity (without trial and error). Despite its approximate nature, the method appears to have advantages over other methods presently available. Estimations based only on molecular weights (which themselves may be estimated or calculated) can only be approximate, and none of the presently available methods will give accurate estimates of specific gravities and boiling points.

(8) A new method for calculating critical properties and acentric factor of petroleum fractions based on an EOS appear to give promising improvements in both volumetric and phase behavior predictions. The method requires only molar volume (ratio of molecular weight to specific gravity) and boiling point. The acentric factor relation is empirical, though it accounts for non-paraffinicity via the Watson characterization factor and simplifies to an accurate relation for paraffins and aromatics. Simply stated, the method matches input molar volume and boiling point with the EOS by adjusting critical pressure and critical temperature. Tables of EOS-based critical properties are given for the Peng/Robinson and Soave/Redlich/Kwong equations.

(9) A method is suggested for calculating the so-called black-oil PVT properties of gas condensates and volatile oils based on constant-volume depletion data. The modified gas/oil ratios and formation volume factors form the basis for modified black-oil numerical simulators which have been shown to have, for certain reservoir processes, comparable accuracy with multicomponent compositional models.

SUMMARY: Chapter 3

(1) Probably the most difficult engineering task facing the multiphase flow problem in porous media is determination of accurate (average) relative permeability relations applicable to fluid flow at reservoir conditions. This leads to the second most difficult task of finding the correct physical/mathematical definition of the relevent saturation relation.

(2) Given the uncertainties associated with the definition of realistic relative permeabilities, complicated mathematical solutions of the saturation/pressure relation for gas/oil flow are probably of questionable merit. More emphasis should be placed on a practical engineering solution to the estimation of two-phase fluid flow. The Evinger/Muskat pseudopressure function provides a reasonable balance between accuracy and simplicity. For many applications, the pressure-squared method suggested by Fetkovich provides a solid engineering approach for analyzing multirate and drawdown/buildup test data.

(3) Based on results of numerical simulations for solution-gas drive depletion, Vogel develops a simple expression for the relation between oil rate and wellflowing pressure. The empirical form of Vogel's relation has been generalized and interpreted in terms of the pressure function proposed by Evinger and Muskat. Having defined the linear form of the pressure function, insight has been gained into alternative and modified inflow performance relations. In particular, it is found that the Standing method for correcting the Vogel relation for nonzero skins has severe limitations for stimulated wells.

(4) A method is proposed for generalizing the analysis of multirate tests. It is based on the observations made by Fetkovich from analyzing over 40 multirate tests on oil wells. A type curve is given for analyzing multirate data; this type curve shows that the common interpretation of a linear log-log deliverability plot is only approximate over a limited range of drawdown. Examples show the use of the type curve and method of analysis for gas and oilwells.

(5) The theoretical considerations of constant-pressure production during depletion have been considered. Different suggestions in the literature about the proper means of normalizing analytical dimensionless rate are discussed. The exponential decline is best approximated using the first root of the Bessel function expression resulting from solution of the differential equation describing flow under constant-pressure conditions. The practical problem with determining this root and calculating Bessel functions to determine the constants of the exponential rate expression are unfortunate. Having compared the various empirical and semi-analytical methods of normalizing the dimensionless rate solution, a suggestion is made as to which relation offers the best compromise between accuracy and simplicity.

(6) The solution to the partial penetration problem proposed by Brons and Marting uses a numerical solution to Nisle's approximate analytical solution. Despite their claim that the key function, G(b), must be solved numerically, it is shown that an exact analytical expression is found in the original Muskat solution, and that its form can be solved directly, without the need of a computing device. While Brons and Marting's suggest that the Muskat solution (and their expression using G(b)) is only valid for 'large' dimensionless heights, it is shown that the corresponding total thicknesses is 25 feet (7.5 m) or less. This means that for all practical purposes the original Muskat solution can be used to estimate partial penetration skin.

Chapter 1

REVIEW AND DEVELOPMENT OF CUBIC EQUATIONS OF STATE

... in memory of J.J. Martin

1.1 WHAT IS A CUBIC EQUATION OF STATE?

What is a cubic equation of state? It is an equation relating pressure, temperature, composition and volume. Slightly oversimplified, we can write a general form of the cubic equation as

$$V^3 + a\cdot V^2 + b\cdot V + c = 0 \quad \ldots\ldots\ldots\ldots\ldots\ldots\ldots \quad (1.1)$$

Constants a, b and c are defined by pressure, temperature, composition and the amount (moles) of fluid. Since the equation is cubic in volume, there may be one, two (seldom) or three real solutions which satisfy the specified conditions. Which volume should be choosen if there are, say, three volumes? In practice the largest volume is defined as vapor and the smallest volume as liquid; if a third volume exists between these two then it is merely ignored. If only one volume satisfies the equation then there is obviously no problem in choosing the correct solution. Negative volumes may result at large supercritical temperatures (e.g., nitrogen at 4006 psia and 163.5 F using the Peng/Robinson EOS), in which case the negative root is ignored.

Why choose a cubic form? The answer lies in the behavior of real fluids. Consider water for a moment. At room conditions water behaves as a liquid and has a density of approximately 1 g/cc. When water is heated its density decreases, though only slightly (mass remains constant while volume increases). However, once 100 ^{o}C is reached the water becomes a vapor (steam) and its density changes abruptly, becoming several orders of magnitude lower. At 100 ^{o}C we can actually say that water has two densities - the saturated vapor density (steam) and saturated liquid density (heated water). To correctly predict this abrupt change in density (i.e., volume, assuming a constant mass), the cubic equation chooses the larger volume solution to describe steam, and the smaller volume solution to describe heated water.

Cubic equations are usually expressed in terms of the compressibility factor, Z, which is defined by the real gas law: $Z = pV/NRT$, where p = pressure, V = volume, N = moles, T = absolute temperature, and R = the universal gas constant. The general form of any cubic equation of state can now be wrhtten,

$$Z^3 + e \cdot Z^2 + f \cdot Z + g = 0 \quad \ldots\ldots\ldots\ldots\ldots\ldots\ldots \quad (1.2)$$

where constants e, f and g are defined by p, T, and composition. Considering only pure compounds, constants e, f and g can be expressed for one of the more popular cubic equations of state - the Peng/Robinson (PR) equation,

$$\begin{aligned} e &= B - 1 \\ f &= A - 3B^2 - 2B \quad \ldots\ldots\ldots\ldots\ldots\ldots\ldots\ldots \quad (1.3) \\ g &= B^3 + B^2 - AB \end{aligned}$$

where

$$A = 0.45724 \cdot \alpha \cdot (p/T^2) \cdot (T_c{}^2/p_c) \quad \ldots\ldots\ldots\ldots\ldots \quad (1.4a)$$

$$B = 0.07780 \cdot (p/T) \cdot (T_c/p_c) \quad \ldots\ldots\ldots\ldots\ldots\ldots \quad (1.4b)$$

and

$$\sqrt{\alpha} = 1 + (0.37464 + 1.54226 \cdot \omega - 0.26992 \cdot \omega^2)(1 - \sqrt{T_r}) \quad .. \quad (1.4c)$$

The expressions for A and B result by forcing the two van der Waals criteria that the first and second derivatives of pressure with respect to volume (at the critical temperature) equal zero. Constants 0.45724 and 0.07780 are usually designated Ω_a and Ω_b, respectively, and are only approximate, rounded here to five significant digits. The term α is an empirical correction factor dependent of the compound (e.g., acentric factor, or another correlating parameter) and reduced temperature, T_r. It is found by matching experimental vapor pressures along the vapor-pressure curve and fitting the results with the equation form (Eq. 1.4c) first suggested by Soave in his modification of the Redlich/Kwong equation.

To calculate volume of a pure compound, first specify component properties ω, p_c, and T_c. Calculate α from Eq. 1.4c, then constants A and B from Eqs. 1.4a and 1.4b, from which constants e, f and g are found from Eq. 1.3. The cubic equation (Eq. 1.2) is solved for Z. Analogous to our previous discussion of multiple-volume roots, the largest Z-factor is assumed to represent vapor and the smallest Z-factor is assumed to represent liquid; no choice is posed if only one Z-factor root exists. Given Z, volume is found from ZNRT/p. Density is merely NM/V or pM/ZRT, where M is molecular weight.

An example calculation is given for methane, which has properties ω=0.0115, p_c=4.604 MPa, and T_c=190.58 K. The boiling point of methane at atmospheric pressure (0.10132 MPa) is 111.6 K (T_r=0.58558). From these data, α=1.0921, A=0.03205, B=0.002924, e=-0.99708, f=0.02617, and g=-0.0000851. Solving the cubic equation gives Z=0.0038, 0.0231, and 0.9702, the smallest root being designated as the liquid factor and the largest root as the vapor factor. Corresponding liquid and vapor densities are 0.461 and 0.001806 g/cc, respectively.

The procedure for finding volume and density is essentially the same for mixtures. Given composition, the terms A and B are calculated using appropriate mixing rules. If the mixture exists in the single-phase region, the procedure can be applied directly to the mixture composition. If the mixture splits into two phases, then the procedure is performed for each phase; this requires, however, the composition of each phase. Vapor/liquid equilibria (VLE) calculations necessary for determining phase compositions are more complicated and will not be reviewed here.

Several points deserve mention. First, the PR EOS is an example of a two-constant cubic equation. The two constants are A and B, as defined by Eqs. 1.4 Second, the critical properties (as well as acentric factor and molecular weight) required for each component in a mixture are not well-defined properties for petroleum fractions. They are usually difficult to estimate, and it may be found that different correlations give considerably different results.

Another observation about two-constant equations is that constant A usually dictates VLE and vapor density predictions, whereas B usually dictates liquid density prediction. Consequently, T_c has more influence on VLE and vapor density predictions than p_c. Also, a second correction factor - the so-called binary interaction parameter - is often used to correct VLE deficiencies for mixtures of compounds with unlike properties. Binary coefficients are also applied to constant A.

1.2 A Short Review of Cubic Equations

Professor Joseph J. Martin from the University of Michigan summarizes the problem resulting from an overabunance of cubic equations of state (EOS) by quoting from none other than Snow White: "Mirror, mirror on the wall, who's the fairest of them all?" Despite Martin's claim to have developed the 'fairest' cubic equation, it is probably safe to say that all equations have inherent limitations and that no single equation performs better than all others.

van der Waals proposed the first cubic EOS in 1873. Since then, the evolution of cubic equations has resulted in new forms such as those proposed by Redlich/Kwong (RK), Martin, Peng/Robinson (PR), and Usdin/McAuliffe (UM), only to name a few. Several alternative forms of these equations have been suggested, but the RK equation has certainly been the most popular basis for modification.

A recent trend (Martin, Abbott, Usdin/McAuliffe, Schmidt/Wenzel, etc.) has been to propose generalized cubic equations which can be simplified to more popular/familiar forms. Most investigators agree that no single equation, no matter how complicated (three, four, or five constants), can accurately predict volumetric and phase behavior of pure compounds or mixtures over a large range of conditions and composition.

Description of pressure/volume/temperature (PVT) behavior of petroleum reservoir fluids has formed the basis for developments given in papers A.2 to A.5. Saturation pressures, densities and two-phase VLE are the properties which have received most attention. Emphasis has also been given to application of EOS's at conditions of pressure and temperature found in the reservoir, production tubulars, surface separators and transportation lines. Low-temperature conditions found in refineries and gas-stripping plants have not been considered.

Most petroluem engineering applications of cubic equations rely on a modification of the RK EOS or Peng-Robinson's original equation. Numerous variants of the RK equation have found acceptance. Soave's modification (SRK) is the simplest and most widely used. Unfortunately it yields poor liquid densities. In an attempt to improve volumetric predictions, Zudkevitch and Joffe (ZJRK) propose a method in which both EOS constants (a and b) are corrected by temperature functions. Several months after the original publication, Joffe, Schroeder and Zudkevitch proposed a slight modification of the original procedure. Others, such as Yarborough and Gray, base their own modifications on the ideas of Zudkevitch, Joffe and Schroeder. The acronym ZJRK is used for all modifications based on the original work by Zudkevitch and Joffe.

The PR EOS is comparable to the SRK equation in simplicity and form. Peng and Robinson report that their equation predicts liquid densities better than the SRK EOS (though they are usually inferior to ZJRK EOS predictions). A distinct advantage of the PR and SRK equations is reproducibility; simple temperature-dependent expressions are used to express the correction to EOS constant A. The ZJRK equations rely on tables or complex best-fit equations to represent highly non-linear correction terms for EOS constants A and B.

A promising three constant EOS was proposed almost simultaneously by Usdin/McAuliffe (UM) and Fuller. Although the equation has not received wide acceptance, it exhibits several qualities which make it an attractive alternative. Martin shares his admiration of the equation by equating Ht in accuracy to his own 'best' equation (his claim that translation in volume is simpler than defining a component-dependent critical compressibility factor seems debatable).

A new concept to cubic equations of state was proposed by Martin in 1979: translation in volume. The application given by Martin is essentially to ease the comparison of his proposed generalized EOS with previously published equations. It also shows similarites/differences in simple volumetric predictions by various equations. In an independent study, Peneloux et al. uses the idea of translation in volume to improve volumetric capabilities of the Soave RK EOS. Peneloux, et al.'s most important observation is that traditional VLE calculations based on component fugacity ratios are not affected by translation in volume. They do not discuss, however, the potential effect which results when using fugacities directly - e.g., with the Peng/Robinson method for predicting semi-solid phase equilibria).

1.3 Redlich/Kwong Modifications

A newcomer introduced to the RK EOS may be intrigued by the simplicity, accuracy and mathematical pleasure which results from deriving its thermodynamic properties. This has lead to inumerable attempts to better, extend and in some cases, bastardize, the original equation.

There are certainly hundreds if not thousands of technical papers, theses, and compendiums written about the RK EOS.

With the advent of advanced numerical computers, this craze developed into what Abbott coined the Redlich/Kwong decade (1967-1977). Abbott claims that the remarkable sucess of the RK EOS results from its excellent prediction of the second viral coefficient (securing good performance at low densities) and reliable predictions at high densities in the supercritical region. This latter observation results from the compromise fit of densities in the near-critical region; all pure components are required by the RK EOS to have a critical compressibility factor of 1/3. This value is reasonable for liqhter hydrocarbons but is less satisfactory for heavier compounds.

Soave/Redlich/Kwong (SRK)

Several attempts have been made to improve vapor-pressure (i.e., VLE) predictions by introducing a correction term for EOS constant A. Soave uses vapor pressures directly to determine the functional relation for the correction factor. The SRK EOS appears to be the most accepted modification proposed to date. Still, it overestimates liquid volumes of petroleum mixtures.

The present use of the SRK EOS results from historical and practical reasons. It offers an excellent predictive tool for systems requiring accurate predictions of VLE and vapor properties. It should be used with caution, however, when liquid volumes are important for the engineering application.

Zudkevitch/Joffe/Redlich/Kwong (ZJRK)

Zudkevitch and Joffe propose a novel procedure for improving the volumetric predictions of the RK EOS without sacrificing VLE capabilities of the original equation. Their method suggests that the same EOS constants, A and B, be used for both the liquid and vapor phases, yet that they be corrected as a function of temperature to match saturated liquid densities and fugacities. They show that errors in vapor fugacities and fugacity ratios (i.e., K-values) remain unaffected for all practical purposes. They do not comment on the effect of their procedure on vapor densities.

Only six months after the original ZJRK modification, Joffe, Schroeder and Zudkevitch proposed an alternative method (similar to one previously used for a modified BWR EOS) whereby liquid fugacity was dropped and vapor pressure used directly. That is, constants A and B are determined by matching the RK EOS to saturated liquid densities and vapor pressures at subcritical temperatures. The procedure for determining A and B is trial and error. The authors claim this procedure only can be used below the critical temperature. Haman, et al. show, however, that a single procedure can, in fact, be used for subcritical and critical temperatures (based on suggestions by Kato, et al.).

The Joffe/Schroeder/Zudkevitch procedure, which is little more than a twist on the original Zudkevitch/Joffe proposal, also is given the acronym ZJRK. To my knowledge, no one uses the original procedure and the acronym should not, therefore, cause confusion.

The ZJRK approach has been used to determine constants A and B for pure paraffins (Haman, et al.) and petroleum fractions (Yarborough and Gray). Unfortunately, the resulting temperature functions are very complex, being represented by higher-order polynomials or cubic splines; the behavior of these functions is highly nonlinear near the critical point. Also, there does not appear to be one set of correlations accepted by the industry, thereby making it difficult to reproduce results. Gray suggests that the ZJRK procedure be performed each time the EOS is used. He claims that it is not necessary to know critical properties of petroleum fractions to use the procedure.

In review, two Relich/Kwong modifications - ZJRK and SRK - seem to have received the most interest in application to petroleum reservoir fluids. The Soave equation is preferred because of its simplicity and overall accuracy. Its primary disadvantage is poor volumetric predictions. The Zudkevitch/Joffe equation is surprisingly accurate for both liquid and vapor property estimation; its main disadvantage is the complexity of functions used to represent temperature-dependent correction factors for EOS constants.

1.4 Peng/Robinson (PR)

In 1975, Peng and Robinson proposed a two-constant equation which created great expectations for improved liquid density predictions. The equation does not produce inferior VLE compared with the RK equations. Also, the relation used to describe the temperature-dependent correction factor for EOS A (Eq. 1.4c) is nearly identical to the Soave correlation.

The largest improvement offered by the PR equation is a universal critical compressibility factor of 0.307401... -somewhat lower than the RK value of 1/3 and closer to experimental values of heavier hydrocarbons. The difference between PR and SRK liquid volumetric predictions can be substantial, though in many cases the errors in oil densities are unacceptable from both equations. There is evidence that the PR equation underpredicts saturation pressure of reservoir fluids and that considerable adjustments of binary interaction coefficients are required to match measured VLE data (re Katz and Firoozabadi).

Availability and considerable publicity have given the PR equation an obvious advantage in recent years. Peng and Robinson certainly make their equation well known by documenting how it can be applied to petroleum and non-hydroocarbon systems. They also have presented numerical solutions to difficult problems near the critical region, as well as proposing novel methods for predicting multiphase and semi-solid phase behavior. In addition to their own efforts, the PR EOS has almost become chic to use for research applications. By virtue of the interest which industry has bestowed upon Peng and Robinson's efforts, it almost seems obligatory to choose the PR over the SRK equation.

To my knowledge, no effort has been made to improve the PR EOS using the ZJRK technique. Neither has the use of volume translation been suggested. It is not obvious why either of the two methods might not be sucessful in improving the original PR EOS.

In review, the PR EOS is a popular, simple and relatively accurate alternative to RK equations. But it is just that - an alternative - and not really a replacement. One good reason for using the PR EOS is that there presently exists extensive sets of binary interaction coefficients for important hydrocarbon/non-hydrocarbon systems. In particular, recent experimental work with carbon dioxide has almost exclusively been fit by the PR EOS using interaction parameters. Considering the practical importance of CO_2 to petroleum reservoirs, the PR EOS will certainly continue as an important tool in describing fluid behavior of complex hydrocarbon mixtures.

1.5 Usdin/McAuliffe (UM)

In 1976, Usdin and McAuliffe presented a three-constant cubic EOS which is claimed to improve liquid density predictions while retaining VLE accuracy and simplicity of RK equations. By specifying critical compressibility factor for each component, Usdin and McAuliffe show that their equation gives greater flexibility, while reducing to more common forms such as the ideal gas law, van der Waals' equation or the RK equation. (Fuller presented the same EOS in an independent studty some six months after Usdin and McAuliffe.)

Usdin and McAuliffe do not suggest that measured critical compressibility factor be used to define EOS constants. Instead they propose a method where Z_c is defined by matching predicted liquid density of a component at a given temperature with its experimental value; e.g., liquid density at standard temperature, usually expressed relative to water as specific gravity.

The temperature-dependent correction factor for EOS A is determined in the same manner as proposed by Soave. Usdin and McAuliffe give, however, a slightly more complicated expression for temperature dependence. They do not indicate if the simpler form proposed by Soave is sufficient (though VLE comparisons presented by Usdin and McAuliffe suggest that little is gained by using the more complicated expression). Also, results are not presented for phase behavior at supercritical temperatures.

The method proposed by Fuller for adjusting UM EOS constants to match vapor pressures and saturated liquid densities is similar to the ZJRK method. In fact the same procedure has been performed in this study without knowledge of the work by Fuller, and not surprisingly gives similar results.

An important difference between the ZJRK and Fuller methods is that EOS constant's variation with temperature is smooth and easily described using the UM EOS (Fuller's choice). This results because critical compressibility factor is specified by the UM EOS and represents a much better estimate if not exact experimental value of Z_c.

In my opinion, the UM EOS provides one of the most practical alternatives to RK and PR equations without complicating thermodynamic predictions. Apparently the improvement in liquid densities has not given sufficient reason to make the UM alternative widely accepted.

1.6 Comparison of Three Cubic Equations

In this section a comparison is given between the predictive capabilities of the Peng/Robinson and two modifications of the Redlich/Kwong equations. The reservoir fluids used to make the comparison are those presented by Standing and Katz. The reason for this choice is that the Standing/Katz data, though somewhat limited in number, form the basis for two of the most widely used density correlations found in the petroleum industry. The Standing/Katz revision of the corresponding states compressibility factor chart is recognized as the industry standard from which all empirical and EOS-based correlations are compared. The liquid density correlation is somewhat limited in the range of temperature but has proven to be both accurate and easy to use. Of upmost importance is that both density correlations resulting from the Standing/Katz data are predictive - i.e., no adjustment of model parameters is necessary.

The SRK and ZJRK equations are chosen to represent the Redlich/Kwong family. Tables of correction terms used by the ZJRK EOS have been read from Yarborough's figures (Hustad, IKU). Critical properties of the petroleum fractions were estimated from correlations (Cavett and Edmister). Complete description of the reservoir fluid mixtures and their properties are given in Appendix B. The Cavett/Edmister property estimations for petroleum fractions are found in Table 1.1.

TABLE 1.1 - Estimated Critical Properties and Acentric Factor for Petroleum Fractions of the Standing/Katz Mixtures using Empirical Correlations of Cavett and Edmister.

	Cavett		Edmister
Fraction	Critical Pressure (MPa)	Critical Temperature (K)	Acentric Factor
F1	3.164	522.7	0.3044
F2	2.630	616.3	0.4358
F3	2.127	690.5	0.5365
F4	1.692	754.9	0.6280
F5	1.442	808.9	0.7000
F6	1.268	857.5	0.7736
F7	1.136	933.0	1.1360

Table 1.2 gives EOS predictions of saturation pressures and vapor/liquid densities. Standing and Katz do not report experimental saturation pressures, although they note that all systems should be above their critical temperature, and therefore the saturation pressures should all be dew points. In fact it is seen from Table 1.2 that PR and SRK equations predict bubble points for systems C, G and H; the ZJRK EOS correctly predicts dew points for all systems. Predicted saturation densities, though not representing the same saturation pressures, give the general qualitative trend that ZJRK densities are greater than PR densities which are greater than SRK densities.

It is unfortunate that Standing and Katz do not report dew point pressures for their systems. Vapor/liquid equilibria data which are reported, however, indicate minimum values of dew point pressures. These are listed in Table 1.2. In nearly all cases, the PR and SRK equations underpredict the minimum saturation pressures considerably (true dew points are probably from 5 to 15 MPa greater than the minimum values listed). The ZJRK EOS always predhcts dew point pressures above the minimum pressures indicated.

Table 1.3 reports experimental and predicted vapor phase densities; it also gives PR and SRK values obtained after adjustment of the methane-C_7+ binary interaction parameters to fit the ZJRK dew point for system A at 322.039 K; binaries are 0.0819 and 0.0702 for the PR and SRK equations, respectively. Also reported in Table 1.3 are predicted vapor densities using the Standing/Katz Z-factor correlation (these values were given in the original work). Qualitatively, the PR and ZJRK equations perform best, though in general all equations underpredict vapor densities.

Table 1.4 reports similar results to Table 1.3 but for liquid phase densities. Also reported in Table 1.4 are predicted liquid densities using the Standing/Katz method based on pseudo-liquid densities of methane and ethane and temperature/pressure correction charts. Qualitatively, EOS predictions of liquid densities are poor, although the PR and ZJRK equations perform better than the SRK equation. PR generally underpredicts, while ZJRK overpredicts; SRK always underpredicts.

Tables 1.5 and 1.6 present results for experimental and predicted properties of the heptanes-plus fraction, including molecular weight and specific gravity. Predictions are not bad in general, although they show considerable scatter. Heptanes-plus properties are not easily determined experimentally, which may explain partly the observed scatter.

Table 1.7 compares experimental and EOS liquid volumes in the two-phase region. It is somewhat difficult to make an objective comparison since saturation pressure of the experimental systems is unknown, and it can be expected that had the EOS been first matched to the saturation pressure that it would better predict VLE.

Tables 1.8a to 1.8d compare experimental and predicted equilibrium constants (K-values) for the Standing/Katz mixtures. Predictions range from poor to good, but they are generally far from desired engineering accuracy. As might be expected from the previous discussion of saturation pressure predictions, the ZJRK equation gives better estimation of heavy-component K-values.

Results of this comparison provide an excellent statement of the problem with which we are dealing: cubic equations of state are seldom predictive tools which can be used, without adjustment, to describe the phase and volumetric behavior of petroleum reservoir mixtures. The three equations used in the comparison certainly indicate large variation in phase behavior prediction, the same indication given in paper A.4. This observation is less valid if critical properties of the petroleum fractions are consistent with the EOS itself, a topic considered in the next chapter.

TABLE 1.2 - COMPARISON OF PREDICTED AND MEASURED SATURATION PRESSURES AND SATURATED DENSITIES FOR THE STANDING/KATZ MIXTURES.

		Saturation Property									
		Pressure (MPa)				Vapor Density (gm/cc)			Liquid Density (gm/cc)		
Sample	Temperature (K)	Exp. c	PR	SRK	ZJRK	PR	SRK	ZJRK	PR	SRK	ZJRK
A	322.039	> 56.7	36.639 (61.678)d	39.753 (61.678)d	61.678	0.4005 (0.4623)d	0.3744 (0.4198)d	0.4413	0.4972 (0.6281)d	0.4603 (0.5565)d	0.8674
B	394.261	> 42.7	40.088	44.223	53.779	0.3162	0.3267	0.3595	0.5063	0.5653	0.8384
C	322.039	> 36.7	31.422a	33.312a	49.125	0.3724	0.3506	0.5082	0.4766	0.4363	0.6249
D	322.039	> 29.8	30.520	32.684	46.742	0.3599	0.3370	0.3905	0.5103	0.4780	0.9494
E	322.039	> 28.9	42.180	46.244	76.117	0.4286	0.4005	0.4790	0.4889	0.4488	0.8134
F	394.261	> 38.1	35.693b	38.426b	46.146	0.4128	0.3806	0.4292	0.4128	0.3806	0.6052
G	274.817	> 34.3	25.404a	27.127a	52.840	0.3563	0.3422	0.5559	0.5178	0.4688	0.6776
H	282.594	> 35.5	26.588a	28.318a	51.766	0.3586	0.3433	0.5477	0.5110	0.4634	0.6656

a Predicted saturation pressure is a bubble point. Experimental indicates a dew point.

b Convergence not achieved. Critical point properties calculated using the Baker-Luks formulation are given instead. For the PR EOS, critical temperature is 382.825 K; for the SRK EOS, critical temperature is 389.517 K.

c Experimental saturation pressures were not reported. Minimum values are listed in this table and correspond to the highest two-phase equilibrium pressure reported; true saturation pressure in most cases will be at least 5-15 MPa higher than the value reported. Standing and Katz note that all systems should be above their critical temperature and therefore all saturation pressures should be dew points.

d Values in parentheses results after having matched the retrograde dew point pressure predicted by the ZJRK EOS. Interaction coefficients between methane and all C7+ fractions were adjusted to 0.0819 and 0.0702 for the PR and SRK equations, respectively.

TABLE 1.3 - COMPARISON OF PREDICTED AND MEASURED VAPOR DENSITIES FOR THE STANDING/KATZ MIXTURES.

	Equilibrium Conditions		Equilibrium Vapor Phase Density (gm/cc)				
Run No.	Pressure (MPa)	Temperature (K)	Exp.	PR	SRK	ZJRK	SK b
A-5	6.882	322.039	0.056	0.0551	0.0534	0.0543	0.0561
....				(0.0550)c	(0.0533)c		
A-4 and 41 ..	11.011	322.039	0.097	0.0951	0.0906	0.0929	0.0981
....				(0.0946)c	(0.0902)c		
A-1	21.919	322.039	0.224	0.2151	0.1983	0.2053	0.2308
....				(0.2079)c	(0.1936)c		
A-2 and 21 ..	36.268	322.039	0.340	0.3911	0.3267	0.3127	0.3333
....				(0.3199)c	(0.2931)c		
A-3	56.570	322.039	0.404	a	a	0.4169	0.4038
....				(0.4324)c	(0.3934)c		
B-3	11.562	394.261	0.091	0.0830	0.0793	0.0816	None
B-1	20.061	394.261	0.154	0.1504	0.1403	0.1463	0.1530
B-2	42.668	394.261	None	a	0.3014	0.2947	None
C-2 and 21 ..	6.951	322.039	0.056	0.0561	0.0544	0.0554	0.0530
C-1	19.820	322.039	0.203	0.1987	0.01839	0.1937	0.2035
C-3 and 31 ..	36.681	322.039	0.400	a	a	0.3703	0.4087
F-1	21.960	394.261	0.192	0.1857	0.1707	0.1817	0.2051
F-2	29.751	394.261	0.277	0.2689	0.2388	0.2537	0.2772
F-3	38.128	394.261	0.349	a	0.3500	0.3326	0.3462
G-1	13.996	274.817	0.176	0.1674	0.1568	0.1595	None
G-2	24.028	274.817	0.383	0.3305	0.2971	0.3008	0.3878
G-3	34.267	274.817	0.463	a	a	0.3969	0.4583
H-4	12.514	282.594	0.140	0.1357	0.1279	0.1302	None
H-2	21.063	282.594	0.296	0.2663	0.2443	0.2515	None
H-3	35.508	282.594	0.474	a	a	0.3989	None
D-1	29.799	322.039	0.327	0.3481	0.3052	0.3017	0.3237
E-1	28.942	322.039	0.261	0.2581	0.2344	0.2376	0.2612

a Pressure higher than predicted saturation pressure; assumed to be a liquid.

b Calculated values reported by Standing and Katz using natural gas compressibility charts.

c Values in parentheses result after having matched the retrograde dew point pressure predicted by the ZJRK EOS. Interaction coefficients between methane and all C7+ fractions were adjusted to 0.0819 and 0.0702 for the PR and SRK equations, respectively.

TABLE 1.4 - COMPARISON OF PREDICTED AND MEASURED LIQUID DENSITIES FOR THE STANDING/KATZ MIXTURES.

	Equilibrium Conditions		Equilibrium Liquid Phase Density (gm/cc)				
Run No.	Pressure (MPa)	Temperature (K)	Exp.	PR	SRK	ZJRK	SK [b]
A-5	6.882	322.039	0.726	0.7112 (0.7228)[c]	0.6352 (0.6435)[c]	0.7874	None
A-4 and 41	11.011	322.039	0.702	0.6809 (0.7021)[c]	0.6094 (0.6246)[c]	0.7601	0.709
A-1	21.919	322.039	0.696	0.6203 (0.6757)[c]	0.5622 (0.6007)[c]	0.7495	0.722
A-2 and 21	36.268	322.039	0.745	0.5059 (0.6637)[c]	0.4984 (0.5905)[c]	0.7865	None
A-3	56.570	322.039	0.814	0.4549[a] (0.6404)[c]	0.4130[a] (0.5684)[c]	0.8568	0.811
B-3	11.562	394.261	None	0.7027	0.6274	0.8077	None
B-1	20.061	394.261	0.697	0.6635	0.5944	0.7823	0.700
B-2	42.668	394.261	None	0.3372[a]	0.5171	0.8152	None
C-2 and 21	6.951	322.039	0.711	0.7025	0.6271	0.7690	0.713
C-1	19.820	322.039	0.652	0.6052	0.5474	0.6968	0.649
C-3 and 31	36.681	322.039	0.712	0.4926[a]	0.4450[a]	0.6747	0.708
F-1	21.960	394.261	0.654	0.5983	0.5409	0.6932	0.668
F-2	29.751	394.261	0.657	0.5396	0.4994	0.6725	0.664
F-3	38.128	394.261	0.677	0.4100[a]	0.4089	0.6506	0.681
G-1	13.996	274.817	0.665	0.6377	0.5742	0.7262	None
G-2	24.028	274.817	0.679	0.5387	0.5023	0.7108	0.676
G-3	34.267	274.817	0.766	0.5388[a]	0.4839[a]	0.7125	0.756
H-4	12.514	282.594	0.682	0.6542	0.5873	0.7326	None
H-2	21.063	282.594	0.659	0.5789	0.5293	0.7055	None
H-3	35.508	282.594	0.752	0.5329[a]	0.4790[a]	0.7037	None
D-1	29.799	322.039	0.731	0.5164	0.4880	0.7411	0.713
E-1	28.942	322.039	0.753	0.6372	0.5829	0.8254	0.736

[a] Pressure higher than predicted saturation pressure; assumed to be a liquid.

[b] Calculated values reported by Standing and Katz using apparent density method.

[c] Values in parentheses result after having matched the retrograde dew point pressure predicted by the ZJRK EOS. Interaction coefficients between methane and all C7+ fractions were adjusted to 0.0819 and 0.0702 for the PR and SRK equations, respectively.

TABLE 1.5 - COMPARISON OF PREDICTED AND MEASURED HEPTANES-PLUS MOLECULAR WEIGHTS FOR THE STANDING/KATZ MIXTURES.

	Equilibrium Conditions		Heptanes-plus Molecular Weight							
			Vapor Phase				Liquid Phase			
Run No.	Pressure (MPa)	Temperature (K)	Exp.	PR	SRK	ZJRK	Exp.	PR	SRK	ZJRK
A-5	6.882	322.039	110.0a	96.76	96.48	96.43	162.0b	193.13	192.69	193.33
....				(96.59)d	(96.35)d			(192.81)d	(192.46)d	
A-4 and 41 ..	11.011	322.039	110.0a	98.54	98.02	97.82	196.0	195.25	194.50	195.53
....				(98.05)d	(97.67)d			(194.60)d	(194.03)d	
A-1	21.919	322.039	127.0	111.34	108.88	106.75	240.0	211.30	209.55	215.59
....				(106.40)d	(105.50)d			(207.84)d	(206.97)d	
A-2 and 21 ..	36.268	322.039	131.0	191.49	157.39	129.06	279.0	226.46	232.76	259.19
....				(127.37)d	(125.82)d			(231.77)d	(230.86)d	
A-3	56.570	322.039	144.0	c	c	173.05	356.0	c	c	324.78
....				(171.42)d	(170.96)d			(253.58)d	(251.94)d	
B-3	11.562	394.261	None	105.82	104.70	104.84	None	228.05	225.35	228.74
B-1	20.061	394.261	115.0a	114.80	112.03	111.88	231.0	240.86	235.84	243.22
B-2	42.668	394.261	None	c	176.78	153.08	None	c	277.57	318.15
C-2 and 21 ..	6.951	322.039	100.0a	96.53	96.29	96.24	186.0	186.85	186.65	186.95
C-1	19.820	322.039	113.0	105.90	104.39	103.17	186.0	191.77	191.34	194.26
C-3 and 31 ..	36.681	322.039	151.0	c	c	134.04	240.0	c	c	218.94
F-1	21.960	394.261	130.0	114.66	111.79	111.38	216.0	210.74	208.56	214.95
F-2	29.751	394.261	139.0	135.04	127.30	124.17	256.0	213.86	212.59	227.30
F-3	38.128	394.261	157.0	c	172.33	146.77	290.0	c	196.14	239.87
G-1	13.996	274.817	None	99.20	98.59	97.65	None	186.28	186.16	186.67
G-2	24.028	274.817	128.0	124.82	119.70	108.52	215.0	186.83	188.84	198.08
G-3	34.267	274.817	145.0	c	c	127.45	315.0	c	c	213.52
H-4	12.514	282.594	None	97.92	97.46	96.95	None	185.56	185.41	185.73
H-2	21.063	282.594	None	110.64	108.43	104.02	None	188.74	189.12	193.10
H-3	35.508	282.594	None	c	c	130.16	None	c	c	214.70
D-1	29.799	322.039	123.0	148.45	136.12	120.65	268.0	213.63	214.00	242.35
E-1	28.942	322.039	130.0	128.26	122.11	114.75	242.0	240.14	237.99	245.68

a Estimated by Standing and Katz.
b Molecular weight for pentanes-plus reported by Standing and Katz.
c Pressure higher than predicted saturation pressure.

TABLE 1.6 - COMPARISON OF PREDICTED AND MEASURED HEPTANES-PLUS SPECIFIC GRAVITIES FOR THE STANDING/KATZ MIXTURES.

Run No.	Equilibrium Conditions		Heptanes-plus Specific Gravity							
			Vapor Phase				Liquid Phase			
	Pressure (MPa)	Temperature (K)	Exp.	PR	SRK	ZJRK	Exp.	PR	SRK	ZJRK
A-5	6.882	322.039	0.742[a]	0.7106 (0.7102)[c]	0.7099 (0.7096)[c]	0.7098	None	0.8441 (0.8438)[c]	0.8437 (0.8435)[c]	0.8442
A-4 and 41	11.011	322.039	0.742[a]	0.7149 (0.7137)[c]	0.7137 (0.7128)[c]	0.7132	0.850	0.8458 (0.8453)[c]	0.8452 (0.8448)[c]	0.8460
A-1	21.919	322.039	0.775	0.7415 (0.7320)[c]	0.7369 (0.7302)[c]	0.7328	0.863	0.8580 (0.8555)[c]	0.8567 (0.8548)[c]	0.8609
A-2 and 21	36.268	322.039	0.788	0.8338 (0.7685)[c]	0.8085 (0.7661)[c]	0.7708	0.904	0.8694 (0.8719)[c]	0.8732 (0.8713)[c]	0.8876
A-3	56.570	322.039	0.802	b (0.8238)[c]	b (0.8233)[c]	0.8253	0.954	b (0.8858)[c]	b (0.8849)[c]	0.9191
B-3	11.562	394.261	None	0.7311	0.7289	0.7292	None	0.8690	0.8673	0.8694
B-1	20.061	394.261	0.753[a]	0.7479	0.7430	0.7428	0.870	0.8769	0.8738	0.8781
B-2	42.668	394.261	None	b	0.8292	0.8029	None	b	0.8985	0.9154
C-2 and 21	6.951	322.039	0.725[a]	0.7100	0.7094	0.7093	0.836	0.8388	0.8386	0.8389
C-1	19.820	322.039	0.750	0.7309	0.7278	0.7253	0.844	0.8429	0.8426	0.8450
C-3 and 31	36.681	322.039	0.800	b	b	0.7783	0.881	b	b	0.8638
F-1	21.960	394.261	0.768	0.7476	0.7424	0.7417	0.862	0.8576	0.8560	0.8605
F-2	29.751	394.261	0.791	0.7800	0.7685	0.7635	0.888	0.8602	0.8592	0.8691
F-3	38.128	394.261	0.808	b	0.8250	0.7955	0.912	b	0.8469	0.8776
G-1	13.996	274.817	None	0.7164	0.7150	0.7128	None	0.8383	0.8382	0.8386
G-2	24.028	274.817	0.765	0.7647	0.7562	0.7361	0.863	0.8388	0.8405	0.8481
G-3	34.267	274.817	0.792	b	b	0.7685	0.903	b	b	0.8599
H-4	12.514	282.594	None	0.7134	0.7123	0.7111	None	0.8377	0.8375	0.8378
H-2	21.063	282.594	None	0.7401	0.7359	0.7271	None	0.8404	0.8407	0.8441
H-3	35.508	282.594	None	b	b	0.7726	None	b	b	0.8608
D-1	29.799	322.039	0.788	0.7994	0.7826	0.7584	0.893	0.8621	0.8621	0.8796
E-1	28.942	322.039	0.771	0.7693	0.7597	0.7474	0.877	0.8761	0.8747	0.8790

[a] Estimated by Standing and Katz.

[b] Pressure higher than predicted saturation pressure.

[c] Values in parentheses result after having matched the retrograde dew point pressure predicted by the ZJRK EOS. Interaction coefficients between methane and all C7+ fractions were adjusted to 0.0819 and 0.0702 for the PR and SRK equations, respectively.

TABLE 1.7 - COMPARISON OF PREDICTED AND MEASURED LIQUID VOLUMES FOR THE STANDING/KATZ MIXTURES.

Run No.	Equilibrium Conditions		Liquid Volume - Percent of Total			
	Pressure (MPa)	Temperature (K)	Exp.	PR	SRK	ZJRK
A-5	6.882	322.039	3.0	5.37 (5.18)c	5.75 (5.59)c	4.57
A-4 and 41	11.011	322.039	9.3	9.58 (8.96)c	10.10 (9.58)c	7.91
A-1	21.919	322.039	15.6	19.28 (16.38)c	19.63 (17.25)c	13.23
A-2 and 21	36.268	322.039	21.0	6.53 (18.22)c	19.48 (19.19)c	11.76
A-3	56.570	322.039	19.1	0.00b (8.59)c	0.00b (9.35)c	3.12
B-3	11.562	394.261	None	4.75	5.15	3.95
B-1	20.061	394.261	8.7	8.24	8.92	6.54
B-2	42.668	394.261	None	0.00b	4.06	5.16
C-2 and 21	6.951	322.039	11.2	11.44	12.18	9.88
C-1	19.820	322.039	33.0	40.58	40.58	29.92
C-3 and 31	36.681	322.039	25.0	100.00b	100.00b	32.31
F-1	21.960	394.261	22.6	24.29	25.29	18.95
F-2	29.751	394.261	22.8	32.66	33.60	21.80
F-3	38.128	394.261	19.0	0.00b	41.69	19.59
G-1	13.996	274.817	34.2	41.44	41.40	30.52
G-2	24.028	274.817	29.0	84.86	74.89	39.42
G-3	34.267	274.817	13.3a	100.00b	100.00b	36.59
H-4	12.514	282.594	28.5	33.04	33.54	25.72
H-2	21.063	282.594	41.0	62.12	59.08	37.84
H-3	35.508	282.594	8.9	100.00b	100.00b	35.76
D-1	29.799	322.039	2.4	4.34	9.61	6.15
E-1	28.942	322.039	18.0	24.79	24.97	16.00

a Evidence of third phase separation reported by Standing and Katz.
b Pressure higher than predicted saturation pressure.
c Values in parentheses result after having matched the retrograde dew point pressure predicted by the ZJRK EOS. Interactionn coefficients between methane and all C7+ fractions were adjusted to 0.0819 and 0.0702 for the PR and SRK equations, respectively.

TABLE 1.8a - COMPARISON OF PREDICTED AND MEASURED K-VALUES FOR THE STANDING/KATZ MIXTURE A.

	Equilibrium Conditions		Equilibrium Constant						
Run No.	Pressure (MPa)	Temperature (K)	C1	C2	C3	n-C4	C5's	n-C6	C7+
A-5	6.882	322.039							
...... Exp. :			4.12	0.97	0.547	0.450	-	-	-
...... PR :			3.4888	1.0334	0.4331	0.1826	0.0864	0.0370	0.0101
...... PRb:			(4.2713)	(1.0251)	(0.4259)	(0.1780)	(0.0837)	(0.0328)	(0.0089)
...... SRK :			3.5631	1.0941	0.4559	0.2025	0.0887	0.0377	0.0092
...... SRKb:			(4.1925)	(1.0884)	(0.4502)	(0.1986)	(0.0864)	(0.0342)	(0.0083)
...... ZJRK :			4.2247	1.2327	0.4847	0.2167	0.0934	0.0389	0.0091
A-4 and 41 ..	11.011	322.039							
...... Exp. :			3.09	0.72	0.388	0.192	0.093	0.065	0.036
...... PR :			2.3834	0.8649	0.4250	0.2101	0.1149	0.0581	0.0166
...... PRb:			(2.9046)	(0.8542)	(0.4131)	(0.2010)	(0.1085)	(0.0473)	(0.0134)
...... SRK :			2.4276	0.9045	0.4392	0.2252	0.1142	0.0575	0.0148
...... SRKb:			(2.8444)	(0.8975)	(0.4300)	(0.2178)	(0.1090)	(0.0490)	(0.0125)
...... ZJRK :			2.8639	1.0141	0.4608	0.2369	0.1177	0.0579	0.0141
A-1	21.919	322.039							
...... Exp. :			2.02	0.703	0.479	0.323	0.242	0.171	0.095
...... PR :			1.4816	0.8484	0.5863	0.4071	0.3012	0.2145	0.0734
...... PRb:			(1.8246)	(0.8252)	(0.5445)	(0.3612)	(0.2575)	(0.1388)	(0.0433)
...... SRK :			1.5130	0.8739	0.5935	0.4166	0.2888	0.2095	0.0642
...... SRKb:			(1.7850)	(0.8597)	(0.5624)	(0.3815)	(0.2551)	(0.1494)	(0.0423)
...... ZJRK :			1.8264	0.9796	0.6076	0.4203	0.2800	0.2688	0.0492
A-2 and 21 ..	36.268	322.039							
...... Exp. :			1.54	0.97	0.81	0.570	0.522	0.324	0.145
...... PR :			1.0732	0.9581	0.8923	0.8320	0.7870	0.7393	0.5338
...... PRb:			(1.4147)	(0.8746)	(0.7042)	(0.5692)	(0.4808)	(0.3038)	(0.1159)
...... SRK :			1.1373	0.9447	0.8318	0.7412	0.6544	0.6024	0.3264
...... SRKb:			(1.3891)	(0.9044)	(0.7234)	(0.5910)	(0.4747)	(0.3329)	(0.1171)
...... ZJRK :			1.4610	1.0138	0.7626	0.6269	0.4957	0.4229	0.1183
A-3	56.570	322.039							
...... Exp. :			1.39	0.90	0.865	0.830	0.728	0.782	0.173
...... PR :			a	a	a	a	a	a	a
...... PRb:			(1.1727)	(0.9300)	(0.8508)	(0.7799)	(0.7296)	(0.5536)	(0.3086)
...... SRK :			a	a	a	a	a	a	a
...... SRKb:			(1.1549)	(0.9500)	(0.8668)	(0.7978)	(0.7252)	(0.5996)	(0.3253)
...... ZJRK :			1.2673	1.0234	0.8632	0.7782	0.6784	0.6388	0.2263

a Pressure higher than predicted saturation pressure.

b Values in parentheses result after having matched the retrograde dew point pressure predicted by the ZJRK EOS. Interaction coefficients between methane and all C7+ fractions were adjsted to 0.0819 and 0.0702 for the PR and SRK equations, respectively.

TABLE 1.8b - COMPARISON OF PREDICTED AND MEASURED K-VALUES FOR THE STANDING/KATZ MIXTURES B AND C.

	Equilibrium Conditions		Equilibrium Constant						
Run No.	Pressure (MPa)	Temperature (K)	C1	C2	C3	n-C4	C5's	n-C6	C7+
B-3	11.562	394.261							
...... Exp. :			None	None	None	None	None	None	None
...... PR :			2.7906	1.2973	0.7525	0.4383	0.2750	0.1641	0.0362
...... SRK :			2.8293	1.3396	0.7749	0.4682	0.2774	0.1659	0.0338
...... ZJRK :			3.2580	1.4601	0.8519	0.4834	0.2922	0.1735	0.0322
B-1	20.061	394.261							
...... Exp. :			2.10	1.11	0.83	0.483	0.320	0.255	0.069
...... PR :			1.8228	1.0472	0.7142	0.4889	0.3549	0.2490	0.0656
...... SRK :			1.8540	1.0723	0.7239	0.5051	0.3468	0.2450	0.0594
...... ZJRK :			2.1339	1.1722	0.7961	0.5178	0.3602	0.2521	0.0527
B-2	42.668	394.261							
...... Exp. :			None	None	None	None	None	None	None
...... PR :			[a]	[a]	[a]	[a]	[a]	[a]	[a]
...... SRK :			1.1607	0.9770	0.8672	0.7784	0.6928	0.6364	0.3158
...... ZJRK :			1.4016	1.0480	0.8849	0.7107	0.6030	0.5314	0.1517
C-2 and 21 ..	6.951	322.039							
...... Exp. :			4.18	1.10	0.520	0.187	0.0695	0.0354	0.005
...... PR :			3.4434	1.0266	0.4322	0.1831	0.0878	0.0375	0.0110
...... SRK :			3.5151	1.0845	0.4543	0.2023	0.0900	0.0382	0.0101
...... ZJRK :			4.1220	1.2122	0.4806	0.2153	0.0945	0.0393	0.0101
C-1	19.820	322.039							
...... Exp. :			1.83	0.86	0.620	0.356	0.276	0.168	0.069
...... PR :			1.5422	0.8439	0.5635	0.3781	0.2724	0.1866	0.0719
...... SRK :			1.5718	0.8695	0.5711	0.3877	0.2625	0.1823	0.0633
...... ZJRK :			1.8313	0.9629	0.5884	0.3974	0.2623	0.1769	0.0553
C-3 and 31 ..	36.681	322.039							
...... Exp. :			1.42	0.98	0.92	0.86	0.78	0.70	0.218
...... PR :			[a]	[a]	[a]	[a]	[a]	[a]	[a]
...... SRK :			[a]	[a]	[a]	[a]	[a]	[a]	[a]
...... ZJRK :			1.2905	1.0178	0.8452	0.7445	0.6409	0.5786	0.2706

[a] Pressure higher than predicted saturation pressure.

TABLE 1.8c - COMPARISON OF PREDICTED AND MEASURED K-VALUES FOR THE STANDING/KATZ MIXTURES F AND G.

	Equilibrium Conditions		Equilibrium Constant						
Run No.	Pressure (MPa)	Temperature (K)	C1	C2	C3	n-C4	C5's	n-C6	C7+
F-1	21.960	394.261							
...... Exp. :			1.89	1.20	0.658	0.520	0.314	0.346	0.141
...... PR :			1.6135	1.0271	0.7539	0.5551	0.4302	0.3229	0.1247
...... SRK :			1.6469	1.0488	0.7594	0.5646	0.4164	0.3133	0.1108
...... ZJRK :			1.8421	1.1262	0.8200	0.5738	0.4281	0.3194	0.1012
F-2	29.751	394.261							
...... Exp. :			1.57	0.98	0.80	0.654	0.561	0.414	0.201
...... PR :			1.2805	0.9829	0.8308	0.7003	0.6089	0.5204	0.2714
...... SRK :			1.3242	1.0017	0.8232	0.6881	0.5714	0.4863	0.2247
...... ZJRK :			1.4996	1.0717	0.8708	0.6796	0.5598	0.4680	0.1772
F-3	38.128	394.261							
...... Exp. :			1.36	1.09	0.87	0.77	0.75	0.77	0.248
...... PR :			a	a	a	a	a	a	a
...... SRK :			1.1052	0.9964	0.9596	0.9273	0.8945	0.8694	0.7287
...... ZJRK :			1.2830	1.0428	0.9224	0.7895	0.7027	0.6378	0.3095
G-1	13.996	274.817							
...... Exp. :			None	None	None	None	None	None	None
...... PR :			1.6371	0.6499	0.3494	0.1892	0.1142	0.0630	0.0208
...... SRK :			1.6694	0.6801	0.3592	0.1990	0.1111	0.0626	0.0183
...... ZJRK :			2.0528	0.7013	0.3664	0.1926	0.1024	0.0541	0.0146
G-2	24.028	274.817							
...... Exp. :			1.44	0.96	0.79	0.585	0.528	0.422	0.217
...... PR :			1.1781	0.8602	0.7065	0.5823	0.5004	0.4187	0.2325
...... SRK :			1.2132	0.8736	0.6970	0.5667	0.4591	0.3918	0.1887
...... ZJRK :			1.5377	0.8792	0.6557	0.4878	0.3584	0.2809	0.0944
G-3	34.267	274.817							
...... Exp. :			1.35	0.96	0.86	0.80	0.71	0.655	0.289
...... PR :			a	a	a	a	a	a	a
...... SRK :			a	a	a	a	a	a	a
...... ZJRK :			1.3211	0.9509	0.8156	0.6977	0.5852	0.5280	0.2248

a Pressure higher than predicted saturation pressure.

TABLE 1.8d - COMPARISON OF PREDICTED AND MEASURED K-VALUES FOR THE STANDING/KATZ MIXTURES H, D, AND E.

Run No.	Equilibrium Conditions		Equilibrium Constant						
	Pressure (MPa)	Temperature (K)	C1	C2	C3	n-C4	C5's	n-C6	C7+
H-4	12.514	282.594							
...... Exp. :			None	None	None	None	None	None	None
...... PR :			1.8288	0.6521	0.3224	0.1605	0.0899	0.0454	0.0144
...... SRK :			1.8650	0.6824	0.3314	0.1697	0.0876	0.0448	0.0126
...... ZJRK :			2.2672	0.6946	0.3440	0.1691	0.0842	0.0408	0.0108
H-2	21.063	282.594							
...... Exp. :			None	None	None	None	None	None	None
...... PR :			1.3176	0.7978	0.5778	0.4204	0.3261	0.2422	0.1060
...... SRK :			1.3469	0.8236	0.5850	0.4272	0.3115	0.2382	0.0927
...... ZJRK :			1.6572	0.8319	0.5795	0.3988	0.2725	0.1947	0.0618
H-3	35.508	282.594							
...... Exp. :			None	None	None	None	None	None	None
...... PR :			a	a	a	a	a	a	a
...... SRK :			a	a	a	a	a	a	a
...... ZJRK :			1.3008	0.9508	0.8300	0.7186	0.6104	0.5540	0.2466
D-1	29.799	322.039							
...... Exp. :			1.58	1.04	0.78	0.575	0.605	0.332	0.147
...... PR :			1.1360	0.9417	0.8356	0.7430	0.6760	0.6079	0.3877
...... SRK :			1.1811	0.9458	0.8109	0.7045	0.6085	0.5442	0.2958
...... ZJRK :			1.4934	1.0231	0.7623	0.6179	0.4850	0.4037	0.1302
E-1	28.942	322.039							
...... Exp. :			1.72	0.94	0.712	0.500	0.357	0.296	0.073
...... PR :			1.3290	0.8558	0.6439	0.4865	0.3874	0.2999	0.0984
...... SRK :			1.3652	0.8758	0.6445	0.4885	0.3625	0.2891	0.0812
...... ZJRK :			1.7114	0.9892	0.6500	0.4793	0.3360	0.2554	0.0516

a Pressure higher than predicted saturation pressure.

1.7 Proposed EOS Modifications

Several methods for improving EOS predictions of petroleum reservoir fluids have been proposed during this study. Although they have not necessarily proven to be major improvements, or even original, their presentation reviews some important aspects of EOS development.

The two-term, four-constant generalized EOS proposed by Martin is given in paper A.5. Several new aspects of his equation have been developed in this work: the fugacity and Z-explicit expressions are formulated; equations for calculating EOS constants are proposed. Two new equations are proposed: a modified UM EOS and an extended PR EOS.

The modified UM EOS is developed using a method similar to the ZJRK procedure. As mentioned in the previous section, this work resembles Fuller's. What is presented here, however, was completed without knowledge of the former and also appears to be simpler and more conducive to petroleum-engineering applications. Details of the proposed modification can be found in paper A.5.

The present discussion will consider the description of several cubic equations in terms of the proposed EOS family. The Z-explicit form of the general Martin equation is,

$$\begin{aligned} &Z^3 + Z^2\{-3B + (C+D-1)\} \\ &\quad + Z\cdot\{3B^2 - 2B(C+D-1) + (A+CD-C-D)\} \\ &\quad + \{-B^3 + B^2(C+D-1) - B(A+CD-C-D) - CD\} = 0 \end{aligned} \qquad \text{... (1.5)}$$

where EOS constants are given by

$$A = a\cdot p/R^2T^2 = \alpha\cdot\Omega_a\cdot p_r/T_r^2 \quad \text{.................... (1.6a)}$$

$$B = b\cdot p/RT = \beta\cdot\Omega_b\cdot p_r/T_r \quad \text{..................... (1.6b)}$$

$$C = c\cdot p/RT = \xi\cdot\Omega_c\cdot p_r/T_r \quad \text{..................... (1.6c)}$$

$$D = d\cdot p/RT = \delta\cdot\Omega_d\cdot p_r/T_r \quad \text{..................... (1.6d)}$$

where $p_r=p/p_c$ and $T_r=T/T_c$. Parameters α, β, ξ, and δ are correction terms to the EOS constants Ω_a, Ω_b, Ω_c, and Ω_d, respectively. The corrections are usually applied to ensure accurate VLE, and perhaps liquid volumetric predictions. They are temperature dependent and commonly rely on acentric factor to correlate variation in temperature dependence for compounds of varying species.

Numerical constants Ω_a, Ω_b, Ω_c, and Ω_d must be determined, typically using the critical constraints of van der Waals: $(\partial p/\partial V)=(\partial^2 p/\partial V^2)=0$ at critical temperature, T_c. These two constaints are only sufficient to define two of the EOS constants, with two more constraints remaining to be specified. An intuitive choice might be to choose critical compressibility factor, Z_c, for each compoud. Martin and Hou show that the combination of van der Waals criteria and specification of Z_c is equivalent to solving the cubic equation $(V-V_c)^3=0$, or its equivalent $(Z-Z_c)^3=0$. Imposing this relation on the general Martin equation results in,

$$-3Z_c = -3\Omega_b + (\Omega_c+\Omega_d-1) \quad \ldots\ldots\ldots\ldots\ldots\ldots \tag{1.7a}$$

$$3Z_c^2 = 3\Omega_b^2 - 2\Omega_b(\Omega_c+\Omega_d-1) + (\Omega_a+\Omega_c\Omega_d-\Omega_c-\Omega_d) \quad .. \tag{1.7b}$$

$$-Z_c^3 = -\Omega_b^3 + \Omega_b^2(\Omega_c+\Omega_d-1) - \Omega_b(\Omega_a+\Omega_c\Omega_d-\Omega_c-\Omega_d) -\Omega_c\Omega_d \quad \ldots\ldots\ldots\ldots\ldots\ldots \tag{1.7c}$$

What can be seen from Eq. 1.7 is that two groups, $\Omega_c+\Omega_d$ and $\Omega_c\Omega_d$, are present. If one more condition is imposed then values of all constants can be determined. Specifying another thermodynamic criterion might be considered, but is should be chosen with care. Consider, for example, the universal sum-chart value, $\sigma=0.62$, suggested by Martin (where $\sigma=Z_c-\partial Z/\partial p_r$ at $p_r=0$ and $T_r=1$). It can be shown that the fourth criterion becomes,

$$Z_c = \Omega_b - \Omega_a + \sigma \quad \ldots\ldots\ldots\ldots\ldots\ldots\ldots\ldots \tag{1.8}$$

and EOS constants are given by

$$\Omega_b^3 + \Omega_b^2(3-3Z_c) + \Omega_b(3Z_c^2-6Z_c+2) + (-Z_c^3+3Z_c^2-2Z_c+1-\sigma) = 0 \quad \ldots\ldots\ldots\ldots\ldots\ldots \quad (1.9a)$$

$$\Omega_a = \Omega_b + \sigma - Z_c \quad \ldots\ldots\ldots\ldots\ldots\ldots \quad (1.9b)$$

$$\Omega_c^2 + \Omega_c(-u-1) + w = 0 \quad \ldots\ldots\ldots\ldots\ldots\ldots \quad (1.9c)$$

$$\Omega_d = w/\Omega_c \quad \ldots\ldots\ldots\ldots\ldots\ldots \quad (1.9d)$$

where

$$u = 3\Omega_b - 3Z_c \quad \ldots\ldots\ldots\ldots\ldots\ldots \quad (1.10a)$$

$$w = Z_c^3 + 2\Omega_b^3 - 3Z_c\Omega_b^2 - 3\Omega_b(Z_c-\Omega_b)^2 \quad \ldots\ldots\ldots \quad (1.10b)$$

The largest root of Eq. 1.9a is chosen for Ω_b, and either of the roots in Eq. 1.9c can be chosen, the second root being equal to Ω_d.

Martin reports the PR EOS gives σ=0.68684. Recalling that Z_c for the PR EOS is 0.307401...; solving Eqs. 1.9a and 1.9b gives Ω_b=0.07780 and Ω_a=0.45723. From Eqs. 1.10, u=-0.6888 and w=0.0121, yielding Ω_c=0.26565 or 0.045548 and Ω_d=0.045548 or 0.26565. Using the sum-chart criterion results in a symetric relation between constants Ω_c and Ω_d, as shown by this example; note, $(2-\sqrt{2})$x0.0778=0.0945548 and $(2+\sqrt{2})$x0.0778=0.26565.

Theoretically we have defined a four-constant EOS using purely thermodynamic criteria. Practically, however, the true (experimental) values of Z_c and σ will not give the best equation. In fact, purely mathematical constraints must be respected, thereby limiting the range of values of σ for a given Z_c. Observation shows that for all Z_c of interest, constants $(3-3Z_c)$ and $(3Z_c^2-6Z_c+2)$ are positive (see Table 1.9). Since Ω_b represents a key parameter in the cubic EOS and its value should be close to 1/10 for the resulting equation to yield reasonable high densities (Abbott), the last constant in Eq. 1.9a must be less than zero. For this to be so, σ must be *larger* than the values listed in the last column of Table 1.9, where the value is dependent on Z_c. Interestingly, the original van der Waals EOS yields σ=0.62, an observation overseen by Martin.

TABLE 1.9 - LIMITATIONS OF THE EOS MODEL USING MARTIN'S SUM-CHART AS A CRITERIA FOR DEFINING EOS CONSTANTS

Z_c	$(3-3Z_c)$	$(3Z_c^2-6Z_c+2)$	Limiting σ = $-Z_c^3+3Z_c^2-2Z_c+1$
0.250	2.250	0.687500	0.671875
0.275	2.175	0.576875	0.656078
0.300	2.100	0.470000	0.643000
0.325	2.025	0.366875	0.632547
1/3	2.000	0.333333	0.629630
0.35	1.950	0.267500	0.624625
0.375	1.875	0.171875	0.619141

This excercise exhibits the limitations and danger in forcing too many and too rigid thermodynamic criteria for the general four-constant EOS. A practical review of popular cubic equations suggests two workable approaches. They both require, however, the use of van der Waals critical criteria - i.e., critical temperature and critical pressure are EOS variables defining the nature of a compound. Thereafter the methods differ as summarized below:

- Set Z_c at a constant, universal value for all compounds and define, somewhat empirically, the relation between constant Ω_c (or Ω_d) and Ω_b. Examples would be the PR EOS where Z_c=0.307401... and $\Omega_c=(2-\sqrt{2})\Omega_b$; or the RK EOS where $Z_c=1/3$ and $\Omega_c=\Omega_b$.

- Allow Z_c to vary for each component, thereby fully utilizing the critical criteria $(Z-Z_c)^3=0$ at T_c, p_c. Once again, an arbitrary relation is specified between Ω_c (or Ω_d) and Ω_b. Examples would be the Usdin/McAuliffe EOS where $\Omega_c=\Omega_b$ and Z_c is specified or given as a function of ω; or the Schmidt/Wenzel EOS which relates Ω_c and Ω_b differently for each compound, dependent on ω (as is Z_c).

With these points in mind, the development of a new family of cubic equations is suggested. It is only one of many possibilities, as can be inferred from the discussion above. It offers, however, a means of generalizing most of the popular cubic equations and studying the behavior of different equations in more general terms.

The proposed family starts from the general four-constant Martin EOS, and applies the full critical criteria for each component, allowing the specification of Z_c different than measured experimentally. The relation between EOS constant Ω_c (or Ω_d) and Ω_b is directly proportional - i.e., $\Omega_c=\lambda\cdot\Omega_b$, where λ is a numerical constant which is not necessarily the same value for all compounds. It merely allows the definition of a specific EOS. The proposed family of cubic equations is now presented in terms of other well known EOS's. The objective is to relate the old equations in terms of the parameters Z_c and λ. The correction factors for EOS constants are also given, resulting in complete definition of the particular equation.

Redlich/Kwong

$\lambda = 1$

$Z_c = 1/3$

- Soave modification:

$\sqrt{\alpha(T_r,\omega)} = 1 + m(1-\sqrt{T_r})$

$m = 0.480 + 1.574\omega - 0.176\omega^2$

Peng/Robinson

$\lambda = 2-\sqrt{2}$ (or $2+\sqrt{2}$)

$Z_c = 0.307401 \ldots$

$\sqrt{\alpha(T_r,\omega)} = 1 + m(1-\sqrt{T_r})$

$m = 0.37464 + 1.54226\omega - 0.26992\omega^2$

Martin, $p=RT/(v-b)-a/(v+c-b)^2$; $c=d$

$\lambda = 0.125/(Z_c-0.25)$

- Kubic modification:

$Z_c = 0.291 - 0.083\cdot\omega'$ (modified Pitzer)

$\alpha(T_r,\omega) = \alpha^0 + \alpha^1\cdot\omega'$

$$\alpha^0 = -0.1514T_r + 0.7895 + 0.3314/T_r + 0.029/T_r^2 + 0.0015/T_r^7$$

$$\alpha^1 = -0.237T_r-0.7846/T_r+1.0026/T_r^2+0.019/T_r^7$$

$\beta = 1$

$$\xi(T_r,\omega')=\delta(T_r,\omega')=(0.043\gamma^0+0.0713\omega'\gamma^1)/(\Omega_c-\Omega_b)$$

$$\gamma^0 = 4.275051 - 8.878889/T_r + 8.508932/T_r^2 - 3.481408/T_r^3 + 0.576312/T_r^4$$

$$\gamma^1 = 12.856404 - 34.744125/T_r + 37.433095/T_r^2 - 18.059421/T_r^3 + 3.514050/T_r^4$$

$$\omega' = 0.000756 + 0.90984\omega + 0.16226\omega^2 + 0.14549\omega^3$$

Usdin/McAuliffe

$\lambda = 1$

$\sqrt{\alpha(T_r,\omega)} = 1 + m(1-\sqrt{T_r})$

$m = 0.48049 + 4.516\omega Z_c + \{0.67713(\omega-0.35)-0.02\}(T_r-0.7)$
for $T_r \le 0.7$

$m = 0.48049 + 4.516\omega Z_c - \{0.67713(\omega-0.35)-0.02\}\times 0.4$
for $T_r \le 0.3$

$m = 0.48049 + 4.516\omega Z_c + \{37.7846\omega Z_c^3 + 0.78662\}(T_r-0.7)^2$
for $0.7<T_r\le 1.0$

Usdin and McAuliffe suggest extrapolation at $T_r>1$ by matching the slope at $T_r=1$ from the preceeding expression. No equation is given, but the following satisfies their criteria of extrapolation,

$$m = 0.48049 + 4.516\omega Z_c + (37.7846\omega Z_c^3+0.78662)\times (0.69-0.6/T_r) \text{ for } T_r>1$$

Usdin and McAuliffe do not suggest experimental values of Z_c be used. Instead, they give best-fit values obtained by matching specific gravity (i.e., density at standard conditions). An extrapolation for heavy petroleum fractions is given by the best-fit equation,

$$Z_c = 0.3328 - 0.0421\cdot\omega$$

- Fuller modification:

The Fuller EOS is equivalent to the UM EOS when both are expressed in their simplest form (without EOS constant correction factors). The equation form given by Fuller is unnecessarily complicated, as is easily seen when trying to make the necessary simplifications to equate it with the UM EOS. Also, the correlating variable for EOS constant Ω_b is parachor instead of acentric factor, an unfortunate choice (and probably without real physical justification). The Fuller relations are therefore not included, and in its place are the equations developed in the present study.

- Proposed modification:

$$Z_c = 0.291 - 0.08\omega \text{ (Pitzer)}$$

$$\sqrt{\alpha(T_r,\omega)} = 1 + m(1-T_r)$$

$$m = 0.46089 + 1.2032\omega - 0.34548\omega^2$$

$$\beta = 1 + (\beta^*-1)\{2/(1+e^{8(T_r-1)})-1\}$$

$$\beta^* = 1.4891 + 0.92175\omega + 0.40116\omega^2 \quad (T_r\le 1)$$

$$\beta^* = 1 \quad (T_r>1)$$

$$\xi = \beta$$

$$\delta = 1 + (\Omega_b/\Omega_d)(\beta-1)$$

Schmidt/Wenzel (modified by Wenzel/Moorwood/Baumgartner)

$\lambda = 3(1+\omega)/2 \pm \{\sqrt{(9(1+\omega)^2-8)}\}/2$

$Z_C = \{3\cdot(1+\omega\cdot\beta_C)\}^{-1}$

where β_C is the smallest root of the cubic equation:

$(6\omega+1)\beta_C{}^3 + 3\beta_C{}^2 + 3\beta_C - 1 = 0$

$\sqrt{\alpha(T_r,\omega)} = 1 + m(1-\sqrt{T_r})$ for $T_r \leq 1$

$\alpha(T_r,\omega) = 1 - (0.4774+1.328\omega)\ln(T_r)$ for $T_r > 1$

$m = m^0$ for $\omega \leq 0.4$

$m = m^1$ for $\omega \geq 0.55$

$m = m^1((\omega-0.4)/0.15) + m^0((0.55-\omega)/0.15)$ for $0.4 < \omega < 0.55$

$m^0 = k^0 + (1/70)(5T_r-3k^0-1)^2$

$m^1 = k^0 + 0.71(T_r-0.779)^2$

$k^0 = 0.465 + 1.347\omega - 0.528\omega^2$ for $\omega \leq 0.3671$

$k^0 = 0.5361 + 0.9593\omega$ for $\omega > 0.3671$

... would be interesting to know what happens physically at acentric factors of 0.3671, 0.4, and 0.55!(?)

Peneloux/Rauzy/Freze

$$\lambda = 1 - 0.40768\cdot(0.29441-Z_{ra})/\Omega_{b,RK}$$

$$Z_c = \{1-\Omega_{b,RK}\cdot(1-\lambda)\}/3$$

$$\sqrt{\alpha(T_r,\omega)} = 1 + m(1-\sqrt{T_r}) \quad \text{(Soave)}$$

$$m = 0.480 + 1.574\omega - 0.176\omega^2$$

where $\Omega_{b,RK} = 0.08664$ ... is the original RK EOS constant and Z_{ra} is the Rackett compressibility factor used to predict saturated liquid densities (see Table 2 in paper A.5).

The table below shows λ and Z_c for several values of the Rackett variable, indicating only a slight modification of the original RK EOS for a rather large variation in Z_{ra}.

Z_{ra}	λ	Z_c
0.28	0.9322	0.3314
0.29	0.9792	0.3327
0.30	1.0263	0.3341
0.31	1.0734	0.3355
0.32	1.1204	0.3368
0.33	1.1675	0.3382

The suggested procedure for calculating Z_{ra} for PNA fractions based on the Robinson/Peng correlations is of questionable merit. Refer to Paper A.4 for a discussion of PNA densities.

Coats

$m_1 = \lambda - 1$

$m_2 = 2 - \lambda - (1-3\cdot Z_c)/\Omega_b$

Values of m_1 and m_2 for the RK and PR equations are, respectively, $m_1=0$ and $m_2=1$, and $m_1=1+\sqrt{2}$ and $m_2=1-\sqrt{2}$. If the Coats EOS becomes popular because of its use by commercial users then the relations above give a simple means of calculating constants m_1 and m_2 where one physical parameter is used (Z_c).

Having already considered the sum-chart as a thermodynamic parameter, it is interesting to consider its relation to Z_c and λ. As shown in paper A.5, the minimum value of σ is 0.67188. This occurs for combinations of Z_c and λ corresponding to the Martin EOS, $p=RT/(v-b)-a/(v+c-b)^2$, which corresponds to $\Omega_c=\Omega_d$. Unfortunately the component fugacity relation derived in paper A.5 for the four-constant Martin EOS assumes $\Omega_c\neq\Omega_d$. The relation which must be used instead is found in the literature (e.g., Kubic),

$$\ln(f/p) = -\ln(Z-B) + B/(Z-B) - 2A/(Z+C-B) + A(C-B)/(Z+C-B)^2 \quad \text{.................... (1.11)}$$

$$\ln(f_i/x_ip) = -\ln(Z-B) + B_i/(Z-B) - 2\cdot \Sigma x_jA_{ij}/(Z+C-B) + A(C_i-B_i)/(Z+C-B)^2 \quad \text{... (1.12)}$$

and also applies to the Kubic modification of the original Martin three-constant EOS.

As an extension of the family of cubic EOS's proposed in this paper, a study was made to find the optimal values of λ and Z_c for several paraffins which minimized the absolute average error, $E(\lambda,Z_c)$, of saturated vapor and liquid densities, after having first fit the EOS to vapor pressure data using correction factor α. Results are shown in Figs. 1.1 to 1.3. Two values of λ have been chosen: $\lambda=1$ and $\lambda=2-\sqrt{2}$, corresponding to the RK and PR EOS's when $Z_c=1/3$ and $Z_c=0.307401...$, repsectively. Calculations were performed at T_r from 0.4 to 0.96 at intervals of 0.02 using the

Lee/Kesler correlation for vapor pressure. If vapor pressure from the Lee/Kesler correlation was less than 0.1 psia then the particular T_r point was not included.

Fig. 1.1 shows the error function, E_{sv}, for saturated vapors as a function of Z_c. Normal paraffins methane, butane, octane, and dodecane are considered. The first observation is that the minimum E_{sv} is approximately the same for all compounds, about 0.3%. In fact, the error is not large (less than 3%) for all values of Z_c in the range 0.24 to 0.40. Interestingly, minima occur at about the same Z_c for both $\lambda=1$ and $\lambda=2-\sqrt{2}$, though somewhat lower for $\lambda=1$. Approximate values of the minima are given in Table 1.10.

Figs. 1.2 and 1.3 show the error function, E_{sl}, for saturated liquids as a function of Z_c. Once again, normal paraffins methane, butane, octane, and dodecane are considered. Fig. 1.2 gives results for $\lambda=1$, and Fig. 1.3 gives results for $\lambda=2-\sqrt{2}$. The minima for E_{sl} are approximately the same for all compounds. However, the minimum for $\lambda=1$ is slightly higher than for $\lambda=2-\sqrt{2}$ (about 2.75% versus 1.75%, respectively), and minimum errors decrease slightly for heavier compounds.

TABLE 1.10 - VALUES OF CRITICAL COMPRESSIBILITY FACTORS MINIMIZING SATURATED VAPOR AND LIQUID DENSITIES FOR VALUES OF λ = 1 AND $2-\sqrt{2}$

	Critical Compressibility Factors Mimimizing Absolute Average Error		
Normal Paraffin	Vapor $\lambda=1,\ 2-\sqrt{2}$	Liquid $\lambda=1$	Liquid $\lambda=2-\sqrt{2}$
methane	0.336	0.330	0.321
butane	0.312	0.322	0.312
octane	0.289	0.314	0.304
dodecane	0.274	0.309	0.298

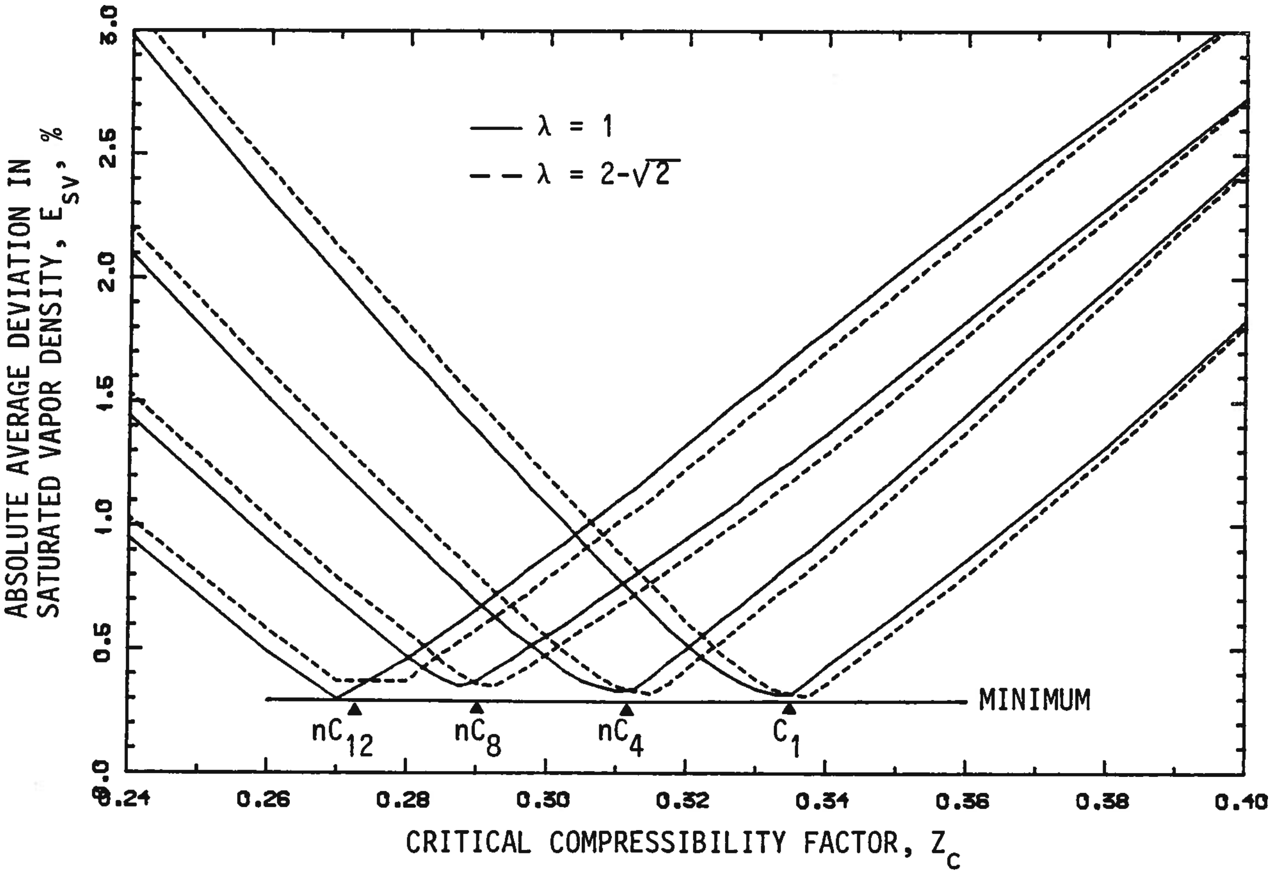

Fig. 1.1 - Calculated Error in Saturated Vapor Density of Four Normal Paraffins as a Function of EOS Critical Compressibility Factor for Two Values of EOS-Defining Constant λ.

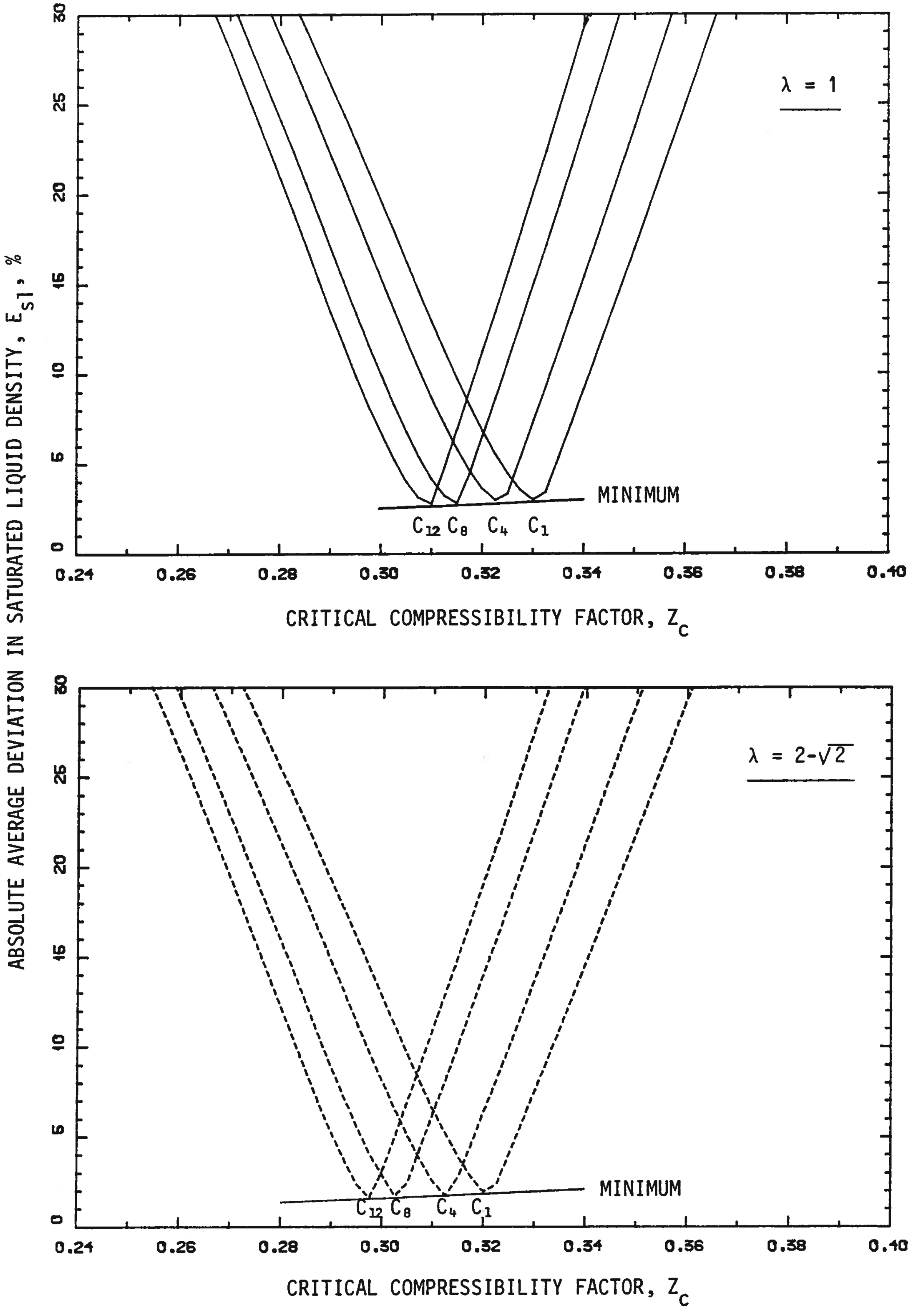

Figs. 1.2 and 1.3 - Calculated Error in Saturated Liquid Density of Four Normal Paraffins as a Function of EOS Critical Compressibility Factor for Two Values of EOS-Defining Constant λ.

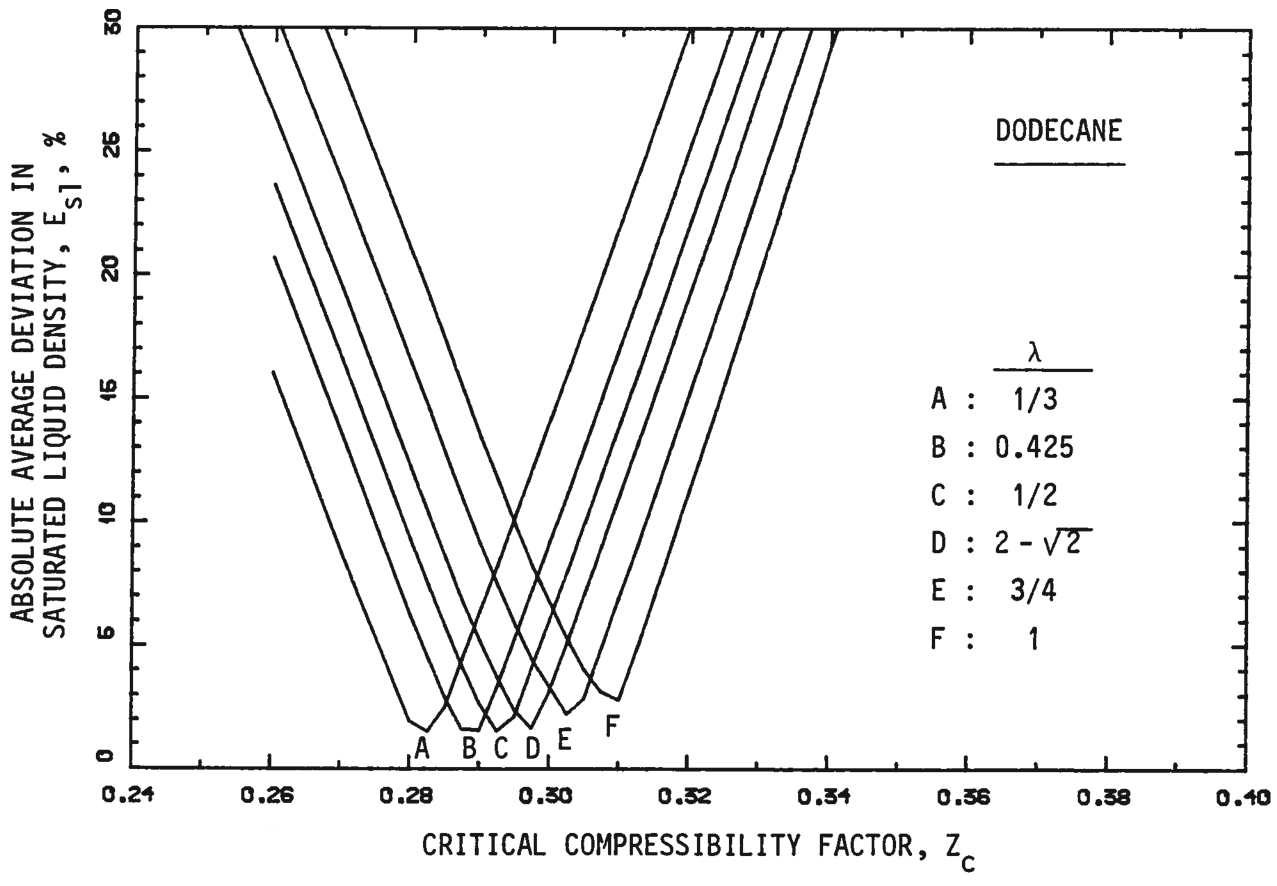

Fig. 1.4 - Calculated Error in Saturated Liquid Density of Dodecane as a Function of EOS Critical Compressibility Factor for Six Values of EOS-Defining Constant λ.

Since minimum errors do not appear to be strongly dependent on the compound, the effect of λ on minimum error is studied by using dodecane only. Also, only the saturated liquid density error is considered. This seems reasonable since the vapor density predictions are less sensitive to λ and Z_c. Fig. 1.4 shows the E_{sl} function for dodecane using several values of λ (1/3, 0.425, 1/2, $2-\sqrt{2}$, 3/4, and 1). It is seen that the minima occur at decreasing values of Z_c and that no improvement occurs at λ values lower than approximately $2-\sqrt{2}$ ($E_{sl} \approx 1.75\%$). There is probably nothing magical about this value of λ, but it is chosen to develop a new three-constant EOS quite similar, but less complicated than the Schmidt/Wenzel EOS.

The first task involves correlating optimal values of Z_c for $\lambda=2-\sqrt{2}$ as a function of acentric factor. The relation is simple and quite accurate,

$$Z_c = 0.3208 - 0.0415\omega \quad \ldots\ldots\ldots\ldots\ldots\ldots\ldots\ldots \quad (1.13)$$

which yields the PR EOS if $\omega=0.3229$ (somewhat between normal hexane and normal heptane).

Next, the correction function, α, is correlated as a function of temperature and acentric factor. The Soave form for α is used,

$$\sqrt{\alpha} = 1 + m(1-\sqrt{T_r}) \quad \ldots\ldots\ldots\ldots\ldots\ldots\ldots\ldots \quad (1.14)$$

where m is a smooth function of acentric factor, as shown in Fig. 1.5,

$$m = 0.40841 + 1.44989\omega - 0.25370\omega^2 \quad \ldots\ldots\ldots\ldots \quad (1.15)$$

What really has been done by utilizing the empirical criteria of minimized saturated liquid density error is best illustrated in Fig. 1.6. The error between calculated and experimental saturated liquid compressibility factors has been plotted as a function of reduced temperature for normal butane (same figure as given by Peng and Robinson). The new equation is compared with the original PR and SRK equations. The important factor is that the shape of all curves is the same (also exhibited by the Schmidt/Wenzel EOS). The new equation results in a shift so that the total absolute error is minimized. To predict liquid (and vapor) densities in the near-critical region requires that correction factor β (and possibly ξ and δ) be used and correlated as a function of reduced temperature and acentric factor, along the lines proposed for the modified Usdin/McAuliffe EOS.

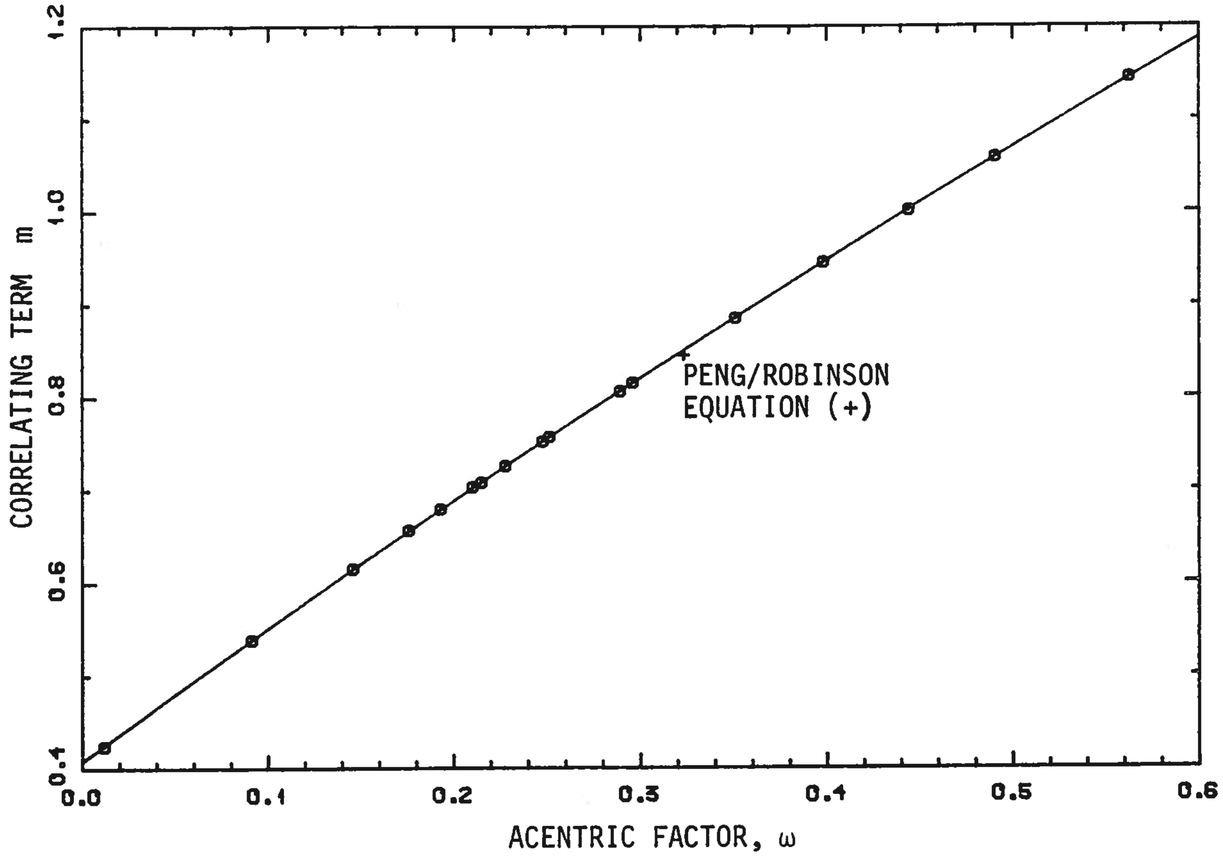

Fig. 1.5 - Relation Between Correlating Parameter m and Acentric Factor for the Proposed EOS.

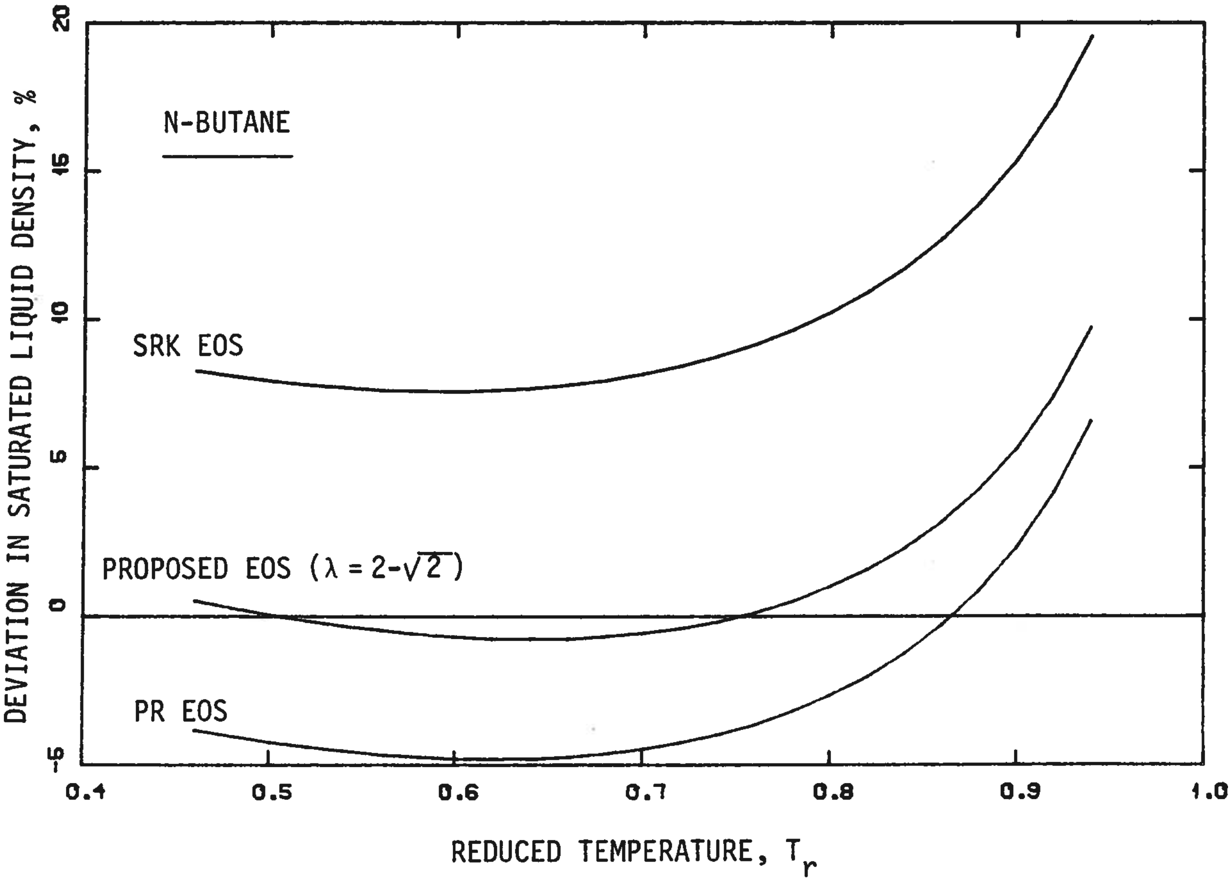

Fig. 1.6 - Error in Saturated Liquid Density of Normal Butane for Three Equations of State.

NOMENCLATURE

a,b,c,d,e,f,g = constants in the general forms of the cubic EOS

A,B,C,D = EOS constants

A_{ij},B_i,C_i,D_i = EOS constants for component i

f = fugacity

f/p = fugacity coefficient of a pure component

$f_i/x_i p$ = fugacity coefficient of component i in a mixture

k^0,k^1 = correlating parameters in the Schmidt/Wenzel EOS for parameter m

K = Watson (Universal Oil Products) characterization factor = $T_b(^{o}R)^{1/3}/\gamma$

m = correlating parameter in the Soave-type correction factor expression for α, usually made a polynomial function of ω

m^0,m^1 = limiting values for m in the Schmidt/Wenzel EOS

m_1,m_2 = defining parameters in the Coats modification of Martin's four-constant EOS

M = molecular weight (mass)

N = number of moles

p = absolute pressure

p_r = reduced pressure, $=p/p_c$

p_c = critical pressure, absolute units

R = universal gas constant

T = absolute temperature

T_c = critical temperature, absolute units

T_r = reduced temperature, $=T/T_c$

u,w = expressions used for defining EOS constants using van der Waals critical criteria

V = volume

Z = compressibility factor, $=pV/NRT$

Z_c = critical compressibility factor

Z_{ra} = Rackett critical compressibility factor used in a correlation for estimating saturated liquid densities of pure compounds

α,β,ξ,δ = correction factors for EOS constants

α^0,α^1 = correlating parameters in the Kubic modification of the Martin three-constant EOS for correction factor α

γ^0,γ^1 = correlating parameters in the Kubic modification of the Martin three-constant EOS for correction factors ξ and δ

β^* = limiting value of the correction factor β in the proposed modification of the Usdin/McAuliffe EOS (termed ’cold temperature beta limit by Fuller)

β_c = defining parameter for expressing the Schmidt/Wenzel EOS in terms of the proposed family of equations

λ = proportionality constant between EOS constants Ω_c and Ω_b, defining the proposed family of cubic equations

ρ = density

σ = sum-chart (proposed by Martin)
= $Z_c - \partial Z/\partial p_r$ at $p_r=0$ and $T_r=1$

ω = acentric factor,
= $-\log(p_v/p_c)-1.0$ at $T_r=0.7$

ω' = corrected acentric factor used by the Kubic modification of the Martin three-constant EOS

$\Omega_a,\Omega_b,\Omega_c,\Omega_d$ = numerical constants defining EOS costants

Chapter 2

CHARACTERIZING PETROLEUM FRACTIONS

... as easy as an Okie sayin 'ae e tronder ae'

2.1 Introduction to the Problem

This chapter reviews and updates work performed on characterization of petroleum fractions. In the present discussion a petroleum fraction is considered any mixture of hydrocarbons with more than six carbon atoms. The petroleum industry usually refers to the entire mixture of such compounds as heptanes-plus, C_{7+}. Depending on the method of chemical analysis, several compounds with six carbon atoms (e.g., benzene) may be found in the heptanes-plus fraction.

The characterization of petroleum fractions may consist of different procedures for different engineering purposes. This study considers characterization as the following:

- Description of the relation between molar quantity (mole fraction) and molecular weight, hereafter referred to as molar distribution,
- Measurement or estimation of specific gravity and normal or average boiling point,
- Estimation of critical pressure, critical temperature, and acentric factor.

Other properties are either difficult or expensive to obtain (e.g., paraffin/naphthene/aromatic content, PNA) or are seldom available to the petroleum engineer (e.g., viscosity, refractive index, cloud point).

Mole fraction has the obvious function of defining composition. Molecular weights are needed to convert from molar quantities calculated by an EOS, to measured volumetric properties such as density. Engineers seldom work in terms of molar quantities, and in the case of petroleum liquids, economics may dictate the choice to quantify in barrels instead of kg-moles.

Specific gravity and boiling point are the two most common physical properties used for defining petroleum fractions. This was true even in the early 1930's, and led to the first characterization schemes by Smith, Watson, and coworkers. From a practical point of view, these two properties are easily determined from distillation experiments and thermodynamically represent two important states: vapor pressure and undersaturated liquid.

Critical pressure and temperature are required by nearly all cubic equations of state. They are chosen to define the EOS constants, e.g., Ω_a and Ω_b, using van der Waals criteria. Acentric factor is usually included in an EOS as a correlating parameter to ensure good VLE predictions.

Traditionally, molar distribution, specific gravity, and boiling point result from high-temperature distillation data. Critical properties and acentric factor are estimated by empirical correlations using specific gravity and boiling point as correlating parameters. Most of the work in this study has been made to help estimate the properties of petroleum fractions when distillation data are not available.

2.2 Proposed Molar Distribution Model

The relation between molar quantity (mole fraction) and molecular weight has earlier been defined as molar distribution. It is somewhat misleading actually, because there is not a direct relation between molecular weight and mole fraction of individual petroleum fractions. For example, plotting mole fraction versus molecular weight will not result in a single curve if petroleum fractions represent single-carbon-number (SCN) groups in the one case, and 10-percent volume cuts in the other. If the same data are plotted as cumulative mole fraction versus cumulative average molecular weight, a single curve results. The cumulative distribution curve is unique. The remaining problem is how to define the cumulative distribution mathematically.

Paper A.2 presents the mathematical model for describing molar distribution. Some of the original applications have been replaced by more practical ones. An example is the method used to match experimental data. The original procedures rely on the use of limited molecular weight boundaries and SCN description. This has been discarded for a more general and easy-to-apply method described below. It should be kept in mind that the concept of describing molar distribution with a probabilistic model is foreign to most petroleum and chemical engineers. Although i don't claim originality, there has been no stimulus from the literature in conceiving the original model or later modifications presented in this chapter.

Instead of repeating the probability model in this section, it is recommended that paper A.2 be read before continuing with this discussion.

The idea of using cumulative quantities to describe molar distribution resulted from a long-time frustration over how to present the probability model in a consise, easy-to-apply form. The solution comes in terms of two cumulative, normalized quantities. The first of these is defined as cumulative normalized mole fraction, X_i,

$$X_i = \sum_{j=n}^{i} x_j \Big/ \sum_{j=n}^{N} x_j \qquad \ldots\ldots \tag{2.1}$$

The second quantity will be referred to as cumulative normalized molecular weight variable, Q_i,

$$Q_i = \frac{\left\{ \sum_{j=n}^{i} x_j \cdot M_j \Big/ \sum_{j=n}^{i} x_j \right\} - \eta}{M_{n+} - \eta} \qquad \ldots\ldots \tag{2.2}$$

where x_j = mole fraction of fraction j
M_j = molecular weight of fraction j
M_{n+} = C_{n+} average molecular weight
η = parameter in the distribution model representing the minimum molecular weight found in the C_{n+} mixture
$j = n, n+1, \ldots, N$

Average molecular weight of the total mixture, M_{n+}, can be expressed as

$$M_{n+} = \sum_{j=n}^{N} x_j \cdot M_j \Big/ \sum_{j=n}^{N} x_j \qquad \ldots\ldots \tag{2.3}$$

and M_{n+} should always be measured experimentally.

Eq. 2.2 can be solved for average molecular weight of a fraction i, M_i, in the C_{n+} mixture,

$$M_i = \eta + (M_{n+}-\eta)(X_i \cdot Q_i - X_{i-1} \cdot Q_{i-1})/(X_i - X_{i-1}) \quad .... \quad (2.4)$$

α is the model parameter defining the form of the distribution function. For $\alpha=1$ the distribution is exponential; for $\alpha<1$ the distribution is accelerated exponential; for $\alpha>1$ the distribution is left-skewed. As $\alpha\to\infty$, the distribution becomes normal, folded at η.

Based on these definitions, values of X_i and Q_i have been calculated and are given in Table 2.1. Fig. 2.1 presents the same quantities graphically. In fact, Fig. 2.1 can be used to fit experimental molar distribution data without the use of a computer. The method is, unfortunately, trial and error, and the best-fit is by eye. However, it greatly simplifies the model and allows the engineer to apply it without knowledge of probability theory, gamma functions, etc.

Instead of presenting a step-by-step procedure, an example calculation is used to show the use of Table 2.1. Consider a heptanes-plus fraction with average molecular weight of 198.7. Suppose detailed compositional data are not available from distillation or chromatographic analysis. If we want to split the fraction into four groups with, say, mole fractions, x_i, 0.3, 0.3, 0.2, and 0.2, then the probability model can be used to calculate molecular weights. With no other information, model parameters α and η are set equal to 1.0 and 92.0 (14·7-6), respectively.

x_{F_1} = 0.3
X_{F_1} = 0.3
Q_{F_1} = 0.16776 (Table 2.1)

M_{F_1} = 92+0.16776(198.7-92)
= 109.90

x_{F_2} = 0.3
X_{F_2} = 0.3+0.3 = 0.6
Q_{F_2} = 0.38914 (Table 2.1)

M_{F_2} = 92 + (198.7-92)(0.6x0.38914-0.3x0.16776)/(0.6-0.3)
= 157.14

x_{F_3} = 0.2
X_{F_3} = 0.3+0.3+0.2 = 0.8
Q_{F_3} = 0.59764 (Table 2.1)

M_{F_3} = 92 + (198.7-92)(0.8x0.59764-0.6x0.38914)/(0.8-0.6)
= 222.51

x_{F_4} = 0.2
X_{F_4} = 0.3+0.3+0.2+0.2 = 1.0
Q_{F_4} = 1.0 (by definition)

M_{F_4} = 92 + (198.7-92)(1.0x1.0-0.8x0.59764)/(1.0-0.8)
= 370.43

Check M_{7+} = 0.3x109.90 + (0.6-0.3)x157.14
+ (0.8-0.6)x222.51 + (1.0-0.8)x370.43
= 198.70 ✓

If distillation data or chromatographic analysis is available then the molar distribution can be fit to the present model. The suggested procedure can be solved either graphically or with a programmable iterative routine. It uses the normalized cumulative quantities, X_i and Q_i, and does not consider molecular weight boundaries for each fraction in the mixture. This greatly simplifies the matching procedure from what is proposed in paper A.2. The cumulative concept also allows a more accurate description and extrapolation of experimental data.

An outline is given below to describe the matching procedure. It assumes mole fractions are available -i.e., molecular weights have been measured and used to convert weight fractions. If only chromatographic analysis is available and generalized SCN molecular weights are not defined from previous distillation studies of similar mixtures, then only weight fractions can be considered. A modification of the procedure below is necessary in this situation.

1. Tabulate mole fractions and molecular weights of groups making up the petroleum fraction mixture.

2. Calculate normalized mole fractions, X_i, using Eq. 2.1

3. Calculate cumulative molecular weight for each group by summing $x_j \cdot M_j$ up to i and dividing by the sum of x_j.

4. Assume several values of model parameter η. Considering a C_{n+} mixture then η values might range from $14 \cdot n-20$ to $14 \cdot n$, but no physical meaning should be given η and its numerical value has no limit (except that it must be less than M_{n+}).

5. For each η, calculate normalized molecular weights, Q_i, using Eq. 2.2.

6. Plot Q_i versus X_i on Fig. 2.1 for each value of η. Determine by eye or a best-fit minimization the optimal value of α and η.

7. If the last group in the mixture is not to be split then calculations are finished, though you might ask why the match was made in the first place.

8. To split the last group requires choosing mole fractions of each subgroup. Thereafter, calculate the corresponding values of X_i and enter either Fig. 2.1 or, preferably, Table 2.1 to find values of Q_i at the optimal α.

9. Calculate molecular weights of the subgroups using Eq. 2.4.

Table 2.2 illustrates the matching procedure using molar distribution data given by Hoffman, et al. for a reservoir oil. Fig. 2.2 shows the plot of Q_i versus X_i for values of η equal to 65, 70, 75, and 80. A best fit of 72.5 was chosen, corresponding to α=2.5. Fig. 2.3 shows the model fit for $(\alpha,\eta)=(2.5,72.5)$. To check the goodness of the match in a physically meaningful way requires that mole fraction (which is common to both the experimental data and the model) be plotted versus molecular weight. Calculated and experimental molecular weights, M_i, are shown in Table 2.2 and plotted in Fig. 2.4 versus mole fraction, x_i. The match is quite satisfactory, particularly when we consider its bimodal shape.

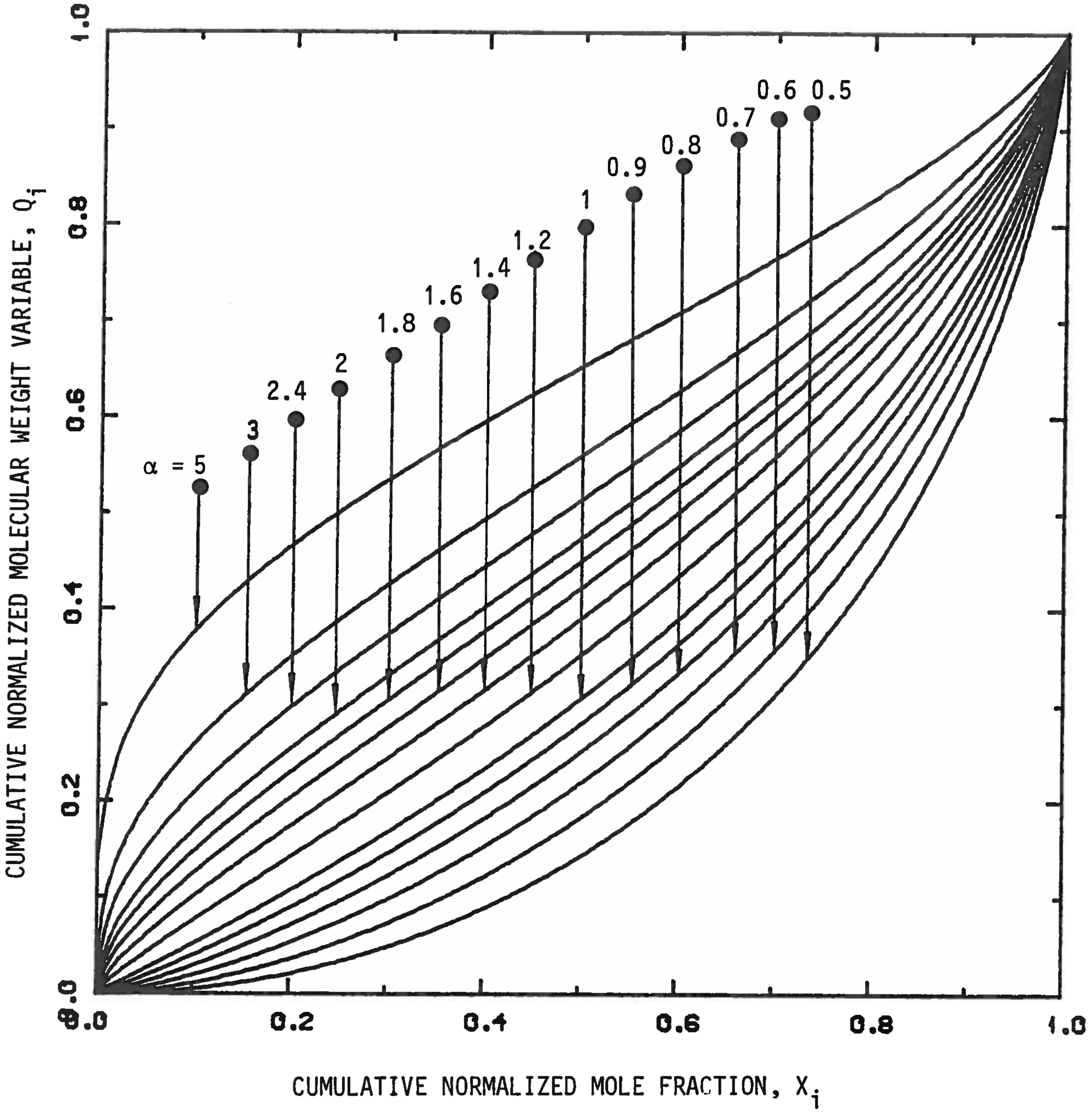

Fig. 2.1 - Probabilistic Model for Molar Distribution Expressed in Cumulative Quantities.

TABLE 2.1 - MOLAR DISTRIBUTION MODEL EXPRESSED IN CUMULATIVE QUANTITIES.

	Cumulative Normalized Molecular Weight, Qi, for Specified α							
Xi	0.3	0.4	0.5	0.6	0.7	0.8	0.9	1.0
0.02	0.00000	0.00003	0.00021	0.00076	0.00192	0.00383	0.00655	0.01007
0.04	0.00001	0.00017	0.00084	0.00243	0.00518	0.00915	0.01423	0.02027
0.06	0.00005	0.00047	0.00189	0.00478	0.00927	0.01524	0.02245	0.03062
0.08	0.00012	0.00096	0.00336	0.00773	0.01403	0.02193	0.03108	0.04111
0.10	0.00025	0.00168	0.00525	0.01124	0.01936	0.02913	0.04006	0.05176
0.12	0.00046	0.00265	0.00757	0.01527	0.02521	0.03676	0.04936	0.06256
0.14	0.00076	0.00389	0.01033	0.01980	0.03154	0.04480	0.05895	0.07352
0.16	0.00119	0.00544	0.01351	0.02481	0.03834	0.05323	0.06882	0.08464
0.18	0.00177	0.00731	0.01714	0.03029	0.04557	0.06202	0.07897	0.09595
0.20	0.00251	0.00953	0.02121	0.03623	0.05323	0.07117	0.08938	0.10743
0.22	0.00345	0.01211	0.02574	0.04264	0.06130	0.08067	0.10007	0.11909
0.24	0.00462	0.01508	0.03072	0.04951	0.06979	0.09051	0.11102	0.13095
0.26	0.00604	0.01846	0.03617	0.05683	0.07869	0.10069	0.12224	0.14301
0.28	0.00774	0.02226	0.04210	0.06461	0.08799	0.11122	0.13374	0.15528
0.30	0.00975	0.02652	0.04852	0.07285	0.09770	0.12209	0.14551	0.16776
0.32	0.01210	0.03125	0.05543	0.08156	0.10783	0.13331	0.15757	0.18047
0.34	0.01484	0.03647	0.06286	0.09074	0.11837	0.14488	0.16993	0.19341
0.36	0.01798	0.04222	0.07081	0.10041	0.12933	0.15681	0.18258	0.20660
0.38	0.02158	0.04850	0.07930	0.11057	0.14073	0.16912	0.19555	0.22005
0.40	0.02566	0.05536	0.08835	0.12124	0.15257	0.18180	0.20883	0.23376
0.42	0.03027	0.06282	0.09797	0.13243	0.16486	0.19487	0.22245	0.24776
0.44	0.03546	0.07090	0.10819	0.14414	0.17762	0.20834	0.23642	0.26205
0.46	0.04125	0.07964	0.11903	0.15641	0.19086	0.22224	0.25074	0.27665
0.48	0.04772	0.08907	0.13050	0.16925	0.20460	0.23657	0.26544	0.29158
0.50	0.05490	0.09924	0.14265	0.18269	0.21886	0.25135	0.28054	0.30685
0.52	0.06285	0.11016	0.15550	0.19674	0.23366	0.26660	0.29605	0.32249
0.54	0.07163	0.12190	0.16908	0.21144	0.24903	0.28235	0.31200	0.33851
0.56	0.08131	0.13450	0.18342	0.22682	0.26499	0.29862	0.32841	0.35494
0.58	0.09195	0.14801	0.19858	0.24290	0.28157	0.31544	0.34530	0.37181
0.60	0.10364	0.16249	0.21459	0.25974	0.29882	0.33285	0.36272	0.38914
0.62	0.11646	0.17799	0.23151	0.27737	0.31676	0.35087	0.38068	0.40696
0.64	0.13051	0.19460	0.24940	0.29584	0.33545	0.36956	0.39924	0.42532
0.66	0.14588	0.21240	0.26832	0.31522	0.35493	0.38895	0.41843	0.44425
0.68	0.16271	0.23147	0.28834	0.33557	0.37526	0.40909	0.43830	0.46380
0.70	0.18113	0.25191	0.30956	0.35695	0.39651	0.43006	0.45891	0.48401
0.72	0.20129	0.27386	0.33207	0.37946	0.41876	0.45192	0.48032	0.50496
0.74	0.22337	0.29746	0.35599	0.40320	0.44209	0.47474	0.50260	0.52670
0.76	0.24759	0.32285	0.38146	0.42829	0.46661	0.49863	0.52586	0.54933
0.78	0.27419	0.35025	0.40864	0.45486	0.49245	0.52371	0.55018	0.57294
0.80	0.30349	0.37989	0.43772	0.48310	0.51976	0.55010	0.57570	0.59764
0.82	0.33583	0.41206	0.46896	0.51320	0.54872	0.57798	0.60257	0.62358
0.84	0.37170	0.44712	0.50265	0.54544	0.57957	0.60755	0.63098	0.65094
0.86	0.41168	0.48555	0.53918	0.58014	0.61261	0.63909	0.66118	0.67993
0.88	0.45654	0.52794	0.57907	0.61775	0.64822	0.67294	0.69348	0.71087
0.90	0.50737	0.57516	0.62302	0.65889	0.68695	0.70960	0.72834	0.74416
0.92	0.56570	0.62841	0.67204	0.70442	0.72956	0.74976	0.76639	0.78037
0.94	0.63397	0.68961	0.72772	0.75571	0.77727	0.79449	0.80860	0.82042
0.96	0.71645	0.76211	0.79284	0.81514	0.83218	0.84569	0.85670	0.86588
0.98	0.82253	0.85323	0.87346	0.88793	0.89886	0.90745	0.91440	0.92016

TABLE 2.1 continued

	Cumulative Normalized Molecular Weight, Qi, for Specified α							
Xi	1.1	1.2	1.3	1.4	1.5	1.6	1.7	1.8
0.02	0.01430	0.01917	0.02456	0.03040	0.03657	0.04302	0.04966	0.05645
0.04	0.02709	0.03452	0.04239	0.05059	0.05899	0.06753	0.07612	0.08471
0.06	0.03950	0.04887	0.05856	0.06843	0.07838	0.08832	0.09818	0.10794
0.08	0.05173	0.06270	0.07385	0.08503	0.09616	0.10716	0.11797	0.12857
0.10	0.06389	0.07622	0.08858	0.10084	0.11293	0.12476	0.13633	0.14758
0.12	0.07603	0.08954	0.10294	0.11611	0.12899	0.14152	0.15368	0.16547
0.14	0.08819	0.10275	0.11704	0.13099	0.14454	0.15765	0.17031	0.18253
0.16	0.10040	0.11588	0.13097	0.14559	0.15971	0.17331	0.18639	0.19896
0.18	0.11268	0.12899	0.14477	0.15998	0.17460	0.18861	0.20204	0.21491
0.20	0.12505	0.14210	0.15850	0.17422	0.18926	0.20363	0.21736	0.23047
0.22	0.13752	0.15524	0.17219	0.18836	0.20377	0.21844	0.23242	0.24573
0.24	0.15012	0.16843	0.18587	0.20243	0.21816	0.23309	0.24727	0.26074
0.26	0.16285	0.18170	0.19956	0.21647	0.23247	0.24762	0.26196	0.27556
0.28	0.17572	0.19505	0.21329	0.23050	0.24673	0.26205	0.27653	0.29024
0.30	0.18875	0.20851	0.22709	0.24455	0.26097	0.27644	0.29102	0.30480
0.32	0.20196	0.22210	0.24096	0.25863	0.27522	0.29080	0.30546	0.31928
0.34	0.21535	0.23582	0.25492	0.27278	0.28949	0.30515	0.31987	0.33371
0.36	0.22893	0.24969	0.26900	0.28700	0.30380	0.31953	0.33427	0.34812
0.38	0.24272	0.26373	0.28321	0.30132	0.31819	0.33394	0.34869	0.36252
0.40	0.25674	0.27795	0.29757	0.31575	0.33266	0.34842	0.36314	0.37694
0.42	0.27099	0.29237	0.31208	0.33032	0.34724	0.36298	0.37766	0.39140
0.44	0.28549	0.30700	0.32678	0.34503	0.36193	0.37763	0.39226	0.40592
0.46	0.30026	0.32185	0.34166	0.35991	0.37677	0.39241	0.40695	0.42052
0.48	0.31532	0.33696	0.35677	0.37497	0.39177	0.40732	0.42176	0.43522
0.50	0.33067	0.35232	0.37210	0.39024	0.40694	0.42238	0.43671	0.45004
0.52	0.34634	0.36797	0.38768	0.40572	0.42231	0.43762	0.45181	0.46500
0.54	0.36236	0.38393	0.40353	0.42145	0.43790	0.45306	0.46708	0.48011
0.56	0.37874	0.40021	0.41968	0.43745	0.45373	0.46871	0.48256	0.49541
0.58	0.39551	0.41684	0.43615	0.45373	0.46981	0.48460	0.49825	0.51090
0.60	0.41270	0.43384	0.45295	0.47032	0.48619	0.50076	0.51419	0.52662
0.62	0.43033	0.45126	0.47013	0.48726	0.50288	0.51721	0.53040	0.54260
0.64	0.44845	0.46911	0.48772	0.50457	0.51992	0.53397	0.54690	0.55885
0.66	0.46708	0.48744	0.50574	0.52228	0.53733	0.55109	0.56373	0.57540
0.68	0.48628	0.50629	0.52423	0.54043	0.55515	0.56859	0.58093	0.59230
0.70	0.50610	0.52571	0.54326	0.55908	0.57343	0.58652	0.59852	0.60958
0.72	0.52658	0.54574	0.56285	0.57825	0.59221	0.60492	0.61656	0.62728
0.74	0.54780	0.56645	0.58308	0.59802	0.61154	0.62384	0.63510	0.64544
0.76	0.56983	0.58791	0.60400	0.61844	0.63149	0.64335	0.65418	0.66413
0.78	0.59276	0.61021	0.62571	0.63960	0.65213	0.66350	0.67389	0.68341
0.80	0.61670	0.63345	0.64830	0.66158	0.67355	0.68440	0.69429	0.70336
0.82	0.64179	0.65775	0.67188	0.68450	0.69585	0.70613	0.71549	0.72406
0.84	0.66819	0.68328	0.69661	0.70849	0.71917	0.72883	0.73761	0.74565
0.86	0.69611	0.71022	0.72267	0.73374	0.74368	0.75265	0.76080	0.76825
0.88	0.72582	0.73884	0.75029	0.76047	0.76959	0.77781	0.78527	0.79207
0.90	0.75771	0.76949	0.77983	0.78900	0.79720	0.80458	0.81128	0.81737
0.92	0.79232	0.80268	0.81175	0.81978	0.82694	0.83339	0.83921	0.84452
0.94	0.83049	0.83918	0.84678	0.85349	0.85947	0.86484	0.86969	0.87409
0.96	0.87367	0.88037	0.88622	0.89136	0.89594	0.90004	0.90373	0.90708
0.98	0.92502	0.92919	0.93281	0.93599	0.93880	0.94131	0.94357	0.94562

TABLE 2.1 continued

	Cumulative Normalized Molecular Weight, Qi, for Specified α							
Xi	1.9	2.0	2.1	2.2	2.3	2.4	2.5	2.6
0.02	0.06333	0.07027	0.07722	0.08417	0.09109	0.09796	0.10478	0.11151
0.04	0.09326	0.10174	0.11011	0.11837	0.12650	0.13448	0.14232	0.15000
0.06	0.11754	0.12697	0.13621	0.14526	0.15409	0.16272	0.17114	0.17935
0.08	0.13893	0.14904	0.15889	0.16848	0.17780	0.18686	0.19567	0.20422
0.10	0.15853	0.16915	0.17945	0.18944	0.19911	0.20849	0.21757	0.22637
0.12	0.17687	0.18790	0.19855	0.20884	0.21878	0.22839	0.23767	0.24664
0.14	0.19430	0.20565	0.21658	0.22710	0.23725	0.24702	0.25645	0.26555
0.16	0.21104	0.22264	0.23379	0.24450	0.25479	0.26470	0.27424	0.28342
0.18	0.22723	0.23904	0.25036	0.26121	0.27162	0.28162	0.29123	0.30047
0.20	0.24299	0.25497	0.26641	0.27737	0.28787	0.29794	0.30760	0.31687
0.22	0.25841	0.27051	0.28206	0.29310	0.30366	0.31376	0.32345	0.33274
0.24	0.27355	0.28575	0.29738	0.30846	0.31906	0.32918	0.33888	0.34817
0.26	0.28847	0.30074	0.31242	0.32354	0.33414	0.34427	0.35396	0.36323
0.28	0.30322	0.31553	0.32724	0.33837	0.34897	0.35909	0.36875	0.37799
0.30	0.31783	0.33017	0.34188	0.35300	0.36359	0.37367	0.38330	0.39249
0.32	0.33233	0.34468	0.35638	0.36748	0.37803	0.38808	0.39765	0.40679
0.34	0.34677	0.35910	0.37077	0.38183	0.39234	0.40233	0.41185	0.42092
0.36	0.36116	0.37346	0.38508	0.39610	0.40654	0.41647	0.42591	0.43491
0.38	0.37552	0.38778	0.39935	0.41029	0.42067	0.43051	0.43988	0.44880
0.40	0.38989	0.40208	0.41358	0.42445	0.43474	0.44450	0.45377	0.46260
0.42	0.40428	0.41640	0.42781	0.43858	0.44878	0.45844	0.46762	0.47634
0.44	0.41872	0.43074	0.44205	0.45273	0.46282	0.47237	0.48144	0.49006
0.46	0.43322	0.44513	0.45633	0.46689	0.47687	0.48630	0.49525	0.50376
0.48	0.44780	0.45959	0.47067	0.48110	0.49095	0.50026	0.50909	0.51746
0.50	0.46249	0.47414	0.48508	0.49538	0.50509	0.51426	0.52296	0.53120
0.52	0.47730	0.48880	0.49959	0.50974	0.51930	0.52833	0.53688	0.54499
0.54	0.49225	0.50359	0.51422	0.52420	0.53361	0.54249	0.55088	0.55884
0.56	0.50736	0.51853	0.52898	0.53880	0.54803	0.55674	0.56498	0.57278
0.58	0.52266	0.53364	0.54390	0.55353	0.56259	0.57113	0.57919	0.58683
0.60	0.53817	0.54894	0.55900	0.56844	0.57730	0.58566	0.59354	0.60101
0.62	0.55392	0.56446	0.57431	0.58353	0.59220	0.60036	0.60805	0.61533
0.64	0.56992	0.58022	0.58984	0.59885	0.60730	0.61525	0.62275	0.62984
0.66	0.58621	0.59626	0.60564	0.61441	0.62263	0.63037	0.63766	0.64455
0.68	0.60283	0.61261	0.62172	0.63024	0.63823	0.64573	0.65280	0.65948
0.70	0.61980	0.62929	0.63813	0.64638	0.65411	0.66138	0.66822	0.67467
0.72	0.63717	0.64635	0.65489	0.66287	0.67033	0.67734	0.68394	0.69016
0.74	0.65499	0.66384	0.67207	0.67975	0.68693	0.69367	0.70000	0.70598
0.76	0.67331	0.68180	0.68970	0.69706	0.70394	0.71039	0.71646	0.72217
0.78	0.69219	0.70031	0.70784	0.71487	0.72143	0.72758	0.73336	0.73879
0.80	0.71170	0.71942	0.72657	0.73324	0.73946	0.74529	0.75076	0.75591
0.82	0.73194	0.73922	0.74597	0.75225	0.75811	0.76359	0.76874	0.77358
0.84	0.75303	0.75984	0.76615	0.77201	0.77748	0.78259	0.78739	0.79190
0.86	0.77509	0.78139	0.78722	0.79264	0.79769	0.80241	0.80683	0.81099
0.88	0.79832	0.80406	0.80938	0.81431	0.81891	0.82320	0.82722	0.83099
0.90	0.82296	0.82810	0.83285	0.83725	0.84134	0.84517	0.84874	0.85210
0.92	0.84937	0.85384	0.85795	0.86177	0.86531	0.86862	0.87171	0.87461
0.94	0.87812	0.88181	0.88521	0.88837	0.89129	0.89402	0.89657	0.89895
0.96	0.91013	0.91294	0.91551	0.91790	0.92011	0.92216	0.92408	0.92588
0.98	0.94748	0.94918	0.95074	0.95219	0.95353	0.95477	0.95592	0.95701

TABLE 2.1 continued

	Cumulative Normalized Molecular Weight, Qi, for Specified α							
Xi	2.7	2.8	2.9	3.0	3.1	3.2	3.3	3.4
0.02	0.11817	0.12474	0.13121	0.13759	0.14387	0.15004	0.15611	0.16208
0.04	0.15752	0.16489	0.17210	0.17915	0.18605	0.19280	0.19940	0.20586
0.06	0.18735	0.19515	0.20276	0.21017	0.21739	0.22443	0.23130	0.23799
0.08	0.21254	0.22062	0.22847	0.23610	0.24352	0.25073	0.25775	0.26458
0.10	0.23489	0.24316	0.25117	0.25895	0.26649	0.27381	0.28092	0.28783
0.12	0.25532	0.26371	0.27183	0.27970	0.28732	0.29471	0.30187	0.30882
0.14	0.27433	0.28281	0.29101	0.29893	0.30660	0.31402	0.32121	0.32817
0.16	0.29227	0.30081	0.30905	0.31700	0.32469	0.33212	0.33931	0.34628
0.18	0.30937	0.31794	0.32620	0.33416	0.34185	0.34928	0.35646	0.36341
0.20	0.32579	0.33437	0.34263	0.35059	0.35826	0.36567	0.37283	0.37975
0.22	0.34166	0.35023	0.35848	0.36642	0.37407	0.38145	0.38857	0.39544
0.24	0.35707	0.36563	0.37385	0.38175	0.38937	0.39670	0.40378	0.41061
0.26	0.37211	0.38063	0.38881	0.39668	0.40424	0.41153	0.41855	0.42533
0.28	0.38683	0.39531	0.40344	0.41125	0.41877	0.42600	0.43296	0.43967
0.30	0.40129	0.40971	0.41779	0.42554	0.43299	0.44016	0.44705	0.45370
0.32	0.41553	0.42389	0.43190	0.43959	0.44697	0.45406	0.46089	0.46746
0.34	0.42959	0.43788	0.44582	0.45343	0.46073	0.46775	0.47450	0.48099
0.36	0.44350	0.45171	0.45957	0.46710	0.47432	0.48126	0.48792	0.49434
0.38	0.45730	0.46543	0.47320	0.48064	0.48777	0.49462	0.50119	0.50752
0.40	0.47101	0.47904	0.48672	0.49407	0.50110	0.50786	0.51434	0.52058
0.42	0.48466	0.49259	0.50016	0.50741	0.51435	0.52100	0.52739	0.53353
0.44	0.49826	0.50608	0.51355	0.52069	0.52753	0.53408	0.54037	0.54641
0.46	0.51184	0.51955	0.52691	0.53394	0.54066	0.54711	0.55329	0.55922
0.48	0.52543	0.53302	0.54025	0.54716	0.55378	0.56011	0.56618	0.57200
0.50	0.53904	0.54649	0.55361	0.56040	0.56689	0.57310	0.57905	0.58477
0.52	0.55268	0.56001	0.56699	0.57365	0.58001	0.58610	0.59194	0.59754
0.54	0.56639	0.57357	0.58042	0.58694	0.59318	0.59914	0.60485	0.61033
0.56	0.58018	0.58721	0.59391	0.60030	0.60640	0.61223	0.61781	0.62316
0.58	0.59407	0.60095	0.60749	0.61373	0.61969	0.62538	0.63083	0.63605
0.60	0.60808	0.61479	0.62118	0.62727	0.63308	0.63863	0.64394	0.64902
0.62	0.62223	0.62878	0.63500	0.64093	0.64659	0.65199	0.65715	0.66210
0.64	0.63655	0.64292	0.64897	0.65474	0.66023	0.66547	0.67049	0.67529
0.66	0.65107	0.65725	0.66312	0.66871	0.67404	0.67912	0.68398	0.68863
0.68	0.66580	0.67178	0.67747	0.68288	0.68803	0.69294	0.69764	0.70213
0.70	0.68078	0.68656	0.69205	0.69727	0.70224	0.70698	0.71150	0.71583
0.72	0.69604	0.70161	0.70689	0.71191	0.71669	0.72125	0.72560	0.72976
0.74	0.71162	0.71697	0.72203	0.72685	0.73143	0.73579	0.73996	0.74394
0.76	0.72757	0.73268	0.73752	0.74211	0.74648	0.75065	0.75462	0.75842
0.78	0.74393	0.74879	0.75339	0.75775	0.76191	0.76586	0.76963	0.77324
0.80	0.76076	0.76535	0.76970	0.77383	0.77775	0.78148	0.78504	0.78844
0.82	0.77814	0.78245	0.78653	0.79040	0.79408	0.79758	0.80092	0.80410
0.84	0.79615	0.80016	0.80396	0.80756	0.81098	0.81423	0.81733	0.82028
0.86	0.81490	0.81860	0.82209	0.82540	0.82854	0.83153	0.83438	0.83709
0.88	0.83454	0.83789	0.84106	0.84406	0.84690	0.84961	0.85218	0.85464
0.90	0.85526	0.85824	0.86105	0.86371	0.86624	0.86864	0.87092	0.87309
0.92	0.87734	0.87990	0.88233	0.88462	0.88680	0.88886	0.89082	0.89269
0.94	0.90120	0.90331	0.90530	0.90718	0.90896	0.91065	0.91226	0.91379
0.96	0.92757	0.92915	0.93065	0.93206	0.93340	0.93466	0.93587	0.93701
0.98	0.95802	0.95897	0.95987	0.96071	0.96151	0.96227	0.96299	0.96367

TABLE 2.1 continued

Cumulative Normalized Molecular Weight, Qi, for Specified α

Xi	3.5	3.6	3.7	3.8	3.9	4.0	4.1	4.2
0.02	0.16795	0.17370	0.17937	0.18492	0.19038	0.19574	0.20101	0.20618
0.04	0.21217	0.21835	0.22438	0.23029	0.23607	0.24173	0.24727	0.25269
0.06	0.24452	0.25089	0.25710	0.26317	0.26909	0.27487	0.28052	0.28604
0.08	0.27123	0.27770	0.28401	0.29015	0.29614	0.30198	0.30767	0.31323
0.10	0.29454	0.30107	0.30742	0.31360	0.31962	0.32548	0.33118	0.33675
0.12	0.31557	0.32212	0.32848	0.33467	0.34069	0.34655	0.35225	0.35780
0.14	0.33493	0.34148	0.34784	0.35402	0.36002	0.36586	0.37154	0.37706
0.16	0.35302	0.35956	0.36591	0.37206	0.37804	0.38384	0.38949	0.39497
0.18	0.37013	0.37664	0.38295	0.38907	0.39501	0.40078	0.40638	0.41183
0.20	0.38644	0.39291	0.39918	0.40526	0.41116	0.41688	0.42243	0.42783
0.22	0.40209	0.40852	0.41475	0.42078	0.42662	0.43229	0.43779	0.44313
0.24	0.41721	0.42359	0.42976	0.43573	0.44152	0.44713	0.45257	0.45785
0.26	0.43187	0.43819	0.44430	0.45021	0.45594	0.46149	0.46687	0.47208
0.28	0.44615	0.45241	0.45845	0.46430	0.46996	0.47544	0.48076	0.48591
0.30	0.46011	0.46630	0.47228	0.47805	0.48364	0.48906	0.49430	0.49938
0.32	0.47380	0.47991	0.48581	0.49152	0.49704	0.50238	0.50755	0.51256
0.34	0.48725	0.49329	0.49911	0.50474	0.51018	0.51545	0.52054	0.52548
0.36	0.50051	0.50647	0.51221	0.51776	0.52312	0.52831	0.53332	0.53818
0.38	0.51361	0.51948	0.52514	0.53061	0.53588	0.54099	0.54592	0.55070
0.40	0.52658	0.53236	0.53793	0.54331	0.54850	0.55352	0.55837	0.56307
0.42	0.53944	0.54512	0.55060	0.55589	0.56099	0.56593	0.57069	0.57531
0.44	0.55221	0.55780	0.56319	0.56838	0.57339	0.57824	0.58291	0.58744
0.46	0.56493	0.57042	0.57570	0.58080	0.58572	0.59047	0.59506	0.59950
0.48	0.57760	0.58299	0.58817	0.59317	0.59799	0.60264	0.60714	0.61149
0.50	0.59026	0.59554	0.60062	0.60551	0.61023	0.61479	0.61919	0.62344
0.52	0.60291	0.60808	0.61305	0.61784	0.62246	0.62691	0.63121	0.63537
0.54	0.61558	0.62064	0.62550	0.63018	0.63469	0.63903	0.64323	0.64729
0.56	0.62829	0.63323	0.63797	0.64254	0.64694	0.65118	0.65527	0.65923
0.58	0.64106	0.64587	0.65049	0.65494	0.65923	0.66336	0.66735	0.67120
0.60	0.65390	0.65858	0.66308	0.66741	0.67158	0.67560	0.67948	0.68322
0.62	0.66684	0.67139	0.67576	0.67997	0.68401	0.68792	0.69168	0.69531
0.64	0.67989	0.68430	0.68855	0.69262	0.69655	0.70033	0.70397	0.70749
0.66	0.69308	0.69735	0.70146	0.70540	0.70920	0.71285	0.71638	0.71978
0.68	0.70644	0.71056	0.71452	0.71833	0.72199	0.72552	0.72892	0.73220
0.70	0.71998	0.72395	0.72777	0.73143	0.73496	0.73835	0.74162	0.74477
0.72	0.73374	0.73756	0.74122	0.74473	0.74811	0.75137	0.75450	0.75753
0.74	0.74775	0.75140	0.75491	0.75827	0.76150	0.76461	0.76761	0.77049
0.76	0.76205	0.76553	0.76887	0.77207	0.77515	0.77811	0.78096	0.78370
0.78	0.77668	0.77998	0.78314	0.78618	0.78909	0.79190	0.79459	0.79720
0.80	0.79169	0.79480	0.79778	0.80064	0.80339	0.80603	0.80857	0.81102
0.82	0.80714	0.81005	0.81284	0.81552	0.81809	0.82055	0.82293	0.82522
0.84	0.82311	0.82581	0.82839	0.83088	0.83326	0.83554	0.83774	0.83986
0.86	0.83968	0.84216	0.84453	0.84680	0.84898	0.85108	0.85310	0.85504
0.88	0.85698	0.85922	0.86136	0.86341	0.86538	0.86728	0.86909	0.87084
0.90	0.87517	0.87715	0.87904	0.88086	0.88260	0.88427	0.88588	0.88743
0.92	0.89447	0.89618	0.89780	0.89936	0.90086	0.90229	0.90367	0.90499
0.94	0.91525	0.91664	0.91797	0.91925	0.92047	0.92164	0.92276	0.92384
0.96	0.93810	0.93914	0.94013	0.94108	0.94200	0.94287	0.94370	0.94451
0.98	0.96432	0.96494	0.96553	0.96609	0.96664	0.96715	0.96765	0.96812

TABLE 2.1 continued

	Cumulative Normalized Molecular Weight, Qi, for Specified α							
Xi	4.3	4.4	4.5	4.6	4.7	4.8	4.9	5.0
0.02	0.21126	0.21625	0.22114	0.22596	0.23068	0.23533	0.23989	0.24437
0.04	0.25799	0.26318	0.26828	0.27326	0.27815	0.28293	0.28763	0.29223
0.06	0.29143	0.29670	0.30186	0.30690	0.31183	0.31666	0.32138	0.32601
0.08	0.31865	0.32395	0.32912	0.33417	0.33911	0.34394	0.34866	0.35328
0.10	0.34217	0.34746	0.35263	0.35767	0.36259	0.36740	0.37210	0.37669
0.12	0.36321	0.36848	0.37362	0.37863	0.38352	0.38830	0.39296	0.39752
0.14	0.38244	0.38768	0.39278	0.39776	0.40261	0.40735	0.41197	0.41648
0.16	0.40031	0.40551	0.41058	0.41551	0.42031	0.42500	0.42958	0.43404
0.18	0.41712	0.42227	0.42729	0.43217	0.43693	0.44156	0.44609	0.45050
0.20	0.43307	0.43817	0.44313	0.44796	0.45266	0.45724	0.46171	0.46607
0.22	0.44832	0.45336	0.45826	0.46303	0.46768	0.47220	0.47661	0.48091
0.24	0.46298	0.46796	0.47280	0.47752	0.48210	0.48657	0.49091	0.49515
0.26	0.47715	0.48207	0.48685	0.49150	0.49602	0.50042	0.50471	0.50889
0.28	0.49091	0.49576	0.50048	0.50506	0.50952	0.51386	0.51808	0.52219
0.30	0.50431	0.50910	0.51375	0.51826	0.52265	0.52692	0.53108	0.53513
0.32	0.51742	0.52213	0.52671	0.53116	0.53548	0.53968	0.54377	0.54775
0.34	0.53026	0.53491	0.53941	0.54379	0.54804	0.55217	0.55619	0.56011
0.36	0.54289	0.54746	0.55189	0.55619	0.56037	0.56443	0.56839	0.57223
0.38	0.55533	0.55982	0.56418	0.56841	0.57251	0.57650	0.58038	0.58416
0.40	0.56762	0.57203	0.57631	0.58046	0.58449	0.58840	0.59221	0.59591
0.42	0.57978	0.58410	0.58830	0.59237	0.59633	0.60017	0.60390	0.60753
0.44	0.59182	0.59607	0.60019	0.60418	0.60805	0.61181	0.61547	0.61902
0.46	0.60379	0.60795	0.61198	0.61589	0.61969	0.62337	0.62695	0.63043
0.48	0.61569	0.61977	0.62371	0.62754	0.63125	0.63485	0.63835	0.64175
0.50	0.62755	0.63153	0.63539	0.63913	0.64276	0.64628	0.64970	0.65302
0.52	0.63939	0.64328	0.64704	0.65070	0.65424	0.65767	0.66101	0.66425
0.54	0.65121	0.65501	0.65869	0.66225	0.66570	0.66905	0.67230	0.67546
0.56	0.66305	0.66675	0.67033	0.67380	0.67716	0.68043	0.68359	0.68667
0.58	0.67492	0.67852	0.68200	0.68538	0.68865	0.69182	0.69490	0.69789
0.60	0.68684	0.69034	0.69372	0.69700	0.70017	0.70325	0.70624	0.70914
0.62	0.69882	0.70221	0.70549	0.70867	0.71175	0.71473	0.71763	0.72044
0.64	0.71089	0.71417	0.71735	0.72042	0.72340	0.72629	0.72909	0.73180
0.66	0.72306	0.72623	0.72930	0.73227	0.73515	0.73793	0.74064	0.74326
0.68	0.73536	0.73842	0.74138	0.74424	0.74701	0.74969	0.75229	0.75482
0.70	0.74781	0.75075	0.75359	0.75634	0.75900	0.76158	0.76408	0.76650
0.72	0.76044	0.76326	0.76598	0.76861	0.77116	0.77363	0.77602	0.77834
0.74	0.77328	0.77597	0.77857	0.78108	0.78351	0.78587	0.78815	0.79036
0.76	0.78635	0.78891	0.79138	0.79377	0.79608	0.79832	0.80049	0.80259
0.78	0.79970	0.80212	0.80446	0.80672	0.80891	0.81102	0.81307	0.81506
0.80	0.81337	0.81565	0.81785	0.81997	0.82203	0.82402	0.82594	0.82781
0.82	0.82742	0.82955	0.83160	0.83358	0.83550	0.83736	0.83915	0.84089
0.84	0.84190	0.84387	0.84577	0.84761	0.84938	0.85110	0.85276	0.85437
0.86	0.85690	0.85870	0.86044	0.86212	0.86375	0.86531	0.86683	0.86830
0.88	0.87253	0.87415	0.87572	0.87723	0.87869	0.88011	0.88147	0.88280
0.90	0.88891	0.89035	0.89173	0.89307	0.89436	0.89560	0.89681	0.89797
0.92	0.90626	0.90749	0.90867	0.90982	0.91092	0.91198	0.91302	0.91401
0.94	0.92488	0.92588	0.92684	0.92777	0.92867	0.92954	0.93038	0.93119
0.96	0.94528	0.94603	0.94674	0.94743	0.94810	0.94875	0.94937	0.94997
0.98	0.96858	0.96902	0.96945	0.96985	0.97025	0.97063	0.97100	0.97135

TABLE 2.2 - EXAMPLE OF HOW THE MOLAR DISTRIBUTION MODEL CAN BE USED TO FIT EXPERIMENTAL DATA: HOFFMAN, *et al*. RESERVOIR OIL.

						Q_i for η=72.5		Calculated	
No.	x_i	x_i ÷36.84	X_i= Σx_i ÷36.84	M_i	$\Sigma x_i M_i$ ÷ Σx_i	Exp.	Calc.	$\Sigma x_i M_i$ ÷ Σx_i	M_i
7	2.630	0.0714	0.0714	99.0	99.0	0.2100	0.1855	95.9	95.9
8	2.340	0.0635	0.1349	110.0	104.2	0.2510	0.2518	104.3	113.7
9	2.350	0.0638	0.1987	121.0	109.6	0.2938	0.3065	111.2	125.8
10	2.240	0.0608	0.2595	132.0	114.8	0.3354	0.3536	117.1	136.5
11	2.412	0.0655	0.3250	145.0	120.9	0.3836	0.4012	123.1	146.9
12	2.457	0.0667	0.3917	158.0	127.2	0.4336	0.4480	129.0	157.8
13	2.657	0.0721	0.4638	172.0	134.2	0.4888	0.4979	135.3	169.5
14	3.262	0.0885	0.5523	186.0	142.5	0.5546	0.5596	143.1	183.9
15	3.631	0.0986	0.6509	203.0	151.7	0.6272	0.6308	152.1	202.5
16	2.294	0.0623	0.7132	222.0	157.8	0.6759	0.6785	158.1	221.0
17	1.714	0.0465	0.7597	238.0	162.7	0.7148	0.7162	162.9	235.8
18	1.427	0.0387	0.7984	252.0	167.0	0.7491	0.7494	167.1	249.2
19	1.303	0.0354	0.8338	266.0	171.2	0.7824	0.7815	171.1	262.7
20	1.078	0.0293	0.8631	279.0	174.9	0.8113	0.8099	174.7	276.7
21	0.871	0.0236	0.8867	290.0	178.0	0.8356	0.8343	177.8	290.2
22	0.715	0.0194	0.9061	301.0	180.6	0.8565	0.8556	180.5	303.3
23	0.575	0.0156	0.9217	315.0	182.9	0.8746	0.8738	182.8	315.9
24	0.481	0.0131	0.9348	329.0	184.9	0.8907	0.8899	184.8	328.2
25	0.394	0.0107	0.9455	343.0	186.7	0.9049	0.9038	186.6	340.2
26	0.335	0.0091	0.9546	357.0	188.3	0.9178	0.9163	188.1	352.0
27	0.280	0.0076	0.9622	371.0	189.8	0.9292	0.9273	189.5	363.9
28	0.250	0.0068	0.9689	385.0	191.1	0.9400	0.9376	190.8	376.1
29	0.232	0.0063	0.9752	399.0	192.5	0.9507	0.9478	192.1	389.6
30	0.912	0.0248	1.0000	444.0	198.7	1.0000	1.0000	198.7	458.3
	36.840	1.0000		198.7					198.7

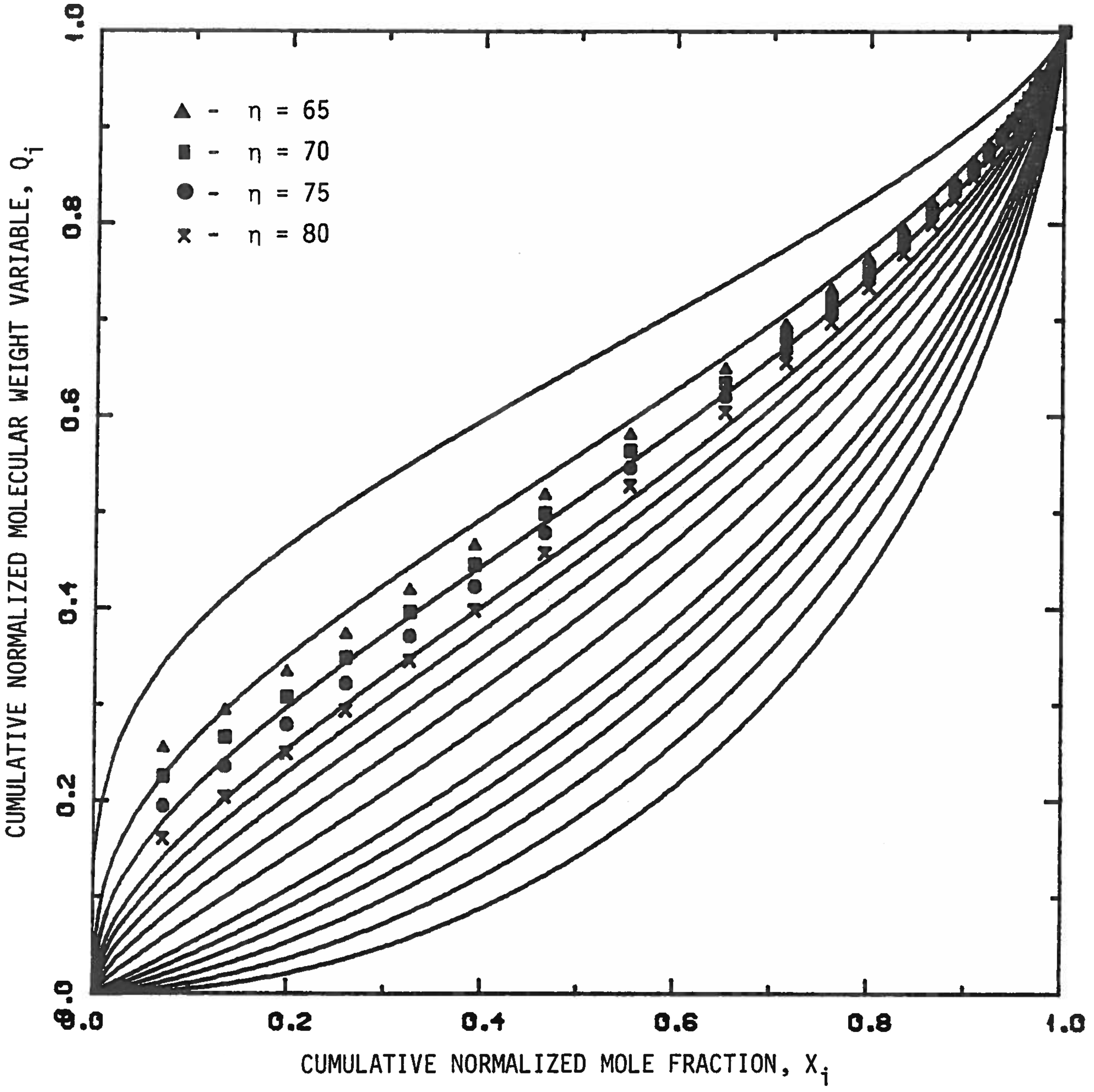

Fig. 2.2 - Example Best-Fit of Experimental Molar Distribution Data (Hoffman, et al. Reservoir Oil) Using the Proposed Probabilistic Model with Four Values of Parameter η.

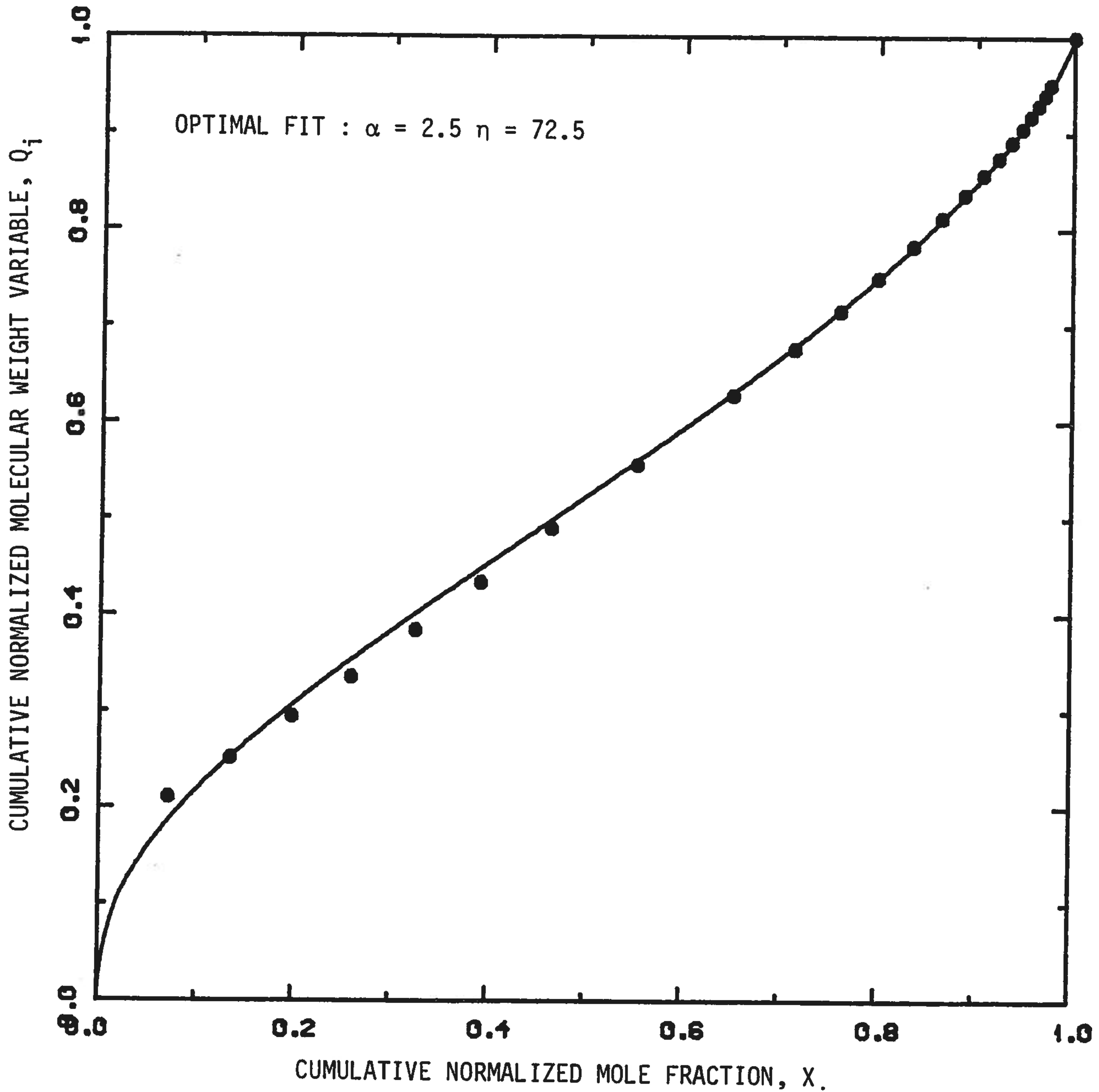

Fig. 2.3 - Best-Fit Match of Experimental Molar Distribution Data for the Hoffman, et al. Reservoir Oil Heptanes-Plus Fraction Using the Proposed Probabilistic Model Expressed in Cumulative Quantities.

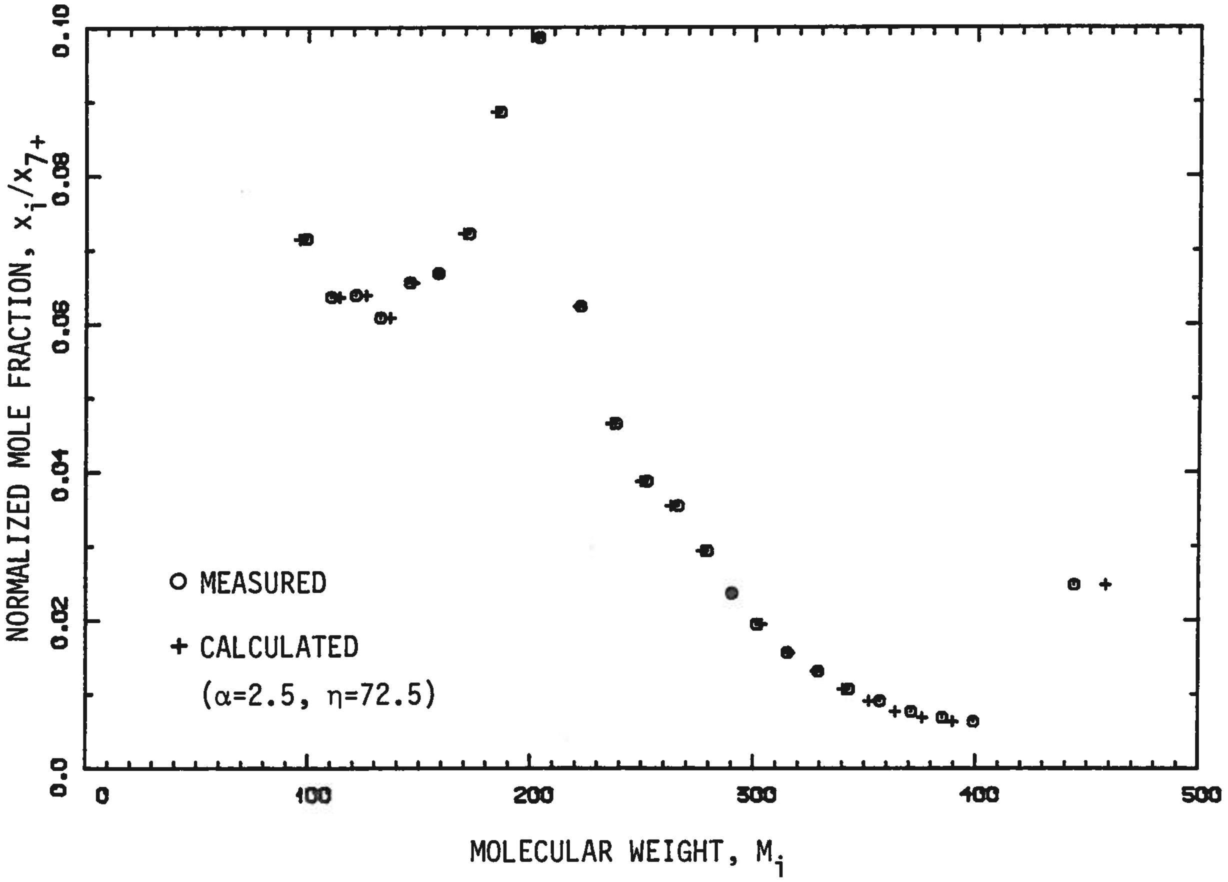

Fig. 2.4 - Best-Fit Match of Experimental Molar Distribution Data for the Hoffman, et al. Reservoir Oil Heptanes-Plus Fraction Expressed Directly as Mole Fraction and Molecular Weight.

2.3 Estimation of Specific Gravity and Boiling Point

If specific gravities and boiling points are not available then their values can be estimated. The proposed procedure is based on the assumption that the Watson characterization factor, K_w, which by definition is the cubic-root of boiling point (^oR) divided by specific gravity: $K_w=\sqrt[3]{T_b}(^oR)/\gamma$, is constant for each fraction. A relation between molecular weight, specific gravity and Watson K_w has been developed from the correlation between molecular weight, specific gravity and boiling point suggested by Riazi and Daubert,

$$K_w = 4.5579 \cdot M^{0.15178} \cdot \gamma^{-0.84573} \quad \text{.................} \quad (2.5)$$

Suppose now that only mole fractions, x_i, and molecular weights, M_i, are defined for the fractions making up a C_{7+} mixture, e.g., from the molar distribution model or chromatographic analysis. Assuming a constant K_w for each fraction, the specific gravity can be calculated from Eq. 2.5,

$$\gamma_i = 6.0108 \cdot M_i^{0.17947} \cdot K_w^{-1.18241} \quad \text{...............} \quad (2.6)$$

It is necessary to choose K_w such that the mixture specific gravity, γ_{7+}, calculated from

$$\gamma_{7+} = x_{7+} \cdot M_{7+} \Big/ \sum_{i=1}^{n} x_i \cdot M_i/\gamma_i \quad \text{...................} \quad (2.7)$$

equals the measured value. It can be shown that the value of K_w necessary to meet this criterion is given by,

$$K_w = \{0.16637 \cdot \gamma_{7+} \cdot S^0 / (x_{7+} \cdot M_{7+})\}^{-0.84573} \quad \ldots\ldots. \quad (2.8)$$

where

$$S^0 = \sum_{i=n}^{N} x_i \cdot M_i^{0.82053} \quad \ldots\ldots\ldots\ldots\ldots\ldots\ldots\ldots\ldots \quad (2.9)$$

The summation is performed for all fractions in the mixture. Having calculated K_w, specific gravity of each fraction is found from Eq. 2.6. Boiling point, T_{bi}, is merely $(K_w \cdot \gamma_i)^3$, found directly from the definition of K_w.

Other methods are available for estimating petroleum fraction specific gravities, although this is the only one which has a simple, direct solution. For example, the method suggested by Yarborough is graphical (specific gravity versus carbon number); the best-fit functions are complex and require interpolation. Haaland's modification of the proposed procedure is perhaps more physical meaningful since K varies for each carbon number. However, neither the Yarborough or Haaland method can be used for random petroleum fractions which are not associated with single carbon numbers.

Continuing with the example from the previous section, specific gravities can be calculated by noting the C_{7+} specific gravity is 0.8409 (corresponding to the M_{7+} of 198.7). Specific gravities of the four fractions are calculated below.

$$\begin{aligned} S^0 &= 0.3\text{x}109.90^{0.82053} + 0.3\text{x}157.14^{0.82053} \\ &\quad + 0.2\text{x}222.51^{0.82053} + 0.2\text{x}370.43^{0.82053} \\ &= 75.70441 \end{aligned}$$

$$K_w = (0.16637\text{x}0.8409\text{x}75.704/1.0/198.7)^{-0.84573}$$

$$= 11.93526$$

and $6.0108\text{x}11.935^{-1.18241} = 0.32039$

$$\gamma_{F1} = 0.32040\text{x}109.9^{0.17947}$$
$$= 0.74469$$
$$\gamma_{F2} = 0.32040\text{x}157.14^{0.17947}$$
$$= 0.79404$$
$$\gamma_{F3} = 0.32040\text{x}222.51^{0.17947}$$
$$= 0.84519$$
$$\gamma_{F4} = 0.32040\text{x}370.43^{0.17947}$$
$$= 0.92615$$

$$\gamma_{7+} = 1.0\text{x}198.7 \,/\, (0.3\text{x}109.9/0.74469 + 0.3\text{x}157.14/0.79404$$
$$+ 0.2\text{x}222.51/0.84519 + 0.2\text{x}370.43/0.92617)$$
$$= 0.8409 \checkmark$$

2.4 Traditional Critical Property Estimation

As noted in the introduction to this chapter, the main purpose of characterizing petroleum fractions is to arrive at estimates of critical pressure, critical temperature, and acentric factor. Presently, experimental determination of these properties is seldom if ever practiced. In the 1930's there was considerable activity in this area, forming the basis for graphical, and later, best-fit correlations. Work by Roess, Smith, Watson, and coworkers provided the foundation, data base, and correlative techniques for critical property estimation. Acentric factor was introduced in 1955 by Pitzer, et al. as a correlating parameter for a corresponding states theory. Edmister provided a simple working relation for estimating acentric factor some three years later. A review of these developments and those which came thereafter is given in paper A.4.

Nearly all correlations for critical properties and acentric factor are functions of specific gravity and boiling point. A few correlations (e.g., Robinson/Peng and Bergman) rely on quantification of the paraffin-naphthene-aromatic (PNA) content of each fraction. These later correlations have several practical drawbacks, the most severe being determination of PNA content.

Critical property correlations for pure compounds have been developed by several workers, perhaps the most important being Lydersen's. The Spencer-Daubert modification of Nokay's relation is more empirical than Lydersen's group contribution theory although it is more easily applied by practicing engineers; specific gravity and boiling point are used instead of pure-compound group contribution parameters. The Lydersen and Spencer/Daubert correlations are of limited use for petroleum fractions unless accurate determination of the chemical nature (e.g., PNA content) can be made.

In general it can be stated that petroleum-fraction critical property correlations are empirical. Most have been developed using the basic data measured in the 1930's. In Paper A.4 it is shown how different correlations effect EOS predictions. Clearly one of the main problems facing the engineer is which correlations to choose. It is reasonable to assume that none of the empirical correlations is best for all applications. The conclusions given in Paper A.4 led to the idea of estimating critical properties based on the EOS itself - the topic of the following section.

A short summary of the observations found in paper A.4 are given below.

- Empirical critical property correlations based on experimental data of petroleum fractions include a wide variety of forms including graphical, tabulated, and best-fit equations. The third type is commonly used by industrial persons because it can be programmed on simple computing machines. Unfortunately there are many forms of best-fit equations, including simple three-constant power equations, polynomials, and complicated multiconstant two/three-variable relations. When used with an EOS, different correlations result in different predictions of VLE and volumetric properties. There does not appear to be agreement in the industry or scientific community as to which correlation is best-suited to EOS's in general, or to particular EOS's.

- Several types of correlations exist for estimating acentric factor. The Edmister relation is best known and gives very good estimates for pure compounds. The Lee/Kesler equations - one for $T_r<0.8$ and one for $T_r>0.8$ - are similar to best-fit critical property correlations. Unfortunately the two correlations are not continuous and are developed from two types of data. Acentric factors estimated from the Lee/Kesler equations may be considereably larger than Edmister estimates. This can have a noticable effect on volumetric predictions by ZJRK-type equations, and to a lesser extent on VLE predictions.

- The Robinson/Peng critical property and acentric factor correlations are highly unreliable. This observation is detailed in paper A.4 and will not be repeated here. If property estimations are to be made by a method based on PNA content then accurate estimation of PNA is necessary. This can best (and perhaps only) be determined using the refractive-index/density correlations. Other methods which have been suggested rely on a material balance and two data such as boiling point and specific gravity. These methods are susceptible to small errors in measured properties, often resulting in negative compositions of one or two of the three constituents. They also rely on description of petroleum fractions as single carbon numbers, a concept which looses validity at relatively low boiling points.

2.5 Equation-of-State Critical Property Estimation

During the comparison of empirical critical property correlations it occured that a basic requirement of petroleum fraction characterization should be that the EOS prediction of specific gravity (i.e., liquid density at standard conditions) and boiling point should reproduce experimental values. It is easily shown that empirical critical property correlations do not have this property - i.e., different equations of state predict different values of specific gravity and boiling point even though they use the same critical properties.

The present work suggests a reasonable estimate of critical properties can be found by fitting the EOS to experimental values of specific gravity and boiling point for each petroleum fraction. One of the problems in developing this method has been definition of acentric factor, ω; i.e., two properties are known - specific gravity and boiling point - but three properties must be determined - critical pressure, critical temperature and acentric factor (in fact, it is the ratio of molecular weight to specific gravity, or molar volume, and not specific gravity alone which is required).

Acentric factor is included in the EOS as a correlating parameter for the correction term to EOS constant A (Ω_a). Hopefully a good estimate of ω will suffice since an experimental vapor pressure is used to determine critical pressure and critical temperature. Paraffin acentric factor is approximately a linear function of boiling point (see Fig. 2.5), given by

$$\omega = -0.477 + 0.00218 \cdot T_b(K) \quad \ldots\ldots\ldots\ldots\ldots\ldots\ldots \quad (2.10)$$

Aromatic acentric factor can be approximated by the linear function,

$$\omega = -0.587 + 0.00218 \cdot T_b(K) \quad \ldots\ldots\ldots\ldots\ldots\ldots\ldots \quad (2.11)$$

Assuming an average Watson characterization factor of 12.7 for paraffins, and 10.0 for aromatics, the following approximate relation for ω in terms of boiling point and Watson K_w is,

$$\omega = -1 + 0.042 \cdot K_w + 0.00218 \cdot T_b(K) \quad \ldots\ldots\ldots\ldots \quad (2.12)$$

If degrees Rankine is used for T_b instead of degrees Kelvin, the second constant in these equations becomes 0.000983. Recall the definition of K_w as $T_b(R)^{1/3}/\gamma$.

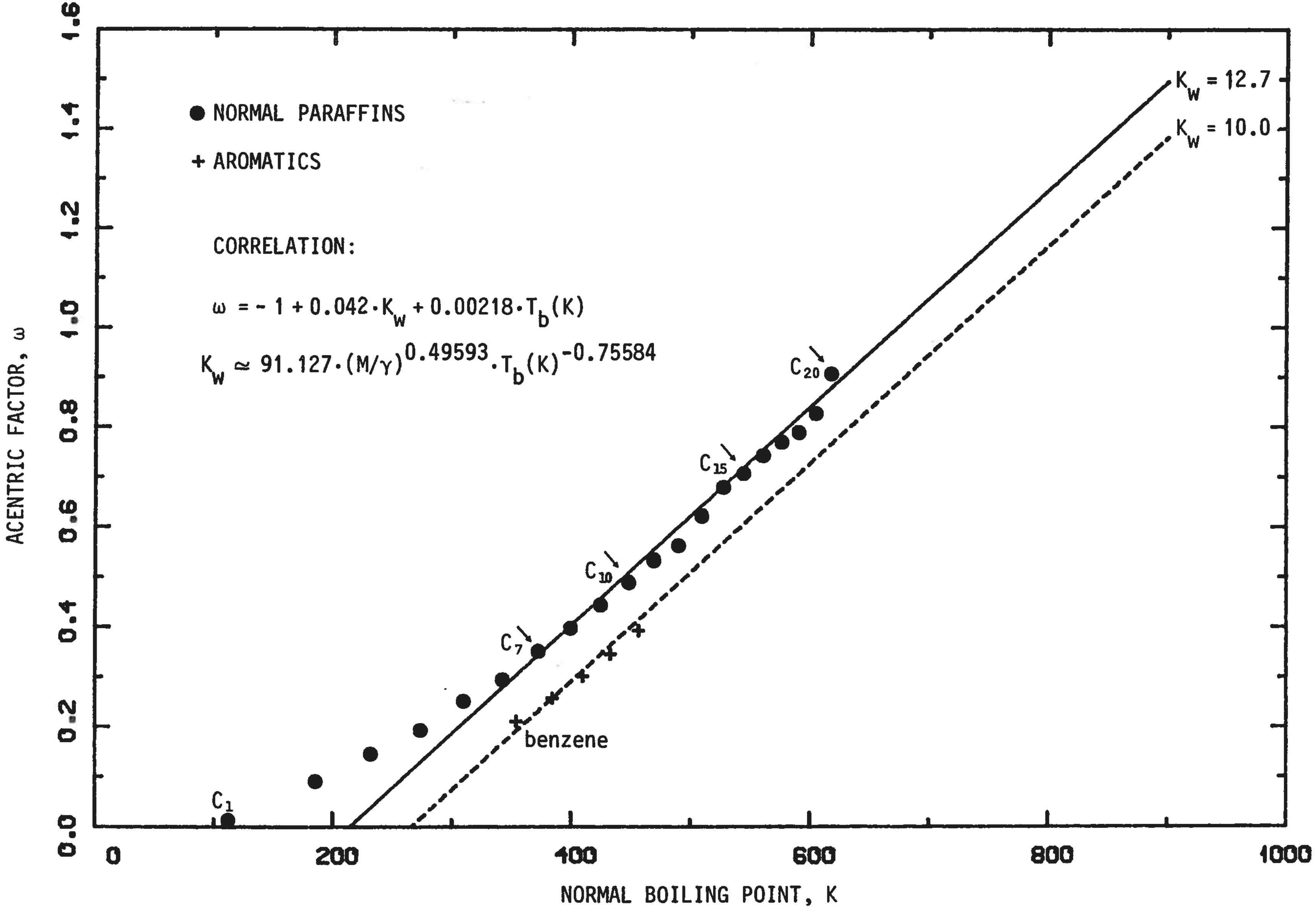

Fig. 2.5 - Acentric Factor as a Function of Normal Boiling Point for Normal Paraffins, Aromatics and Two Values of Watson Characterization Factor Using the Proposed Acentric Factor Correlation.

A problem with using the original definition of K_w is that the resulting critical property correlation, though based on an EOS, requires three data: molar volume, boiling point and specific gravity, used to define K_w; Criticals = Criticals $(M/\gamma, T_b, \gamma)$. An estimate of K_w based on M/γ and T_b can be developed from the Riazi-Daubert correlation in an analogous manner used to develop Eq. 2.5,

$$K_w = 91.127 \cdot (M/\gamma)^{0.49593} \cdot T_b(K)^{-0.75584} \quad \ldots\ldots\ldots \quad (2.13)$$

If T_b is given in degrees Rankine instead, constant 91.127 becomes 142.1. Now the critical property correlation based on an EOS can be determined in terms of only M/γ and T_b; Criticals = Criticals $(M/\gamma, T_b)$.

It will be shown in the following section that using Eqs. 2.12 and 2.13 is not considerably better than merely using the paraffin relation, Eq. 2.11. Eqs. 2.12 and 2.13 are adopted in the event that EOS predictions may be enhanced for mixtures with relatively aromatic petroleum fractions.

Critical pressures and temperatures have been calculated for the PR and SRK EOS's. They are presented in Tables 2.3 to 2.6 and Figs. 2.6 to 2.9. The ratio T_c/T_b is used instead of T_c directly.

After the present procedure was developed it was found that Schmidt and Wenzel had suggested that an EOS could be used to predict critical properties. They use their own EOS (see Chapter 1) and rely on two vapor pressure measurements and one density measurement to determine critical pressure, critical temperature, and acentric factor. They conclude that the EOS predictions are accurate for a wide range of pure compounds when compared with experimental data. Not surprisingly they show that critical pressure is mostly influenced by molar volume, while critical temperature is mostly affected by vapor pressure. It is interesting to note that their EOS predicts critical properties and acentric factors better than the PR or SRK equations.

Application to petroleum fractions is not discussed by Schmidt and Wenzel, and the most obvious problem is determination of the second vapor pressure data. Also, the experimental determination of molecular weight for petroleum fractions is, at best, 2 to 3 percent, and even worse for heavy constituents. The same problem is inherent in the present method. Perhaps the major difference between the

Schmidt/Wenzel study and the proposed procedure is that the former tries to show the application of a specific EOS for accurate prediction of true critical properties and acentric factor, whereas the aim of this study has been to find a method for (1) consistently defining the critical properties of petroleum fractions given a specific EOS, and (2) improving liquid density and VLE predictions for any EOS chosen.

From prelimenary calculations with the proposed method for the PR EOS, it appears that VLE predictions are improved considerably. Liquid density (i.e., volumetric) predictions are also improved, though it seems that instead of underestimated liquid densities, as is usually shown by the PR EOS with traditional critical property correlations, it now overpredicts liquid densities. It has not been established if the same problem exists for the SRK EOS.

PENG/ROBINSON EQUATION OF STATE

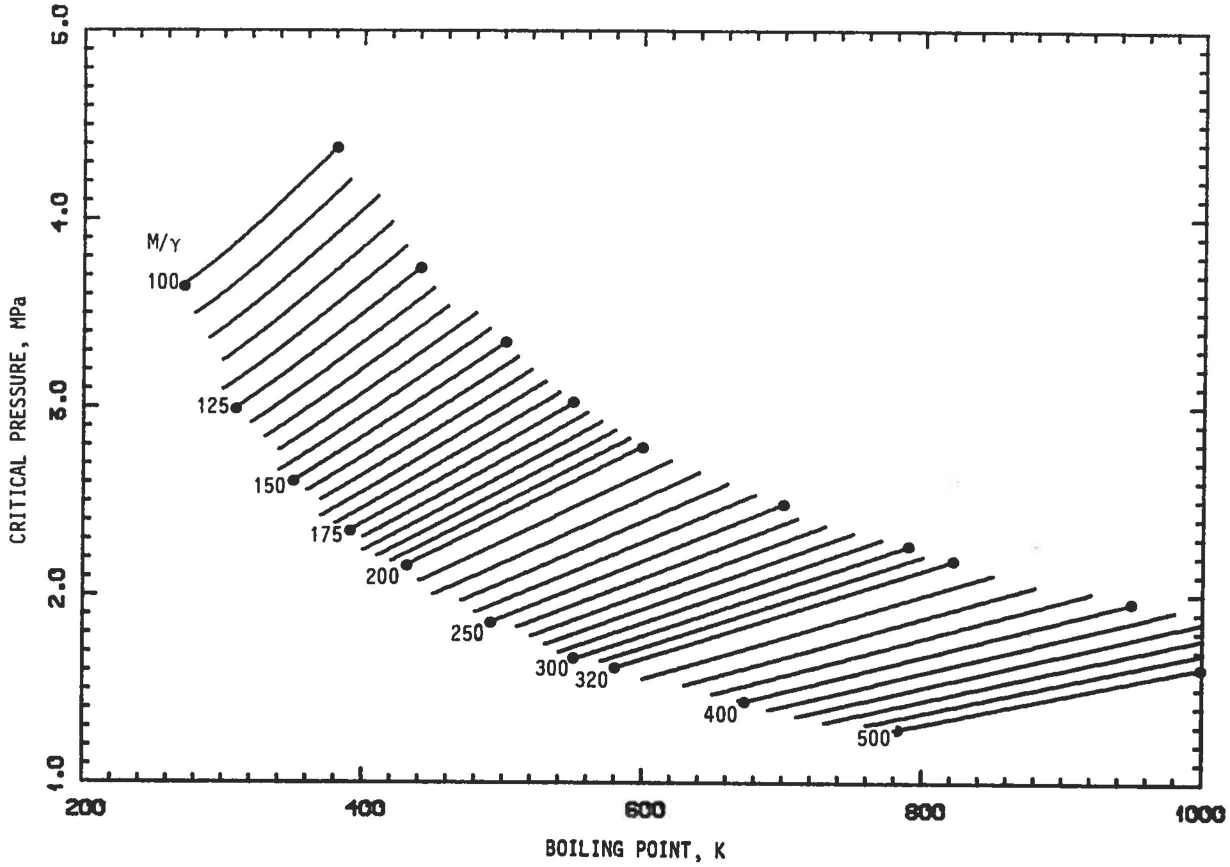

SOAVE/REDLICH/KWONG EQUATION OF STATE

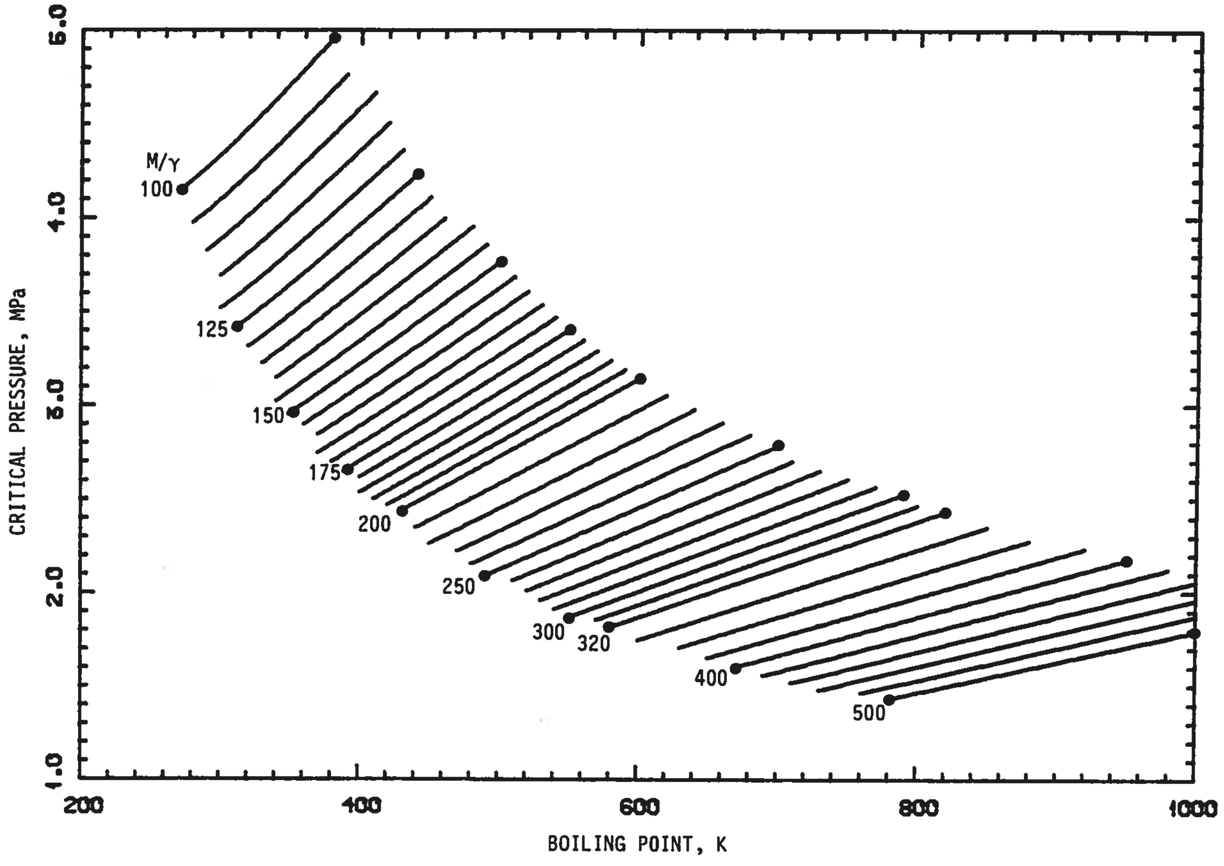

Figs. 2.6 and 2.7 - EOS-Based Critical Pressure for PR and SRK EOS's as a Function of Boiling Point and Molar Volume.

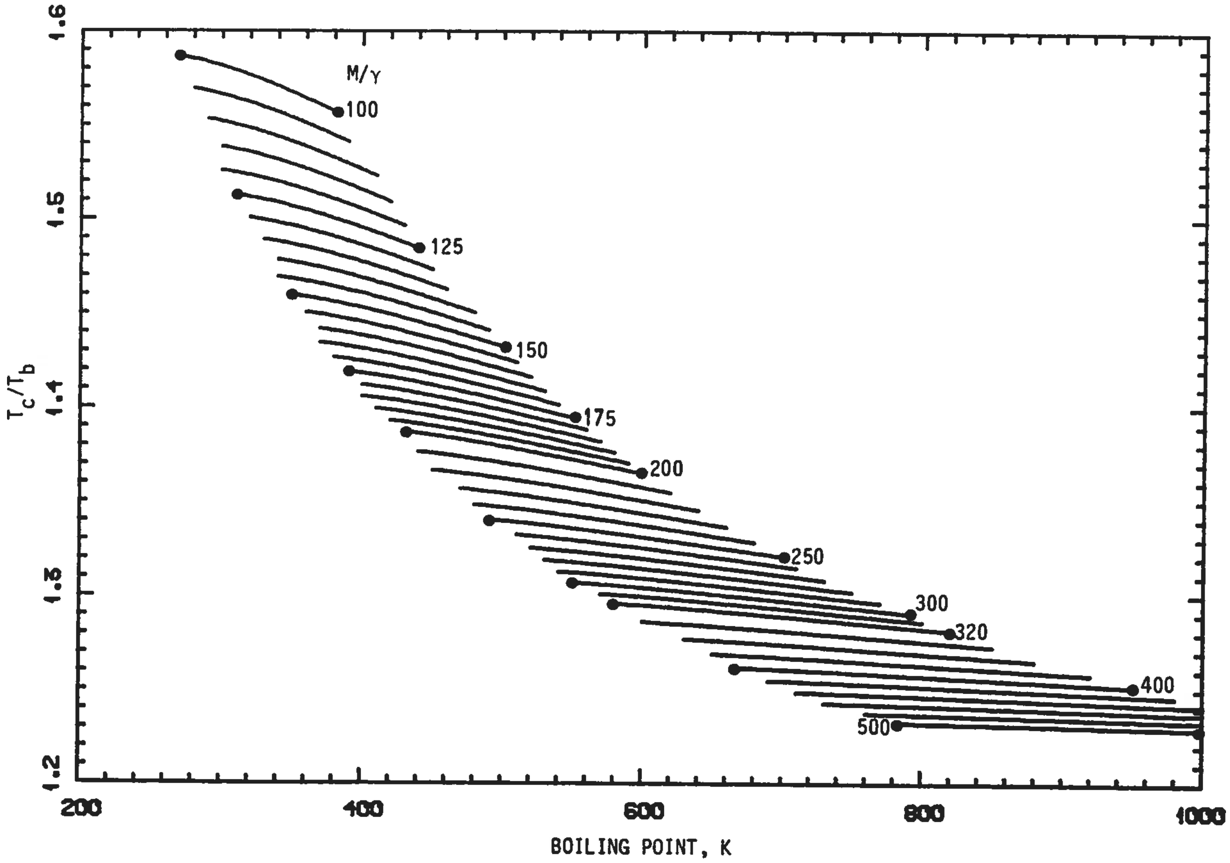
PENG/ROBINSON EQUATION OF STATE

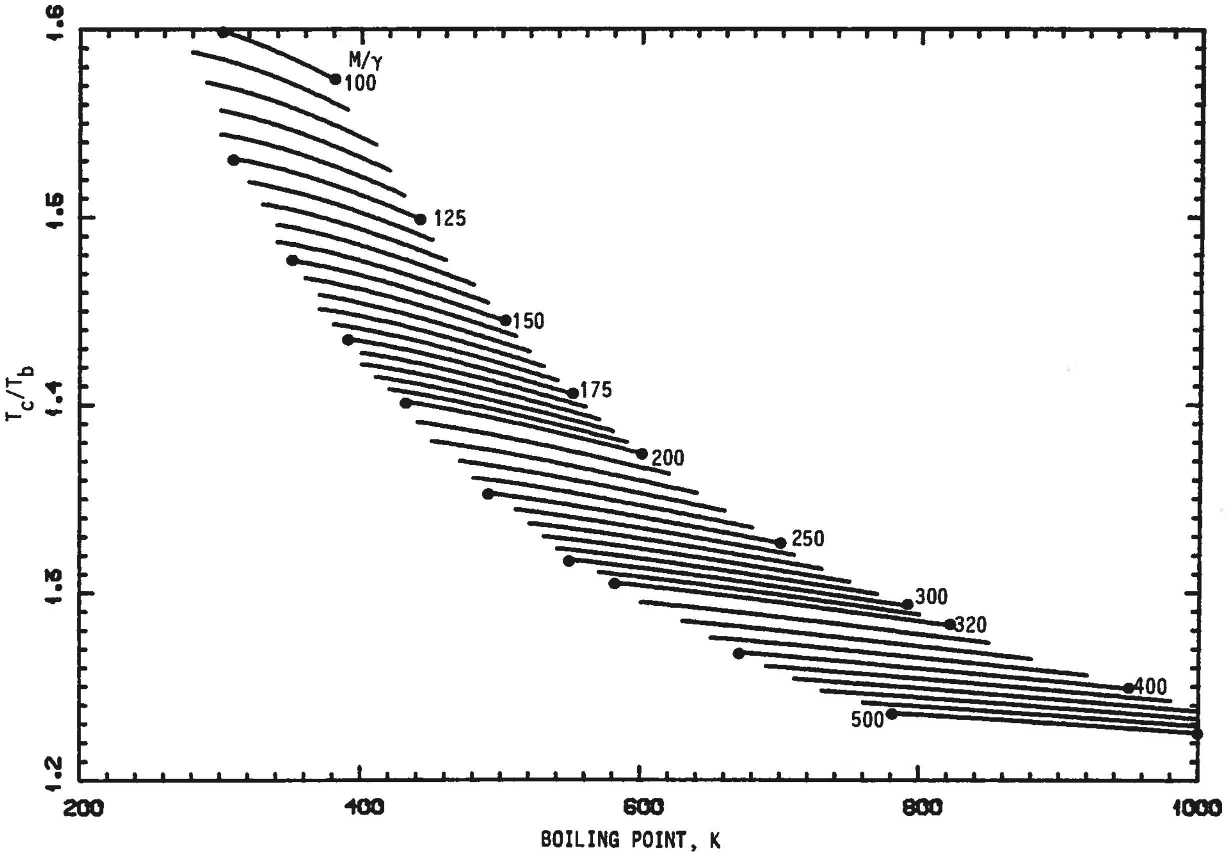
SOAVE/REDLICH/KWONG EQUATION OF STATE

Figs. 2.8 and 2.9 - EOS-Based Critical-Temperature/Boiling Point Ratio for PR and SRK EOS's as a Function of Boiling Point and Molar Volume.

TABLE 2.3 - EOS-BASED CRITICAL PRESSURE (MPa) FOR THE PR EOS.

PENG/ROBINSON EQUATION OF STATE

Boiling Point		Molar Volume (Mol Weight/Specific Gravity)					
(K)	(R)	100	105	110	115	120	125
270	486	3.6456					
280	504	3.6959	3.4952				
290	522	3.7523	3.5475	3.3630			
300	540	3.8132	3.6044	3.4162	3.2459	3.0910	
310	558	3.8775	3.6647	3.4729	3.2993	3.1415	2.9974
320	576	3.9442	3.7276	3.5323	3.3555	3.1947	3.0478
330	594	4.0129	3.7924	3.5937	3.4137	3.2499	3.1004
340	612	4.0830	3.8588	3.6566	3.4734	3.3068	3.1547
350	630	4.1542	3.9263	3.7207	3.5345	3.3650	3.2102
360	648	4.2264	3.9947	3.7858	3.5964	3.4241	3.2667
370	666	4.2991	4.0638	3.8515	3.6592	3.4841	3.3241
380	684	4.3724	4.1335	3.9179	3.7225	3.5446	3.3820
390	702		4.2036	3.9847	3.7863	3.6056	3.4405
400	720			4.0518	3.8504	3.6670	3.4993
410	738			4.1192	3.9148	3.7287	3.5584
420	756				3.9795	3.7906	3.6179
430	774					3.8527	3.6775
440	792						3.7372

PENG/ROBINSON EQUATION OF STATE

Boiling Point		Molar Volume (Mol Weight/Specific Gravity)					
(K)	(R)	130	135	140	145	150	155
320	576	2.9133					
330	594	2.9634	2.8374				
340	612	3.0152	2.8869	2.7685	2.6590		
350	630	3.0683	2.9377	2.8173	2.7058	2.6023	
360	648	3.1224	2.9896	2.8671	2.7536	2.6484	2.5505
370	666	3.1773	3.0423	2.9177	2.8023	2.6953	2.5957
380	684	3.2329	3.0957	2.9690	2.8517	2.7429	2.6416
390	702	3.2890	3.1495	3.0208	2.9016	2.7910	2.6881
400	720	3.3454	3.2038	3.0731	2.9520	2.8396	2.7350
410	738	3.4023	3.2585	3.1257	3.0027	2.8886	2.7823
420	756	3.4593	3.3134	3.1786	3.0537	2.9378	2.8299
430	774	3.5166	3.3685	3.2317	3.1050	2.9873	2.8777
440	792	3.5741	3.4238	3.2850	3.1564	3.0369	2.9257
450	810	3.6316	3.4792	3.3384	3.2079	3.0868	2.9739
460	828		3.5348	3.3920	3.2596	3.1367	3.0222
470	846			3.4456	3.3114	3.1868	3.0707
480	864			3.4993	3.3633	3.2369	3.1192
490	882				3.4152	3.2871	3.1678
500	900					3.3374	3.2164
510	918						3.2651

TABLE 2.3 - EOS-BASED CRITICAL PRESSURE (MPa) FOR THE PR EOS.

PENG/ROBINSON EQUATION OF STATE

Boiling Point		Molar Volume (Mol Weight/Specific Gravity)					
(K)	(R)	160	165	170	175	180	185
370	666	2.5028	2.4160				
380	684	2.5471	2.4588	2.3761			
390	702	2.5920	2.5023	2.4182	2.3393		
400	720	2.6374	2.5462	2.4607	2.3805	2.3050	2.2340
410	738	2.6831	2.5904	2.5036	2.4221	2.3454	2.2732
420	756	2.7292	2.6350	2.5468	2.4640	2.3861	2.3127
430	774	2.7755	2.6798	2.5902	2.5061	2.4270	2.3525
440	792	2.8219	2.7249	2.6339	2.5485	2.4682	2.3925
450	810	2.8686	2.7701	2.6778	2.5911	2.5095	2.4327
460	828	2.9154	2.8154	2.7217	2.6338	2.5510	2.4730
470	846	2.9623	2.8609	2.7658	2.6766	2.5926	2.5135
480	864	3.0093	2.9064	2.8100	2.7195	2.6343	2.5540
490	882	3.0563	2.9521	2.8543	2.7625	2.6761	2.5947
500	900	3.1034	2.9978	2.8987	2.8056	2.7180	2.6354
510	918	3.1506	3.0435	2.9431	2.8487	2.7599	2.6762
520	936	3.1978	3.0893	2.9875	2.8919	2.8018	2.7170
530	954		3.1351	3.0320	2.9351	2.8439	2.7579
540	972			3.0765	2.9783	2.8859	2.7988
550	990				3.0216	2.9280	2.8397
560	1008					2.9701	2.8807
570	1026						2.9217

TABLE 2.3 - EOS-BASED CRITICAL PRESSURE (MPa) FOR THE PR EOS.

PENG/ROBINSON EQUATION OF STATE

Boiling Point		Molar Volume (Mol Weight/Specific Gravity)					
(K)	(R)	190	195	200	210	220	230
410	738	2.2050					
420	756	2.2434	2.1780				
430	774	2.2821	2.2157	2.1527			
440	792	2.3210	2.2535	2.1896	2.0715		
450	810	2.3601	2.2916	2.2267	2.1068	1.9985	
460	828	2.3994	2.3298	2.2639	2.1422	2.0322	
470	846	2.4387	2.3681	2.3012	2.1777	2.0661	1.9648
480	864	2.4782	2.4066	2.3387	2.2133	2.1000	1.9972
490	882	2.5178	2.4451	2.3763	2.2490	2.1341	2.0298
500	900	2.5574	2.4837	2.4139	2.2849	2.1683	2.0624
510	918	2.5971	2.5224	2.4516	2.3207	2.2025	2.0951
520	936	2.6369	2.5611	2.4893	2.3567	2.2368	2.1279
530	954	2.6767	2.5999	2.5271	2.3926	2.2711	2.1607
540	972	2.7165	2.6387	2.5650	2.4287	2.3054	2.1935
550	990	2.7563	2.6775	2.6028	2.4647	2.3398	2.2264
560	1008	2.7962	2.7164	2.6407	2.5008	2.3743	2.2594
570	1026	2.8361	2.7552	2.6786	2.5369	2.4087	2.2923
580	1044	2.8761	2.7942	2.7166	2.5730	2.4432	2.3253
590	1062		2.8331	2.7545	2.6092	2.4777	2.3583
600	1080			2.7925	2.6453	2.5123	2.3913
610	1098				2.6815	2.5468	2.4244
620	1116				2.7177	2.5813	2.4574
630	1134					2.6159	2.4905
640	1152					2.6505	2.5236
650	1170						2.5566
660	1188						2.5898

TABLE 2.3 - EOS-BASED CRITICAL PRESSURE (MPa) FOR THE PR EOS.

PENG/ROBINSON EQUATION OF STATE

Boiling Point		Molar Volume (Mol Weight/Specific Gravity)					
(K)	(R)	240	250	260	270	280	290
480	864	1.9036					
490	882	1.9347	1.8477				
500	900	1.9659	1.8777				
510	918	1.9972	1.9077	1.8254			
520	936	2.0286	1.9378	1.8543	1.7774		
530	954	2.0600	1.9679	1.8833	1.8053	1.7332	
540	972	2.0915	1.9981	1.9123	1.8332	1.7601	1.6923
550	990	2.1230	2.0283	1.9414	1.8612	1.7871	1.7183
560	1008	2.1546	2.0586	1.9704	1.8892	1.8140	1.7444
570	1026	2.1861	2.0889	1.9996	1.9172	1.8410	1.7704
580	1044	2.2177	2.1192	2.0287	1.9452	1.8681	1.7965
590	1062	2.2494	2.1496	2.0579	1.9733	1.8951	1.8226
600	1080	2.2810	2.1799	2.0871	2.0014	1.9222	1.8488
610	1098	2.3126	2.2103	2.1163	2.0295	1.9493	1.8749
620	1116	2.3443	2.2407	2.1455	2.0577	1.9764	1.9011
630	1134	2.3760	2.2711	2.1747	2.0858	2.0036	1.9273
640	1152	2.4077	2.3016	2.2040	2.1140	2.0307	1.9535
650	1170	2.4394	2.3320	2.2332	2.1422	2.0579	1.9797
660	1188	2.4711	2.3625	2.2625	2.1703	2.0851	2.0060
670	1206	2.5029	2.3929	2.2918	2.1985	2.1123	2.0322
680	1224	2.5346	2.4234	2.3211	2.2268	2.1395	2.0585
690	1242		2.4539	2.3504	2.2550	2.1667	2.0847
700	1260		2.4844	2.3797	2.2832	2.1939	2.1110
710	1278			2.4091	2.3115	2.2211	2.1373
720	1296				2.3397	2.2484	2.1636
730	1314				2.3680	2.2756	2.1899
740	1332					2.3029	2.2162
750	1350					2.3301	2.2425
760	1368						2.2689
770	1386						2.2952

TABLE 2.3 - EOS-BASED CRITICAL PRESSURE (MPa) FOR THE PR EOS.

PENG/ROBINSON EQUATION OF STATE

Boiling Point		Molar Volume (Mol Weight/Specific Gravity)					
(K)	(R)	300	310	320	340	360	380
550	990	1.6545					
560	1008	1.6796					
570	1026	1.7048	1.6436				
580	1044	1.7300	1.6680	1.6101			
590	1062	1.7552	1.6924	1.6337			
600	1080	1.7805	1.7168	1.6573	1.5495		
610	1098	1.8057	1.7413	1.6810	1.5717		
620	1116	1.8310	1.7657	1.7047	1.5940		
630	1134	1.8563	1.7902	1.7284	1.6163	1.5172	
640	1152	1.8817	1.8147	1.7521	1.6386	1.5383	
650	1170	1.9070	1.8392	1.7759	1.6609	1.5593	1.4690
660	1188	1.9324	1.8638	1.7996	1.6833	1.5804	1.4889
670	1206	1.9577	1.8883	1.8234	1.7056	1.6015	1.5089
680	1224	1.9831	1.9128	1.8472	1.7280	1.6226	1.5289
690	1242	2.0085	1.9374	1.8710	1.7503	1.6437	1.5489
700	1260	2.0339	1.9620	1.8948	1.7727	1.6649	1.5689
710	1278	2.0593	1.9865	1.9186	1.7951	1.6860	1.5889
720	1296	2.0847	2.0111	1.9424	1.8175	1.7071	1.6089
730	1314	2.1101	2.0357	1.9662	1.8399	1.7283	1.6289
740	1332	2.1356	2.0603	1.9900	1.8624	1.7495	1.6490
750	1350	2.1610	2.0850	2.0139	1.8848	1.7706	1.6690
760	1368	2.1865	2.1096	2.0377	1.9072	1.7918	1.6891
770	1386	2.2119	2.1342	2.0616	1.9297	1.8130	1.7091
780	1404	2.2374	2.1589	2.0855	1.9521	1.8342	1.7292
790	1422	2.2629	2.1835	2.1094	1.9746	1.8554	1.7493
800	1440		2.2082	2.1332	1.9971	1.8766	1.7694
810	1458			2.1571	2.0196	1.8979	1.7895
820	1476			2.1811	2.0421	1.9191	1.8096
830	1494				2.0646	1.9403	1.8297
840	1512				2.0871	1.9616	1.8498
850	1530				2.1096	1.9829	1.8699
860	1548					2.0041	1.8901
870	1566					2.0254	1.9102
880	1584					2.0467	1.9304
890	1602						1.9506
900	1620						1.9708
910	1638						1.9910
920	1656						2.0112

TABLE 2.3 - EOS-BASED CRITICAL PRESSURE (MPa) FOR THE PR EOS.

PENG/ROBINSON EQUATION OF STATE

Boiling Point		Molar Volume (Mol Weight/Specific Gravity)					
(K)	(R)	400	420	440	460	480	500
670	1206	1.4260					
680	1224	1.4450					
690	1242	1.4639	1.3875				
700	1260	1.4829	1.4055				
710	1278	1.5019	1.4236	1.3527			
720	1296	1.5209	1.4417	1.3700			
730	1314	1.5399	1.4598	1.3872	1.3213		
740	1332	1.5589	1.4779	1.4045	1.3378		
750	1350	1.5780	1.4960	1.4218	1.3543		
760	1368	1.5970	1.5141	1.4391	1.3708	1.3085	
770	1386	1.6161	1.5322	1.4564	1.3874	1.3243	
780	1404	1.6351	1.5504	1.4737	1.4039	1.3402	1.2818
790	1422	1.6542	1.5685	1.4910	1.4204	1.3560	1.2970
800	1440	1.6733	1.5867	1.5083	1.4370	1.3719	1.3122
810	1458	1.6923	1.6048	1.5256	1.4535	1.3877	1.3274
820	1476	1.7114	1.6230	1.5429	1.4701	1.4036	1.3426
830	1494	1.7305	1.6412	1.5603	1.4867	1.4195	1.3579
840	1512	1.7496	1.6594	1.5776	1.5033	1.4354	1.3731
850	1530	1.7688	1.6776	1.5950	1.5199	1.4513	1.3883
860	1548	1.7879	1.6958	1.6124	1.5365	1.4671	1.4036
870	1566	1.8070	1.7140	1.6297	1.5531	1.4831	1.4189
880	1584	1.8262	1.7322	1.6471	1.5697	1.4990	1.4341
890	1602	1.8453	1.7504	1.6645	1.5863	1.5149	1.4494
900	1620	1.8645	1.7687	1.6819	1.6030	1.5308	1.4647
910	1638	1.8837	1.7869	1.6993	1.6196	1.5468	1.4800
920	1656	1.9029	1.8052	1.7167	1.6363	1.5627	1.4953
930	1674	1.9220	1.8235	1.7342	1.6529	1.5787	1.5106
940	1692	1.9413	1.8418	1.7516	1.6696	1.5946	1.5259
950	1710	1.9605	1.8601	1.7691	1.6863	1.6106	1.5412
960	1728		1.8784	1.7865	1.7030	1.6266	1.5566
970	1746		1.8967	1.8040	1.7197	1.6426	1.5719
980	1764		1.9150	1.8215	1.7364	1.6586	1.5873
990	1782			1.8390	1.7531	1.6746	1.6026
1000	1800			1.8565	1.7699	1.6907	1.6180
1010	1818			1.8740	1.7866	1.7067	1.6334
1020	1836				1.8034	1.7228	1.6488
1030	1854				1.8201	1.7388	1.6642
1040	1872				1.8369	1.7549	1.6796

TABLE 2.4 - EOS-BASED T_c/T_b RATIO FOR THE PR EOS.

PENG/ROBINSON EQUATION OF STATE

Boiling Point		Molar Volume (Mol Weight/Specific Gravity)					
(K)	(R)	100	105	110	115	120	125
270	486	1.5866					
280	504	1.5850	1.5692				
290	522	1.5832	1.5677	1.5531			
300	540	1.5811	1.5659	1.5516	1.5382	1.5256	
310	558	1.5788	1.5639	1.5499	1.5367	1.5243	1.5126
320	576	1.5762	1.5617	1.5480	1.5351	1.5229	1.5113
330	594	1.5734	1.5592	1.5458	1.5332	1.5212	1.5099
340	612	1.5704	1.5565	1.5434	1.5311	1.5194	1.5083
350	630	1.5672	1.5537	1.5409	1.5288	1.5173	1.5064
360	648	1.5639	1.5506	1.5381	1.5263	1.5151	1.5045
370	666	1.5604	1.5475	1.5352	1.5237	1.5127	1.5023
380	684	1.5568	1.5442	1.5322	1.5209	1.5102	1.5000
390	702		1.5408	1.5291	1.5181	1.5076	1.4976
400	720			1.5259	1.5151	1.5049	1.4951
410	738			1.5226	1.5120	1.5020	1.4925
420	756				1.5089	1.4991	1.4898
430	774					1.4962	1.4870
440	792						1.4842

PENG/ROBINSON EQUATION OF STATE

Boiling Point		Molar Volume (Mol Weight/Specific Gravity)					
(K)	(R)	130	135	140	145	150	155
320	576	1.5004					
330	594	1.4991	1.4889				
340	612	1.4977	1.4877	1.4781	1.4690		
350	630	1.4961	1.4863	1.4769	1.4679	1.4594	
360	648	1.4943	1.4847	1.4755	1.4667	1.4583	1.4502
370	666	1.4924	1.4830	1.4740	1.4653	1.4571	1.4492
380	684	1.4903	1.4811	1.4723	1.4638	1.4557	1.4479
390	702	1.4881	1.4791	1.4704	1.4621	1.4542	1.4466
400	720	1.4858	1.4770	1.4685	1.4604	1.4526	1.4451
410	738	1.4834	1.4747	1.4664	1.4585	1.4508	1.4435
420	756	1.4809	1.4724	1.4643	1.4565	1.4490	1.4418
430	774	1.4783	1.4700	1.4621	1.4544	1.4471	1.4400
440	792	1.4757	1.4676	1.4598	1.4523	1.4451	1.4382
450	810	1.4730	1.4650	1.4574	1.4501	1.4430	1.4363
460	828		1.4625	1.4550	1.4478	1.4409	1.4343
470	846			1.4526	1.4455	1.4388	1.4323
480	864			1.4501	1.4432	1.4366	1.4302
490	882				1.4408	1.4343	1.4281
500	900					1.4321	1.4259
510	918						1.4238

TABLE 2.4 - EOS-BASED T_c/T_b RATIO FOR THE PR EOS.

PENG/ROBINSON EQUATION OF STATE

Boiling Point		Molar Volume (Mol Weight/Specific Gravity)					
(K)	(R)	160	165	170	175	180	185
370	666	1.4415	1.4342				
380	684	1.4405	1.4333	1.4264			
390	702	1.4393	1.4322	1.4254	1.4189		
400	720	1.4379	1.4310	1.4243	1.4179	1.4117	1.4057
410	738	1.4365	1.4297	1.4231	1.4168	1.4107	1.4048
420	756	1.4349	1.4283	1.4218	1.4156	1.4097	1.4039
430	774	1.4333	1.4267	1.4204	1.4144	1.4085	1.4028
440	792	1.4315	1.4251	1.4190	1.4130	1.4072	1.4016
450	810	1.4297	1.4235	1.4174	1.4115	1.4059	1.4004
460	828	1.4279	1.4217	1.4158	1.4100	1.4045	1.3991
470	846	1.4260	1.4199	1.4141	1.4084	1.4030	1.3977
480	864	1.4240	1.4181	1.4124	1.4068	1.4015	1.3963
490	882	1.4220	1.4162	1.4106	1.4051	1.3999	1.3948
500	900	1.4200	1.4143	1.4088	1.4034	1.3983	1.3932
510	918	1.4180	1.4123	1.4069	1.4017	1.3966	1.3917
520	936	1.4159	1.4104	1.4051	1.3999	1.3949	1.3901
530	954		1.4084	1.4032	1.3981	1.3932	1.3885
540	972			1.4013	1.3963	1.3915	1.3868
550	990				1.3945	1.3897	1.3852
560	1008					1.3880	1.3835
570	1026						1.3818

TABLE 2.4 - EOS-BASED T_c/T_b RATIO FOR THE PR EOS.

PENG/ROBINSON EQUATION OF STATE

Boiling Point		Molar Volume (Mol Weight/Specific Gravity)					
(K)	(R)	190	195	200	210	220	230
410	738	1.3991					
420	756	1.3983	1.3928				
430	774	1.3973	1.3920	1.3868			
440	792	1.3962	1.3910	1.3859	1.3762		
450	810	1.3951	1.3899	1.3850	1.3754	1.3664	
460	828	1.3939	1.3888	1.3839	1.3745	1.3657	
470	846	1.3926	1.3876	1.3828	1.3736	1.3648	1.3566
480	864	1.3912	1.3864	1.3816	1.3725	1.3640	1.3558
490	882	1.3898	1.3850	1.3804	1.3715	1.3630	1.3550
500	900	1.3884	1.3837	1.3791	1.3703	1.3620	1.3542
510	918	1.3869	1.3823	1.3778	1.3692	1.3610	1.3533
520	936	1.3854	1.3808	1.3764	1.3680	1.3599	1.3523
530	954	1.3839	1.3794	1.3750	1.3667	1.3588	1.3513
540	972	1.3823	1.3779	1.3736	1.3654	1.3577	1.3503
550	990	1.3807	1.3764	1.3722	1.3641	1.3565	1.3492
560	1008	1.3791	1.3749	1.3707	1.3628	1.3553	1.3481
570	1026	1.3775	1.3733	1.3692	1.3614	1.3540	1.3470
580	1044	1.3759	1.3718	1.3678	1.3601	1.3528	1.3459
590	1062		1.3702	1.3663	1.3587	1.3515	1.3447
600	1080			1.3648	1.3573	1.3503	1.3435
610	1098				1.3559	1.3490	1.3424
620	1116				1.3546	1.3477	1.3412
630	1134					1.3464	1.3400
640	1152					1.3451	1.3388
650	1170						1.3376
660	1188						1.3364

TABLE 2.4 - EOS-BASED T_c/T_b RATIO FOR THE PR EOS.

PENG/ROBINSON EQUATION OF STATE

Boiling Point		Molar Volume (Mol Weight/Specific Gravity)					
(K)	(R)	240	250	260	270	280	290
480	864	1.3481					
490	882	1.3474	1.3402				
500	900	1.3467	1.3396				
510	918	1.3459	1.3389	1.3322			
520	936	1.3451	1.3381	1.3315	1.3252		
530	954	1.3442	1.3374	1.3309	1.3246	1.3187	
540	972	1.3432	1.3365	1.3301	1.3240	1.3181	1.3125
550	990	1.3423	1.3357	1.3294	1.3234	1.3176	1.3120
560	1008	1.3413	1.3348	1.3286	1.3226	1.3169	1.3115
570	1026	1.3403	1.3339	1.3278	1.3219	1.3163	1.3109
580	1044	1.3393	1.3330	1.3269	1.3211	1.3156	1.3103
590	1062	1.3382	1.3320	1.3261	1.3204	1.3149	1.3096
600	1080	1.3371	1.3310	1.3252	1.3195	1.3142	1.3090
610	1098	1.3361	1.3300	1.3243	1.3187	1.3134	1.3083
620	1116	1.3350	1.3290	1.3233	1.3179	1.3126	1.3076
630	1134	1.3339	1.3280	1.3224	1.3170	1.3118	1.3069
640	1152	1.3328	1.3270	1.3214	1.3161	1.3110	1.3061
650	1170	1.3316	1.3259	1.3205	1.3153	1.3102	1.3054
660	1188	1.3305	1.3249	1.3195	1.3144	1.3094	1.3046
670	1206	1.3294	1.3239	1.3186	1.3135	1.3086	1.3039
680	1224	1.3283	1.3228	1.3176	1.3126	1.3077	1.3031
690	1242		1.3218	1.3166	1.3117	1.3069	1.3023
700	1260		1.3208	1.3157	1.3108	1.3061	1.3015
710	1278			1.3147	1.3099	1.3052	1.3008
720	1296				1.3090	1.3044	1.3000
730	1314				1.3081	1.3035	1.2992
740	1332					1.3027	1.2984
750	1350					1.3019	1.2976
760	1368						1.2968
770	1386						1.2961

TABLE 2.4 - EOS-BASED T_c/T_b RATIO FOR THE PR EOS.

PENG/ROBINSON EQUATION OF STATE

Boiling Point		Molar Volume (Mol Weight/Specific Gravity)					
(K)	(R)	300	310	320	340	360	380
550	990	1.3067					
560	1008	1.3062					
570	1026	1.3057	1.3007				
580	1044	1.3052	1.3002	1.2955			
590	1062	1.3046	1.2997	1.2950			
600	1080	1.3040	1.2992	1.2946	1.2858		
610	1098	1.3034	1.2987	1.2941	1.2854		
620	1116	1.3028	1.2981	1.2936	1.2850		
630	1134	1.3021	1.2975	1.2930	1.2846	1.2767	
640	1152	1.3014	1.2969	1.2925	1.2841	1.2763	
650	1170	1.3007	1.2962	1.2919	1.2837	1.2759	1.2687
660	1188	1.3000	1.2956	1.2913	1.2832	1.2756	1.2684
670	1206	1.2993	1.2950	1.2907	1.2827	1.2752	1.2681
680	1224	1.2986	1.2943	1.2901	1.2822	1.2747	1.2677
690	1242	1.2979	1.2936	1.2895	1.2817	1.2743	1.2674
700	1260	1.2972	1.2930	1.2889	1.2811	1.2739	1.2670
710	1278	1.2964	1.2923	1.2883	1.2806	1.2734	1.2666
720	1296	1.2957	1.2916	1.2876	1.2801	1.2730	1.2663
730	1314	1.2950	1.2909	1.2870	1.2795	1.2725	1.2659
740	1332	1.2942	1.2902	1.2863	1.2790	1.2720	1.2655
750	1350	1.2935	1.2895	1.2857	1.2784	1.2715	1.2651
760	1368	1.2928	1.2889	1.2851	1.2778	1.2710	1.2646
770	1386	1.2921	1.2882	1.2844	1.2773	1.2706	1.2642
780	1404	1.2913	1.2875	1.2838	1.2767	1.2701	1.2638
790	1422	1.2906	1.2868	1.2832	1.2762	1.2696	1.2634
800	1440		1.2861	1.2825	1.2756	1.2691	1.2630
810	1458			1.2819	1.2751	1.2686	1.2625
820	1476			1.2813	1.2745	1.2681	1.2621
830	1494				1.2740	1.2677	1.2617
840	1512				1.2734	1.2672	1.2613
850	1530				1.2729	1.2667	1.2609
860	1548					1.2662	1.2605
870	1566					1.2658	1.2600
880	1584					1.2653	1.2596
890	1602						1.2592
900	1620						1.2588
910	1638						1.2584
920	1656						1.2581

TABLE 2.4 - EOS-BASED T_c/T_b RATIO FOR THE PR EOS.

PENG/ROBINSON EQUATION OF STATE

Boiling Point		Molar Volume (Mol Weight/Specific Gravity)					
(K)	(R)	400	420	440	460	480	500
670	1206	1.2614					
680	1224	1.2611					
690	1242	1.2608	1.2546				
700	1260	1.2605	1.2544				
710	1278	1.2602	1.2542	1.2484			
720	1296	1.2599	1.2539	1.2483			
730	1314	1.2596	1.2537	1.2481	1.2427		
740	1332	1.2593	1.2534	1.2478	1.2425		
750	1350	1.2589	1.2531	1.2476	1.2424		
760	1368	1.2586	1.2529	1.2474	1.2422	1.2372	
770	1386	1.2582	1.2526	1.2472	1.2420	1.2371	
780	1404	1.2579	1.2523	1.2469	1.2418	1.2370	1.2323
790	1422	1.2575	1.2520	1.2467	1.2416	1.2368	1.2322
800	1440	1.2572	1.2517	1.2464	1.2414	1.2367	1.2321
810	1458	1.2568	1.2513	1.2462	1.2412	1.2365	1.2320
820	1476	1.2564	1.2510	1.2459	1.2410	1.2363	1.2318
830	1494	1.2561	1.2507	1.2456	1.2408	1.2361	1.2317
840	1512	1.2557	1.2504	1.2454	1.2406	1.2360	1.2316
850	1530	1.2553	1.2501	1.2451	1.2403	1.2358	1.2314
860	1548	1.2550	1.2498	1.2448	1.2401	1.2356	1.2313
870	1566	1.2546	1.2495	1.2446	1.2399	1.2354	1.2312
880	1584	1.2543	1.2492	1.2443	1.2397	1.2352	1.2310
890	1602	1.2539	1.2489	1.2440	1.2395	1.2351	1.2309
900	1620	1.2536	1.2486	1.2438	1.2392	1.2349	1.2307
910	1638	1.2532	1.2483	1.2435	1.2390	1.2347	1.2306
920	1656	1.2529	1.2480	1.2433	1.2388	1.2345	1.2304
930	1674	1.2525	1.2477	1.2430	1.2386	1.2343	1.2303
940	1692	1.2522	1.2474	1.2428	1.2384	1.2342	1.2301
950	1710	1.2519	1.2471	1.2425	1.2382	1.2340	1.2300
960	1728		1.2468	1.2423	1.2379	1.2338	1.2298
970	1746		1.2465	1.2420	1.2377	1.2336	1.2297
980	1764		1.2463	1.2418	1.2375	1.2335	1.2296
990	1782			1.2416	1.2374	1.2333	1.2294
1000	1800			1.2414	1.2372	1.2332	1.2293
1010	1818			1.2411	1.2370	1.2330	1.2292
1020	1836				1.2368	1.2328	1.2291
1030	1854				1.2366	1.2327	1.2289
1040	1872				1.2365	1.2326	1.2288

TABLE 2.5 - EOS-BASED CRITICAL PRESSURE (MPa) FOR THE SRK EOS.

SOAVE/REDLICH/KWONG EQUATION OF STATE

Boiling Point		Molar Volume (Mol Weight/Specific Gravity)					
(K)	(R)	100	105	110	115	120	125
270	486	4.1446					
280	504	4.2020	3.9741				
290	522	4.2657	4.0333	3.8239			
300	540	4.3341	4.0973	3.8838	3.6905	3.5147	
310	558	4.4060	4.1648	3.9474	3.7505	3.5713	3.4077
320	576	4.4806	4.2351	4.0137	3.8132	3.6308	3.4642
330	594	4.5572	4.3074	4.0822	3.8781	3.6925	3.5229
340	612	4.6352	4.3813	4.1522	3.9447	3.7558	3.5833
350	630	4.7144	4.4563	4.2235	4.0125	3.8205	3.6450
360	648	4.7945	4.5323	4.2958	4.0814	3.8862	3.7078
370	666	4.8753	4.6090	4.3688	4.1509	3.9526	3.7714
380	684	4.9566	4.6863	4.4423	4.2211	4.0197	3.8356
390	702		4.7639	4.5163	4.2918	4.0873	3.9003
400	720			4.5906	4.3627	4.1552	3.9654
410	738			4.6651	4.4340	4.2234	4.0308
420	756				4.5054	4.2918	4.0965
430	774					4.3604	4.1623
440	792						4.2282

SOAVE/REDLICH/KWONG EQUATION OF STATE

Boiling Point		Molar Volume (Mol Weight/Specific Gravity)					
(K)	(R)	130	135	140	145	150	155
320	576	3.3115					
330	594	3.3674	3.2244				
340	612	3.4251	3.2795	3.1452	3.0209		
350	630	3.4841	3.3361	3.1994	3.0729	2.9556	
360	648	3.5442	3.3937	3.2547	3.1261	3.0067	2.8956
370	666	3.6051	3.4521	3.3109	3.1801	3.0587	2.9458
380	684	3.6667	3.5113	3.3677	3.2348	3.1115	2.9967
390	702	3.7288	3.5709	3.4251	3.2901	3.1648	3.0481
400	720	3.7913	3.6310	3.4829	3.3458	3.2185	3.1000
410	738	3.8541	3.6914	3.5411	3.4019	3.2726	3.1523
420	756	3.9171	3.7520	3.5995	3.4582	3.3270	3.2049
430	774	3.9804	3.8129	3.6581	3.5148	3.3816	3.2577
440	792	4.0437	3.8739	3.7169	3.5715	3.4364	3.3107
450	810	4.1072	3.9350	3.7758	3.6283	3.4914	3.3638
460	828		3.9961	3.8348	3.6853	3.5464	3.4170
470	846			3.8938	3.7423	3.6015	3.4703
480	864			3.9529	3.7993	3.6566	3.5237
490	882				3.8564	3.7118	3.5771
500	900					3.7670	3.6305
510	918						3.6840

TABLE 2.5 - EOS-BASED CRITICAL PRESSURE (MPa) FOR THE SRK EOS.

SOAVE/REDLICH/KWONG EQUATION OF STATE

Boiling Point		Molar Volume (Mol Weight/Specific Gravity)					
(K)	(R)	160	165	170	175	180	185
370	666	2.8404	2.7420				
380	684	2.8896	2.7895	2.6957			
390	702	2.9393	2.8375	2.7422	2.6527		
400	720	2.9895	2.8861	2.7893	2.6983	2.6128	2.5323
410	738	3.0400	2.9350	2.8367	2.7443	2.6575	2.5756
420	756	3.0909	2.9843	2.8844	2.7906	2.7024	2.6193
430	774	3.1420	3.0338	2.9324	2.8372	2.7476	2.6632
440	792	3.1933	3.0835	2.9805	2.8839	2.7930	2.7074
450	810	3.2447	3.1333	3.0289	2.9308	2.8386	2.7517
460	828	3.2962	3.1832	3.0773	2.9779	2.8843	2.7961
470	846	3.3479	3.2333	3.1259	3.0250	2.9301	2.8407
480	864	3.3996	3.2834	3.1745	3.0722	2.9760	2.8853
490	882	3.4513	3.3336	3.2232	3.1195	3.0220	2.9300
500	900	3.5031	3.3838	3.2719	3.1669	3.0680	2.9748
510	918	3.5549	3.4340	3.3207	3.2142	3.1140	3.0196
520	936	3.6067	3.4843	3.3695	3.2616	3.1601	3.0644
530	954		3.5345	3.4183	3.3090	3.2062	3.1092
540	972			3.4671	3.3564	3.2523	3.1541
550	990				3.4038	3.2984	3.1989
560	1008					3.3445	3.2438
570	1026						3.2887

TABLE 2.5 - EOS-BASED CRITICAL PRESSURE (MPa) FOR THE SRK EOS.

SOAVE/REDLICH/KWONG EQUATION OF STATE

Boiling Point		Molar Volume (Mol Weight/Specific Gravity)					
(K)	(R)	190	195	200	210	220	230
410	738	2.4984					
420	756	2.5409	2.4668				
430	774	2.5836	2.5083	2.4371			
440	792	2.6265	2.5501	2.4778	2.3441		
450	810	2.6696	2.5921	2.5186	2.3830	2.2605	
460	828	2.7129	2.6342	2.5597	2.4220	2.2976	
470	846	2.7562	2.6764	2.6008	2.4611	2.3349	2.2204
480	864	2.7997	2.7187	2.6420	2.5003	2.3723	2.2561
490	882	2.8432	2.7611	2.6833	2.5396	2.4098	2.2920
500	900	2.8867	2.8035	2.7247	2.5790	2.4474	2.3278
510	918	2.9304	2.8460	2.7661	2.6184	2.4850	2.3638
520	936	2.9740	2.8885	2.8076	2.6579	2.5226	2.3998
530	954	3.0177	2.9311	2.8491	2.6974	2.5603	2.4358
540	972	3.0613	2.9736	2.8905	2.7369	2.5980	2.4719
550	990	3.1050	3.0162	2.9321	2.7764	2.6357	2.5080
560	1008	3.1487	3.0588	2.9736	2.8160	2.6735	2.5441
570	1026	3.1924	3.1013	3.0151	2.8555	2.7112	2.5802
580	1044	3.2361	3.1439	3.0566	2.8951	2.7490	2.6163
590	1062		3.1865	3.0981	2.9346	2.7867	2.6524
600	1080			3.1396	2.9741	2.8245	2.6885
610	1098				3.0137	2.8622	2.7246
620	1116				3.0532	2.9000	2.7607
630	1134					2.9377	2.7968
640	1152					2.9754	2.8329
650	1170						2.8690
660	1188						2.9050

TABLE 2.5 - EOS-BASED CRITICAL PRESSURE (MPa) FOR THE SRK EOS.

SOAVE/REDLICH/KWONG EQUATION OF STATE

Boiling Point		Molar Volume (Mol Weight/Specific Gravity)					
(K)	(R)	240	250	260	270	280	290
480	864	2.1502					
490	882	2.1845	2.0862				
500	900	2.2189	2.1192				
510	918	2.2533	2.1522	2.0593			
520	936	2.2878	2.1853	2.0911	2.0043		
530	954	2.3223	2.2184	2.1229	2.0350	1.9536	
540	972	2.3568	2.2515	2.1548	2.0656	1.9832	1.9068
550	990	2.3914	2.2847	2.1867	2.0963	2.0128	1.9353
560	1008	2.4260	2.3179	2.2186	2.1270	2.0424	1.9639
570	1026	2.4606	2.3511	2.2505	2.1577	2.0720	1.9924
580	1044	2.4952	2.3843	2.2824	2.1885	2.1016	2.0210
590	1062	2.5298	2.4175	2.3144	2.2192	2.1313	2.0497
600	1080	2.5644	2.4508	2.3463	2.2500	2.1609	2.0783
610	1098	2.5990	2.4840	2.3782	2.2807	2.1906	2.1069
620	1116	2.6336	2.5172	2.4102	2.3115	2.2202	2.1355
630	1134	2.6682	2.5504	2.4421	2.3423	2.2499	2.1642
640	1152	2.7028	2.5836	2.4741	2.3730	2.2795	2.1928
650	1170	2.7374	2.6168	2.5060	2.4038	2.3092	2.2214
660	1188	2.7720	2.6501	2.5379	2.4345	2.3388	2.2501
670	1206	2.8066	2.6832	2.5699	2.4653	2.3685	2.2787
680	1224	2.8411	2.7164	2.6018	2.4960	2.3981	2.3073
690	1242		2.7496	2.6337	2.5267	2.4278	2.3359
700	1260		2.7828	2.6656	2.5575	2.4574	2.3645
710	1278			2.6975	2.5882	2.4870	2.3931
720	1296				2.6189	2.5166	2.4217
730	1314				2.6496	2.5462	2.4503
740	1332					2.5758	2.4789
750	1350					2.6054	2.5075
760	1368						2.5361
770	1386						2.5646

TABLE 2.5 - EOS-BASED CRITICAL PRESSURE (MPa) FOR THE SRK EOS.

SOAVE/REDLICH/KWONG EQUATION OF STATE

Boiling Point		Molar Volume (Mol Weight/Specific Gravity)					
(K)	(R)	300	310	320	340	360	380
550	990	1.8633					
560	1008	1.8909					
570	1026	1.9185	1.8496				
580	1044	1.9461	1.8763	1.8111			
590	1062	1.9738	1.9031	1.8371			
600	1080	2.0015	1.9299	1.8630	1.7416		
610	1098	2.0291	1.9566	1.8889	1.7660		
620	1116	2.0568	1.9834	1.9148	1.7904		
630	1134	2.0845	2.0102	1.9408	1.8148	1.7035	
640	1152	2.1122	2.0370	1.9667	1.8392	1.7265	
650	1170	2.1398	2.0637	1.9926	1.8636	1.7496	1.6481
660	1188	2.1675	2.0905	2.0186	1.8880	1.7726	1.6699
670	1206	2.1952	2.1173	2.0445	1.9124	1.7956	1.6917
680	1224	2.2228	2.1441	2.0704	1.9368	1.8187	1.7136
690	1242	2.2505	2.1708	2.0964	1.9612	1.8417	1.7354
700	1260	2.2782	2.1976	2.1223	1.9856	1.8647	1.7572
710	1278	2.3058	2.2244	2.1482	2.0100	1.8878	1.7790
720	1296	2.3335	2.2511	2.1741	2.0344	1.9108	1.8008
730	1314	2.3611	2.2779	2.2001	2.0588	1.9338	1.8226
740	1332	2.3887	2.3046	2.2260	2.0831	1.9569	1.8444
750	1350	2.4163	2.3313	2.2519	2.1075	1.9799	1.8662
760	1368	2.4440	2.3581	2.2778	2.1319	2.0029	1.8880
770	1386	2.4716	2.3848	2.3036	2.1563	2.0259	1.9098
780	1404	2.4992	2.4115	2.3295	2.1806	2.0489	1.9316
790	1422	2.5268	2.4382	2.3554	2.2050	2.0719	1.9534
800	1440		2.4649	2.3813	2.2293	2.0949	1.9752
810	1458			2.4072	2.2537	2.1179	1.9970
820	1476			2.4330	2.2780	2.1409	2.0188
830	1494				2.3024	2.1639	2.0405
840	1512				2.3267	2.1869	2.0623
850	1530				2.3510	2.2098	2.0841
860	1548					2.2328	2.1058
870	1566					2.2558	2.1276
880	1584					2.2788	2.1494
890	1602						2.1711
900	1620						2.1929
910	1638						2.2146
920	1656						2.2364

TABLE 2.5 - EOS-BASED CRITICAL PRESSURE (MPa) FOR THE SRK EOS.

SOAVE/REDLICH/KWONG EQUATION OF STATE

Boiling Point		Molar Volume (Mol Weight/Specific Gravity)					
(K)	(R)	400	420	440	460	480	500
670	1206	1.5987					
680	1224	1.6195					
690	1242	1.6402	1.5544				
700	1260	1.6609	1.5742				
710	1278	1.6816	1.5939	1.5145			
720	1296	1.7023	1.6136	1.5333			
730	1314	1.7230	1.6333	1.5522	1.4783		
740	1332	1.7437	1.6531	1.5710	1.4963		
750	1350	1.7645	1.6728	1.5898	1.5143		
760	1368	1.7852	1.6925	1.6086	1.5323	1.4627	
770	1386	1.8059	1.7122	1.6274	1.5503	1.4799	
780	1404	1.8266	1.7319	1.6462	1.5683	1.4971	1.4319
790	1422	1.8473	1.7516	1.6650	1.5863	1.5143	1.4484
800	1440	1.8680	1.7713	1.6838	1.6042	1.5316	1.4649
810	1458	1.8886	1.7910	1.7026	1.6222	1.5488	1.4815
820	1476	1.9093	1.8107	1.7214	1.6402	1.5660	1.4980
830	1494	1.9300	1.8304	1.7402	1.6582	1.5832	1.5145
840	1512	1.9507	1.8501	1.7590	1.6761	1.6005	1.5311
850	1530	1.9714	1.8698	1.7778	1.6941	1.6177	1.5476
860	1548	1.9920	1.8895	1.7966	1.7121	1.6349	1.5641
870	1566	2.0127	1.9092	1.8154	1.7300	1.6521	1.5806
880	1584	2.0334	1.9288	1.8341	1.7480	1.6693	1.5971
890	1602	2.0540	1.9485	1.8529	1.7660	1.6865	1.6136
900	1620	2.0747	1.9682	1.8717	1.7839	1.7037	1.6301
910	1638	2.0954	1.9879	1.8905	1.8019	1.7209	1.6467
920	1656	2.1160	2.0075	1.9092	1.8198	1.7381	1.6632
930	1674	2.1367	2.0272	1.9280	1.8378	1.7553	1.6797
940	1692	2.1573	2.0469	1.9468	1.8557	1.7725	1.6962
950	1710	2.1780	2.0665	1.9655	1.8737	1.7897	1.7127
960	1728		2.0862	1.9843	1.8916	1.8069	1.7292
970	1746		2.1058	2.0031	1.9095	1.8241	1.7457
980	1764		2.1255	2.0218	1.9275	1.8413	1.7622
990	1782			2.0406	1.9454	1.8585	1.7787
1000	1800			2.0593	1.9634	1.8756	1.7952
1010	1818			2.0781	1.9813	1.8928	1.8117
1020	1836				1.9992	1.9100	1.8282
1030	1854				2.0172	1.9272	1.8446
1040	1872				2.0351	1.9444	1.8611

TABLE 2.6 - EOS-BASED T_c/T_b RATIO FOR THE SRK EOS.

SOAVE/REDLICH/KWONG EQUATION OF STATE

Boiling Point		Molar Volume (Mol Weight/Specific Gravity)					
(K)	(R)	100	105	110	115	120	125
270	486	1.6049					
280	504	1.6033	1.5876				
290	522	1.6014	1.5860	1.5715			
300	540	1.5992	1.5841	1.5699	1.5565	1.5439	
310	558	1.5967	1.5819	1.5680	1.5549	1.5425	1.5308
320	576	1.5940	1.5795	1.5659	1.5530	1.5409	1.5294
330	594	1.5910	1.5769	1.5635	1.5509	1.5390	1.5277
340	612	1.5878	1.5740	1.5610	1.5486	1.5370	1.5259
350	630	1.5844	1.5709	1.5582	1.5461	1.5347	1.5238
360	648	1.5809	1.5677	1.5552	1.5434	1.5323	1.5216
370	666	1.5772	1.5643	1.5521	1.5406	1.5296	1.5192
380	684	1.5733	1.5607	1.5489	1.5376	1.5269	1.5167
390	702		1.5571	1.5455	1.5345	1.5240	1.5140
400	720			1.5420	1.5312	1.5210	1.5112
410	738			1.5384	1.5279	1.5179	1.5083
420	756				1.5245	1.5147	1.5054
430	774					1.5114	1.5023
440	792						1.4992

SOAVE/REDLICH/KWONG EQUATION OF STATE

Boiling Point		Molar Volume (Mol Weight/Specific Gravity)					
(K)	(R)	130	135	140	145	150	155
320	576	1.5184					
330	594	1.5170	1.5067				
340	612	1.5153	1.5053	1.4957	1.4866		
350	630	1.5135	1.5037	1.4943	1.4853	1.4767	
360	648	1.5115	1.5019	1.4926	1.4838	1.4754	1.4673
370	666	1.5093	1.4999	1.4908	1.4822	1.4739	1.4659
380	684	1.5070	1.4977	1.4889	1.4804	1.4723	1.4645
390	702	1.5045	1.4955	1.4868	1.4785	1.4705	1.4628
400	720	1.5019	1.4931	1.4846	1.4764	1.4686	1.4611
410	738	1.4992	1.4905	1.4822	1.4742	1.4666	1.4592
420	756	1.4964	1.4879	1.4798	1.4720	1.4645	1.4572
430	774	1.4936	1.4852	1.4773	1.4696	1.4622	1.4552
440	792	1.4906	1.4825	1.4747	1.4671	1.4599	1.4530
450	810	1.4876	1.4796	1.4720	1.4646	1.4576	1.4508
460	828		1.4768	1.4693	1.4621	1.4551	1.4485
470	846			1.4665	1.4594	1.4526	1.4461
480	864			1.4637	1.4568	1.4501	1.4437
490	882				1.4541	1.4475	1.4413
500	900					1.4449	1.4388
510	918						1.4363

TABLE 2.6 - EOS-BASED T_c/T_b RATIO FOR THE SRK EOS.

SOAVE/REDLICH/KWONG EQUATION OF STATE

Boiling Point		Molar Volume (Mol Weight/Specific Gravity)					
(K)	(R)	160	165	170	175	180	185
370	666	1.4583	1.4509				
380	684	1.4570	1.4497	1.4428			
390	702	1.4555	1.4484	1.4416	1.4350		
400	720	1.4539	1.4469	1.4402	1.4337	1.4275	1.4214
410	738	1.4521	1.4453	1.4387	1.4324	1.4262	1.4203
420	756	1.4503	1.4436	1.4371	1.4309	1.4249	1.4190
430	774	1.4483	1.4418	1.4354	1.4293	1.4234	1.4177
440	792	1.4463	1.4399	1.4336	1.4276	1.4218	1.4162
450	810	1.4442	1.4379	1.4318	1.4259	1.4202	1.4147
460	828	1.4420	1.4358	1.4298	1.4241	1.4185	1.4130
470	846	1.4398	1.4337	1.4278	1.4222	1.4167	1.4113
480	864	1.4375	1.4315	1.4258	1.4202	1.4148	1.4096
490	882	1.4352	1.4293	1.4237	1.4182	1.4129	1.4078
500	900	1.4328	1.4271	1.4215	1.4162	1.4110	1.4059
510	918	1.4304	1.4248	1.4193	1.4141	1.4090	1.4040
520	936	1.4280	1.4225	1.4171	1.4120	1.4069	1.4021
530	954		1.4201	1.4149	1.4098	1.4049	1.4001
540	972			1.4126	1.4077	1.4028	1.3981
550	990				1.4055	1.4007	1.3961
560	1008					1.3986	1.3941
570	1026						1.3920

TABLE 2.6 - EOS-BASED T_c/T_b RATIO FOR THE SRK EOS.

SOAVE/REDLICH/KWONG EQUATION OF STATE

Boiling Point		Molar Volume (Mol Weight/Specific Gravity)					
(K)	(R)	190	195	200	210	220	230
410	738	1.4145					
420	756	1.4134	1.4079				
430	774	1.4121	1.4067	1.4015			
440	792	1.4108	1.4055	1.4004	1.3906		
450	810	1.4093	1.4041	1.3991	1.3895	1.3803	
460	828	1.4078	1.4027	1.3977	1.3883	1.3793	
470	846	1.4062	1.4012	1.3963	1.3870	1.3782	1.3699
480	864	1.4045	1.3996	1.3948	1.3857	1.3770	1.3688
490	882	1.4028	1.3980	1.3933	1.3843	1.3758	1.3677
500	900	1.4010	1.3963	1.3917	1.3828	1.3745	1.3665
510	918	1.3992	1.3945	1.3900	1.3813	1.3731	1.3653
520	936	1.3974	1.3928	1.3883	1.3798	1.3717	1.3640
530	954	1.3955	1.3910	1.3866	1.3782	1.3703	1.3627
540	972	1.3936	1.3891	1.3848	1.3766	1.3688	1.3613
550	990	1.3916	1.3873	1.3831	1.3749	1.3672	1.3599
560	1008	1.3897	1.3854	1.3813	1.3733	1.3657	1.3585
570	1026	1.3877	1.3835	1.3794	1.3716	1.3641	1.3571
580	1044	1.3857	1.3816	1.3776	1.3699	1.3625	1.3556
590	1062		1.3797	1.3757	1.3681	1.3609	1.3541
600	1080			1.3739	1.3664	1.3593	1.3526
610	1098				1.3647	1.3577	1.3510
620	1116				1.3629	1.3560	1.3495
630	1134					1.3544	1.3480
640	1152					1.3528	1.3464
650	1170						1.3448
660	1188						1.3433

TABLE 2.6 - EOS-BASED T_c/T_b RATIO FOR THE SRK EOS.

SOAVE/REDLICH/KWONG EQUATION OF STATE

Boiling Point		Molar Volume (Mol Weight/Specific Gravity)					
(K)	(R)	240	250	260	270	280	290
480	864	1.3610					
490	882	1.3600	1.3527				
500	900	1.3590	1.3518				
510	918	1.3579	1.3508	1.3440			
520	936	1.3567	1.3497	1.3431	1.3367		
530	954	1.3555	1.3486	1.3421	1.3358	1.3298	
540	972	1.3542	1.3475	1.3410	1.3349	1.3289	1.3232
550	990	1.3530	1.3463	1.3400	1.3339	1.3280	1.3224
560	1008	1.3516	1.3451	1.3388	1.3328	1.3271	1.3216
570	1026	1.3503	1.3439	1.3377	1.3318	1.3261	1.3207
580	1044	1.3489	1.3426	1.3365	1.3307	1.3251	1.3198
590	1062	1.3475	1.3413	1.3353	1.3296	1.3241	1.3188
600	1080	1.3461	1.3400	1.3341	1.3284	1.3230	1.3178
610	1098	1.3447	1.3386	1.3328	1.3273	1.3219	1.3168
620	1116	1.3433	1.3373	1.3316	1.3261	1.3208	1.3158
630	1134	1.3418	1.3359	1.3303	1.3249	1.3197	1.3147
640	1152	1.3403	1.3346	1.3290	1.3237	1.3186	1.3136
650	1170	1.3389	1.3332	1.3277	1.3225	1.3174	1.3126
660	1188	1.3374	1.3318	1.3264	1.3212	1.3163	1.3115
670	1206	1.3359	1.3304	1.3251	1.3200	1.3151	1.3104
680	1224	1.3345	1.3290	1.3238	1.3187	1.3139	1.3092
690	1242		1.3276	1.3224	1.3175	1.3127	1.3081
700	1260		1.3262	1.3211	1.3162	1.3115	1.3070
710	1278			1.3198	1.3150	1.3103	1.3059
720	1296				1.3137	1.3091	1.3047
730	1314				1.3125	1.3079	1.3036
740	1332					1.3067	1.3024
750	1350					1.3055	1.3013
760	1368						1.3002
770	1386						1.2990

TABLE 2.6 - EOS-BASED T_c/T_b RATIO FOR THE SRK EOS.

SOAVE/REDLICH/KWONG EQUATION OF STATE

Boiling Point		Molar Volume (Mol Weight/Specific Gravity)					
(K)	(R)	300	310	320	340	360	380
550	990	1.3170					
560	1008	1.3163					
570	1026	1.3154	1.3104				
580	1044	1.3146	1.3096	1.3048			
590	1062	1.3137	1.3088	1.3041			
600	1080	1.3128	1.3080	1.3033	1.2945		
610	1098	1.3119	1.3071	1.3025	1.2938		
620	1116	1.3109	1.3062	1.3017	1.2930		
630	1134	1.3099	1.3053	1.3008	1.2923	1.2843	
640	1152	1.3089	1.3043	1.2999	1.2915	1.2837	
650	1170	1.3079	1.3034	1.2990	1.2908	1.2830	1.2757
660	1188	1.3069	1.3024	1.2981	1.2900	1.2823	1.2751
670	1206	1.3058	1.3014	1.2972	1.2891	1.2816	1.2745
680	1224	1.3048	1.3004	1.2963	1.2883	1.2808	1.2738
690	1242	1.3037	1.2994	1.2953	1.2874	1.2801	1.2731
700	1260	1.3026	1.2984	1.2943	1.2866	1.2793	1.2725
710	1278	1.3015	1.2974	1.2934	1.2857	1.2785	1.2718
720	1296	1.3005	1.2964	1.2924	1.2848	1.2777	1.2711
730	1314	1.2994	1.2953	1.2914	1.2840	1.2769	1.2703
740	1332	1.2983	1.2943	1.2904	1.2831	1.2761	1.2696
750	1350	1.2972	1.2933	1.2894	1.2822	1.2753	1.2689
760	1368	1.2961	1.2922	1.2884	1.2813	1.2745	1.2681
770	1386	1.2950	1.2912	1.2875	1.2804	1.2737	1.2674
780	1404	1.2940	1.2901	1.2865	1.2795	1.2729	1.2666
790	1422	1.2929	1.2891	1.2855	1.2785	1.2720	1.2659
800	1440		1.2881	1.2845	1.2776	1.2712	1.2651
810	1458			1.2835	1.2767	1.2704	1.2643
820	1476			1.2825	1.2758	1.2695	1.2636
830	1494				1.2749	1.2687	1.2628
840	1512				1.2740	1.2679	1.2620
850	1530				1.2731	1.2670	1.2613
860	1548					1.2662	1.2605
870	1566					1.2654	1.2597
880	1584					1.2646	1.2590
890	1602						1.2582
900	1620						1.2575
910	1638						1.2567
920	1656						1.2560

TABLE 2.6 - EOS-BASED T_c/T_b RATIO FOR THE SRK EOS.

SOAVE/REDLICH/KWONG EQUATION OF STATE

Boiling Point		Molar Volume (Mol Weight/Specific Gravity)					
(K)	(R)	400	420	440	460	480	500
670	1206	1.2677					
680	1224	1.2672					
690	1242	1.2666	1.2604				
700	1260	1.2660	1.2599				
710	1278	1.2654	1.2593	1.2536			
720	1296	1.2647	1.2587	1.2531			
730	1314	1.2641	1.2582	1.2526	1.2472		
740	1332	1.2634	1.2576	1.2520	1.2467		
750	1350	1.2628	1.2570	1.2515	1.2463		
760	1368	1.2621	1.2564	1.2510	1.2458	1.2408	
770	1386	1.2614	1.2558	1.2504	1.2453	1.2404	
780	1404	1.2607	1.2551	1.2498	1.2448	1.2399	1.2353
790	1422	1.2600	1.2545	1.2493	1.2443	1.2395	1.2349
800	1440	1.2593	1.2539	1.2487	1.2437	1.2390	1.2345
810	1458	1.2586	1.2532	1.2481	1.2432	1.2385	1.2340
820	1476	1.2579	1.2526	1.2475	1.2427	1.2380	1.2336
830	1494	1.2572	1.2520	1.2469	1.2421	1.2375	1.2331
840	1512	1.2565	1.2513	1.2463	1.2416	1.2370	1.2327
850	1530	1.2558	1.2506	1.2457	1.2410	1.2365	1.2322
860	1548	1.2551	1.2500	1.2451	1.2405	1.2360	1.2318
870	1566	1.2544	1.2493	1.2445	1.2399	1.2355	1.2313
880	1584	1.2537	1.2487	1.2439	1.2394	1.2350	1.2308
890	1602	1.2530	1.2480	1.2433	1.2388	1.2345	1.2303
900	1620	1.2523	1.2474	1.2427	1.2382	1.2340	1.2299
910	1638	1.2516	1.2467	1.2421	1.2377	1.2334	1.2294
920	1656	1.2509	1.2461	1.2415	1.2371	1.2329	1.2289
930	1674	1.2502	1.2454	1.2409	1.2365	1.2324	1.2284
940	1692	1.2495	1.2448	1.2403	1.2360	1.2319	1.2279
950	1710	1.2488	1.2441	1.2397	1.2354	1.2314	1.2274
960	1728		1.2435	1.2391	1.2349	1.2308	1.2270
970	1746		1.2429	1.2385	1.2343	1.2303	1.2265
980	1764		1.2422	1.2379	1.2338	1.2298	1.2260
990	1782			1.2373	1.2332	1.2293	1.2255
1000	1800			1.2367	1.2327	1.2288	1.2250
1010	1818			1.2361	1.2321	1.2283	1.2246
1020	1836				1.2316	1.2277	1.2241
1030	1854				1.2310	1.2272	1.2236
1040	1872				1.2305	1.2267	1.2231

2.6 EOS Predictions using EOS-Based Critical Properties

This section gives results of application of the method just described for estimating critical properties and acentric factor of petroleum fractions. Reservoir fluids reported in the literature have been chosen Detailed discussion and tabulation of data can be found in Appendix B.

Hoffman, Crump, and Hocott present compositional and PVT data for a reservoir oil and its gas cap fluid. Extended analysis of the heptanes-plus mixture to C_{35} is given for the oil. Mole fractions, molecular weights, and specific gravities correspond to fractions with boiling points of normal paraffins. Methane content is 52 mol-% and heptanes-plus consists of 36.84 mol-% with an average molecular weight of 198.7 and specific gravity of 0.8409. Reported bubble point pressure is 3840 psia (26.47 MPa) at 201 ^{o}F (93.89 ^{o}C).

Katz and Firoozabadi report that a match of the measured bubble point can be achieved using the PR EOS with increasing interaction coefficients between methane and all C_{7+} groups, with a value of 0.17 for the heaviest fraction, C_{35}. They do not give the critical properties and acentric factor used, although it is assumed one of the empirical correlations is used (probably Cavett and Edmister). Using critical properties based on the PR EOS (see Appendix B), an estimated bubble point is predicted as 3829 psia, or 0.3% low. Interaction coefficients are not used. The predicted saturated oil density is 0.6867 g/cc, compared with the experimental value of 0.6672, or 2.9% high; estimated density is not reported by Katz and Firoozabadi.

The gas-cap fluid reported by Hoffman, et al. is analyzed in SCN fractions up to C_{22} (see Appendix B); properties are close, but not exactly the same as for the equilibrium reservoir oil. Methane content is 91.35 mol-% and heptanes-plus consists of 1.54 mol-% with average molecular weight of 141.25 and specific gravity of 0.7867. Predicted composition from the bubble point VLE calculation above resulted in methane content of 91.70 mol-%, heptanes-plus consisting of 1.318 mol-% with average molecular weight of 128.00 and specific gravity of 0.7854; note the specific gravity is in good agreement with the experimental value, but molecular weight is less accurate, possibly suggesting that the use of paraffin molecular weights by Hoffman, et al. is not satisfactory.

If the resulting composition from the bubble point flash is used, retaining only components up to C_{22}, the point at which Hoffman, et al. end their analysis and the point at which predicted composition (from the bubble point calculation) equals 0.001 mol-%, a dew point is predicted at 3706 psia. If the exact composition to C_{35} is used, the dew point will be exactly equal to the bubble point (3865 psia). This shows the sensitivity in dew point prediction due to a round-off error in composition of less than 0.001 mol-%!

Using the gas compositions reported by Hoffman, et al. the PR EOS predicts a dew point at 201 °F of 4044 psia, some 5.3% high. This is worse than the prediction given by Katz and Firoozabadi (+0.8%). Unfortunately they do not report the critical properties of petroleum fractions (or the correlation used). Also, Katz and Firoozabadi use an empirical relation to calculate methane interaction coefficients for petroleum fractions as a function of specific gravity. Table 2.7 illustrates how different critical properties affect predicted dew point pressures. Apparently Katz and Firoozabadi use the Cavett and Edmister correlations. It is obvious that the dew point prediction is dependent on the properties used to describe the petroleum fractions.

TABLE 2.7 - EFFECT OF CRITICAL PROPERTIES USED WITH THE PENG/ROBINSON EOS TO PREDICT THE HOFFMAN ET AL. RESERVOIR GAS DEW POINT PRESSURE.

	Dew Point Pressure (psia)	
Correlation	Predicted without Methane Binaries	With Katz/ Firoozabadi Methane Binaries
Experimental ....:	3841	
1. PR-Based ....:	4044 (+5.3)	
2. PR-Based[1] ....:	3706 (-3.5)	
3. Katz/Firoozabadi results (same as 5?) ....:		3870 (+0.8)
4. Riazi/Daubert + Edmister:	3322(-13.5)	3632 (-5.4)
5. Cavett + Edmister ......:	3668 (-4.5)	3866 (+0.7)
6. Lee/Kesler ....:	3523 (-8.3)	4049 (+5.4)

[1] PR-2 represents the prediction using gas composition up to C_{22} resulting from the PR EOS prediction of bubble point pressure for the reservoir oil (using PR-based properties).

Calculated liquid densities and yields are compared with experimental values in Table 2.8. The various PR predictions correspond to the six listed in Table 2.7, where PR-3, PR-4, PR-5, and PR-6 use methane binaries suggested by Katz and Firoozabadi.

Table 2.8 - COMPARISON OF MEASURED AND EXPERIMENTAL LIQUID DENSITIES FOR THE HOFFMAN, ET AL. RESERVOIR GAS

Press.	Liquid Density, g/cc (Liquid Yield, bbl/MMscf)						
(psia)	Exp.	PR-1	PR-2	PR-3	PR-4	PR-5	PR-6
2915	0.6565	0.6637	0.6749	-	0.5921	0.6364	0.6300
	(9.07)	(9.31)	(4.53)	(9.69)	(8.37)	(9.75)	(10.21)
2515	0.6536	0.6709	0.6798	-	0.6020	0.6475	0.6392
	(12.44)	(11.97)	(6.61)	(12.49)	(12.01)	(12.61)	(12.93)
2015	0.6538	0.6822	0.6885	-	0.6159	0.6619	0.6520
	(15.56)	(14.53)	(8.75)	(15.02)	(15.33)	(15.23)	(15.48)
1515	0.6753	0.6967	0.7003	-	0.6315	0.6779	0.6665
	(16.98)	(16.09)	(10.2)	(16.51)	(17.30)	(16.74)	(17.00)
1015	0.7160	0.7148	0.7172	-	0.6486	0.6957	0.6834
	(16.94)	(16.45)	(10.68)	(16.80)	(17.79)	(17.01)	(17.30)
515	0.7209	0.7390	0.7420	-	0.6675	0.7164	0.7029
	(15.08)	(14.97)	(9.56)	(15.29)	(16.17)	(15.45)	(15.73)
Absolute Average Error (%)		2.32	3.07		2.80	1.50	2.48
		(3.65)	(42.36)		(4.46)	(2.54)	(3.93)

Results indicate that the Cavett/Edmister (PR-5) combination performs best, though the proposed EOS-based properties give excellent results as well. Interestingly, liquid yields for predictions based on calculated gas composition (from the bubble point prediction) are very poor, despite the good predictions of liquid densities. This indicates that measured compositions are reliable and that determination of composition from the bubble point calculation can lead to erroneous VLE predictions in the two-phase region.

Next we consider the data presented by Olds, Sage, and Lacey in 1945. Extensive experimental results are given for six recombined systems, each measured at three temperatures (100, 190, and 250 °F). The hexanes-plus fraction was fractionated into seven cuts with approximately equal weight fractions (~10%). Properties of the separator gas and liquid are given in the original work, however recombined reservoir mixtures are given in Appendix B including a split of the hexanes-plus fraction for each reservoir mixture.

Critical properties of the petroleum fractions are calculated using the EOS-based method and the PR EOS. Comparisons are presented in Table 2.9 for saturation pressures, and saturated vapor and liquid densities. Binary interaction coefficients are set equal to zero in all cases.

Absolute average deviation for saturation pressure is 4.57% not including the leanest mixture (GOR=14440 scf/stb), and 5.45% for all mixtures. Dew points for very lean condensates are difficult to measure experimentally, and therefore it should be reasonable to question measurements of the 14440-GOR mixture. Maximum error is less than 10% otherwise. Considering the range of temperatures and compositions and lack of any adjustment or use of binary interaction coefficients, the predictions are very good. Also, the transition from bubble- to dew-point is correctly predicted.

Saturated liquid and vapor densities are all overpredicted. Absolute average deviation is 5.14% with maximum error of 8.1%. Saturated liquid densities are predicted more accurately than vapor densities. The general trend for overprediction is opposite that which is usually observed with the PR EOS, using empirical property correlations.

Predictions of the Olds/Sage/Lacey data presented in 1949 are reviewed in Table 2.10. Once again the PR EOS is used and properties are calculated using the procedure given in the previous section. No binary interaction coefficients are used.

Absolute average deviation for saturation pressures (all are bubble points) is 5.61%, with a maximum error of 13.7%. The errors are random in nature which is somewhat unexpected, although bubble points at 100°F were always worse than at higher temperatures. Excluding the 100 °F data gives an absolute average deviation in bubble point pressur of 3.0% with a maximum error of 4.0%. Descrepencies at lower temperatures are difficult to explain experimentally.

Saturated liquid densities are predicted with an absolute average deviation of 3.30% with a maximum error of 6.3%.

Interestingly, the best predictions occured at the lowest temperature of 100 ^{o}F; predictions of density were made at the experimental bubble point pressure and not at the predicted value.

From results presented in this section it can be concluded that the present method of defining critical properties based on an EOS is reasonably accurate for providing predictions of saturation pressures and mixture densities. It also appears that VLE predictions are good. The method is certainly not inferior to empirical correlations and has the advantage of being consistent with the EOS used, allowing for easy reproduction of results. For accurate predictions it is absolutely necessary to have accurate chemical analysis of the reservoir mixture, preferably including distillation data with measurements of specific gravity and molecular weight for each fraction.

TABLE 2.9 - COMPARISON OF SATURATED PROPERTIES FOR OLDS-SAGE-LACEY RESERVOIR MIXTURES (1945).

Temperature (F)	Saturation Pressure (psia)			Saturated Density (lb/ft^3)		
	Meas.	Calc.	Δ(%)	Exp.	Calc.^{3}	Δ(%)
Gas/Oil Ratio (scf/bbl) : 552 (0.0571)^2						
100	1112	1065 (1072)^1	-4.2	42.55	43.34 (43.36)	+1.8
190	1410	1383 (1389)	-1.9	39.68	40.52 (40.53)	+2.1
250	1675	1549 (1552)	-7.5	37.52	38.50 (38.50)	+2.6
Gas/Oil Ratio (scf/bbl) : 940 (0.1213)^2						
100	1870	1723 (1748)	-7.9	39.65	40.88 (40.91)	+3.1
190	2210	2174 (2196)	-1.6	36.13	37.78 (37.79)	+4.6
250	2380	2375 (2394)	-0.2	33.66	35.44 (35.52)	+5.3
Gas/Oil Ratio (scf/bbl) : 2205 (0.2867)^2						
100	3430	3102 (3136)	-9.6	34.13	35.44 (35.47)	+3.8
190	3542	3691 (3715)	+4.2	29.61	31.52 (31.54)	+6.5
250	3595	3880 (3896)	+7.9	27.07	28.75 (28.75)	+6.2
Gas/Oil Ratio (scf/bbl) : 5361 (0.5335)^2						
100	4490	4348 (4408)	-3.2	27.01	28.54 (28.56)	+5.7
190	4590	4836 (4878)	+5.4	22.90	24.40 (24.41)	+6.6
250	4630	4869 (2901)	+5.2	20.37	21.85 (21.86)	+7.3
Gas/Oil Ratio (scf/bbl) : 7393 (0.6292)^2						
100	4560	4615 (4579)	+1.2	24.05	25.99 (26.01)	+8.1
190	4730	4981 (5027)	+5.3	20.46	22.02 (22.03)	+7.6
250	4780	4933 (4969)	+3.2	18.35	19.65 (19.65)	+7.1
Gas/Oil Ratio (scf/bbl) : 14440 (0.8111)^2						
100	3835	4556 (4614)	+18.8	19.08	20.05 (20.06)	+5.1
190	4305	4709 (4754)	+9.4	16.24	16.96 (16.97)	+4.4
250	4440	4504 (4540)	+1.4	14.49	15.15 (15.16)	+4.6

TABLE 2.10 - COMPARISON OF SATURATED PROPERTIES FOR OLDS-SAGE-LACEY RESERVOIR MIXTURES (1945).

Temperature (F)	Bubble-Point Pressure (psia)			Bubble-Point Density (lb/ft^3)		
	Meas.	Calc.	Δ(%)	Exp.	Calc.[3]	Δ(%)
			Gas/Oil Ratio (scf/bbl) : 274 (0.02066)[2]			
100	817	796 (779)[1]	-3.8	49.12	49.87 (49.81)	+1.5
190	1020	1067 (1056)	+4.6	46.36	47.96 (47.89)	+3.5
250	1170	1236 (1223)	+5.6	44.66	46.54 (46.46)	+4.2
			Gas/Oil Ratio (scf/bbl) : 460 (0.05082)[2]			
100	1540	1361 (1346)	-11.6	47.96	48.34 (48.28)	+0.8
190	1830	1805 (1785)	-1.4	44.92	46.29 (46.22)	+3.0
250	2020	2051 (2027)	+1.5	43.08	44.78 (44.68)	+3.9
			Gas/Oil Ratio (scf/bbl) : 620 (0.07539)[2]			
100	2085	1799 (1778)	-13.7	46.62	47.19 (47.13)	+1.2
190	2439	2360 (2329)	-3.2	43.55	45.04 (44.98)	+3.4
250	2670	2656 (2620)	-0.5	41.53	43.50 (43.42)	+4.7
			Gas/Oil Ratio (scf/bbl) : 811 (0.10311)[2]			
100	2656	2273 (2242)	-14.4	44.68	45.96 (45.90)	+2.9
190	3067	2944 (2901)	-9.0	41.98	43.73 (43.67)	+4.2
250	3384	3284 (3235)	-3.0	39.70	42.21 (42.14)	+6.3

[1] Values in parentheses are predictions using EOS-based critical properties but assuming the paraffin relation for acentric factor (Eq. 2.10).

[2] Values in parentheses are weight fraction of the separator gas used to make the mixture.

[3] Saturated densities are calculated at the experimental saturation pressure assuming the mixture is a single phase.

NOMENCLATURE

K_w = Watson (Universal Oil Products) characterization factor

M_i = molecular weight of i

M_{n+} = average molecular weight of a mixture of petroleum fractions with a lowest carbon number n, e.g., C_{7+}

p_c = critical pressure, absolute units

Q_i = cumulative normalized molecular weight variable of i

S^0 = sum used to calculate K_w which results in the measured C_{n+} specific gravity

T_b = boiling point, absolute units

T_c = critical temperature, absolute units

x_i = mole fraction of i

X_i = cumulative normalized mole fraction of i

x_{n+} = mole fraction of a mixture of petroleum fractions with a lowest carbon number n, e.g., C_{7+}

α = parameter in the molar distribution model defining the form of the distribution

γ_i = specific gravity of i

γ_{n+} = average specific gravity of a mixture of petroleum fractions with a lowest carbon number n, e.g., C_{7+}

Δ = deviation, %
= 100x(calculated-measured)/measured

η = parameter in the molar distribution model representing the approximate minimum molecular weight of compounds found in a mixture

ω = acentric factor,
= $-\log(p_v/p_c)-1.0$ at $T/T_c=0.7$

Chapter 3

FLOW IN POROUS MEDIA

... "don't get no respect" said Morris the cat

3.1 Introduction to Fluid Flow in Porous Media

Darcy's law first appeared in 1856. It states that an incompressible fluid of constant viscosity, μ, flowing a given distance in a porous media of uniform quality has a velocity, v, directly proportional to the pressure drop, Δp. Written in equation form,

$$v = C \cdot \Delta p \quad \text{(3.1)}$$

where it is assumed that the direction of flow is from high to low pressure; both v and Δp are considered positive by definintion. The constant C is inversely proportional to viscosity and dependent on the flow geometry and porous material. For linear flow along a distance L, Darcy's law can be written

$$v = k(\Delta p/\mu L) \quad \text{(3.2)}$$

where k is a constant defined by Darcy as permeability. Permeability is a property of the porous media dependent on pore size distribution and tortuosity (relative path of fluid flow). The original units used by Darcy were v(centimeter/second), Δp(atmosphere), μ(centipoise), and L(centimeter), resulting in the unit for permeability (in abbreviated notation) as $(cm^2/s)(cp)/atm$, since defined as a darcy.

For most reservoir engineering applications the unit millidarcy - one-thousandth of a darcy - is used. This results because permeabilities usually encountered range from 1 to 100 md. 'Low-permeability' reservoirs lie below the value of 1 md, and 'high-permeability' resevoirs go beyond 100 md up to tens of darcies. High permeabilities are not always a blessing due to mechanical instability of the rock/pore system. Low-permeability reservoirs are becoming more important as a resource since they represent the reserves which were left behind when oil and gas were plentiful.

Darcy's law has probably been written in hundreds, if not thousands of forms - all with different nomenclature! These include generalizations to radial/cylindrical and spherical geometries, vector, finite-difference, and differential forms. It doesn't take long before one forgets the most important aspect of Darcy's law - that of simplicity.

Muskat gives numerous invaluable examples of the application of Darcy's law, ranging from simple to difficult applications. i recall from one of my lectures at Stanford U. where Dr. Ramey said that if you think you discover a new solution to a fluid flow problem, it is best to first check Muskat's books and papers to make sure it hasn't already been solved. Two excellent examples appear in the sections of this chapter on multiphase flow and effects of partially penetrating wells. Sometimes it seems that the craze over numerical simulation is a result of those who don't have the patience to read Muskat, but would rather rediscover Darcy's law in finite-difference form; exceptions are well taken.

The following section reviews multiphase flow in porous media, which relies on extension of Darcy's law to each phase. Similar to equilibrium constants and phase behavior calculations, description of multiphase flow relies on the definition of relative permeabilities. Analogous to the equation of state for describing two-phase equilibria, models exist for estimating relative permeabilities based on the characterization of the porous media. Unfortunately the character of reservoir rocks, with which we are concerned, varies considerably from point to point. Also, the models for describing relative permeability are more primitive than those for describing phase equilibria, and they are limited in their ability to predict the effects of pressure, temperature, and composition. This results in the very difficult engineering task of defining 'average' relative permeabilities.

Where Darcy's law has been shown to be applicable to multiphase flow, it is deficient in describing the relation between velocity and pressure drop when flow is not laminar. High velocity flow requires another model, the most accepted being Forscheimer's equation,

$$v + Bv^2 = C \cdot \Delta p \quad \text{.................................} \quad (3.3)$$

where B is proportional to density, as well as having the same relation to viscosity and geometry as constant C. Section 3.4 considers application of the Forsheimer equation to multirate testing of oil and gas wells.

Another application of Darcy's law is to help solve the diffusivity equation relating pressure, position, and time to rate. The simplest solution to this problem results by assuming incompressible flow, thereby eliminating the time variable. Muskat uses this assumption to develop many useful engineering solutions to difficult problems. Amoung these are multiphase flow and partial penetration effects, two subjects consider in this chapter.

Compressible flow, on the other hand, must consider transient (time-dependent) effects. Solution of compressible flow problems has been an important tool to the study of oil and gas well performance. The simplest solution assumes, amoung other conditions, a fully penetrating well in an infinite system (no boundaries) producing at a constant rate. After some time, the pressure drop at the wellbore is closely approximated by a logarithmic function of time,

$$\Delta p(r_w,t) \simeq D \cdot \log(t) + E \quad \text{.......................} \quad (3.4)$$

Constants D and E are dependent on rate (assumed constant), permeability, well geometry (e.g, wellbore radius and total thickness), compressibility of the formation and fluid, viscosity, and porosity.

Considering the pressure drop at any radius in the system, Eq. 3.4 can be rewritten in a more general form as,

$$\Delta p(r,t) = -D \cdot Ei(-r^2/t) + F \text{ .... } (3.5)$$

where Ei is the exponential integral, which for large times or small radii simplifies to the logarithmic approximation given by Eq. 3.4. As time proceeds, the pressure drop at the no-flow boundary will begin to effect the pressure drop at the wellbore. That is, Eqs. 3.4 and 3.5 assume an infinite reservoir with no boundaries, an assumption which is no longer valid when Δp at r_e reaches some value (say 1 psi).

When boundary effects become prominent, a more rigorous solution to the diffusivity equation must be used. The exact solution for pressure drop <u>at the wellbore</u> in a circular bounded system is a linear function of time plus an infinite series of exponential and Bessel function expressions,

$$\Delta p(r_w,t) = G \cdot t + H + SUM(t,r_e/r_w) \text{ .... } (3.6)$$

where constants G and H also are dependent on rate, permeability, well geometry (particularly the ratio, r_e/r_w), total compressibility, viscosity, and porosity. It can be shown that after only a very short time the sum of exponential and Bessel functions becomes neglible and that pressure drop is a linear function of time. In fact, the transition from when the pressure drop in an infinite system changes to pressure drop in a bounded sytem is so short that the semi-log relation and the linear relations (G·t+H) are sufficient for most practical applications. This is not the case for other reservoir geometries which may have long transition periods.

To simplify discussion of pressure-drop solutions to transient flow problems, the common practice is to use dimensionless quantities - dimensionless pressure, p_D, dimensionless time, t_D, and dimensionless radius, r_D, defined below assuming consistent units,

$$p_D = (q\mu B/kh)\cdot\Delta p \quad \text{.............................} \quad (3.7a)$$

$$t_D = (k/\phi\mu c_t r_w{}^2)\cdot t \quad \text{...........................} \quad (3.7b)$$

$$r_D = r/r_w \quad \text{..................................} \quad (3.7c)$$

$$r_{De} = r_e/r_w \quad \text{..................................} \quad (3.7d)$$

where q = rate (velocity times area), μ = viscosity, B = formation volume factor, k = permeability, h = thickness, ϕ = porosity, c_t = total compressibility (rock plus fluid), r_w = wellbore radius, and r_e = external boundary radius.

Using Eqs. 3.7, earlier relations for pressure drop can be written exactly,

$$p_D(r_D{=}1,t_D) = 0.5\cdot\ln(t_D) + 0.404535 \quad \text{..........} \quad (3.4)$$

$$p_D(r_D,t_D) = -0.5\cdot Ei(-r_D{}^2/t_D) \quad \text{.................} \quad (3.5)$$

$$p_D(r_D{=}1,t_D) = 2\cdot t_D/r_{De}{}^2 + \ln(r_{De}) - 3/4 + 2\cdot\sum_{n=1}^{\infty}\frac{\exp(-a_n{}^2 t_D)\cdot J_1{}^2(a_n r_{De})}{a_n{}^2(J_1{}^2(a_n r_{De}) - J_1{}^2(a_n))} \quad \text{..} \quad (3.6)$$

where a_n are the roots of $J_1(a_n r_{De})Y_1(a_n) - J_1(a_n)Y_1(a_n r_{De})$ equal to 0.0.

A topic which receives almost no attention in the traditional petroleum-engineering curricula is constant-pressure production, and the resulting rate decline. This indicates, perhaps, the lack of understanding about what the petroleum engineer is suppose to do - determine the rates of oil, gas, and water as a function of time and producing conditions. It is also due to the fact that for many years oil and gas production were regulated, either by economic or political forces. Translated into simple terms, the wells could produce more than they were allowed to produce. Those days are over now, at least for the most part, and a result is that most wells producing today are produced to their potential (or are regulated by a minimum surface pressure). In practical terms this means that many wells produce at a constant bottomhole pressure, with a natural decline in rate. The flow equations dictating constant-pressure production is unknown to most petroleum engineers, and its inclusion in traditional university studies is emminent. The topic is covered in Section 3.5 of this chapter.

Another very useful dimensionless quantity is the skin factor suggested by Hurst and van Everdingen. Actually Muskat suggests the same concept when discussing the effect of perforations on well productivity (he called the factor C, and subsequently discussed its equivalence with a reduced wellbore radius, $r_w' = r_w \cdot e^{-C}$). Skin, as it will be referred to hereafter, offers a convenient way to describe the increase or decrease in pressure drop at the wellbore due to nonideal effects. The most common skin is due to damage from mud filtration during drilling; permeability in the near-wellbore region is reduced, causing an extra pressure drop. In this study we consider the skin due to partial penetration of a formation, resulting in nonradial stream lines near the well. It is shown that the original Muskat solution is equivalent to the Brons and Marting solution, but can be expressed in analytical form.

3.2 Corey/Burdine Relative Permeability Model

The flow of more than one fluid phase in porous media can be classified into several groups:

- immiscible without mass transfer between phases
- immiscible with mass transfer between phases
- miscible
- partially miscible

amoung several other categories including non-Newtonian flow. An example of immiscible flow without mass transfer is oil displacement by water, assuming the two do not create an emulsion. An example of immiscible flow with mass transfer is flow of saturated oil and its solution gas. An example of miscible flow is carbon-dioxide injection in an oil reservoir where first-contact miscibility is achieved. In this case there are three phases: the untouched oil, the injected CO_2, and the resulting mixture. An example of partially miscible flow is injection of dry gas into an oil reservoir, in which the injected gas, after numerous contacts with the reservoir oil, becomes progressively richer until it is almost (i.e., partially) miscible with the original reservoir oil.

The present discussion will only cover immiscible fluid flow, and it will concentrate on definition of relative permeabilities. Most of this section repeats or extends the exellent notes on relative permeability relations written by Standing at NTH in 1975. Although no 'new' results or developments are given (for which i am responsible), its inclusion is justified when we consider the importance of relative permeability to multiphase flow in porous media. The work by Svein Havig (one of my students at NTH) should be considered as a serious contribution to the application and characterization of relative permeability theory to North Sea chalk reservoirs.

The following definitions should be helpful to the following discussion:

Relative Permeability:

$k_{rw} = k_w/k$

$k_{ro} = k_o/k$

$k_{rg} = k_g/k$

$k_{rx} = k_{ox}/k = k_{gx}/k$

k = absolute permeability to nonreactive liquid

k_w = effective permeability to water phase

k_o = effective permeability to oil phase

k_g = effective permeability to gas phase

$k_{ox} = k_{gx}$ = effective permeability to oil or gas in a two phase system where water, the second phase, is at its irreducible saturation, S_{iw}

Somewhat logically, relative permeability of a given phase is a strong function of the saturation of that phase. Saturation is merely the volume of a given phase divided by the total pore volume contained by fluid. Although relative permeability has also been shown to vary with surface tension between phases and rock/water affinity (wettability), the strongest factors affecting relative permeability are saturation, saturation history, and pore size distribution.

The Corey/Burdine model is perhaps the most widely known and commonly used relation in the petroleum industry. It accounts for the three important factors mentioned above, and it has been modified to account for trapping effects of a third phase. No account is made for either surface tension or wettability. In general, saturation history - re drainage versus imbibition is only considered for the nonwetting phase.

The model relies on estimates of pore size distribution, λ, which can be determined from capillary pressure measurements, and irreducible wetting-phase saturation (assumed to be water in the present discussion), S_{iw}. The first step is to calculate effective saturations. Considering three-phase drainage relative permeability, the following definitions can be used:

Effective Saturations:

$$S_{we} = (S_w - S_{iw})/(1 - S_{iw}) \quad \text{(3.8a)}$$

$$S_{oe} = S_o/(1 - S_{iw}) \quad \text{(3.8b)}$$

$$S_{ge} = S_g/(1 - S_{iw}) \quad \text{(3.8c)}$$

where S_{iw} is the irreducible water (wetting-phase) saturation, S_o is the oil saturation, S_g is the gas saturation, and S_w is the total water saturation (mobile plus irreducible).

The drainage relative permeability relations for three phase flow (which simplifies to two phase flow when the third phase, gas or oil, is not present) are:

Three-Phase Drainage Relative Permeabilities:

$$k_{rw} = S_{we}^{(2+3\lambda)/\lambda} \quad \text{(3.9a)}$$

$$k_{ro} = k_{rx} \cdot S_{oe}^{2}\{(S_{oe} - S_{we})^{(2+\lambda)/\lambda} - S_{we}^{(2+\lambda)/\lambda}\} \quad \text{(3.9b)}$$

$$k_{rg} = k_{rx} \cdot S_{ge}^{2}\{1 - (S_{oe} - S_{we})^{(2+\lambda)/\lambda}\} \quad \text{(3.9c)}$$

where k_{rx} is defined above as the relative permeability of oil or gas in a two-phase system where water, the second phase, is at its irreducible saturation. These relations should be applicable to the following processes:

- solution gas drive
- gas displacing or replacing oil during gas injection or gravity drainage
- gas displacing water during storage

It has been found that using the traditional definition of effective gas saturation is not usually sufficient due to critical gas saturation and stratification effects. A modified effective gas saturation is usually preferred,

$$S_{ge} = (S_g+S_m-1)/(S_m-S_{iw}) \quad \ldots\ldots\ldots\ldots\ldots\ldots\ldots\ldots \quad (3.10)$$

where S_m will be called the Corey saturation variable. Its value is not equal to $1-S_{gc}$, where S_{gc} is the trapped gas saturation. Such an interpretation might be assumed based on the mathematical character of S_m - i.e., when $S_g=1-S_m$, S_{ge} becomes zero as does gas relative permeability. If S_m is less than unity then such an interpretation might be argued. In fact, Corey shows from interpretation of two-phase gas/oil relative permeability data that $S_m>1$ results due to stratification parallel to flow, while $S_m<1$ results due to stratification perpendicular to flow. Critical gas effects will obviously influence the value of S_m as well. My experience based on interpretation of carbonate relative permeabilities (relying mainly on results given by Havig) suggests that S_m is always greater than unity when both λ and S_m are used to fit experimental k_{rg}/k_{ro} data.

Concerning the estimate of λ, it can be theoretically determined using capillary pressure data. From a plot of capillary pressure versus effective water saturation, S_{we}, on log-log paper, the value of λ is found from the negative reciprocal of the slope. If capillary pressure data are not available from the same core on which relative permeability data are measured, the value of λ can be determined simultaneously with the value of S_m by fitting relative permeability data.

A minimization routine must be used to determine the best-fit of λ and S_m. The simplest approach, used in my own applications, is to determine the possible range of λ and S_m (e.g., $\lambda=0.5,3.0$ and $S_m=0.9,1.3$), calculate the absolute average deviation between $\ln(X_{exp})$ and $\ln(X_{calc})$ where X is either a relative permeability or relative permeability ratio, and plot a histogram of the average deviation to allow easy determination of λ and S_m by eye. The graphical method also helps determine the sensitivity of the match to λ and S_m.

Havig, has fit gas/oil relative permeability data from over fifty carbonate samples, taken from five North Sea reservoirs in the Ekofisk area. He uses an advanced numerical routine for determing the λ and S_m which minimizes the sum of squares of the logarithm to gas/oil relative permeability ratios. Part of his results are presented in Table 3.1. Note that all best-fits have S_m greater than unity. i have checked this tendency on other samples from the North Sea.

Havig analyzes the data using trend analysis and proposed the following generalized correlation,

$$\lambda = 1.9953 - 4.0659 \cdot S_{iw} \quad \text{(3.11)}$$

$$S_m = 1.0444 + 0.0516 \cdot \lambda \quad \text{(3.12)}$$

Comparison with experimental data using Eqs. 3.11 and 3.12 gives excellent results considering the range of data and general difficulty in correlating the parameters λ and S_m.

able 3.1 - SAMPLE OF MATCHING THE COREY MODEL TO MEASURED RELATIVE PERMEABILITY DATA USING PARAMETERS λ and S_m (Havig)

Sample[1]	λ	S_m	S_{iw}	ϕ	k_{air} (md)	Error[2]
A/X-1	1.569	1.206	0.108	0.399	7.5	0.369
A/X-2	2.240	1.150	0.123	0.395	6.2	0.819
A/X-3	0.969	1.145	0.126	0.258	0.34	0.207
A/X-4	0.671	1.286	-	0.360	2.0	0.026
B/X-1	1.224	1.144	0.145	0.402	2.6	0.207
B/X-2	0.993	1.093	0.148	0.383	2.5	0.073
B/X-3	1.467	1.108	0.178	0.400	2.1	0.101
B/X-4	1.223	1.100	0.171	0.401	2.0	0.537
B/X-5	1.025	1.115	0.137	0.387	1.9	0.134
B/X-6	1.056	1.093	0.170	0.392	1.8	0.100
B/X-7	1.174	1.093	0.139	0.377	1.7	0.282
B/X-8	0.997	1.103	0.220	0.329	1.7	0.158
B/X-9	0.961	1.121	0.165	0.367	1.6	0.293
B/X-10	1.096	1.082	0.158	0.356	1.2	0.172
B/X-11	1.004	1.098	0.176	0.350	1.0	0.119
B/X-12	1.058	1.059	0.192	0.324	0.62	0.341
C/Y-1	2.496	1.149	0.130	0.383	7.4	0.567
C/Y-2	2.072	1.188	0.113	0.336	3.8	0.440
C/Y-3	1.715	1.089	0.124	0.333	3.2	0.766
C/Y-4	2.326	1.252	0.123	0.313	2.8	0.567
C/Y-5	3.369	1.204	0.184	0.314	2.3	0.630
C/Y-6	1.884	1.120	0.154	0.305	1.9	0.375
C/Y-7	1.594	1.100	0.141	0.288	1.7	0.781
C/Y-8	1.068	1.227	0.133	0.270	1.3	0.709
C/Y-9	1.116	1.155	0.130	0.228	0.85	0.136
D/Y-1	1.533	1.124	0.043	0.309	2.8	0.064
D/Y-2	4.779	1.246	0.091	0.327	2.4	0.493
D/Y-3	1.096	1.144	0.076	0.288	1.7	0.059
D/Y-4	3.778	1.416	0.061	0.271	1.4	0.334
D/Y-5	1.743	1.203	0.117	0.231	1.4	0.181
D/Y-6	1.449	1.085	0.035	0.264	1.14	0.423
D/Y-7	2.503	1.101	0.110	0.247	0.83	0.377
E/Z-1	1.103	1.062	-	0.362	1.6	0.531
E/Z-2	0.859	1.009	-	0.302	0.9	0.263
F/Z-1	1.095	1.072	-	0.372	1.93	0.082
F/Z-2	1.441	1.294	-	0.374	1.14	0.071
F/Z-3	1.459	1.180	-	0.373	1.69	0.072
F/Z-4	1.921	1.107	0.084	0.358	5.9	0.653
F/Z-5	1.889	1.125	0.075	0.322	4.2	0.685

[1] Field/Formation-Sample

[2] Sum of squares of $\ln(k_{rg}/k_{ro})_{exp} - \ln(k_{rg}/k_{ro})_{calc}$. The match of data is usually excellent when this value is less than 1.0.

The relation for k_{rx} given by Havig is,

$$k_{rx} = 1.0 - 4.538 \cdot S_{iw} + 3.876 \cdot S_{iw}^2 \quad \ldots\ldots\ldots\ldots \quad (3.13)$$

which gives values considerably lower than calculated using the relation suggested by Standing (developed at Chevron Research Laboratory),

$$k_{rx} = 1.08 - 1.11 \cdot S_{iw} - 0.73 \cdot S_{iw}^2 \quad \ldots\ldots\ldots\ldots \quad (3.14)$$

Havig also compares pore size distribution factors calculated by matching k_{rg}/k_{ro} data (Table 3.1) with λ calculated from capillary pressure data. Table 3.2 shows his results. It appears that the values fit by matching gas/oil relative permeabilities are lower than those found from capillary pressure data. If capillary pressure data were available for the same samples analyzed for gas/oil relative permeabilities then the match could have been performed holding λ constant (equal to the capillary pressure determined value) and varying only S_m. Unfortunately it is seldom the case that both capillary pressure and gas/oil relative permeability data are available from the same sample.

Table 3.2 - COMARISON OF PORE SIZE DISTRIBUTION FACTORS CALCULATED BY FITTING GAS/OIL RELATIVE PERMEABILITY DATA AND BY ANALYZING CAPILLARY PRESSURE DATA.

Formation	Fit[1]	No.	p_c Data[1]	No.
X	1.14	17	2.24	18
Y	2.17	17	2.61	9
Z	1.33	8	2.12	1

[1] Represent arithmetic averages for the samples listed in Table 3.1.

The imbibition relation for the nonwetting phase in a two-phase system (e.g., gas-water) is given by

$$k_{rg} = S_{geF}{}^{2}\cdot\{1-(1-S_{geF})^{(2+\lambda)/\lambda}\} \quad \ldots\ldots\ldots\ldots\ldots (3.15)$$

where S_{geF} is the effective free gas saturation, given by

$$S_{geF} = 0.5\cdot\{(S_{ge}-S_{ger})+\sqrt{(S_{ge}-S_{ger})^{2}+4(S_{ge}-S_{ger})/C}\}$$

$$\ldots (3.16)$$

and C is the trapping constant. It is determined experimentally by measuring the trapped gas resulting from water flooding a core, starting at different initial gas saturations. i have tabulated C for several data sets reported in the literature:

TABLE 3.3 - TRAPPING CONSTANTS FOR SEVERAL ROCK TYPES

Formation/Type	S_{iw}	λ	ϕ	C
Chalk	0.152	0.464	0.350	1.98
Abo	0.200	0.769	0.130	0.597
Lansing K.C.	0.121	0.644	0.251	0.387
Smackover(TX)	0.045	0.458	0.311	1.603
Smackover(MS)	0.210	0.632	0.137	0.739
Alendum	0.020	10.0(∞)	0.450	4.617[1]
Berea	0.190	10.0(∞)	0.230	1.273[1]
Torpedeo	-	-	0.230	1.273

[1] Values determined by fitting relative permeability data were 1.8 and 0.8, respectively, for the Alendum and Berea samples.

Imbibition water relative permeability can be calculated using the drainage relation (Eq. 3.9a) without great error. Three-phase imbibition relative permeability relations based on the Burdine/Corey model have not appeared in the literature.

Application of imbibition relative permeabilities has direct application to the following reservoir processes:

- water displacing oil or gas during water injection or water influx
- oil condensation during depletion of gas-condensate reservoirs

3.3 Constant-Rate Testing of Solution-Gas Drive Reservoirs

The analysis of well test data obtained from wells producing from saturated oil reservoirs involves accounting for two-phase gas/oil effects. Several nonideal conditions violating the liquid-like assumptions implicit in traditional solutions of the diffusivity equation are:

- two phases flow, instead of one

- the second phase, gas, and in some cases the saturated oil are not slightly compressible but show relatively large volumetric changes due to pressure variation

- saturation becomes an additional variable in the diffusivity equation which can not, a priori, be related to pressure, position, or time

- the phase behavior re gas/oil exchange between phases is not well defined but must be approximated using solution gas/oil ratios and formation volume factors

These problems are serious obstacles to the analytical solution of the constant rate two-phase problem. The best that can be hoped for is an approximate solution, and one which must be varified by numerical calculations and field data. Papers A.7 and A.8 consider some of the problems associated with arriving at approximate solutions. The first of these deals mainly with well testing during transient flow (before boundary effects become important). The second deals more with pseudosteady state flow which is mainly dominated by depletion effects resulting from boundary conditions. This section reviews paper A.7 and poses practical questions to the potential application of methods proposed in that work.

Raghavan gives results of numerical simulations for a well producing at constant oil rate from an initially saturated reservoir. His purpose is to investigate the use of a pseudopressure function, m(p), to linearize - at least approximately - the diffusivity equation. As first defined by Evinger and Muskat for steady state flow, and later suggested by Fetkovich for analysis of transient flow, the pseudopressure function has the form,

$$m(p) = \int k_{ro}/\mu_o B_o \, dp \quad \text{.........................} \quad (3.17)$$

where integration proceeds from a reference pressure, p_{ref}, to the wellbore pressure, p_w. Both viscosity, μ_o, and oil formation volume factor (FVF), B_o, are for all practical purposes <u>only</u> functions of pressure (assuming isothermal conditions).

Oil relative permeability, k_{ro}, is essentially a function of saturation, saturation history, and pore size distribution. Neglecting the latter two effects, k_{ro} can be considered only a function of saturation. This simplifies the analysis considerably, and is assumed by all those who have attempted to derive an approximate solution to the two-phase gas/oil problem. It should be remembered, however, that these two assumptions are clearly violated in practical situations -i.e., (1) saturation changes during drawdown/buildup and multirate tests are not in the same direction, and (2) rock properties are never homogeneous throughout the reservoir.

Starting based on the assumption that k_{ro} is a sole function of saturation, the problem with solving the integral in Eq. 3.17 involves relating saturation to pressure. Raghavan rationalizes two empirical saturation/pressure relations - one for drawdown and one for buildup - based on his results and interpretation of numerical simulations. Although empirical, he shows that the m(p) solution can be applied sucessfully to drawdown and buildup test interpretation. Results are better for drawdown analysis during the infinite-acting period, and his interpretation method for buildup is only considered for a well producing under depletion (pseudosteady state) prior to shutin. Despite the limitations and approximate nature of his results, Raghavan shows the applicability of the pseudopressure approach to oil well testing in saturated reservoirs.

Paper A.7 proposes a semi-analytical relation between saturation and pressure. It is developed from the diffusivity equations for oil and gas phases separately. The main assumption is that saturation is only a function of pressure and not time or position. The saturation-pressure relation reduces to Martin's relation at early times when pressure gradients are small. At long times it reduces to a relation equivalent to assuming constant gas/oil ratio, R, which is equivalent to the original Evinger/Muskat proposal. This is interesting when we consider that the relation developed in paper A.8 should only apply during the infinite-acting period while the Evinger/Muskat relation is developed for application during steady or pseudosteady state conditions. The transition from the Martin relation to the Evinger/Muskat relation is usually very short, and the merit of the general relation is therefore minor.

What is of value in paper A.7, and interestingly is not mentioned by Raghavan, is that producing gas/oil ratio is essentially constant during the entire infinite-acting period. The practical significance is that the original Evinger/Muskat approach - an engineering approach which can be solved by a simple graphical procedure - applies to constant rate transient drawdown analysis. Interestingly, the buildup procedure suggested by Raghavan is also equivalent to the Evinger/Muskat procedure. This is not discussed by either Raghavan or Boe, et al., probably because the Evinger/Muskat method already existed and would lessen the apparent significance of their work.

Paper A.7 suggests an alternative method for calculating the buildup m(p) function - i.e., applying the Martin saturation-pressure relation during buildup. This is supported theoretically by arguing that pressure gradient at the wellbore is zero during shutin. The difference between Raghavan's buildup procedure (equivalent to the constant GOR Evinger/Muskat assumption) and the one based on Martin's saturation relation is not discussed. It was found in extra simulations during our work on paper A.7 that the buildup procedure is not exact, as might be inferred from results we present. This is despite the correct calculation of saturation at all points in the reservoir during buildup using the Martin relation. Apparently the theory of superposition has its limitations when using the pseudopressure function, which itself is only an approximate linearization of the diffusivity equation.

An interesting feature of the Evinger/Muskat constant GOR method is that saturation is not directly involved in the calculations. The relative permeability relation which is important is oil relative permeability as a function of gas/oil relative permeability ratio. The form of this function, examples of which can be found in the original

Evinger/Muskat work and paper A.8, does not vary considerably for various rock types. Conceivably the relation could be determined from production data, and perhaps with less accuracy, from well test data. Equations given in the previous section (drainage functions) can be used to generate a series of k_{rg}/k_{ro} versus k_{ro} curves for various values of λ and S_m. Independent of how the relation is obtained, it should be the same relation which is used for material balance calculations for the entire reservoir. It is unlikely that individual curves for specific wells can be determined, and moreover the pseudopressure approach should not be considered an exact solution, but merely a means to obtain a better answer than if pressure alone had been used.

What can be concluded from this discussion, as is stated in paper A.8, is that the original Evinger/Muskat method of relating saturation to pressure is reliable for evaluating the pseudopressure function used for interpretation of test data from drawdown and buildup in wells producing from saturated reservoirs. Results should be as accurate as calculated using methods proposed by Raghavan and Boe, et al. during infinite-acting and depletion. Once more, it appears that had Muskat's contributions been considered more seriously, that considerable time and effort (and many numerical simulations) had been saved.

3.4 Deliverability Performance Using Multirate Testing

As mentioned in the introduction, Darcy's law is not applicable when fluids flow at very high velocities. Recalling the expression for velocity (Eq. 3.2) but written in terms of radial/cylindrical geometry, we have

$$v = (k/\mu)dp/dr = (k/\mu r)\Delta p/\ln(r_e/r_w) \quad \text{..........} \quad (3.18)$$

where Δp represents the pressure drop between external radius, r_e, and the radius to the wellbore, r_w. Two observations can be made: first, high velocities result for low viscosities, and second, high velocities occur at small radii. On the average, gas viscosities are two orders of magnitude less than oil viscosities (e.g., 0.01 vs 1 cp). We should therefore expect high velocity flow and subsequent breakdown of Darcy's law for gases flowing near the wellbore. This is, in fact, what has been observed in experimental studies and field production testing. Recently, Fetkovich has shown that high velocity flow (HVF) also occurs in oil wells producing at high rates.

Traditional well testing has several purposes, including the determination of deliverability. That is, given an allowable pressure drop in the reservoir - dictated by factors between the wellbore and surface transportation - what rate will result. If Darcy's law is applicable, then surface rate, q, equals velocity multiplied by area perpendicular to flow, $A=2\pi rh$, divided by a conversion factor, B, relating volume at reservoir conditions to volume at surface conditions,

$$q = v \cdot A/B = 2\pi kh\Delta p/\mu B\ln(r_e/r_w) \quad \text{..............} \quad (3.19)$$

Depending on whether <u>steady state</u> or <u>pseudosteady state</u> conditions are considered, Δp represents pressure drop between the external reservoir pressure, p_e, or average reservoir pressure, p_R, and wellbore flowing pressure, p_{wf}, respectively; for a given test, however, this distinction is not really important.

The first observation to make about Eq. 3.19 is that a plot of rate, q, versus pressure drop, Δp, should result in a straight line with slope proportional to the permeability thickness product, kh. This suggests that a single rate test, producing long enough to reach steady or pseudosteady state conditions, will provide the information necessary to predict rate at other pressure drops. This concept is used extensively by Muskat and other early reservoir engineers, and it has been termed productivity index, $J=q/\Delta p$.

It was soon realized that the effect of high velocity flow near the wellbore causes problems in applying productivity index to gas wells. In practical terms, the rate predicted by the relation $q=J\cdot\Delta p$ where J is determined at rate, q_1, and pressure drop, Δp_1, is too large if the new pressure drop, Δp_2, is larger than Δp_1, and too small if the new pressure drop is smaller than Δp_1. By applying the Forscheimer equation (Eq. 3.3), a new relation can be written for surface flow rate,

$$q = 2\pi kh\Delta p/\mu B\{\ln(r_e/r_w)+Dq\} \quad \text{..................} \quad (3.20)$$

where D is a constant dependent on rock and fluid properties. Unfortunately, Eq. 3.20 is nonlinear in rate. Practical experience shows that a good approximation is,

$$q \simeq J'(\Delta p)^n \quad \text{..................................} \quad (3.21)$$

where exponent n represents the correction for Dq. If D is large then n approaches 0.5, and for small D, n approaches 1.0 and Darcy's law is valid.

The essential difference between the relation $q=J\cdot\Delta p$ and Eq. 3.21 is the first has only one unknown, J, whereas the second has two unknowns, J' and n. The logical result is that at least two rates are needed for wells experiencing HVF. Usually the reservoir engineer requests more than two rates during a production test to ensure accurate determination of the two constants.

The most common multirate tests are <u>true isochronal</u>, <u>flow-after-flow</u> (FAF), and <u>modified isochronal</u>. An <u>isochronal test</u>, as suggested by the name, produces a well for a specified period, Δt, followed by an extended shutin until pressure builds up to its original value, repeats production at a different rate for the same length of time, Δt, repeats another extended buildup, and so on. Four rates and three buildups are common, the last rate usually being produced long enough to reach pseudosteady state flow. It can be shown for a true isochronal test that production periods do not need to be the same length, only that the pressures chosen for analysis occur at the same time after start of the flow period. Since transients from previous flows and buildups should, theoretically, disappear before the next flow starts, it does not matter if the rates are increasing or decreasing (time for transients to die out is not dependent on the rate, only the length of the flow period).

The flow-after-flow test should only be run if, during each flow period, pseudosteady state is reached. The analysis is not dependent on the length of each test or if rates increase or decrease. This type of testing is seldom applicable unless the reservoir formation has high permeability and/or limited drainage area and surrounding producers.

The modified isochronal test was suggested to eliminate the long buildup periods often required by true isochronal tests. The length of buildup is a strong function of permeability, and therefore many tight gas reservoirs requires excessive shutin periods (equivalent with lost production revenue) to obtain deliverability performance. The modified test is based on an approximation of the superposition principle. Work i have completed suggests that the approximate nature of the modified isochronal test has validity if flow is radial (i.e., Eq. 3.4 applies) but that problems arise when flow is linear or in transition between linear and radial flow.

Modified isochronal testing is identical to true isochronal testing with the exception that buildup periods are of the same duration as drawdowns, and that average pressure used to analyzes each rate is the pressure at the end of the buildup just prior to start of production for the given rate.

Paper A.8 proposes a log-log type curve and generalized procedure for analyzing multirate test data. It is applicable to oil and gas wells and has the advantage of yielding the value of D directly, without making the assumption inherent in the traditional analysis that $\log(q)$ vs $\log(\Delta p)$ is linear for all drawdowns (Eq. 3.21). The method also is superior to the alternative (mathematically equivalent) method of plotting $\Delta p/q$ versus q on linear paper, the problem with which is the difficulty in conceptualizing the quantity $\Delta p/q$ and shifting the resulting curve due to transient effects. The proposed method plots q versus Δp on log-log paper, and the best-fit match is easily shifted to account for transient changes. It also allows direct graphical determination of absolute open flow potential, both for the transient condition and stabilized flow.

3.6 Constant-Pressure Rate Solution During Depletion

Traditionally, solution of the diffusivity equation using the constant-pressure inner boundary condition has been equated with Hurst and van Everdingen's application to water influx. Interestingly, their historical paper on the subject does not tabulate or present graphically the dimensionless rate solution. This is despite the fact that roots of the Bessel function which must be solved to determine constant-pressure flux (cumulative rate) are the same needed to calculate dimensionless rate. The logical reasoning for their omission is that the application of constant-pressure rate analysis was not obvious when the solution was found. Most producing wells at that time were regulated, which meant they used only part of the reservoir energy (pressure drop) available and had no problem with maintaining the allowable rates. Also, the energy crisis had not occured and only the best reservoirs were produced, meaning those with high permeabilities. Stimulation had not become popular or necessary, and the concept of a well with an effective dimensionless radius, $r_{De}=r_e/r_w$, of 10, 50, or even 100 was unheard of. For these reasons it was not obvious that the constant-pressure rate solution had a function.

Today it might be guessed that over half the wells producing oil and gas are produced at a constant bottomhole flowing pressure. In fact, any well requiring stimulation will, sooner or later, produce at constant pressure - and probably sooner! The first tabulations of dimensionless rate solutions for bounded reservoirs appeared in the Russian literature in the mid-1950's by Tsarevich and Kuranov. They reorganize the original analytical solution of Hurst and van Everdingen, resolve (and present) the first five roots of the Bessel function expression, and tabulate/plot the results. Since values of the roots are not found in the Western literature, they have been recalculated for a large number of dimensionless radii and are presented in Table 3.4.

The exact solution for dimensionless rate is an infinite sum of exponential terms,

$$q_D = \sum_{n=1}^{\infty} c_n \cdot \exp\{-(b_n/r_{De})^2 t_D\}, \quad \ldots\ldots\ldots\ldots\ldots\ldots \quad (3.22)$$

and cumulative influx, Q_D, which is merely $\int q_D(t_D)dt_D$ evaluated from 0 to t_D, given by,

$$Q_D = (r_{De}-1)/2 - \sum_{n=1}^{\infty} c_n \cdot (r_{De}/b_n)\exp\{-b_n/r_{De})^2 t_D\} \quad \ldots \quad (3.23)$$

where q_D is dimensionless rate, $q(t)\mu B/kh(p_i - p_{wf})$, t_D is dimensionless time, $kt/\phi\mu c_t r_w^2$, and r_{De} is dimensionless external radius, r_e/r_w. Constant b_1 is the first and smallest root of the equation

$$Y_1(b_n) \cdot J_0(b_n/r_{De}) - J_1(b_n) \cdot Y_0(b_n/r_{De}) = 0 \quad \ldots. \quad (3.24)$$

which results from the exact solution to the constant-pressure problem originally solved by Hurst. Constant c_n is given by

$$c_n = \frac{2 \cdot Y_1^2(b_n)}{Y_1^2(b_n/r_{De}) - Y_1^2(b_n)}, \quad \ldots\ldots\ldots\ldots\ldots\ldots \quad (3.25)$$

where J_0, J_1, Y_0, and Y_1, are regular Bessel functions of order zero and one.

Not until the late 1970's and early 1980's did the Western literature begin taking notice of the applications offered by the constant-pressure solution. Fetkovich shows that rate decline resulting from constant-pressure production is exponential, an observation made in the work by Tsarevich and Kuranov (and reported by Arp's the same year, based on field data). Fetkovich also suggests that the analytical constant-pressure solution be combined with the empirical Arp's decline equations to form a powerful diagnostic tool relating production and time - the relation most critical to engineering and economic considerations.

TABLE 3.4 - FIRST FIVE ROOTS OF THE BESSEL FUNCTION EXPRESSION (EQ. 3.24) AND THE DIMENSIONLESS TIME tD* AT WHICH THE EXPONENTIAL EXPRESSION IS WITHIN 1% ACCURACY.

Dimensionless Radius	tD*	n	bn	cn
1.5	5.706E-02	1	4.33482E+00	4.41653E+00
		2	1.40172E+01	4.04006E+00
		3	2.34902E+01	4.01428E+00
		4	3.29355E+01	4.00721E+00
		5	4.23717E+01	4.00416E+00
2.0	2.243E-01	1	2.72155E+00	2.41705E+00
		2	9.29180E+00	2.03945E+00
		3	1.56283E+01	2.01407E+00
		4	2.19343E+01	2.00724E+00
		5	2.82301E+01	2.00436E+00
3.0	8.729E-01	1	1.87679E+00	1.40979E+00
		2	6.91216E+00	1.04157E+00
		3	1.16863E+01	1.01567E+00
		4	1.64255E+01	1.00809E+00
		5	2.11529E+01	1.00370E+00
4.0	1.925E+00	1	1.57382E+00	1.06666E+00
		2	6.10644E+00	7.10766E-01
		3	1.03633E+01	6.84021E-01
		4	1.45823E+01	6.75872E-01
		5	1.87882E+01	6.72357E-01
5.0	3.371E+00	1	1.41180E+00	8.90488E-01
		2	5.69608E+00	5.46042E-01
		3	9.69592E+00	5.18995E-01
		4	1.36560E+01	5.10351E-01
		5	1.76020E+01	5.06480E-01
6.0	5.201E+00	1	1.30843E+00	7.81811E-01
		2	5.44496E+00	4.46993E-01
		3	9.29138E+00	4.20395E-01
		4	1.30968E+01	4.11379E-01
		5	1.68874E+01	4.07239E-01
7.0	7.416E+00	1	1.23557E+00	7.07293E-01
		2	5.27416E+00	3.81835E-01
		3	9.01868E+00	3.54910E-01
		4	1.27214E+01	3.45626E-01
		5	1.64087E+01	3.41263E-01
8.0	1.001E+01	1	1.18079E+00	6.52581E-01
		2	5.14964E+00	3.35051E-01
		3	8.82141E+00	3.09227E-01
		4	1.24512E+01	2.98809E-01
		5	1.60650E+01	2.94271E-01

TABLE 3.4 continued

Dimensionless Radius	tD*	n	bn	cn
10.0	1.631E+01	1	1.10269E+00	5.76811E-01
		2	4.97885E+00	2.72455E-01
		3	8.55430E+00	2.48732E-01
		4	1.20868E+01	2.36630E-01
		5	1.56029E+01	2.31845E-01
12.0	2.410E+01	1	1.04869E+00	5.26121E-01
		2	4.86589E+00	2.32426E-01
		3	8.37994E+00	2.06639E-01
		4	1.18509E+01	1.97230E-01
		5	1.53052E+01	1.92306E-01
14.0	3.335E+01	1	1.00849E+00	4.89355E-01
		2	4.78479E+00	2.04509E-01
		3	8.25629E+00	1.79797E-01
		4	1.16847E+01	1.70025E-01
		5	1.50963E+01	1.65046E-01
16.0	4.407E+01	1	9.77006E-01	4.61214E-01
		2	4.72322E+00	1.83868E-01
		3	8.16353E+00	1.59684E-01
		4	1.15607E+01	1.50111E-01
		5	1.49411E+01	1.45062E-01
18.0	5.623E+01	1	9.51463E-01	4.38822E-01
		2	4.67459E+00	1.67935E-01
		3	8.09076E+00	1.44369E-01
		4	1.14642E+01	1.34899E-01
		5	1.48208E+01	1.29863E-01
20.0	6.982E+01	1	9.30177E-01	4.20469E-01
		2	4.63500E+00	1.55234E-01
		3	8.03207E+00	1.32157E-01
		4	1.13867E+01	1.22888E-01
		5	1.47244E+01	1.17876E-01
25.0	1.101E+02	1	8.89299E-01	3.86060E-01
		2	4.56145E+00	1.32353E-01
		3	7.92432E+00	1.10579E-01
		4	1.12455E+01	1.01570E-01
		5	1.45500E+01	9.66404E-02
30.0	1.592E+02	1	8.59514E-01	3.61715E-01
		2	4.51000E+00	1.16972E-01
		3	7.85018E+00	9.61935E-02
		4	1.11493E+01	8.75311E-02
		5	1.44318E+01	8.27094E-02

TABLE 3.4 continued

Dimensionless Radius	tD*	n	bn	cn
40.0	2.837E+02	1	8.17934E-01	3.28786E-01
		2	4.44127E+00	9.73492E-02
		3	7.75275E+00	7.81798E-02
		4	1.10243E+01	7.00636E-02
		5	1.42797E+01	6.54739E-02
50.0	4.429E+02	1	7.89445E-01	3.06991E-01
		2	4.39638E+00	8.51618E-02
		3	7.69032E+00	6.72065E-02
		4	1.09451E+01	5.95321E-02
		5	1.41842E+01	5.51553E-02
100.0	1.749E+03	1	7.16692E-01	2.54234E-01
		2	4.28994E+00	5.86124E-02
		3	7.54643E+00	4.40421E-02
		4	1.07663E+01	3.77283E-02
		5	1.39720E+01	3.40733E-02
200.0	6.844E+03	1	6.60753E-01	2.16711E-01
		2	4.21634E+00	4.25008E-02
		3	7.45082E+00	3.06613E-02
		4	1.06510E+01	2.55277E-02
		5	1.38382E+01	2.25461E-02
500.0	4.130E+04	1	6.03471E-01	1.81181E-01
		2	4.14842E+00	2.95441E-02
		3	7.36585E+00	2.04155E-02
		4	1.05512E+01	1.64977E-02
		5	1.37249E+01	1.42285E-02
1000.0	1.605E+05	1	5.68803E-01	1.61125E-01
		2	4.11089E+00	2.32612E-02
		3	7.32030E+00	1.56657E-02
		4	1.04989E+01	1.24338E-02
		5	1.36667E+01	1.05721E-02
2000.0	6.238E+05	1	5.39461E-01	1.45044E-01
		2	4.08123E+00	1.87680E-02
		3	7.28503E+00	1.23717E-02
		4	1.04591E+01	9.67663E-03
		5	1.36228E+01	8.13277E-03
4000.0	2.424E+06	1	5.14223E-01	1.31865E-01
		2	4.05722E+00	1.54506E-02
		3	7.25699E+00	1.00054E-02
		4	1.04278E+01	7.73025E-03
		5	1.35887E+01	6.43498E-03

TABLE 3.4 continued

Dimensionless Radius	tD*	n	bn	cn
10000.0	1.458E+07	1	4.85704E-01	1.17711E-01
		2	4.03172E+00	1.22540E-02
		3	7.22776E+00	7.78092E-03
		4	1.03954E+01	5.93389E-03
		5	1.35538E+01	4.88921E-03
25000.0	8.780E+07	1	4.61458E-01	1.06288E-01
		2	4.01137E+00	9.95097E-03
		3	7.20473E+00	6.21915E-03
		4	1.03703E+01	4.69244E-03
		5	1.35269E+01	3.83470E-03
100000.0	1.330E+09	1	4.30803E-01	9.26732E-02
		2	3.98738E+00	7.52598E-03
		3	7.17803E+00	4.61482E-03
		4	1.03415E+01	3.43797E-03
		5	1.34963E+01	2.78251E-03
250000.0	8.024E+09	1	4.13591E-01	8.54380E-02
		2	3.97474E+00	6.37797E-03
		3	7.16415E+00	3.87056E-03
		4	1.03267E+01	2.86469E-03
		5	1.34807E+01	2.30682E-03
1000000.0	1.219E+11	1	3.91084E-01	7.64036E-02
		2	3.95909E+00	5.08188E-03
		3	7.14712E+00	3.04481E-03
		4	1.03086E+01	2.23491E-03
		5	1.34617E+01	1.78848E-03

Unfortunately the new interest in constant-pressure solutions is still in a stage of infancy, being mainly used by theoreticians as a new field within which to publish. The most obvious applications of constant-pressure and decline curve analysis reported in the recent literature have been attacked with three-dimensional simulators, not even first having plotted rate-time data on log-log paper to satisfy their preconceived opinions that decline curve analysis is, as stated by Nind, "merely a convenience, a method that is amenable to mathematical or graphical treatment, and has no basis in physical laws governing the flow of oil and gas through the formation."

3.6 Partial Penetration Effects on Fluid Flow

One of the most common reductions in productivity is due to partial penetration, which results when the producing interval of a well constitutes only a fraction of the total contributing (pay) thickness. Reasons for partial penetration include:

- avoiding water and gas coning
- avoiding intervals with weak mechanical rock properties
- lost hole due to mechanical problems
- selective production testing during exploration
- poor log interpretation by the service company
- inability of air rigs to drill while producing liquids
- malfunction of the perforating gun

The partial-penetration problem is one which has been studied and solved for many years. Muskat presented one of the first solutions in 1927 for the analogous problem of an electrode partially penetrating a large cylindrical conducting disk; Kozeny gave the problem a slightly different treatment in 1933, resulting in a simple and useful expression for partial penetration skin (or its equivalent, which didn't have a name then). These earliest solutions assume steady state flow, and only later - first with numerical solutions and later analytically - did the transient problem receive attention. For practical purposes it is the steady state solution which is important since the transient effects die out extremely early, with the possible exceptions of low-permeability reservoirs or infintesimal penetration.

Probably because the problem is so obvious and has such profound practical implications - so much so that even theoreticians see them - it has received more attention than it really merits. Consider, for example, what is most commonly referred to in the petroleum literature as the first solution for partial penetration skin: Brons and Marting's results based on a numerical solution of Nisle's approximate analytical solution. Their purpose was to propose a simple relation for skin, expressed as

$$s = (1/b-1)\{\ln(h/r_w)-G(b)\} \quad \text{.....................} \quad (3.26)$$

"where G(b) is a function of b (the fraction of the total formation, h, penetrated by the well). Since this function *cannot* be expressed analytically, it has been calculated numerically ... for a range of b values."

If we now move back to Muskat's solution some 30 years earlier, we can rearrange (Eq. 6 in *Physical Principles of Oil Production*) and derive the analytical expression for G(b),

$$G(b) = M/2(1-b) - \ln(4) \quad \text{......................} \quad (3.27)$$

where

$$M = \exp\{\Gamma(0.875b)\Gamma(0.125b)/\Gamma(1-0.875b)\Gamma(1-0.125b)\}$$

$$\text{...} \quad (3.28)$$

and $\Gamma(x)$ is the gamma function of x. Table 3.2 compares numerical values of G(b) with *analytical* values.

TABLE 3.2 - COMPARISON OF ANALYTICAL AND NUMERICAL VALUES OF THE PARTIAL PENETRATION FACTOR G(b).

b	G(b) Brons/ Marting	G(b) Muskat (3.27)	M (3.28)
0.1	2.337	2.337	6.7022
0.2	1.862	1.862	5.1966
0.4	1.569	1.569	3.5470
0.6	1.621	1.620	2.4051
0.8	1.995	1.992	1.3507

Brons and Marting state that the Muskat solution (and their form using G(b)) is only valid if the ratio h/r_w is not too small; the quantity should actually be $\sqrt{k_h/k_v} \cdot h/r_w$, and a minimum value of 50 marks the point when Eq. 3.27 can be used. Considering the extreme case when $\sqrt{k_h/k_v}=1$ (usually a realistic value is about 3), $r_w=0.5$ feet (a very large wellbore) suggests that the total thickness of the reservoir can not be less than 25 feet. The limitation is obviously of little importance since reservoirs with thicknesses less than 25 feet probably never have partial penetration problems!

Eqs. 3.27 and 3.28 provide the analytical solution to partial penetration skin as formulated by Brons and Marting. The form is general and easy to solve, requiring only four values of the gamma function. And most of all, the solution came from Muskat some fifty years ago, desguised in a form so close to the present-day skin factor that it boggles the mind.

NOMENCLATURE

a_n = root of the Bessel function expression resulting from solution of the diffusivity equation assuming constant rate production

A = area perpendicular to flow

b_n = root of the Bessel function expression resulting from solution of the diffusivity equation assuming constant wellbore flowing pressure

b = fraction of the formation penetrated and open to flow

B = constant in the Forcheimer equation;
= formation volume factor, res/std volume

B_o = oil formation volume factor, res/std volume

c_n = constant in the dimensionless rate solution

C = constant defining Darcy's law;
= constant defined by Muskat, equivalent to skin factor;
= trapping constant in Corey/Burdine relative permeability relations

c_t = total rock plus fluid compressibility at initial or average reservoir pressure

D,E,F,G,H = arbitrary constants in the general expressions for pressure drop

$\exp(x)$ = e^x

$-Ei(-x)$ = exponential integral of x

$G(b)$ = analytical expression suggested by Brons and Marting for relating partial penetration ratio, b, to skin effect

h = total reservoir thickness

J = productivity index, $=q/\Delta p$

J' = constant in the approximate rate equation for wells experiencing high velocity flow, approaching J as n approaches 1

J_0, J_1, Y_0, Y_1 = regular Bessel functions of order 0 and 1

k = absolute permeability

k_{air} = permeability to air

k_h/k_v = ratio of horizontal to vertical permeability

k_{ox}, k_{gx} = effective permeability to nonwetting phase (oil or gas) in a two-phase, oil/water or gas/water system at irreducible water saturation

k_{rw}, k_{ro}, k_{rg} = relative permeabilities to water, oil, and gas phases, respectively

k_{rx} = relative permeabiliaty at k_{ox} (or k_{gx})

k_w, k_o, k_g = effective permeabilities to water, oil, and gas phases, respectively

L = length traversed during flow

$m(p)$ = oil pseudopressure function

M = factor relating $G(b)$ to its analytical expression given by Muskat

n = exponent in the approximate rate equation for wells experiencing high velocity flow,
= 0.5 for turbulence-dominated flow
= 1.0 for laminar, Darcy flow

p_D = dimensionless pressure

Δp = pressure drop causing flow

p_R = average reservoir pressure

p_{wf} = wellbore flowing pressure

q_D = dimensionless rate

Q_D = dimensionless cumulative rate or flux

q = volumetric flow rate

r = radius from well centerline

r_e = external radius defining no-flow boundary

r_D = dimensionless radius, $=r/r_w$

r_{De} = dimensionless external radius, $=r_e/r_w$

r_w = wellbore radius

r_w' = apparent wellbore radius, different from the true value to skin effects

s = skin factor, equivalent to a dimensionless pressure drop

S_{geF} = effective free gas (nonwetting-phase) saturation

S_{iw} = irreducible water (wetting-phase) saturation

S_m = Corey saturation variable

SUM = expression for a sum of Bessel functions

S_w, S_o, S_g = saturations of water, oil, and gas phases, respectively

S_{we}, S_{oe}, S_{ge} = effective saturations of water, oil, and gas phases, respectively

S_{wi} = initial water (wetting-phase) saturation

t = time

t_D = dimensionless time

v = velocity

$\Gamma(x)$ = gamma function of x

ϕ = porosity, fraction of bulk volume

μ = dynamic viscosity

λ = pore size distribution factor

REFERENCES: Chapters 1 and 2

Abbott, M.M.: "Cubic Equations of State: An Interpretive Review," Equations of State in Engineering and Research, K.C. Chao and R.L. Robinson, Jr. (eds.).

Bergman, D.F.: "Predicting the Phase Behavior of Natural Gas in Pipelines," PhD Dissertation, U. Michigan, Ann Arbor (1976).

Cavett, R.H.: "Physical Data for Distillation Calculations - Vapor-Liquid Equilibrium," Proc. 27th Meeting, API, San Francisco (1962)351-366.

Coats, K.H.: "Simulation of Gas Condensate Reservoir Performance," paper SPE 10512 presented at the Sixth SPE Symposium on Reservoir Simulation, New Orleans, Jan.31-Feb.3,1982.

Edmister, W.C.: Pet. Refiner (1958)37,173.

Fuller, G.G.: "A Modified Redlich-Kwong-Soave Equation of State Capable of Representing the Liquid State," Ind.Eng.Chem.Fund. (1976)15,4,254-257.

Gray, R.D., Jr.: "Industrial Experience in Applying the Redlich-Kwong Equation to Vapor-Liquid Equilibria," Equations of State in Engineering and Research, K.C. Chao and R.L. Robinson, Jr. (eds.).

Haaland, S.: "Characterization of North Sea Crude Oils and Petroleum Fractions," MS thesis, Norwegian Institute of Technology (NTH), The Univ. of Trondheim, Norway.

Haman, S.E.M., Chung, W.K., Eishayal, I.M. and Lu, B.C.-Y.: "Generalized Temperature-Dependent Parameters of the Redlich-Kwong Equation of State for Vapor-Liquid Equilibrium Calculations," Ind.Eng.Chem., Proc.Des.Dev. (1977)16,1, 51-59.

Hoffmann, A.E., Crump, J.S. and Hocott, C.R.: Equilibrium Constants for a Gas-Condensate System," Trans. AIME(1953) 198,1-10.

Joffe, J, Schroeder, G.M. and Zudkevitch, D.: "Vapor-Liquid Equilibria with the Redlich-Kwong Equation of State," AIChE J. (1970)16,3,496-498.

Katz,D.L.andFiroozabadi,A.: "Predicting Phase Behavior of Condensate/Crude-Oil Systems Using Methane Interaction Coefficients," J.Pet.Tech. (Nov. 1978)1649-1655 Trans. AIME, 228.

Kesler, M.G. and Lee, B.I.: "Improve Predictions of Enthalpy of Fractions," Hydro. Proc. (March 1977)153-158.

Kubic, W.L.: "A Modification of the Martin Equation of State for Calculating Vapor-Liquid Equilibria," Fluid Phase Equilibria (1982)9,79-97.

Lee, B.I. and Kesler, M.G.: AIChE (1975)21,510.

Lydersen, A.L.: "Estimation of Critical Properties of Organic Compounds," U. Wisconsin, Eng. Experimental Station Report 3, Madison, Wisconsin (April 1955).

Martin, J.J. and Hou, Y.C.: AIChE J. (1955)1,142.

Martin, J.J.: "Equations of State," Applied Thermodynmaics Symposium (1967)59,12,34-52.

Martin, J.J.: "Cubic Equations of State - Which," Ind.Eng.Chem.Fund. (1979)18,2,81-97.

Nokay, R.: "Estimate Petrochemical Properties," Chem.Eng. (1959)147-148.

Peneloux, A., Rauzy, E., and Freze, R.: "A Consistent Correction for Redlich-Kwong-Soave Volumes," Fluid Phase Equilibria,(1982)8,7-23.

Peng, D.-Y. and Robinson, D.B.: "A New Two-Constant Equation of State," Ind.Eng.Chem.Fund. (1976)15,1,59-64.

Pitzer, K.S., et al.: "The Volumetric and Thermodynamic Properties of Fluids. II. Compressibility Factor, Vapor Pressure, and Entropy of Vaporization," J.Amer.Chem.Soc. (1955)77,3433-3440.

Redlich, O. and Kwong, J.N.S.: "On the Thermodynamics of Solutions. V: An Equation of State. Fugacities of Gaseous Solutions," Chem.Reviews (1948)44,233-244.

Riazi, M.R. and Daubert, T.E.: "Simplify Property Predictions", Hydro. Proc. (March 1980),115-116.

Robinson, D.B. and Peng, D.-Y.: "The Characterization of the Heptanes and Heavier Fractions," Research Report 28, GPA Tulsa, Oklahoma (1978).

Schmidt, G. and Wenzel, H.: "A Modified van der Waals Type Equation of State," Chem.Eng.Sci. (1980)35,1503-1512.

Smith, R.L. and Watson, K.M.: "Boiling Points and Critical Properties of Hydrocarbon Mixtures," Ind.Eng.Chem. (1937) 1408-1414.

Soave, G.: "Equilibrium Constants from a Modified Redlich-Kwong Equation of State," Chem.Eng.Science (1972)27, 1197-1203.

Spencer, C.F. and Daubert, T.E.: "A Critical Evaluation of Methods for the Prediction of Critical Properties of Hydrocarbons," AIChE J. (May 1973)19,3,482-486.

Standing, M.B. and Katz, D.L.: "Density of Natural Gases," Trans. AIME (1942)146,140-149.

Standing, M.B. and Katz, D.L.: "Density of Crude Oils Saturated with Natural Gas," Trans. AIME (1942)146,159-165.

Standing, M.B. and Katz, D.L.: "Vapor-Liquid Equilibria of Natural Gas-Crude Oil Systems", Trans. AIME (1944)155,232.

Standing, M.B.: Volumetric and Phase Behavior of Oil Field Hydrocarbon Systems, 8th Printing, Society of Petroleum Engineers of AIME, Dallas (1977).

Usdin, E. and McAuliffe, J.C.: "A One Parameter Family of Equations of State," Chem.Eng.Sci. (1976)31, 1077-1084.

van der Waals, J.D.: Doctoral Dissertation, Leiden, Holland, 1873.

Watson, K.M., Nelson, E.F. and Murphy, G.B.: "Characterization of Petroleum Fractions," Ind.Eng.Chem. (1935)27,1460-1464.

Yarborough, L.: "Application of a Generalized Equation of State to Petroleum Reservoir Fluids," Equations of State in Engineering and Research, K.C. Chao and R.L. Robinson, Jr. (eds.).

Zudkevitch, D. and Joffe, J.: "Correlation and Prediction of Vapor-Liquid Equilibrium with the Redlich-Kwong Equation of State," AIChE J. (1970)16,112-119.

REFERENCES: Chapter 3

Arps, J.J.: "Analysis of Decline Curves," *Trans.* AIME (1945) *160*,228-247.

Brons, F. and Marting, V.E.: "The Effect of Restricted Fluid Entry on Well Productivity," *Trans.* AIME (1961)*222*, 172-174.

Darcy, H.: "Les Fontaines Publiques de la Ville de Dijon," Victor Dalmont, Paris.

Evinger, H.H. and Muskat, M.: "Calculation of Theoretical Productivity Factor," *Trans.* AIME (1942)*146*,126-139.

Fetkovich, M.J.: "The Isochronal Testing of Oil Wells," paper SPE 4529 presented at the SPE-AIME 48th Annual Fall Meeting, Las Vegas, Nevada, Sept.30-Oct.3, 1973.

Fetkovich, M.J.: "Decline Curve Analysis Using Type Curves," *J.Pet.Tech.* (June 1980) 1067-1077; *Trans.* AIME, *269*.

Havig, S.O.: "Gas-Oil Relative Permeability Correlations for Some North Sea Chalk Reservoirs," Norwegian Institute of Technology (1981), held confedential by the Norwegian Petroleum Directorate.

Hurst, W.: "Unsteady Flow of Fluids in Oil Reservoirs," *Physics* (Jan. 1934)*5*,20-30.

Hurst, W. "Establishment of the Skin Effect and Its Impediment to Fluid Flow Into a Wellbore," *Pet.Eng.* (Oct. 1953)*25*,B-6.

Kozeny, *Wasserkraft und Wasserwirtschaft*: (1933)*28*,101.

Nisle, R.G.: "The Effect of Partial Penetration on Pressure Buildup in Oil Wells," *Trans.* AIME (1958)*213*,85.

Muskat, M.: *Physical Principles of Oil Production*, International Human Resources Development Corporation, Boston (1981).

Raghavan, R.: "Well Test Analysis: Wells Producing by Solution Gas Drive," *J.Pet.Tech.* (Aug. 1976) 196-208; *Trans.* AIME, *261*.

Standing, M.B.: "Inflow Performance Relationships for Damaged Wells Producing by Solution-Gas Drive," J.Pet.Tech. (Nov. 1970),1399-1400.

Standing, M.B.: "Concerning the Calculation of Inflow Performance of Wells Producing from Solution Gas Drive Reservoirs," J.Pet.Tech. (Sept. 1971),1141-1142.

Standing, M.B.: Notes on Relative Permeability Relationships, Norwegian Institute of Technology (1975), Trondheim, Norway.

Tsarevich, K.A. and Kuranov, I.F.: "Calculation of the Flow Rates for the Center Well in a Circular Reservoir Under Elastic Conditions," Problems of Reservoir Hydrodynamics, Leningrad (1956)I,9-34.

van Everdingen, A.F.: "The Skin Effect and Its Influence on the Productive Capacity of a Well," Trans. AIME(1953)198, 171-176.

Vogel, J.V.: "Inflow Performance Relationships for Solution-Gas Drive Wells," J.Pet.Tech. (Jan. 1968),83-92.

JPT Forum

JPT **Forum** articles are limited to 1,500 words (including 250 per table or figure) or a maximum of two pages. **Forum** articles may present preliminary results or conclusions from continuing investigations or may impart general technical information that does not require publication as a full-length paper. **Forum** articles are subject to approval by an editorial committee. Letters to the editor are published as **Dialog** and may cover technical or nontechnical topics. SPE reserves the right to edit letters for style and content.

The Accuracy of PVT Parameters Calculated From Computer Flash Separation at Pressures Less Than 1,000 psia

Ø.S. Glasø, SINTEF/U. of Trondheim
C.H. Whitson, Rogaland District C.,

Introduction

Standing[1] derived a set of equations that fit the equilibrium constant data of Katz and Hachmuth[2] at pressures less than 1,000 psia (6.895 MPa) and temperatures below 250°F (121°C). A standard deviation (SD) of 3.5% between calculated and chart K values is reported by Standing.

Not reported, however, is the accuracy of the Katz and Hachmuth K values applied to reservoir fluids of various paraffinicities and containing significant amounts of nonhydrocarbons. Because the data of Katz and Hachmuth were for an Oklahoma City crude oil containing no nonhydrocarbons, it was necessary to investigate their general applicability.

A separator flash program was developed that incorporates the Standing K-value equations. The program was used to analyze 15 crude oils from various regions of the world, some containing substantial amounts of nonhydrocarbons. Flash parameters were calculated and compared with experimental values obtained from a PVT analysis of the fluid samples. GOR, average gas gravity, stock-tank oil gravity, and bubble-point formation volume factor were used in the comparisons.

Flash Program Description

Our vapor and liquid equilibrium calculations involved use of the Katz and Hachmuth K values fitted by Standing. The algorithm used for calculations is described by Standing.[3] The basic equation for fitting K-value data given by Hoffman *et al.*[4] was used in this study:

$$K=\frac{1}{p_{sp}}10^{(a+cF)}, \quad \text{(1)}$$

where coefficients a and c are functions of separator pressure. p_{sp} is measured in psia, and F is a characterization factor. Equations for constants a and c appear in Ref. 1.

The characterization factor, F, as defined by Hoffman *et al.*,[4] is

$$F=b(1/T_b-1/T_{sp}), \quad \text{(2)}$$

where separator temperature, T_{sp}, is in °R, T_b is the average boiling-point temperature in °R, and coefficient b is defined for the pure components C_3, iC_4, nC_4, iC_5, nC_5, and C_6 as

$$b=\frac{\log\left(\frac{p_c}{14.7}\right)}{(1/T_b-1/T_c)}. \quad \text{(3)}$$

All other fractions except C_{7+} (i.e., C_1, C_2, CO_2, N_2, and H_2S) have modified values of b and T_b, and these values can be determined by the procedure outlined in Ref. 1.

The K value for the C_{7+} fraction was determined by the equation[2]

$$K_{C_{7+}}=0.15\times K_{C_7}, \quad \text{(4)}$$

where K_{C_7} was calculated as a pure component. Ref. 1 provides an alternative method to determine $K_{C_{7+}}$. This method was not available to the authors at the time this study was conducted. We recommend that the procedure given in Ref. 1 be used to determine $K_{C_{7+}}$. A check was made to see what, if any, error resulted from using Eq. 4. It was found that there is no significant loss of accuracy in calculated flash parameters unless the oil contains a large C_{7+} fraction (greater than 0.70).

The flash program assumes that 1 mol of reservoir

0149-2136/82/0008-8033$00.25

TABLE 1—SURFACE PROPERTIES AND EXPERIMENTALLY DETERMINED OIL FORMATION VOLUME FACTOR AT SATURATION PRESSURE

Sample	R (scf/STB)	γ_g (air = 1)	γ_{API}	F_p	T (°F)	B_{ob} (RB/STB)	Nonhydrocarbon Content in Total Surface Gas (mol%) N_2	CO_2	H_2S
Middle East	770	0.729	44.8	12.40	210	1.450			
North Sea	786	0.755	36.7	11.90	196	1.435			
California	104	0.881	27.0	11.42	102	1.061			
Michigan	230	0.935	26.0	11.82	83	1.109			
California	788	0.850	33.7	11.66	242	1.498			
California	710	—	35.1	11.66	242	1.433			
Mississippi	326	0.864	37.2	11.74	253	1.313	9	7	5
FA-1	840	1.248	27.9	11.38	240	1.593	—	6	57
GL-1	1,344	0.985	48.1	12.00	248	1.850	24	4	—
GL-2	1,452	1.034	47.7	12.00	249	1.901	21	4	2
North Sea	497	0.936	36.9	11.80	150	1.253			
North Sea	497	0.936	36.9	11.80	280	1.363			
North Sea	1,052	0.746	33.8	11.75	215	1.512			

fluid is flashed at first-stage separator pressure and temperature. Liquid from each subsequent stage of separation is flashed until the final liquid feed is flashed at stock-tank (nth-stage) conditions, p_{st} and T_{st}. At each stage, the composition and moles of liquid and vapor are calculated and converted to a basis of 1 STB (0.2 stock-tank m^3) oil. From these data, total GOR, average gas gravity, stock-tank oil gravity, and bubble-point formation volume factor are calculated.

Two methods are used to calculate bubble-point formation volume factor. The first combines gas and stock-tank oil weights with bubble-point oil density as follows.

$$B_{ob}=\frac{\sum_{j=1}^{n} W_{gj}+W_{sto}}{5.6146\,\rho_{ob}} \quad \text{.....................(5)}$$

The bubble-point oil density either is reported from PVT analysis or is calculated from the Alani and Kennedy[5] correlation. The second method of determining B_{ob} uses a North Sea correlation by Glasø.[6] This correlation was developed for North Sea crude oils but has been proved equally applicable to oils of varying paraffinicity. A comparable correlation was developed by Standing[7] for mixtures of California oils and gases. The paraffinicity of the samples used was calculated from a method developed by Whitson.[8] Some of these examples are compared in Tables 1 and 2. Four of the 15 samples contained relatively large amounts of nonhydrocarbons CO_2, N_2, and H_2S, as shown in Table 1.

Results and Discussion

Experimental and calculated values of total GOR, average gas gravity, stock-tank oil gravity, and formation volume factor for the 15 samples were compared in this study. Samples marked "California" were analyzed at several separator conditions. Separator pressure and temperature were varied for separator designs from one to three stages.

TABLE 2—COMPARISON OF EXPERIMENTAL AND CALCULATED FLUID PROPERTIES

	Computer Flash Data						Bubble-Point Formation Volume Factor, RB/STB			
							From Correlation[6]		From Bubble-Point Density[5]	
Sample	R (scf/STB)	GOR Deviation (%)	γ_g (air = 1)	γ_g Deviation (%)	γ_{API}	γ_{API} Deviation (%)	B_{ob} (RB/STB)	Deviation (%)	B_{ob} (RB/STB)	Deviation (%)
Middle East	740	3.90	0.702	3.70	45.8	−2.23	1.400	3.45	1.412	2.62
North Sea	758	3.55	0.758	−0.40	36.5	0.54	1.407	1.95	1.408	1.88
California	107	−2.88	0.914	−3.75	27.3	−1.11	1.048	1.23	1.058	0.28
Michigan	219	4.78	0.886	5.24	26.4	−1.54	1.085	2.16	1.094	1.35
California	820	−3.90	0.894	−5.18	34.5	−2.37	1.507	−0.60	1.494	0.27
California	677	4.65	0.711		37.0	−5.41	1.380	3.70	1.395	2.65
Mississippi	296	9.20	0.969	−12.15	37.7	−1.34	1.219	7.16	1.243	5.33
FA-1	860	−2.38	1.221	2.16	27.2	2.51	1.609	−1.00	1.574	1.19
GL-1	1,301	3.20	0.916	7.01	50.3	−4.57	1.844	0.32	1.765	4.59
GL-2	1,359	6.40	0.945	8.61	49.9	−4.61	1.912	−0.58	1.851	2.63
North Sea	495	0.40	0.971	−3.74	37.0	−0.27	1.279	−2.08	1.279	−2.08
North Sea	495	0.40	0.971	−3.74	37.0	−0.27	1.349	1.03	1.386	−1.69
North Sea	1,057	−0.48	0.758	−1.61	36.0	−6.51	1.580	−4.50	1.549	−2.45

Summary for All Samples					
Number of samples compared*	18	15	18	20	20
Average deviation, %	2.18	−0.35	−2.49	0.99	0.96
SD, %	4.16	5.37	3.50	2.75	2.39

*Some comparisons involve the same sample.

Statistical analysis of the data gave average deviation, SD, and number of comparisons for each parameter. Results are found in Table 2. Although 15 samples do not constitute an exhaustive analysis, applicability of the correlations is supported by the wide range of oil types studied.

Comparison of the calculated and experimental data for these samples did not deviate substantially from pure hydrocarbon samples, suggesting that the modified parameters for nonhydrocarbon K values are sufficiently accurate for estimating their phase behavior.

Conclusions

1. The Katz and Hachmuth[2] K-value data seem to be applicable to most black oils, independent of paraffinicity and large content of nonhydrocarbons in the surface gases, at pressures below 1,000 psia (6.895 MPa) and temperatures below 250°F (121°C).

2. The usefulness of Katz and Hachmuth's work is extended by equations developed by Standing[1] that fit the K-value data of Katz and Hachmuth. Modified parameters are presented to generate K values for the light components (C_1, C_2, CO_2, N_2, and H_2S), with a special correlation given for the C_{7+} fraction.

3. Results from a computer flash separator program that used Standing's equations for calculating K values yielded average deviations of 2.18, −0.35, and −2.49% and SD's of 4.16, 5.37, and 3.50% for GOR, average gas gravity, and stock-tank oil gravity, respectively. Bubble-point formation volume factor, calculated with bubble-point oil density and a correlation by Glasø,[6] yielded average deviations of 0.96 and 0.99% and SD's of 2.39 and 2.75%.

Nomenclature

a = variable in K-value equation
b = variable in characterization factor equation
B_{ob} = oil formation volume factor at bubble-point (saturation) pressure, RB/STB (res m^3/stock-tank m^3)
c = variable in K-value equation
f_{Vi} = volume fraction of component i
F = characterization factor
F_p = $\left(\sum_{i=1}^{n} f_i \times T_{bi}{}^{1/3}\right) \times (1/\gamma_o)$ = paraffinicity characterization factor
p_c = critical pressure, psia (MPa)
p_{sp} = separator pressure, psia (MPa)
R = total producing GOR from flash separation, scf/STB (std m^3/stock-tank m^3)
T = reservoir temperature, °F (°C)
T_b = average boiling-point temperature, °R (K)
T_c = critical temperature, °R (K)
T_{sp} = separator temperature, °R (K)
W_g = weight of gas [basis: 1 STB (0.2 stock-tank m^3) oil], lbm (kg)
W_{sto} = weight of 1 STB (0.2 stock-tank m^3) oil, lbm (kg)
γ_{API} = $(141.5/\gamma_o) - 131.5$ = stock-tank oil gravity from flash separation
γ_g = average specific gravity of total surface gases from flash separation (air = 1)
ρ_{ob} = bubble-point oil density, lbm/cu ft (kg/m^3)

Subscripts

i = components (e.g., C_1, C_2, etc.)
j = stage number, where $j = 1, 2, \ldots n$

References

1. Standing, M.B.: "A Set of Equations for Computing Equilibrium Ratios of a Crude Oil/Natural Gas System at Pressures Below 1,000 psia," *J. Pet. Tech.* (Sept. 1979) 1193-1195.
2. Katz, D.L. and Hachmuth, D.H.: "Vaporization Equilibrium Constants in a Crude Oil-Natural Gas System," *Ind. and Eng. Chem.* (Sept. 1937) **29**, 1072-1077.
3. Standing, M.B.: *Volumetric Phase Behaviour of Oil Field Hydrocarbon Systems*, Chevron Oil Field Research Co., La Habra, CA (Sept. 1970), 43-56.
4. Hoffman, A.E., Crump, J.S., and Hocott, C.R.: "Equilibrium Constants for a Gas-Condensate System," *Trans.*, AIME (1953) **198**, 1-10.
5. Alani, G.H. and Kennedy, T.H.: "Volumes of Liquid Hydrocarbons at High Temperatures and Pressures, *Trans.*, AIME (1960) **219**, 288-292.
6. Glasø, Ø.: "Generalized Pressure-Volume-Temperature Correlations," *J. Pet. Tech.* (May 1980) 784-795.
7. Standing, M.B.: "A Pressure-Volume-Temperature Correlation for Mixtures of California Oils and Gases," *Drill. and Prod. Prac.*, API (1947) 275.
8. Whitson, C.H.: "Characterizing Hydrocarbon Plus Fractions," paper EUR 183 presented at the European Offshore Petroleum Conference and Exhibition, London, Oct. 21-24, 1980.

SI Metric Conversion Factors

bbl × 1.589 873 E−01 = m^3
°F (°F−32)/1.8 = °C
scf × 2.863 64 E−02 = std m^3

*Conversion factor is exact

JPT

Original manuscript received in Society of Petroleum Engineers office May 11, 1979.
Revised manuscript received Feb 23, 1982.

A.2-1

Characterizing Hydrocarbon Plus Fractions

Curtis H. Whitson,* SPE, U. of Trondheim

Abstract

Methods are developed for characterizing the molar distribution (mole fraction/molecular weight relation) and physical properties of petroleum fractions such as heptanes-plus (C_7+). These methods should enhance equation-of-state (EOS) predictions when experimental data are lacking.

The three-parameter gamma probability function is used to characterize the molar distribution, as well as to fit experimental weight and molar distributions and to generate synthetic distributions of heptanes-plus fractions.

Equations are provided for calculating physical properties such as critical pressure and temperature of single-carbon-number (SCN) groups. A simple three-parameter equation is also presented for calculating the Watson characterization factor from molecular weight and specific gravity.

Finally, a regrouping scheme is developed to reduce extended analyses to only a few multiple-carbon-number (MCN) groups. Two sets of mixing rules are considered, giving essentially the same results when used with the proposed regrouping procedure.

Introduction

During the development of the application of EOS's to naturally occurring hydrocarbon mixtures, it has become clear that insufficient description of heavier hydrocarbons (e.g., heptanes and heavier) reduces the accuracy of PVT predictions. Volatile oil and gas-condensate volumetric phase behavior is particularly sensitive to composition and properties of the heaviest components.

Until recently there has not been published in technical journals a comprehensive method for characterizing compositional variation, which we call "molar distribution." Several authors[1-5] have given lucid descriptions of petroleum fraction characterization, though they deal mainly with physical property estimation. Usually, only a single heptanes-plus (C_7+) fraction lumps together thousands of compounds with a carbon number higher than six. Molecular weight and specific gravity (or density) of the C_7+ fraction may be the only measured data available.

Preferably, a complete true-boiling-point (TBP) analysis should be performed on fluids to be matched by an EOS. Distillation experiments yield boiling points, specific gravities, and molecular weights, from which molar distribution is found directly. Special analyses of TBP data can also provide estimates of the paraffin/napthene/aromatic (PNA) content of SCN groups, which are useful in some property correlations.[5]

Unfortunately, such high-quality data are seldom available for fluids being matched or predicted by an EOS. If data other than lumped C_7+ properties are available, they might include a partial component analysis (weight distribution) from chromatographic measurements. In this case, only weight fractions of SCN groups are reported: normal boiling points, specific gravities, and molecular weights (needed to convert to a molar basis) simply are not available.

Compositional simulation based on an EOS involves two major problems: (1) how to "split" a C_7+ fraction into SCN groups with mole fractions, molecular weights, and specific gravities that match measured C_7+ properties, and (2) if a partial extended analysis (e.g., $C_{11}+$) is available, how to extend it to higher carbon numbers.

The first step in addressing these problems is to find a versatile, easy-to-use probability function for describing molar distribution. The distribution function should allow consistent matching and reasonable extension of partial analyses. Also, it should not contain too many unknown or difficult-to-determine parameters. This paper presents such a probabilistic model and describes its application to several reservoir fluids under "Molar Distribution."

The second step in characterizing plus fractions involves estimating SCN group specific gravities, which, together with estimated molecular weights (from the probabilistic model), could be used to estimate critical properties required by EOS's. We address this problem and suggest a simple method for specific gravity estimation under "Physical Properties Estimation." The

---

*Now at Rogaland Dist. C.

0197-7250/83/0081-2233$00.25

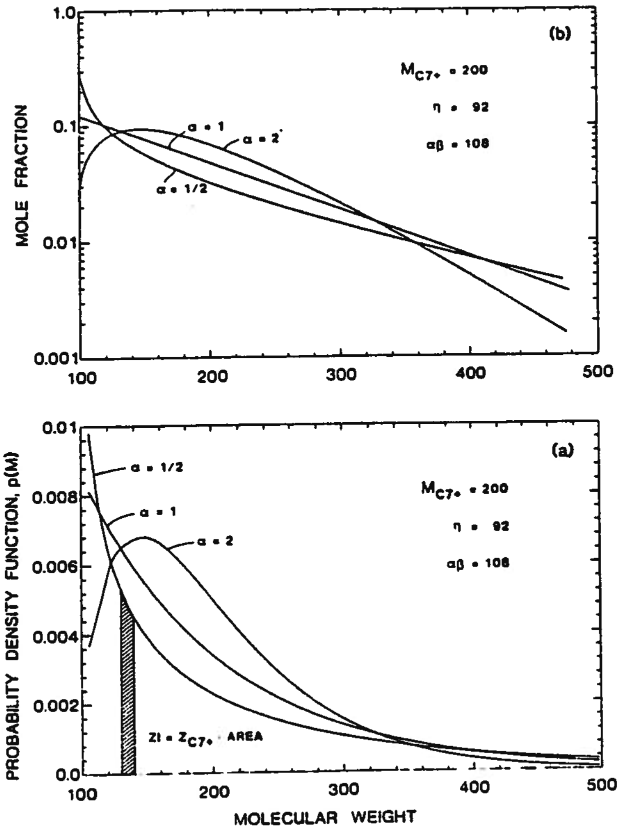

Fig. 1—Illustration of the probabilistic model for several values of parameter α.

method is based on the Watson characterization factor,[6] which is shown to relate specific gravity, molecular weight, and boiling point by a simple three-parameter equation. A second alternative is based on the generalized properties proposed by Katz and Firoozabadi,[7] somewhat modified to make their use more consistent.

The last section, "Regrouping (Pseudoization) and Mixing Rules," deals with the problem of reducing the complexity of fully extended characterizations to only a few MCN groups. Several mixing rules are proposed for the pseudoization (regrouping) process. Also, simple relations are given to estimate how many MCN groups are required and how the regrouping can be performed consistently.

Several examples are given to illustrate some of the capabilities and limitations of the proposed methods. They also indicate the sensitivity of EOS predictions to C_7+ characterization.

Molar Distribution

The problem of estimating reservoir-fluid molar distributions was encountered when a commercial EOS PVT package was used. It became evident that proper characterization of heavier components was important for obtaining a reasonable match of experimental data. It was decided to examine existing molar-distribution (mole fraction/molecular weight) data for similarities and characteristics that could be used to describe hydrocarbon systems. An important requirement for the distribution model was its ability to match weight fractions reported from chromatographic studies.

Probabilistic Model

The three-parameter gamma function (Type 3 of the Pearson system[8]) was chosen for describing molar distribution. Fig. 1a shows three examples of the probability model. Each curve has the same expected value of x (for our purposes this corresponds to measured C_7+ molecular weight). For $\alpha=1$, the distribution is exponential. Values less than one give accelerated exponential distributions, while values greater than one yield left-skewed distributions. Note that as α approaches infinity, the distribution becomes normal, though "folded" at η, the minimum molecular weight included in the C_7+ fraction.

The probability density function, $p(x)$, is given by

$$p(x)=\frac{(x-\eta)^{\alpha-1}\exp[(x-\eta)/\beta]}{\beta^{\alpha}\Gamma(\alpha)}, \quad \ldots\ldots\ldots\ldots (1)$$

where α, β, and η are parameters defining the distribution. η can be estimated accurately since it represents the minimum molecular weight to be included in the C_n+ fraction. If α is given, β is found directly from η, α, and the measured C_n+ molecular weight, M_n+. α can be fit to measured molar- and weight-distribution data, or estimated using an empirical relation.

The cumulative probability function, $P(X\leq x)$, is the integral of $P(x)$ from η to x,

$$P(X\leq x)=\int_{\eta}^{x} p(x)\,dx, \quad \ldots\ldots\ldots\ldots (2a)$$

and represents the frequency of occurrence (normalized mole fraction) in the interval η to x. The analytical expression for the cumulative probability function is[8]

$$P(X\leq x)=e^{-y}\cdot\sum_{j=0}^{\infty}[y^{\alpha+j}/\Gamma(\alpha+j+1)], \quad \ldots\ldots (2b)$$

with $y=(x-\eta)/\beta$.

To apply Eq. 2 to the molar distribution problem it is necessary to define variables in practical terms and to show how the relation can be used to calculate mole fractions, molecular weights, and from them weight fractions (see Fig. 1).

The variable x in Eq. 2 is merely the SCN-group molecular weight, or

$$x\equiv M. \quad \ldots\ldots\ldots\ldots (3a)$$

The parameter η is defined as the minimum molecular weight expected to occur in the C_n+ fraction. That is, there is zero probability $[p(x)=0]$ for occurrence of compounds with molecular weight less than η. If the C_7+ fraction is considered, then $\eta=92$ (the molecular weight of toluene) would be a good estimate for η. Experience has shown that a good approximation of η is given by

$$\eta=14n-6 \quad \ldots\ldots\ldots\ldots (3b)$$

for a C_n+ fraction. Eq. 3b is a useful empirical relation but should not be considered a restraint on the model.

Considering the remaining two parameters in Eq. 2, α and β, a useful property of the three-parameter gamma function is that the product $\alpha\beta$ equals the arithmetic average molecular weight, M_n+, minus η, or

$$M_n+ - \eta = \alpha\beta, \quad \text{(3c)}$$

where M_n+ is measured directly.

There are several empirical correlations available for estimating α from randomly sampled data such as a fully extended molar distribution. β is easily calculated from the other variables.

$$\beta = (M_n+ - \eta)/\alpha. \quad \text{(3d)}$$

The cumulative frequency of occurrence, f_i, for compounds having molecular weight boundaries M_{i-1} and M_i is merely

$$f_i = \int_{M_{i-1}}^{M_i} p(x)\,dx = P(r)(M \le M_i) - P(r)(M \le M_{i-1}). \quad \text{(4)}$$

The frequency, f_i, is directly proportional to mole fraction z_i.

$$z_i \equiv f_i \cdot z_n+. \quad \text{(5)}$$

The average molecular weight in the same interval is given by

$$\bar{M}_i = \eta + \alpha\beta \frac{P(M \le M_i, \alpha+1) - P(M \le M_{i-1}, \alpha+1)}{P(M \le M_i, \alpha) - P(M \le M_{i-1}, \alpha)}. \quad \text{(6)}$$

where all $P(X \le x)$ functions, independent of the α used (i.e., α or $\alpha+1$), use β as defined in Eq. 3d [$\beta = (M_n+ - \eta)/\alpha$].

Fig. 1a shows how Eqs. 2 through 6 were used to convert the probability density functions in Fig. 1a to molar distributions.

Given SCN mole fractions (z_i) and molecular weights ($\bar{M}_i$), weight fraction, f_{wi}, is given by

$$f_{wi} = z_i \bar{M}_i / (z_n+ M_n+). \quad \text{(7)}$$

The $P(r)$ function, given by Eq. 2, can be simplified to facilitate its calculation on a computer by avoiding inclusion of the gamma function inside the summation. Using the recurrence property of the gamma function, Γ, yields

$$P(r)\,(X \le x) = \frac{e^{-y} y^{\alpha}}{\Gamma(\alpha)} \cdot \sum_{j=0}^{\infty} \frac{y^j}{(\alpha+j)!}. \quad \text{(8)}$$

where the summation can be ceased when

$$\Sigma_{j+1} - \Sigma_j < 10^{-6}. \quad \text{(9)}$$

The proposed probabilistic model is not a true physical model. One assumption is the continuous relation between molecular weight and mole fraction. This assumption, however, along with others implicit in its mathematical form, seems as reasonable as, for example, the assumption in distillation (TBP) analysis that cumulative volume and boiling point have a continuous relation.[9,10]

Application of the Molar Distribution Model

Direct Estimate of α

An estimator of α can be calculated using the following proposed empirical relation.[11]

$$\alpha = Y^{-1}\,(0.5000876 + 0.1648852\,Y - 0.0544174\,Y^2), \quad \text{(10)}$$

where

$$Y = \ln[(M_n+ - \eta)/m_G)], \quad \text{(11)}$$

and

$$m_G = \left[\prod_{i=n}^{N} (M_i - \eta)^{z_i}\right]^{1/z_n+}. \quad \text{(12)}$$

Eq. 10 is valid for $0 < Y < 0.5772$ (i.e., $\alpha \geqq 1.0$). m_G merely represents a geometric average molecular-weight variable. For Eq. 10 to be useful for the molar distribution problem, it is necessary to have measured SCN mole fractions and molecular weights accurately. They should also constitute a full compositional analysis, preferably having a diminishing or neglible quantity of the last fraction, N. Since such analyses are nearly nonexistent, a set of correction tables* has been developed when only partial analyses are available (the limitation of $\alpha \geqq 1.0$ mentioned previously is also lifted in the present use of Eq. 10).

Determining α by Minimization

The error function, $E(\alpha)$, used to optimize α is defined as the sum of the squares of differences in measured and calculated compositions and is given by

$$E(\alpha) = \sum_{i=n}^{N} (z_i - \tilde{z})^2 \quad \text{(13a)}$$

if a molar distribution is to be fit, and

$$E(\alpha) = \sum_{i=n}^{N} (f_{wi} - \tilde{f}_{wi})^2 \quad \text{(13b)}$$

if a weight distribution is to be fit (the more common case). Calculated values are marked with a tilde (e.g., $\tilde{z}_i$).

The minimization of E may proceed by a simple secant or half-interval method. Two procedures for performing the minimization have proved useful. Reasonable limits for α are 0.5 to 3.0.

The first method, called the "constant molecular weight interval" (CMWI), is the simpler. In this case, a value of η is chosen (e.g., from Eq. 3b), and the length between molecular weight boundaries is set to a constant, such as 14, the molecular weight of a CH_2 group: this technique is called CMWI-1. An alternative is to define the molecular weight of the first component, C_n, and the molecular weight interval (e.g., 14), and then find the value of η that satisfies this condition (trial-and-error procedure): this technique is called CMWI-2. In both cases molecular weight boundaries are separated by a constant, except for the last fraction, which has infinity as its upper boundary.

---

*These tables can be obtained directly from the author: NTH, Petroleum Dept., 7034 Trondheim, Norway.

TABLE 1—CONSTANTS *a*, *b*, AND *c* USED IN THE GENERALIZED PHYSICAL PROPERTIES CORRELATION (Eq. 14)

Property	Constants Used in Eq. 14 *a*	*b*	*c*	Data Points	Range	Average Absolute Deviation (%)	Maximum Deviation (%)
M (mass/mole)	4.56730×10^{-5}	2.1962	−1.0164	186	general*	2.6	11.8
(mass/mole)	1.66070×10^{-4} (SI)†						
T_c (°R)	2.42787×10^{1}	0.58848	0.3596	126	general*	1.3	10.6
(K)	1.90623×10^{1} (SI)						
p_c (psia)	3.12281×10^{9}	−2.3125	2.3201	103	general*	3.1	9.3
(kPa)	5.53028×10^{9} (SI)						
p_c (psia)	2.41490×10^{14}	−3.86618	4.2448	48	$T_b>850$°R**	0.11	13.2
(kPa)	1.71589×10^{14} (SI)						
V_{cm} (cu ft/lbm-mole)	7.04340×10^{-7}	2.3829	−1.683	102	general*	2.9	11.2
(m^3/kg·mole)	1.78420×10^{-7} (SI)						
V_c (cu ft/lb)	7.52140×10^{-3}	0.2896	−0.7666	103	general*	2.3	9.1
(m^3/kg)	5.56680×10^{-4} (SI)						
V_{lm} (cm^3/g-mole)	7.62110×10^{-5}	2.1262	−1.8688	128	general*	2.8	9.5
(m^3/kg·mole)	2.65940×10^{-1} (SI)						
ρ (g/cm^3)	9.82554×10^{-1}	0.002016	1.0055	128	general*	0.028	0.91
(kg/m^3)	9.83719×10^{2} (SI)						

*Constants *a*, *b*, and *c* are those originally reported by Riazi and Daubert,[17] who claim the correlations are reliable for boiling points up to 850°F. Except in the case of critical pressure, the correlations appear to be acceptable at higher boiling points; for example, the original constants yielded an absolute average deviation of only 1.52% in the 850 to 1200°F range.

**Constants *a*, *b*, and *c* were determined from multiple regression analysis on data reported in Ref. 18.

†Use of SI units implies that boiling point is given in degrees Kelvin, with the calculated property having the appropriate SI units given in Col. 1.

The second method, called "variable molecular weight interval" (VMWI), allows the interval between boundaries to vary between two limits, such as $14i-10$ and $14i+2$. The first lower boundary is set by η (Eq. 3b or by defining molecular weight of the first component). The upper boundary is then varied until either the measured SCN mole or weight fraction is matched or the upper or lower boundary is exceeded. The resulting upper boundary is then used as the lower boundary for the next SCN. If VMWI is used, the minimization of E must proceed by interval halving.

Physical Properties Estimation

Since the 1930's, process and chemical engineers have been using physical property correlations based on the boiling point and specific gravity of SCN and MCN groups.[12,13] The chemical makeup of petroleum mixtures was later characterized by Watson[6,13] using the same two properties.

Physical property correlations have been revised and extended several times; Ref. 18 presents numerous correlations commonly used in industry. Tabular and graphical forms of the correlations have slowly been replaced by multiconstant equations used for programming. Generally these equations are complex best-fit polynomials.[14-16]

A recent physical property correlation was proposed by Riazi and Daubert.[17] It was chosen for this study because it is simple to use, having only three constants, and is claimed to be based on EOS principles. Also, it was found that it led to simple relations for estimating the Watson characterization factor.

The equation form of all correlations is the same,

$$\Theta=a\,T_b^b\gamma^c, \quad\text{.......................... (14)}$$

where Θ is a physical property: critical pressure or temperature, molecular weight, etc. If Θ is the property of an SCN group, then T_b is the normal boiling point of that group. If Θ is a property of an MCN group, then T_b is an average boiling point, the type being dependent on which property is estimated [see Regrouping (Pseudoization) and Mixing Rules].

Constants *a*, *b*, and *c* are presented in Table 1 for several properties relevant to EOS calculations. Concerning the original constants developed for Eq. 14, Ref. 17 states that "prediction accuracy is reasonable over the boiling point range 100 - 850°F [310 - 730 K]." It was found, however, that the accuracy using the original constants for critical temperature was good for the boiling-point range up to 925 K (1200°F). Critical pressure predictions did not, however, show good accuracy using the original constants for boiling points greater than 730 K (850°F). It was necessary to determine constants for extending Eq. 14 using data from Ref. 18.

Watson Characterization Factor

The Watson characterization factor, K, is given by

$$K\equiv T_b^{1/3}/\gamma, \quad\text{.......................... (15)}$$

where T_b is normal or cubic-average boiling point in degrees Rankine and γ is specific gravity at 290 K (60°F). If SI units are used (i.e., T_b is given in degrees Kelvin), the right side of Eq. 15 should be multiplied by $1.21644\ (=1.8^{1/3})$. (Appendix A presents a discussion of another characterization factor and compares it with the Watson factor.) K defines relative paraffinicity of a hydrocarbon fraction, with a typical range from 10.0 (highly aromatic) to 13.0 (highly paraffinic).

A useful relation between K, molecular weight, and specific gravity can be developed by using the Riazi-Daubert relation for molecular weight,

$$M=4.5673\times10^{-5}\,T_b^{2.1962}\,\gamma^{-1.0164}, \quad\text{.......... (16)}$$

which, when combined with the definition of K, yields

$$K=4.5579\ M^{0.15178}\ \gamma^{-0.84573}. \qquad (17)$$

To test the validity of Eq. 17, data from 12 systems given in Ref. 19, 9 from Ref. 12, and 4 pure compounds were compared. K factors calculated from experimental data and the definition of K (Eq. 15), using cubic average boiling point and specific gravity, are compared with values estimated by Eq. 17 (see Table 2).

A procedure based on the Watson characterization factor is proposed for estimating SCN boiling points and specific gravities. It is assumed that SCN molecular weights are available, for example from the molar distribution model, and C_n+ specific gravity is determined experimentally. First, K is assumed constant for all SCN fractions. SCN specific gravities are calculated from Eq. 17 and molecular weights. A trial-and-error procedure is performed until a value of K gives SCN specific gravities with an average that matches the measured value. (Haaland[20] recently modified this procedure by generalizing the variation in K for SCN groups up to C_{40}.) SCN boiling points are calculated from K and SCN specific gravities (Eq. 15).

As an alternative to this procedure, a set of generalized properties is presented. They are modified from data presented by Katz and Firoozabadi.[7] Unfortunately, it may be difficult to match measured C_n+ specific gravity if generalized SCN values are used.

Generalized Physical Properties

It was found that tabulated molecular weights (Table 1 of Ref. 7) were inconsistent with plotted data (Fig. 2 of Ref. 7). Molecular weights for SCN groups 22 through 45 are clearly inconsistent. An analysis and comparison of both sets of data with sources from which they were developed indicated that the graphically presented molecular weights were more correct (the tabulated extrapolation for C_{22} through C_{45} results merely from addition of 14 to the previous molecular weight).

Instead of reading numerical values from Fig. 1 of Ref. 7, the extrapolation was performed using the Riazi-Daubert correlation form (Eq. 16) based on generalized boiling points and specific gravities. Since tabulated and graphical values of molecular weight in the region C_6 through C_{22} were consistent, these values were fit by nonlinear regression, yielding modified constants: $a=2.4820\times10^{-7}$, $b=2.9223$, and $C=2.4750$. Molecular weights in Table 3 for C_{22} through C_{45} were calculated using these constants in Eq. 14 instead of those in Eq. 16. Other molecular weights (C_6 through C_{22}) are the same as originally presented in Ref. 7. SCN normal boiling points and specific gravities (converted from densities) are also the same as originally reported.

Critical properties of SCN groups 6 through 45 were calculated using Eq. 14 and appropriate constants in Table 1. [Modified constants with boiling points greater than 730 K (850°F) were used for critical pressure estimation.] Acentric factors were calculated using the Edmister equation.[21]

Binary interaction coefficients between methane and SCN groups are also presented in Table 3. They were estimated from the graphical correlation proposed by Katz and Firoozabadi,[7] represented by

$$\delta_{C_1-C_i}=0.14\cdot\gamma_i-0.0668. \qquad (18)$$

Eq. 18 and binary interaction coefficients presented in Table 3 should be used only with the Peng-Robinson EOS.[22]

TABLE 2—COMPARISON OF TRUE (Eq. 15) AND ESTIMATED (Eq. 17) WATSON CHARACTERIZATION FACTORS

Sample	Molecular Weight	Specific Gravity	Watson Characterization Factor*	
			Measured	Calculated
A 1 to A 4	243	0.888	11.6	11.60
A 5 to A 10	191	0.828	11.9	11.86
A 11	187	0.837	11.7	11.72
A 13	205	0.867	11.6	11.54
B 1 to B 3	106	0.733	12.0	12.03
B 4	114	0.739	12.0	12.08
B 8 to B 9	167	0.813	11.8	11.81
B 10 to B 12	158	0.800	11.9	11.87
B 13	114	0.765	11.7	11.73
B 14	171	0.802	12.0	11.99
B 15	207	0.827	12.0	12.02
B 16	167	0.812	11.8	11.82
C 1	116	0.757	11.88	11.87
C 2	205	0.936	10.70	10.81
C 3	245	0.848	11.92	12.07
C 4	132	0.800	11.54	11.55
C 5	152	0.850	11.23	11.21
C 6	176	0.894	10.95	10.98
C 7	160	0.804	11.9	11.84
C 8	195	0.826	11.91	11.93
C 9	107	0.771	11.55	11.54
n-C_5	72.1	0.636	12.94	12.80
C_6H_6	78.05	0.882	9.75	9.82
n-C_6	114.13	0.707	12.65	12.54
C_7H_8	92.06	0.870	10.16	10.19

*Samples labeled A and B are C_7+ fractions, whereas samples labeled C are stock-tank oil samples. The last four samples are pure components.

Regrouping (Pseudoization) and Mixing Rules

The cost and resources required for simulating phase and volumetric behavior increases considerably with the number of components used to describe the fluid.

Some authors have suggested that as few as 2 or as many as 50 components may be required to predict reservoir-fluid behavior. In general, it might be reasoned that the accuracy of EOS predictions increases with the number of components used to describe the reservoir fluid. Based on experience, two observations can be made: (1) it is not merely the number of fractions used, but what spectra of components they represent that affects the accuracy of predictions, and (2) with proper grouping, the increase in accuracy resulting from more fractions diminishes rapidly.

Questions arising in this regard include the following.

1. How many pseudocomponents are required?
2. How should they be chosen from a partial or complete C_7+ analysis?
3. What mixing rules should be used for calculating properties of the pseudocomponents?

Based on preliminary results of EOS predictions for reservoir fluids, several guidelines are proposed for the pseudoization process.

TABLE 3—GENERALIZED SINGLE-CARBON-NUMBER PHYSICAL PROPERTIES

SCN	Normal Boiling Point (K)	Normal Boiling Point (°R)	Specific Gravity (60/60)	Watson Characterization Factor	Molecular Weight	Critical Temperature (K)	Critical Temperature (°R)	Critical Pressure (kPa)	Critical Pressure (psia)	Acentric Factor	PR EOS Methane Interaction Coefficient
6	337	607	0.690	12.27	84	512	923	3340	483	0.250	0.0298
7	366	658	0.727	11.96	96	548	985	3110	453	0.280	0.0350
8	390	702	0.749	11.87	107	575	1036	2880	419	0.312	0.0381
9	416	748	0.768	11.82	121	603	1085	2630	383	0.348	0.0407
10	439	791	0.782	11.83	134	626	1128	2420	351	0.385	0.0427
11	461	829	0.793	11.85	147	648	1166	2230	325	0.419	0.0442
12	482	867	0.804	11.86	161	668	1203	2080	302	0.454	0.0458
13	501	901	0.815	11.85	175	687	1236	1960	286	0.484	0.0473
14	520	936	0.826	11.84	190	706	1270	1860	270	0.516	0.0488
15	539	971	0.836	11.84	206	724	1304	1760	255	0.550	0.0502
16	557	1002	0.843	11.87	222	740	1332	1660	241	0.582	0.0512
17	573	1032	0.851	11.87	237	755	1360	1590	230	0.613	0.0523
18	586	1055	0.856	11.89	251	767	1380	1530	222	0.638	0.0530
19	598	1077	0.861	11.91	263	778	1400	1480	214	0.662	0.0537
20	612	1101	0.866	11.92	275	790	1421	1420	207	0.690	0.0544
21	624	1124	0.871	11.94	291	801	1442	1380	200	0.717	0.0551
22	637	1146	0.876	11.95	300	812	1461	1330	193	0.743	0.0558
23	648	1167	0.881	11.95	312	822	1480	1300	188	0.768	0.0565
24	659	1187	0.885	11.96	324	832	1497	1260	182	0.793	0.0571
25	671	1207	0.888	11.99	337	842	1515	1220	177	0.819	0.0575
26	681	1226	0.892	12.00	349	850	1531	1190	173	0.844	0.0581
27	691	1244	0.896	12.00	360	859	1547	1160	169	0.868	0.0586
28	701	1262	0.899	12.02	372	867	1562	1130	165	0.894	0.0591
29	709	1277	0.902	12.03	382	874	1574	1110	161	0.915	0.0595
30	719	1294	0.905	12.04	394	882	1589	1090	158	0.941	0.0599
31	728	1310	0.909	12.04	404	890	1603	984	143	0.897	0.0605
32	737	1326	0.912	12.05	415	898	1616	952	138	0.909	0.0609
33	745	1341	0.915	12.05	426	905	1629	926	134	0.921	0.0613
34	753	1355	0.917	12.07	437	911	1640	896	130	0.932	0.0616
35	760	1368	0.920	12.07	445	917	1651	877	127	0.942	0.0620
36	768	1382	0.922	12.08	456	924	1662	850	124	0.954	0.0623
37	774	1394	0.925	12.08	464	929	1673	836	121	0.964	0.0627
38	782	1407	0.927	12.09	475	935	1683	811	118	0.975	0.0630
39	788	1419	0.929	12.10	484	940	1693	795	115	0.985	0.0633
40	796	1432	0.931	12.11	495	947	1703	771	112	0.997	0.0635
41	801	1442	0.933	12.11	502	951	1712	760	110	1.006	0.0638
42	807	1453	0.934	12.13	512	955	1720	741	108	1.016	0.0640
43	813	1464	0.936	12.13	521	960	1729	727	105	1.026	0.0642
44	821	1477	0.938	12.14	531	967	1739	706	103	1.038	0.0645
45	826	1487	0.940	12.14	539	971	1747	696	101	1.048	0.0648

Regrouping Scheme

Consider EOS predictions using two groupings of C_{7+} SCN fractions: (1) C_7, C_8, C_9, C_{10}, C_{11}, and C_{12+}, and (2) $C_{7\text{-}10}$, $C_{11\text{-}14}$, $C_{15\text{-}18}$, $C_{19\text{-}25}$, and $C_{26\text{-}35}$. It will be shown that the latter choice yields considerably better results than the former, with a complete SCN description of the C_{7+} fraction used as the base of comparison. (See Figs. 2a and 2b.)

A method is proposed for estimating the number of MCN groups needed for adequate plus-fraction description, as well as which SCN groups belong to the MCN group. It is based on Sturge's rule and the observation that the proposed distribution model is similar to a folded log-normal distribution. The number of MCN groups, N_g, is given by

$$N_g = \text{Int}[1+3.3\cdot\log_{10}(N-n)]. \quad \text{(19)}$$

For black-oil systems, this number probably can be *reduced* by one.

The molecular weights separating each MCN group are taken as

$$M_I = M_n\{\exp[(1/N_g)\cdot\ln(M_N/M_n)]\}^I, \quad \text{(20)}$$

where M_N is the molecular weight of the last SCN group (which may actually be a plus fraction), and $I=1, 2 \ldots N_g$. Molecular weights of SCN groups falling within the boundaries of these values are included in the MCN group, I.

Mixing Rules

Two sets of mixing rules for calculating critical properties (including acentric factor and specific gravity) of MCN groups are discussed. The pseudoization process does not appear, from preliminary calculations, to influence EOS predictions greatly. For completeness, however, both methods of pseudoization are compared. Method 1 employs simple molar weighting.[23] Method 2 relies on various average boiling points to calculate MCN properties.

Molar and volumetric properties of MCN groups are always calculated using the mixing rules

$$M_I = \sum^{I} (z_i/z_I)\, M_i \quad \text{(21)}$$

and

$$\gamma_I = 1.0\Big/\Big[\sum^{I} (f_{wi}/f_{wI})/\gamma_i\Big]. \quad \text{(22)}$$

and Ref. 12 suggests that pseudocritical volume should be calculated using weight fractions

$$V_{pcI}=\sum^{I}(f_{wi}/f_{wI})\cdot V_{ci}, \quad \text{.................}(23)$$

where z_I and f_{wI} are the sums of z_i and f_{wi} found in MCN group I.

MCN acentric factors are usually calculated using Kay's mixing rule, though Robinson and Peng[5] suggest a considerably more complicated expression,

$$\omega_I=-\log_{10}$$

$$\left\{\left[\sum^{I}(z_i/z_I)\cdot p_{ci}\cdot 10^{-(1+\omega_i)}\right]/p_{cI}\right\}-1.0, \quad \text{...}(24)$$

for averaging the acentric factor of PNA groups with a given SCN. No comparison is given to document the advantage of using Eq. 24.

Method 1: Pseudocritical Mixing Rules. On the basis of results given in Ref. 24, one can use pseudocritical pressure and temperature calculated using Kay's mixing rule in the Peng-Robinson EOS[22] with reasonable matching success of thermal processes. No indication was given, however, whether the same was true for more complicated systems such as miscible gas injection. However, since the mixing rules are simple and easy to apply, they are presented as Method 1 in this paper.

$$p_{pcI}=\sum^{I}(z_i/z_I)\cdot p_{ci}, \quad \text{..................}(25)$$

$$T_{pcI}=\sum^{I}(z_i/z_I)\cdot T_{ci}, \quad \text{..................}(26)$$

and

$$\omega_I=\sum^{I}(z_i/z_I)\cdot\omega_i. \quad \text{....................}(27)$$

Method 2: Average Boiling Points. This method is based on relations developed between molal-, weight-, and mean-average boiling points, and pseudocritical and critical properties.[12]

Molal-average boiling point for MCN groups is calculated using Kay's mixing rule.

$$T_{bmI}=\sum^{I}(z_i/z_I)\cdot T_{bi} \quad \text{.................}(28a)$$

Weight-average boiling point for MCN groups is calculated using weight fractions as the mixing parameter and is given by

$$T_{bwI}=\sum^{I}(f_{wi}/f_{wI})\cdot T_{bi} \quad \text{.................}(28b)$$

Cubic-average boiling point is given by

$$T_{bcI}=\left[\sum^{I}(f_{vi}/f_{vI})\cdot T_{bi}^{1/3}\right]^3, \quad \text{.............}(28c)$$

where volume fractions f_v are merely given by

$$f_{vi}=f_{wi}/\gamma_i,\ f_{vI}=\sum^{I}f_{vi} \quad \text{.................}(29)$$

Mean-average boiling point, T_{bI}, is defined as the arithmetic average of true molal- and cubic-average boiling points.

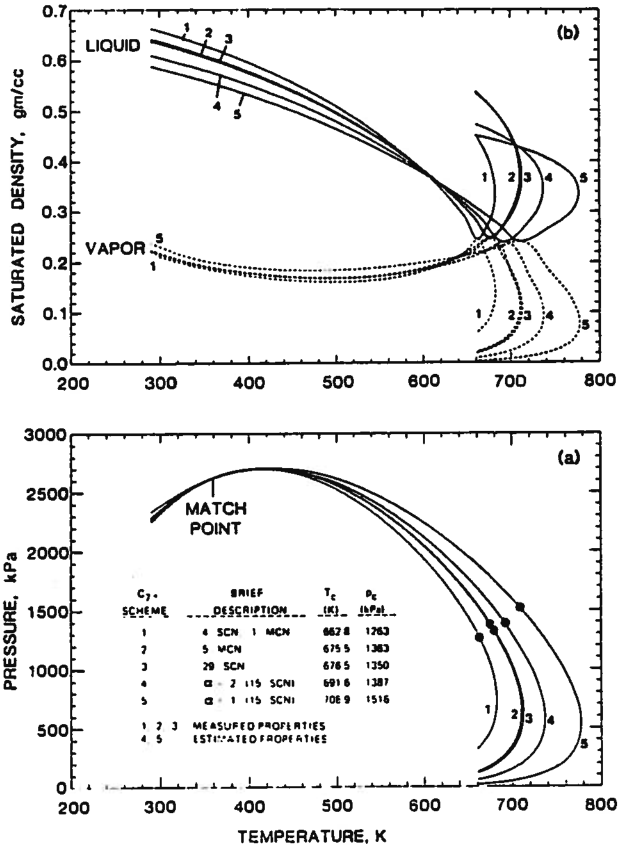

Fig. 2—Effect of several C_7+ characterizations on Peng-Robinson EOS predictions for the Hoffman *et al.* reservoir oil.

True critical temperature of MCN groups is calculated using weight-average boiling point.

$$T_{cI}=a\,T_{bwI}^{b}\,\gamma^{c}. \quad \text{.......................}(30a)$$

Pseudocritical temperatures are calculated using molal-average boiling points.

$$T_{pcI}=a\,T_{bmI}^{b}\,\gamma^{c}. \quad \text{......................}(30b)$$

Pseudoreduced critical temperature, used for calculating pseudocritical pressure, is then defined by

$$T_{prcI}\equiv T_{cI}/T_{pcI}. \quad \text{.......................}(30c)$$

Pseudocritical pressures are calculated using mean-average boiling point.

$$p_{pcI}=a\bar{T}_{bI}^{\,b}\,\gamma^{c} \quad \text{.......................}(31a)$$

The graphical relation between pseudoreduced critical temperature and pseudoreduced critical pressure[12] was curve-fit to give

$$p_{prcI}=1+8.467\cdot\Upsilon+1.654\cdot\Upsilon^2+29.56\cdot\Upsilon^3. \quad \text{..}(31b)$$

where $\Upsilon\equiv T_{prcI}-1$. Combining Eqs. 31a and 31b yields the relation for calculating critical pressure of MCN groups.

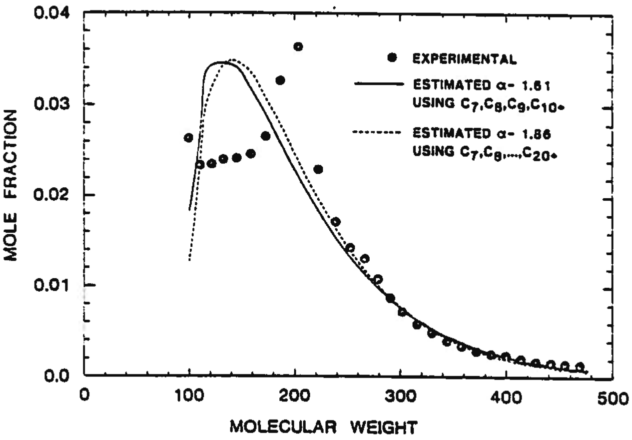

Fig. 3—Comparison of experimental and estimated molar distribution for the Hoffman *et al.* reservoir oil C_{7+} fraction (CMWI's used).

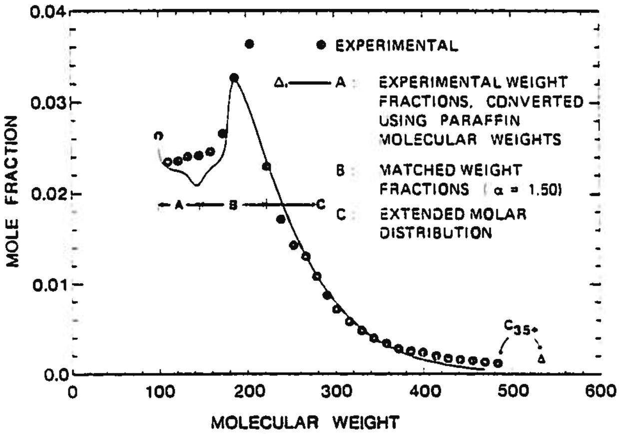

Fig. 4—Comparison of experimental and converted/matched/extended molar distributions for the Hoffman *et al.* reservoir oil C_{7+} fraction (VMWI's used in Region B).

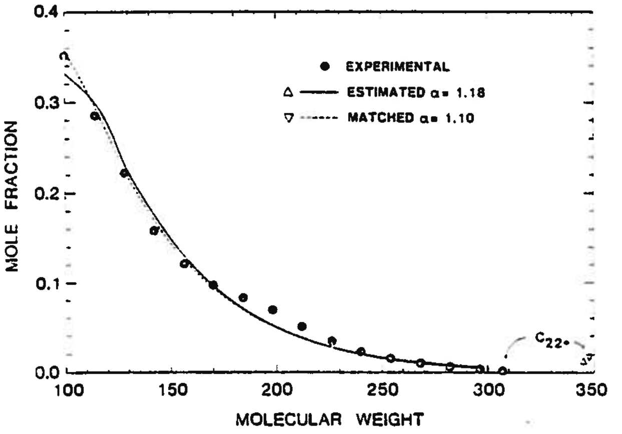

Fig. 5—Comparison of experimental and estimated/matched molar distributions for the Hoffman *et al.* reservoir gas C_{7+} fraction (CMWI's used).

$$p_{cl}=p_{prcl}p_{pcl} \quad \ldots\ldots (32)$$

Critical volumes can be estimated using mean-average boiling point,

$$V_{cl}=a\,\bar{T}^{b}_{bl}\gamma^{c}_{l} \quad \ldots\ldots (33)$$

Constants *a*, *b*, and *c* are those found in Table 1, depending on which property is being estimated.

Results and Discussion

Molar Distribution Example: Reservoir Oil

Experimental data presented by Hoffman *et al.*[25] for calculating critical properties of a reservoir black oil constitute one of the most comprehensive analyses available in the literature: mole fractions, molecular weights, specific gravities, and normal boiling points are reported for SCN groups 7 through 35.

The Ref. 25 oil was chosen to illustrate the versatility of the proposed molar distribution model. It exhibits a bimodal molar distribution, which is unusual. This special case reveals limitations of the proposed model, but also shows its flexibility.

The complete C_7-through-C_{35} molar analysis was reduced to three partial analyses: (1) C_7, C_8, C_9, C_{10+}; (2) C_7, C_8 . . . C_{15+}; and (3) C_7, C_8 . . . C_{20+}. These were first used to estimate α using Eq. 10 and correction tables. Next, the partial molar distributions were fit using the CMWI-2 method. Finally, the partial weight distribution C_{11}, C_{12} . . . C_{15+} was fit using the variable VMWI method.

Estimates of α calculated from Eq. 10 and correction tables were 1.61, 1.81, and 1.86 for the three partial analyses, respectively. Corresponding values of η were 91.6, 91.2 and 91.1. Using these parameters in the proposed probabilistic model gave the two molar distributions presented in Fig. 3 for α=1.61 and α=1.86.

When the same three partial molar distributions were fit using the CMWI-2 procedure ($\Delta M_i=14$ and $\bar{M}_7=100$), optimal values of α=1.78, 1.93, and 1.64 were calculated. Corresponding values of η were 91.2, 91.0, and 91.5. Each distribution was extended to C_{35} by using the same molecular weight interval. Results were nearly identical to those presented in Fig. 3.

Although matches of molar distributions presented in Fig. 3 are reasonable, the proposed model did not reproduce bimodal behavior. Another approach was chosen to extend the C_{15+} partial analysis.

Fig. 4 presents the matched and extended molar distribution. First, weight fractions of SCN groups 7 through 10 were converted to mole fractions by using paraffin molecular weights. Weight fractions of carbon number groups 11 through 15+ were then fit by using η=148 (calculated from Eq. 3b) and the VMWI method. Optimal α was 1.5, although values 1.4 to 1.6 yielded near-perfect matches.

Molar Distribution Example: Reservoir Gas

Hoffman *et al.*[25] present experimental data for the C_{7+} fraction of the gas-cap fluid associated with the previous reservoir oil. The complete molar distribution was reduced to the same three partial analyses as in the previous example. Estimated values of α from Eq. 10

TABLE 4—COMPARISON OF SCN CRITICAL PROPERTIES BASED ON EXPERIMENTAL AND ESTIMATED BOILING POINTS AND SPECIFIC GRAVITIES

	Based on Experimental Boiling Points and Specific Gravities			Based on K Factors From Eqs. 18a through 18d and Paraffin Mole Weights				
	Critical					Critical		
SCN	Pressure (kPa)	Temperature (K)	Acentric Factor	Normal Boiling Point (K)	Specific Gravity (60/60)	Pressure (kPa)	Temperature (K)	Acentric Factor
7	3223	559.1	0.2763	349.1	0.6981	3162	525.5	0.2679
8	2814	585.3	0.3228	379.0	0.7253	2857	559.1	0.3080
9	2603	612.8	0.3565	407.7	0.7513	2620	591.0	0.3457
10	2348	634.4	0.3981	435.2	0.7764	2430	621.5	0.3815
11	2179	656.0	0.4328	462.0	0.8008	2275	651.0	0.4155
12	2056	676.8	0.4632	484.4	0.8120	2105	672.8	0.4526
13	1957	696.6	0.4912	505.7	0.8212	1956	692.8	0.4896
14	1908	717.2	0.5107	526.1	0.8295	1828	711.7	0.5263
15	1811	733.4	0.5404	546.0	0.8382	1718	730.1	0.5626
16	1682	745.6	0.5800	565.3	0.8462	1621	747.7	0.5989
17	1519	753.2	0.6350	583.6	0.8526	1533	764.0	0.6357
18	1465	767.2	0.6623	601.3	0.8586	1454	779.5	0.6729
19	1406	779.6	0.6926	618.8	0.8651	1385	794.9	0.7100
20	1409	796.5	0.7002	636.2	0.8723	1324	810.4	0.7468
21	1368	808.6	0.7248	652.7	0.8780	1266	824.7	0.7847
22	1328	820.0	0.7499	669.3	0.8845	1216	839.1	0.8225
23	1311	827.1	0.7625	685.1	0.8896	1168	852.5	0.8617
24	1274	836.8	0.7879	700.9	0.8955	1125	866.0	0.9008
25	1239	846.3	0.8130	716.7	0.9022	1087	879.9	0.9397
26	1204	855.2	0.8396	732.3	0.9087	961	893.4	0.9033
27	1171	863.9	0.8661	747.6	0.9150	913	906.5	0.9245
28	1142	872.4	0.8924	762.6	0.9211	870	919.4	0.9460
29	1111	880.2	0.9203	777.3	0.9270	830	932.0	0.9678
30	1083	887.8	0.9479	791.9	0.9327	793	944.3	0.9900
31	972	895.1	0.9036	806.2	0.9383	759	956.3	1.0125
32	937	902.1	0.9161	820.3	0.9437	728	968.1	1.0354
33	906	908.7	0.9281	834.2	0.9490	698	979.7	1.0587
34	874	914.7	0.9400	847.8	0.9542	671	991.1	1.0826
35	846	920.3	0.9513	958.9	0.9942	496	1081.3	1.3149
	Multi-Carbon-Number properties using Kay's mixing rule					Multi-Carbon-Number properties using average boiling points		
	2765	596.4	0.3359			2816	599.6	0.3359
	2014	689.3	0.4777			2044	691.3	0.4777
	1669	745.5	0.5875			1671	746.6	0.5875
	1356	807.9	0.7315			1370	809.6	0.7315
	1065	883.1	0.9004			1112	885.2	0.9004

and correction tables were 1.18, 1.20, and 1.21, respectively. The value of η was 92.6 for all three estimates of α.

The three partial analyses were fit by the CMWI-2 method ($\Delta M_i = 14$ and $\bar{M}_7 = 100$). Optimal values of α were 1.10, 1.07, and 1.08, with corresponding values of $\eta = 93.0$, 93.1, and 93.1

Fig. 5 presents the predicted molar distributions. There was essentially no difference between predicted distributions for the three partial distributions—i.e., it was sufficient to use only C_7, C_8 . . . $C_{10}+$ mole (or weight) fractions to yield an excellent match of the complete molar distribution. •

Physical Properties Example: Reservoir Oil

This example is divided into two parts: (1) estimation of SCN physical properties and (2) pseudoization or regrouping of SCN physical properties.

Two sets of SCN physical properties were estimated using the Riazi-Daubert correlations (Eq. 14 and Table 1); Table 4 gives these results. The first set was calculated from measured boiling points and specific gravities reported by Hoffman *et al.* The second set was calculated using the variable *K*-factor correlation proposed by Haaland[20] and molecular weights resulting from the match and extension of C_7, C_8, C_9, and $C_{10}+$ data presented earlier. This case might represent a typical situation when few experimental data are available—i.e., a worst-case example.

SCN physical properties calculated from measured boiling points and specific gravities were then regrouped using the two procedures outlined previously under "Regrouping (Pseudoization) and Mixing Rules." Table 4 presents these results. Little difference in MCN properties is observed, though it may be more pronounced as the number of MCN groups decreases.

EOS Application: Reservoir Oil

The previous examples are attempts to illustrate how the proposed methods can be used. They have also given an indication of the accuracy these methods provide. Since the purpose of C_7+ characterization is to improve EOS predictions, several examples were generated using the Peng-Robinson EOS. The Hoffman *et al.* reservoir oil was chosen since it offered a sound basis for comparison—i.e., EOS predictions based on complete, experimental molar distribution and properties.

Three EOS predictions were used to compare various

C_7+ characterizations: (1) phase envelope estimation (bubble- and dewpoint loci), (2) critical point estimation and (3) equilibrium phase density estimation. Although critical point and dewpoint regions of this system were clearly outside realistic operating conditions, the example still gives an indication of C_7+ characterization on EOS predictions.

Figs. 2a and 2b present results of EOS predictions for five different C_7+ characterizations. Brief descriptions of the five follow this section. All data used by the EOS can be found in Table 4 or can be calculated using equations presented in the text. For all cases, the measured bubble-point pressure [2640 kPa at 366.9 K (383 psi at 200.8°F)] was matched using the binary interaction coefficient between methane and the last component (be it an SCN or MCN fraction).

Case 3 represents the base case. All SCN measured properties were used to estimate critical properties, acentric factors, and methane binary interaction coefficients. The complete C_7-through-C_{35} molar distribution was also used.

Case 2 represents a regrouping of the SCN properties from Case 3 using the pseudocritical Kay's mixing rule.[23] As indicated in Table 4 and substantiated by EOS calculations, the two different mixing rules did not alter predictions appreciably.

Case 1 used the first four SCN properties from Case 3, but lumped all remaining groups into a $C_{12}+$ fraction. The $C_{12}+$ properties were calculated using Kay's mixing rule.

Cases 4 and 5 should be compared with each other, as well as with Case 3 (base case). They represent, in a sense, the worst possible cases. That is, molar distributions were merely assigned values of $\alpha=1$ and 2. Also, they were extended only to $C_{22}+$. The C_7+ specific gravity and variable K factors[20] were used to estimate specific gravities and boiling points. These cases indicate (1) the influence of molar distribution and (2) the accuracy one might expect from EOS predictions using only C_7+ properties and proposed methods of characterization.

Conclusions

An attempt has been made to develop a systematic characterization scheme for describing the molar distribution and physical properties of hydrocarbon plus fractions. Its purpose is to enhance the predictive capabilities of EOS's applied to naturally occurring hydrocarbon mixtures. Proposed methods, as summarized here, were developed with the assumption that minimal experimental data are available and that a certain degree of estimation and extrapolation is necessary.

1. A probabilistic model based on the gamma distribution function is proposed for describing the molar distribution of plus fractions such as C_7+. This model can be used to estimate, match, or extend experimental molar distributions. Examples are presented to illustrate several uses of the proposed model.
2. The Riazi-Daubert generalized physical properties correlation is extended for critical pressure estimation at boiling points higher than 730 K (850°F). The correlation is also used to develop a generalized relation between molecular weight, specific gravity, and the Watson characterization factor.
3. A method is proposed for estimating specific gravities and boiling points of SCN groups. It is based on the Watson characterization factor, which is assumed constant for all SCN groups.
4. As an alternative to this method, a set of generalized physical properties is proposed. It is based on boiling points, specific gravities, and molecular weights originally presented by Katz and Firoozabadi. Molecular weights for SCN groups 22 through 45 are extrapolated in a more consistent manner. The Riazi-Daubert correlations are used to calculate generalized critical properties; acentric factors and methane binary interaction coefficients (for the Peng-Robinson EOS) are calculated using other correlations.
5. A procedure is proposed for regrouping SCN groups into a minimum number of pseudocomponents. It estimates the number of MCN groups needed and determines which SCN groups constitute each MCN group. Two sets of mixing rules are proposed for calculating MCN critical properties.
6. Examples show that the accuracy of EOS predictions is not dependent merely on the number of C_7+ fractions but also on which components are found in each fraction.

Nomenclature

a,b,c = constants in the generalized physical-properties correlation
$E(\alpha)$ = error function
f = frequency of occurrence
f_w = weight fraction
i = single carbon number index ($=n$, $n+1 \ldots N$)
I = multiple carbon number index ($=1, 2, 3 \ldots$ Ng)
J_a = Jacoby aromaticity factor, fraction
K = Watson Characterization Factor, $°R^{1/3}$
m_G = geometric average molecular weight
M = molecular weight, kg/mol
M_n^+ = molar average molecular weight, kg/mol
$\bar{M}$ = average molecular weight, kg/mol
n = first SCN in a C_n+ fraction
N = last SCN (or MCN) in a C_n+ fraction
N_g = number of MCN groups
p = pressure, kPa (psia)
$p(x)$ = probability density function
$P(X \leq x)$ = cumulative probability function
T = temperature, °R (K)
T_{tb} = true boiling point
T_b = boiling point
$\bar{T}_b$ = mean average boiling point
V = volume, m^3 (cu ft)
x = measured variable
X = all values of variable
y = normalized molecular weight variable
Y = variable in α estimation equation
z = mole fraction

Subscripts

b = boiling point

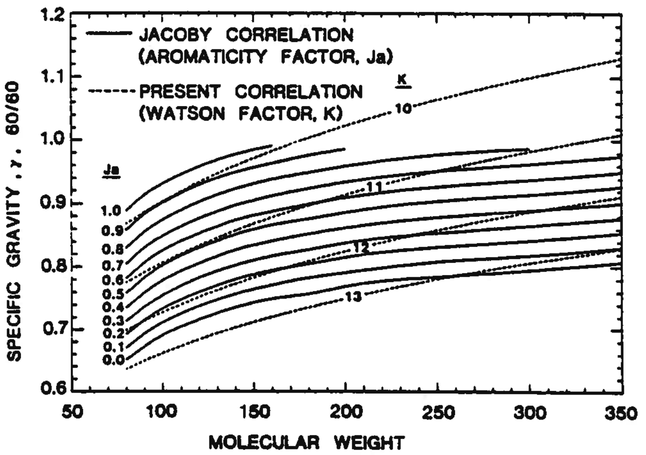

Fig. A-1—Comparison of specific gravity and molecular weight relations based on two different characterization factors.

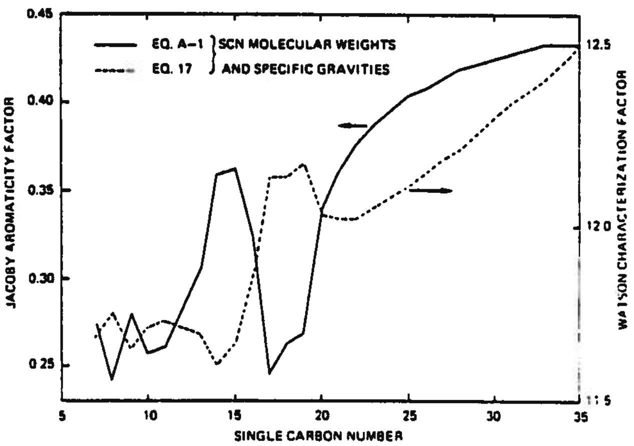

Fig. A-2—Comparison of the variation in two characterization factors as a function of SCN for the Hoffman *et al.* reservoir oil C_7+ fraction.

bc = cubic volume average boiling point
bi = normal boiling point of SCN i
bm = molal average boiling point
bw = weight average boiling point
c = critical property
cm = molar critical property
G = geometric average
lm = liquid molar
n = first SCN group in the C_n+ fraction
N = last SCN (or MCN) in the C_n+ fraction
n^+ = plus fraction beginning with SCN group C_n
N^+ = last MCN group in the C_n+ fraction
pc = pseudocritical property
pr = pseudoreduced critical property (from Θ_c/Θ_{pc})
w = weight

Greek

α,β,η = parameters in the gamma distribution function
γ = specific gravity at 60°F and 60 psia
Γ = gamma function
δ = binary interaction coefficient
$\bar{\Delta}$ = average deviation = (calculated-measured)/measured
Θ = property
ρ = liquid density, kg/m^3 (lbm/cu ft)
Υ = variable in property correlation
ω = acentric factor

Acknowledgments

I thank E.E. and T.C. Whitson, L. and B.P. Walker, J. Faust and the late John Hassler—all independent oil and gas persons—for continual encouragement during preparation and completion of this work. Support from Frying Pan Publications Inc. is gratefully acknowledged.

References

1. Hopke, S.W. and Lin, C.J.: "Applications of the BWRS Equation to Absorber Systems," *Proc.*, 53rd Gas Processors Assn. Convention (1974) 63-71.
2. Bergman, D.F.: "Predicting the Phase Behavior of Natural Gas in Pipelines," PhD dissertation, U. of Michigan, Ann Arbor (1976).
3. Erbar, J.H.: "Prediction of Absorber Oil K-Values and Enthalpies," Research Report 13, Gas Processors Assn., Tulsa (1977).
4. Cavett, R.H.: "Physical Data for Distillation Calculations—Vapor-Liquid Equilibrium," *Proc.*, 27th API Meeting, San Francisco (1962).
5. Robinson, D.B. and Peng, D.-Y.: "The Characterization of the Heptanes and Heavier Fractions," Research Report 28, Gas Processors Assn., Tulsa (1978).
6. Watson, K.M., Nelson, E.F., and Murphy, G.B.: "Characterization of Petroleum Fractions," *Ind. and Eng. Chem.* (1935) **27**, 1460-64.
7. Katz, D.L. and Firoozabadi, A.: "Predicting Phase Behavior of Condensate/Crude-Oil Systems Using Methane Interaction Coefficients," *J. Pet. Tech.* (Nov. 1978) 1649-55; *Trans.*, AIME, **228**.
8. Pearson, K.: "Contributions to the Mathematical Theory of Evolution. II. Skew Variations in Homogeneous Material," *Philosophical Trans.*, Royal Society of London, Series A (1895) **186**, 343-414.
9. Edmister, W.C.: "Improved Integral Technique for Petroleum Distillation Calculations," *Ind. and Eng. Chem.* (1955) **47**, 1685-90.
10. Taylor, D.L. and Edmister, W.C.: "Solutions for Distillation Processes Treating Petroleum Fractions," *AIChE J.* (Nov. 1971) **17**, 1324-29.
11. Greenwood, J.A. and Durand, D.: "Aids for Fitting the Gamma Distribution by Maximum Likelihood," *Technometrics* (1960) **2**, 35-65.
12. Smith, R.L. and Watson, K.M.: "Boiling Points and Critical Properties of Hydrocarbon Mixtures," *Ind. and Eng. Chem.* (1937) **29**, 1408-14.
13. Watson, K.M. and Nelson, E.F.: "Improved Methods for Approximating Critical and Thermal Properties of Petroleum Fractions," *Ind. and Eng. Chem.* (1933) **25**, 880-87.
14. Kesler, M.G., Lee, B.I., and Sandler, S.I.: "A Third Parameter for Use in General Thermodynamic Correlations," *Ind. and Eng. Chem. Fund.* (1979) **18**, 49-54.
15. Kesler, M.B. and Lee, B.I.: "Improve Predictions of Enthalpy of Fractions," *Hydrocarbon Processing* (March 1976) 153-58.
16. Hariu, O.H. and Sage, R.C.: "Crude Split Figured by Computer," *Hydrocarbon Processing* (April 1969) 143-48.
17. Riazi, M.R. and Daubert, T.E.: "Simplify Property Predictions," *Hydrocarbon Processing* (March 1980) 115-16.
18. "Selected Values of Properties of Hydrocarbons and Related Compounds," API Project 44, Texas A&M U., College Station, (1969).

TABLE A-1—COEFFICIENTS USED IN THE YARBOROUGH SPECIFIC GRAVITY CORRELATION

Jacoby Aromaticity (Fraction)	b_0	b_1	b_2	b_3
0.0	-7.43855×10^{-2}	$-1.72341\times10^{+0}$	1.38058×10^{-3}	-3.34169×10^{-2}
0.1	-4.25800×10^{-1}	-7.00017×10^{-1}	-3.30947×10^{-5}	8.65465×10^{-2}
0.2	-4.47553×10^{-1}	-7.65111×10^{-1}	1.77982×10^{-4}	1.07746×10^{-1}
0.3	-4.39105×10^{-1}	-9.44068×10^{-1}	4.93708×10^{-4}	1.19267×10^{-1}
0.4	-2.73719×10^{-1}	$-1.39960\times10^{+0}$	3.80564×10^{-3}	5.92005×10^{-2}
0.6	-7.39412×10^{-3}	$-1.97063\times10^{+0}$	5.87273×10^{-3}	-1.67141×10^{-2}
0.8	-3.17618×10^{-1}	-7.78432×10^{-1}	2.58616×10^{-3}	1.08382×10^{-3} — -1

$$c J_a - d\frac{J_a}{M} = \gamma - a + \frac{b}{M} \Rightarrow \gamma = a + cJ_a - d\frac{J_a}{M} - \frac{b}{M}$$

a b c d

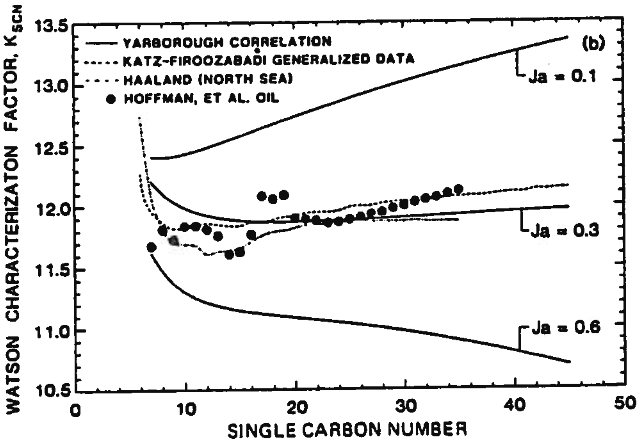

Fig. A-3—Variation in Watson characterization factor as a function of SCN.

19. Simon, R. and Yarborough, L.: "A Critical Pressure Correlation for Gas-Solvent-Reservoir Oil Systems," *J. Pet. Tech.* (May 1963) 556-60; *Trans.*, AIME, **228**.
20. Haaland, S.: "Characterization of North Sea Crude Oils and Petroleum Fractions," MS thesis, Norwegian Inst. of Technology, U. of Trondheim, Norway, June 1981.
21. Edmister, W.C.: *Pet. Refiner* (1958) **37**, 173.
22. Peng, D.-Y. and Robinson, D.B.: "A New Two-Constant Equation of State," *Ind. and Eng. Chem. Fund.* (1976) **15**, 59-64.
23. Kay, W.B.: "Density of Hydrocarbon Gases and Vapors at High Temperature and Pressure," *Ind. and Eng. Chem.* (1936) **28**, 1014-19.
24. Lee, S.T., *et al.*: "Experimental and Theoretical Studies on the Fluid Properties Required for Simulation of Thermal Processes," *Soc. Pet. Eng. J.* (Oct. 1981) 535-50.
25. Hoffman, A.E., Crump, J.S., and Hocott, C.R.: "Equilibrium Constants for a Gas-Condensate System," *Trans.*, AIME (1953) **198**, 1-10.
26. Jacoby, R.: "NGPA Phase Equilibrium Project," *Proc.*, API (1964) 288.
27. Yarborough, L.: "Application of a Generalized Equation of State to Petroleum Reservoir Fluids," *Equation of State in Engineering and Research*, K.C. Chao and R.L. Robinson Jr. (eds.), Advances in Chemistry Series, Amer. Chem. Soc. (1978) **182**, 386-439.

APPENDIX

An Alternative Characterization Parameter: The Jacoby Aromaticity Factor

Although the Watson characterization factor was chosen to correlate molecular weight, specific gravity, and boiling point, an alternative would have been the Jacoby aromaticity factor, J_a.[26] Fig. A-1 shows the variation in specific gravity with molecular weight for several values of J_a. The original curves presented by Jacoby were fit by the equation

$$J_a=(\gamma-0.8468+15.8/M)/(0.2456-1.77/M). \quad \text{(A-1)}$$

Also shown in Fig. A-1 are several curves generated using Eq. 17 and the Watson characterization factor. The difference in correlations seems to be only qualitative. For example, where the Watson factor indicates increasing paraffinicity, the Jacoby factor indicates decreasing aromaticity. This is illustrated in Fig. A-2, which plots each characterization factor vs. SCN for the Hoffman *et al.* reservoir oil.

Yarborough[27] used the Jacoby correlation to generate a set of curves relating specific gravity to SCN. Unfortunately, the relation has an unusual behavior for low SCN groups. This may be a result of his attempt "to reflect the behavior of the distillation fractions for carbon numbers up to C_{13}."

The proposed best fit of Yarborough's Fig. 19 is

$$\gamma_i=\exp[b_0+b_1/i+b_2\cdot i+b_3\cdot\ln(i)], \quad \text{........ (A-2)}$$

where constants b_0, b_1, b_2, and b_3 are given in Table A-1 for values of J_a=0.0, 0.1, 0.2, 0.3, 0.4, 0.6, and 0.8. Linear interpolation between values of specific gravity is recommended—i.e., if J_a=0.5, use coefficients for J_a=0.4 and 0.6 to calculate two specific gravities, from which specific gravity for J_a=0.5 is found.

Yarborough's curves for J_a=0.1, 0.3, and 0.6 were converted to Watson characterization factors using Eq. 17 and paraffin molecular weights. Results are plotted in Fig. A-3, showing that the variation in K is dissimilar for each value of J_a, though the curve for J_a=0.3 has a variation similar to the one proposed by Haaland.

There does not appear to be any real advantage to the Jacoby aromaticity factor or Yarborough's modification. Although the Watson K factor was used in this study, this should not alter the general conclusions made concerning C_7+ characterization and its effect on EOS predictions.

SI Metric Conversion Factors

°R	(°R/1.8)		=	K
psi	× 6.894 757	E+00	=	kPa

*Conversion factor is exact.

SPEJ

Original manuscript received in Society of Petroleum Engineers office Aug. 3, 1980. Paper accepted for publication Nov. 20, 1981. Revised manuscript received Dec. 28, 1982. Paper (SPE 12233) first presented at the 1980 European Offshore Petroleum Conference and Exhibition held in London, Oct. 21–24.

A.3-1

Evaluating Constant-Volume Depletion Data

Curtis H. Whitson, Rogaland District C.
Stein B. Torp,* Norwegian Inst. of Technology

Abstract

This paper presents methods for evaluating constant-volume depletion (CVD) data obtained from experimental analyses of gas condensates and volatile oils. Theoretical and practical developments are supported by experimental data from a North Sea gas-condensate fluid.

The three major contributions of the work are: (1) presentation of material-balance equations to calculate fluid properties from measured CVD data, (2) a simple method for calculating black-oil formation volume factors and solution GOR's using material-balance results and a separator flash program, and (3) investigation of the Peng-Robinson (PR) equation of state (EOS) as a tool for matching measured PVT data and studying vapor/liquid phase behavior during CVD.

Introduction

CVD experiments are performed on gas condensates and volatile oils to simulate reservoir depletion performance and compositional variation. Measured data can be used in a variety of reservoir engineering calculations, among the most useful being material-balance calculations, generating black-oil PVT properties and, more recently, the tuning of empirical EOS. All these applications are addressed in this paper.

Few engineers are aware of useful fluid properties that can be derived from CVD data—e.g., *liquid* composition (and therefrom K-values), density, and molecular mass of the C_{7+} fraction, *vapor* density, and *total* system molecular mass. Only experimental CVD data and simple material-balance equations are used to calculate these data. A procedure outlining these calculations was first presented by Reudelhuber and Hinds.[1] Their description, however, is somewhat difficult to follow and not extensively known or used by petroleum engineers. The material-balance relations are presented here in equation form using current SPE nomenclature.

Based on material-balance-derived properties, a method is proposed for calculating black-oil PVT properties — i.e., FVF's and solution GOR's used in two-phase flow equations and reservoir material balances. The method was first suggested by Dodson *et al.*[2] in 1953 for solution-gas/crude-oil systems. Their method, however, requires expensive and time-consuming liquid sample removals and experimental flash separations. The proposed method follows the Dodson *et al.* procedure but uses experimentally determined vapor compositions and material-balance-derived liquid compositions together with a multistage separator flash program. PVT properties calculated using this method are compared with those predicted by the PR EOS.

Though more complicated, empirical equations of state are also used to evaluate CVD data. Several investigators[3,4] have used the PR EOS to simulate PVT studies of light gas condensates and crude oils. Unfortunately most studies have emphasized K-value predictions instead of volumetric predictions, and most have avoided systems operating near the critical point. Results have varied considerably, depending on which properties are compared. Conrad and Gravier[4] propose a method to improve liquid-density estimations by adjusting properties of the heaviest-plus fraction (boiling point and methane interaction coefficient). Firoozabadi *et al.*[3] studied another lean gas condensate and found that by adjusting only the methane-heavy fraction interaction coefficient, the PR EOS highly overestimated liquid volumes.

About 30 CVD studies performed by commercial and private laboratories were analyzed using the material-balance approach. A North Sea rich gas condensate was

---

*Now with Esso E&P Norway Inc.

0149-2136/83/0031-0067$00 25

chosen to be analyzed using the PR EOS. This choice was based on consistency of measured CVD data as indicated by material-balance calculations and availability of extended compositional data for the heptanes-plus fraction.

Description of CVD Process

A CVD experiment is conducted at reservoir temperature and begins at saturation pressure. Cell volume, V_{cell}, or the volume contained by the saturated fluid, is used as a reference volume.

Mercury is withdrawn from the bottom of the cell, thereby lowering the pressure as fluid expands. During this process, a second phase evolves — either retrograde liquid (for gas condensates) or solution gas (for volatile oils).

Mercury withdrawal is ceased when a predetermined pressure is reached. Some laboratories measure liquid volumes at several pressures before any vapor has been removed; these volumes, reported relative to V_{cell}, represent constant-composition depletion. They closely approximate volumes that would have been measured if the process had been CVD. (This was checked using the PR EOS simulator for lean and rich condensates: see also Ref. 5.)

Mercury is reinjected into the cell at constant pressure while simultaneously withdrawing an equivalent volume of vapor. When initial cell volume is reached, mercury injection is ceased. Withdrawn vapor is analyzed using gas chromatography to determine composition, y_j. Moles of vapor produced, n_p, are calculated using the real gas law and are reported as a cumulative percent of initial moles. Compressibility factor, Z, also is calculated by noting produced vapor surface volume and equivalent cell volume (at pressure and temperature). From measured vapor gravity and composition, heptanes-plus molecular mass is back-calculated. Liquid volume is measured visually and reported as a percent of cell volume, which is actually a type of hydrocarbon liquid saturation, S_L.

The experimental procedure is repeated several times until a low pressure is reached. The remaining liquid is removed, distilled, and analyzed using gas chromatography. Measured liquid composition should check with material-balance-derived composition. (Some major laboratories smooth and adjust measured vapor compositions until the material balance checks. This procedure is discouraged. It is good practice to ask if a laboratory reports measured or smoothed data, and to what extent material-balance-derived data are used in final CVD reports.)

Material-Balance Equations

Liquid Composition and *K*-Value Calculations

Perhaps the most useful application of constant-volume depletion data is for calculating liquid compositions that, together with measured vapor compositions, yield high-pressure *K*-values having several important reservoir- and process-engineering applications. To arrive at the final expression for liquid composition in terms of measured CVD data, we first state mole and component material balances, respectively, as

$$n_{tk} = n_{Lk} + n_{vk} \quad \ldots\ldots (1)$$

and

$$n_{tk}\cdot z_{jk} = n_{Lk}\cdot x_{jk} + n_{vk}\cdot y_{jk}\ , \quad \ldots\ldots (2)$$

where n_L is moles of liquid with composition x_j, n_v is moles of vapor with composition y_j, and n_t is total moles in the system with composition z_j, each associated with pressure stage *k*. Subscript *j* designates components methane, ethane, etc. Eq. 1 states that total moles of the two-phase system equals the sum of liquid and vapor moles, while Eq. 2 states that total moles of component *j* in the two-phase system equals moles of *j* in the liquid plus moles of *j* in the vapor. The only data measured directly and appearing in either of the equations is vapor composition. The remaining unknowns can be determined from reported CVD data and modified forms of the material-balance relations.

Then we note that total moles at stage *k* equals initial moles minus cumulative moles of vapor produced.

We assume a basis of one mole initial fluid, $n_{t1} = 1$, yielding

$$n_{tk} = 1 - \sum_{i=2}^{k} \Delta n_{pi}\ . \quad \ldots\ldots (3)$$

The same material balance can be applied on a component basis, resulting in

$$n_{tk}\cdot z_{jk} = z_{j1} - \sum_{i=2}^{k} \Delta n_{pi}\cdot y_{ji}\ , \quad \ldots\ldots (4)$$

where Δn_{pi} is the incremental moles of vapor produced from the cell during stage *i*, and z_{j1} is the initial fluid composition at Stage 1 (saturated conditions).

Moles of vapor remaining in the cell can be calculated using a volumetric balance and the real gas law ($pV = nZRT$).

Recalling the basis of 1 mol initial fluid, cell volume can be calculated from initial fluid properties, which for gas condensates is

$$V_{\text{cell}} = \frac{Z_d\cdot R\cdot T}{p_d}\ , \quad \ldots\ldots (5a)$$

and, for volatile oils (existing as a liquid at bubble-point pressure),

$$V_{\text{cell}} = M_b/\rho_b \quad \ldots\ldots (5b)$$

where R = 8.3143 J/mol-K for preferred SI units, and R = 10.732 psia-cu ft/mol-°R for field units. M_b and ρ_b are bubble-point molecular mass and density, respectively. Z_d and p_d are dewpoint fluid compressibility factor and pressure, respectively.

At each depletion pressure, liquid volume is measured visually and reported as a fraction, S_{Lk}, of cell volume. Liquid volume, V_{Lk}, then can be calculated from

$$V_{Lk} = S_{Lk}\cdot V_{\text{cell}}\ . \quad \ldots\ldots (6)$$

and, from a volume balance, vapor volume, V_{vk}, is

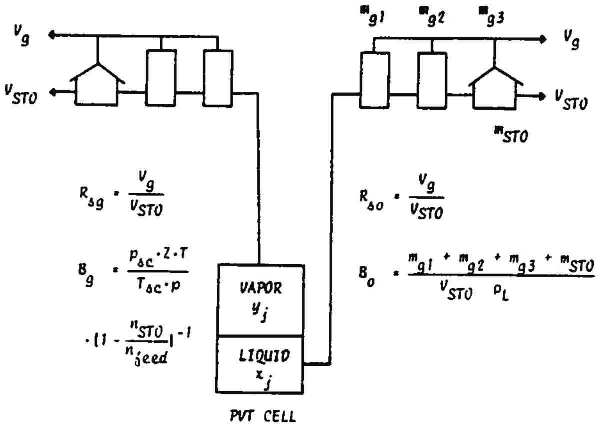

Fig. 1—Schematic of the procedure for calculating black-oil PVT properties.

$$V_{vk} = (1 - S_{Lk}) V_{\text{cell}} \quad \ldots \ldots \ldots \ldots \ldots \ldots \ldots \quad (7)$$

Using the real gas law, the corresponding moles of vapor n_{vk} are calculated from

$$n_{vk} = \frac{p_k \cdot V_{vk}}{Z_k \cdot R \cdot T}, \quad \ldots \ldots \ldots \ldots \ldots \ldots \ldots \quad (8)$$

where vapor compressibility factor, Z_k, which is measured at each stage k, corresponds to pressure p_k.

All unknowns in Eq. 1 now have been defined in terms of measured CVD data except liquid composition, which when written in terms of the other variables becomes

$$x_{jk} = \frac{n_{tk} \cdot z_{jk} - n_{vk} \cdot y_{jk}}{n_{tk} - n_{vk}} \quad \ldots \ldots \ldots \ldots \ldots \ldots \quad (9)$$

Equilibrium constants or K-values are defined as the ratio of equilibrium vapor to liquid composition, or

$$K_{jk} = y_{jk} / x_{jk} \quad \ldots \ldots \ldots \ldots \ldots \ldots \ldots \ldots \quad (10)$$

An effective means of correlating and checking the consistency of calculated K-values (i.e., liquid compositions) is to plot log Kp vs. the component characterization factor, F, as suggested by Hoffman *et al.*[6]

Physical Property Calculations

CVD data also can be used to calculate physical properties of equilibrium vapor and liquid. A mass balance is employed to carry out the necessary calculations:

$$m_{tk} = m_{Lk} + m_{vk}, \quad \ldots \ldots \ldots \ldots \ldots \ldots \ldots \ldots \quad (11)$$

where m_t is total mass of the system, m_L is liquid mass and m_v is vapor mass at stage k. Another way of stating the mass balance is that total mass at stage k equals initial mass minus cumulative vapor mass produced from the cell. Recalling the basis of 1 mol initial fluid, and thereby equating initial mass with initial (saturation) molecular mass, M_s, gives

$$m_{tk} = M_s - \sum_{i=2}^{k} \Delta n_{pi} \cdot M_{vi}, \quad \ldots \ldots \ldots \ldots \ldots \quad (12)$$

where M_{vi} is the vapor phase molecular mass at stage i.

Both M_s and M_v can be calculated using Kay's mixing rule and appropriate component molecular masses.

Vapor mass can be calculated by noting that mass equals molecular mass times moles, or

$$m_{vk} = n_{vk} \cdot M_{vk} \quad \ldots \ldots \ldots \ldots \ldots \ldots \ldots \ldots \quad (13)$$

Liquid mass then is calculated as the difference between total mass and vapor mass,

$$m_{Lk} = m_{tk} - m_{vk} \quad \ldots \ldots \ldots \ldots \ldots \ldots \ldots \ldots \quad (14)$$

Having calculated masses and volumes of equilibrium liquid and vapor, respective densities can be calculated directly: $\rho = m/V$ (where volumes come from Eqs. 6 and 7).

An independent check of vapor density can be used to check the consistency of measured Z factors. The relation is derived directly from the real gas law and can be stated as

$$\rho_{vk} = \frac{M_{vk} \cdot p_k}{Z_k \cdot R \cdot T} \quad \ldots \ldots \ldots \ldots \ldots \ldots \ldots \quad (15)$$

We also can calculate molecular mass of the equilibrium liquid, and specifically its heptanes-plus fraction. Rewriting the mass balance as

$$m_{tk} = M_{Lk} \cdot n_{Lk} + M_{vk} \cdot n_{vk}, \quad \ldots \ldots \ldots \ldots \ldots \quad (16)$$

we can solve for liquid molecular mass, M_{Lk},

$$M_{Lk} = \frac{m_{tk} - M_{vk} \cdot n_{vk}}{n_{Lk}} \quad \ldots \ldots \ldots \ldots \ldots \ldots \quad (17)$$

Using Kay's mixing rule, the heptanes-plus molecular mass can be back-calculated to yield

$$M_{Lk7+} = \frac{M_{Lk} - \sum_{i=1}^{N-1} M_i x_{ki}}{x_{k7+}}, \quad \ldots \ldots \ldots \ldots \quad (18)$$

where M_i are molecular masses of pure components.

The average C_{7+} molecular mass of the two-phase system should be calculated using the relation

$$M_{7+} = \frac{n_{Lk} x_{k7+} M_{Lk7+} + n_{vk} y_{k7+} M_{vk7+}}{n_{Lk} x_{k7+} + n_{vk} y_{k7+}} \quad \ldots \ldots \quad (19)$$

Black-Oil PVT Properties

Dodson *et al.*[2] suggested an experimental procedure for determining so-called black-oil PVT properties used in two-phase flow equations and solution-gas drive material-balance relations. Current laboratory procedures for estimating oil formation volume factor, B_o, and solution GOR, R_{so}, only approximate the Dodson *et al.* method without flashing the liquid phase at each stage of the differential vaporization process. For medium to low volatile crudes, this procedure appears valid for most engineering calculations. Also, vapor solution GOR, R_{sg}, is assumed to equal infinity — i.e., liquid condensation is neglected.

Highly volatile oils and gas condensates usually can-

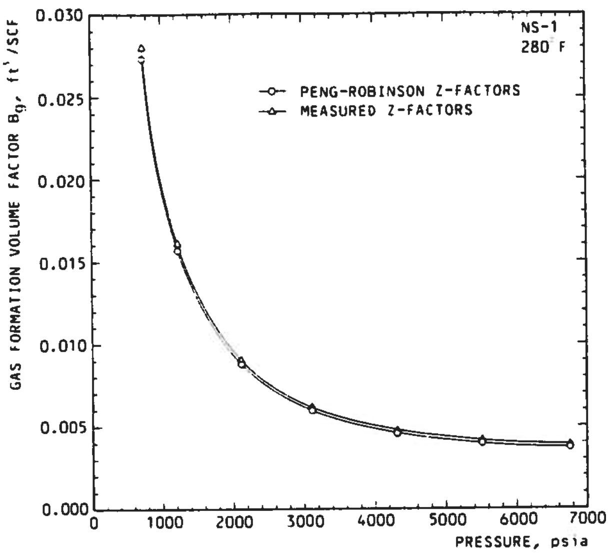

Fig. 2—Gas FVF vs. pressure for NS-1 at 280°F.

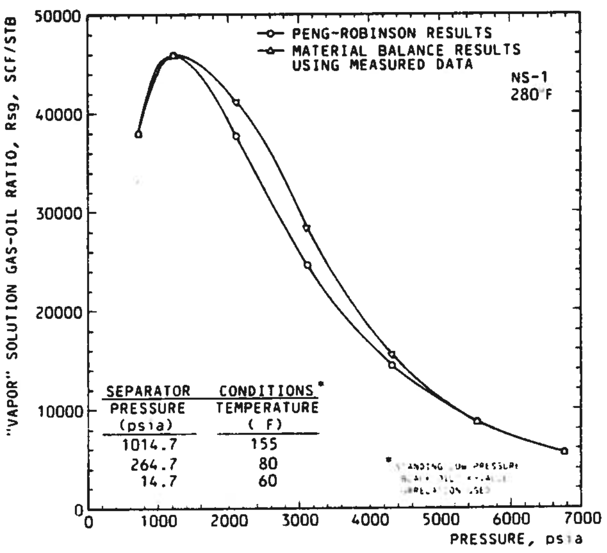

Fig. 3—Vapor solution GOR vs. pressure for NS-1 at 280°F.

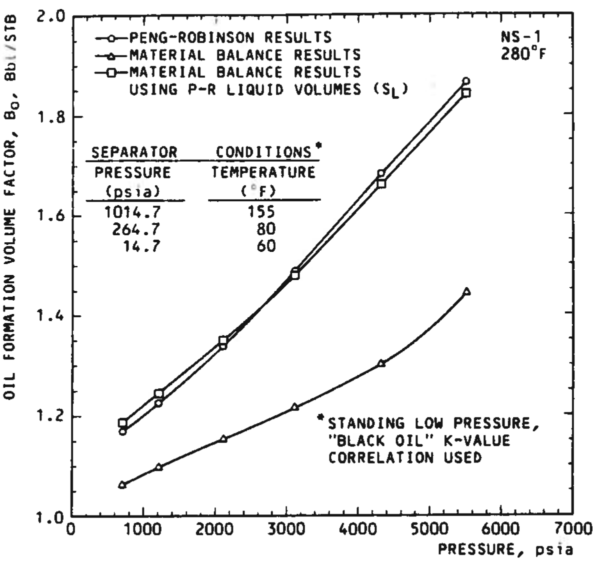

Fig. 4—Oil FVF vs. pressure for NS-1 at 280°F.

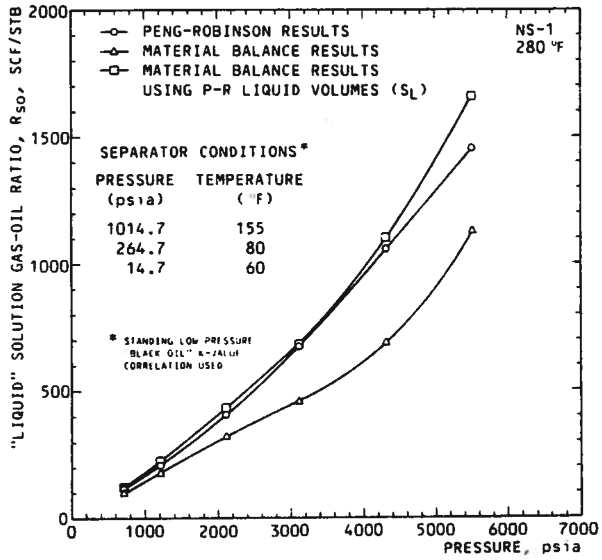

Fig. 5—Liquid solution GOR vs. pressure for NS-1 at 280°F.

not be described by the same differential process. The basic problem posed by these more volatile fluids is that during two-phase flow there exist both two phases and two components. That is, flowing oil contains solution gas that, when undergoing pressure reduction, evolves and mixes with the existing vapor phase. Likewise, flowing gas contains retrograde liquid that also evolves and mixes with the existing liquid when pressure declines. This complex thermodynamic phenomenon is, for all practical purposes, impossible to simulate in the laboratory.

An alternative method is suggested that, by making certain simplifying assumptions, approximates the true model described previously. Individual phase compositions determined from CVD analysis (measured or calculated) are flashed through a multistage separator simulator representing field conditions. Fig. 1 describes the process diagrammatically.

Before beginning our discussion of the proposed method, let us define the four basic PVT properties used in two-phase flow and reservoir material-balance equations: B_o is liquid volume of x_j at reservoir conditions divided by stock-tank oil volume resulting from flash of x_j; R_{so} is surface gas volume resulting from the flash of x_j divided by stock-tank oil volume resulting from flash of x_j; B_g is vapor volume of y_i at reservoir conditions divided by surface gas volume resulting from the flash of y_i; and R_{sg} is surface gas volume resulting from the

TABLE 1—MEASURED CONSTANT-VOLUME DEPLETION DATA FOR THE NS-1 FLUID AT 280°F (psia)

	Compositions								
	Equilibrium Vapor							Equilibrium Liquid	
								Experimental	Calculated
Component	6764.7	5514.7	4314.7	3114.7	2114.7	1214.7	714.7	714.7	714.7
Carbon dioxide	2.37	2.40	2.45	2.50	2.53	2.57	2.60	0.59	0.535
Nitrogen	0.31	0.32	0.33	0.34	0.34	0.34	0.33	0.02	0.017
Methane	73.19	75.56	77.89	79.33	79.62	78.90	77.80	12.42	10.704
Ethane	7.80	7.83	7.87	7.92	8.04	8.40	8.70	3.36	3.220
Propane	3.55	3.47	3.40	3.41	3.53	3.74	3.91	2.92	2.896
isobutane	0.71	0.67	0.65	0.64	0.66	0.72	0.78	0.91	0.916
n-butane	1.45	1.37	1.31	1.30	1.33	1.44	1.56	2.09	2.103
isopentane	0.64	0.59	0.55	0.53	0.54	0.59	0.64	1.40	1.417
n-pentane	0.68	0.62	0.58	0.56	0.57	0.61	0.66	1.60	1.624
Hexanes	1.09	0.97	0.88	0.83	0.82	0.85	0.90	3.68	3.755
Heptanes-plus	8.21	6.20	4.09	2.64	2.02	1.84	2.12	71.01	72.815
Totals	100.000	100.000	100.000	100.000	100.000	100.000	100.000	100.000	100.000
$M_{C_{7+}}$	184.0	160.0	142.0	127.0	119.0	115.0	114.0	213.0	207.8
$\gamma_{C_{7+}}$	0.816	0.799	0.783	0.770	0.762	0.758	0.757	0.833	0.843
Z	1.238	1.089	0.972	0.913	0.914	0.937	0.960		
n_p, %	0.000	9.024	21.744	38.674	55.686	72.146	81.301		
S_L, %	0.0	14.1	19.7	21.6	21.3	20.2	19.3		

flash of y_j divided by stock-tank oil volume resulting from flash of y_j, where x_j are liquid compositions determined from material-balance equations and y_j are vapor compositions measured experimentally.

First, liquid composition x_j is flashed using a set of appropriate K-values and basic vapor/liquid equilibria equations. [Glasø and Whitson[7] have documented that Standing's[8] low-pressure K-value equations are quite accurate for flash calculations of black oils. We have since found that they are also accurate for flash calculations of many gas condensates — e.g., systems with GOR's less than about 50,000 scf/STB (9000 std m^3/stock-tank m^3).] The sum of surface gas volumes divided by stock-tank oil volume is defined as the liquid GOR, R_{so}.

Oil FVF, B_o, is calculated from the relation

$$B_o = \frac{\sum_{i=1}^{\text{stages}} m_{gi} + m_{\text{sto}}}{V_{\text{sto}} \cdot \rho_L}, \qquad (20)$$

where V_{sto} is stock-tank oil volume [e.g., 1 bbl (0.16 m^3)], and m_g and m_{sto} are masses of total surface gases and stock-tank oil, respectively. Liquid density, ρ_L, can be determined either from material-balance calculations (m_L from Eq. 14 and V_L from Eq. 6) or from one of several compositional density correlations available[9,10] using material-balance-derived liquid compositions.

At the same depletion stage k, vapor phase with composition y_j is separated through the flash simulator using identical K-values. The resulting surface gas volumes divided by stock-tank oil volume defines the vapor solution GOR, R_{sg}. Gas FVF, on the other hand, can be calculated from the CVD compressibility factor, Z, using the real gas law:

$$B_g = \frac{p_{sc} \cdot Z \cdot T}{p \cdot T_{sc}} \left(1 - \frac{n_{\text{sto}}}{n_{\text{feed}}}\right)^{-1}, \qquad (21)$$

where n_{sto} is moles of stock-tank oil resulting from the flash of n_{feed} moles of reservoir vapor.

The major assumption implicit in the proposed method is that liquid and vapor compositions are solely dependent on pressure. That is, the composition/pressure relation is unique and not altered by physical flow.

Examples of PVT properties for a rich gas condensate (NS-1) are presented in Figs. 2 through 5. Here we have compared properties calculated using material-balance results with those calculated using PR EOS simulated data. Identical low-pressure K-values were used for both sets of data. Vapor solution GOR's are nearly the same for both methods of calculation. Liquid solution GOR's and oil FVF's are both low for material-balance-derived properties. The difference is a result of the underestimated liquid densities calculated by the PR equation.

Application of the Peng-Robinson Equation of State

Measured CVD data and material-balance-derived properties were controlled using a fluid properties package based on the PR EOS. Pure component properties (critical pressure, critical temperature, acentric factor, and molecular mass) were used for nonhydrocarbons and hydrocarbons from methane to n-pentane. Only n-hexane was considered for the C_6 fraction. Heptanes and heavier properties were estimated using the procedure and equations suggested by Whitson.[11]

To manipulate the retrograde liquid-volume curve, the Watson characterization factor of the heaviest component was adjusted, making sure that adjusted critical properties were physically realistic.

Binary interaction coefficients were set equal to zero except[12]: $N_2-N_2 = -0.02$, CO_2 – hydrocarbons = 0.15, N_2 – hydrocarbons = 0.12, and C_1-C_n, $n = 6$,

TABLE 2—COMPOSITIONAL AND PROPERTIES DATA OF FLUID NS-1B SAMPLED FROM A WELL OFFSETTING NS-1 COMPARED WITH CALCULATED DATA GENERATED USING THE METHOD PRESENTED IN REF. 11

	Measured			Calculated*				
Single Carbon Number	Mole Percent	Molal Mass	Specific Gravity	K_{uop} Factor	Boiling Point (°R)	Mole Percent	Molal Mass	Upper Molal Mass
7	0.94	95	0.7158	12.05	641.7	0.935	95.1	99.6
8	0.84	104	0.7365	11.93	678.3	0.838	105.4	111.9
9	0.74	118	0.7557	11.90	727.3	0.739	118.9	126.8
10	0.60	132	0.7639	11.99	768.4	0.600	134.2	142.4
11	0.41	144	0.7723	12.04	804.0	0.410	148.7	155.5
12	0.34	154	0.7814	12.04	832.7	0.340	161.7	168.4
13	0.31	167	0.7939	12.03	871.2	0.310	175.0	182.2
14	0.26	180	0.8053	12.02	907.0	0.260	188.7	195.7
15	0.22	197	0.8096	12.13	947.1	0.220	202.1	209.1
16	0.19	212	0.8152	12.30	1008.1	0.190	215.4	222.4
17	0.17	226	0.8255	12.19	1019.0	0.170	228.9	236.1
18	0.15	234	0.8303	12.20	1039.4	0.150	242.8	250.1
19	0.13	250	0.8341	12.26	1069.4	0.130	256.8	264.1
20	0.11	262	0.8400	12.28	1097.6	0.110	270.6	277.8
21	0.08	277	0.8477	12.29	1130.8	0.080	283.0	289.0
22	0.07	292	0.8531	12.32	1161.0	0.070	294.1	299.9
23	0.06	308	0.8577	12.36	1191.4	0.060	304.8	310.3
24	0.06	329	0.8666	12.38	1234.9	0.070	316.7	324.0
25+	0.51	471	0.8826	12.87	1465.6	0.508	439.1	∞
	6.19	177	0.8061	12.25 (12.02)**		6.190	177.0	

*The gamma distribution (Ref. 11) was used where an optimal alpha of 0.712 was found for eta (minimum molecular mass in the C_{7+} fraction) of 92. Upper molecular masses were found by fitting the measured compositions.

**The higher average K_{uop} value was calculated using a weight-average mixing rule, whereas the lower value was estimated using the Whitson correlation.

7..., which were estimated using a linear fit of the Katz and Firoozabadi[12] data (their Table 2),

$$\delta_{C_1-C_n} = 0.14 \cdot \gamma_n - 0.0668 \quad \text{. . . . . (22)}$$

The interaction coefficient between methane and the heaviest component then was adjusted until a match of the measured dewpoint pressure was obtained.

Fluid Description: Rich Gas Condensate NS-1

NS-1 is a rich gas condensate first tested at a GOR of 5,500 scf/STB (980 std m^3/stock-tank m^3) from an initial reservoir pressure of 7,300 psia (50 MPa) and temperature of 280°F (138°C). Stock-tank oil gravity was 44°API (0.8055 g/cm^3). Separator samples were taken while flowing the well at 16.3 MMscf/D (460 × 10^3 std m^3/d) and a flowing bottomhole pressure of 7,260 psia (50 MPa). Table 1 presents constant-volume depletion data measured on the recombined reservoir fluid.

Heptanes-Plus Characterization

Extended compositional data of the C_{7+} fraction were not available for the NS-1 fluid, only molecular mass and specific gravity. Complete true-boiling-point (TBP) data were, however, available from an offset well. These data were adapted to the NS-1 fluid using the methods presented in Ref. 11.

Molar distribution (mole fraction vs. molecular mass) of the offset well fluid was fit using the gamma distribution parameter alpha and variable upper-boundary molecular masses. The optimal alpha was 0.712 for eta (minimum molecular mass in the C_{7+} fraction) of 92. Table 2 gives results of the match. Molar distribution of the NS-1 C_{7+} fraction then was calculated using α = 0.712, η = 92, and M_{C7+} = 184 (as compared to 177 for the NS-1b fluid). Results are presented in Table 3.

Tuning the Peng-Robinson Equation of State

Single carbon number groups were combined into five multiple carbon number (MCN) groups: C_7 through C_9, C_{10} through C_{13}, C_{14} through C_{17}, C_{18} through C_{24}, and C_{25}+, as suggested in Ref. 11. Group properties were calculated using Kay's mixing rule. Methane interaction coefficients were estimated using MCN specific gravities and Eq. 22.

Using these data, the PR EOS yielded a dewpoint pressure much lower than measured. The C_1 through C_{25+} interaction coefficient then was increased until dewpoint pressure was matched.

The CVD program was run using the MCN properties (Table 3). The overall match was good to excellent, except for liquid volumes, which were much too high (32% simulated maximum vs. 22% measured maximum). To check whether measured volumes were low, we compared material-balance liquid densities with Alani-Kennedy[10] densities (using material-balance compositions and molecular masses). Table 4 shows results of the comparison, indicating that measured volumes are consistent except for perhaps small errors in the first two volume measurements.

On the basis of these results, we decided to lower the

TABLE 3—PHYSICAL PROPERTIES OF THE C_{7+} SINGLE AND MULTIPLE CARBON NUMBER GROUPS USED IN THE PENG-ROBINSON EQUATION OF STATE TO DESCRIBE RESERVOIR FLUID BEHAVIOR OF THE NS-1 FLUID

					Critical			
Single Carbon Number	Mole Percent	Molal Mass	Specific Gravity	Boiling Point (°R)	Temperature (°R)	Pressure (psia)	Acentric Factor	Methane Interaction Coefficient
7	1.2136	95.3	0.7177	646.8	971.6	457.5	0.2742	
8	1.1730	106.5	0.7409	690.6	1021.4	423.4	0.3056	
9	0.8600	120.7	0.7599	739.4	1073.4	383.2	0.3454	
10	0.6872	134.7	0.7682	781.4	1112.9	345.9	0.3861	
11	0.5681	148.7	0.7781	822.2	1152.1	316.8	0.4251	
12	0.4783	162.7	0.7908	863.1	1192.3	294.0	0.4622	
13	0.4074	176.7	0.8034	902.8	1231.2	274.9	0.4984	
14	0.3498	190.7	0.8153	941.2	1268.3	258.4	0.5342	
15	0.3021	204.7	0.8168	972.6	1294.2	240.4	0.5740	
16	0.2621	218.7	0.8210	1029.8	1321.5	225.7	0.6127	
17	0.2282	232.7	0.8310	1039.5	1354.0	214.6	0.6486	
18	0.1992	246.6	0.8389	1072.0	1383.6	204.3	0.6855	
19	0.1744	260.6	0.8432	1104.7	1408.7	194.0	0.7246	
20	0.1529	274.6	0.8486	1131.6	1434.4	185.1	0.7634	
21	0.1343	288.6	0.8554	1161.9	1461.0	177.4	0.8016	
22	0.1182	302.6	0.8602	1190.2	1484.9	170.0	0.8416	
23	0.1041	316.5	0.8639	1217.4	1507.0	162.9	0.8830	
24	0.0918	330.5	0.8690	1245.1	1530.2	156.8	0.9241	
25+	0.7054	462.3	0.9292	1488.0	1734.6	91.4	1.0590	
	8.2100	184.0	0.8160					
Multiple Carbon Number Properties Used in the Final CVD Simulation								
7 through 9	3.2466	106.1	0.7385	688.3	1016.5	425.5	0.3044	0.03659*
10 through 13	2.1410	152.7	0.7837	835.0	1163.6	313.1	0.4348	0.04292*
14 through 17	1.1421	209.2	0.8205	984.4	1304.5	237.4	0.5856	0.04807*
18 through 24	0.9749	281.5	0.8524	1146.9	1446.0	182.7	0.7832	0.05254*
25+	0.7054	462.3	0.9192	1276.1**	1584.2**	168.8**	0.8819**	0.18400†
	8.2100	184.0	0.8160					

*Calculated using the Katz and Firoozabadi correlation, curve-fit to yield the relation $\delta_{C_1-C_n} = 0.14\ \gamma_n - 0.0668$. Though not shown in this table, the methane/hexane interaction coefficient also was calculated using this relation.

**Adjusted values representing a K_{uop} factor of 11.80. The original values correspond to a K_{uop} factor of 12.42 and are given above (e.g., 1488.0).

†Adjusted value used to match the measured dewpoint pressure.

TABLE 4—CALCULATED LIQUID DENSITIES AS A FUNCTION OF PRESSURE FOR NS-1 FLUID

	Calculated Liquid Densities (g/cm³)			
	Measured CVD Data		Simulated CVD Data	
Pressure (psia)	Material-Balance Density	Alani-Kennedy Density (Material-Balance Liquid Properties)*	PR Density**	Alani-Kennedy Density (PR Liquid Properties)*
5,514.7	0.670	0.608	0.541	0.570
4,314.7	0.680	0.649	0.554	0.596
3,114.7	0.688	0.670	0.580	0.632
2,114.7	0.700	0.682	0.608	0.664
1,214.7	0.711	0.700	0.636	0.692
714.7	0.722	0.711	0.653	0.707

*The Alani-Kennedy density correlation requires liquid compositions, total liquid molecular mass, heptanes-plus molecular mass, and specific gravity (as well as pressure and temperature). These data were available from either material-balance calculations or PR simulation results.

**The PR simulation used properties given in Table 3 with an adjusted K_{uop} = 11.8 for the C_{25+} fraction. Using the original K_{uop} factor of 12.42 gave even lower liquid densities than those given above, with a larger deviation from the Alani-Kennedy values.

TABLE 5—SIMULATED CONSTANT-VOLUME DEPLETION DATA FOR THE NS-1 FLUID AT 280°F USING THE PENG-ROBINSON EQUATION OF STATE (psia)

	Compositions								
	Equilibrium Vapor							Equilibrium Liquid	
								Experimental	Calculated
Component	6764.7	5514.7	4314.7	3114.7	2114.7	1214.7	714.7	714.7	714.7
Carbon dioxide	2.370	2.403	2.447	2.497	2.541	2.576	2.583	0.590	0.595
Nitrogen	0.310	0.323	0.336	0.344	0.343	0.334	0.321	0.020	0.029
Methane	73.190	75.549	77.644	79.135	79.712	79.242	77.772	12.420	11.939
Ethane	7.800	7.779	7.793	7.878	8.057	8.372	8.711	3.360	3.623
Propane	3.550	3.474	3.405	3.383	3.444	3.660	3.989	2.920	3.133
isobutane	0.710	0.686	0.660	0.644	0.647	0.691	0.778	0.910	0.967
n-butane	1.450	1.390	1.326	1.281	1.282	1.375	1.567	2.090	2.314
isopentane	0.640	0.604	0.564	0.530	0.516	0.548	0.638	1.400	1.509
n-pentane	0.680	0.639	0.592	0.550	0.532	0.563	0.659	1.600	1.770
Hexanes	1.090	0.996	0.889	0.789	0.727	0.744	0.877	3.680	4.223
Heptanes-plus	8.210	6.157	4.343	2.969	2.198	1.895	2.105	71.010	69.897
Totals	100.000	100.000	100.000	100.000	100.000	100.000	100.000	100.000	100.000
$M_{C_{7+}}$	184.0	161.0	142.7	129.1	121.2	116.4	114.5	213.0	209.1
$\gamma_{C_{7+}}$	0.816	0.799	0.783	0.770	0.762	0.758	0.757	0.833	0.843
Z	1.203	1.037	0.937	0.890	0.886	0.911	0.936		
n_p, %	0.000	9.637	22.581	39.492	56.196	72.413	81.535		
S_L, %	0.00	19.55	26.11	26.65	25.11	23.00	21.58		

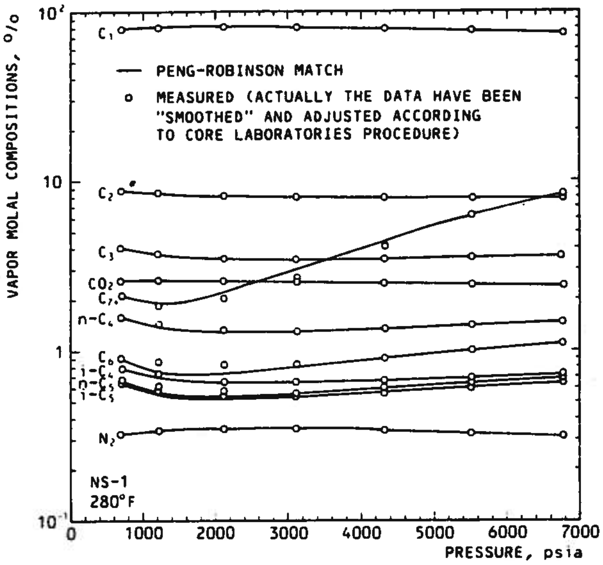

Fig. 6—Calculated and measured vapor compositions vs. pressure for NS-1 at 280°F.

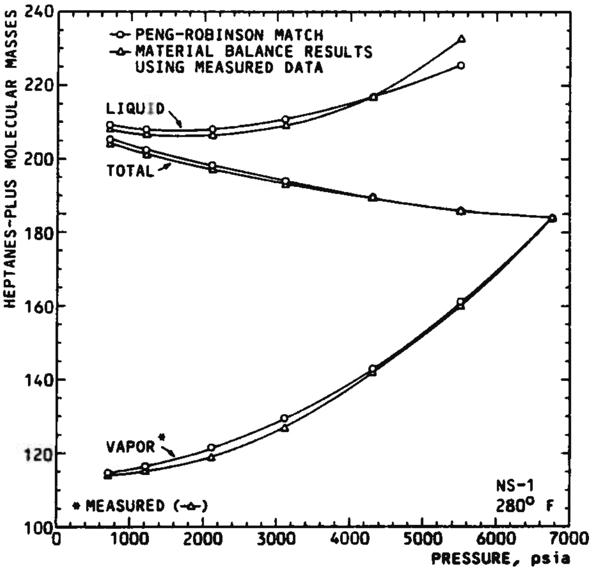

Fig. 7—Calculated heptanes-plus molecular masses vs. pressure for NS-1 at 280°F.

PR liquid volumes by adjusting the characterization factor of the C_{15+} fraction. Lowering the factor from 12.24 to 11.80 resulted in an 8% decrease of the liquid volumes for the maximum drop-out (from 32% to 26%). The adjustment had little effect on other estimated data. To have lowered the K_{uop} factor more would have created a physically unrealistic system. Adjusted physical properties for the C_{15+} fraction are found in Table 3, as is the methane interaction coefficient used to adjust dewpoint pressure. Complete results of the CVD simulation are presented in Table 5. PR liquid densities are compared with Alani-Kennedy estimates in Table 4.

Many other adjustments of the C_{7+} characterization procedure were tried. None of these were particularly helpful, though some are worth mentioning: (1) extending the C_{7+} split to C_{40+} such that the last component was very heavy, (2) increasing the number of MCN groups used to nine, C_{25+} inclusive, (3) splitting the

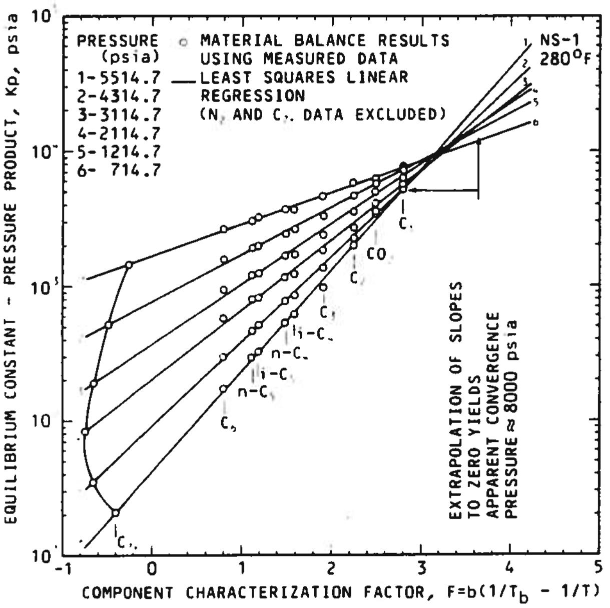

Fig. 8—NS-1 *K*-values at 280°F calculated using the material-balance approach.

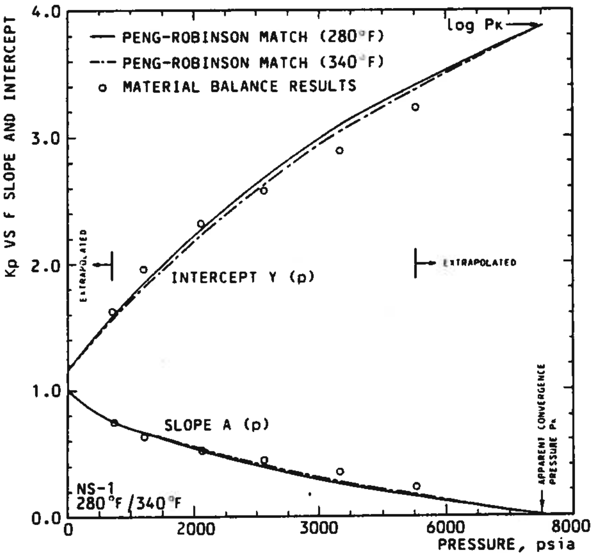

Fig. 10—Slopes and intercepts of log *Kp* vs. *F* plots vs. pressure for NS-1 at 280 and 340°F.

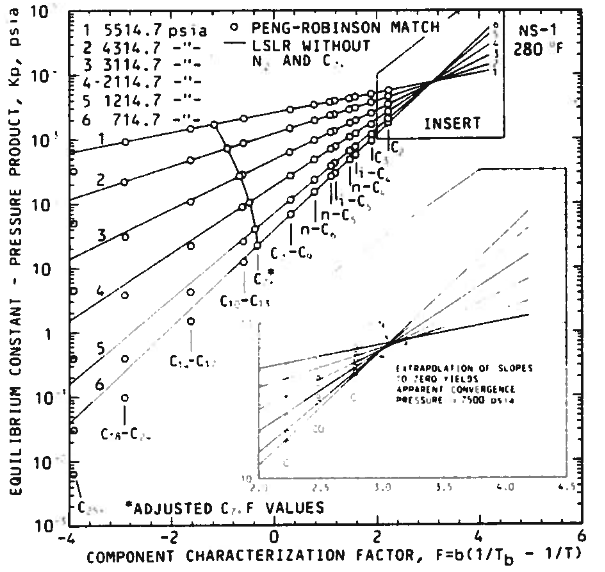

Fig. 9—NS-1 *K*-values at 280°F calculated using the PR EOS.

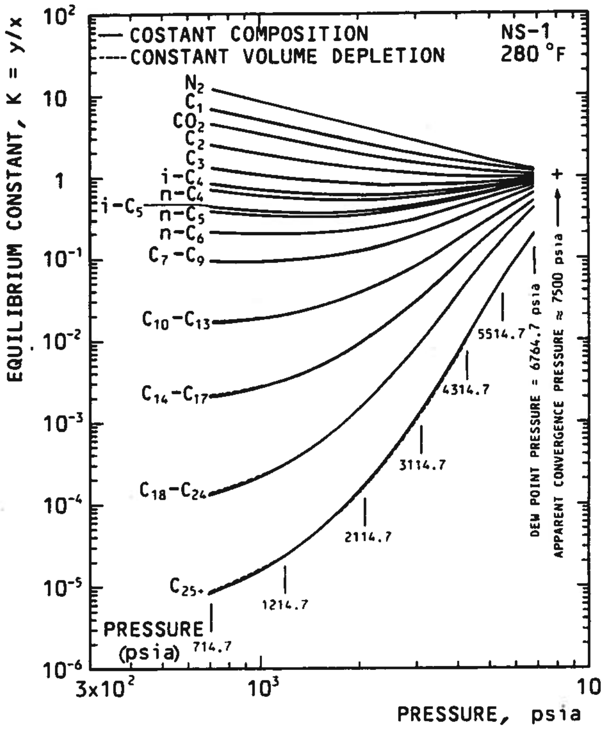

Fig. 11—PR *K*-values for NS-1 at 280°F representing two depletion processes.

C_{7+} fraction into eight SCN groups and a C_{15+} fraction, and (4) using TBP K_{uop} factors instead of those estimated from Eq. 23.

Results and Discussion

Fig. 6 compares measured (or more correctly, "smoothed") vapor compositions with those simulated using the PR EOS. The match is excellent, showing only slight deviation for the C_{7+} and C_6 components. Deviation of the hexane component is probably because of its incorrect characterization as n-hexane.

Fig. 7 presents heptanes-plus molecular masses of liquid and vapor phases and the total system. Simulated and material-balance-derived values match well. Our experience has shown that a good match of C_{7+} molecular mass using the PR EOS is usually difficult and very dependent on proper characterization of the plus fraction.

Calculated equilibrium constants were correlated using the Hoffman *et al.*[6] method. Fig. 8 presents NS-1 *K*-values calculated using material-balance relations. The log *Kp* vs. *F* plots are linear and appear to approach a common point. The convergence point can give an estimate of the apparent convergence pressure. Actually, the most accurate value is obtained by extrapolating the slope vs. pressure curve to zero, as done in Fig. 10. The resulting estimate of p_K is 8,000 psia (55 MPa).

Fig. 9 presents NS-1 *K*-values calculated from the EOS. Once again linear plots of log *Kp* vs. *F* converge to a point. From the extrapolation of slope to zero in Fig. 10, $p_K \approx$ 7,500 psia (52 MPa). Another interesting feature shown in Fig. 9 is that heavy components are better correlated using the log *Kp* vs. *F* methods at higher pressures.

Temperature effects on the log *Kp* vs. *F* plots of NS-1 were investigated by running the EOS simulator at 340°F (171.1°C), about 60°F (15.5°C) higher than reservoir temperature. Results indicate that temperature influence is (1) largest for heavy components at large pressures, (2) negligible at low pressures (as was found in Ref. 8), (3) relatively small compared to the influence of pressure, and (4) not significant in changing the apparent convergence pressure of the system.

For lighter systems, there does not always appear such a unique convergence point for log *Kp* vs. *F* plots. We thought that this perhaps resulted from a change in the total composition of the system or from alteration in the heptanes-plus properties. We investigated these possibilities by running a constant-composition simulation of NS-1. Resulting *K*-values were compared with CVD *K*-values and are presented as log *K* vs. log *p* plots in Fig. 11. This plot indicates that compositional change during constant volume depletion is not significant enough to influence *K*-values or convergence pressure.

Conclusions

1. Measured CVD data for a gas condensate were analyzed using simple material balances and the PR EOS.

2. A simple method was proposed for calculating black-oil PVT properties (FVF's and solution GOR's) of gas condensates and volatile oils.

3. Simulated constant-composition and CVD studies of lean and rich gas condensates using the EOS indicate that *K*-values are independent of the depletion process.

4. Equations of state usually overestimate liquid volumes of petroleum reservoir fluids. The problem was improved by reducing the Watson characterization factor of the heaviest component.

Nomenclature

A or $A(p)$ = slope of log*Kp* vs. *F* plot
b = slope of the straight line connecting the critical point and atmospheric boiling point on a log vapor pressure vs. $1/T$ plot, cycle-°R (cycle-K)
B = formation volume factor, bbl/STB (m^3/stock-tank m^3)
F or $F(T)$ = component characterization factor, cycle
K = equilibrium constant (*K*-value)
K_{uop} = Watson characterization factor
m = mass, lbm (kg)
M = molecular mass, lbm/lbm-mol (kg/kg-mol)
n = moles, lbm-mol (kg-mol), exponent in *K*-value correlation
p = pressure, psia (kPa)
R = universal gas constant, 10.732 psia-cu ft/mol-°R (9.3143 J/mol-K)
R_{sg} = vapor solution GOR, scf/STB (std m^3/stock-tank m^3)
R_{so} = liquid solution GOR, scf/STB (std m^3/stock-tank m^3)
S = saturation, fraction or %
T = absolute temperature, °R (K)
V = volume, cu ft (m^3)
x = liquid composition, fraction or %
y = vapor composition, fraction or %
Y or $Y(p)$ = intercept of log *Kp* vs. *F* plot
z = total system composition
Z = vapor compressibility factor
γ = specific gravity relative to air or water (60/60)
δ = interaction coefficient
Δ = incremental
ρ = density, lbm/cu ft (kg/m^3)
ω = acentric factor

Subscripts

a = atmospheric
b = bubble point (p_b) or boiling (T_b)
c = critical
cell = cell, pertaining to PVT cell volume
d = dewpoint
g = gas
i = index for summation
j = component identifier
k = depletion stage
K = convergence

L = liquid phase
n = carbon number
o = oil
p = produced
r = reduced
s = saturated (bubble- or dewpoint)
sc = standard conditions
sto = stock-tank oil
t = total (two-phase)
v = vapor phase

Acknowledgments

We thank H. Norvik, H. Asheim, D. Murphy, V. Dalen, and G. Nielsen for useful comments concerning this paper. We also acknowledge computer time and facilities provided by Rogaland Dist. C., Norwegian Inst. of Technology, and Continental Shelf Inst. We thank Phillips Petroleum Co. Norway for contributing needed fluid data to the petroleum literature. Support from Frying Pan Publications Inc. is appreciated.

References

1. Reudelhuber, F.O. and Hinds, R.F.: "A Compositional Material Balance Method for Prediction of Recovery from Volatile Oil Depletion Drive Reservoir," *Trans.*, AIME (1957) **210**, 19-26.
2. Dodson, C.R., Goodwill, D., and Mayer, E.H.: "Application of Laboratory PVT Data to Reservoir Engineering Problems," *Trans.*, AIME (1953) **198**, 287—98.
3. Firoozabadi, A., Hekim, Y., and Katz, D.L.: "Reservoir Depletion Calculations for Gas Condensates Using Extended Analyses in the Peng-Robinson Equation of State," *Cdn. J. Chem. Eng.* (Oct. 1978) **56**, 610-15.
4. Conrad, P.G. and Gravier, J.F.: "Peng-Robinson Equation of State Checks Validity of PVT Experiments," *Oil and Gas J.* (April 21, 1980) 77-86.
5. Standing, M.B.: ***Volumetric and Phase Behavior of Oil Field Hydrocarbon Systems***, SPE, Dallas (1977).
6. Hoffmann, A.E., Crump, J.S., and Hocott, C.R.: "Equilibrium Constants for a Gas-Condensate System," *Trans.*, AIME (1953) **198**, 1-10.
7. Glasø, Ø. and Whitson, C.H.: "The Accuracy of PVT Parameters Calculated from Computer Flash Separation at Pressures Less Than 1,000 psia," *J. Pet. Tech.* (Aug. 1982) 1811-13.
8. Standing, M.B.: "A Set of Equations for Computing Equilibrium Ratios of a Crude Oil/Natural Gas System at Pressures Below 1,000 psia," *J. Pet. Tech.* (Sept. 1979) 1193-95.
9. Standing, M.B. and Katz, D.L.: "Vapor/Liquid Equilibria of Natural Gas-Crude Oil Systems," *Trans.*, AIME (1944) **155**, 232-45.
10. Alani, G.H. and Kennedy, H.T.: "Volumes of Liquid Hydrocarbons at High Temperatures and Pressures," *Trans.*, AIME (1960) **219**, 288-92.
11. Whitson, C.H.: "Characterizing Hydrocarbon Plus Fractions," paper EUR 183 presented at the 1980 European Offshore Petroleum Conference and Exhibition, London, Oct. 21-24.
12. Katz, D.L. and Firoozabadi, A.: "Predicting Phase Behavior of Condensate/Crude-Oil Systems Using Methane Interaction Coefficients," *Trans.*, AIME (1978) **265**, 1649-55.

SI Metric Conversion Factors

°API	141.5/(131.5+°API)		= g/cm^3
bbl ×	1.589 873	E−01	= m^3
cu ft ×	2.831 685	E−02	= m^3
°F	(°F−32)/1.8		= °C
psi ×	6.894 757	E+00	= kPa
scf ×	2.863 640	E−02	= std m^3

JPT

Original manuscript received in Society of Petroleum Engineers office July 22, 1981. Paper accepted for publication Sept. 5, 1982. Revised manuscript received Dec. 15, 1982. Paper (SPE 10067) first presented at the 1981 SPE Annual Technical Conference and Exhibition held in San Antonio Oct. 5–7.

Society of Petroleum Engineers of AIME

SPE 11200

Effect of Physical Properties Estimation on Equation-of-State Predictions

by Curtis H. Whitson, *Rogaland Regional College*
Member SPE

This paper was presented at the 57th Annual Fall Technical Conference and Exhibition of the Society of Petroleum Engineers of AIME, held in New Orleans, LA, Sept. 26-29, 1982. The material is subject to correction by the author. Permission to copy is restricted to an abstract of not more than 300 words. Write 6200 N. Central Expressway, P.O. Drawer 64706, Dallas, Texas 75206.

ABSTRACT

The aim of this work was to document the influence of various hepatanes-plus characterization schemes on equation-of-state predictions. Both the Peng-Robinson and a modified Redlich-Kwong cubic equation were used. Numerous characterization procedures were chosen from the literature. Six reservoir fluids with detailed heptanes-plus analysis were chosen to represent a broad range of fluid types. Pressure-volume-temperature measurements for these fluids were performed over a relatively wide range of conditions.

One part of the study dealt with methods for estimating specific gravities and boiling points of petroleum fractions. These two properties are usually required by critical property correlations. Four methods were studied, including two based on the Watson characterization factor, one based on the aromaticity factor proposed by Jacoby and Yarborough, and the generalized properties proposed by Katz and Firoozabadi. Equation-of-state predictions were made using critical properties based on the estimated specific gravities and boiling points; these were compared with predictions made using critical properties based on measured specific gravities and boiling points.

Another part dealt with various critical property correlations, and their influence on equation-of-state predictions. A thorough review of commonly used correlations was presented. Four sets of correlations were compared. Results indicate that relatively small differences in critical properties and acentric factor can result in significant differences in equation-of-state predictions.

Finally, a study was performed to document the influence of adjustments in heptanes-plus critical properties, equation-of-state constants (a and b) and binary interaction coefficients. Graphical presentations illustrate the influence of individual and combined adjustments of these parameters. They provide a guide to engineers involved with matching experimental data measured on reservoir fluids.

References and illustrations at end of paper.

INTRODUCTION

In recent years, there has been an increasing interest in enhanced oil recovery (EOR) methods. One result has been the need to develop more advanced numerical models for simulating EOR processes. Some of these models use an equation of state (EOS) to predict vapor-liquid equilibrium (VLE) and volumetric phase behavior. The validity of EOS application to EOR processes has been well-documented elsewhere.[1,2,4,5,10,14,15,21,25,27,46,46]

One significant problem with using an EOS is the difficulty in describing heavy fractions found in reservoir fluids. These fractions, usually constituting a heptanes-plus (C_7+) fraction, have a significant effect on EOS predictions.[1,2,4,5,15,16,27,37,44-46] Few data may be available for the heavy fractions. Even so, accurate estimates of critical properties - critical pressure, critical temperature, acentric factor - and molecular weight are required by most equations of state.

Several methods and correlations exist for characterizing heptanes-plus fractions. Some of these were developed for EOS applications, while others were developed to improve or replace previous methods. Most of the correlations are polynomial or exponential equations. Equation constants were fit to existing experimental data or graphical correlations based on experimental data.

Some of the more recent methods try to provide a better characterization by estimating the chemical "make-up" of petroleum fractions.[1,2,34] The most common approach has been to assume heavy fractions are composed of three hydrocarbon groups: paraffins (P), naphthenes (N) and aromatics (A). Several schemes have been proposed for determining the PNA content of petroleum fractions,[1,2,6,34] though it is shown in this work that only a few of these are reliable.

All of the above property correlations are aimed at obtaining accurate estimates of critical properties required by equations-of-state. However, each method is based on one or more properties which can be measured directly. The most common "correlating variables" are specific gravity and boiling point, originally proposed by Smith and Watson.[38]

Fractional distillation is the only reliable method for obtaining direct measurements of both correlating variables. In recent years, however, advances in chromatography have made distillation less common. As a result, it was necessary to develop methods for estimating specific gravities and boiling points of petroleum fractions without experimental data.[44,46] Unfortunately, these methods do not meet standards of generalized correlations since they are based on specific fluids and have not been compared with data from other sources.

Several investigators[2,15] have presented results which indicate that the choice of critical property correlations may be as important as the choice of EOS. The present work was designed to investigate this hypothesis for reservoir fluids at reservoir conditions. Another purpose was to investigate the influence of manual adjustments to properties, constants and interaction coefficients commonly used to "match" measured PVT data.

To perform a reliable comparative study, it was necessary to isolate the effects of each factor. The three factors chosen in this investigation were (1) methods for estimating correlating variables (specific gravity and boiling point) of SCN groups, (2) correlations or procedures for estimating critical properties (pressure and temperature, and acentric factor), and (3) manual adjustments of critical properties, EOS constants (Ω_a and Ω_b) and binary interaction coefficients (particularly between methane/CO_2 and heavy fractions).

The primary basis for choosing reservoir fluids for this study was the availability of distillation data for the C_7+ fraction. PVT measurements performed at reservoir conditions were also a requirement. Based on these criteria, six fluids were chosen from the literature.[9,13,14,17] The types of fluid ranged from a lean gas to a non-volatile oil. PVT measurements were performed at several temperatures for all but one system. This gave an opportunity to illustrate the apparent temperature-dependence of methane-hydrocarbon binary interaction coefficients used to match saturation pressures of reservoir fluids.

Two cubic equations of state were used for the study. The Peng-Robinson[29] (PR) EOS was chosen because of its wide-spread industrial use. It also yields better liquid-density estimates than the comparable Soave-Redlich-Kwong equation. As a representative of the Redlich-Kwong family, Yarborough's version of the modified Zudkevich-Joffe-Redlich-Kwong* (ZJRK) EOS[46] was chosen. Although not as widely adopted as the PR or SRK equations, the ZJRK EOS gave considerably better estimates of liquid densities and saturation pressures for reservoir fluids used in this study.

All results from this work suggest that the C_7+ characterization has a significant influence on EOS predictions for reservoir fluids. The numerous examples presented and systematic approach followed allow the reader to observe the degree of influence each property and estimation procedure has. It was suspected at the beginning of the project that no single characterization scheme would prove to be substantially more accurate than all others. This proved to be the case.

In general, there were too many degrees of freedom - too many unknowns - to make concrete, objective conclusions from this study. Also, it should be noted that some of the guidelines and conclusions presented are based on my experience with a larger number of fluids than are presented in this work. They are therefore subject to criticism. I feel, however, that practicing engineers confronted with the problem of "which characterization scheme to use" should have some guidelines, however subjective, with which to make their final decision.

PHYSICAL PROPERTIES CORRELATIONS: A REVIEW

The critical point of a pure compound is defined as the pressure and temperature at which the vapor phase has properties identical with the equilibrium liquid phase. These conditions also define the end point of the vapor pressure curve. All equations of state require critical pressure and temperature of individual components in a mixture.

Most equations also require the acentric factor.[30] Molecular weights are needed to convert molar volumes to densities. Some recent cubic equations have included critical compressibility factor as a parameter.[41]

There are numerous correlations for estimating physical properties of petroleum fractions. Most of these use specific gravity, γ, and boiling point, T_b, as correlating variables. Correlations commonly used in the petroleum and chemical engineering fields are presented in Tables 1 and 2. Graphical correlations[43,47] are not considered in the present study.

Most correlations were developed when English units were the industry standard. In recent years, many engineering Societies have converted to an SI standard. To help facilitate using these correlations with SPE preferred SI units, the following variables and correlating factors are used:

$$T_c = \frac{5}{9} \cdot T_c^* \quad \ldots\ldots\ldots\ldots\ldots\ldots \quad (1a)$$

$$p_c = 6.894759 \cdot p_c^* \quad \ldots\ldots\ldots\ldots\ldots\ldots \quad (1b)$$

$$t = 1.8 \cdot T_b - 459.67 \quad \ldots\ldots\ldots\ldots\ldots\ldots \quad (1c)$$

$$\gamma = \rho(15.5^{\circ}C) \; / \; \rho_{water}(15.5^{\circ}C) \quad \ldots\ldots\ldots \quad (1d)$$

$$\gamma_{API} = \frac{141.5}{\gamma} - 131.5 \quad \ldots\ldots\ldots\ldots\ldots\ldots \quad (1e)$$

---

* By convention[4] the abbreviation ZJRK is used. Actually, RKJSZ would be more correct since the RK modification which has been most accepted was proposed by Joffe, Schroeder and Zudkevich.[19] This modification was an almost-instantaneous modification of the Zudkevich-Joffe modification (not referenced here).

$$\theta = T_b/T_c \tag{1f}$$

$$K_w = [1.8 \cdot T_b]^{1/3} / \gamma \tag{1g}$$

$$J_A = \frac{\gamma - 0.8468 + 15.8/M}{0.2456 - 1.77/M} \tag{1h}$$

$$x_{wA} = 0.7 \cdot (12.1 - K_w) \tag{1i}$$

where T_b and T_c have units Kelvin (K) and p_c has units kPa. t, T_c^* and p_c^* are merely variables (though they actually represent English unit equivalents of T_b, T_c and p_c).

A short review and discussion of each correlation is provided to help the reader decipher differences between correlations. If several correlations are taken from the same source, they are discussed together. The order of presentation is chronologic to avoid the appearance of personal preference. I have tried to give an objective critique of each correlation based on claims of the original authors and my experience with the correlation. Limitations are stated if they are available.

ROESS[36]

In 1936, Roess presented correlations for critical temperature and pressure. They were developed from flow data on petroleum fractions in a pioneering work previous to most correlation development. The API Technical Data Book has retained the original form of the Roess critical temperature equation (the critical pressure equation is not generally used). It has been modified using recent data from U.S. and North Sea oils.

The main limitation of the Roess correlation is that it should not be used for fractions heavier than C_{20}. It highly underestimates critical temperatures for heavier fractions and is not, therefore, reliable for many reservoir applications.

EDMISTER[7]

In 1948, Edmister proposed a simple but accurate equation for estimating acentric factor of pure compounds. It requires boiling point, critical pressure and critical temperature. The equation has also been applied sucessfully to petroleum fractions. If acentric factor is available from another source, the Edmister equation can be rearranged to solve for any of the three other properties (assuming, of course, the other two are known).

Edmister acentric factors tend to be *lower* than Kesler-Lee values for fractions heavier than C_{20}. The difference is most significant for EOS predictions when the ZJRK EOS is used.

NOKAY[28]

In 1959, Nokay presented seven simple equations for estimating parachor, boiling points, specific gravity and critical temperature. The critical temperature correlation is perhaps the most important because it introduced a simple equation form which was later shown to be applicable to many other physical properties (see Riazi-Daubert correlations below).

Nokay's original relation for critical temperature has been improved by Spencer and Daubert[39] by fitting the three constants to data for each hydrocarbon family.

CAVETT[3]

In 1962, Cavett proposed correlations for estimating critical pressure and temperature of petroleum fractions. The correlations were built into a program designed to simulate tray-to-tray distillation up to pressures of 7000 kPa (1000 psia).

Although these correlations have been widely adapted, they are presented without reference to which data were used for their development, and no limitations or comparison with previous correlations are offered.

HARIU-SAGE[12]

In 1969, Hariu and Sage presented a method (program) for simulating fractional distillation of crude oils. In their procedure they give an equation for estimating molecular weight from boiling point and specific gravity (viz the Watson characterization factor, K_w). It represents a surface-fit of the Winn nomograph. They claim the equation gives a reasonable extrapolation to boiling points over 1090 K.

This correlation can be rearranged to solve directly for specific gravity. It cannot, however, be solved directly for boiling point. Even though a trial and error method is needed, the Hariu-Sage equation provides a necessary link between three important properties. It appears to be more accurate than the Kesler-Lee molecular weight correlation, though the difference may result from using different data to develop the equations.

BERGMAN[1,2]

In 1976, Bergman presented a comprehensive study of the retrograde condensation effects on natural gas pipelines. One result from this study was experimental data which were correlated to give molecular weight and specific gravity as a function of boiling point. Only lean gases and gas condensates with relatively light plus fractions were used in this study, thereby limiting the general applicability of these correlations.

BERGMAN (continued)

A PNA approach is developed to estimate critical properties of the heavy fractions. Only some of the limitations found in the Robinson-Peng method are shared by the Bergman method (see below). The basic difference between these two methods is that Bergman assumes all three constituents (PNA) have the same boiling point, but different properties otherwise. Robinson and Peng use carbon number as the linking property.

The method for estimating PNA content is outlined below. Although there is less chance of obtaining negative PNA compositions, the method is based on scattered data and has not been tested for fractions heavier than C_{20}.

First, the boiling point and specific gravity are used to calculate the Watson characterization factor, K_w (Eq. 1g). Another relation (Eq. 1i) is then used to estimate the weight fraction of the aromatic component; its value is limited to between 0.03 and 0.3. Paraffin and naphthene weight fractions are then calculated from

$$x_{wP} = [\frac{1}{\gamma} - \frac{1}{\gamma_N} - x_{wA}\cdot(\frac{1}{\gamma_A} - \frac{1}{\gamma_N})]\cdot(\frac{1}{\gamma_P} - \frac{1}{\gamma_N})^{-1} \quad \ldots \text{(2a)}$$

$$x_{wN} = 1 - x_{wP} - x_{wA} \quad \ldots\ldots\ldots\ldots\ldots\ldots\ldots\ldots \text{(2b)}$$

Paraffin weight fraction is limited to a minimum of 0.20. If this criterion is not met, the aromatic content is increased in increments of 0.03 until $x_{wP} > 0.20$. Bergman suggests that the procedure may be repeated up to 15 times, and is satisfactory for fractions up to C_{15}.

Bergman's logic for using the PNA method is that critical property correlations were originally developed for wider boiling point cut fractions. This reasoning loses some validity when he suggests that the traditional correlations be used for fractions heavier than C_{15}. It appears, in fact, that the PNA approach may merely complicate the characterization process unnecessarily, without any noticable advantages.

KESLER-LEE[23, 24]

In 1976, Kesler and Lee presented correlations for molecular weight, critical pressure, critical temperature and acentric factor. They were proposed for improving enthalpy predictions. Kesler and Lee claim that critical pressure and temperature equations yield nearly identical results when compared with graphical correlations found in the API Technical Data Book. This claim holds up to a boiling point of 920 K. Modifications are introduced to extend the correlations beyond this limit by ensuring that critical pressure approaches atmospheric pressure as boiling point approaches critical temperature.

Two acentric factor correlations are proposed. One is designed for petroleum fractions with a reduced boiling point, $\theta = T_b/T_c$, less than 0.8, and the other for heavier fractions. These correlations usually predict acentric factors larger than the Edmister equation.

Daubert[6] made comparisons of the Kesler-Lee and Edmister equations and found that for pure compounds (of unspecified type and number) that the Edmister correlation performed better. This comparison should not, however, be considered valid for petroleum fractions.

The molecular weight correlation was developed from data with molecular weights ranging from 60 to 650. Less weighting was given to isomers not commonly found in petroleum fractions. There is an unexplained difference between the resulting correlation and values in the API Technical Data Book.

STANDING[40]

In 1977, Standing presented equations for estimating critical* pressure and temperature of heptanes-plus fractions. The data of Matthews, Roland and Katz were used to develop the correlations. Molecular weight and specific gravity are the correlating variables.

Although Standing claims the correlation is for C_7+ fractions, it appears to be valid for narrower boiling point cuts as well. The use of molecular weight instead of boiling point could be an advantage for characterization methods such as proposed by Yarborough. That is, instead of using molecular weight and specific gravity to estimate boiling point, which is then used with specific gravity to estimate critical properties, they can be estimated directly. The correlation should be used with caution for fractions heavier than C_{25}.

KATZ-FIROOZABADI[21]

In 1978, Katz and Firoozabadi presented generalized properties of single carbon number (SCN) fractions. Because it has become popular to use these properties when measured data are not available, they were correlated in the present work. Molecular weight and specific gravity were made functions of boiling point using third and fourth degree polynomials, respectively.

Molecular weights above C_{22} are somewhat lower than reported by Katz and Firoozabadi. This results from the choice to use values presented by Whitson instead of the original values which were merely extrapolated by adding 14 to the previous molecular weight.

Specific gravities fit the original density data with an absolute average deviation of 0.19%, and a maximum deviation of 0.4% (for C_6). Extrapolation beyond C_{45} is not suggested.

---

* Actually, the equations estimate pseudocritical properties. For narrow boiling cuts, however, critical and pseudocritical properties are nearly equal.

ROBINSON-PENG [34]

In 1978, Robinson and Peng proposed a detailed procedure for characterizing heavy fractions. It was to be used in conjunction with the GPA Peng-Robinson Programs, though its applicability is obviously not restricted to the Peng-Robinson EOS.

The proposed property correlations are based on the paraffin-naphthene-aromatic concept. Equations for PNA properties are provided, including boiling point, specific gravity, molecular weight, critical pressure, critical temperature and acentric factor (amoung others). The critical pressure correlation is taken from Lydersen.[26] The critical temperature is back-calculated from acentric factor, boiling point and critical pressure. Acentric factor is assumed to be a linear function of carbon number.

The procedures and equations are based on the requirement that each heavy fraction represent a single carbon number (SCN). *Naphthenes and aromatics have carbon numbers one less than paraffins in the Robinson-Peng correlations. This assumption is built into the equations in Tables 1 and 2. Do not reduce the carbon number by one for naphthenes and aromatics when using these equations.*

No indication of the maximum carbon number is given. Robinson indicated in a verbal communication that the maximum value was "C_{25}. No, I wouldn't stop there if I had to get an answer. Because I wouldn't know any better way to go if I had C_{30} or C_{40} than to just go ahead with the same scheme. I would recognize that the backup gets shakier and shakier." [35]

Experience with the Robinson-Peng method has led to the following observations:

(1) As shown in Fig. 1, SCN specific gravities can not exceed 0.875, the aromatic value for C_7. This is, of course, unacceptable.

(2) Boiling point data must be converted to cuts with paraffin boiling point intervals. This is often both time-consuming and unnecessary. An example is the Hoffman, et al. fluid.

(3) The use of a mass accumulation curve to determine SCN densities (from its tangent) is highly unreliable.

(4) Methods proposed for estimating the PNA content from boiling point, molecular weight and specific gravity are easily subject to error, resulting in negative compositions. Fig. 1 illustrates the problem by showing the regions which yield non-negative PNA compositions. The problem worsens when we note that boiling points found using the proposed method will almost always equal the arithmetic average of neighboring paraffin boiling points (exactly if the distillation curve is linear between these two values). This makes the region (or line) in which realistic non-negative PNA compositions can be obtained very small, and in many cases non-existent.

(5) Acentric factors for fractions heavier than C_{20} are considerably higher than when estimated from either the Edmister or Kesler-Lee equation. They reach a value of 2.0 for C_{45}. It appears that the linear extrapolation is not appropriate for heavier fractions. An indirect result is that critical temperatures are too low.

(6) The assumption that naphthene and aromatic fractions have one less carbon number than paraffins is only approximate and loses credibility at higher boiling points.

Because of these limitations, the Robinson-Peng method is not suggested for reservoir fluids containin fractions heavier than C_{20} (about the same limitation as imposed on the Bergman PNA method). Unless an accurate estimate of the PNA content is available from mass spectrometry or the density-viscosity-refractive-index correlation of Riazi-Daubert, the method should probably not be used at all.

ROWE [37]

In 1978, Rowe presented equations for estimating boiling point, critical pressure and critical temperature of paraffin hydrocarbons. He suggested that the correlations could be used to characterize C_7+ fractions found in reservoir fluids. Although it is not clear that his assumption is correct, the correlations are presented because of their simplicity. Carbon number is used as the only correlating variable, and Rowe suggests it be calculated from molecular weight, $C_N = (M-2)/14$.

YARBOROUGH [46]

In 1978, Yarborough presented a method for characterizing the heavy fractions of reservoir fluids. A graphical correlation relating specific gravity to carbon number for various aromaticity factors[18] is the basis for this method. These curves have been fit by a four constant equation. The constants are a function of aromaticity.

The Yarborough method assumes that the C_7+ molecular weight and specific gravity are measured. It also assumes that mole fractions are measured from chromatographic analysis (paraffin molecular weights are assumed to convert weight to mole fractions).

The procedure begins by assuming an aromaticity factor. A good estimate can be calculated from Eq. 1h using C_7+ properties. SCN specific gravities are calculated from the specific gravity - carbon number correlation. The plus specific gravity is then calculated using the proper mixing rule. This value is compared with the measured value, and the aromaticity factor adjusted until a match is achieved.

Using SCN specific gravities and assumed molecular weights, boiling points are estimated from the charts in Ref.47, or an appropriate correlation. Critical properties are estimated using boiling points and specific gravities. Acentric factor is estimated from the Edmister equation.

RIAZI-DAUBERT [32]

In 1980, Riazi and Daubert presented simple equations for estimating numerous physical properties of pure compounds and petroleum fractions. The same equation form is used for all properties. It is identical to the equation proposed by Nokay for critical temperature.

The correlations are compared with the Winn nomograph and Mobil nomograph for critical pressure and critical temperature, respectively. The original claim was that the correlations gave "equivalent" results. A later publication by Daubert gives more detailed comparisons with nomographs and other correlations. In the boiling point range 255-590 K, the Riazi-Daubert correlations perform better (though only slightly) than other "best" methods.

The most serious drawback with the Riazi-Daubert correlations is the limitation of boiling point to 730 K for critical pressure and molecular weight. Whitson proposed an extension to the critical pressure correlation, but the resulting constants create a discontinuity.

For systems without components heavier than C_{25}, the Riazi-Daubert correlations are probably the most accurate and easiest to use.

WHITSON [14]

In 1981, Whitson proposed a scheme for characterizing heptanes-plus fractions found in reservoir fluids. A method is proposed for estimating single carbon number specific gravities using SCN molecular weights and a generalized function for the Watson characterization factor, K_w. The method is similar to the Yarborough scheme, except that the characterization factor is directly related to boiling point. The aromaticity factor is not.

The equation proposed for relating K_w, specific gravity and molecular weight is

$$K_w = 4.5579 \cdot M^{0.15178} \cdot \gamma^{-0.84573} \quad \ldots\ldots\ldots\ldots (3)$$

Unfortunately, Eq. 3 is only valid up to a boiling point of 730 K. The Hariu-Sage correlation is preferred for heavier fractions. The Whitson equation is probably more useful for correlating C_7+ molecular weights and specific gravities. Such a relation has been found very useful for a variety of reservoir engineering applications.

The Whitson procedure begins by assuming an average K_w for the plus fraction. Eq. 3 can be used with C_7+ molecular weight and specific gravity. SCN characterization factors are then estimated using the following correlation developed by Haaland, [11]

$$K_{C_N}/K_{C_{7+}} = -0.0110 \cdot C_N + 1.1010 \quad \text{for } C_N = 6\ 11$$

$$K_{C_N}/K_{C_{7+}} = 0.0025 \cdot C_N + 0.9525 \quad \text{for } C_N = 11\text{-}19$$

$$K_{C_N}/K_{C_{7+}} = 0.0014 \cdot C_N + 0.9734 \quad \text{for } C_N = 19\text{-}24$$

$$K_{C_N}/K_{C_{7+}} = 1.0070 \quad \text{for } C_N = 24\text{-}\infty$$

SCN specific gravities are calculated from SCN characterization factors and molecular weights using the Hariu-Sage equation (originally Eq. 3 was suggested). Average C_7+ specific gravity is calculated using the proper mixing rule and compared with the measured value. If the two do not match, a new estimate of $K(C_{7+})$ is made. This procedure is repeated until calculated and measured C_{7+} specific gravities match.

Boiling points are calculated from SCN characterization factors and specific gravities by rearranging Eq. 1g: $T_b = (\gamma \cdot K_w)^3 / 1.8$. Critical properties are estimated using the Riazi-Daubert correlations. The original critical pressure equation is only used for boiling points less than 730 K. A revised set of constants are used for heavier fractions. Unfortunately, the revision causes a discontinuity in critical pressure and acentric factor (the Edmister equation uses critical pressure) near C_{30-32}.

SUGGESTIONS AND COMMENTS

From my experience, there is not one correlation or characterization scheme which is better than all others. Observations made from EOS predictions have led me to make the following general, albeit subjective conclusions about physical properties estimation:

CRITICAL PRESSURE - The Kesler-Lee correlation is suggested. Nearly identical results are obtained, however, from the Riazi-Daubert equation* Cavett's correlation deviates slightly from these two at higher boiling points.

CRITICAL TEMPERATURE - The Kesler-Lee correlation is suggested. The Riazi-Daubert and Cavett correlations are nearly identical, with estimates slightly higher than Kesler-Lee.

ACENTRIC FACTOR - The Kesler-Lee correlations are suggested, though with acknowledged reservation. I have observed that the higher acentric factor estimations help density estimates when using the ZJRK EOS. It can also be reasoned that since the Kesler-Lee equations were developed specifically for narrow boiling petroleum fractions (first relation) and unusually heavy petroleum fractions (second relation), that they should perform better than the Edmister equation. This is only a hypothesis.

MOLECULAR WEIGHT - The Hariu-Sage correlation is suggested. A comparison should probably be made between this correlation and the one proposed by Kesler and Lee using experimental data.

* Recall the Riazi-Daubert p_c correlation has a discontinuity because two sets of constants are required to cover the entire boiling point range.

EQUATION OF STATE CONSTANTS

Several recent publications[4,27] have suggested that EOS constants a and b (or Ω_a and Ω_b) can be adjusted to match experimental PVT data. It can be shown, however, that this method is essentially the same as the earlier practice of adjusting individual component critical properties.

For the Peng-Robinson and Soave-Redlich-Kwong equations,

$$a = \Omega_a^o \cdot \frac{R^2 \cdot T_c^2}{p_c} \cdot [1 + \kappa \cdot (1 - T_r^{1/2})]^2 \quad \dots\dots\dots\dots \text{(5a)}$$

$$b = \Omega_b^o \cdot \frac{R \cdot T_c}{p_c} \quad \dots\dots\dots\dots \text{(5b)}$$

$$\kappa = k_0 + k_1 \cdot \omega + k_2 \cdot \omega^2 \quad \dots\dots\dots\dots \text{(5c)}$$

	PR	SRK
k_0	0.37464	0.480
k_1	1.54226	1.574
k_2	-0.26992	-0.176

Ω_a^o (PR) = 0.45724
Ω_b^o (PR) = 0.07780
Ω_a^o (SRK) = 0.42748
Ω_b^o (SRK) = 0.08664

If we define adjusted constants $\hat{\Omega}_a^o = \alpha \cdot \Omega_a^o$ and $\hat{\Omega}_b^o = \beta \cdot \Omega_b^o$ where α and β are correction factors, then equivalent results may be obtained using

$$\hat{T}_c = \frac{\alpha}{\beta} \cdot T_c \quad \dots\dots\dots\dots \text{(6a)}$$

$$\hat{p}_c = \frac{\alpha}{\beta^2} \cdot p_c \quad \dots\dots\dots\dots \text{(6b)}$$

$$\hat{\omega} = \frac{-k_1 + \sqrt{k_1^2 - 4 \cdot k_2 \cdot (k_0 - \hat{\kappa})}}{2 \cdot k_2} \quad \dots\dots\dots\dots \text{(6c)}$$

$$\hat{\kappa} = \kappa \cdot \frac{1 - \sqrt{T/T_c}}{1 - \sqrt{T/\hat{T}_c}} \quad \dots\dots\dots\dots \text{(6d)}$$

instead of corrections applied to constants Ω_a and Ω_b. Eqs. 6a-6d illustrate that adjustments of a and b can be directly translated to adjustments of T_c, p_c and ω. If $\alpha/\beta = 1$, only p_c is adjusted. If $\alpha/\beta^2 = 1$, only T_c and ω are adjusted. All other combinations of α and β correspond to an adjustment of all three critical properties.

The engineer should not adjust a and b more than will result in altered critical properties which are physically meaningful. Eqs. 6a-6d should help prevent misuse of adjustments to EOS constants. They were used in this study to investigate the the influence of the adjustment process on EOS predictions.

Although it can be shown that alternative relations can be used instead of Eqs. 6a-6d, the proposed equations are considerably less complicated. and should be useful interpretive tools.

RESULTS

Calculations were performed on six reservoir fluids taken from the literature[9,13,14,17] Several characterization shcemes were used to describe the heavy fractions. Each example illustrates the effect of one or more physical properties on EOS predictions. In all cases, the C_7+ fraction was split into SCN groups.

The PR and ZJRK equations were used exclusively for all calculations. Although detailed input data are not presented for each example, they can be obtained from the author.

Eilerts OO-L-544 Gas Condensate[9]

The OO-L-544 fluid presented by Eilerts is a gas condensate containing 90.162 mol-% methane and 1.51 mol-% heptanes-plus. The C_7+ fraction has a molecular weight of 167.3 and specific gravity of 0.8051. Fractional distillation data are available up to C_{24}. These data were converted to SCN groups according to the method of Robinson-Peng (except for density determination). Dew point pressure is reported to be 33.85 MPa at reservoir temperature of 394.8 K; the reservoir was initially undersaturated at a pressure of 35.00 MPa.

Dew point pressure was estimated with the ZJRK EOS at 394.8 K. Measured specific gravities and boiling points were used to estimate critical properties from five* correlations. Acentric factors were estimated from the Edmister equation except when using the Kesler-Lee and Robinson-Peng correlations. For all cases, the interaction coefficients between methane and all C_7+ fractions were adjusted to match the measured dew point pressure. Saturation pressures were then calculated at temperatures from 290-440 K. Results are presented in Fig. 2a.

The matching procedure was repeated at 310 K using only two of the property correlations. The matched dew point was 39.40 MPa. Extrapolation in temperature was also performed. Results are given in Fig. 2b.

A continual match of dew point pressure was made in the temperature range 290-440 K using the Riazi-Daubert correlations. The resulting interaction coefficients are presented in Fig. 2c.

Liquid-gas ratios** were calculated as a function of depletion pressure at reservoir temperature using the five property correlations; the match point was once again 394.8 K and 33.85 MPa. Using this match, the same calculations were performed at a lower temperature of 310.9 K. Results are found in Fig. 3a.

The same procedure was repeated, but the match point was reversed. In this case, only two of the property correlations were used. Liquid-gas ratios are plotted versus pressure in Fig. 3b.

---

* The first correlation, labeled "Eilerts (Paraffin)" is merely the set of critical properties which Eilerts proposed. They represent paraffin values and were not calculated from a correlation. Acentric factor was estimated from the Edmister equation.

** As used by Eilerts, the liquid-gas ratio, LGR, is liquid volume at p,T divided by gas volume at standard conditions. Its relation to liquid volume, relative to total (L+G) volume, v_{rL}, is: ρ_g(g/cc); LGR($m^3/10^6 Sm^3$) ⇒ $LGR = 42.26 \frac{M_g}{\rho_g} \cdot \frac{v_{rL}}{1 - v_{rL}}$

Eilerts OO-L-544 (continued)

The Peng-Robinson EOS was used to illustrate the effect of adjusting the methane - C_7+ interaction coefficient. Fig.4 shows dewpoint pressure, gas density and liquid density as functions of interaction coefficient.* Calculations were made at 394.8 K.

Eilerts CH-P-843 [8,9]

The CH-P-843 fluid is a gas condensate containing 76.432 mol-% methane and 2.992 mol-% heptanes-plus. The C_7+ molecular weight is 125 with a specific gravity of 0.7385. Fractional distillation data did not indicate hydrocarbons heavier than C_{13}. There are consierably more intermediates in this fluid than in OO-L-544. Extensive experimental data are provided by Eilerts. These include: the phase diagram from 220-310 K, critical point, cricondenbar, cricondentherm and two-liquid phase region. Some liberty has been taken in this work when extrapolating the saturation-pressure - temperature diagram.

The Peng-Robinson EOS was used to predict some of the experimental PVT observations. Paraffin critical properties suggested by Eilerts were used together with Edmister acentric factors.

Figs. 5a-5e show the effect of adjusting C_7+ critical properties. Dew point pressure and liquid volume, relative to total volume, were estimated at 310.9 K. Curves labeled 1 and 2 are the same for all figures. Curve 1 was determined from experimental data, whereas Curve 2 is the PR prediction using unaltered paraffin properties for the C_7+ fractions.

The effects of simultaneously adjusting critical pressure and temperature are shown in Figs. 5a and 5b. Results of adjusting only critical pressure are shown in Fig. 5d; results of adjusting only critical temperature are shown in Fig.5c ; results of adjusting only acentric factor are shown in Fig. 5e.

Figs. 6a-6c show the effect of adjusting EOS constants a and b. Both constants are adjusted in Fig. 6a. Only constant b is adjusted in Fig. 6b, whereas only constant a is adjusted in Fig. 6c. Note that Curve 3 in Fig. 6a (decreasing both a and b) results in an excellent prediction of dewpoint pressure and liquid dropout.

The saturation-pressure - temperature diagram was predicted using three C_7+ characterization schemes. The first merely used unaltered paraffin critical properties without adjusting interaction coefficients. The second was identical with Curve 3 in Fig. 6a. The third alternative used unaltered paraffin critical properties, but matched dewpoint pressure at 310.9 K with the methane-C_7+ interaction coefficient of -0.12. Phase diagrams and critical points are presented in Fig. 7.

Jacoby Synthetic Mixtures [17]

The synthetic mixtures presented by Jacoby were studied using the PR and ZJRK equations of state. Several critical property correlations were chosen to describe the eight boiling point fractions constituting hexanes-plus.

Fig. 8 shows results for the S-3 mixture. The phase diagram was predicted by matching saturation pressure of 27.4 MPa at 370.5 K with a methane-C_6+ interaction coefficient of 0.0536. Experimental data show a dew point at this temperature. A bubble point was predicted using both PR and ZJRK equations, independent of the property correlation. Extrapolation in temperature was reliable for all correlations (two which are shown in Fig. 8). However, the estimated critical temperatures were always 70 to 100 degrees (K) high.

Numerous attempts were made to predict the phase diagram created by recombining separator samples at various gas-oil ratios. For all critical property correlations, both equations of state predicted reasonable (± 5%) saturation pressures up to the last two gas-oil ratios (S-6 and S-7). The estimated critical composition (gas-oil ratio) was considerably different than measured experimentally. Bubble points were predicted until a gas-oil ratio between 890-1340 Sm^3/Sm^3 (S-4 to S-5). Experimental data suggest that the last bubble point should have been between 620-710 Sm^3/Sm^3 (S-2 to S-3).

Hoffman-Crump-Hocott Reservoir Oil [13]

The Hoffman-Crump-Hocott (HCH) reservoir oil was used to study the effect of property correlations on typical PVT behavior. The oil was saturated at initial conditions of 26.4 MPa and 367.0 K. It contains 52.00 mol-% methane and 36.84 mol-% heptanes-plus. The C_7+ molecular weight is 198.7 with a specific gravity of 0.8412. Distillation analysis is available to C_{35}; boiling point cuts approximate SCN groups with paraffin boiling points.

Several aspects of C_7+ characterization were investigated using the HCH oil. First, a comparison was made between three schemes for estimating specific gravities and boiling points of SCN fractions. Fig. 9 compares experimental and estimated values of γ and T_b. The Kesler-Lee correlations were used to estimate critical properties and acentric factors.

Figs. 10a-e present results of EOS predictions for a simulated differential liberation experiment at 367 K. A swelling test (described in the next paragraph) was also simulated. There was essentially no effect on EOS predictions from the various methods for estimating specific gravity and boiling point.

EOS predictions were also performed using four different critical property correlations. One case (1') used variable C_{7-21} - methane interaction coefficients, matching bubble point pressure with the C_1-C_{22}+ coefficient. Results of differential liberation simulations are found in Figs. 11a-11e. Swelling test predictions are found in Figs. 12a-12b and 13. Injection gas used in the swelling test is given in Table 3. It was determined by optimizing a three stage flash process for maximum C_2-C_6 content in the separator gases.

---

* As should be obvious from Fig. 4, deviations are calculated relative to *predicted* EOS properties - albeit matched at the measured dew point pressure.

Hoffman-Crump-Hocott Reservoir Gas [13]

Hoffman, et al. also presented extensive data for the gas-cap fluid loacted in the same formation as the abovementioned reservoir oil. The gas contains 91.35 mol-% methane and 1.54 mol-% heptanes-plus. The C_7+ molecular weight is 141 with a specific gravity of 0.7867. Dewpoint pressure equals bubble point pressure of the oil (26.4 MPa) at reservoir temperature of 367 K.

The same comparisons made in the previous example were made for this fluid (except the case with varying interaction coefficients). Instead of simulating a differential liberation experiment, a constant composition (mass) expansion (CCE) and constant volume depletion (CVD) were simulated. Only some results are included in this work. CCE predictions were compared with experimental data reported by Hoffman, et al.

Figs. 14a-14d present results of the comparisons made between different methods of estimating specific gravities and boiling points. Kesler-Lee properties were used in the ZJRK EOS.

Figs. 15a-15d present results of the comparisons made between different property correlations. Both PR and ZJRK equations were used.

Hong Reservoir Oil A - CO_2 System [14]

A recent publication by Hong gives experimental data for a reservoir oil - CO_2 system. The oil contains 31.00 mol-% methane and 32.43 mol-% heptanes-plus. C_7+ molecular weight is 199. No distillation data or C_7+ specific gravity are reported. Mole fractions and "tuned" critical properties are given for C_7-C_{12} SCN groups and the remaining C_{13}+ fraction. Bubble point pressure of the initial oil is 11.4 MPa at 327.6 K.

The Hong oil - CO_2 system was chosen to illustrate the effect of carbon dioxide - hydrocarbon (CO_2-HC) binary interaction coefficients on predicted phase behavior. The Peng-Robinson EOS is used by Hong. Both PR and ZJRK equations were used in this study.

Using the PR EOS, four methods were used to describe the CO_2-HC interaction coefficients. The first method used guidelines provided by Hong. Coefficients were varied from 0.14 to 0.20, decreasing as a function of acentric factor. The second method used the empirical equation suggested by Kato.[20] Fig. 16 shows the graphical form of this correlation. The third method used a constant, molar average of coefficients from the first method. The last method used a constant CO_2-HC coefficient of 0.145. This value was determined by matching the bubble point pressure at 50 mol-% CO_2.

Results of the first three cases are shown in Figs. 17a and 17b. For the first case (A), saturation pressures matched experimental data up to CO_2 concentrations of 80 mol-%. The critical CO_2 concentration was overestimated by 10 mol-%. This predicted phase diagram is similar to the one using a constant CO_2-HC coefficient of 0.145.

Using the Kato coefficients (B), saturation pressures were grossly underestimated. Bubble point pressures were predicted up to a CO_2 concentration of 70 mol-%.

Using the average CO_2-HC coefficient of 0.175 (from A) resulted in overestimates of saturation pressures. At 60 mol-% CO_2, no saturation pressure was predicted below 30 MPa. The experimental critical pressure at this concentration was 17.7 MPa.

Phase behavior of this system was also predicted using the ZJRK EOS. Only a slight change (from 0.137 to 0.147) in CO_2-C_3+ coefficients was necessary to match the entire phase envelope. The adjusted value is nearly identical with the one found using the PR EOS (0.145); note that the ZJRK EOS used slighly lower values for CO_2-C_1 and CO_2-C_2 coefficients. As in all other cases, critical CO_2 concentration was overestimated.

DISCUSSION

Discussion of the results begins by disclaiming any attempt to present a conclusive document of the effects C_7+ characterization has on EOS predictions. The examples which are presented were designed to give an indication of the influence certain characterization schemes may have on EOS predictions. Examples were also limited to the examination of PVT properties important to reservoir engineering.

Interaction Coefficients

The effect of increasing binary interaction coefficients between methane and heavy fractions is to increase saturation pressure prediction. This observation appears to be general for both the bubble point and retrograde dew point regions.

Fig. 4 presents the general trend one can expect in saturated liquid and gas densities and saturation pressure when adjusting the C_1-C_7+ interaction coefficients. The primary reason for variation in saturated densities is the variation in saturation pressure. At constant pressure and temperature, interaction coefficients have a small influence on phase densities.

In general, the Peng-Robinson EOS requires positive coefficients to match saturation pressure, whereas the ZJRK EOS often requires negative values. This rule does not always hold, as shown in Fig. 2a. Apparently the critical properties influence the value of interaction coefficients needed to match saturation pressure. This observation leads me to conclude that adjusting interaction coefficients is more a correction due to inadequate characterization of the heavy fractions than a physical description of interaction between large and small compounds.

It appears that C_1-C_7+ interaction coefficients have a relatively strong temperature dependence for many reservoir fluids. An important consequence is that saturation pressures may be overestimated if coefficients matched at one temperature are used to estimate saturation pressure (VLE) at lower temperatures. An example of this situation might be when matching the dew point at reservoir temperature, then using the same interaction coefficients to predict VLE properties at temperatures expected in the tubing and process equipment. Underestimation seems to be less significant if the match at one temperature is extrapolated to higher temperatures (see Fig. 2b).

Several attempts have been made to correlate methane-hydrocarbon interaction coefficients.[21,25] The trend is that coefficients increase with increasing molecular size. A comparison between using a constant C_1-C_7+ coefficient and using variable (increasing) values had little effect on most EOS predictions. Some properties were influenced however. These included gas compressibility and gravity (i.e. molecular weight), swelling factor, saturation pressure increase due to gas injection, and interfacial tension (calculated using a compositional correlation).

Concerning the use of CO_2-hydrocarbon binary interaction coefficients, it appears that there is little advantage in using coefficients which vary as a function of molecular size. This conclusion is based on studies of only two systems. It may not be valid if near-critical phase behavior is to be predicted accurately.

EOS Parameter Adjustments

Several generalizations appear valid concerning the adjustment of heavy fraction critical properties and EOS constants. They are interpretations of results presented in Figs. 5 and 6 for a gas condensate. A summary of important observations is given below:

(1) A decrease in critical temperature results in a decrease of both saturation pressure and maximum liquid drop-out.

(2) An increase in critical pressure results in an increase in saturation pressure and a decrease in maximum liquid drop-out.

(3) Acentric factor has little or no effect on maximum liquid drop-out. This is only true for the PR and Soave RK equations; acentric factor only affects EOS constant a, which is mostly related to VLE calculations. For these two equations, a decrease in acentric factor results in a decrease in saturation pressure.

Constants a and b in the ZJRK EOS are both dependent on acentric factor. For this equation, values of acentric factor will strongly influence volumetric properties such as maximum liquid drop-out. This results from the strong connection between b and volumetric predictions.

(4) A decrease in constant a results in a decrease in both saturation pressure and maximum liquid drop-out. The greater influence is on saturation pressure (i.e. VLE predictions).

(5) A decrease in constant b results in a relatively large increase in saturation pressure and decrease in maximum liquid drop-out. This observation suggests that constant b has influence on both VLE and volumetric predictions.

By noting that maximum liquid drop-out is strongly, though not completely dependent on liquid density, one can draw similar conclusions about volumetric phase behavior of reservoir oils. Effects on dew point pressure should be analogous to effects on bubble point pressure for oil systems; therefore the term saturation pressure has been used above.

General Observations

The influence of heptanes-plus characterization on EOS predictions appears to be substantial for reservoir fluids. The choice of critical property correlation usually has more influence on EOS predictions than the method used to estimate specific gravities and boiling points (when these properties are not available). This was somewhat unexpected. The reason may be that reservoir fluids have heavy components with properties which reach the limits of some, if not all correlations. The methods used for estimating specific gravities and boiling points appear to be reliable for even very heavy fractions.

Several observations not directly related to C_7+ characterization are worth noting. The two equations of state used in this study always overestimated critical temperature (see Figs. 7 and 8). The same behavior has been observed for several other systems. This problem can be particularly important if a rich (near critical point) gas condensate is being studied. That is, it may be difficult to predict a dew point at reservoir temperature.

Although it is not my intention to suggest one EOS over another, the ZJRK EOS gave an overal better performance than the PR EOS. The major difference was seen in liquid density (volumetric) predictions. On the other hand, the PR EOS has a simple form which can be readily reproduced. This is not the case for most of the ZJRK variants. For example, constants a and b presented by Yarborough have the shortcoming that they must be digitized from figures. The method of representing these values - equations versus tables - varies from program to program. The ZJRK EOS lacks an essential property of being reproducible.[4, 10, 19, 27, 46]

CONCLUSIONS

Results indicate that equation of state predictions are highly sensitive to characterization of the heptanes-plus fraction. This observation has also been made by others. The present study offers direct comparison between various physical property correlations & their effect on predicted phase behavior using the Peng-Robinson and Zudkevich-Joffe-Redlich-Kwong equations of state.

Too many unknown factors are involved in the characterization of heavy fractions to make objective conclusions concerning which property correlations are best. This is compounded by inconsistencies and different extrapolative capabilities of various property correlations.

Most engineers will probably rely on adjusting EOS parameters to achieve satisfactory predictions of PVT properties. To this end, guidelines are provided for making such adjustments.

NOMENCLATURE

a = equation-of-state constant

A = constant in property correlation

b = equation-of-state constant

B = constant in property correlation

C_N = carbon number

C_7+ = heptanes-plus fraction

J_A = Jacoby aromaticity factor

k = constants in Eqs. 5 and 6

K_w, K = Watson characterization factor

LGR = liquid-gas ratio, $m^3/10^6 Sm^3$

M = molecular mass, mass per mole

p_c = critical pressure, kPa

p_c^* = critical pressure variable

PNA = Paraffin, Naphthene, Aromatic

R = universal gas constant, 8.3143 J/(mol·K)

t = boiling point variable

T = absolute temperature, K

T_b = normal boiling point, K

T_c = critical temperature, K

T_c^* = critical temperature variable

T_r = reduced temperature $(=T/T_c)$

v_{rL} = liquid volume, relative to total volume

x_w = weight fraction

$\mathring{x}$ = adjusted value of variable x

Greek Symbols

α = correction factor for EOS constant a

β = correction factor for EOS constant b

γ = specific gravity, relative to water at 15.5°C

γ_{API} = liquid gravity, degrees API

θ = reduced normal boiling point $(=T_b/T_c)$

κ = constant in Eq. 5

ρ = density, gm/cc

ω = acentric factor

Ω_a^o = equation-of-state constant in Eq. 5a

Ω_b^o = equation-of-state constant in Eq. 5b

ACKNOWLEDGMENTS

i would like to thank V. Dalen and G.Ø. Nielsen for helpful comments and criticism of this paper. The work was performed at the Continental Shelf Institute (IKU) during 1982, and the equation of state used was developed under a joint project by IKU and Norsk AGIP A/S. Continuing support from frying pan publications, inc. is greatly appreciated.

REFERENCES

1. Bergman, D.F.: "Predicting the Phase Behvaior of Natural Gas in Pipelines," PhD Dissertation, U. of Michigan, Ann Arbor (1976)

2. Bergman, D.F., Tek, M.R. and Katz, D.L.: "Retrograde Condensation in Natural Gas Pipelines," Project PR26-69 of the Pipelines Research Committee AGA (Jan. 1977)

3. Cavett, R.H.: "Physical Data for Distillation Calculations - Vapor-Liquid Equilibrium," Proc. 27th Meeting, API, San Francisco (1962)351-366

4. Coats, K.H.: "Simulation of Gas Condensate Reservoir Performance," paper SPE 10512 presented at the Sixth SPE Symposium on Reservoir Simulation, New Orleans, Jan. 31 - Feb. 3, 1982

5. Conrard, P.G. and Gravier, J.F.: "Peng-Robinson Equation of State Checks Validity of PVT Experiments," Oil and Gas J. (Apr. 21 1980)77-86

6. Daubert, T.E.: "Characterization Parameters for Hydrocarbons for Physical and Thermodynamic Property Prediction," Proc. 53rd GPA Convention (1979)17-24

7. Edmister, W.C.: "Applied Hydrocarbon Thermodynamics Part 4: Compressibility Factors and Equations of State," Pet. Refiner (Apr. 1958)37,173-179

8. Eilerts, C.K., Barr, V.L., Mullens, N.B. and Hanna, B.: "Phase Relations of a Gas-Condensate Fluid at Low Temperatures, Including the Critical State," The Pet. Engineer (Feb. 1948)154-180

9. Eilerts, C.K. and Others: Phase Relations of Gas-Condensate Fluids, Monograph 10, Bureau of Mines American Gas Association, New York (1957)Vol. 1

10. Gray, R.D., Jr.: "Industrial Experience in Applying the Redlich-Kwong Equation to Vapor-Liquid Equilibria," Equations of State in Engineering and Research, K.C. Chao and R.L. Robinson, Jr. (eds.), Advances in Chemistry Series 182, Amer. Chem. Soc. (1978)386-439

11. Haaland, S.: "Characterization of North Sea Crude Oils and Petroleum Fractions," MS Thesis, Norwegian Institute of Technology (NTH), The Univ. of Trondheim, Norway

12. Hariu, O.H. and Sage, R.C.: "Crude Split Figured by Computer," Hydro. Proc. (April 1969)143-148

13. Hoffman, A.E., Crump, J.S. and Hocott, C.R.: "Equilibrium Constants for a Gas-Condensate System" Trans.,AIME(1953)198,1-10

14. Hong, K.C.: "Lumped-Component Characterization of Crude Oils for Compositional Simulation," paper SPE 10691 presented at the SPE/DOE Third Joint Symposium on Enhanced Oil Recovery, Tulsa, April 4-7, 1982

15. Hughes, D.S., Matthews, J.D. and Mott, R.E.: "Theoretical Aspects of Calculating the Performance of CO_2 as an EOR Process in North Sea Reservoirs," presented at the Symposium on Enhanced Oil Recovery Bournemouth, England, Sept. 21-23, 1981, 247-266

16. Jacoby, R.H. and Berry, V.J.: "A Method for Predicting Pressure Maintaenance Performance For Reservoirs Producing Volatile Crude Oil," Trans., AIME(1958)213,59-64

17. Jacoby, R.H., Koeller, R.C. and Berry, V.J.: "Effect of Composition and Temperature on Phase Behavior and Depletion Performance of Rich Gas-Condensate Systems," Trans.,AIME(1959)216,406-411

18. Jacoby, R.H.: "NGPA Phase Equilibrium Project," Proc. Amer. Pet. Inst., Sect. 3 (1964)288

19. Joffe, J., Schroeder, G.M. and Zudkevich, D.: "Vapor-Liquid Equilibria with the Redlich-Kwong Equation of State," AIChE J., Vol. 16, No. 3 (May 1970)496-498

20. Kato, K., Nagahama, K. and Hirata, M.: "Generalized Interaction Parameter for Systems Containing CO_2 and Normal Paraffins," Fluid Phase Equilibria, 7 (1981)219-231

21. Katz, D.L. and Firoozabadi, A.: "Predicting Phase Behavior of Condensate/Crude-Oil Systems Using Methane Interaction Coefficients," J. Pet. Tech. (Nov. 1978)1649-1655; Trans.,AIME,228

22. Kay, W.B.: "Density of Hydrocarbon Gases and Vapors at High Temperature and Pressure," Ind. and Eng. Chem. (1936)28,1014

23. Kesler, M.G. and Lee, B.I.: "Improve Predictions of Enthalpy of Fractions," Hydro. Proc. (March 1977)153-158

24. Lee, B.I. and Kesler, M.G.: AIChE J. (1975)21,510

25. Lee, S.T., Jacoby, R.H. Chen, W.H. and Culham, W.E.: "Experimental and Theoretical Studies on the Fluid Properties Required for Simulation of Thermal Processes," paper SPE 8398 presented at the SPE 54th Annual Fall Technical Conference and Exhibition, Las Vegas, Sept. 23-26, 1979

26. Lydersen, A.L.: "Estimation of Critical Properties of Organic Compounds," Univ. of Wisconsin, Eng. Experimental Station Report 3, Madison, Wisconsin (Apr. 1955)

27. Mott, R.E.: "Calculating PVT Behavior in Gas Condensate Reservoirs," Oil Recovery Projects Division, Atomic Energy Establishment, Winfrith Great Britian (Apr. 1982)

28. Nokay, R.: "Estimate Petrochemical Properties," Chem. Eng. (Feb. 23 1959)147-148

29. Peng, D.-Y. and Robinson, D.B.: "A New Two-Constant Equation of State," Ind. and Eng. Chem. Fund., Vol. 15, No. 1(1976)59-64

30. Pitzer, K.S., Lippman, D.Z., Curl, R.F., Jr., Huggins, C.M. and Petersen, D.E.: "The Volumetric and Thermodynamic Properties of Fluids. II. Compressibility Factor, Vapor Pressure and Entropy of Vaporization," J. Amer. Chem. Soc. (1955)77,3433-3440

31. Reid, R.C., Prausnitz, J.M. and Sherwood, T.K.: The Properties of Gases and Liquids, 3rd edition, McGraw-Hill, New York (1977)

32. Riazi, M.R. and Daubert, T.E.: "Simplify Property Predictions," Hydro. Proc. (March 1980)115-116

33. Riazi, M.R. and Daubert, T.E.: "Prediction of the Composition of Petroleum Fractions," Ind. and Eng. Chem. Process Dev. (1980)19,289-294

34. Robinson, D.B. and Peng, D.-Y.: "The characterization of the Heptanes and Heavier Fractions," Research Report 28, GPA Tulsa (1978)

35. Robinson, D.B.: "Peng-Robinson Correlations," Proc. 56th GPA Convention (1977)102-104

36. Roess, L.C.: "Determination of Critical Temperature and Pressure of Petroleum Fractions by a Flow Method," J. Petrol. Tech. (1936)22,665

37. Rowe, A.M.: "Internally Consistent Correlations for Predicting Phase Compositions for Use in Reservoir Compositional Simulators," paper SPE 7475 presented at the 53rd Annual Fall Technical Conference and Exhibition, Houston, Oct. 1-3, 1978

38. Smith, R.L. and Watson, K.M.: "Boiling Points and Critical Properties of Hydrocarbon Mixtures," Ind. and Eng. Chem. (1937)1408-1414

39. Spencer, C.F. and Daubert, T.E.: "A Critical Evaluation of Methods for the Prediction of Critical Properties of Hydrocarbons," AIChE J. Vol. 19, No. 3 (May 1973)482-486

40. Standing, M.B.: Volumetric and Phase Behavior of Oil Field Hydrocarbon Systems, Society of Petroleum Engineers, Dallas (1977)124

41. Usdin, E. and McAuliffe, J.C.: "A One Parameter Family of Equations of State," Chem. Eng. Data (1976)31,1077-1084

42. Watson, K.M., Nelson, E.F. and Murphy, G.B.: "Characterization of Petroleum Fractions," Ind. and Eng. Chem. (1935)27,1460-1464

43. Watson, K.M. and Nelson, E.F.: "Improved Methods for Approximating Critical and Thermal Properties of Petroleum Fractions," Ind. and Eng. Chem., (1933)25,880-887

44. Whitson, C.H.: "Characterizing Hydrocarbon Plus Fractions," paper EUR 183 presented at the EUROPEC Conference, London, Oct. 21-24, 1980

45. Whitson, C.H. and Torp, S.B.: "Evaluating Constant Volume Depletion Data," paper SPE 10067 presented at the SPE 56th Annual Fall Technical Conference and Exhibition, San Antonio, Oct. 5-7, 1981

46. Yarborough, L.: "Application of a Generalized Equation of State to Petroleum Reservoir Fluids," Equations of State in Engineering and Research, K.C. Chao and R.L. Robinson, Jr. (eds.)

47. "Technical Data Book - Petroleum Refining," American Petroleum Institute, Washington, D.C. (1976)Chpts. 1-6

TABLE IA - CRITICAL PRESSURE CORRELATIONS

KESLER-LEE

$$\begin{aligned} \ln p_c^* = {} & 8.3634 - 0.0566/\gamma - (0.24244 + 2.2898/\gamma + 0.11857/\gamma^2)\cdot 10^{-3}\cdot(1.8\cdot T_b) \\ & + (1.46850 + 3.6480/\gamma + 0.47277/\gamma^2)\cdot 10^{-7}\cdot(1.8\cdot T_b)^2 \\ & - (0.42019 + 0.0000/\gamma + 1.69770/\gamma^2)\cdot 10^{-10}\cdot(1.8\cdot T_b)^3 \end{aligned}$$

CAVETT

$$\begin{aligned} \log p_c^* = {} & 2.8290406 + 0.94120109\cdot 10^{-3}\cdot t - 0.30474749\cdot 10^{-5}\cdot t^2 \\ & - 0.20876110\cdot 10^{-6}\cdot \gamma_{API}\, t + 0.15184103\cdot 10^{-8}\cdot t^3 \\ & + 0.11047899\cdot 10^{-7}\cdot \gamma_{API}\cdot t^2 - 0.48271599\cdot 10^{-7}\cdot \gamma_{API}^2\cdot t \\ & + 0.13949619\ 10^{-9}\cdot \gamma_{API}^2\cdot t^2 \end{aligned}$$

RIAZI-DAUBERT (WHITSON EXTENSION)

$$p_c^* = 3.12281\cdot 10^{9}\cdot(1.8\cdot T_b)^{-2.31250}\cdot\gamma^{2.3201} \qquad T_b(K) < 475$$

$$p_c^* = 2.41490\cdot 10^{14}\cdot(1.8\cdot T_b)^{-3.86618}\cdot\gamma^{4.2448} \qquad T_b(K) > 475$$

LYDERSEN (ROBINSON-PENG; PNA)

P: PARAFFIN: $p_c^* = 14.69600\cdot\dfrac{14.026\cdot C_N + 2.016}{(0.227\cdot C_N + 0.340)^2}$

N: NAPHTHENE: $p_c^* = 14.69600\cdot\dfrac{14.026\cdot C_N - 14.026}{(0.227\cdot C_N - 0.137)^2}$

A: AROMATIC: $p_c^* = 14.69600\cdot\dfrac{14.026\cdot C_N - 20.074}{(0.227\cdot C_N - 0.325)^2}$

BERGMAN (PNA)

P: $p_c^* = 573.011 - 1.13707\cdot t + 0.13162\cdot 10^{-2}\cdot t^2 - 0.85103\cdot 10^{-6}\cdot t^3$

N: $p_c^* = 726.414 - 1.32750\cdot t + 0.98460\cdot 10^{-3}\cdot t^2 - 0.45169\cdot 10^{-6}\cdot t^3$

A: $p_c^* = 1184.514 - 3.44681\cdot t + 0.45312\cdot 10^{-2}\cdot t^2 - 0.23416\cdot 10^{-5}\cdot t^3$

STANDING (MATTHEWS, ROLAND, KATZ)

$$p_c^* = 1188 - 431\cdot\log(M-61.1) + [2319 - 852\cdot\log(M-53.7)]\cdot(\gamma-0.8)$$

ROWE

$$p_c^* = 10^5\cdot 10^{-0.0137726826\cdot C_N + 0.6801481651} / (1.8\cdot T_c)$$

EDMISTER

$$p_c^* = 14.69600\cdot 10^{\frac{7}{3}(\omega+1)[(T_c/T_b)-1]}$$

TABLE IB - CRITICAL TEMPERATURE CORRELATIONS

KESLER-LEE

$$\begin{aligned} T_c^* = {} & 341.7 + 811\cdot\gamma + (0.4244 + 0.1174\cdot\gamma)\ (1.8\cdot T_b) \\ & + (0.4669 - 3.2623\cdot\gamma)\cdot 10^5/(1.8\cdot T_b) \end{aligned}$$

CAVETT

$$\begin{aligned} T_c^* = {} & 768.07121 + 0.17133693\cdot 10^{+1}\ t - 0.10834003\cdot 10^{-2}\cdot t^2 \\ & - 0.89212579\cdot 10^{-2}\ \gamma_{API}\cdot t + 0.38890584\cdot 10^{-6}\cdot t^3 \\ & + 0.53094920\cdot 10^{-5}\cdot \gamma_{API}\cdot t^2 + 0.32711600\cdot 10^{-7}\cdot t^2 \end{aligned}$$

RIAZI-DAUBERT

$$T_c^* = 24.2787\cdot(1.8\cdot T_b)^{0.58848}\cdot\gamma^{0.3596}$$

NOKAY

$$T_c^* = 19.0780\cdot(1.8\cdot T_b)^{0.62164}\cdot\gamma^{0.2985}$$

ROESS

$$\begin{aligned} T_c^* = {} & 645.83 + 1.6667\cdot[\gamma(1.8\cdot T_b - 359.67)] \\ & - 0.7127\cdot[\gamma(1.8\cdot T_b - 359.67)]^2\cdot 10^{-3} \end{aligned}$$

EDMISTER (ROBINSON-PENG; PNA)

$$T_c^* = 1.8\cdot T_b\cdot\left[1 + \frac{3\cdot\log(p_c/101.325)}{7\cdot(1+\omega)}\right]$$

BERGMAN (PNA)

P: $T_c^* = 734.86 + 1.2061\cdot t - 0.32984\cdot 10^{-3}\cdot t^2$

N: $T_c^* = 616.56 + 2.6077\cdot t - 0.38010\cdot 10^{-2}\cdot t^2 + 0.25440\cdot 10^{-5}\cdot t^3$

A: $T_c^* = 749.20 + 1.7017\cdot t - 0.15843\cdot 10^{-2}\cdot t^2 + 0.82358\cdot 10^{-6}\cdot t^3$

SPENCER-DAUBERT (PNA)

P: $T_c^* = 1.8\cdot[22.87689\cdot T_b^{0.562244}\cdot\gamma^{0.436843}]$

N: $T_c^* = 1.8\cdot[\ 4.55116\cdot T_b^{0.811961}\cdot\gamma^{-0.071646}]$

A: $T_c^* = 1.8\cdot[11.40300\cdot T_b^{0.669286}\cdot\gamma^{0.227320}]$

ROWE

$$T_c^* = 1.8\cdot[961 - 10^{(2.95597 - 0.090597\cdot C_N^{2/3})}]$$

STANDING (MATTHEWS, ROLAND, KATZ)

$$T_c^* = 608 + 364\cdot\log(M-71.2) + [2450\cdot\log(M) - 3800]\cdot\log(\gamma)$$

TABLE IC - ACENTRIC FACTOR CORRELATIONS

PITZER (DEFINITION)

$$\omega = -\log[p_v(\text{at } T_r=0.7)/p_c] - 1$$

EDMISTER

$$\omega = \frac{3[\log(p_c) - 2.0057]}{7\cdot(T_c/T_b - 1)} - 1$$

KESLER-LEE (θ < 0.8)

$$\omega = \frac{-\ln(p_c/101.325) - 5.92714 + 6.09648\theta^{-1} + 1.28862\ln\theta - 0.169347\theta^6}{15.2518 - 15.6875\theta^{-1} - 13.4721\ln\theta + 0.43577\theta^6}$$

KESLER-LEE (θ > 0.8)

$$\omega = -7.904 + 0.1352\cdot K_w - 0.007465\cdot K_w^2 + 8.359\cdot\theta + (1.408 - 0.01063\cdot K_w)/\theta$$

ROBINSON-PENG (PNA)

P: $\omega = 0.0432\cdot C_N + 0.0457$

N: $\omega = 0.0432\cdot C_N - 0.0880$

A: $\omega = 0.0445\cdot C_N - 0.0995$

BERGMAN (PNA)

P: $\omega = 0.140 + 0.900\cdot 10^{-3}\cdot t + 0.233\cdot 10^{-6}\cdot t^2$

N: ω = PARAFFIN VALUE - 0.075

A: ω = PARAFFIN VALUE - 0.100

and for NAPHTHENES (N),

$\omega(C_8) = 0.26$; $\omega(C_9) = 0.27$; $\omega(C_{10}) = 0.35$

TABLE 2A - SPECIFIC GRAVITY CORRELATIONS

HARIU-SAGE

$\gamma = [-b - (b^2 - 4ac)^{\frac{1}{2}}] / (2a)$

$a = -\log(M) + A_{00} + A_{10} \cdot t + A_{20} \cdot t^2$

$b = (t+459.67)^{1/3} \cdot (A_{01} + A_{11} \cdot t + A_{21} \cdot t^2)$

$c = (t+459.67)^{2/3} \cdot (A_{02} + A_{12} \cdot t + A_{22} \cdot t^2)$

YARBOROUGH

$\gamma = \exp[B_0 + B_1/C_N + B_2 \cdot C_N + B_3 \cdot \ln(C_N)]$

r_A	B_0	B_1	B_2	B_3
0.0	$-7.43855 \cdot 10^{-2}$	$-1.72341 \cdot 10^{0}$	$1.38058 \cdot 10^{-3}$	$-3.34169 \cdot 10^{-2}$
0.1	$-4.25800 \cdot 10^{-1}$	$-7.00017 \cdot 10^{-1}$	$-3.30947 \cdot 10^{-5}$	$4.65465 \cdot 10^{-2}$
0.2	$-4.47553 \cdot 10^{-1}$	$-7.65111 \cdot 10^{-1}$	$1.77982 \cdot 10^{-4}$	$1.07746 \cdot 10^{-1}$
0.3	$-4.39105 \cdot 10^{-1}$	$-9.34068 \cdot 10^{-1}$	$4.33708 \cdot 10^{-4}$	$1.19267 \cdot 10^{-1}$
0.4	$-2.73719 \cdot 10^{-1}$	$-1.39960 \cdot 10^{0}$	$1.80564 \cdot 10^{-3}$	$5.92005 \cdot 10^{-2}$
0.6	$-7.39412 \cdot 10^{-3}$	$-1.97063 \cdot 10^{0}$	$5.67273 \cdot 10^{-3}$	$-1.67141 \cdot 10^{-2}$
0.8	$+3.17618 \cdot 10^{-1}$	$-7.78432 \cdot 10^{-1}$	$2.58616 \cdot 10^{-3}$	$1.08382 \cdot 10^{-1}$

BERGMAN (GENERAL)

$$\gamma = [0.4189 + 2.786 \cdot 10^{-3} \cdot t - 8.685 \cdot 10^{-6} \cdot t^2 + 1.336 \cdot 10^{-8} \cdot t^3 - 7.092 \cdot 10^{-12} \cdot t^4] / 0.9991$$

KATZ-FIROOZABADI (GENERAL)

$$\gamma = [0.5516 + 1.208 \cdot 10^{-3} \cdot t - 2.231 \cdot 10^{-6} \cdot t^2 + 2.265 \cdot 10^{-9} \cdot t^3 - 8.614 \cdot 10^{-13} \cdot t^4] / 0.9991$$

ROBINSON-PENG (PNA)

$$P:\ \gamma = \left[\frac{14.026 \cdot C_N + 2.016}{16.280 \cdot C_N + 31.1016}\right] / 0.9991$$

$$N:\ \gamma = \left[\frac{14.026 \cdot C_N - 14.026}{16.376 \cdot C_N - 5.5844}\right] / 0.9991$$

$$A:\ \gamma = \left[\frac{14.026 \cdot C_N - 20.074}{16.108 \cdot C_N - 25.7697}\right] / 0.9991$$

BERGMAN (PNA)

$$P:\ \gamma = [0.582486 + 0.694810 \cdot 10^{-3} \cdot t - 0.757281 \cdot 10^{-6} \cdot t^2 + 0.320776 \cdot 10^{-9} \cdot t^3] / 0.9991$$

$$N:\ \gamma = [0.694208 + 0.490627 \cdot 10^{-3} \cdot t - 0.659736 \cdot 10^{-6} \cdot t^2 + 0.311366 \cdot 10^{-9} \cdot t^3] / 0.9991$$

$$A:\ \gamma = [0.916103 - 0.250418 \cdot 10^{-3} \cdot t + 0.357967 \cdot 10^{-6} \cdot t^2 - 0.166318 \cdot 10^{-9} \cdot t^3] / 0.9991$$

KESLER-LEE

[illegible] $1.25906 - 0.42922 \cdot 10^{-2} \cdot T_b +$ [illegible] $\cdot T_b^2 - 111.665/T_b$

TABLE 2B - BOILING POINT CORRELATIONS

ROBINSON-PENG (PNA)

$$P:\ \ln(T_b) = \sum_{i=1}^{6} a_i (C_N - 6)^{i-1}$$

$$N:\ \ln(T_b) = \sum_{i=1}^{6} a_i (C_N - 7)^{i-1}$$

$$A:\ \ln(T_b) = \sum_{i=1}^{6} a_i (C_N - 7)^{i-1}$$

CONSTANT	PARAFFIN	NAPHTHENE	AROMATIC
a_1	$+5.83451830$	$+5.85793320$	$+5.86717600$
a_2	$+0.84909035 \cdot 10^{-1}$	$+0.79805995 \cdot 10^{-1}$	$+0.80436947 \cdot 10^{-1}$
a_3	$-0.52635428 \cdot 10^{-2}$	$-0.43949101 \cdot 10^{-2}$	$-0.47136506 \cdot 10^{-2}$
a_4	$+0.21252908 \cdot 10^{-3}$	$+0.14783123 \cdot 10^{-3}$	$+0.18233365 \cdot 10^{-3}$
a_5	$-0.34933363 \cdot 10^{-5}$	$-0.27095216 \cdot 10^{-5}$	$-0.38327239 \cdot 10^{-5}$
a_6	$+0.37285365 \cdot 10^{-7}$	$+0.19907794 \cdot 10^{-7}$	$+0.32550576 \cdot 10^{-7}$

TABLE 2C - MOLECULAR WEIGHT CORRELATIONS

HARIU-SAGE

$$\log(M) = \sum_{j=0}^{2} \sum_{i=0}^{2} A_{ij} \cdot t^i \cdot K_w^j$$

$A_{00} = +0.6670202 \cdot 10^{1}$; $A_{10} = +4.5837050 \cdot 10^{-3}$; $A_{20} = -2.6986930 \cdot 10^{-6}$

$A_{01} = +0.1552531 \cdot 10^{1}$; $A_{11} = -5.7555850 \cdot 10^{-4}$; $A_{21} = +3.8759500 \cdot 10^{-7}$

$A_{02} = -5.3784960 \cdot 10^{-1}$; $A_{12} = +2.5005840 \cdot 10^{-5}$; $A_{22} = -1.5662280 \cdot 10^{-8}$

KESLER-LEE

$$\begin{aligned} M = & -12272.6 + 9486.4 \cdot \gamma + (4.6523 - 3.3287 \cdot \gamma)(1.8 \cdot T_b) \\ & + (1 - 0.77084 \cdot \gamma - 0.02058 \cdot \gamma^2)[1.3437 - 720.79/(1.8 \cdot T_b)] \cdot 10^7 / (1.8 \cdot T_b) \\ & + (1 - 0.80882 \cdot \gamma + 0.02226 \cdot \gamma^2)[1.8828 - 181.98/(1.8 \cdot T_b)] \cdot 10^{12} / (1.8 \cdot T_b)^3 \end{aligned}$$

RIAZI-DAUBERT

$$M = 4.5673 \cdot 10^{-5} \cdot (1.8 \cdot T_b)^{2.1962} \cdot \gamma^{-1.0164}$$

BERGMAN (GENERAL)

$$M = 58.7208 + 1.3806 \cdot 10^{-1} \cdot t + 2.2369 \cdot 10^{-4} \cdot t^2 + 1.4598 \cdot 10^{-7} \cdot t^3$$

KATZ-FIROOZABADI (GENERAL)

$$M = 72.5257 + 1.1389 \cdot 10^{-1} \cdot t + 5.5708 \cdot 10^{-4} \cdot t^2 - 1.1995 \cdot 10^{-7} \cdot t^3$$

ROBINSON-PENG (PNA)

$P:\ M = 14.026 \cdot C_N + 2.016$

$N:\ M = 14.026 \cdot C_N - 14.026$

$A:\ M = 14.026 \cdot C_N - 20.074$

TABLE 3 - INJECTION-GAS COMPOSITION FOR HOFFMAN ET AL. SWELLING TEST EXAMPLE

COMPONENT	MOLE PERCENT
C_1	90.29
C_2	5.14
C_3	2.24
$i\text{-}C_4$	0.48
$n\text{-}C_4$	0.52
$i\text{-}C_5$	0.22
$n\text{-}C_5$	0.14
C_6	0.29
C_7	0.51
C_8	0.17
	100.00

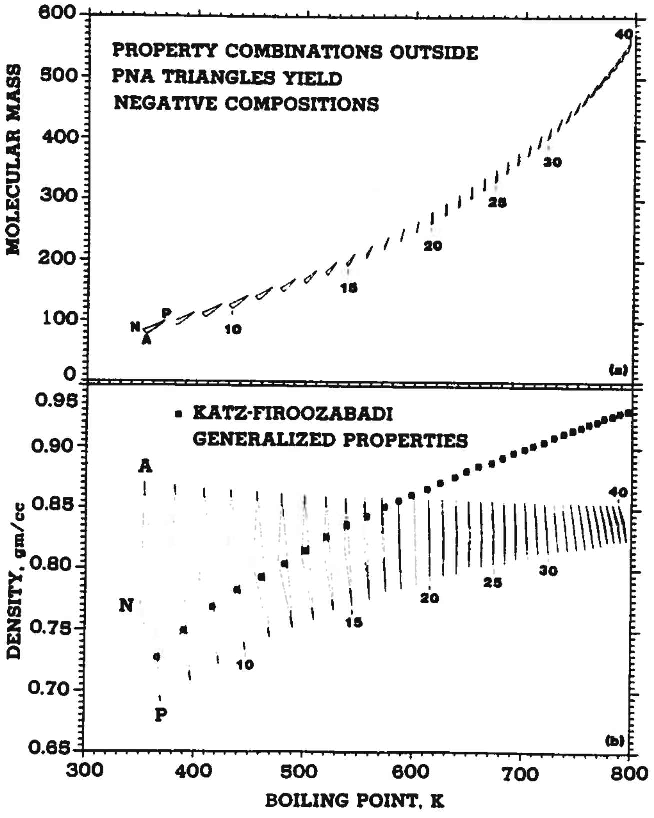

Fig. 1—Robinson-Peng PNA molecular weight and density vs. boiling point.

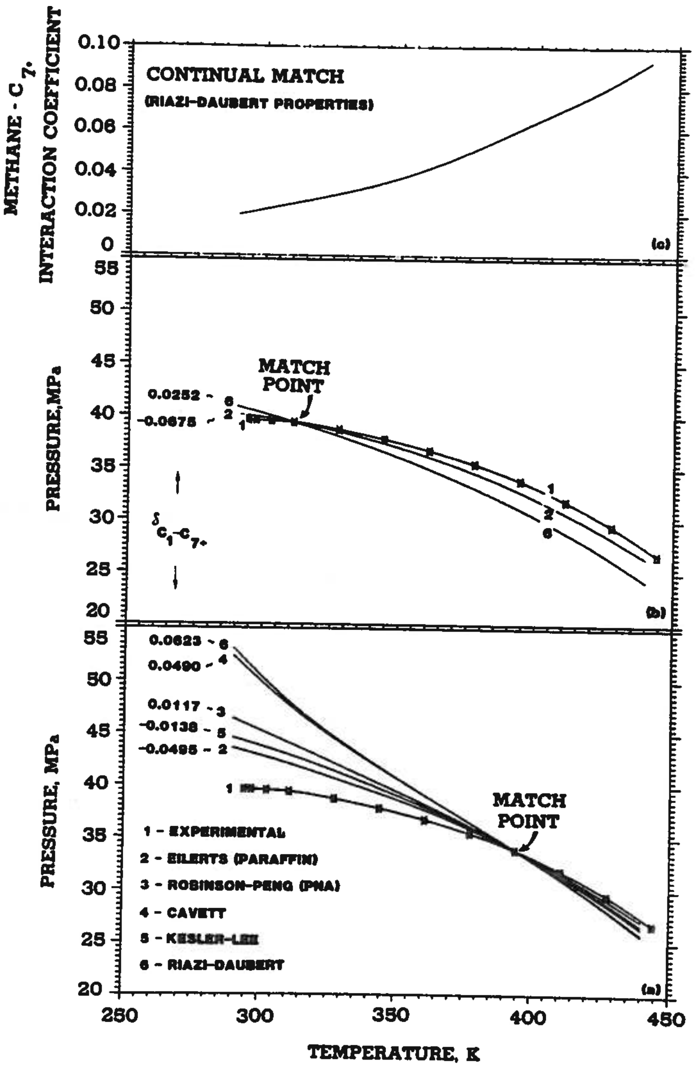

Fig. 2—ZJRK EOS predictions of Eilerts OO-L-544 gas condensate: phase diagram.

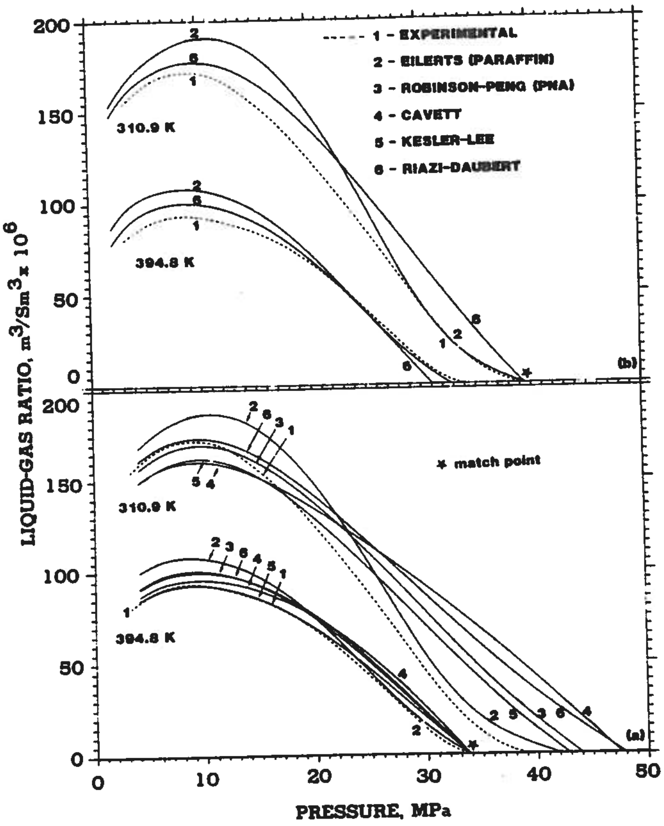

Fig. 3—ZJRK EOS predictions of Eilerts OO-L-544 gas condensate: liquid/gas ratio.

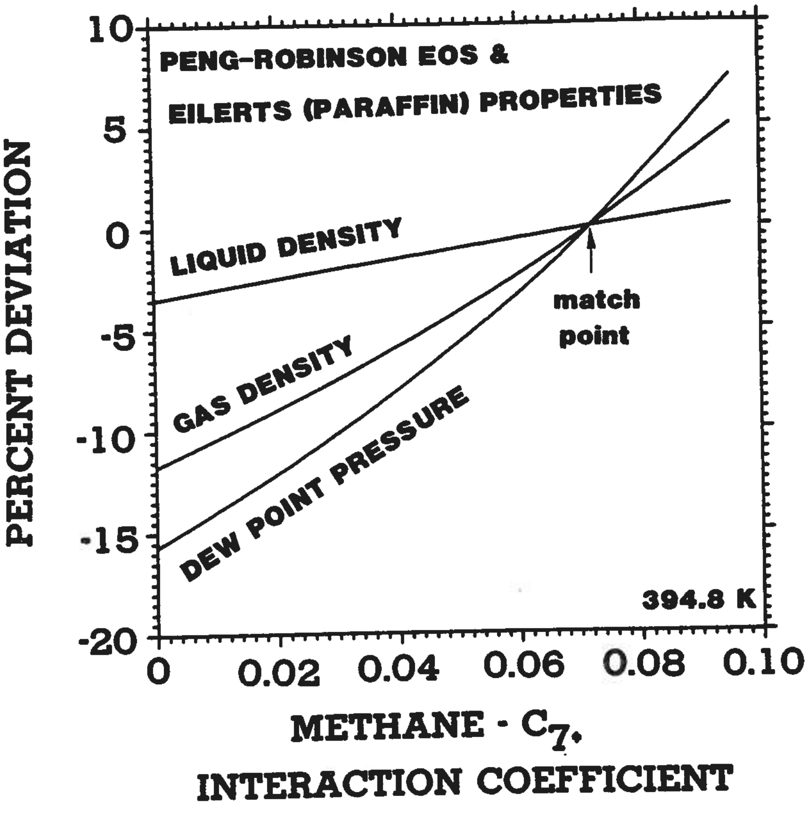

Fig. 4—PR EOS predictions of Eilerts OO-L-544 gas condensate: $C_1 - C_7+$ interaction coefficient.

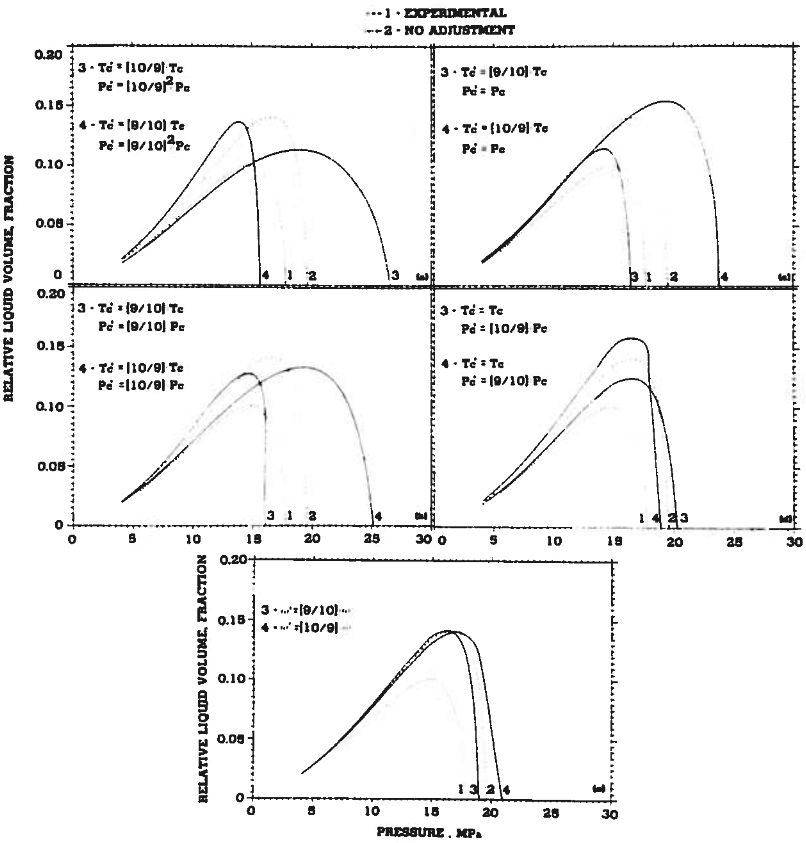

Fig. 5—PR EOS predictions of Eilerts CH-P-843 gas condensate: critical properties adjustment.

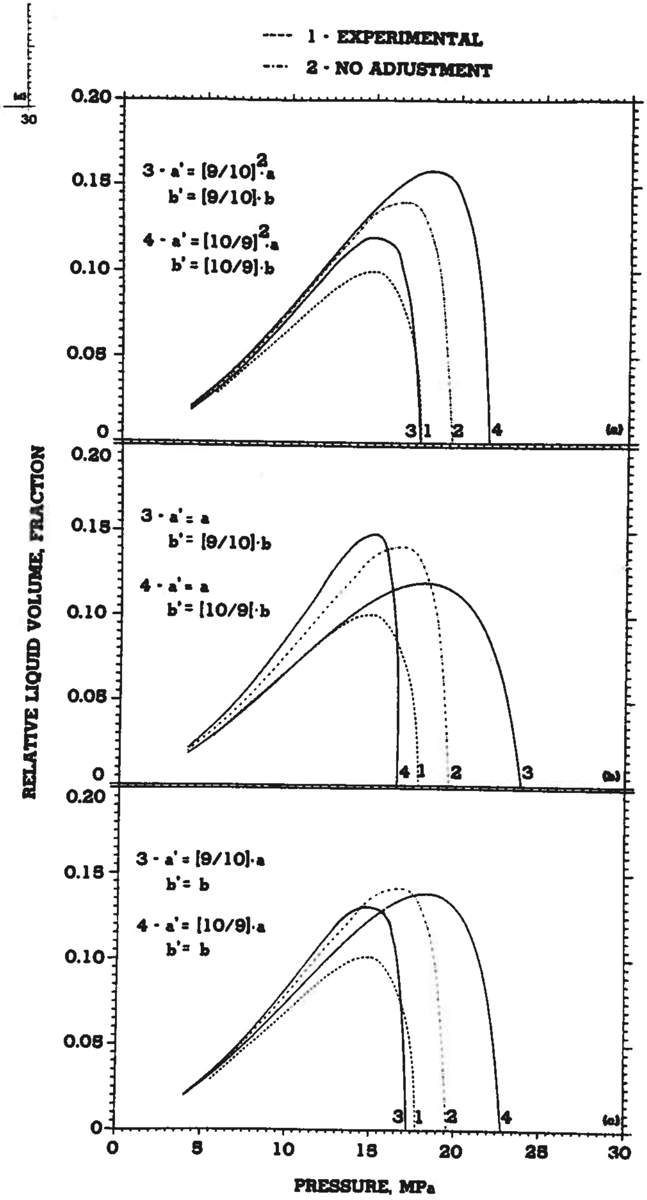

Fig. 6—PR EOS predictions of Eilerts CH-P-843 gas condensate: EOS constants adjustment.

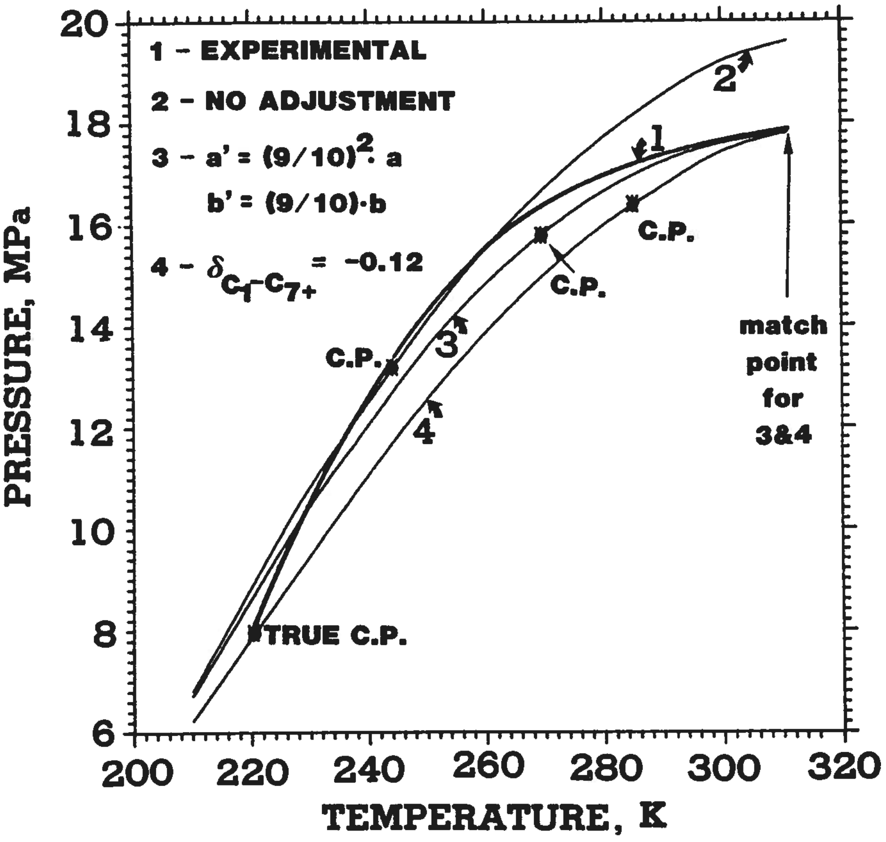

Fig. 7—PR EOS predictions of Eilerts CH-P-843 gas condensate: phase diagram.

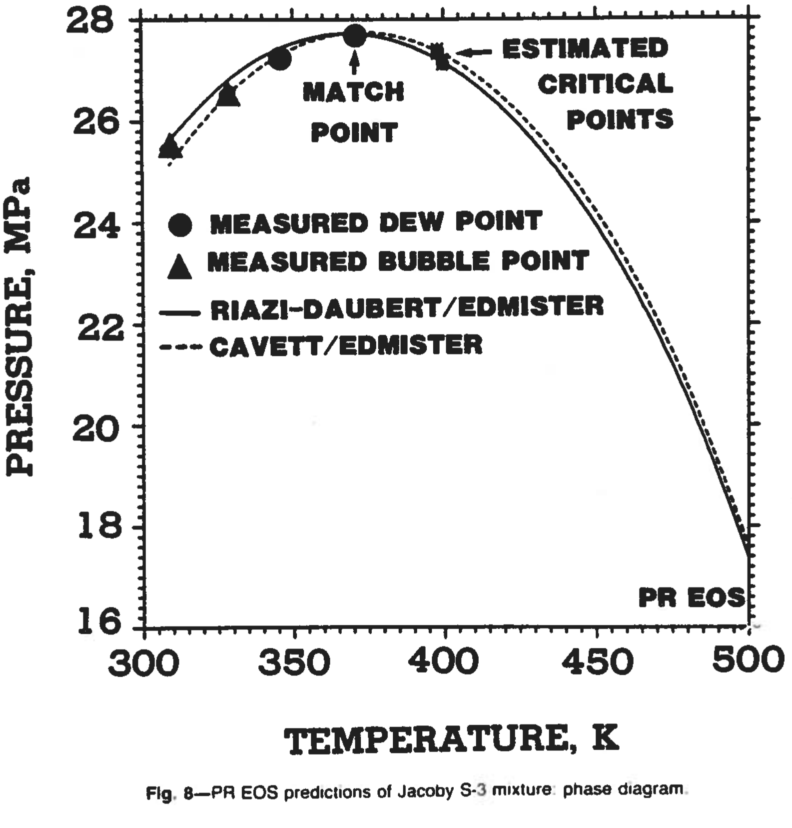

Fig. 8—PR EOS predictions of Jacoby S-3 mixture: phase diagram.

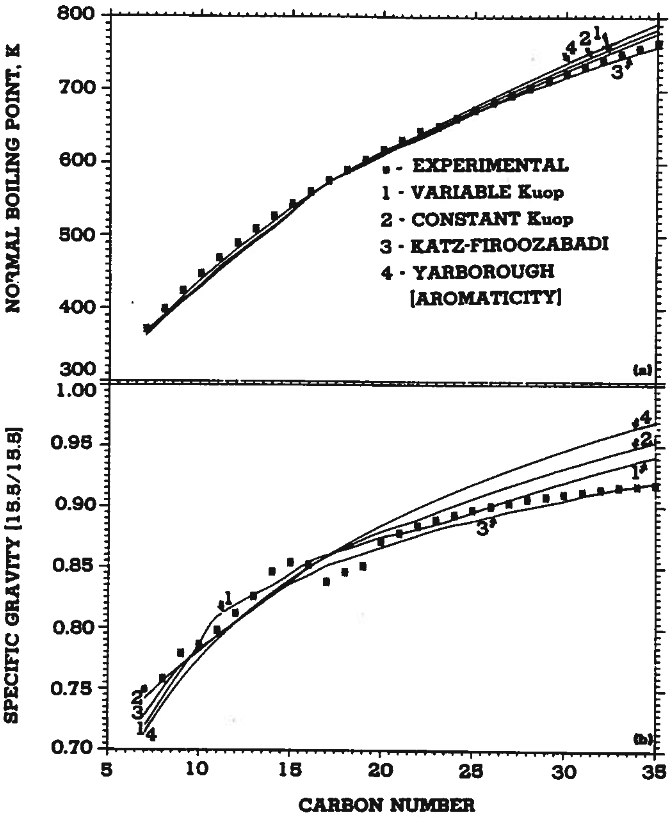

Fig. 9—Experimental vs. estimated boiling points and specific gravities: Hoffman oil.

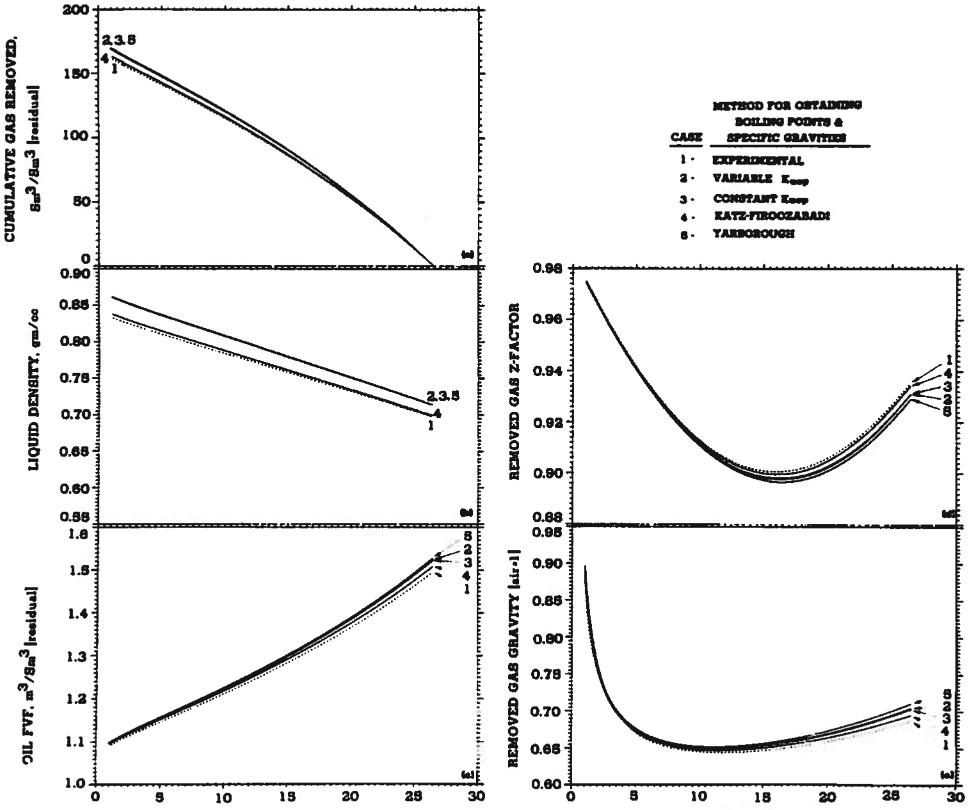

Fig. 10—ZJRK EOS predictions of Hoffman oil: simulated differential liberation test.

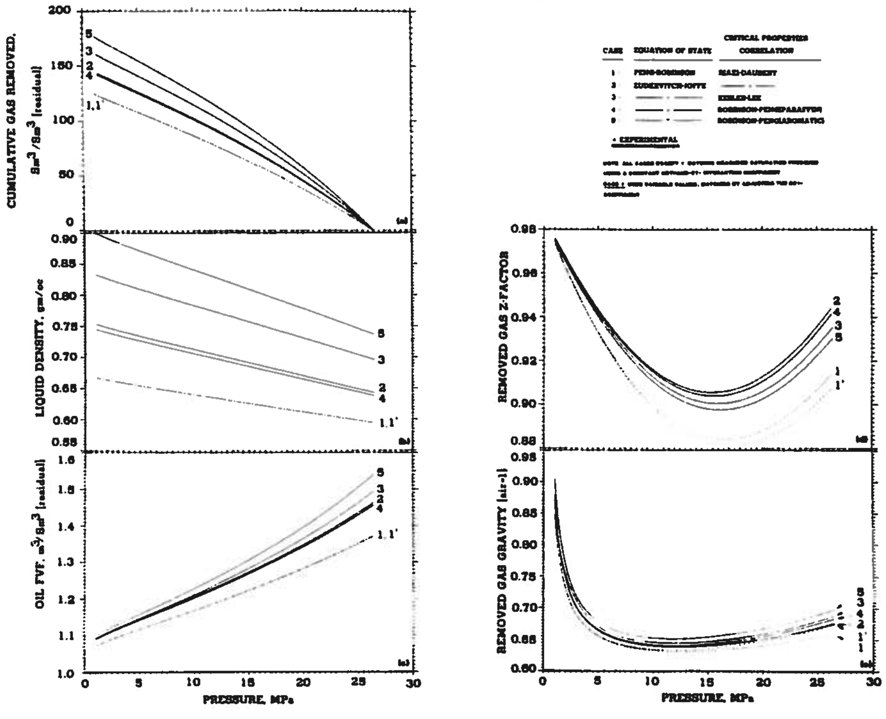

Fig. 11—ZJRK and PR EOS predictions of Hoffman oil: simulated differential liberation test.

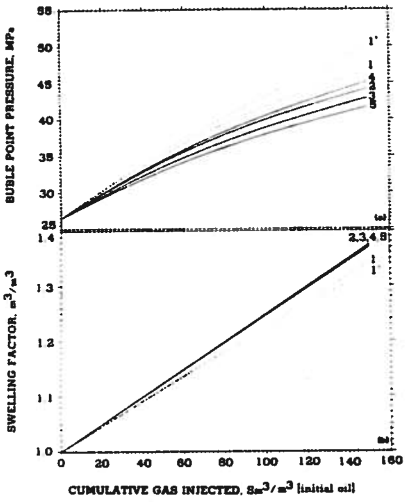

Fig. 12—ZJRK and PR EOS predictions of Hoffman oil: simulated swelling test.

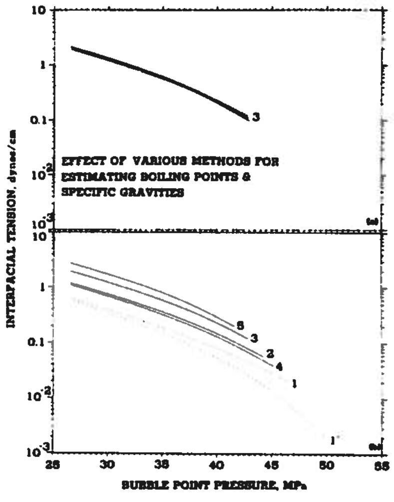

Fig. 13—ZJRK and PR EOS predictions of Hoffman oil: simulated swelling test—interfacial tension.

CASE	EQUATION OF STATE	CRITICAL PROPERTIES CORRELATION
1	PENG-ROBINSON	RIAZI-DAUBERT
2	ZUDKEVITCH-JOFFE	—— · ——
3	—— · ——	KESLER-LEE
4	—— · ——	ROBINSON-PENG(PARAFFIN)
5	—— · ——	ROBINSON-PENG(AROMATIC)

NOTE: ALL CASES EXCEPT 1' MATCHED MEASURED SATURATION PRESSURE USING A CONSTANT METHANE-C7+ INTERACTION COEFFICIENT.

CASE 1' USES VARIABLE VALUES, MATCHING BY ADJUSTING THE C7+ COEFFICIENT

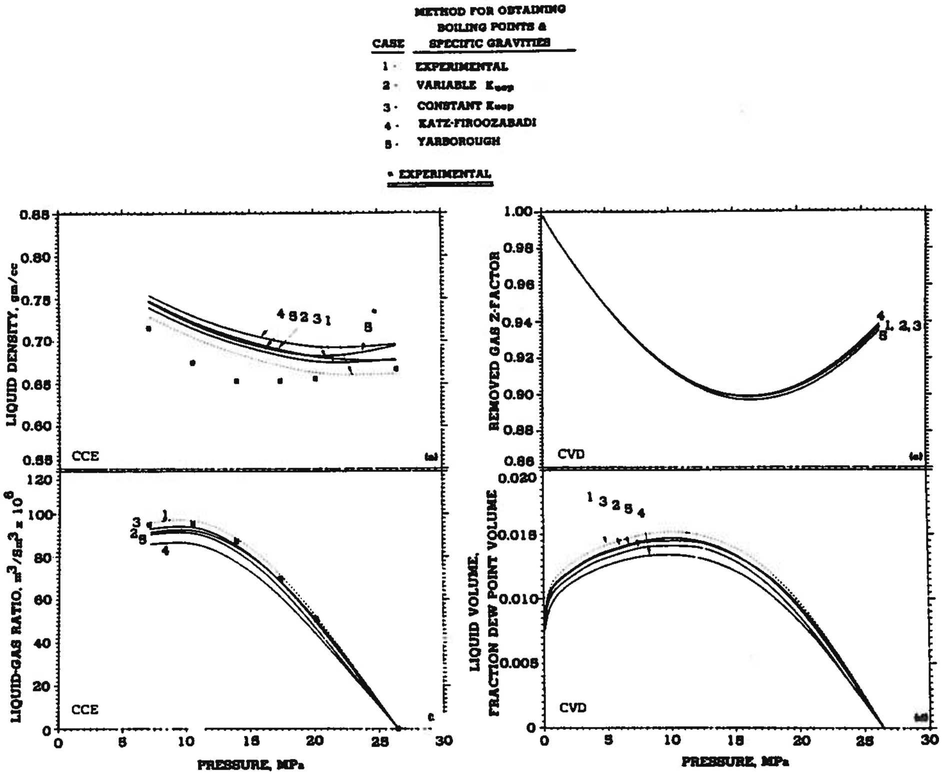

Fig. 14—ZJRK EOS predictions of Hoffman gas: simulated expansion tests.

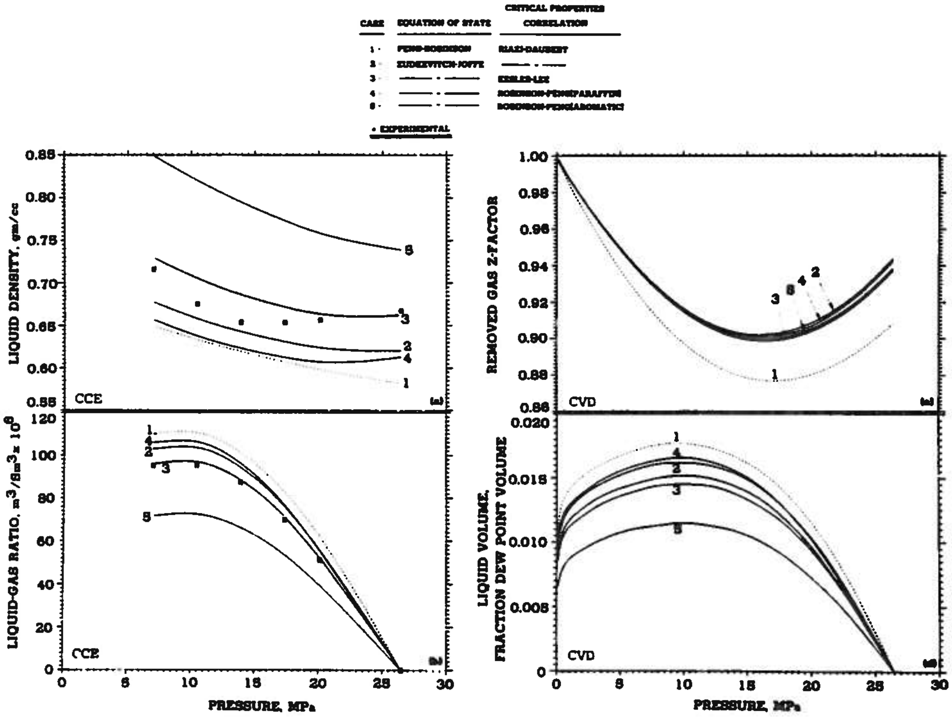

Fig. 15—ZJRK and PR EOS predictions of Hoffman gas: simulated expansion tests.

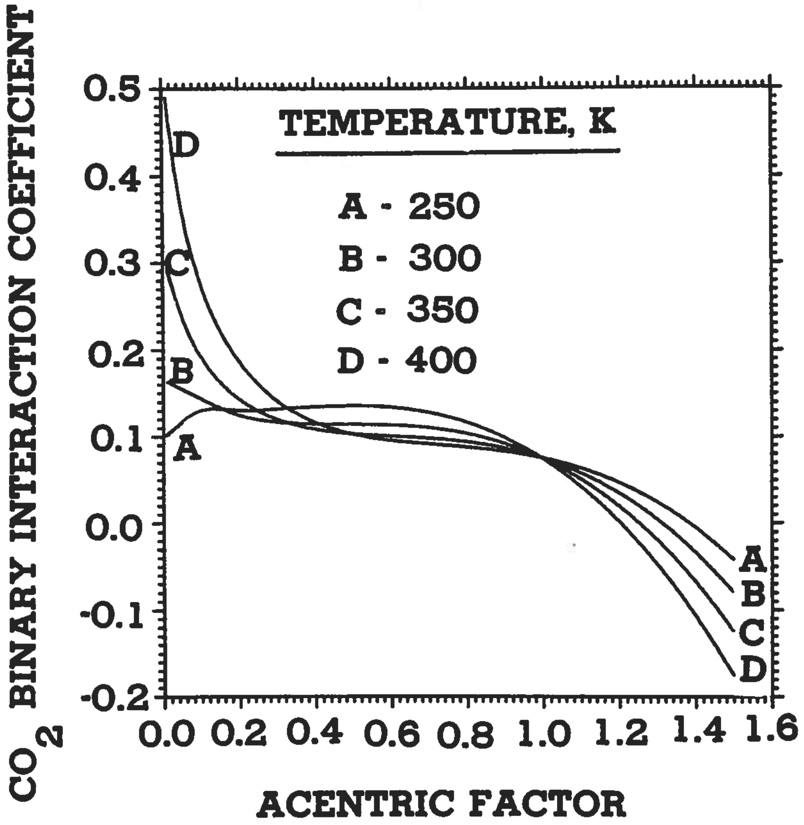

Fig. 16—Kato correlation for carbon dioxide-hydrocarbon interaction coefficients.

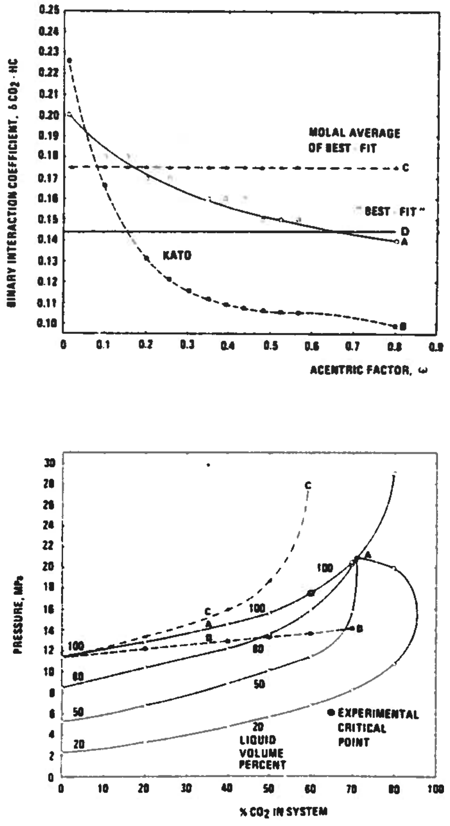

Fig. 17—PR EOS predictions of Hong oil: phase diagram and interaction coefficients.

A FAMILY OF CUBIC EQUATIONS OF STATE

Curtis H. Whitson
Rogaland Regional College
Ullandhaug
4000 Stavanger, Norway

January, 1983

INTRODUCTION

The Usdin-McAuliffe[1] (UM) and Peng-Robinson[2] (PR) equations of state (EOS) are two of the more useful cubic equations available for predicting volumetric and phase behavior of fluids. The former is a three-constant equation which reduces to the Redlich-Kwong[3] (RK) EOS, van der Waals[4] EOS or the real gas law. The PR EOS, a two-constant equation, has gained wide-spread acceptance in the petroleum industry because of its simplicity and improved liquid-density estimation.

A family of cubic equations of state is proposed which incorporates both the UM and PR equations. It stems from the development of Martin's[5] general two-term, four-constant EOS. Thermodynamic expressions presented for the general equation are not limited by restraints which define the proposed cubic family. They are shown, for example, to be applicable to the recent Schmidt-Wenzel (SW) EOS.[6]

The UM EOS has been modified by matching vapor pressures and saturated liquid densities with correction factors for EOS constants. The resulting expressions for these factors are not complicated like some which have been proposed for the RK EOS.[7-10] Only acentric factor is used as a correlating variable, making the modified UM EOS comparable in simplicity to the PR and Soave-RK[11] (SRK) equations. The new equation should also give better predictions of liquid densities for petroleum reservoir fluids containing considerable amounts of heavier fractions.

MARTIN FOUR-CONSTANT EQUATION OF STATE

The basis for EOS development in this study is the general four-constant, two-term equation proposed by Martin,[5]

$$p = \frac{RT}{(v-b)} - \frac{a}{(v-b+c)(v-b+d)} \quad \ldots\ldots\ldots\ldots\ldots\ldots\ldots\ldots \quad (1)$$

which has been translated in volume by constant b. Actually, Eq. 1 is a special case of the Abbott[13] equation, where the denominator of the second term (v-b+c)(v-b+d) replaces the more general quadratic form. Using the definition of compressibility factor, $Z=pv/RT$, allows Eq. 1 to be rewritten as

$$\begin{aligned} &Z^3 + Z^2[-3B + (C+D-1)] \\ &\quad + Z\,[\,3B^2 - 2B(C+D-1) + (A+CD-C-D)] \\ &\quad + \;[-B^3 + B^2(C+D-1) - B(A+CD-C-D) - CD] = 0 \ \ldots \quad (2) \end{aligned}$$

Using the definition of fugacity, f, for a single component,

$$\ln(f/p) = \int_0^p (v/RT - 1/p)dp \quad \ldots\ldots\ldots\ldots\ldots\ldots\ldots\ldots \quad (3)$$

gives

$$\begin{aligned} \ln(f/p) = -\ln(Z-B) + \frac{B}{Z-B} + \frac{A}{D-C}\left[\frac{B-D}{Z-B+D} + \frac{C-B}{Z-B+C}\right] \\ + \frac{A}{C-D}\cdot\ln\left(\frac{Z-B+D}{Z-B+C}\right) \quad \ldots\ldots\ldots\ldots\ldots \quad (4) \end{aligned}$$

For a mixture the fugacity relation can be written

$$\ln(f_i/x_ip) = \int_{\infty}^{V} [\frac{1}{V} - \frac{1}{RT}\cdot(\frac{\partial p}{\partial Ni})]dV - \ln Z \quad \ldots\ldots\ldots\ldots \quad (5a)$$

or

$$\begin{aligned}\ln(f_i/x_ip) = &-\ln(Z-B) + \frac{B_i}{Z-B} \\ &+ \frac{A}{D-C}[\frac{B_i-D_i}{Z-B+D} + \frac{C_i-B_i}{Z-B+C}] \\ &+ [\frac{2\cdot\Sigma x_jA_{ij}}{(C-D)} + \frac{A(D_i-C_i)}{(C-D)^2}]\cdot\ln(\frac{Z-B+D}{Z-B+C}) \quad .. \quad (5b)\end{aligned}$$

where traditional mixing rules have been used for EOS constants: $a=\Sigma_i\Sigma_j\ x_ix_ja_{ij}$ where $a_{ij}=(1-\kappa_{ij})(a_ia_j)^{½}$, $b=\Sigma_i\ x_ib_i$, $c=\Sigma_i\ x_ic_i$ and $d=\Sigma_i\ x_id_i$.

EOS constants are defined as follows,

$$A = a\cdot p/R^2T^2 = \alpha\cdot\Omega_a\cdot p_r/T_r^2 \quad \ldots\ldots\ldots\ldots\ldots\ldots\ldots\ldots \quad (6a)$$

$$B = b\cdot p/RT \quad = \beta\cdot\Omega_b\cdot p_r/T_r \quad \ldots\ldots\ldots\ldots\ldots\ldots\ldots\ldots \quad (6b)$$

$$C = c\cdot p/RT \quad = \xi\cdot\Omega_c\cdot p_r/T_r \quad \ldots\ldots\ldots\ldots\ldots\ldots\ldots\ldots \quad (6c)$$

$$D = d\cdot p/RT \quad = \delta\cdot\Omega_d\cdot p_r/T_r \quad \ldots\ldots\ldots\ldots\ldots\ldots\ldots\ldots \quad (6d)$$

where numerical constants Ω_a, Ω_b, Ω_c and Ω_d must be determined, usually by critical-point restraints. Liberty has been taken to include terms α, β, ξ and δ in Eqs. 6. These represent corrections to the numerical constants Ω_a, Ω_b, etc. and are typically functions of reduced temperature and acentric factor. The terms ξ and δ are usually considered constants (unity) or can be written in terms of β.

PROPOSED EQUATION-OF-STATE FAMILY

Martin[5] shows that Eq. 1 can be simplified to yield the RK, UM and PR equations, amoung several others. Table 1 shows the necessary definitions required to make the simplifications. Since the SRK, UM and PR equations are amoung the most promising, an EOS family is proposed which incorporates all three.

First the constraint

$$c = \lambda \cdot b \quad \text{or} \quad \Omega_c = \lambda \cdot \Omega_b \qquad \ldots\ldots\ldots\ldots\ldots\ldots\ldots\ldots \quad (7)$$

is imposed, where λ is a numerical constant. For the UM (and RK) EOS, $\lambda=1,2$; for the PR EOS, $\lambda=2\pm\sqrt{2}$. The following critical-point restraints,[12]

$$Z = Z_c$$

$$(\partial v/\partial p) = (\partial^2 v/\partial p^2) = 0 \qquad \text{at } T_c,\ p_c \qquad \ldots\ldots\ldots\ldots \quad (8)$$

$$\text{or } (Z-Z_c)^3 = 0$$

are sufficient to yield

$$\Omega_b^3 - \Omega_b^2(\lambda^2-3\lambda+3Z_c) + \Omega_b(\lambda-3\lambda Z_c+3Z_c^2) - Z_c^3 = 0 \ \ldots\ldots\ldots\ldots \quad (9a)$$

$$\Omega_d = \Omega_b(3-\lambda) - 3Z_c + 1 \qquad \ldots\ldots\ldots\ldots\ldots\ldots\ldots\ldots \quad (9b)$$

$$\Omega_a = \Omega_b^2(\lambda^2-3\lambda+3) + \Omega_b(3\lambda Z_c-\lambda-6Z_c+3) + (3Z_c^2-3Z_c+1) \quad \ldots\ldots \quad (9c)$$

The smallest real root of Eq. 9a is taken for Ω_b, while Ω_d and Ω_a follow directly from Eqs. 9b and 9c. Z_c is a critical compressibility factor to be specified. For the PR EOS, Z_c is 0.307401...; for the RK EOS, Z_c is 1/3; for the UM EOS, Z_c can be specified individually for each component in a mixture.

The restriction that $\Omega_c = \lambda \cdot \Omega_b$, combined with the critical-point criteria, define the family of equations. Other choices could have been made, of course, and the Z-chart sum proposed by Martin,[5] ($\Sigma = 0.62$) was considered but eventually rejected during this study. Although Eqs. 7 and 8 constitute a specific family of equations, Eqs. 1 to 6 are completely general expressions.

One observation to be made at this point is that critical compressibility factor Z_c of 0.307401 is not unique to the PR two-constant EOS. Neither is Z_c of 1/3 claimed by the RK EOS. Any choice of λ leaves the remaining option to choose Z_c. There is no reason given by Peng and Robinson, for example, why the value of $2\pm\sqrt{2}$ is better than, say 2. One might contemplate if a specific pair of λ and Z_c gives better overall predictions of pure component and mixture phase behavior; the optimal pair would obviously depend on which physical properties were chosen, and in which p-T-x_i regions they exist.

A study was made to determine the pair λ^*, Z_c^* which minimize the Σ-chart defined by Martin,[5]

$$\Sigma = Z_c - (\partial Z/\partial p_r)_{T_r=1,\ p_r=0} \quad \text{.........................} \quad (10a)$$

which is easily shown to be given by:

$$\Sigma = Z_c + \Omega_a - \Omega_b \quad \text{....................................} \quad (10b)$$

Fig. 2 shows Σ versus Z_c for four values of λ (1, 2, $2\pm\sqrt{2}$), and values defining the SW EOS (see Eq. 16); curves for λ=1,2 define the UM EOS. An interesting observation is that the minimum Σ-chart value, Σ^* is always 0.67188, the same value given by Martin for his "best" three-constant equation. Fig. 3 shows the variation in optimal λ^* with optimal Z_c^*. All values on the curve give a Σ^* of 0.67188. Points representing the RK and PR equations are also noted; Σ_{RK} = 0.67417 and Σ_{PR} = 0.68684.

MODIFIED USDIN-MCAULIFFE EQUATION OF STATE

An effort has been made to improve the UM EOS by matching vapor pressures and saturated liquid densities (calculated from correlations[15]; see Appendix). Specifically, correction factors α and β were adjusted in the subcritical region $0.4<T_r<1.0$, where

$$\alpha = \alpha(T_r,\omega) \quad \text{(11a)}$$

$$\beta = \beta(T_r,\omega) \quad \text{(11b)}$$

$$\xi = \beta(T_r,\omega) \quad \text{(11c)}$$

$$\delta = 1 + (\Omega_b/\Omega_d)[\beta(T_r,\omega)-1] \quad \text{(11d)}$$

The last expression results from not correcting what is introduced in the original form of the UM EOS as a third constant ("d" as denoted by Usdin and McAuliffe). The PR and SRK equations only consider α as a function of T_r and ω, where $\beta=\xi=\delta=1$.

As shown by Fuller,[16] the α and β functions are more well-behaved for the UM EOS than the RK EOS (as modified by Zudkevitch and Joffe,[7] Haman,[9] and Yarborough[10]). This results from specifying Z_c for each component close to its true value. Unfortunately this procedure lessens the accuracy of EOS predictions for lighter components such as methane.

The present correlations for α and β differ from Fuller's and are easier to apply,

$$\alpha^{\frac{1}{2}} = 1 + m(1-T_r) \quad \text{.................................} \quad (12a)$$

$$m = 0.46089 + 1.2032 \cdot \omega - 0.34548 \cdot \omega^2 \quad \text{...............} \quad (12b)$$

$$\beta = 1 + (\beta^{*}-1)\{2/[1+e^{8(Tr-1)}] - 1\} \quad \text{................} \quad (12c)$$

$$\beta^{*} = 1.4891 + 0.92175 \cdot \omega + 0.40116 \cdot \omega^2 \quad \text{................} \quad (12d)$$

For $T_r > 1$, β is set equal to one. More accurate results would probably result if a second correlation were used for α at supercritical temperatures.

The Pitzer correlation was chosen to estimate Z_c,

$$Z_c = 0.291 - 0.08 \cdot \omega \quad \text{..............................} \quad (13)$$

Fig. 1 shows variation in experimental Z_c with ω for paraffins. The Pitzer correlation (Eq. 13) is also shown. Its main advantage in the present context is simplicity and that its close estimate of true critical compressibility factor contributes to the smooth, simple behavior of α and β relations.

Figs. 4 and 5 show variation in m and β^{*} with acentric factor. Figs. 6 and 7 show variation in α and β with reduced temperature for methane and benzene. Table 2 reviews properties of compounds used to develop the modified UM EOS.

SCHMIDT-WENZEL EQUATION OF STATE

It might be argued that a better choice for the Z_c-ω relation would be one which had 1/3 as its intercept, ensuring RK capabilities for methane and the ligher components. This arguement is used by Schmidt and Wenzel to develop specific criteria for determining EOS constants. They try to incorporate characteristics of the RK, PR and Harmens[17] equations by noting that each seems better suited for components with increasing acentric factors - specifically, ω=0.0, 0.33 and 0.67.

Retaining the previous notation that $c=\lambda \cdot b$, but now allowing λ to vary for each component (i.e. acentric factor), the SW equation is solved by first calculating the constant β_c,

$$(6\omega+1)\beta_c^3 + 3\beta_c^2 + 3\beta_c - 1 = 0 \quad \ldots\ldots\ldots\ldots\ldots\ldots\ldots\ldots \quad (14)$$

where β_c is the smallest positive root of Eq. 14. Z_c is then defined by the relation:

$$Z_c = \frac{1}{3(1+\omega \cdot \beta_c)} \quad \ldots\ldots\ldots\ldots\ldots\ldots\ldots\ldots\ldots\ldots \quad (15)$$

which is shown in Fig. 1 and can be compared with the Pitzer correlation. EOS constants follow directly from Eqs. 9 where λ is given by:

$$\lambda = \frac{3}{2}(1+\omega) \pm \frac{1}{2}[9(1+\omega)^2 - 8]^{1/2} \quad \ldots\ldots\ldots\ldots\ldots\ldots\ldots \quad (16)$$

Note that EOS constants and Z_c are defined explicitly by acentric factor. Schmidt and Wenzel suggest that only α be considered temperature-dependent, where $\beta=\xi=\delta=1$. The $\alpha(T_r,\omega)$ function is given by two expressions, one for $T_r \leq 1$ and the other for $T_r > 1$.

CONCLUSIONS

1. General thermodynamic expressions are developed for the Martin two-term, four-constant equation of state.

2. A family of cubic equations of state is proposed which includes the Peng-Robinson, Redlich-Kwong and Usdin-McAuliffe equations. It is based on the general Martin EOS which is simplified by introducting a correlating parameter, λ, having a specific numerical value for each equation.

3. For the proposed EOS family it is shown that the values of λ and Z_c which minimize the Σ-chart defined by Martin form a smooth function and that the minimum Σ-chart value is always 0.67188.

4. The Usdin-McAuliffe equation is generalized by matching vapor pressures and saturated liquid densities. The EOS-constant correction factors are expressed as simple functions of acentric factor and reduced temperature. This equation should predict more accurate liquid densities of petroleum mixtures containing considerable amounts of heavy fractions.

5. The Schmidt-Wenzel equation is expressed in terms of the general Martin EOS and is shown to be a specialization of the proposed EOS family where λ is a function of acentric factor instead of a numerical constant.

TABLE 1 - Definition of Martin EOS quantities for three common equations of state.

Quantity	Redlich-Kwong	Peng-Robinson	Usdin-McAuliffe
a	a	a	a
b	b	b	b
c	b	$(2+\sqrt{2})b$	b
d	2b	$(2-\sqrt{2})b$	$b+\tilde{d}$
Z_c	1/3	0.307401...	Z_c
λ	1	$2+\sqrt{2}$	1

Note: $\tilde{d}$ represents the constant found in the original UM EOS. Definitions of c and d are interchangable because of symetry; this suggests that λ can have either of two values - e.g. PR: $2\pm\sqrt{2}$, RK: 1,2.

TABLE 2 - Compound properties used to develop modified UM EOS.

Compound Name	Molecular Weight	Critical Pressure (MPa)	Critical Temperature (K)	Acentric Factor	True Z_c	Rackett Z_{ra}
methane	16.043	4.604	190.58	0.0115	0.288	0.2876
ethane	30.070	4.880	305.42	0.0908	0.284	0.2789
propane	44.097	4.249	369.82	0.1454	0.280	0.2763
i-butane	58.124	3.648	408.14	0.1756	0.282	0.2750
n-butane	58.124	3.797	425.18	0.1928	0.274	0.2728
i-pentane	72.151	3.383	460.43	0.2273	0.270	0.2716
n-pentane	72.151	3.369	469.65	0.2510	0.262	0.2685
benzene	78.114	4.898	562.16	0.2100	0.271	0.2696
cycloheaxane	84.162	4.075	553.54	0.2144	0.273	0.2729
2,3-dimethylbutane	86.178	3.127	499.98	0.2473	0.269	0.2694
n-hexane	86.178	3.012	507.43	0.2957	0.264	0.2635
2,2-dimethylpentane	100.205	2.773	520.50	0.2886	0.267	0.2673
n-heptane	100.205	2.736	540.26	0.3506	0.263	0.2611
n-octane	114.232	2.486	568.83	0.3978	0.259	0.2567
n-nonane	128.259	2.289	594.64	0.4437	0.254	0.2547
n-decane	142.286	2.096	617.65	0.4902	0.246	0.2503
n-dodecane	170.330	1.820	658.26	0.5622	0.237	0.2466

REFERENCES

1. Usdin, E. and McAuliffe, J.C.: "A One Parameter Family of Equations of State," Chem.Eng.Sci. (1976)31, 1077-1084

2. Peng, D.-Y. and Robinson, D.B.: "A New Two-Constant Equation of State," Ind.Eng.Chem.Fund. (1976)15,1, 59-64

3. Redlich, O. and Kwong, J.N.S.: "On the Thermodynamics of Solutions. V: An Equation of State. Fugacities of Gaseous Solutions," Chem.Reviews (1948)44, 233-244

4. van der Waals, J.D.: Doctoral Dissertation, Leiden, Holland, 1873

5. Martin, J.J.: "Cubic Equations of State - Which," Ind.Eng.Chem.Fund. (1979)18,2, 81-97

6. Schmidt, G. and Wenzel, H.: "A Modified van der Waals Type Equation of State," Chem.Eng.Sci. (1980)35, 1503-1512

7. Zudkevitch, D. and Joffe, J.: "Correlation and Prediction of Vapor-Liquid Equilibrium with the Redlich-Kwong Equation of State," AIChE J. (1970)16, 112-119

8. Joffe, J, Schroeder, G.M. and Zudkevitch, D.: "Vapor-Liquid Equilibria with the Redlich-Kwong Equation of State," AIChE J. (1970)16,3, 496-498

9. Haman, S.E.M., Chung, W.K., Eishayal, I.M. and Lu, B.C.-Y.: "Generalized Temperature-Dependent Parameters of the Redlich-Kwong Equation of State for Vapor-Liquid Equilibrium Calculations," Ind.Eng.Chem., Proc.Des.Dev. (1977)16,1, 51-59

10. Yarborough, L.: "Application of a Generalized Equation of State to Petroleum Reservoir Fluids," Equations of State in Engineering and Research, K.C. Chao and R.L. Robinson, Jr. (eds.)

11. Soave, G.: "Equilibrium Constants from a Modified Redlich-Kwong Equation of State," Chem.Eng.Science (1972)27, 1197-1203

12. Martin, J.J. and Hou, Y.C.: AIChE J. (1955)1, 142

13. Abbott, M.M.: "Cubic Equations of State," AIChE J. (1973)19,3, 596-601

14. Martin, J.J.: "Equations of State," Applied Thermodynmaics Symposium (1967)59,12, 34-52

15. Technical Data Book - Petroleum Refining, American Petroleum Institute, Washington, D.C. (1976)Vol.1, 3rd ed.; Procedures 5A1.10 (Lee-Kesler) and 6A2.13 (modified Rackett)

16. Fuller, G.G.: "A Modified Redlich-Kwong-Soave Equation of State Capable of Representing the Liquid State," Ind.Eng.Chem.Fund. (1976)15,4, 254-257

17. Harmens, A.: Cryogenics (1977)17, 519

NOMENCLATURE

a, b, c, d = EOS constants
A, B, C, D = EOS constants
$\alpha, \beta, \xi, \delta$ = EOS constant correction factors
$\Omega_a, \Omega_b, \Omega_c, \Omega_d$ = EOS numerical constants
f = fugacity
κ = binary interaction coefficient
m = correlating parameter for α
M = molecular weight
p = absolute pressure
p_c = critical pressure
p_v = vapor pressure
R = universal gas constant
T = absolute temperature
T_c = critical temperature
v = molar volume
x_i = mole fraction of component i
Z = compressibility factor
Z_{ra} = Rackett correlating parameter ($\cong Z_c$)
Z_c = critical compressibility factor
β_c = correlating parameter for SW EOS
β^* = correlating parameter for β
κ_{ij} = binary interaction parameter between i and j
λ = correlating numerical constant
ρ_{sL} = saturated liquid density
Σ = Z-sum chart
ω = acentric factor

APPENDIX

The correlations for vapor pressure and saturated liquid density were taken from Ref. 15, procedures 5A1.10 and 6A2.13. They are repeated here because Ref. 15 is often not available.

Vapor pressure, p_v, is estimated from critical properties and acentric factor (see Table 2):

$$\ln(p_v/p_c) = A_0 + A_1 \cdot \omega \quad \text{(A-1)}$$

where

$$A_0 = 5.92714 - 6.09648/T_r - 1.28862 \cdot \ln T_r + 0.169347 \cdot T_r^6 \quad \text{(A-2a)}$$

$$A_1 = 15.2518 - 15.6875/T_r - 13.4721 \cdot \ln T_r + 0.435770 \cdot T_r^6 \quad \text{(A-2b)}$$

and $T_r = T/T_c$. Units are arbitrary, though temperature and pressure should always have absolute units.

Saturated liquid density, ρ_{sL}, is estimated from a modified Rackett equation using critical properties, molecular weight and a correlating parameter Z_{ra} (closely approximated by true critical compressibility factor):

$$\rho_{sL} = M \cdot [p_c/RT_c] \cdot Z_{ra}^{-[1.0+(1.0-T_r)^{2/7}]} \quad \text{(A-3)}$$

where the units of ρ_{sL} depend on the units of R and critical properties. Values of Z_{ra} are given in Table 2 for several compounds.

It is only suggested to use these two correlations for reduced temperatures greater than 0.4 and less than or equal to 1.0. The accuracy should be less than 0.5% in this region and only applies to pure hydrocarbons.

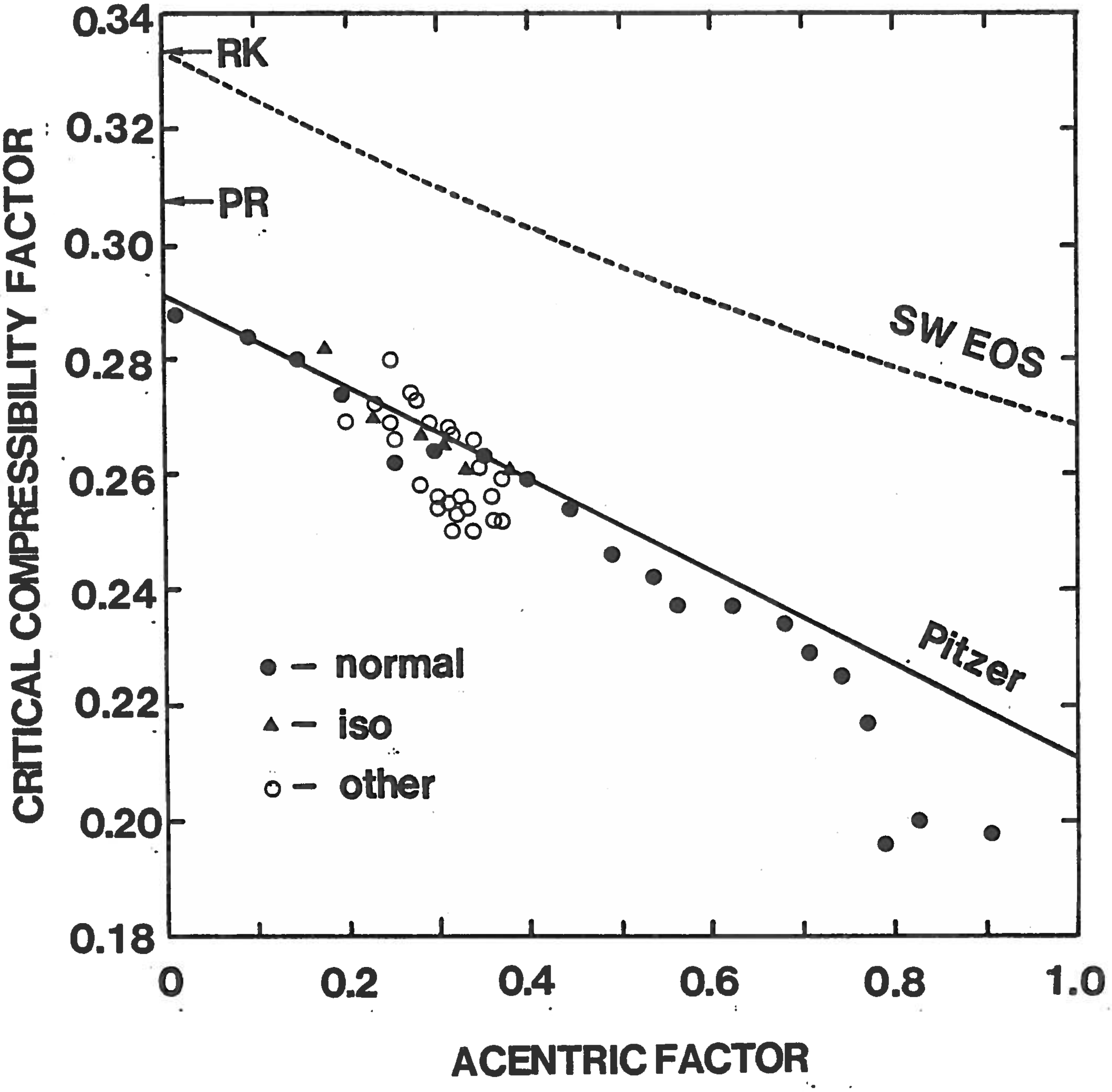

FIG. 1 - Experimental Z_c-ω data for paraffins; Pitzer Z_c-ω correlation and Z_c-ω correlation defining the Schmidt-Wenzel EOS.

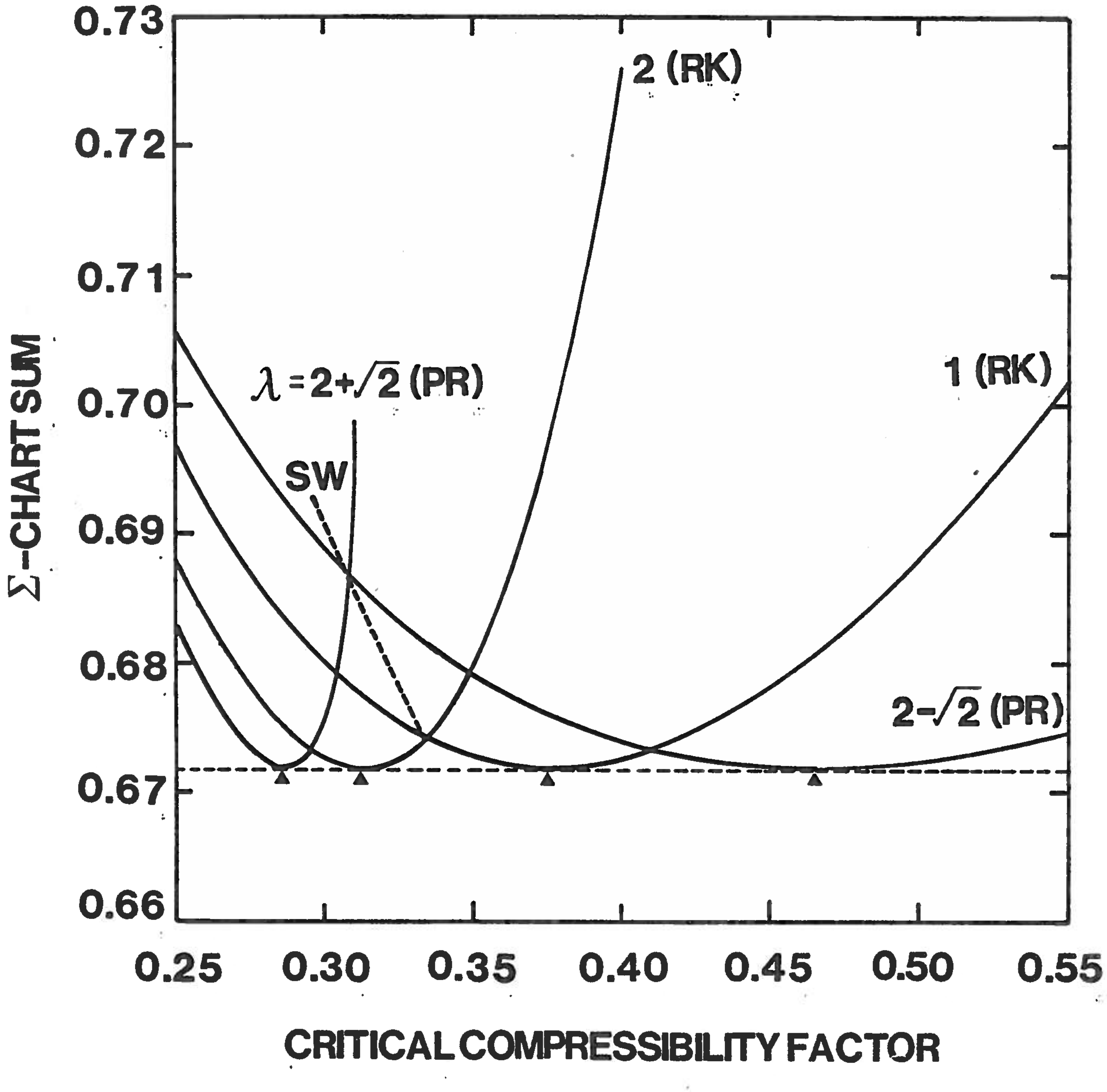

FIG. 2 - Behavior of the Σ-chart sum as a function of Z_c for several values of correlating parameter λ.

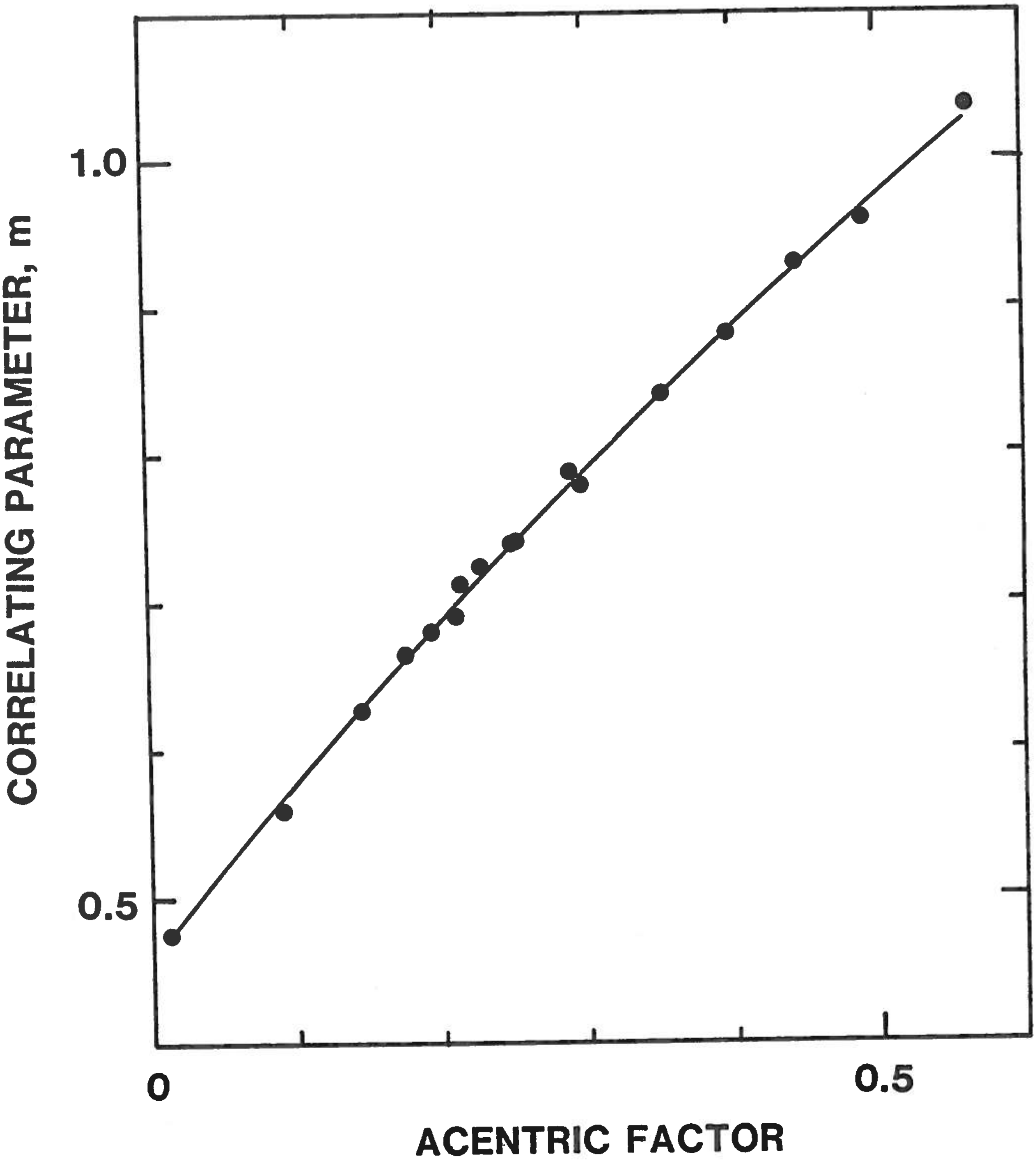

FIG. 4 - Relation between correlating parameter m and acentric factor for the modified Usdin-McAuliffe EOS.

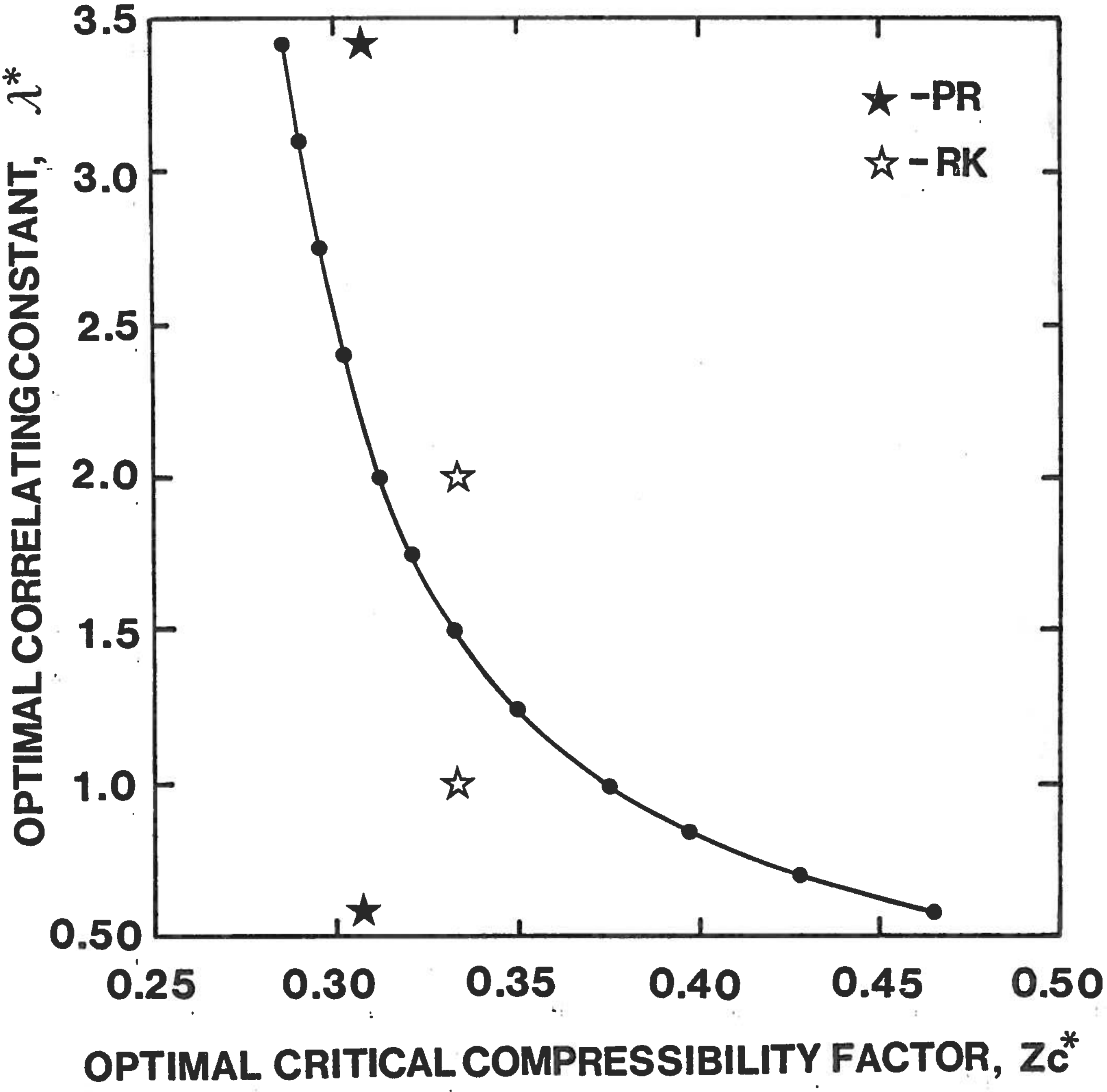

FIG. 3 - Optimal parameters λ^* and Z_c^* for minimizing the Σ-chart sum (to its universal value of 0.67188).

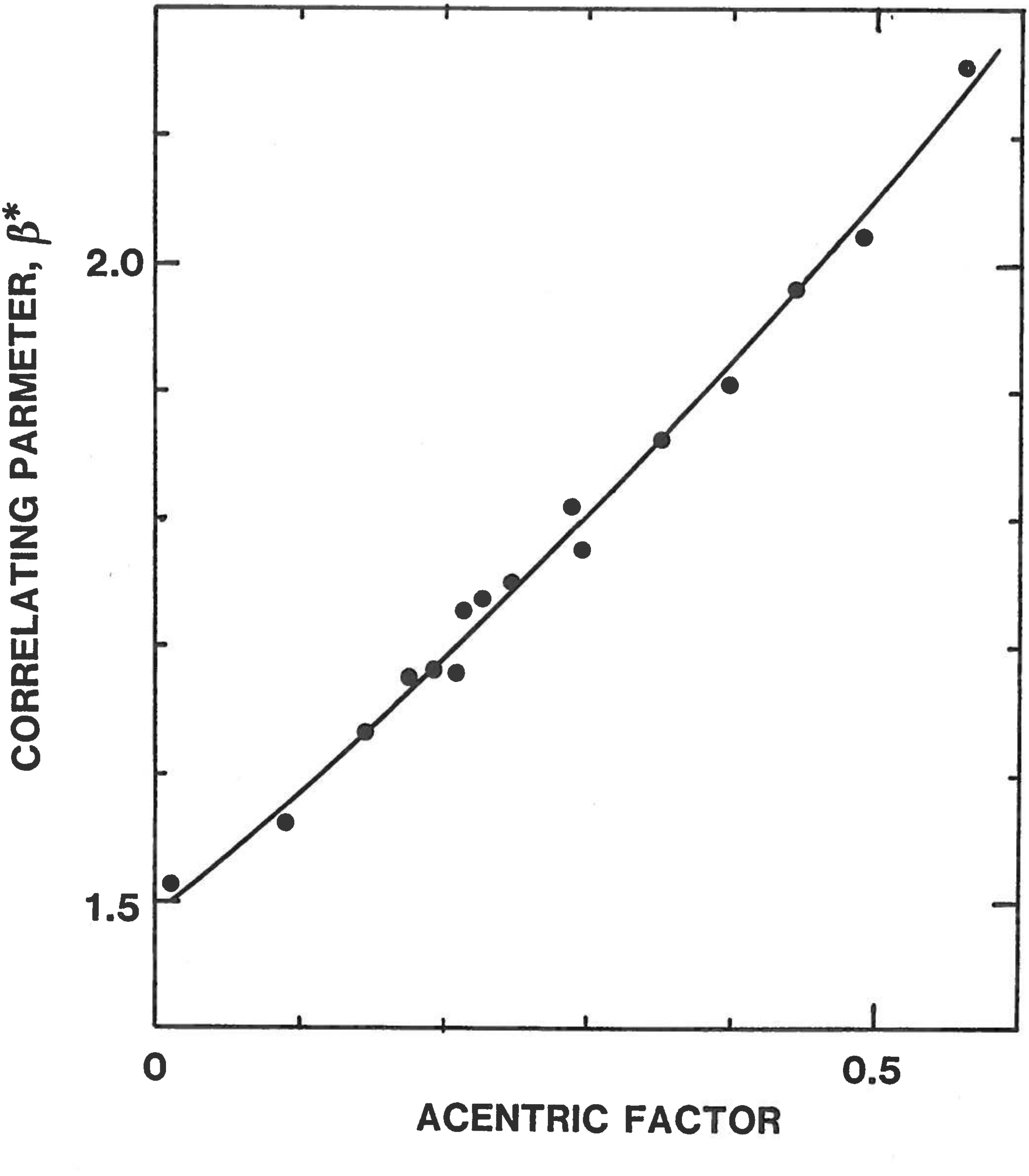

FIG. 5 - Relation between correlating parameter β* and acentric factor for the modified Usdin-McAuliffe EOS.

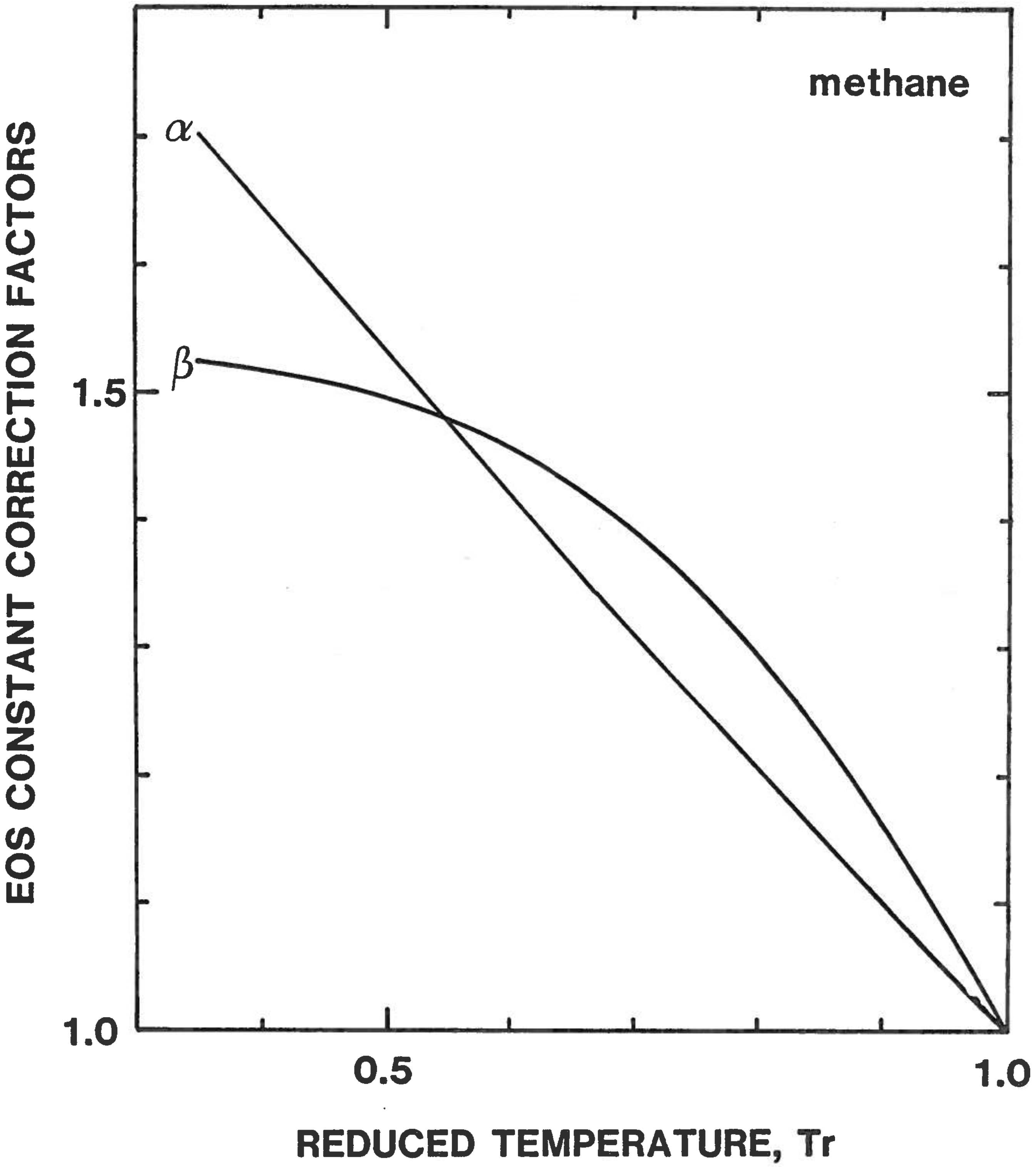

FIG. 6 - Relation between EOS-constant correction factors α and β and reduced temperature for methane.

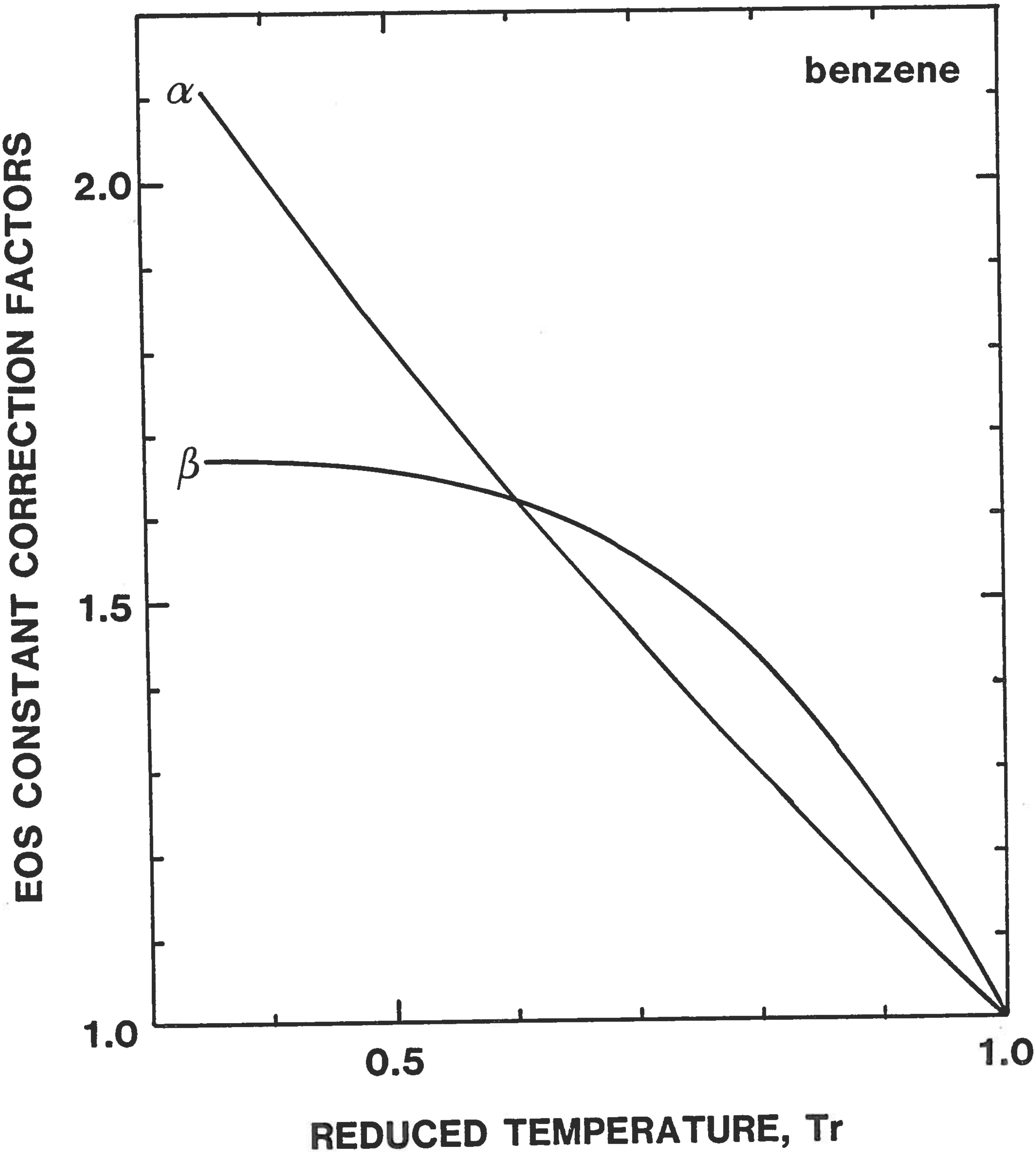

FIG. 7 - Relation between EOS-constant correction factors α and β and reduced temperature for benzene.

PRACTICAL ASPECTS OF CHARACTERIZING PETROLEUM FLUIDS

by

Tor Austad[1]

John Hvidsten[2]

Haakon Norvik[2]

Curtis H. Whitson[1]

[1] Rogaland Regional College
[2] Rogaland Research Institute

presented at the conference on

North Sea Condensate Reservoirs and Their Development

May 24-25, 1983

London

INTRODUCTION

This paper describes the essential aspects of chemical and pressure-volume-temperature (PVT) analysis of gas condensates. It also discusses the use of cubic equations of state (EOS) for modelling gas-condensate phase behavior. Particular emphasis is placed on characterization of petroleum fractions defining the heptanes-plus (C_7+) group. Although we have chosen to concentrate our discussion on gas condensates, in keeping with the conference theme, most parts of the paper are equally applicable to black oils.

A gas condensate is, by definition, a naturally occuring petroleum mixture found at reservoir temperature greater than the mixture's critical temperature and less than its cricondentherm (see Fig. 1). The most distinguishing feature of a gas condensate is retrograde condensation, defined in the present context as an increasing accumulation of liquid (condensate) during isothermal pressure reduction. Other typical characteristics of gas condensates include producing gas-oil ratios greater than 3000 scf/STB (535 Sm^3/Sm^3), stock-tank oil gravity greater than 45 degrees API (0.8 g/cc), and reservoir temperatures often greater than 200 °F (95 °C).

The first part of the paper concerns chemical analysis of separator samples. Description of experimental techniques is supplemented with North Sea gas-condensate data measured at Rogaland Research Institute (RRI). These data typify the fluid character of richer North Sea fluids.

The chemical characterization of heptanes-plus is discussed in detail. Numerous experimental procedures are reviewed and data from North Sea condensate samples are presented. Also, a complete distillation analysis up to C_{20} is presented for a mixture of North Sea heptanes-plus fractions representing black-oil and gas-condensate systems. Properties of carbon-number groups should give useful estimates for normal boiling points, specific gravities, and molecular weights when experimental distillation data are not available.

Next we review the most common PVT analyses offered by commercial and in-house laboratories. The constant-volume depletion procedure is considered in more detail since it closely simulates the physical process a gas condensate undergoes during depletion.

Finally, we describe the use of cubic equations of state (Peng-Robinson's equation in particular) for modelling phase behavior. Heptanes-plus characterization is reviewed and its importance to EOS predictions is emphasized. A procedure for matching experimental PVT data is given, and it is tested on a North Sea gas condensate previously published in the literature.

A convenient literature guide is given following the References section. These sources give access to a wide range of information on gas-condensate fluids.

CHEMICAL ANALYSIS

Analytical information yielding compositional data for petroleum reservoir fluids is useful during exploration, production and gas-cycling phases of a gas-condensate reservoir. Analytical data, in combination with PVT analysis, can be used to accurately describe phase behavior and physical properties. Fig. 2 illustrates schematically several processes which are highly dependent on proper fluid characterization - near-wellbore effects, vertical flow, surface separation, platform or wellsite processing, transportation, refining, and miscible/immiscible gas displacement.

The obvious first step in properly characterizing a reservoir fluid is to determine its composition. Petroleum in general, and gas condensates specifically, are very complex mixtures of hydrocarbons and light non-hydrocarbons. On a routine basis it is only possible to define the molar quantities of a few relatively light components, including hydrogen sulphide (H_2S), carbon dioxide (CO_2), nitrogen (N_2) - the most common non-hydrocarbons - methane (C_1), ethane (C_2), propane (C_3), iso-butane (iC_4), normal butane (nC_4), iso-pentane (iC_5), normal pentane (nC_5), grouped hexanes and similar-sized compounds (C_6), and the heptanes-plus fraction (C_7+) combining all remaining heavier constituents.

The heptanes-plus fraction may consist of hundreds or thousands of paraffinic, naphthenic and aromatic compounds. The C_7+ fraction is commonly described by experimental molecular weight, density (i.e, specific gravity, relative to water) and sulfur content. Other properties used to characterized the lumped C_7+ fraction include viscosity, refractive index and Watson characterization factor.

Fluid samples used for chemical analysis during exploration and production phases are normally sampled from a test separator. The well is produced through separator equipment at monitored pressure and temperature (e.g., 1500 psia and 100 °F; 10000 kPa and 40 °C). After producing gas-oil ratio (GOR) stabilizes, equilbrium is assumed and samples are collected. Gas and oil samples are taken in stainless steel cylinders to prevent leakage and contamination. Usually 200 to 300 cc samples of both oil and gas are available (measured at separator conditions).

Rogaland Research Institute (RRI) has developed a routine procedure for analyzing separator oil and gas samples. Having determined respective compositions on weight and molar bases, the wellstream composition is calculated using separator GOR, temperature and pressure. The following is a discussion of RRI's procedure.

Laboratory Equipment

The laboratory is equipped with standard equipment such as a low-temperature distillation apparatus, gas chromatograph (GC), density meter (atmospheric pressure), freezing-point depression molecular weight apparatus, and X-ray fluorescence used for determining sulfur content.

Additional equipment used for detailed analysis of the heptanes-plus fraction include a high-temperature distillation column, high-pressure liquid chromatograph, GC equipped with a capillary column, and a mass spectrometer facility based on GC. Necessary data processing equipment includes micro- and mini-computers.

Separator-Gas Analysis

Prior to GC analysis, the gas-sample cylinder is heated about 10 °C above sampling temperature. Instrumentation includes an HP-5880, level four GC with two detectors. The GC run is made using a thermal conductivity detector (TCD) to determine the content of non-hydrocarbons and paraffin constituents from methane to butane. The second GC run is made using a flame ionization dector (FID). This run first determines pentanes and hexanes content, then uses backflush to quantify heptanes-plus. Fig. 3 illustrates the procedure for analyzing separator-gas samples.

The chromatograph detects mass of certain substances and responds by drawing a peak on the chromatogram (see Fig. 4). The area under the curve for a given peak indicates the relative mass of that substance (weight fraction). From previous calibration it is known when a specific compound will be detected by the chromatograph. Assigning the area to the specific compound, it is then possible to define the composition of the gas. Identical injected quantities (moles) of gas is ensured for each run by temperature control and a back-pressure gauge.

Results from each run are stored on tape and then recombined automatically to yield weight and molar compositions. Molecular weight of hexanes and heptanes-plus used to convert to molar basis are 86.0 and 100.0, respectively; these values represent the molecular weights of normal hexane and heptane. Table 1 gives an example report of separator-gas analysis from a North Sea gas-condensate sample.

Separator-Oil Analysis

The pressured-oil sample is distilled roughly into three batches. First, the lighter components including non-hydrocarbons and methane to butanes are separated by boiling the separator oil to about 23 °C. Pentanes and hexanes are then separated by boiling up to 94 °C. The remaining mixture is considered heptanes-plus. Fig. 3 illustrates the distillation procedure.

The first distillation batch is collected in preevacuated receivers. By recording temperature, pressure and volume it is possible to calculate the mass of gas collected. The pentanes-to-hexanes batch is weighed directly, as is the remaining heptanes-plus fraction.

GC analysis is used to determine weight fractions of components found in the first two distillation batches (see Fig. 3); each batch is analyzed separately and results are stored on tape. The C_7+ fraction is characterized by measuring its specific gravity, molecular weight and sulfur content. When combined with the GC results for the two lighter batches, the total separator oil composition is determined. Compounds with seven carbon atoms which are carried over in the pentanes-to-hexanes batch are detected by the GC. The measured C_7+ molecular weight and specific gravity is corrected for these constituents by assuming they have properties of normal heptane. Table 2 gives an example of separator-oil analysis for a North Sea gas-condensate sample. Fig. 5 shows chromatograms for runs 1 and 2 (distillation batches 1 and 2) of a North Sea gas condensate.

Recombination and Consistency Check

It is usually of interest to recombine the separator gas and oil compositions to yield a composite wellstream composition. This is done by a simple material balance if separator GOR, pressure and temperature are known. An example of recombination is given in Table 3 for the separator samples given above.

To check the consistency of separator-fluid compositions it may be helpful to use a method proposed by Hoffman, Crump and Hocott for correlating equilibrium constants (K-values). By definition, K-value is the ratio of normalized mole fraction in the vapor (gas) phase to the normalized mole fraction in the liquid (oil or condensate) phase. Hoffman, Crump and Hocott noted that if the product Kp is plotted versus a temperature function, F, on semi-log paper, then the resulting curve is linear. This relation is particularly accurate at pressures and temperatures encountered at separator conditions.

The temperature function F is different for each component. It is defined as the product of b and the quantity $(1/T_b-1/T)$, where T_b is the normal boiling point of the component and b is a composite function of critical pressure and temperature and normal boiling point. Standing gives modified values for b and T_b for light compounds which should be used instead of the true values. Table 3 shows an example calculation of Kp vs F for the same gas condensate fluid analysed earlier. A plot of the function is given in Fig. 6. Note that the C_7+ F-value is not well-defined, so it can not be included in the consistency check directly.

Inconsistent compositions due to leakage, improper analysis or lack of equilibrium during sampling may be spotted on a log Kp vs F plot which is nonlinear. Such an example is given in Fig. 6.

Another helpful consistency check is to estimate the Watson characterization factor using measured C_7+ molecular weight and specific gravity. The correlation given by Whitson is,

$$K_w = 4.5579 \cdot M^{0.15178} \cdot \gamma^{-0.84573} \quad .... \ (1)$$

We have found that the K_w value for a given oil or gas-condensate field varies only slightly (e.g., 12.00±0.02) for the C_7+ fraction. This is illustrated in Table 4 for several North Sea gas-condensate and black-oil reservoirs. Fig. 7a shows the very slight variation in K_w value for a North Sea gas-condensate reservoir. Fig. 7b shows an anologous plot for a North Sea black-oil reservoir.

If a laboratory can establish the characterization factor K_w for a given field (or even a given well), then each time new measurements of C_7+ molecular weight and specific gravity are made, the resulting K_w value can be checked to see if it is close to the field average. If the value deviates more than ± 0.01 to 0.02 then the molecular weight measurement (which is much more difficult to perform) should be questioned; a new measurement of both specific gravity and molecular weight should probably be made.

In the last column of Table 4 we have calculated C_7+ molecular weight using Eq. 1 with measured specific gravity and the field-average characterization factor. It is seen that the range in K_w of ± 0.02 suggests a maximum error in molecular weight of approximately 2 to 3 (usually less than 1.5%).

SPECIAL ANALYSIS OF HEPTANES-PLUS FRACTION

Characterizing all compounds with more than six carbon numbers as a single component is acceptable for many engineering applications. It may be necessary, however, to better define the constituents making up heptanes-plus. One example would be for the pricing of oil or condensate; i.e, it is necessary to determine the relative quantities of fuel oils, gasolines, etc. which can be refined from the produced fluid. Another example would be if an equation of state is used for predicting phase behavior at conditions other than those measured experimentally. The predictive capability of all equations of state is severly limited if only heptanes-plus properties can be defined; in general it is necessary to split C_7+ into at least three to five pseudocomponents.

There are many ways to extend the analysis of heptanes-plus fractions. Perhaps the oldest and most common is true boiling point (TBP) distillation. Because this technique is both time consuming and expensive, it may be replaced by simulated distillation using gas chromatography. Although simulated distillation may only require a small fraction of the time and expenses required by TBP analysis, it does not provide the engineer with the same data base for each fraction. Instead of measuring boiling point, volume distilled, specific gravity and perhaps molecular weight, viscosity and refractive index of each fraction, the only real data simulated distillation gives is weight fraction and a calculated estimate of boiling point.

The research laboratory at RRI has developed a special analysis procedure for characterizing heptanes-plus fractions. Starting with the previously mentioned procedure for analysing separator oil, the C_7+ mixture is subjected to one or more of the following analyses:

- carbon-number distillation from C_7 to C_{20} with a remaining C_{21}+ residue; normal paraffin boiling points are used to define single carbon-number groups (ASTM D 2892-78).
- TBP distillation using predefined volume-percent cuts to separate the petroleum fractions - e.g., 3% per cut.
- simulated distillation using GC with high-precision slice widths of 6 seconds (240 detector readings per slice).
- aromatic analysis of carbon-number fractions up to C_{20} using high-pressure liquid chromatography.
- paraffin-naphthene-aromatic analysis of carbon-number fractions up to C_{10} using mass spectrometry based on GC.
- molecular weight and specific gravity measurements of all petroleum fractions determined by carbon-number or TBP distillation.

Depending on the particular need, some or all of the above procedures may be justified. Usually, however, only simulated distillation can be run on a routine basis. This might be practical for analysis of production fluids where calibration of the GC has been determined based on more reliable TBP or carbon-number distillation results. The other analyses would need to be justified for a specific use requiring particularly detailed description of the C_7+ fraction. Some results from experimental work on North Sea heptanes-plus mixtures are presented in the following discussion.

Carbon-Number Distillation

Results of a carbon-number distillation based on the ASTM D 2892-78 method is presented in Table 5 and Fig. 8. There are several aspects of interpreting distillation data worth noting. First let us start off by asking "what is the normal boiling point of a given fraction?" First, by normal it is inferred that the boiling point corresponds to atmospheric (normal) pressure - i.e., the vapor pressure equals atmospheric pressure at its normal boiling point temperature.

Suppose the distillation cut we are considering starts boiling at 68 °C and stops boiling at 98 °C (boiling points of normal paraffins C_6 and C_7). If 8 volume percent of the initial C_7+ mixture boils off in this interval, then one point on the distillation curve would be 0% and 68 °C and another would be 8% and 98 °C. Suppose that 6 volume percent boils between 98 °C and 126 °C. The next point on the distillation curve would be 14% (8% + 6%) and 126 °C. Having three points on the distillation curve, a smooth line can be drawn. The normal boiling point for the first (C_7) cut would be read from the curve at the mid-volume point - i.e., at 4%. The normal boiling point for the second cut (C_8) would be read from the curve at its mid-volume point - i.e., at 11% (8% + 14% divided by two). The engineer who does not have a background in petroleum distillation might consider working through the example data given in Table 5.

If distillation is performed to high carbon-number groups such as C_{20}, then the resulting residue ($C_{21}+$) will be a semi-solid at room temperature. To avoid large losses the column should be rinsed with a volatile solvent after distillation is completed. The extracted residue can be retrieved by evaporating the solvent. We have found that total distillation losses can be minimized using this procedure.

Properties of the residue are not readily obtained by direct measurement due to its semi-solid character at room conditions. It may be necessary to back-calculate residue properties using measured C_7+ properties and mass/mole balances. Unfortunately, small errors in C_7+ molecular weight may result in unphysical values of residue molecular weight. Engineering judgement should be used, though direct estimation of residue molecular weight is desirable.

The example distillation presented in Table 5 and Fig. 8 represents a mixture of numerous C_7+ fractions separated using the procedure outlined in the previous section. Both black-oil and gas-condensate samples were mixed, though the properties of the mixture suggest a more gas-condensate character. Carbon-number boiling points, specific gravities and molecular weights up to C_{20} can probably be used as estimates for most North Sea fluids if measured data are not available.

Simulated Distillation

A chromatogram for simulated distillation by GC is shown in Fig. 9. It is for the same C_7+ mixture analyzed in the previous section. Normal hexane is used as the internal standard. For paraffinic oils it is easy to locate normal paraffin peaks on the chromatogram. Instead of using peak integration mode, area slice mode is chosen. This mode is useful because simulated distillation analysis depends on the distribution of area under the chromatographic curve, rather than on the amount of specific peaks. The area slice mode provides this basic area distribution data.

A nine-foot by 1/8-inch stainless steel colum packed with 10% SP-2100 on 80/100 supelcoport was used to conduct the present analysis. A blank test showed that normal C_{20} eluted prior to any significant bleeding of the column material. This observation suggests that base-line shift will not be observed up to C_{20}.

A flame ionization detector was applied and normal hexane was used as an internal standard (2.5 weight percent of the injected sample). Although the FID should give similar response on a weight basis for various hydrocarbons, we found it gave values systematically low. By increasing the response factor of the internal standard by 15.5%, we found that simulated results match true distillation data very well. Also, reproducibility was good. Fig. 10 shows a comparison of distillation curves on a weight basis.

It should be noted that the correction to response factor is probably dependent on the particular fluid. If a fluid has not been studied previously, then a TBP or carbon-number distillation should probably be run to calibrate the internal-standard response factor.

PNA Analysis Using Mass Spectometry

Using GC-based mass spectometry, RRI has been able to determine the paraffin-naphthene-aromatic (PNA) content of carbon-number distillation fractions C_7 to C_{10}. The basic technique is to identify compounds showing responses with mass-to-charge values, m/z, approximately equal to molecular weights of the compounds in a given family for a given carbon number. These values are approximately $14 \cdot n + a$, where n is the number of carbon atoms and a equals +2 for paraffins, 0 for naphthenes, and -6 for aromatics (for the C_{10} fraction, values of -6 and -8 are used for aromatics). Having located all compounds with the specified m/z ratio, relative amounts are found by integrating the various peaks in the total-ion-count, TIC, chromatogram.

An example spectrogram is given in Fig. 11 for the naphthene family. Only those peaks found in the proper time interval are integrated; others are ions which result from the breakdown of large compounds.

Presently the identification and integration of TIC peaks is done manually for each carbon number group. A program is now being developed to automate the calculations; it is based on a procedure somewhat different than presently performed manually. Such a program should make PNA analysis from mass spectrometry more routine.

Alternative methods for estimating PNA content have been proposed. These methods rely on measured physical properties including refractive index, viscosity and density.

CONVENTIONAL PVT ANALYSIS

The conventional experimental procedures performed on gas condensates include

- constant-volume depletion (CVD)
- constant-composition (-mass) expansion (CCE)
- separator flash

The first two experiments are conducted in a high-pressure cell with some means of visually observing phase behavior during pressure changes. Mercury is usually used as an injection medium for changing the pressure. Reservoir temperature is maintained by a circulating-air system enclosing the cell.

Separator flash experiments are designed with the intention of (1) checking the recombined fluid composition and (2) analyzing the effect of separator pressure and temperature on oil gravity and total surface gas-oil ratio. Using the Hoffman-Crump-Hocott method it may be possible to determine a low-pressure K-value correlation from compositional data reported from separator flash tests.

Constant-composition expansion is merely an isothermal pressure-volume experiment. Starting at or above initial reservoir pressure with a known number of moles of resevoir fluid, pressure is reduced and volume is measured. At undersaturated conditions (above the dew point), volume measurements can be converted into compressibility factors ($Z=pV/NRT$). Below the dew point (at saturated conditions) retrograde condensation can be observed. The volume of liquid condensate is reported as a percent of dew-point volume. CCE data are not sufficient to calculate compressibility factors of saturated vapor in equilibrium with liquid condensate; number of moles in the vapor phase is not known, only its volume.

Description of the constant-volume depletion procedure is taken from Whitson and Torp:

"A CVD experiment is conducted at reservoir temperature and begins at saturation pressure. Cell volume, or the volume contained by the saturated fluid, is used as a reference volume."

"Mercury is withdrawn from the bottom of the cell, thereby lowering the pressure as fluid expands. During this process, a second phsase evolves - either retrograde liquid (for gas condensates) or solution gas (for volatile oils)."

"Mercury withdrawal is ceased when a predetermined pressure is reached. Some laboratories measure liquid volumes at several pressures before any vapor has been removed; these values, reported relative to cell volume, represent CCE. They closely approximate volumes that would have been measured if the process had been CVO..."

"Mercury is reinjected into the cell at constant pressure while simultaneously withdrawing an equivalent volume of vapor. When initial cell volume is reached, mercury injection is ceased. Withdrawn vapor is analyzed using gas chromatography to determine compositions. Moles of vapor produced are calculated using the real gas law and are reported as a cumulative percent of initial moles. Compressibility factor also is calculated noting produced vapor surface volume and equivalent cell volume (at pressure and temperature). From measured vapor gravity and composition, heptanes-plus molecular mass is back-calculated. Liquid volume is measured visually and reported as a percent of cell volume, which is actually a type of hydrocarbon liquid saturation."

"The experimental procedure is repeated several times until a low pressure is reached. The remaining liquid is removed, distilled, and analyzed using gas chromatography. Measured liquid composition should check with material-balance derived composition. (Some major laboratories smooth and adjust measured vapor compositions until the material balance checks. This procedure is discouraged. It is good practice to ask if a laboratory reports measured or smoothed data, and to what extent material-balance-derived data are used in final CVD reports.)"

Whitson and Torp also show that reported CVD data are sufficient to calculate other physical properties, including liquid density, composition, and heptanes-plus molecular weight, vapor density (using two independent methods), K-values at depletion pressures, and black-oil PVT properties used by numerical reservoir simulators.

Engineers working with gas-condensate phase behavior should certainly become familiar with the CVO procedure and data which are reported in conventional reports. There are numerous concepts such as two-phase Z-factors and wellstream surface volumes which are not well-documented or understood in the industry.

CUBIC EQUATIONS-OF-STATE APPLICATION

What is a cubic equation of state? It is an equation relating pressure, temperature, composition and volume. Slightly oversimplified, we write a general form of the cubic equation as

$$V^3 + a \cdot V^2 + b \cdot V + c = 0 \quad \ldots\ldots\ldots\ldots\ldots\ldots\ldots\ldots \quad (2)$$

Constants a, b and c are defined by pressure, temperature, composition and moles of the fluid. Since the equation is cubic in volume, there may be one, two or three volumes which satisfy the specific conditions. Which one do you choose if there are, say, three volumes? In practice we merely define the largest volume as a vapor and the smallest volume as a liquid; if a third volume exists between these two then it is merely ignored. If only one volume satisfies the equation defined by specified conditions, then there is obviously no problem in choosing the correct volume.

Why do we choose a cubic form? The answer lies in the behavior of real fluids. Consider water for a moment. At room conditions water behaves as a liquid and has a density of approximately 1 g/cc. When we begin to heat water its density decreases slightly (mass remains constant while volume increases). However, once we reach 100 °C the water becomes a vapor (steam) and its density changes abruptly, becoming several orders of magnitude lower than at 99 °C. At 100 °C we can actually say that water has two densities - the saturated vapor density (steam) and saturated liquid density (heated water). To correctly predict this abrupt change in density (i.e., volume, assuming a constant mass), the cubic equation merely chooses the larger volume solution to describe steam, and the smaller volume solution to describe heated water.

Cubic equations are usually expressed in terms of the compressibility factor, Z, which is defined by the real gas law: $Z = pV/NRT$. The general form of any cubic equation then becomes,

$$Z^3 + e \cdot Z^2 + f \cdot Z + g = 0 \quad \text{..........................} \quad (3)$$

where constants e, f and g are defined by pressure, temperature, and composition. If we consider only pure compounds for the moment, then we can express e, f and g for one of the more popular cubic equations of state - the Peng-Robinson (PR) equation,

$$\begin{aligned} e &= B - 1 \\ f &= A - 3B^2 - 2B \quad \text{................................} \quad (4) \\ g &= B^3 + B^2 - AB \end{aligned}$$

where

$$\left.\begin{aligned} A &= 0.45724 \cdot (p/T^2) \cdot (T_c^2/p_c) \\ B &= 0.07780 \cdot (p/T) \cdot (T_c/p_c) \end{aligned}\right\} \quad \text{.....................} \quad (5)$$

To calculate volume of a pure compound, first specify pressure, p, temperature, T, and critical constants p_c and T_c. Calculate A and B using Eqs. 5; actually Peng and Robinson introduce a correction factor for the A-term, dependent on reduced temperature (T/T_c) and acentric factor (along the same line as suggested by Soave). Having calculated A and B, constants e, f and g are found. The cubic equation (Eq. 3) is solved for Z. Analogous to our previous discussion of multiple-volume roots, the largest Z-factor is assumed to represent vapor and the smallest Z-factor is assumed to represent liquid; no choice is posed if only one Z-factor root exists. Given Z, volume is found from ZNRT/p. Density is merely NM/V or pM/ZRT, where M is molecular weight.

The procedure for finding volume and density is essentially the same for mixtures. Given composition, the terms A and B are calculated using appropriate mixing rules. If the mixture lies in the single-phase region, this simplified procedure can be applied directly to the mixture composition. If the mixture splits into two phases, then the procedure is performed for each phase; this requires, however, that the composition of each phase be known. Vapor-liquid equilibria (VLE) calculations necessary for determining phase compositions are complicated and will not be discussed here.

Three points deserve mention at this point in the discussion. First, the PR EOS is an example of a two-constant equation. The two constants are A and B, as defined by Eq. 5. Second, the numerical constants - 0.45724 and 0.07780 (approximate) - result from forcing two rigid thermodynamic criteria proposed by van der Waals. Third, the critical properties (as well as acentric factor and molecular weight) required for each component in a mixture are not well-defined properties for petroleum fractions. In fact they are very difficult to estimate, and one may find that different correlations give considerably different estimates.

Another general observation about two-constant equations is that constant A usually dictates VLE and vapor density predictions, whereas B usually dictates liquid density prediction. Consequently, T_c has more influence on VLE and vapor density predictions than p_c. Also, a second correction factor - the so-called binary interaction parameter - is often used to correct VLE deficiencies for mixtures of compounds with unlike properties. Binary coefficients are also applied to constant A.

This short explanation of cubic equations of state has been given to help the reader understand methods presently used for tuning or matching an EOS to measured PVT data. Adjustments made to an EOS during the tuning process are usually localized to the components describing the $C_{7}+$ fraction. This is logical when one realizes that the greatest uncertainty lies in proper definition of critical properties for components which are actually mixtures of tens or hundreds of pure compounds. In addition to adjustment of heavy-fraction critical properties, the interaction parameter between methane (or carbon dioxide) and heavy fractions may be adjusted to match saturation pressure.

MATCHING AN EQUATION OF STATE TO MEASURED PVT DATA

None of the cubic equations of state presently available have been able to accurately predict VLE and volumetric properties of petroleum reservoir fluids without some kind of adjustment. This is really not difficult to understand when you consider our inability to define constituents found in petroleum fractions, as well as inherent limitations of cubic equations. In fact, a new field of research has evolved to develop more accurate methods of correcting EOS predictions. A few of these efforts are summarized below.

One method for improving EOS predictions is to improve the equation itself. This can be done in a number of ways. What we might consider as the purest modification is exemplified by the work of Peng and Robinson. Their conclusions give a summary of their goals and the limitations of the proposed equation:

"By modifying the attraction pressure term of the semi-empirical van der Waals equation a new equation of state has been obtained. This equation can be used to accurately predict vapor pressures of pure substances and equilibrium ratios of mixtures."

"While the new equation offers the same simplicity as the SRK (Soave-Redlich-Kwong) equation and although both equations predict vapor densities and enthalpy values with reasonable accuracy, more accurate liquid densities can be obtained with the new equation. In regions where engineering calculations are frequently required the new equation gives better agreement between predictions and experimental PVT data."

"Since two-constant equations have their inherent limitations, and the equation obtained in this study is no exception, the justification for the new equation is the compromise of simplicity and accuracy." (our emphasis)

Similar efforts by numerous other researchers and engineers has led to an enormous availability of cubic equations of state (mostly two-constant equations). The Peng-Robinson equation is certainly one of the more well-accepted and widely used equations.

Another approach which has gained considerable acceptance in the petroleum industry was proposed by Joffe, Schroeder and Zudkevich. They suggested that a second correction term be used for the Redlich-Kwong EOS constant B. According to their method, the correction terms for A and B are found simultaneously by matching vapor pressures and saturated liquid densities of pure components. Unfortunately the resulting corrections can not be readily expressed in functional form. The net result of the method is to improve liquid-density predictions. In general, the improvement in liquid density using this method is superior, though certainly more complicated, than results given by Peng and Robinson.

The last approach we will consider does not directly change the form of the equation by using pure component data. Instead, a set of measured PVT data are chosen to represent the true phase behavior of the reservoir fluid. Selected parameters used by the EOS are chosen as regression variables and can be altered to match the measured PVT data. Commonly the critical properties of C_7+ fractions are considered regression variables. Binary interaction parameters between methane (or carbon dioxide) and C_7+ fractions allow a simple means of matching saturation pressure.

An alternative to adjustment of critical properties and acentric factor is, as suggested by Coats, to adjust the two numerical constants (e.g., 0.45724 and 0.07780 for the PR EOS) in the defining equations for A and B. It should be noted that for isothermal processes (e.g., CVD), only two of the three properties (T_c, p_c, and ω) are independent. Thus only two of them need (should be) adjusted simultaneously. The disadvantages of Coats approach are 1) its unclear physical implications, and 2) the resulting EOS constants can not be used in other simulators based on the PR EOS.

One problem with the matching procedure is that no assurance can be made that a global minimum of the error function can be found. This is illustrated by an example match of a North Sea gas condensate previously presented in the literature (called NS-1 by Whitson and Torp, and Condensate B by Coats).

Coats introduced three pseudocomponents to describe the C_7+ fraction; Whitson and Torp originally give carbon-number groups up to C_{20}, plus a C_{21}+ residue, as well as a proposed five-pseudocomponent regrouping. The original Whitson-Torp match of CVD data was excellent except for liquid dropout, which was overestimated by several volume-percent. An automatic regression routine was not used, and manual adjustments were made based on previous experience with matching condensate fluid behavior.

Coats improved the liquid dropout match at the expense of a poorer C_7+ description (molecular weight and mole fraction). The adjustment of EOS constants for methane is probably responsible for better gas densities (Z-factors). Unfortunately they infer a substance with properties similar to argon; this alteration is not entirely satisfactory.

We started the present analysis using Coats final three-pseudocomponent C_7+ characterization but retain methane as a pure compoent. Equivalent critical properties were calculated as suggested by Whitson.

The error function used in this study was the average of absolute deviation of dew-point pressure and root-mean-square of all other CVD data, The regression routine is a simplex algorithm for minimization (Nelder and Mead).

Regression variables included critical temperature, critical pressure and acentric factor for all three C_7+ pseudocomponents. Also, interaction coefficient between methane and the heaviest C_7+ fraction (F13). All ten parameters were not adjusted simultaneously. Instead, repeated minimization was made with groups of three parameters. Table 6 shows the sequence of parameter adjustment. For early runs the methane-F13 interaction coefficients was adjusted to give an exact match of dew-point pressure. For the two final runs these coefficients were included in the optimalization routine as a fourth regression variable. Table 7 gives the complete fluid characterization used by the Peng-Robinson EOS for the "best" match. The choice of three-parameter groups for each regression was made arbitrarily.

Total error reduction during the entire regression sequence (manual and automatic) was more than 2.4 %, resulting in a final error slightly greater than 2.0%. The initial error was undefined because of convergence problems.

This procedure does not guarantee a global minimum will be found. In fact this example shows an interesting feature. If only critical pressure and temperature of the heaviest C_7+ fraction are used as regression variables then the resulting error function is found to have a valley of local minima as shown in Fig. 12. The valley is actually bounded; the 10-% contour encircles the valley only slightly outside the p_c-T_c bounds in Fig. 12. Two test runs show approaches to local minima along the valley (A1 to A5 and B1 to B6). Although local minima have numerical values nearly identical (ca. 2 %), the resulting liquid dropout curve has a distinctly different character at the upper and lower ends of the valley (see Fig. 12). Global minima have been located for other examples we have studied.

Fig. 13 shows results of predicted CVD data using the PR EOS. Note that C_{7+} molecular weights are poorly predicted, similar to Coats results. Vapor compressibility factor is not predicted as well as by Coats. In general, however, the present match is as good or better than matches previously obtained by Whitson and Torp and Coats.

CONCLUSIONS

Proper characterization of petroleum reservoir fluids, and particularly gas condensates, can be divided into three categories.

1. Chemical analysis, based on chromatography, distillation and mass spectrometry, provides the necessary data to determine composition and properties of pure compounds and petroleum fractions making up reservoir fluids.

2. PVT analysis provides phase behavior data of the reservoir fluid as a whole. These data, including volumetric and vapor-liquid equilibria, can be used directly in engineering calculations or as the basis for matching an equation of state.

3. Prediction of reservoir fluid behavior at conditions other than those measured experimentally is made possible by thermodynamic property correlations. One of the more powerful correlations is the cubic equation of state (EOS). Simulation of complex physical processes such as development of miscibility can be achieved by an EOS due to its consistent behavior in near-critical regions.

Our purpose has been to review these three areas of fluid characterization. Most of our observations are based on experience we have gained by working with gas-condensate fluids from the North Sea. Hopefully some of the measured data we present will be useful for those working with North Sea gas condensates.

In closing, we would like to thank American Petrofina Exploration Company of Norway and Phillips Petroleum Company Norway for support which has allowed us to perform much of the analysis presented in this paper.

REFERENCES

1. Annual Book of ASTM Standards: "Standard Method for Distillation of Crude Petroleum (15-Theoretical Plate Column)," ASTM D 2892 (1979), Part 24, 802-839.
2. Coats, K.H.: "Simulation of Gas-Condensate Reservoir Performance," Paper SPE 10512 presented at the Sixth SPE Symposium on Reservoir Simulation, New Orleans, Jan. 31 - Feb. 3, 1982.
3. Coats, K.H. and Smart, G.T.: "Application of a Regression-Based EOS PVT Program to Laboratory Data," Paper SPE 11197 presented at the 57th Annual Fall Technical Conference and Exhibition, New Orleans, Sept. 27-29, 1982.
4. Hoffman, A.E., Crump, J.S., and Hocott, C.R.: "Equilibrium Constants for a Gas-Condensate System," Trans. AIME (1953) 198, 1-10.
5. Joffe, J., Schroeder, G.M., and Zudkevich, D.: "Vapor-Liquid Equilibria with the Redlich-Kwong Equation of State," AIChE J. (May, 1970),16,3, 496-498.
6. Katz, D.L. and Firoozabadi, A.: "Predicting Phase Behavior of Condensate/Crude-Oil Systems using Methane Interaction Coefficients," J.Pet.Tech. (Nov., 1978), 1649-1655; Trans. AIME, 228.
7. Nelder, J.A. and Mead, R.: "A Simplex Method for Function Minimization," Comp.J. (1965),7, 308-313.
8. Norvik, H.: PVT Program, User's Manual and Documentation, Report Number T4-83, Rogaland Research Institute, Stavanger, Norway.
9. Peng, D.-Y. and Robinson, D.B.: "A New Two-Constant Equation of State," Ind. and Eng. Chem. Fund. (1976),15,1, 59-64.
10. Soave, G.: "Equilibrium Constants from a Modified Redlich-Kwong Equation of State," Chem. Eng. Sci. (1972) 27,6, 1197-1203
11. Standing, M.B.: "A Set of Equations for Computing Equilibrium Ratios of a Crude Oil/Natural Gas System at Pressures Below 1000 psia," J.Pet.Tech. (Sept. 1979) 1193-1195.
12. Whitson, C.H.: "Characterizing Hydrocarbon Plus Fractions," EUR 183, presented at the EUROPEC Conference, London, Oct. 21-24, 1980.
13. Whitson, C.H. and Torp, S.B.: "Evaluating Constant Volume Depletion Data," J.Pet.Tech. (March, 1983) 610-620.
14. Whitson, C.H.: "Effect of Physical Properties Estimation on Equation-of-State Predictions," Paper SPE 11200 presented at the 57th Annual Fall Technical Conference and Exhibition, New Orleans, Sept. 26-29, 1982.

LITERATURE GUIDE TO GAS CONDENSATE FLUID BEHAVIOR

1. Eaton, B.A. and Jacoby, R.H.: "A New Depletion Performance Correlation for Gas-Condensate Reservoir Fluids," J.Pet.Tech. (July, 1965) 852-856 Trans. AIME, 234
2. Eilerts, C.K., et al.: Phase Relations of Gas-Condensate Fluids, Monograph 10, USBM, Washington D.C. (1957).
3. Jacoby, R.H., Koeller, R.C., and Berry, V.J., Jr.: "Effect of Composition and Temperature on Phase Behavior and Depletion Performance of Rich Gas-Condensate Systems," J.Pet.Tech. (July, 1959) 58-63; Trans. AIME, 216, 406-411.
4. Katz, D.L. and Kurata, F.: "Retrograde Condensation," Ind.Eng.Chem. (1940), 32, 817-827.
5. Katz, D.L., et al.: Handbook of Natural Gas Engineering, McGraw Hill Book Co., Inc., New York City (1959).
6. Reid, R.C., Prausnitz, J.M., and Sherwood, T.K.: Properties of Gases and Liquids, 3rd Edition, McGraw Hill Co., Inc., New York City (1977).
7. Standing, M.B.: Volumetric and Phase Behavior of Oil Field Hydrocarbon Systems, Society of Petroleum Engineers, Dallas, 1977.
8. Yarborough, L.: "Application of a Generalized Equation of State to Petroleum Reservoir Fluids," Equations of State in Engineering and Research, Advances in Chemistry Series No. 182, ACS, Washington, D.C. (1979), 385-439.

TABLE 1 - Example Analysis of a Separator-Gas Sample.

ANALYSIS OF NATURAL GAS

Sample arrived	83.04.07	Sample analysed	83.04.14
Field	NSCC/1B	Sampling date	83.03.13
Well No	8	Sampling time	20:37:33 hrs

Sampling conditions:

Sep temperature	146.0	°F	Specific gravity (Operator enter value)	0.6814	
Sep pressure	664.7	PSIG	Oil flow	525.0	BOPD
Choke size		/64 inches	Gas flow	13475	MSCFPD
Flowing density	2.140	LBS/CUFT	H_2S (Drager)	10	ppm
Mass flow	705580	LBS/DAY	CO_2 (Drager):	2.3 volume-%	

PR: 15:30 April 14, 1983

Component	Weight-%	Mole-%	Molecular Weight
nitrogen	0.82	0.59	28.02
carbon dioxide	4.57	2.09	44.01
methane	66.90	83.84	16.04
ethane	11.40	7.63	30.07
propane	6.61	3.01	44.09
iso-butane	1.41	0.49	58.12
normal butane	2.73	0.95	58.12
iso-pentane	1.28	0.36	72.15
normal pentane	1.44	0.40	72.15
hexanes	2.24	0.52	86.17*
heptanes-plus	0.60	0.12	100.20*
total	100.00	100.00	20.11**

$$y_i = w_i \cdot \frac{\overline{M}}{M_i}$$

where

y_i = mole-%

w_i = weight-%

M_i = molecular weight

$\overline{M}$ = average molecular weight

$= 100 / (\Sigma w_i/M_i)$

$= (\Sigma y_i \cdot M_i) / 100$

* Assumed

** Specific Gravity = 0.6942 (air=1).

Analysed by

TABLE 2 - Example Analysis of a Separator-Oil Sample.

ANALYSIS OF PRESSURED OIL

Sample arrived	83.04.07	Sample analysed	83.04.22
Field	NSGC/1B	Sampling date	83.03.13
Well No	8	Sampling time	20:38:01 hrs

Sampling conditions:

Sep. temperature	157.6	°F	Specific gravity (Operator enter value)	0.6954	
Sep. pressure	707.2	PSI	Oil flow	525.0	BOPD
Choke size		/64 inches	Gas flow	13475	MSCFPD
Flowing density	226.6	LB/BBL	Water flow		BBL/D
Mass flow	232440	LBS/DAY			

PR: 13:31 April 22, 1983

Component	Weight-%	Mole-%	Molecular Weight
nitrogen	0.01	0.04	28.02
carbon dioxide	0.27	0.63	44.01
methane	2.12	13.37	16.04
ethane	1.36	4.56	30.07
propane	1.99	4.57	44.09
iso-butane	0.86	1.49	58.12
normal butane	2.39	4.16	58.12
iso-pentane	1.82	2.55	72.15
normal pentane	2.40	3.36	72.15
hexanes	8.78	10.30	86.17*
heptanes-plus	78.00	54.97	143.4 **
total	100.00	100.00	101.07

$$y_i = w_i \cdot \frac{\overline{M}}{M_i}$$

where

y_i = mole-%

w_i = weight-%

M_i = molecular weight

$\overline{M}$ = average molecular weight

$= 100 / (\Sigma w_i/M_i)$

$= (\Sigma y_i \cdot M_i) / 100$

* Assumed

** Heptanes-plus Specific Gravity = 0.7802 (water=1)

Analysis of C7+:

Real spesific gravity 60/60F	0.7747	
Average mol. wt.	143.4	
Sulfur content	0.03	wt%

Analysis of non-pressurized oilsample:

BS&W < 0.06 wt%. Salt < 0.00011 wt%

Analysed by

TABLE 3 - Results of Recombination and Consistency Check for Separator-Gas and Oil Samples.

Sample Description .... : Field NSGC/1B, Well 8 (83.03.13)
Separator Pressure (psia) .... : 700.6
Separator Temperature (°F) .... : 151.8
Separator Gas-Oil Ratio (scf/STB) ... : 25670

Component	Compositions (mole-%) x	y	z	Hoffman-Crump-Hocott Analysis F	K (=y/x)	Kp	b (~·°R)	T_b (°R)
nitrogen	0.04	0.59	0.57	3.544	14.75	10330.	470.0	109.0
carbon dioxide	0.63	2.09	2.04	2.295	3.317	2324.	652.0	194.0
methane	13.37	83.84	81.48	2.701	6.272	4394.	300.0	94.0
ethane	4.56	7.63	7.53	1.907	1.673	1172.	1145.0	303.0
propane	4.57	3.01	3.06	1.384	0.659	461.5	1799.0	416.0
iso-butane	1.49	0.49	0.52	0.995	0.329	230.4	2037.0	471.0
normal butane	4.16	0.95	1.06	0.866	0.228	160.0	2153.0	491.0
iso-pentane	2.55	0.36	0.43	0.498	0.141	98.91	2368.0	542.0
normal pentane	3.36	0.40	0.50	0.399	0.119	83.41	2480.0	557.0
hexanes	10.30	0.52	0.85	0.013	0.050	35.37	2780.0	616.0
heptanes-plus	54.97	0.12	1.96	-	0.00218	1.53	*	*
	100.00	100.00	100.00					

C_{7+} Sp. Gravity :	0.7802	-	0.7789
C_{7+} Mol. Weight :	143.4	100.2	142.0
C_{7+} Watson K_w :	11.95	-	11.95
Tot. Mol. Weight :	101.1	20.11	22.84

Summary of Results From Same Well During First Flow Test (81.05.21)

Separator Pressure (psia) .... : 1099.9
Separator Temperature (°F) .... : 193.7
Separator Gas-Oil Ratio (scf/STB) ... : 9929

C_{7+} Sp. Gravity :	0.7911	-	0.7898
C_{7+} Mol. Weight :	162.7	100.2	161.1
C_{7+} Watson K_w :	12.04	-	12.04
Tot. Mol. Weight :	102.6	19.40	26.1

* b and T_b are not readily defined for C_{7+} fractions. T_b can be approximated by the relation, $T_b = (K_w \cdot \gamma)^3$, where γ is the C_{7+} specific gravity of the wellstream fluid. The value of b can be back-calculated, where $F(C_{7+})$ is read from the log Kp vs F straight line, extrapolated to the measured Kp value.

TABLE 4a - Heptanes-Plus Characterization Based on Molecular Weight and Specific Gravity Measurements: Field NSGC/1A.

Well No.	Date Tested	Measured Molecular Weight	Measured Specific Gravity	K_w	Calculated Molecular Weight (K_w=12.02)
NSGC/1A-16	81.02.14	154.3	0.7872	11.99	156.9
	81.07.24	161.8	0.7907	12.03	160.8
	81.10.01	150.3	0.7810	12.02	150.2
	82.01.09	150.9	0.7830	12.00	152.3
	82.02.04	155.9	0.7875	12.00	157.2
	82.05.08	148.5	0.7815	11.99	150.7
	82.06.19	151.2	0.7809	12.03	150.0
	82.07.07	155.2	0.7843	12.04	153.7
	83.01.09	150.1	0.7798	12.04	148.9
NSGC/1A-3	81.02.13	164.9	0.7947	12.01	165.4
	81.04.03	166.7	0.7950	12.03	165.8
	81.06.28	164.1	0.7928	12.03	163.2
	81.08.28	165.9	0.7942	12.03	164.8
	81.10.06	163.8	0.7936	12.02	164.2
	81.12.04	162.4	0.7917	12.02	162.0
	82.01.09	161.5	0.7935	11.99	164.0
	82.04.01	160.0	0.7905	12.01	160.6
	82.06.15	161.2	0.7902	12.03	160.3
NSGC/1A-19	81.02.16	159.6	0.7909	12.00	161.1
	81.04.09	160.9	0.7907	12.02	160.8
	81.07.22	162.9	0.7913	12.04	161.5
	81.08.31	155.5	0.7879	11.99	157.7
	81.09.30	159.9	0.7878	12.05	157.6
	81.12.05	154.4	0.7858	12.01	155.4
	82.01.10	154.8	0.7848	12.03	154.3
	82.04.08	152.9	0.7826	12.01	151.9
	82.07.07	150.1	0.7813	12.02	150.5
	82.10.06	150.6	0.7813	12.02	150.5
	83.01.07	149.0	0.7792	12.03	148.2
NSGC/1A-20	81.04.09	165.3	0.7958	12.00	166.7
	82.05.01	170.9	0.7986	12.03	170.0
	82.08.08	164.5	0.7936	12.02	164.2
	82.11.04	163.0	0.7935	12.01	164.0
	83.02.21	169.9	0.7990	12.01	170.5

TABLE 4a - continued

Well No.	Date Tested	Measured Molecular Weight	Measured Specific Gravity	K_w	Calculated Molecular Weight (K_w=12.02)
NSGC/1A-13	81.06.28	170.2	0.7970	12.04	168.1
	81.08.30	172.7	0.7976	12.06	168.8
	82.02.04	163.4	0.7935	12.01	164.0
	82.06.17	164.3	0.7920	12.04	162.3
	82.09.02	161.1	0.7908	2.02	161.0
NSGC/1A-10	81.07.14	159.0	0.7881	12.03	157.9
	81.08.30	152.6	0.7861	11.98	155.7
	81.11.11	150.3	0.7904	11.98	160.5
	81.12.04	153.7	0.7849	12.01	154.4
	82.06.16	151.9	0.7821	12.03	151.3
	82.09.03	149.8	0.7813	12.01	150.5
	82.12.03	148.4	0.7801	12.01	149.2
NSGC/1A-15	81.06.30	163.0	0.7896	12.06	159.6
	82.03.04	155.0	0.7846	12.03	154.0
	82.05.10	150.9	0.7822	12.01	151.4
	82.06.17	154.2	0.7835	12.03	152.8
	82.09.02	153.6	0.7823	12.04	151.5
NSGC/1A-1	81.08.31	172.5	0.7999	12.03	171.6
	81.11.10	167.8	0.7948	12.04	165.5
	82.02.01	164.2	0.7939	12.02	164.5
	82.05.02	158.8	0.7919	11.98	162.2
	83.02.21	171.6	0.7992	12.03	170.7
NSGC/1A-4	81.08.29	165.3	0.7918	12.06	162.1
	81.11.06	164.4	0.7929	12.03	163.4
	82.05.04	158.3	0.7873	12.03	157.0
	82.11.02	157.6	0.7869	12.03	156.6

TABLE 4b - Heptanes-Plus Characterization Based on Molecular Weight and Specific Gravity Measurements: Field NSGC/1B.

Well No.	Date Tested	Measured		K_w	Calculated Molecular Weight (K_w=12.02)
		Molecular Weight	Specific Gravity		
NSGC/1B-16	81.03.11	172.3	0.7989	12.04	170.4
	81.05.12	166.8	0.7967	12.01	167.8
	82.02.14	151.0	0.7834	12.00	152.7
	82.07.13	149.2	0.7793	12.03	148.3
	82.09.14	148.9	0.7793	12.03	148.3
	82.11.04	146.4	0.7774	12.02	146.4
	83.02.04	143.7	0.7765	12.00	145.4
NSGC/1B-20	81.03.11	174.9	0.8001	12.05	171.8
	81.05.11	172.2	0.7991	12.04	170.6
	81.10.07	166.7	0.7953	12.03	166.1
	82.02.04	161.2	0.7925	12.00	162.9
	82.05.21	159.5	0.7903	12.01	160.4
	82.07.16	159.7	0.7904	12.01	160.5
	82.12.09	155.6	0.7875	12.00	157.2
NSGC/1B-9	81.03.11	177.7	0.8031	12.04	175.4
	81.05.10	168.4	0.7955	12.04	166.4
	82.04.10	151.5	0.7827	12.01	152.0
	82.05.16	151.5	0.7824	12.02	151.6
	82.06.17	152.9	0.7826	12.03	151.9
	83.02.13	153.0	0.7855	12.00	155.0
NSGC/1B-6	81.03.31	181.4	0.8040	12.07	176.5
	81.10.08	166.6	0.7960	12.02	166.9
	81.11.29	163.2	0.7930	12.02	163.5
	82.05.16	157.0	0.7873	12.02	157.0
	82.07.13	154.7	0.7845	12.03	153.9
	82.09.13	153.5	0.7839	12.02	153.3
	82.11.03	150.1	0.7835	11.99	152.8
	83.02.03	148.2	0.7813	11.99	150.5
NSGC/1B-3	81.04.01	181.6	0.8058	12.05	178.7
	81.06.14	174.0	0.8000	12.04	171.7
	82.01.23	164.3	0.7963	11.99	167.3
	82.05.15	159.8	0.7898	12.02	159.8
	82.08.12	165.3	0.7935	12.03	164.0
	82.10.10	160.5	0.7900	12.03	160.0
	82.12.09	158.3	0.7896	12.01	159.6
	83.01.09	169.3	0.7975	12.03	168.7

TABLE 4b - continued

Well No.	Date Tested	Measured		K_w	Calculated Molecular Weight (K_w=12.02)
		Molecular Weight	Specific Gravity		
NSGC/1B-18	81.04.01	174.2	0.7995	12.05	171.1
	81.06.10	170.0	0.7976	12.03	168.8
	82.01.23	155.9	0.7873	12.01	157.0
	82.05.19	154.0	0.7851	12.01	154.6
	82.08.09	151.3	0.7821	12.02	151.3
	82.10.07	149.0	0.7804	12.01	149.5
	83.01.06	148.5	0.7785	12.03	147.5
NSGC/1B-8	81.06.14	162.4	0.7904	12.04	160.5
	81.10.08	158.3	0.7877	12.03	157.5
	82.01.23	150.8	0.7833	12.00	152.6
	82.02.14	147.8	0.7804	12.00	149.5
	82.04.11	149.4	0.7804	12.02	149.5
	82.06.19	146.9	0.7780	12.02	147.0
	82.09.14	145.1	0.7765	12.02	145.4
	82.11.04	145.0	0.7755	12.03	144.4
NSGC/1B-5	81.08.30	164.0	0.7936	12.02	164.2
	81.11.28	152.2	0.7838	12.01	153.2
	82.04.09	150.4	0.7817	12.01	150.9
	82.05.21	158.0	0.7898	12.00	159.8
	82.06.18	154.7	0.7864	12.00	156.0
	82.08.07	154.0	0.7858	12.00	155.4
	82.10.05	156.0	0.7881	12.00	157.9
	83.01.01	155.5	0.7878	12.00	157.6

TABLE 4c - Heptanes-Plus Characterization Based on Molecular Weight and Specific Gravity Measurements: Field NSGC/2.

Well No.	Date Tested	Measured Molecular Weight	Measured Specific Gravity	K_w	Calculated Molecular Weight (K_w=11.99)
NSGC/2-5	81.04.22	143.6	0.7774	11.99	143.9
	81.09.24	142.2	0.7763	11.98	142.8
	82.06.22	139.4	0.7720	12.00	138.5
	83.02.18	134.1	0.7683	11.98	134.8
NSGC/2-9	81.03.14	150.6	0.7840	11.99	150.9
	82.01.09	139.1	0.7719	12.00	138.4
	82.02.10	137.0	0.7730	11.96	139.5
	82.07.18	138.7	0.7718	12.00	138.3
	82.12.23	134.1	0.7678	11.99	134.3
NSGC/2-8	81.03.13	148.3	0.7817	11.99	148.4
	81.09.24	141.6	0.7760	11.98	142.5
	82.12.23	134.4	0.7685	11.98	135.0
NSGC/2-1	81.03.13	151.6	0.7848	11.99	151.7
	81.09.26	142.7	0.7756	12.00	142.1
	82.03.21	138.8	0.7721	11.99	135.0
NSGC/2-4	81.04.21	144.9	0.7783	11.99	144.9
	82.01.10	140.4	0.7740	11.99	140.5
	82.02.12	139.4	0.7740	11.98	140.5
	82.05.16	139.6	0.7733	11.99	139.8
	82.07.18	138.7	0.7718	11.99	138.3
	82.12.23	134.1	0.7678	11.99	134.3
NSGC/2-3	81.04.22	145.1	0.7771	12.01	143.6
	82.01.08	137.4	0.7722	11.97	138.7
	82.02.11	137.3	0.7714	11.98	137.9
	83.02.17	133.5	0.7670	11.99	133.5

TABLE 4d - Heptanes-Plus Characterization Based on Molecular Weight and Specific Gravity Measurements: Field NSBO/3B.

Well No.	Date Tested	Measured Molecular Weight	Measured Specific Gravity	K_w	Calculated Molecular Weight (K_w=11.90)
NSBO/3B-1	81.10.25	217.7	0.8446	11.90	217.4
	81.12.17	229.8	0.8535	11.89	230.5
	82.04.19	228.9	0.8532	11.89	230.0
NSBO/3B-14	81.02.13	245.5	0.8621	11.90	243.7
	81.09.13	247.8	0.8646	11.90	247.7
	81.10.08	245.7	0.8637	11.90	246.2
	82.03.24	245.9	0.8636	11.90	246.1
	82.10.04	244.3	0.8637	11.89	246.2
	82.12.02	246.7	0.8634	11.91	245.8
NSBO/3B-19	81.02.13	251.0	0.8669	11.90	251.4
	82.02.09	251.6	0.8672	11.90	251.9
	82.06.16	255.7	0.8670	11.93	251.5
	83.02.08	250.9	0.8658	11.91	249.6
NSBO/3B-11	81.06.14	228.0	0.8530	11.89	229.7
	81.12.08	222.2	0.8502	11.87	225.6
	82.04.19	223.7	0.8506	11.88	226.1
NSBO/3B-10	81.06.08	257.9	0.8711	11.90	258.2
	82.08.07	256.6	0.8704	11.90	257.1
	83.02.05	252.8	0.8702	11.87	256.8
NSBO/3B-18	81.06.11	242.7	0.8607	11.91	241.5
	82.03.16	241.3	0.8605	11.90	241.2
	82.06.12	240.5	0.8610	11.89	242.0
	83.03.09	244.0	0.8618	11.91	243.2
NSBO/3B-6	81.10.08	223.9	0.8490	11.90	223.8
	82.02.12	219.6	0.8482	11.88	222.6
	82.06.14	223.7	0.8486	11.90	223.2
	82.08.08	219.6	0.8468	11.89	220.6
	82.10.04	219.7	0.8474	11.89	221.4
	82.10.04	219.0	0.8470	11.88	220.9
NSBO/3B-9	82.03.18	241.6	0.8596	11.91	239.8
	82.08.08	242.2	0.8610	11.90	242.0
NSBO/3B-7	82.04.22	244.1	0.8628	11.89	244.8
	82.10.24	245.8	0.8654	11.89	249.0
	82.12.07	242.6	0.8613	11.90	242.5

TABLE 6 - Minimization Procedure for Matching CVD Data with the Peng-Robinson Equation of State.

Run No.	Adjusted Parameter (C_7+ Fraction)	Initial Value	Final Value	Data Matched	Error Reduction
1	δ (C_1-F3)	0.2	0.3368	p_d	undefined
2	T_c (F1)	976.1	1018.0	CVD	undefined
	T_c (F2)	1168.0	1261.0		
	T_c (F3)	1408.0	1395.0		
3	δ (C_1-F3)	0.3368	0.3380	p_d	0.6
4	p_c (F1)	419.8	429.0	CVD	0.6
	p_c (F2)	268.9	260.2		
	p_c (F3)	148.5	151.7		
5	δ (C_1-F3)	0.3380	0.3385	p_d	-0.4
6	ω (F1)	0.5844	0.6040	CVD	0.1
	ω (F2)	0.6801	0.6800		
	ω (F3)	0.8042	0.8030		
7	δ (C_1-F3)	0.3385	0.3388	p_d	-0.3
8	T_c (F3)	1395.0	1320.0	CVD and p_d	1.8
	p_c (F2)	260.2	303.1		
	ω (F1)	0.6040	0.4887		
	δ (C_1-F3)	0.3388	0.3840		
9	T_c (F1)	1018.0	1010.0	CVD and p_d	0.2
	p_c (F2)	303.1	302.3		
	ω (F3)	0.8027	0.8040		
	δ (C_1-F3)	0.3840	0.3840		

Notes:

- δ (C_1-F3) = binary interaction parameter between methane and the heaviest C_7+ fraction, F3.
- p_d = dew-point pressure
- Undefined error reductions result from convergence problems with Run 1.
- Critical temperature, T_c, and critical pressure, p_c, have units °R and psia, resepectively; acentric factor, ω, is dimensionless.
- The error function after Run 2 was 4.8 %. The final error function after Run 9 was 2.2 %. The error function is the average of the absolute deviation in saturation pressure and the root mean square of errors for CVD data.

TABLE 7 - Final "best-fit" Properties used in the Peng-Robinson EOS to Predict Constant-Volume Depletion Data from Field NSGC/1B.

Component	z (%)	M (g/mol)	T_c (°R)	p_c (psia)	ω	γ (water=1)
1 - carbon dioxide	2.37	44.010	547.57	1071.0	0.2250	
2 - nitrogen	0.31	28.013	227.27	493.0	0.0400	
3 - methane	73.19	16.043	343.04	667.8	0.0104	
4 - ethane	7.80	30.070	549.76	707.8	0.0986	
5 - propane	3.55	44.097	665.68	616.3	0.1524	
6 - iso-butane	0.71	58.124	734.65	529.1	0.1848	
7 - normal butane	1.45	58.124	765.32	550.7	0.2010	
8 - iso-pentane	0.64	72.151	828.77	490.4	0.2223	
9 - normal pentane	0.68	72.151	845.37	488.6	0.2539	
10 - hexanes	1.09	84.000	931.97	483.0	0.2500	0.690
11 - fraction 1	4.04	125.3	1010.37b	429.0b	0.4887b	0.758
12 - fraction 2	3.44	213.2	1261.27b	302.3b	0.6804b	0.825
13 - fraction 3	0.73	370.1	1319.87b	151.7b	0.8040b	0.907

Binary Interaction Coefficients[a]

	1	2	3	4	5	6	7	8	9	10	11	12	13
1		-.200	.100	.130	.135	.130	.130	.125	.125	.125	.110	.110	.110
2			.036	.050	.080	.095	.090	.095	.100	.100	.100	.100	.100
3											.039	.049	.384[b]

a. Equal to zero except where specified otherwise.
b. Adjusted during regression.

Table 5 - Carbon-Number Distillation (ASTM D 2892-78) Results for a Mixture of Numerous Heptanes-Plus Fractions Sampled from North Sea Gas-Condensate and Black-Oil Reservoirs.

Initial Weighed Amount of C_7+ Material ...... : 2073.1 g
Reflux Ratio .... : 5 to 1
Reflux Cycle .... : 18 seconds

Distillation at Atmospheric (Normal) Pressure : 94 to 175 °C
Distillation at 100 mm Hg .... : 175 to 244 °C
Distillation at 10 mm Hg .... : 244 to 345 °C

Carbon No.	Normal Boiling-Point Range (°C)	Normal Boiling Point (°C)	Weight (g)	Density (g/cc)	Molecular Weight (g/mol)	Volume (cc)	Moles (mol)	Cumulative Volume (%)	Cumulative Weight (%)	Moles (%)
7	69 - 98[a]	90	90.2[b]	0.7276	96	124.1	0.940	4.83	4.35	8.05
8	98 - 126	113	214.6	0.7452	110	288.0	1.951	16.03	14.70	16.70
9	126 - 151	139	225.3	0.7651	122	294.5	1.847	27.49	25.57	15.81
10	151 - 175	163	199.3	0.7704	137	258.7	1.455	37.56	35.18	12.46
11	175 - 194	184	128.8	0.7823	151	164.6	0.853	43.96	41.40	7.30
12	194 - 216	205	136.8	0.7902	161	173.1	0.850	50.70	48.00	7.28
13	216 - 235	226	123.8	0.8040	181	154.0	0.684	56.69	53.97	5.86
14	235 - 256	246	120.5	0.8214	193	146.7	0.624	62.40	59.78	5.34
15	256 - 273	265	101.6	0.8229	212	123.5	0.479	67.20	64.68	4.10
16	273 - 288	281	74.1	0.8271	230	89.6	0.322	70.69	68.26	2.76
17	288 - 304	296	76.8	0.8283	245	92.7	0.313	74.29	71.96	2.68
18	304 - 318	311	58.2	0.8370	259	69.5	0.225	77.00	74.77	1.93
19	318 - 332	325	50.2	0.8458	266	59.4	0.189	79.31	77.19	1.62
20	332 - 345	339	45.3	0.8528	280	53.1	0.162	81.37	79.37	1.39
21+	345 -		427.6	0.8933[c]	545[c]	478.7	0.785	100.00	100.00	6.72
Total/Average			2073.1	0.8066	177	2570.2	11.679			100.00

a. Most likely some of the C_7 cut was lost during distillation of C_5 to C_6 fractions and the period of storage during which samples were analyzed (ca. 2 years).
b. Distillation loss was 5.0 grams (0.3 %); this weight was added to the C_7 cut.
c. Not measured, but back-calculated from measured C_7+ properties.

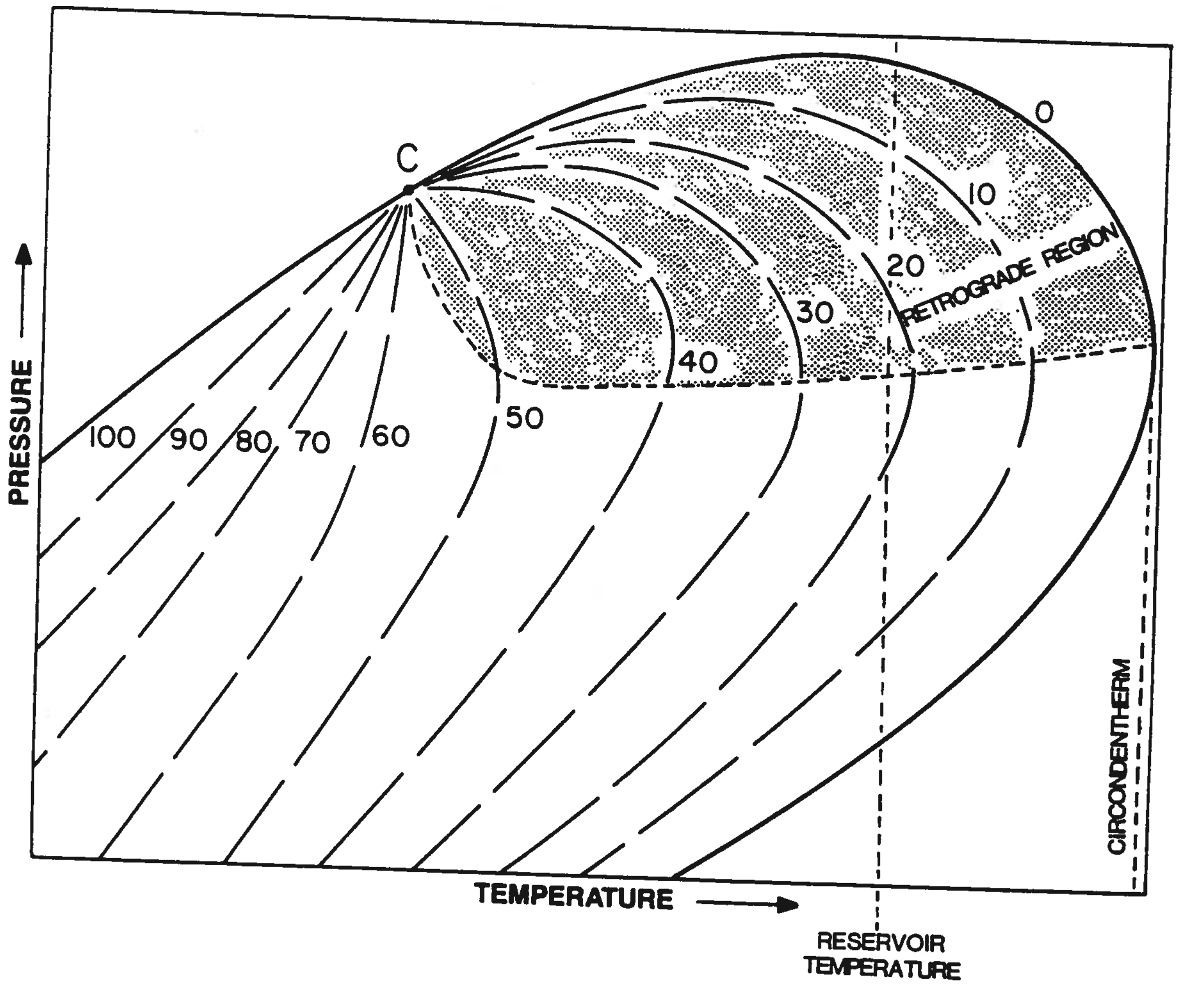

Fig. 1 - Hypothetical pressure-temperature phase diagram showing the isothermal retrograde region for a gas condensate.

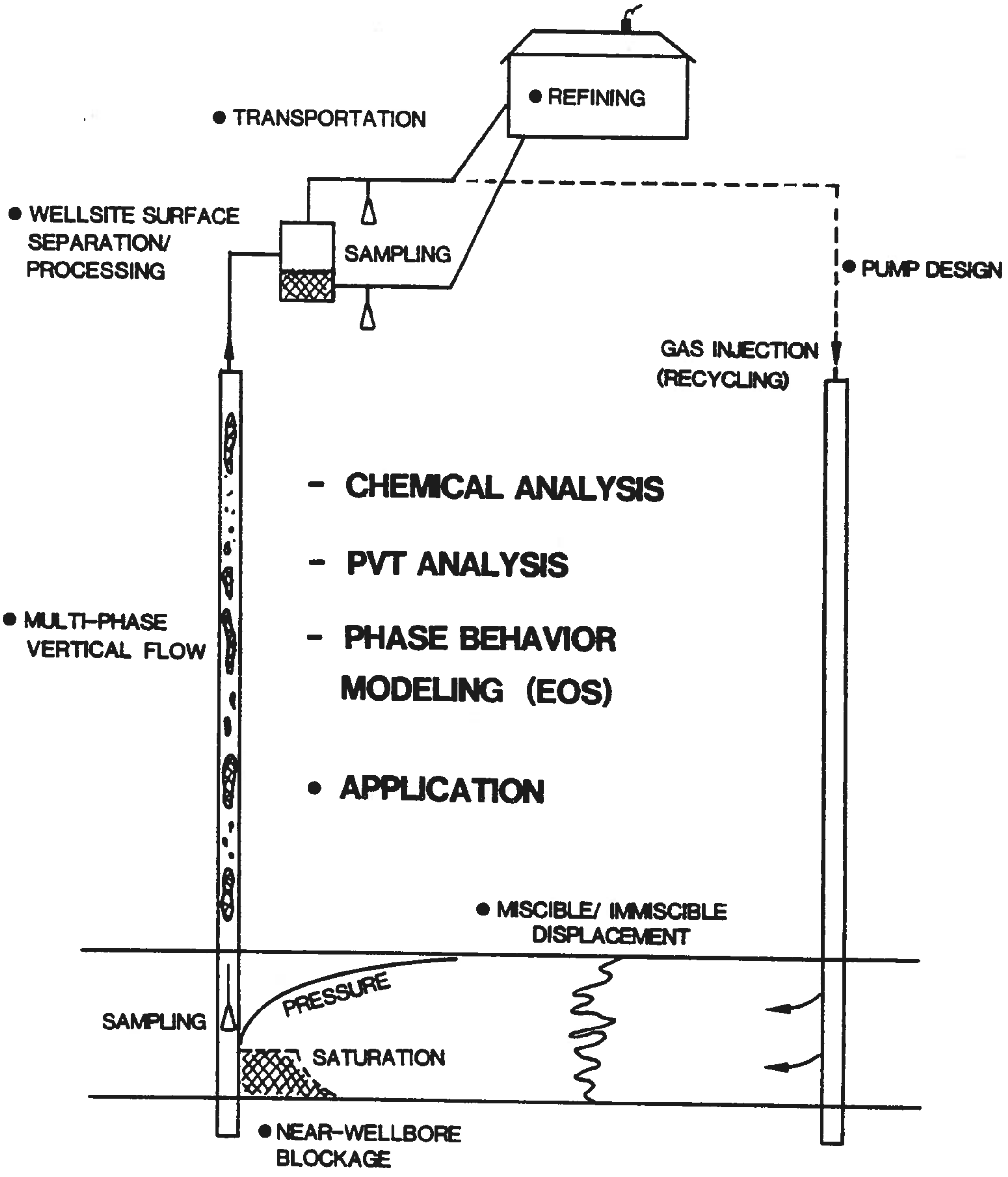

Fig. 2 - Schematic illustrating processes which are highly dependent on proper fluid characterization of gas condensate fluids.

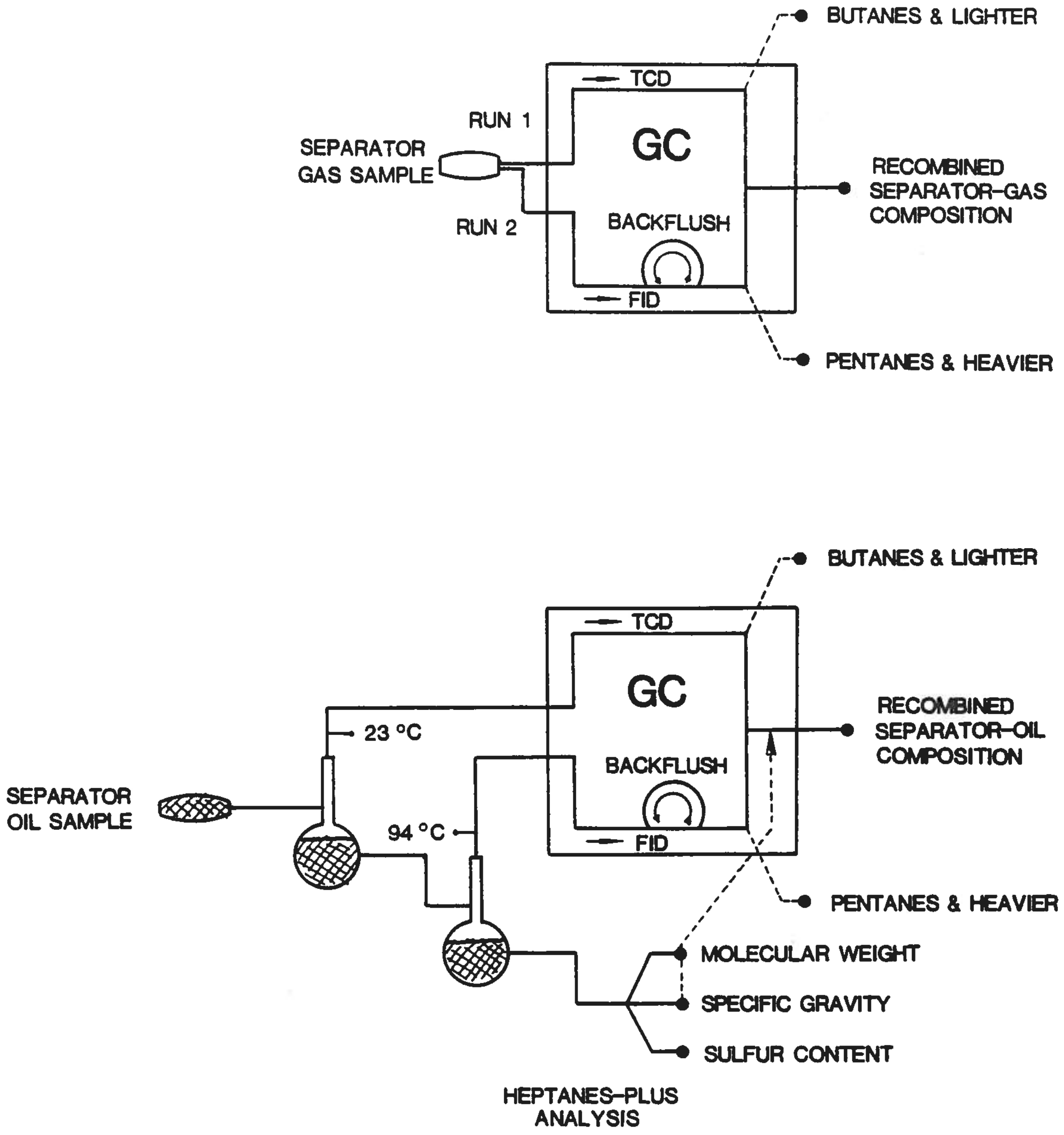

Fig. 3 - Schematic of separator-gas and separator-oil analyses using programmed gas chromatography, low-temperature distillation, and heptanes-plus characterization.

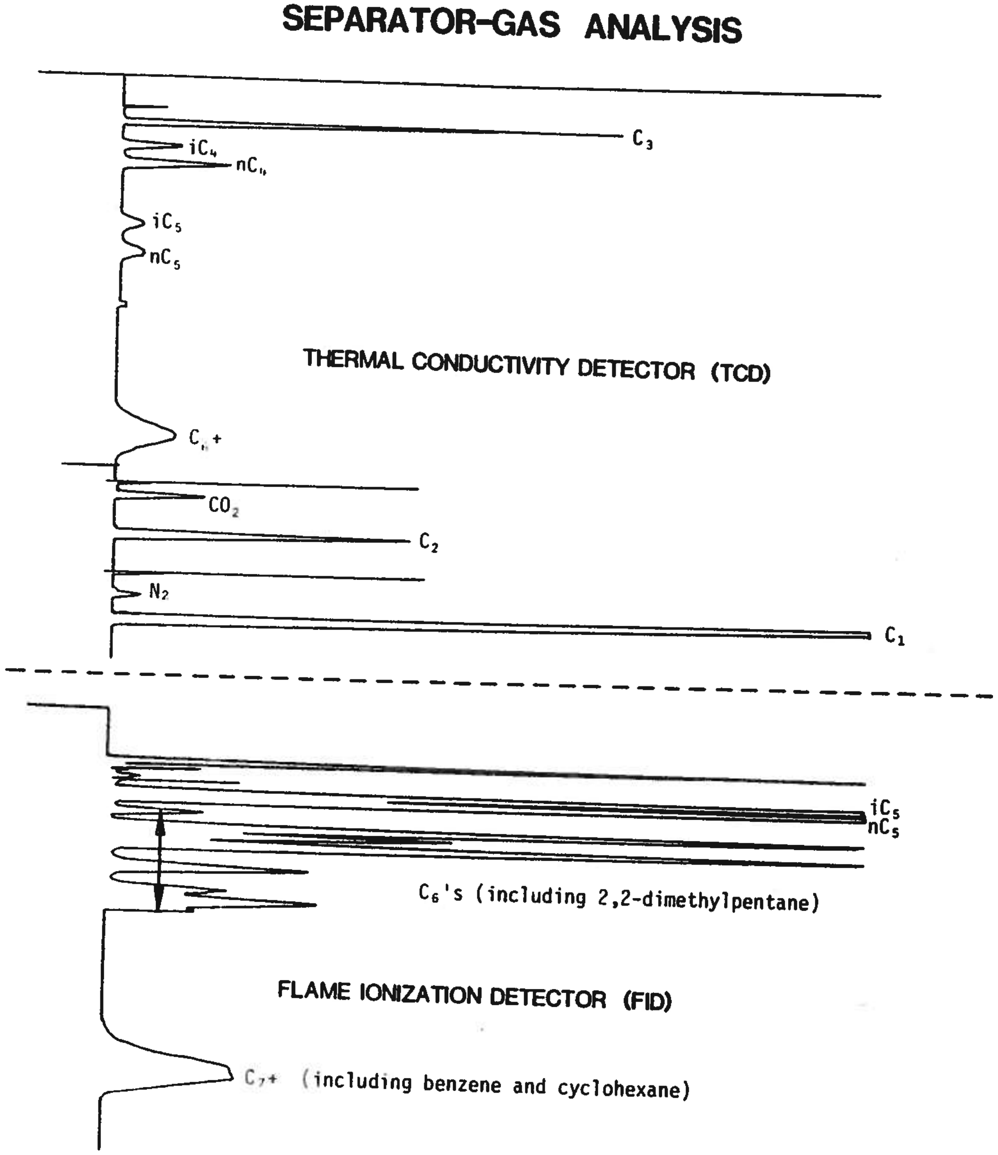

Fig. 4 - Two gas chromatograph runs (TCD and FID) used to analyze separator gas from Well 8, Field NSGC/1B, tested 83.03.13.

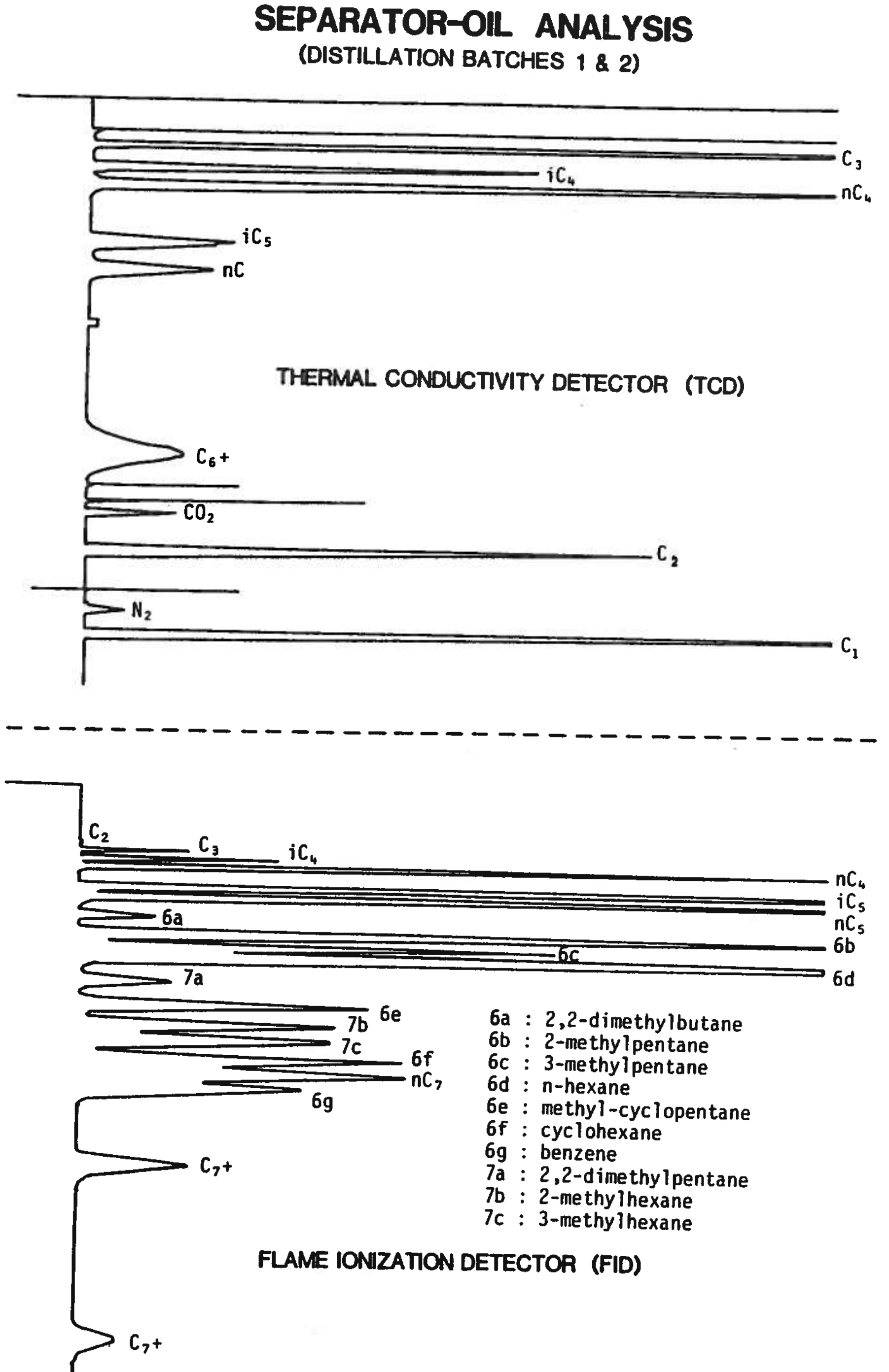

Fig. 5 - Two gas chromatograph runs (TCD and FID) used to analyze distillation batches 1 and 2 (respectively) from separator oil from Well 8, Field NSGC/1B, tested 83.03.13

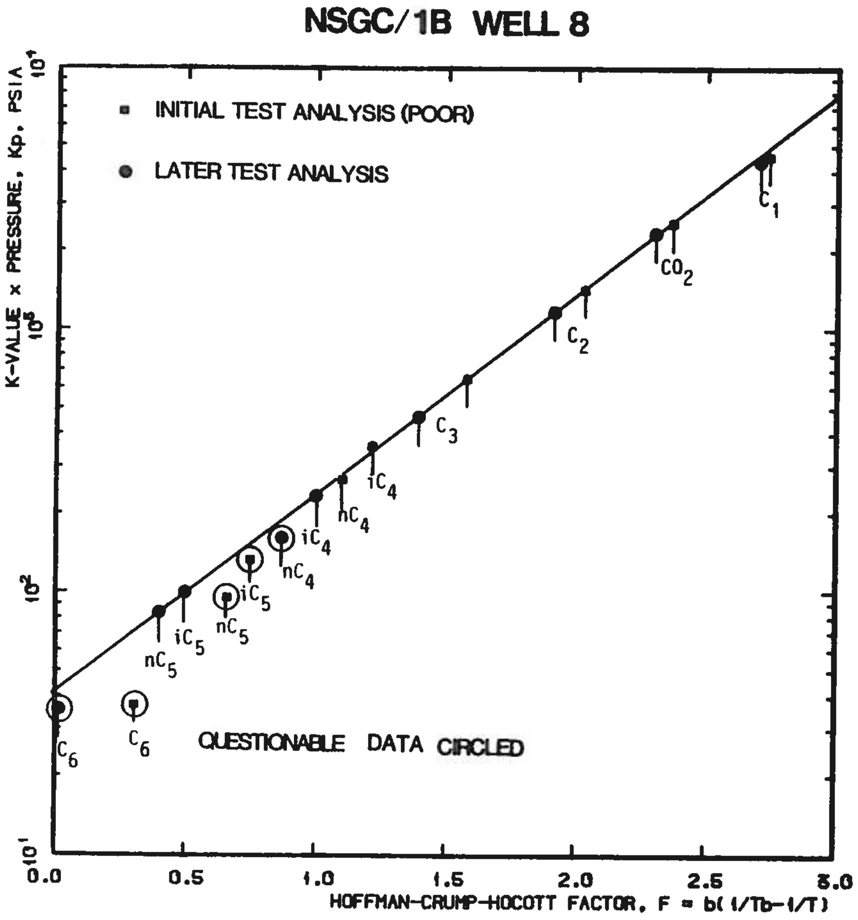

Fig. 6 - Illustration of how the Hoffman-Crump-Hocott method can be used to isolate possible errors in separator-fluid analysis due to sample-container leakage, inaccurate analysis or lack of equilibrium during sampling.

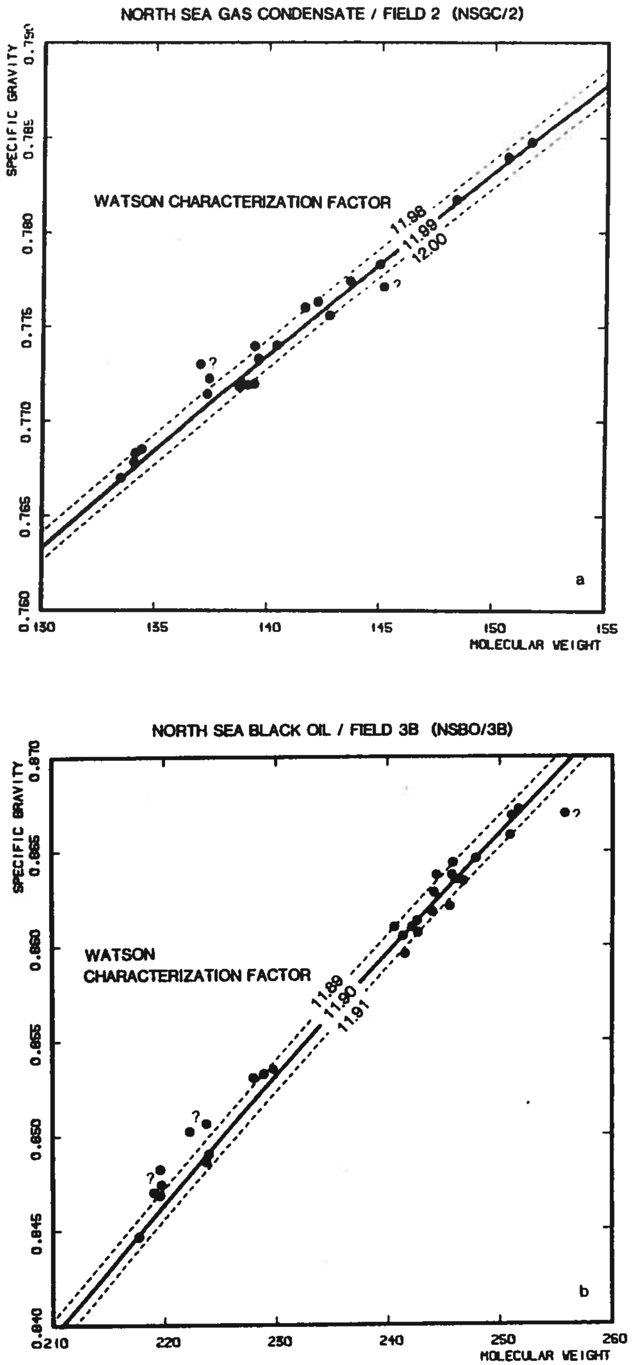

Fig. 7 - Heptanes-plus characterization based on measured molecular weight and specific gravity using the Watson characterization factor.

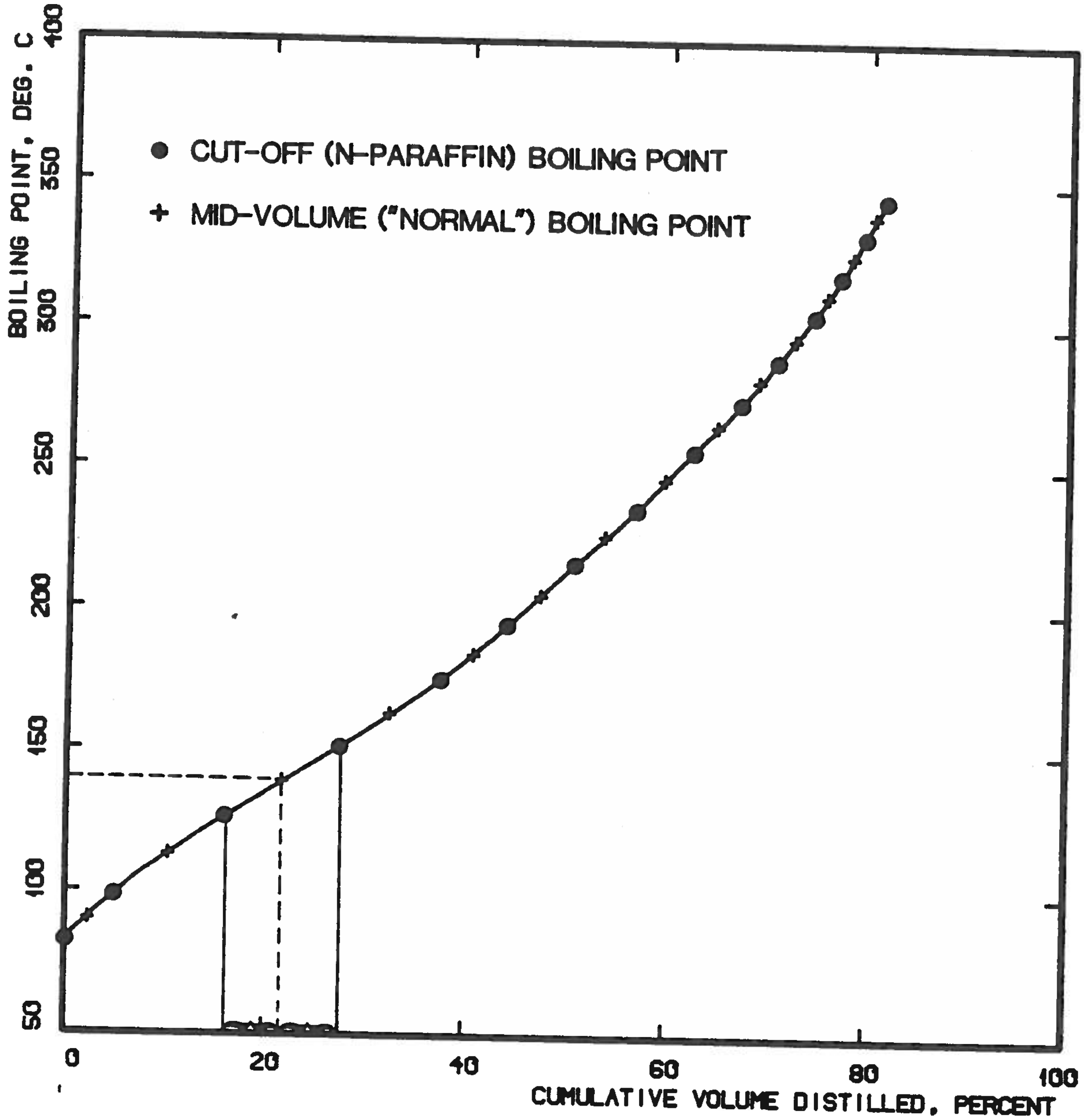

Fig. 8 - Carbon-number distillation (ASTM D 2892-78) boiling point curve for a blend of heptanes-plus fractions from gas-condensate and black-oil reservoirs in the North Sea.

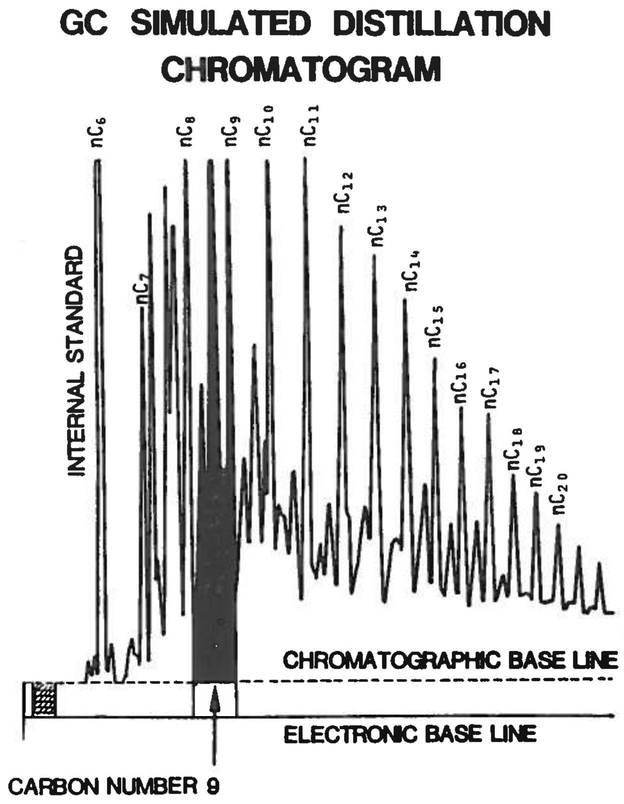

Fig. 9 - Simulated distillation gas chromatogram for a blend of heptanes-plus fractions from gas-condensate and black-oil reservoirs in the North Sea.

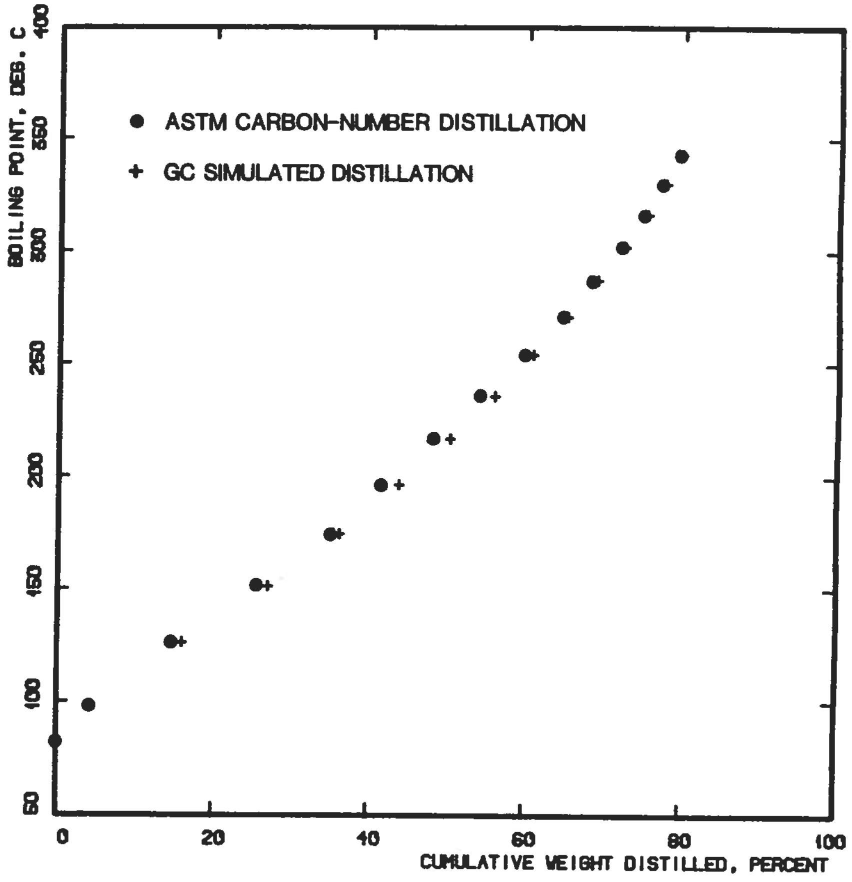

Fig. 10 - Comparison of ASTM carbon-number and GC-simulated boiling point curves (on weight-percent basis) for a blend of heptanes-plus fractions from gas-condensate and black-oil reservoirs in the North Sea.

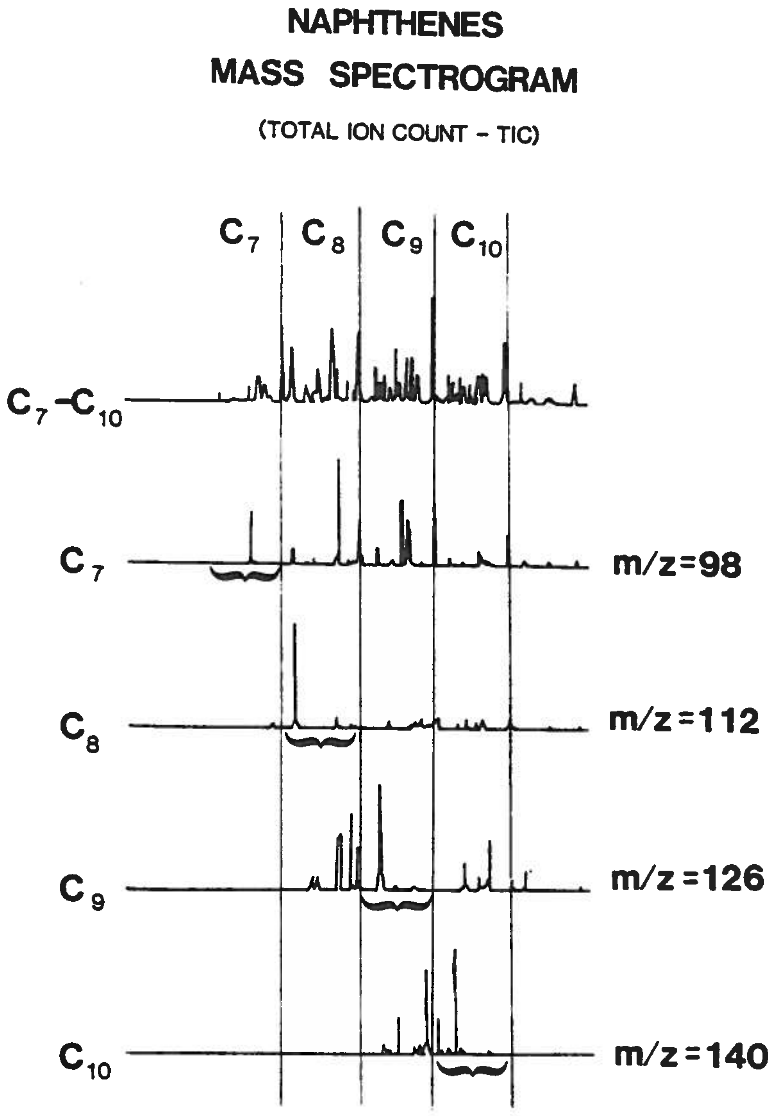

Fig. 11 - Example of GC-based mass spectrography used to isolate and quantify the content of a particular hydrocarbon family (naphthenes) in carbon-number distillation fractions up to C_{10}; analogous spectrograms can be made for paraffin and aromatic hydrocarbon families.

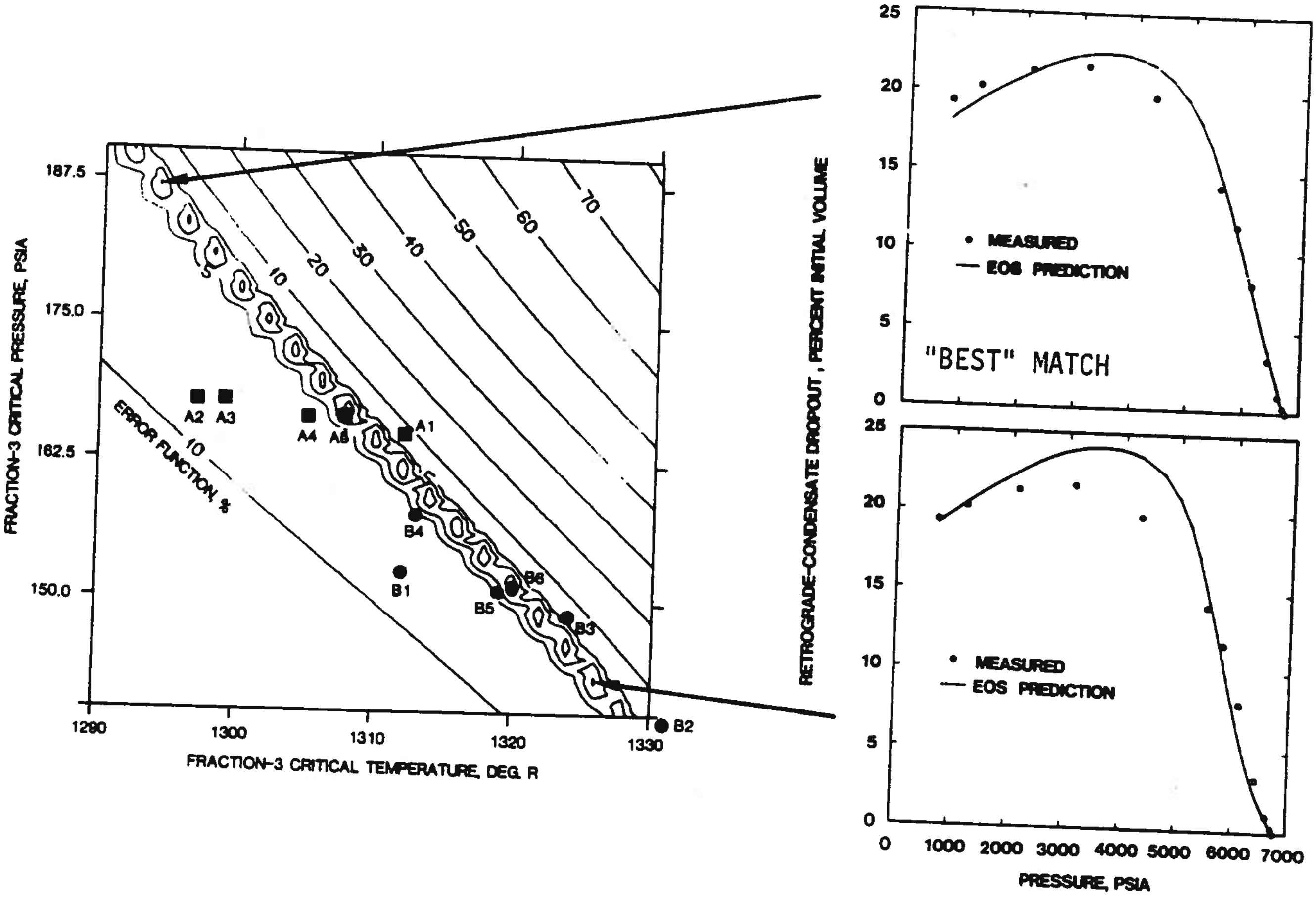

Fig. 12 - Results of Peng-Robinson EOS match for constant-volume depletion data from Field NSGC/1B illustrating two retrograde-condensation dropout curves for EOS predictions with the same overall error function (approximately 2 percent).

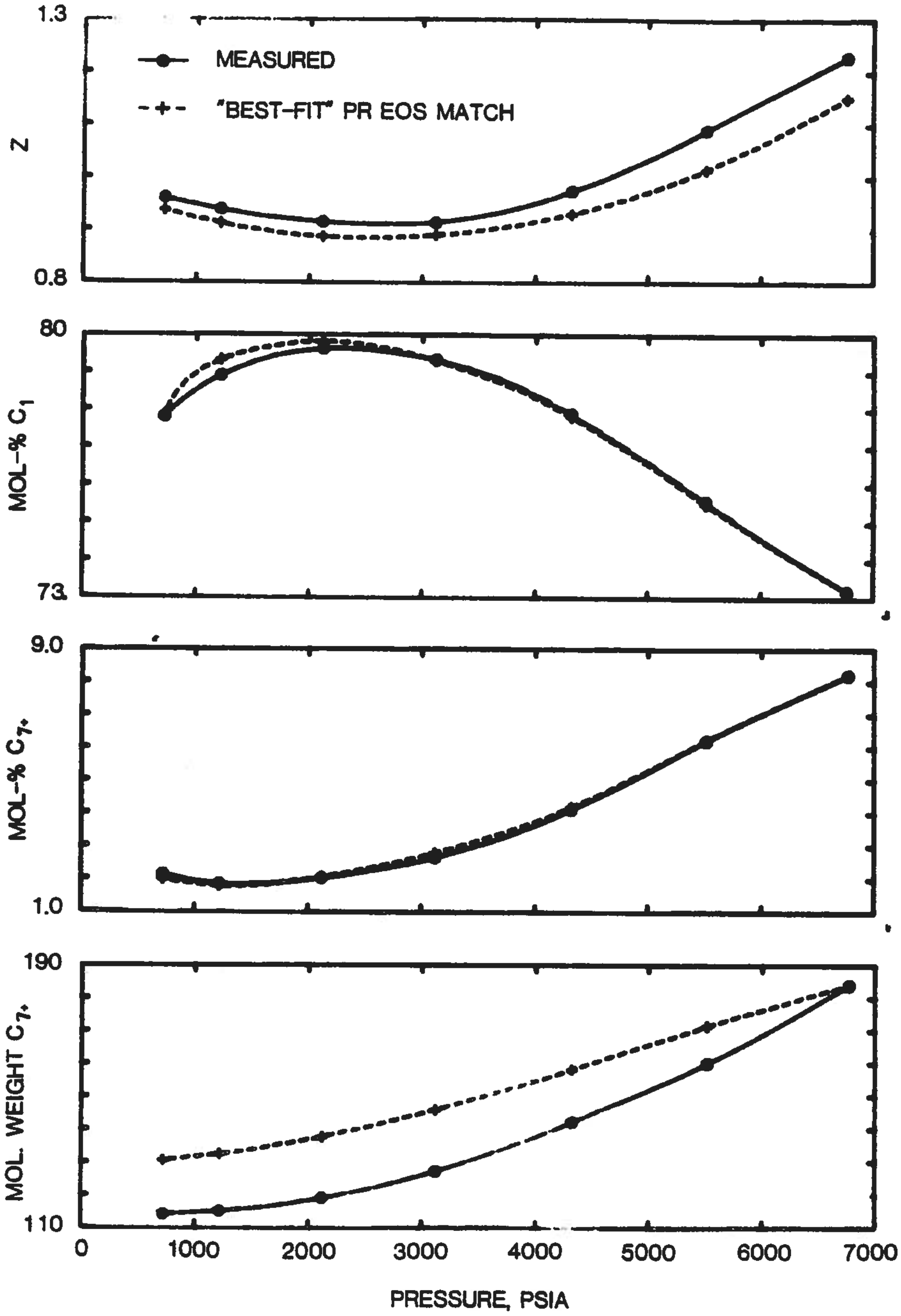

Fig. 13 - Results of predicted CVD data using the Peng-Robinson EOS and the proposed minimization routine ("best" match corresponds to liquid dropout curve in Fig. 12, upper inset).

SPE 10224

SPE
Society of Petroleum Engineers of AIME

Two-Phase Pressure Test Analysis

by Arild Bøe, *Rogaland Research Institute*; Svein M. Skjaeveland*
and Curtis H. Whitson, *Rogaland Regional College*

*Members SPE-AIME

This paper was presented at the 56th Annual Fall Technical Conference and Exhibition of the Society of Petroleum Engineers of AIME, held in San Antonio, Texas, October 5-7, 1981. The material is subject to correction by the author. Permission to copy is restricted to an abstract of not more than 300 words. Write: 6200 N. Central Expressway, Dallas, Texas 75206.

ABSTRACT

A theoretical basis is given for well test analysis of solution-gas and gas-condensate reservoirs in the infinite-acting period. The study is limited to radial flow with a fully penetrating well in the center of the drainage area. Porosity and absolute permeability are constants and gravitational and capillary effects are neglected. The tests are conducted at constant surface rate.

An analytical expression for the pressure - saturation relationship is derived from the time-dependent gas- and oil-flow equations. This relationship can be used at the wellbore to generate pseudopressure functions for drawdown and buildup that allow test interpretation using the liquid analogy.

The pressure-saturation relation for buildup is a limiting case of that for drawdown. They can both be used together with the Boltzman transform to generate saturation profiles as functions of radius at any stage of the tests conducted during the infinite-acting period.

Theoretical developments are examplified by simulated drawdown and buildup tests in a solution-gas drive reservoir.

INTRODUCTION

Many transient pressure tests can be interpreted using solutions of the diffusivity equation based on the liquid analogy of reservoir fluids. In the liquid model the reservoir fluids are represented by a single-phase liquid with small and constant compressibility and constant viscosity. The corresponding diffusivity equation is linear and solutions for a variety of boundary conditions have been presented in the literature. Single-phase gas test can be interpreted within the liquid analogy by introducing an integral transform, the pseudopressure function, originally suggested by Al-Hussainy et al.[1]. This pseudopressure function is uniquely dependent on pressure and can therefore be used both for drawdown and buildup analyses.

Multiphase-flow effects can also, to a certain extent, be adapted to the liquid model solutions if total mobility and compressibility are used[2,3]. The interpretation of the test will yield the effective permeability. For solution-gas reservoirs, this method becomes less reliable with increasing gas saturation[4]. A better adaption to the liquid analogy can be achieved by introducing a pseudopressure function into the multiphase-flow equations, as suggested by Fetkovich[5], in analogy to the single-phase gas case. This suggestion was persued by Raghavan[6] who gave practical methods for calculating the pseudopressure function for oil in solution-gas drive reservoirs, and showed that the standard, liquid analogy, semilog plots could be used to calculate the absolute formation permeability from computer-generated test data. In order to evaluate the oil pseudopressure function, the relation between oil saturation and pressure must be known. Raghavan did not, however, present a theoretically-based relation, but demonstrated, through examples, that the instantaneous, measured, producing GOR could be used for drawdown interpretation. He also suggested that the producing GOR at shutin could be used for buildup analysis.

The main objective of this paper is to present theoretical relationships between pressure and saturation that can be used to evaluate pseudopressure functions in the infinite-acting period. The suggested method should be valid for any multiphase system provided the fluid flow can be described by diffusivity equations based on "beta"-formulation, i.e. formation volume factors. The examples, based on computer-generated test data, are limited to solution-gas drive reservoirs.

THEORY

For simplicity, consider only the oil and gas phases to be mobile and the irreducible water to be incompressible. The flow equations are then

---

References and illustrations at end of paper.

$$\text{Gas:}\quad \nabla\cdot\left[\left(\frac{R_{so}k_{ro}}{\mu_o B_o}+\frac{k_{rg}}{\mu_g B_g}\right)\nabla p\right]=\frac{\phi}{k}\frac{\partial}{\partial t}\left(\frac{R_{so}S_o}{B_o}+\frac{S_g}{B_g}\right)\quad ..\ (1)$$

$$\text{Oil:}\quad \nabla\cdot\left[\left(\frac{r_{sg}k_{rg}}{\mu_g B_g}+\frac{k_{ro}}{\mu_o B_o}\right)\nabla p\right]=\frac{\phi}{k}\frac{\partial}{\partial t}\left(\frac{r_{sg}S_g}{B_g}+\frac{S_o}{B_o}\right)\quad ..\ (2)$$

where $S_o + S_g + S_{iw} = 1$.

The term R_{so} denotes gas dissolved in the oil phase and r_{sg} denotes oil dissolved in the gas phase. This last term is included to make the system of equations equally applicable to gas-condensate reservoirs. The formation volume factors, B_o, r_{sg}, R_{so}, B_g, can, in this case, be derived from a constant volume depletion experiment, as proposed by Whitson, et al.[7].

The following simplifying notation is introduced

$$S \equiv S_o$$

$$a \equiv \frac{R_{so}k_{ro}}{\mu_o B_o} + \frac{k_{rg}}{\mu_g B_g}$$

$$\alpha \equiv \frac{r_{sg}k_{rg}}{\mu_g B_g} + \frac{k_{ro}}{\mu_o B_o} \quad \dots\dots\dots\dots\dots\dots \quad (3)$$

$$b \equiv \frac{R_{so}S_o}{B_o} + \frac{S_g}{B_g}$$

$$\beta \equiv \frac{r_{sg}S_g}{B_g} + \frac{S_o}{B_o}$$

In these expressions, R_{so}, r_{sg}, B_o, B_g, μ_o, μ_g only depend on pressure p, and k_{rg}, k_{ro} only depend on saturation S.

We also introduce the following notations

$\dot{x} = (\frac{\partial x}{\partial S})_p$ = partial derivative of x with respect to S, p constant,

$x' = (\frac{\partial x}{\partial p})_S$ = partial derivative of x with respect to p, S constant,

where $x \in \{a, \alpha, b, \beta\}$.

Eqs. 1 and 2 may then be written as

$$\text{Gas:}\quad \nabla\cdot(a\nabla p) = \frac{\phi}{k}\frac{\partial b}{\partial t} \quad \dots\dots\dots\dots\dots\dots \quad (4)$$

$$\text{Oil:}\quad \nabla\cdot(\alpha\nabla p) = \frac{\phi}{k}\frac{\partial \beta}{\partial t} \quad \dots\dots\dots\dots\dots\dots \quad (5)$$

Formally, the non-linearities of Eqs. 4 and 5 given by the coefficients a and α can be eliminated by introducing an integral transform of the pressure, the pseudopressure function m, defined by Fetkovich[5]. Actually, several pseudopressure functions can be used:

$$\text{Oil:}\quad m_o(p) = \int_{p_o}^{p} \alpha\, dp \quad \dots\dots\dots\dots\dots\dots \quad (6)$$

$$\text{Gas:}\quad m_g(p) = \int_{p_o}^{p} a\, dp \quad \dots\dots\dots\dots\dots\dots \quad (7)$$

$$\text{Total:}\quad m_t(p) = \int_{p_o}^{p} (a+\alpha)\, dp \quad \dots\dots\dots\dots\dots\dots \quad (8)$$

Also, any linear combination of a and α can be used in the definition of m_t, for example normalizing Eqs. 4 and 5 before adding.

In practical use, the choice of definition depends on the characteristics of the reservoir and the boundary conditions of the test. For an oil reservoir with constant surface-oil rate, Eq. 6 would be used. With constant surface-gas rate during the test, Eq. 7 would be used. Eq. 8 would require constant total rate of gas plus oil at surface conditions.

In order to evaluate the integrals, Eqs. 6 - 8, the relationship between S and p must be known. This relationship must be consistent with the pressure and saturation profiles developed around the well during the test. In contrast to the single-phase pseudopressure function, the multiphase pseudopressure functions are not uniquely dependent on pressure, in general, but also depend on the history of the test, e.g. $m_o(p)$ for a drawdown test is different from $m_o(p)$ for buildup following the drawdown[6].

Line source solution

For radial flow, and with the Boltzman transform $y = \frac{\phi r^2}{4kt}$, Eq. 5 yields

$$\frac{d}{dy}\left(\alpha y \frac{dp}{dy}\right) = -\,y\,\frac{d\beta}{dy} \quad \dots\dots\dots\dots\dots\dots \quad (9)$$

From Eq. 6 we have $\alpha \frac{dp}{dy} = dm_o/dy$, and

$$\frac{d\beta}{dy} = \dot{\beta}\frac{dS}{dy} + \beta'\frac{dp}{dy}$$

$$= \left(\dot{\beta}\frac{dS}{dp} + \beta'\right)\alpha^{-1}\frac{dm_o}{dy}$$

Substituted in Eq. 9 this gives

$$\frac{d}{dy}\left(y\frac{dm_o}{dy}\right) = -\left(\frac{c}{\lambda}\right)^{*} y\,\frac{dm_o}{dy} \quad \dots\dots\dots\dots\dots\dots \quad (10)$$

where

$$\left(\frac{c}{\lambda}\right)^{*} = \left(\dot{\beta}\frac{dS}{dp} + \beta'\right)\alpha^{-1} \quad \dots\dots\dots\dots\dots\dots \quad (11)$$

The term $(c/\lambda)^*$ is a generalized compressibility-mobility ratio. For single-phase flow it corresponds to the compressibility-viscosity product, and to the total compressibility divided by the total mobility for two-phase flow in the approximation given by Martin[3], as will be verified below.

If the $(c/\lambda)^*$ term, Eq. 11, can be considered a constant, Eq. 10 has the standard line source solution, in logarithmic approximation

$$m_{ow} = m_{oi} - \frac{141.2\ q_o}{kh} \cdot [\tfrac{1}{2}(\ln t_D + 0.80907)] \qquad (12)$$

where q_o is the constant surface rate, and dimensionless time t_D is defined by

$$t_D = 0.0002637 \frac{kt}{\phi r_w^2 (c/\lambda)^*} \quad \dots\dots\dots\dots\dots\dots \quad (13)$$

Field units are used consistently.

Although $(c/\lambda)^*$ can be shown to vary with pressure, our simulation results, as well as Raghavan's[6], show that the pseudopressure function plots as a semilog straight line during the entire infinite-acting period. This can be explained from the boundary condition

$$\lim_{y \to 0} \left(y \frac{dm_o}{dy}\right) = \frac{141.2\ q_o}{2kh} \quad \dots\dots\dots\dots\dots\dots\dots\dots \quad (14)$$

used in deriving Eq. 12. That is, when the producing time becomes sufficiently large, Eq. 14 can be solved directly and yields logarithmic time dependence, independent of $(c/\lambda)^*$.

Interpreted results from simulated tests correlate fairly well with the liquid reference curve if the initial value, $(c/\lambda)_i^*$, is used in Eq. 13. To correlate exactly with the liquid reference curve, $(c/\lambda)_i^*$ has to be adjusted by a constant correction factor, usually between 1.0 and 2.0. This is also necessary in Raghavan's[6] example. The slight error in using $(c/\lambda)_i^*$ can be seen as a skin, usually small and negligible.

When the well during a drawdown test reaches pseudosteady state, the Boltzman transform is no longer valid and the boundary condition, Eq. 14, breaks down. In this flow period then, the pressure dependence of $(c/\lambda)^*$ can be expected to cause deviations from the liquid reference curve.

Line source solutions for other choices of pseudopressure functions, Eqs. 7 - 8, can be derived similarly using different expressions for $(c/\lambda)^*$.

Relationship between saturation and pressure

From the oil equation, Eq. 9, and the corresponding gas equation we get

$$\text{Gas: } a \frac{d}{dy}\left(y \frac{dp}{dy}\right) + \frac{da}{dy} y \frac{dp}{dy} = - y \frac{db}{dy} \quad \dots\dots\dots\dots \quad (15)$$

$$\text{Oil: } \alpha \frac{d}{dy}\left(y \frac{dp}{dy}\right) + \frac{d\alpha}{dy} y \frac{dp}{dy} = - y \frac{d\beta}{dy} \quad \dots\dots\dots\dots\dots \quad (16)$$

Here $\frac{da}{dy} = \dot{a} \frac{dS}{dy} + a' \frac{dp}{dy}$ and similarly for the other terms.

For convenience, introduce

$$N = y \frac{dp}{dy} \quad \text{and} \quad K = y \frac{dS}{dy}$$

and the flow equations become

$$\text{Gas: } a \frac{dN}{dy} + N \cdot [a' \frac{N}{y} + b'] + K \cdot [\dot{a} \frac{N}{y} + \dot{b}] = 0$$

$$\text{Oil: } \alpha \frac{dN}{dy} + N \cdot [\alpha' \frac{N}{y} + \beta'] + K \cdot [\dot{\alpha} \frac{N}{y} + \dot{\beta}] = 0$$

Eliminating dN/dy between the two equations and noting that K/N = dS/dp, we get the general saturation - pressure relation

$$\frac{dS}{dp} = \frac{(\alpha a' - a\alpha') \frac{N}{y} + (\alpha b' - a\beta')}{(a\dot{\alpha} - \alpha\dot{a}) \frac{N}{y} + (a\dot{\beta} - \alpha\dot{b})} \quad \dots\dots\dots \quad (17)$$

Estimation of $\frac{N}{y}$ - term

At radius r and time t, from Darcy's law:

$2\pi rkh\alpha(y) \frac{\partial p(y)}{\partial r} = q_o(y)$ where $q_o(y)$ is the surface oil rate. Hence

$$N = y \frac{dp}{dy} = \frac{q_o(y)}{4\pi kh\alpha(y)}$$

which shows that N is bounded for all values of y.

At the wellbore:

$$\frac{N}{y} = \frac{q_o \cdot t}{\pi r_w^2 h \phi \alpha}$$

or

$$\frac{N}{y} = \frac{1}{\alpha} \frac{t}{t_w} \quad \dots\dots\dots\dots\dots\dots\dots\dots\dots\dots\dots\dots \quad (18)$$

where $t_w = 13.44 \frac{\phi r_w^2 h}{q_o}$, Field Units.

Eq. 18 has to be solved iteratively together with Eq. 17 since α depends on both saturation and pressure. Note that Eq. 18 is independent of absolute permeability k. Therefore, m_o-values can be generated without knowledge of k.

Limiting cases.

We will first examine the two limiting cases of short and long producing times for a constant surface-oil rate drawdown test. In these cases Eq. 17 is solved without estimation of the N/y-term.

A. Initial flow, $y \to \infty$ $(t \to 0)$

Since N is bounded, $\frac{N}{y} \to 0$ as $y \to \infty$ and Eq. 17 reverts to

$$\frac{dS}{dp} = \frac{\alpha b' - a\beta'}{a\dot{\beta} - \alpha\dot{b}} \quad \ldots\ldots\ldots\ldots\ldots\ldots\ldots \quad (19)$$

In order to compare with the results of Martin[3], we set $r_{sg} = 0$, substitute the expressions from Eq. 3 and get

$$\alpha b' - a\beta' = \frac{\lambda_t}{B_o B_g}\left(S_o \frac{B'_o}{B_o} + \frac{\lambda_o}{\lambda_t} c_t\right)$$

$$a\dot{\beta} - \alpha\dot{b} = \frac{\lambda_t}{B_o B_g}$$

where total mobility is

$$\lambda_t = \lambda_o + \lambda_g = \frac{k_{ro}}{\mu_o} + \frac{k_{rg}}{\mu_g}$$

and

$$c_t = -\frac{S_o B'_o}{B_o} + \frac{S_o B_g R'_{so}}{B_o} - \frac{S_g B'_g}{B_g}$$

is the total compressibility of the fluids.

Hence

$$\frac{dS_o}{dp} = S_o \frac{B'_o}{B_o} + \frac{\lambda_o}{\lambda_t} c_t \quad \ldots\ldots\ldots\ldots\ldots\ldots\ldots \quad (20)$$

as shown by Martin[3].

Eq. 19 can be derived directly from Eqs. 15 and 16 by neglecting the second-order flow terms[3]. Substituting Eq. 20 into Eq. 11 we find $(c/\lambda)^* = c_t/\lambda_t$. Therefore, in the limiting case when $t \to 0$, or, if the second-order flow terms can be neglected, the standard interpretation procedure is applicable[2]. Our simulation runs show, however, that Eq. 19 is only valid at the wellbore for very short producing times, only a few minutes for the presented example.

B. Long producing times, $y \to 0$.

In this case Eq. 17 reduces to

$$\frac{dS}{dp} = \frac{\alpha a' - a\alpha'}{a\dot{\alpha} - \alpha\dot{a}} \quad \ldots\ldots\ldots\ldots\ldots\ldots\ldots \quad (21)$$

The consequences of this expression can be seen as follows. The producing gas-oil ratio R is given by $R = a/\alpha$. The total derivative of R with respect to pressure is then

$$\frac{dR}{dp} = \dot{R}\,\frac{dS}{dp} + R'$$

Substituting from Eq. 21, we find

$$\frac{dR}{dp} = 0$$

that is, the gas-oil ratio is a constant, independent of pressure (and time). This is an important observation. For a drawdown test in the infinite-acting period, when Eq. 21 becomes valid, the gas-oil ratio will stabilize. The level of stabilization depends strongly on the rate and may be higher or lower than the initial gas-oil ratio, as determined from our simulation runs. The stabilization and the shift from Eq. 19 to Eq. 21 occurs after a very short producing time, only a few minutes for the presented example.

Eq. 21 can also easily be derived directly from Eqs. 15 and 16 by neglecting the expansion terms on the right hand side of the equations.

Saturation as function of radius.

In the infinite-acting period, when the Boltzman transform is valid, saturation and pressure profiles can easily be generated if S and p are known functions of time at the wellbore.

For a drawdown test, at radius r and time t, the saturation will be equal to the saturation at the wellbore at a time

$$t' = \frac{r_w^2}{r^2}\,t$$

During buildup, the saturation change ΔS from the shutin profile, at radius r and shutin time Δt, will be equal to the saturation change at the wellbore at a shutin time

$$\Delta t' = \frac{r_w^2}{r^2}\,\Delta t$$

Integration paths.

Raghavan[6] points out that the pseudopressure function should reflect the pressure and saturation profiles occurring in the drainage area during the test. To achieve this, the integral

$$\int_{p_w}^{p_i} \alpha\, dp$$

could, for a given time, be evaluated by integration over the saturation and pressure profiles, i.e. over radius r. This approach is consistent with the pseudopressure equations suggested for steady-state and pseudosteady flow, Fetkovich[5]. When the Boltzman transform is valid, however, the integration over radius for a fixed time is equivalent to integration over time for a fixed radius $r = r_w$. In the infinite acting period, the pseudopressure function can therefore be evaluated simply by using the correct pressure-saturation relationship at the wellbore.

Interpretation procedures, infinite acting period.

A. Drawdown.

Eqs. 17 and 18 are used to generate a table of S vs p_{wf}. The pseudopressure function m_o is calculated from Eq. 6. A semilog plot of m_o vs producing time t gives a straight line and absolute permeability k is calculated from the slope. The dimensionless pseudopressure function m_{wD} can then be calculated and compared with the liquid reference curve,

$$m_{wD} = \frac{kh}{141.2\ q_o} m_w \quad \ldots\ldots\ldots\ldots\ldots\ldots \quad (22)$$

where

$$m_w = m_o(p_i) - m_o(p_{wf}) = \int_{p_{wf}}^{p_i} \alpha\, dp$$

This method is similar to that suggested by Raghavan[6]. He used the gas-oil ratio equation, $R = a/\alpha$, to relate saturation to pressure based on measured R values.

B. Buildup.

The saturation-pressure relation at the wellbore during buildup differs from the drawdown case. After shutin, the pressure gradient at the wellbore is zero and $N/y = 0$. Hence Eq. 19 is valid during the whole buildup period.

To interpret a buildup test, the saturation at the wellbore at shutin must be known. This value can be found from the drawdown S vs p or directly from the gas-oil ratio equation and the observed constant level of R. A table of S vs p_{ws} is then generated using Eq. 19. The pseudopressure function m_w is calculated from

$$m_w = m_o(p_{ws}) - m_o(p_{wf,s}) = \int_{p_{wf,s}}^{p_{ws}} \alpha\, dp$$

A Horner or MDH plot will give the absolute permeability k and the dimensionless pseudopressure function

$$m_{wD} = \frac{kh}{141.2\ q_o} m_w \quad \ldots\ldots\ldots\ldots\ldots\ldots \quad (23)$$

can be calculated.

This procedure is different from the one suggested by Raghavan[6]. He used the gas-oil ratio equation with R constant, equal to the value at shutin, to generate the S vs p_{ws} relationship.

Pseudosteady state (PSS)

A. Drawdown.

When the well reaches PSS, the Boltzman transform is no longer compatible with the boundary conditions. If the use of Eq. 17 is extended into this flow period, deviation from the liquid analogy will occur. Even if the correct S vs p relation at the wellbore were used, from the observed $R = a/\alpha$, it is not obvious to us that a continued integration only of wellbore data would give a pseudopressure function that properly describes the conditions within the drainage area. Also, $(c/\lambda)^*$ in the expression for dimensionless time, Eq. 13, varies with pressure and will give departure from the liquid reference curve. It is therefore not presently evident how the liquid analogy of multiphase flow can be extended into the PSS period in order to accurately determine the drainage area.

B. Buildup from PSS.

It can easily be shown, without the use of Boltzman transform, that the p vs S relationship at the wellbore is still given by Eq. 19. This is verified in the presented example. But, if the pseudopressure function is evaluated only based on wellbore data of S and p, the corresponding Horner plot will not be a straight line with the correct slope, as shown in the example. This indicates that for buildup from PSS, a pseudopressure function evaluated from correct wellbore data will not properly describe the saturation and pressure profiles occurring in the reservoir during the test. It appears that Raghavan's[6] suggested procedure for buildup better covers this case. This lack of a liquid analogy makes it difficult to accurately determine the average reservoir pressure from the test.

EXAMPLE

Numerical model.

The test data were generated by a radial, one-dimensional, three-phase simulator with variable bubble-point pressure developed at Rogaland Research Institute. The formulation is implicit finite difference with simultaneous and direct solution of pressures and saturations.

The validity of the model was checked by simulation and interpretation of several single-phase liquid pressure tests. Trial runs were also made to eliminate time and space discretization errors. All the example runs were finally made with a 40-block numerical grid, the block lengths increasing logarithmically with radius, and with the time-step size controlled by a maximum saturation change of 0.025 and a maximum pressure change of 43.5 psi (3 bar).

Reservoir and test characteristics.

The example tests are limited to a well fully penetrating the center of a radial oil reservoir with solution-gas drive. In all calculations, the oil pseudopressure function, Eq. 6, is therefore used. All runs were made with a constant surface-oil rate of 125.8 STB/D (20 SM3/D) and with incompressible water at a irreducible saturation of 0.30. All tests started with initial reservoir pressure equal to the bubble-point pressure. The absolute permeability and porosity were constant and gravitational and capillary effects excluded. The common reservoir properties, fluid properties and relative permeabilities for the tests are presented in Tables 1, 2 and 3, respectively.

Dimensionless variables.

All plots are presented in dimensionless form with the pseudopressure functions, m_{wD}, for drawdown and buildup defined by Eqs. 22 and 23. Dimensionless time, t_{Di}, based on wellbore radius is defined by Eq. 13, with $(c/\lambda)^*$ evaluated at initial pressure. Dimensionless time based on drainage area, t_{DAi}, is given by

$$t_{DAi} = t_{Di}\,\frac{r_w^2}{\pi r_e^2}$$

Dimensionless wellbore pressures, p_{wD}, for drawdown and buildup, respectively, are defined by

$$p_{wD} = \frac{kh}{141.2\,q_o}\,(p_i - p_{wf})$$

and

$$p_{wD} = \frac{kh}{141.2\,q_o}\,(p_{ws} - p_{wf,s})$$

All definitions are given in field units.

It should be noted that k_{roi} is not included in the definition of p_{wD}. Correct slope of a p_{wD} vs t_{Di} semilog plot should therefore be $1.151/k_{roi}$ per log cycle, while for the corresponding m_{wD}-plots, the slope should be 1.151 per log cycle.

The dimensionless liquid-reference pressure is denoted by p_D on the plots.

Test cases.

1. Drawdown to 100 hrs which corresponds to a t_{DAi} = 0.17. The test therefore extends slightly into PSS ($t_{DAi}>0.10$).
2. Buildup following a drawdown of 5 hrs. The entire test is performed in the infinite-acting period.
3. Buildup following the 100 hrs. drawdown. This test examplifies buildup from PSS.

We also ran a drawdown to t_{DAi} = 2.7 followed by a buildup to further check the conclusions from the 100 hrs drawdown-buildup. The results are not presented here since the main objective of the study is to demonstrate the validity of the pseudopressure approach in the infinite-acting period.

Results.

Case 1.

Fig. 1 shows a semilog plot of pseudopressure function m_{wD}, liquid reference pressure p_D and wellbore pressure p_{wD}. The m_{wD}-curve is a straight line with the correct slope in the infinite acting period, parallel to the liquid reference curve. A slight shift between the two curves corresponds to a correction factor of 1.62 on $(c/\lambda)_i^*$, or a skinfactor equal to -0.48, which should have been zero since no fixed skin zone is used in the model and the gas blockage around the well is incorporated in the m_{wD}-function. The m_{wD}-plot will therefore give the correct absolute permeability, but a slightly erroneous skinfactor if $(c/\lambda)_i^*$ is used in the dimensionless time, t_{Di}. The p_{wD}-values do not plot as a straight line and cannot be used to interpret the test.

The results are replotted in Fig. 2 on a linear t_{DAi}-scale. The infinite-acting S vs p relation, Eq. 17, has been used to evaluate m_{wD} also in the PSS period ($t_{DAi}>0.10$). The slope of m_{wD}-curve is close to the correct value 2π, but the shift between the p_D- and m_{wD}-curves makes determination of drainage area uncertain. Further extension of the drawdown to t_{DAi} = 2.7 shows that the m_{wD}-values do not plot as a straight line, as also noted by Raghavan[6]. Neither of the two suggested methods are therefore applicable for a liquid analogy interpretation in the PSS period.

Fig. 3 shows the development of producing gas-oil ratio with time. The simulated and calculated R values from Eq. 17 agree closely. R drops down from 267 SM3/SM3 within about 5 minutes ahd then stays constant throughout the infinite-acting period. Curve 3 has been generated by using Eq. 19 until dS/dp becomes equal to the value calculated from Eq. 21 and then using Eq. 21. Only a coarse estimate of the constant R level is achieved.

Fig. 4 plots simulated and calculated values of the oil saturation at the wellbore. There is a close agreement between simulated values and those from Eq. 17.

Case 2.

Fig. 5 depicts the results from buildup following the 5 hrs drawdown in an MDH plot. The m_{wD}-values plot parallel to the liquid reference curve p_D, as long as $\Delta t \ll t$, and have been calculated using Eq. 19. The m_{wD}-curve can be shifted to the p_D-curve by correcting the value $(c/\lambda)_i^*$. Any constant formation skinfactor can then be calculated using the corrected $(c/\lambda)_i^*$. This procedure cannot be used for a drawdown test since a parallel shift in that case is equivalent to a nonzero skinfactor. The Horner plot is given in Fig. 6. The m_{wD} values fall on a straight line with slope 1.15 while the p_{wD}-data do not form a straight line.

Fig. 7 shows an excellent match between simulated and calculated values of oil saturation, Eq. 19, at the wellbore during the buildup.

Simulated and calculated saturation profiles as functions of radius, at shutin and after 5 min buildup, are given in Fig. 8. The calculated saturations are generated from wellbore data and by the use of the Boltzman transform, as explained in the text. The excellent agreement verifies the validity of the Boltzman transform in the infinite-acting period.

Case 3.

The results from buildup following the 100 hrs drawdown are shown in Figs. 9 and 10. The m_{wD}-values do not plot parallel to the liquid reference curve and the Horner line has a slope of 1.30, a 13% deviation from the correct value 1.15. If the buildup is performed further out in PSS, these discrepancies become more pronounced and the Horner plot ceases to give a straight line for the pseudopressure function. Fig. 11 shows that the match between simulated and calculated oil saturations, from Eq. 19, is still excellent. Although the correct relationship between pressure and saturation at the wellbore is used, the m_{wD}-function generated from these data departs from the liquid analogy. The reason for this is probably that wellbore data alone will not properly represent the saturation and pressure profiles occuring in the reservoir during the buildup from PSS.

CONCLUSIONS

Methods have been presented for interpretation of multiphase drawdown and buildup tests in the infinite-acting period through the pseudopressure approach. In this period the pseudopressure functions are calculated based on wellbore data only, with theoretically consistent relations between pressure and saturation. The relation for buildup is a special case of the general drawdown relation.

Results from an example solution-gas drive reservoir correlate with the liquid reference curve with $(c/\lambda)^*$ close to the initial value.

During the drawdown test the producing gas-oil ratio quickly stabilizes and remains constant throughout the infinite acting period. The saturation profiles during this period can, both for drawdown and buildup, be generated based only on wellbore data.

The proposed interpretation methods are not readily extended to the pseudosteady state.

NOMENCLATURE

a, α, b, β = defined by Eq. 3
B = formation volume factor
c = compressibility
$(\frac{c}{\lambda})^*$ = defined by Eq. 11
h = formation height
K = $y\frac{dS}{dy}$
k = absolute permeability
k_r = relative permeability
m = pseudopressure function
N = $y\frac{dp}{dy}$
p = pressure
p_o = base pressure in evaluation of pseudopressure function
p_{wf} = flowing well pressure
$p_{wf,s}$ = flowing well pressure at shutin
p_{ws} = shutin well pressure
q = surface rate
r = radius
R = producing gas-oil ratio
r_{sg} = dissolved oil-gas ratio
R_{so} = solution gas-oil ratio
S = saturation or oil saturation
S_{iw} = irreducible water saturation
t = time or producing time
t_D = dimensionless producing time based on wellbore radius
Δt_D = dimensionless shutin time based on wellbore radius
t_{DA} = dimensionless producing time based on drainage area
x = dummy variable
$\dot{x}$ = partial derivative of x with respect to S, constant p
x' = partial derivative of x with respect to p, constant S
y = $\frac{\phi r^2}{4kt}$
Δ = difference (change in)
∇ = gradient
$\nabla\cdot$ = divergence
ϕ = porosity
λ = mobility
μ = viscosity

Subscripts

o = oil
g = gas
w = well or water
i = initial
t = total
D = dimensionless

ACKNOWLEDGEMENTS

We appreciate the economic support from the Royal Norwegian Council for Industrial and Scientific Research (Grant No. 1840.07425) and from Statoil.

REFERENCES

1. Al-Hussainy, R., Ramey, H.J., Jr., and Crawford, P.B.: "The Flow of Real Gases Through Porous Media," J. Pet. Tech. (May 1966), 624-636; Trans., AIME, Vol. 237.

2. Perrine, R.L.: "Analysis of Pressure Buildup Curves," Drill. and Prod. Prac., API (1956) 482.

3. Martin, J.C.: "Simplified Equations of Flow in Gas Drive Reservoirs and the Theoretical Foundation of Multiphase Pressure Buildup Analyses," Trans., AIME (1959) Vol. 216, 309-311.

4. Weller, W.T.: "Reservoir Performance During Two-Phase Flow," J. Pet. Tech. (Feb. 1966) 240-246; Trans., AIME, Vol. 237.

5. Fetkovich, M.J.: "The Isochronal Testing of Oil Wells," paper SPE 4529 presented at the SPE-AIME 48th Annual Fall Meeting, Las Vegas, Nev., Sept. 30 - Oct. 3, 1973.

6. Raghavan, R.: "Well Test Analysis: Wells Producing by Solution-Gas Drive," Soc.Pet. Eng. J. (Aug. 1976) 196 - 208; Trans., AIME, Vol. 261.

7. Whitson, C.H. and Torp, S.B.: "Evaluating Constant Volume Depletion Data," Paper SPE 10067, presented at the 56th Annual Fall Meeting of SPE of AIME, in San Antonio, Texas, October 5-7, 1981

TABLE 1 - RESERVOIR PROPERTIES

Porosity	0.30
Absolute permeability, md	10.0
Initial pressure, bar	393.3
Initial bubblepoint pressure, bar	393.3
Connate water saturation, incompressible	0.30
Initial gas saturation	0.0
Initial system compressibility, bar^{-1}	1.303 E-04
Well radius, m	0.10
External radius, m	200.0
Height, m	4.74

TABLE 2 - FLUID PROPERTIES*

p (bar)	B_o (Res m^3/Sm^3)	μ_o (cp)	R_{so} (Sm^3/Sm^3)	B_g (Sm^3/Res m^3)	μ_g (cp)
393.330	1.806	0.298	266.964	298.85	0.0298
388.390	1.791	0.300	261.867	296.99	0.0295
358.780	1.702	0.317	232.513	285.12	0.0281
324.240	1.605	0.348	200.793	269.48	0.0263
289.690	1.516	0.391	171.590	251.30	0.0246
255.140	1.434	0.446	144.715	229.88	0.0228
220.600	1.360	0.515	119.997	204.59	0.0210
190.990	1.302	0.587	100.408	179.63	0.0195
161.370	1.249	0.671	82.196	151.96	0.0181
131.760	1.202	0.768	65.275	122.42	0.0166
102.150	1.159	0.881	49.553	92.32	0.0152
72.540	1.121	1.011	34.925	63.03	0.0138
42.930	1.088	1.164	21.218	35.63	0.0125
13.320	1.058	1.350	7.887	10.55	0.0113

*PVT properties represent a crude oil system with 35°API, spesific gas gravity 0.75, initial solution gas-oil ratio 1500 SCF/STB, and reservoir temperature 200°F.

TABLE 3 - RELATIVE PERMEABILITIES*

S_g	k_{rg}	k_{ro}
0.0	0.0	0.700
0.0102	0.000004	0.660
0.0204	0.000034	0.622
0.0306	0.000115	0.585
0.0408	0.000269	0.550
0.0510	0.000522	0.517
0.0612	0.000896	0.485
0.0714	0.00141	0.455
0.0816	0.00209	0.426
0.0918	0.00295	0.399
0.102	0.00402	0.373
0.112	0.00531	0.348
0.122	0.00684	0.324
0.133	0.00863	0.302
0.143	0.0107	0.281
0.153	0.0130	0.261
0.163	0.0157	0.242
0.173	0.0187	0.224
0.184	0.0220	0.207
0.194	0.0256	0.191
0.204	0.0296	0.176

*Generated from $k_{ro} = 0.7(S_o^*)^4$

$k_{rg} = 0.7(1-S_o^*)^2(1-(S_o^*)^2)$

$S_o^* = S_o/(1-S_{iw})$, $S_{iw} = 0.3$

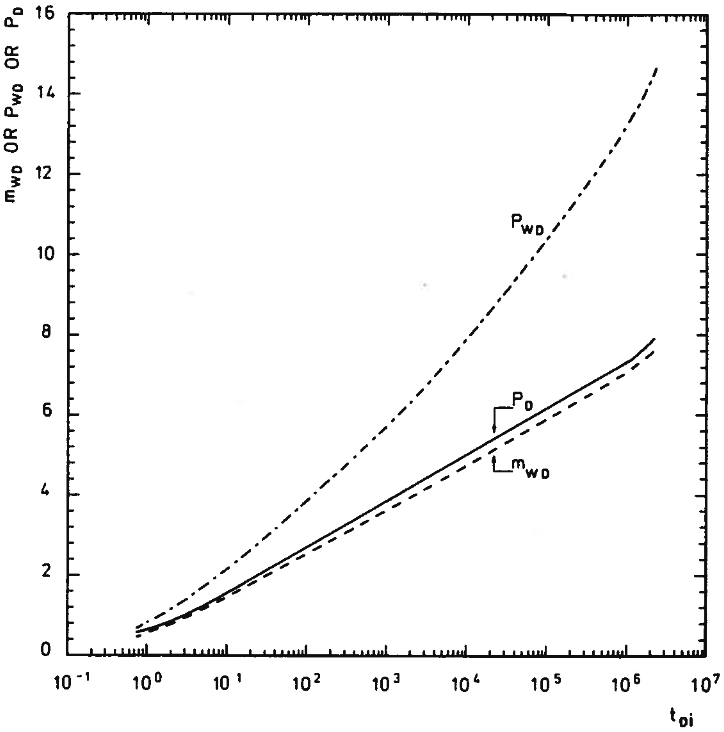

Fig. 1 – Dimensionless pressure functions vs. dimensionless producing time, t_{Di}. Case 1.

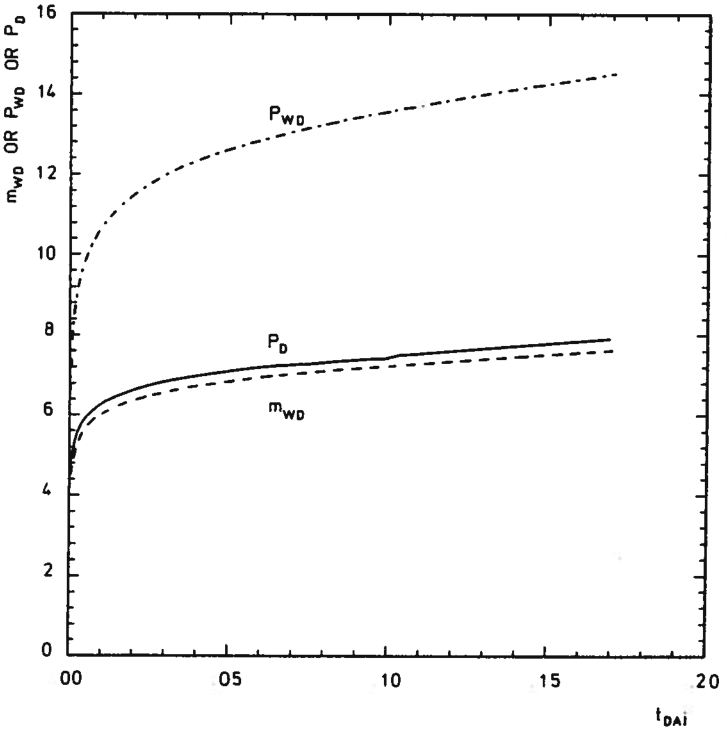

Fig. 2 – Dimensionless pressure functions vs. dimensionless time, t_{DAi}. Case 1.

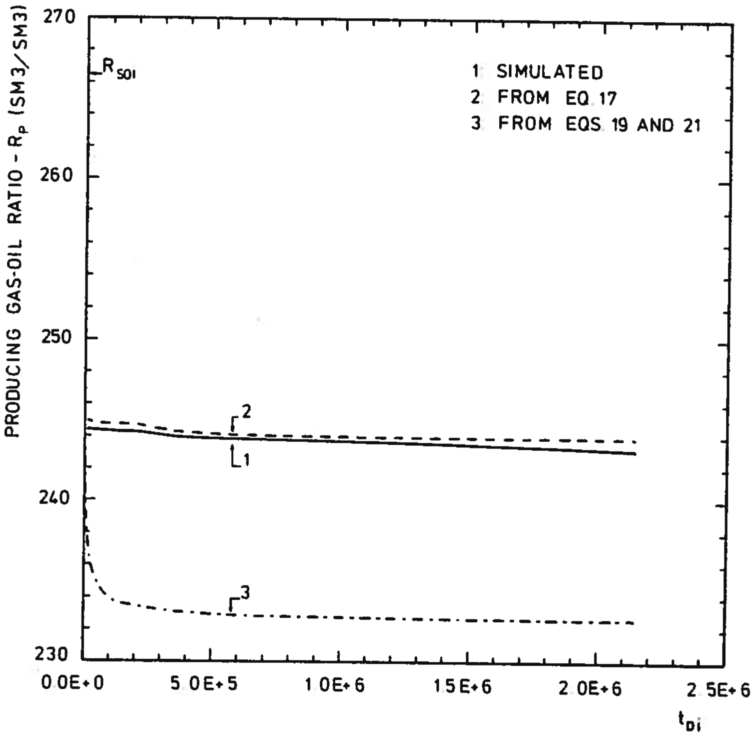

Fig. 3 – Producing gas-oil ratio vs. dimensionless time, t_{Di}, Case 1.

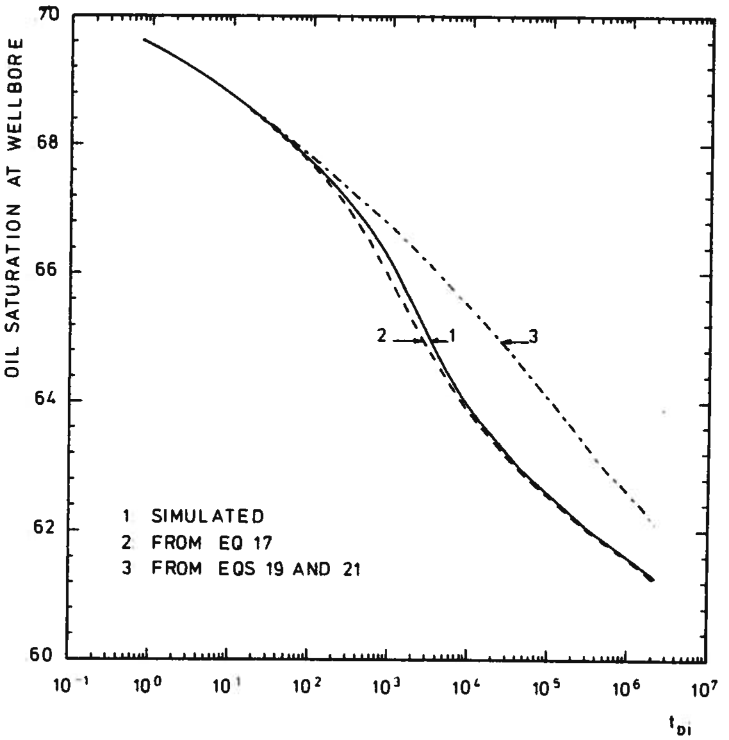

Fig. 4 – Oil saturation at wellbore vs. dimensionless time, t_{Di}, Case 1.

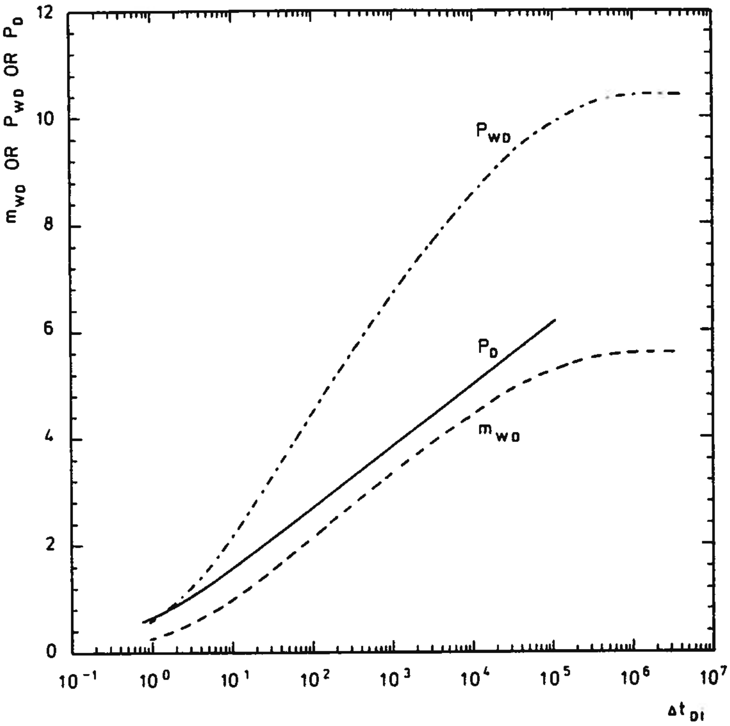

Fig. 5 – Dimensionless pressure functions vs. dimensionless shut-in time, Δt_{DI}. Case 2.

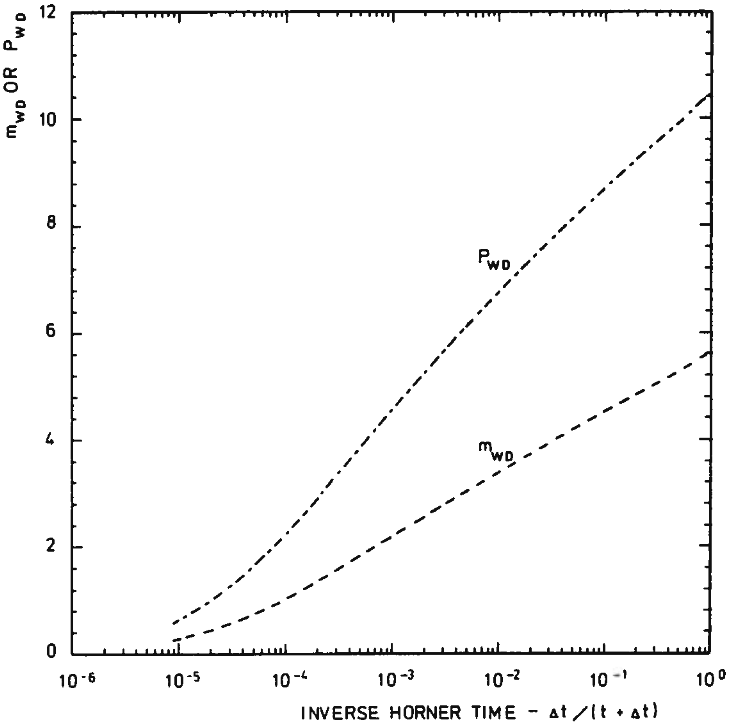

Fig. 6 – Dimensionless pressure functions vs. inverse Horner time, $\Delta t/(t+\Delta t)$. Case 2.

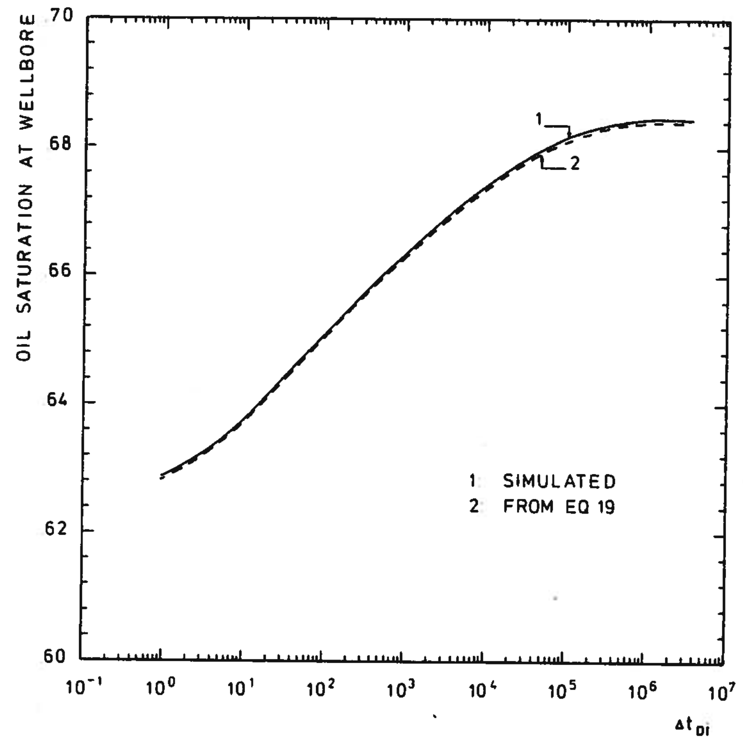

Fig. 7 – Oil saturation at wellbore vs. dimensionless shut-in time, Δt_{Di}. Case 2.

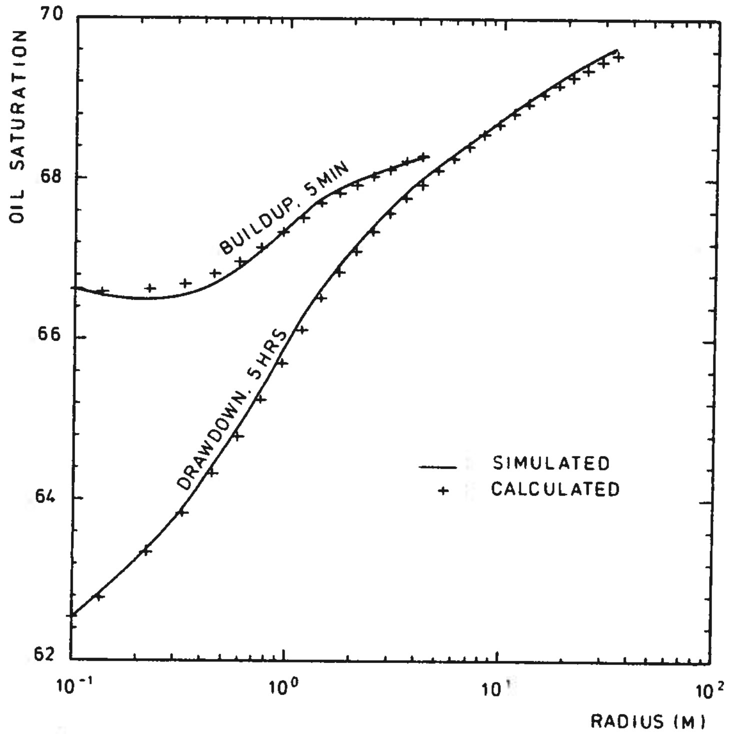

Fig. 8 – Saturation profiles vs. radius at the end of 5 hrs drawdown and after 5 min buildup. Case 2.

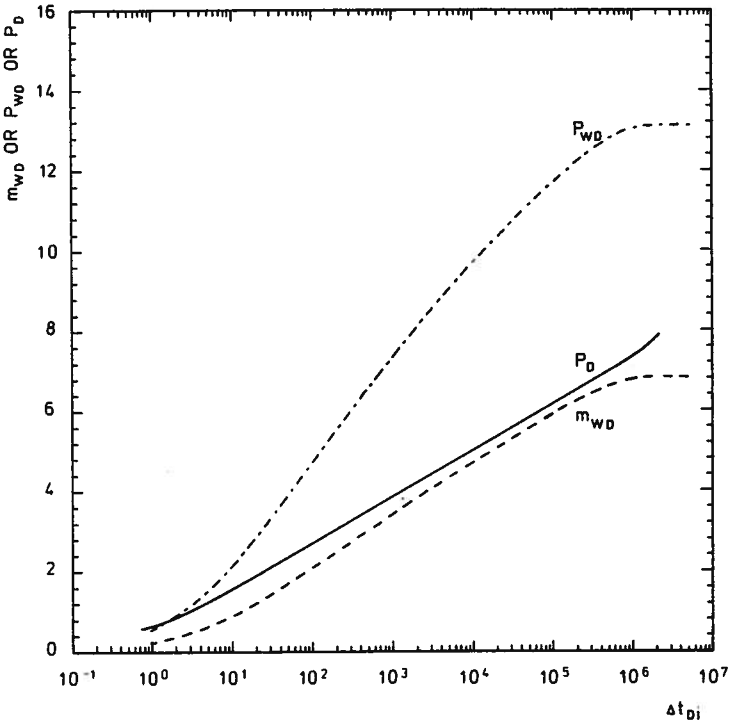

Fig. 9 – Dimensionless pressure functions vs. dimensionless shut-in time, Δt_{Di}. Case 3.

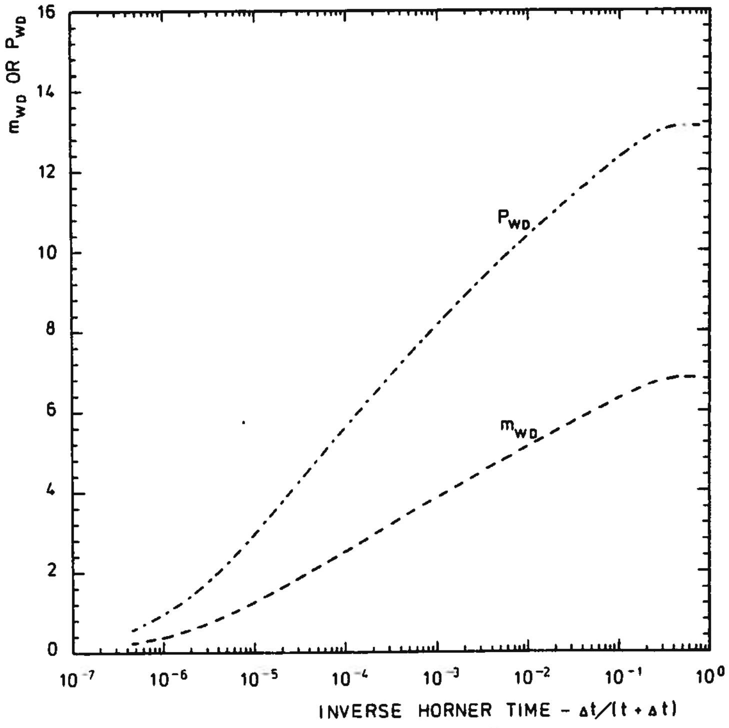

Fig. 10 – Dimensionless pressure functions vs. inverse Horner time, $\Delta t/(t+\Delta t)$. Case 3.

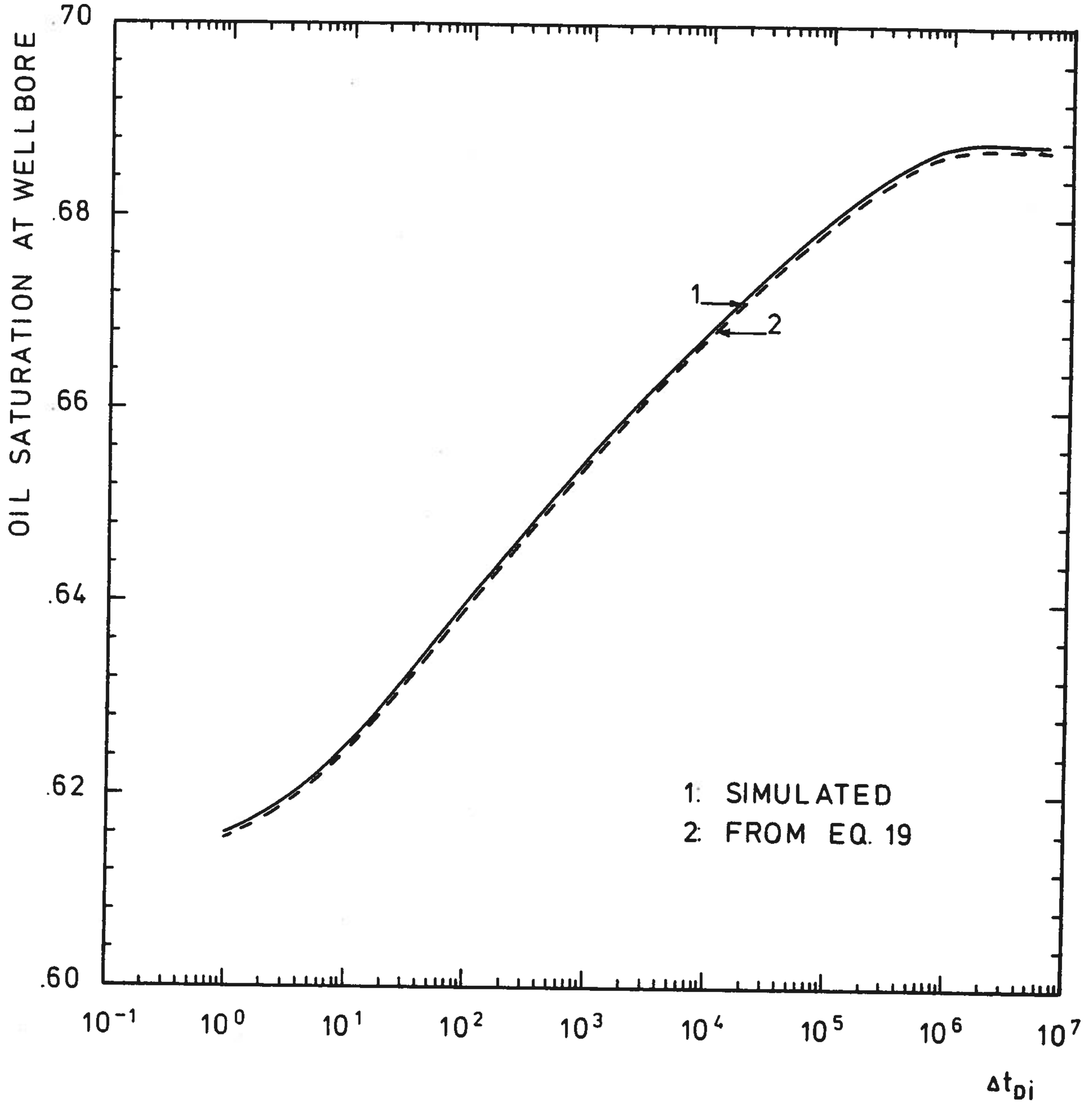

Fig. 11 – Oil saturation at wellbore vs. dimensionless shut-in time, Δt_{Di}. Case 3.

RESERVOIR WELL PERFORMANCE
AND
PREDICTING DELIVERABILITY

by

Curtis H. Whitson

Rogaland Regional College
Ullandhaug
4000 Stavanger, Norway

INTRODUCTION

Numerous publications address the subject of well performance and stabilized deliverability. Only a few, however, have received general acceptance for solving traditional production and reservoir engineering problems. Simplicity plays a significant role since the relation between rate and wellbore flowing pressure is often used by production teams only interested in approximate answers to design problems.

Productivity index, PI, is defined as the ratio of rate to pressure drop in the resevoir ($q/\Delta p$). It plays an important role in describing a well's inflow performance. PI is nearly constant for oil wells with wellbore flowing pressure above the bubble point, leading to the simplest of all inflow performance relations. Muskat[1] was one of the first to use the PI concept to understand the role of physical factors such as partial penetration, perforation density and two-phase, gas-oil flow.

The concept of skin factor, usually attributed to Hurst[2] and van Everdingen,[3] and its subsequent expression as a flow efficiency, E_F, provides a simple means to account for nonideal fluid flow. The idea can actually be found in Muskat's treatment of perforation effects on well productivity. The Hurst-van Everdingen concept of skin is a steady-state dimensionless pressure drop occuring at the wellbore. It has since been modified to account for high-velocity-flow (HVF) or turbulence effects, blockage due to the buildup of a gas or oil saturation in the near-wellbore region, and other nonideal reservoir behavior. Application of skin factor to predicting deliverability has become as important as the concept of productivity index.

An important case of oilwell inflow performance is when pressure in the reservoir sinks below the bubble point. Gas evolves and reduces oil productivity. Evinger and Muskat[4] show that PI decreases as oil rate increases. They suggest a method to estimate the reduction in oil productivity based on steady-state flow.

The method presented by Evinger and Muskat has never been widely used. The first study on two-phase, gas-oil flow to gain acceptance by engineers came in 1968. Vogel[5] presented a simple relation between oil rate and wellbore flowing pressure based on numerical simulation of saturated-oil systems with varying rock and fluid properties. This relation has been and probably still is the industry standard for predicting oilwell performance.

The Vogel relation has been modified by several workers. Standing proposes simple extensions when a well experiences a change in flow efficiency[6] (damage or stimulation) or average reservoir pressure drops below the bubble point.[7] Patton and Goland[8] extend the Vogel relation for undersaturated reservoirs with wells experiencing drawdown below the bubble point. A recent work by Richardson and Shaw[9] proposes a generalization of the Vogel relation based on mathematical intuition. It appears from results in this study that the generalization has a physical basis.

Fetkovich[10] presents an excellent correlation of oilwell performance on data collected from over 40 multirate tests. He shows that HVF effects are present in oil wells and that absolute open flow potential (AOFP) is overestimated if such effects are not considered. He also draws the analogy between gas-and oilwell performance by comparing pressure functions which dictate the respective flow equations. It would appear that Fetkovich's study answers the request in Vogel's paper for field verification; the Vogel correlation cannot be used without first determining that HVF effects are insignificant, and this can only be done by running a multirate test.

The present study builds on the suggestion that gas-and oilwell performance are similar and can be studied using a single approach. In particular, a dimensionless solution of the radial flow equation including HVF effects is presented in terms of the pseudopressure function. A simple correlation is given to estimate if HVF should be considered.

The oil pressure function is defined for both saturated and undersaturated oils with wellbore flowing pressures above and below the bubble point. The resulting expressions for dimensionless pseudopressure are simple to use (similar to Vogel's relation) and readily determined. It is shown that the Evinger-Muskat (EM) steady-state method of estimating oil pseudopressure is accurate enough to reproduce Vogel's results based on a numerical simulator. The EM method is simplified by the introduction of a generalized relative permeability relation. It also appears that the EM pseudopressure can be used to analyze transient well tests.

EQUATIONS AND DEFINITIONS

A general expression for the rate-pressure relation of a given phase (oil, gas, or water) is

$$q = C \cdot \int_{p_{wf}}^{p_R} F(p)dp, \quad \ldots\ldots\ldots\ldots\ldots\ldots\ldots\ldots\ldots\ldots \quad (1)$$

where q is surface rate; C is a constant composed of formation rock properties, drainage geometry, and nonideal characteristics such as partial penetration; F(p) is a pressure function evaluated from wellbore flowing pressure, p_{wf}, to average reservoir pressure, p_R.

Using the pressure function suggested by Al-Hussainy, Ramey, and Crawford[11] for real gas flow, Eq. 1 can be written

$$q_g = \frac{\pi akhT_{sc}}{Tp_{sc}\{\ln(r_e/r_w)-3/4+s\}} \cdot \int_{p_{wf}}^{p_R} (2p/\mu_g Z)dp. \quad \ldots. \quad (2)$$

Using the pressure function suggested by Evinger and Muskat for oil flow, Eq. 1 can be written

$$q_o = \frac{2\pi akh}{\{\ln(r_e/r_w)-3/4+s\}} \cdot \int_{p_{wf}}^{p_R} \frac{k_{ro}}{\mu_o B_o} dp. \quad \ldots\ldots\ldots\ldots \quad (3)$$

The definition of C and F(p) should be obvious for Eqs. 2 and 3. kh is the permeability-thickness product; r_e/r_w is the ratio of external-to-wellbore radius, suggesting a radial drainage area; -3/4 results from the assumption of pseudosteady-state flow, as does the use of p_R instead of initial or external boundary pressure; T is the reservoir temperature in absolute units, while T_{sc} and p_{sc} define standard conditions; s is the steady-state skin factor reflecting the composite effect of nonideal conditions; μ_g and μ_o are gas and oil viscosities; Z is the gas compressibility factor; a is a units conversion constant given in Table 1 for field and SPE preferred SI units.

The centered-well, radial-drainage assumption can be corrected by a skin factor (as suggested by M.J. Fetkovich in a personal communication) equal to $0.5 \cdot \ln(31.62/C_A)$, where C_A is the Dietz shape factor. Earlougher[12] gives values of C_A for numerous drainage shapes. By inspection it is seen that the effect of nonradial drainage boundaries is usually small: if C_A=0.1 (very nonradial or off-centered) then s=2.9, if C_A=10 (moderately nonradial) then s=0.6. The same observation is made qualitatively by Muskat.[1]

Transient Deliverability

The pseudosteady-state (pss) assumption is only valid if production time is long enough that the outer boundary has felt the effect of production. For tight, low-permeability formations or short production tests the pss assumption may need to be replaced by a transient (time-dependent) formulation. This is done by replacing p_R with initial reservoir pressure and the term $\ln(r_e/r_w)-3/4$ with an appropriate expression for dimensionless pressure.

In most situations, an expression for the transient form of $\ln(r_e/r_w)-3/4$ is the logarithmic approximation to dimensionless pressure, p_D, (t_D>10):

$$\ln(r_e/r_w)-3/4 \nLeftrightarrow p_D \simeq \tfrac{1}{2}\{\ln(t_D)+0.80907\}. \quad \ldots\ldots\ldots \quad (4a)$$

For stimulated wells with induced-vertical-fracture half-length , x_f, an early-time expression (t_D<0.1) is the uniform-flux approximation:

$$\ln(r_e/r_w)-3/4 \nLeftrightarrow p_D \simeq \sqrt{\pi t_D}, \quad \ldots\ldots\ldots\ldots\ldots\ldots\ldots \quad (4b)$$

which may apply for months or years in low-permeability reservoirs.

Dimensionless time, t_D, is given by

$$t_D = \frac{a_t k}{\phi \mu_i c_{ti} r_w^2} \cdot t. \quad \ldots\ldots\ldots\ldots\ldots\ldots\ldots\ldots\ldots\ldots \quad (5a)$$

If the well is vertically fractured then x_f should replace r_w in Eq. 5a; also, if Eq. 4a applies, then 0.80907 should be replaced by 2.80907. Other p_D solutions can be used instead of Eqs. 4a and 4b. Earlougher gives numerous p_D solutions applying to a variety of wellbore and external-boundary geometries for large ranges of t_D.

Production time required to use the simplified pss formulation is given by

$$t_{pss} = \frac{\phi \mu_i c_{ti} A}{a_t k} \cdot t_{DApss}. \quad \ldots\ldots\ldots\ldots\ldots\ldots\ldots\ldots \quad (5b)$$

For most applications, t_{DApss} of 0.1 can be used; this also applies to vertically fractured wells. Values of t_{DApss} for nonradial geometries can be found in Ref. 12. In Eqs. 5a and 5b, ϕ is porosity; μ_i and c_{ti} are viscosity and total compressibility at initial pressure; A is the drainage area; k is the absolute permeability and a_t is a units conversion factor given in Table 1 for field and SPE preferred SI units. For partially depleted reservoirs μ_i and c_{ti} should be evaluated at average reservoir pressure.

For many reservoirs it may take from a few hours to several weeks to reach pss conditions. In these cases the stabilized deliverability curve can be determined from a transient multirate test and should apply for long periods of time. The only change in deliverability results from changes in the pressure integral in Eq. 1.

Low-permeability (k<1md) formations may require years or even decades to reach stabilized flow. In such cases the concept of stabilized deliverability is no longer valid. The constant C in Eq. 1 changes continually and the deliverability relation must be updated accordingly. Both low- and moderate-permeability reservoirs may produce at a constant wellbore or surface pressure. Once again the concept of stabilized deliverability is not directly useful; inflow performance is a rate-time instead of a rate-pressure relation.

High Velocity Flow (Turbulence)

The effect of turbulence or high velocity flow (HVF) is not included in Eqs. 1 to 3. It is commonly accepted that gas flow can be influenced by HVF. This effect is usually expressed as a rate-dependent skin, Dq_g. Fetkovich gives conclusive evidence that HVF also exists in saturated and undersaturated oil systems. Field data suggest that HVF can dominate the oil-rate equation and that rate-dependent skin is equally applicable. Based on these observations the following developments were made to generalize the analysis of multirate gas- and oilwell tests, including prediction of stabilized deliverability.

First, an equation was developed to estimate the minimum rate, q_{HVF}, at which HVF effects might be expected,

$$q_{HVF} = a_{HVF} \frac{r_w h_p \mu}{\gamma}, \quad \ldots\ldots\ldots\ldots\ldots\ldots\ldots\ldots \quad (6)$$

where r_w is the wellbore radius; h_p is the perforated producing thickness; μ is gas or oil viscosity at the minimum-expected wellbore flowing pressure; γ is specific gravity of gas or oil at standard conditions, relative to air or water, respectively; a_{HVF} is a units conversion factor given in Table 1 for field and SPE preferred SI units. Eq. 6 is derived by assuming a Reynold's number of one at the onset of HVF, and an average grain diameter of 0.5mm.[1,10] The assumptions were made intentionally to give a pessimistic estimate of q_{HVF}.

For saturated-oil reservoirs, q_{HVF} for gas should be compared with gas rate calculated from $q_o(R-R_s)$ where q_o is the maximum oil rate expected during stabilized production, R is the producing gas-oil ratio (GOR) and R_s is the solution GOR at the minimum-expected wellbore flowing pressure. A multirate test should be run if either gas or oil q_{HVF} is lower than the maximum gas or oil rate expected during stabilized production.

Rewriting Eq. 1 and including rate-dependent skin, Dq, gives

$$q = C \frac{\ln(r_e/r_w)-3/4+s}{\ln(r_e/r_w)-3/4+s+Dq} \cdot \int_{p_{wf}}^{p_R} F(p)dp. \quad \ldots\ldots\ldots\ldots \quad (7)$$

The following definitions are made to simplify the following development:

$$m(p) = \int_{p_a}^{p} F(p)dp, \quad \ldots\ldots\ldots\ldots \quad (8a)$$

$$m_d = 1 - m(p_{wf})/m(p_R), \quad \ldots\ldots\ldots\ldots \quad (8b)$$

$$Q_{max} = C \cdot m(p_R), \quad \ldots\ldots\ldots\ldots \quad (8c)$$

$$q_d = q/Q_{max}, \quad \ldots\ldots\ldots\ldots \quad (8d)$$

$$D_d = \frac{Q_{max}}{\ln(r_e/r_w)-3/4+s} D. \quad \ldots\ldots\ldots\ldots \quad (8e)$$

The definition of pseudopressure function, m(p), uses atmospheric reference pressure (the lower integration limit) according to the definition of AOFP. m_d is a dimensionless form of the pseudopressure drop which equals q/Q_{max} if D=0. Q_{max} is a theoretical (no-HVF) AOFP, whereas the true AOFP, q_{max}, may only be a small fraction of Q_{max} if HVF effects are significant. The definition of dimensionless rate-dependent-skin term, D_d, results from the previous definitions.

Solving Eq. 7 in terms of dimensionless parameters gives

$$D_d \cdot q_d^2 + q_d - m_d = 0, \tag{9}$$

or

$$q_d = \frac{1 + (1 + 4 \cdot D_d \cdot m_d)^{0.5}}{2 \cdot D_d} \; ; \; D_D \neq 0, \tag{10a}$$

$$q_d = m_d \; ; \; D_d = 0. \tag{10b}$$

Fig. 1 presents the solutions of Eq. 9 graphically for several values of D_d. This log-log type curve has proven useful for analyzing multirate test data and predicting stabilized deliverability.

PRESSURE FUNCTIONS

The pressure function, F(p), in Eq. 1 is defined differently for gas and oil systems. The gas function only considers pressure effects caused by fluid properties; note that $p/\mu_g Z$ is directly porportional to $1/\mu_g B_g$. The oil function includes the pressure dependence of oil relative permeability, implying two-phase gas-oil flow. Gas condensate reservoirs also exhibit two-phase gas-oil flow. They are not considered here because of insufficient understanding and estimation of their PVT properties.

Gas Reservoirs

Calculation of the pseudopressure function can be simplified by making certain assumptions about the behavior of the pressure function.[13] F(p) for gases can be separated into three regions as shown in Fig. 2. The low-pressure region (<10000 kPa or 1500 psia) can be approximated by a straight line with zero intercept, yielding:

$$F(p) = 2\cdot\left(\frac{1}{\mu_g Z}\right)_{p*}\cdot p, \ \ldots\ldots\ldots\ldots\ldots\ldots\ldots\ldots\ldots \quad (11a)$$

and

$$m_d = 1 - (p_{wf}/p_R)^2, \ \ldots\ldots\ldots\ldots\ldots\ldots\ldots\ldots\ldots \quad (11b)$$

where $p*$ is any low pressure in the linear region. Eqs. 11 can actually be used in any pressure region if the drawdown is small enough and $p*$ is taken as the average of p_R and p_{wf}. Unfortunately this latter case is seldom found in practice and it should not be used unless the assumptions on which it is based are fully understood.

At high pressures (>22500 kPa or 3500 psia) the gas F(p) function is nearly constant and the following simplification results:

$$F(p) = 2\cdot\left(\frac{p}{\mu_g Z}\right)_{p*} \simeq \text{constant}, \;\ldots\ldots\ldots\ldots\ldots\ldots \quad (12a)$$

and

$$m_d = 1 - (p_{wf}/p_R), \;\ldots\ldots\ldots\ldots\ldots\ldots\ldots\ldots\ldots \quad (12b)$$

where $p*$ is any pressure in the region where F(p) is constant, though the value at p_R is often used. This case corresponds to a constant productivity index. The problem with using Eqs. 12 is that wellbore flowing and average reservoir pressure must always remain in the high-pressure region where F(p) is constant.

As the search for gas reservoirs goes deeper and to lower-permeability formations, the range p_R to p_{wf} often stretches over all three pressure regions, thus making both the low- and high-pressure assumptions invalid. In general the integral form of m(p) given in Eq. 2 should be solved numerically, graphically or analytically. The resulting m(p) function is valid for both wellbore flowing and average reservoir pressures during the entire production life of a gas well.[11]

Oil Reservoirs: Simplified Approach

Fetkovich suggests that F(p) for oil systems can be approximated by two straight lines joined at the bubble point. This is shown schematically in Figs. 3. Above the bubble point, F(p) only reflects the pressure dependence of oil viscosity and formation volume factor. Defining y as the ratio of $F(p_R)$ to $F(p_b)$, then

$$y = \frac{(\mu_o B_o)_{p_b}}{(\mu_o B_o)_{p_R}} . \qquad \ldots\ldots\ldots\ldots\ldots\ldots\ldots\ldots\ldots\ldots \quad (13)$$

for $p_R \geq p_b$.

Defining x as the ratio of $F(p_a)$ (i.e., at atmospheric pressure) to $F(p_b)$, then

$$x = \frac{(k_{ro}/\mu_o B_o)_{p_a}}{(k_{ro}/\mu_o B_o)_{p_b}} . \qquad \ldots\ldots\ldots\ldots\ldots\ldots\ldots\ldots\ldots\ldots \quad (14)$$

for $p_R \geq p_b$.

For undersaturated reservoirs there are two cases to consider, as shown in Figs. 3a and 3b. Case I corresponds to a completely undersaturated reservoir where $p_b \leq p_{wf} \leq p_R$. Case II corresponds to an undersaturated reservoir with wells producing at flowing pressures below the bubble point, or $p_{wf} \leq p_b \leq p_R$. For both cases the F(p) function is given by

$$F(p \geq p_b) = F_b + \frac{(1-y)F_b}{(p_b - p_R)} \cdot (p - p_b) \quad \ldots\ldots\ldots\ldots\ldots\ldots \quad (15a)$$

and

$$F(p \leq p_b) = x \cdot F_b + \frac{(1-x)F_b}{p_b} \cdot p. \quad \ldots\ldots\ldots\ldots\ldots\ldots \quad (15b)$$

Fig. 3c shows Case III for a saturated oil reservoir at or below its bubble point. Generalizing the definition of x as the ratio of $F(p_a)$ to $F(p_R)$ at $p_R \leq p_b$, and assuming it remains constant at all stages of depletion, the general form of the saturated-pressure function is

$$F(p \leq p_b) = x \cdot F_R + \frac{(1-x)F_R}{p_R} \cdot p. \quad \ldots\ldots\ldots\ldots\ldots\ldots \quad (16)$$

Using the linear relations suggested by Eqs. 15 and 16, the following three expressions for dimensionless pseudopressure, m_d, result:

$p_b \leq p_{wf} \leq p_R$: Completely Undersaturated

$$m_d = 2 \cdot v \cdot y \cdot (p_R/p_b - p_{wf}/p_b) + \frac{v \cdot (1-y)}{(p_R/p_b - 1)} \cdot (p_R/p_b - p_{wf}/p_b)^2, \quad \ldots\ldots\ldots\ldots\ldots \quad (17)$$

$p_{wf} \leq p_b \leq p_R$: Undersaturated; Saturated Flowing Pressure

$$m_d = 1 - 2 \cdot v \cdot x \cdot (p_{wf}/p_b) - v \cdot (1-x) \cdot (p_{wf}/p_b)^2, \quad \ldots\ldots \quad (18)$$

where

$$v = \frac{1}{(x+1)+(y+1)(p_R/p_b-1)}; \quad \ldots\ldots\ldots\ldots\ldots\ldots\ldots\ldots \quad (19)$$

$p_{wf} \leq p_R \leq p_b$: Completely Saturated

$$m_d = 1 - V(p_{wf}/p_R) - (1-V)(p_{wf}/p_R)^2, \quad \ldots\ldots\ldots\ldots \quad (20)$$

where

$$V = \frac{2 \cdot x}{(x+1)}. \quad \ldots\ldots\ldots\ldots\ldots\ldots\ldots\ldots\ldots\ldots\ldots\ldots \quad (21)$$

It was found that the minimum value of y for physically realistic systems ranges from 1.0 to 0.885 for p_R/p_b of 1.0 to 2.0, as shown in Fig. 4a. The effect of y on m_d (i.e., q_o/q_{omax} if D=0) is negligible, as shown in Fig. 4c. If y is set to one, then approximate expressions can be written for Eqs. 17, 18 and 19,

$p_b \leq p_{wf} \leq p_R$: Completely Undersaturated

$$m_d = 2 \cdot v \cdot (p_R/p_b - p_{wf}/p_b), \quad \ldots\ldots\ldots\ldots\ldots\ldots\ldots\ldots \quad (22)$$

$p_{wf} \leq p_b \leq p_R$: Undersaturated; Saturated Flowing Pressure

$$m_d = 1 - 2 \cdot v \cdot x \cdot (p_{wf}/p_b) - v \cdot (1-x) \cdot (p_{wf}/p_b)^2, \quad \ldots\ldots \quad (23)$$

where

$$v = \frac{1}{(x+1)+2(p_R/p_b-1)}; \quad \ldots\ldots\ldots\ldots\ldots\ldots\ldots\ldots \quad (24)$$

The general quadratic relation for saturated oils, Eqs. 20 and 21, can probably be used for both undersaturated and saturated conditions. The resulting simplicity should usually outweigh any loss in accuracy. The dashed curves in the lower half of Fig. 4c illustrate the potential error in using Eqs. 20 and 21. Fig. 5a shows the saturated-oil pressure function, relative to its value at average reservoir pressure, corresponding to various values of V in Eq. 20.

It cannot be overemphasized that **if HVF effects are** neglible ($D \approx 0$) then $m_d = q/q_{max}$. For example, the simplest relation, as suggested by **Fetkovich**, assumes the pressure function has zero intercept ($x=0; V=0$), resulting in

$$q/q_{max} = 1 - (p_{wf}/p_R)^2, \quad \ldots\ldots\ldots\ldots\ldots\ldots\ldots\ldots \quad (25)$$

which can be compared with **Vogel's relation** ($x=1/9; V=0.2$),

$$q/q_{max} = 1 - 0.2(p_{wf}/p_R) - 0.8(p_{wf}/p_R)^2. \;........\; (26)$$

Actually, Eq. 20 is a special case of Eq. 18 when $p_R/p_b=1$. The same quadratic form is given by Richardson and Shaw (see Fig. 5b). They suggest the equation as an intuitive generalization of Vogel's relation (V=0.2, D=0) for saturated reservoirs. Vogel's results actually show a variation in V from 0.1 to 0.7. It appears that V remains constant during most of depletion and increases after recoveries of 8 to 10% initial oil in place. Vogel's average value of V=0.2 corresponds to early depletion.

Physically, V of 0.2 for saturated reservoirs corresponds to a linear F(p) function with intercept equal to one-nineth the value at average reservoir pressure (see Fig. 5a). The value of $F(p_R)$ changes according to conditions dictated by the material balance, as shown schematically in Fig. 3c.

For all field examples given by Fetkovich (except Field A, which is a highly depleted, low-pressure reservoir), maximum drawdown is 20% or less. It can be shown that independent of the pressure function used, backpressure slope n appears the same at low drawdowns, though extrapolated AOFP's differ. Using delta-pressure-squared versus rate corresponds to assuming x of zero (V=0), which results in a relatively pessimistic AOFP. The error in AOFP and stabalized deliverability may vary, depending on the nature of the true pressure function. If HVF effects are not present (D=0) then the error caused by using the delta-pressure-squared plotting technique can be expressed as $-100 \cdot x/(1+x)$ percent.

Fig. 6 shows a Fetkovich example plotted as oil rate versus $1-(p_{wf}/p_R)^2$, corresponding to x of 0.0 or V of 0.0, and oil rate versus $1-0.4(p_{wf}/p_R)-0.6(p_{wf}/p_R)^2$, corresponding to x of 0.25 or V of 0.4. Backpressure slope, n, is the same for both curves ($\simeq$ 0.62), but AOFP's are 795 and 890 Sm^3/d (5000 and 5600 STB/D), respectively. The insert figure shows pressure functions corresponding to the two definitions of m_d. Fetkovich gives an analogous example (his Fig. 22) showing that delta-pressure (V=1, x=1) versus rate yields an AOFP of 5406 Sm^3/d (34000 STB/D), whereas using delta-pressure-squared (V=0,x=0) versus rate yields an AOFP of 1526 Sm^3/d (9600 STB/D); backpressure slopes of both plots are the same (n=0.81).

Oil Reservoirs: Evinger-Muskat Method

Evinger and Muskat suggest a method for calculating the m(p) function from PVT and relative permeability data. It assumes that producing GOR is constant at all points in the reservoir. This method is probably the most rigorous available without access to a simulator. It is shown in this study that Vogel's results, based on a numerical model, can be reproduced using the steady-state method of Evinger and Muskat (see Fig. 7).

First, PVT properties (R_s, B_o, μ_o, B_g and μ_g) are tabulated from initial to atmospheric pressure (see Table 2). The producing GOR, R, is specified. At each tabulated pressure the gas-oil relative permeability ratio, k_{rg}/k_{ro}, is calculated from the relation

$$k_{rg}/k_{ro}(p) = \{R-R_s(p)\} \frac{\mu_g(p)B_g(p)}{\mu_o(p)B_o(p)} \quad .... \quad (27)$$

If experimental relative permeability data are available, k_{rg}/k_{ro} should be plotted directly versus k_{ro}, as shown in Fig. 8. If experimental data are not available, then one of the curves in Fig. 8 can be used. Pore size distribution factor of one should be used for most reservoirs; ten applies to unconsolidated sandstones and one-half to highly consolidated sandstones.

Having calculated $k_{rg}/k_{ro}(p)$ from Eq. 27, $k_{ro}(p)$ is found from the relative permeability relation. The pressure function $k_{ro}/\mu_o B_o$ is tabulated and plotted versus pressure. The m(p) function can be calculated numerically as follows. First, $F(p)\cdot\Delta p$ is calculated at p_k, where F(p) is the average of values evaluated at pressures p_k and p_j, and $\Delta p=p_k-p_j$. The m(p) function is calculated by summing the

$F(p)\cdot\Delta p$ values, starting at atmospheric pressure. The calculation procedure is shown in Table 2.

Dimensionless pseudopressure, m_d, can be calculated and plotted versus p/p_R as shown in Fig. 7. The best-fit value of V for Vogel's results is 0.2. The Evinger-Muskat methoa usually reproduces simulated results with good accuracy.

The EM method also can be applied to analysis of transient well tests. Although this application is not rigorous it appears to be accurate enough for practical puposes.

Raghavan[14] suggests separate drawdown and buildup pseudopressure functions. The calculation procedure for each is essentially the same as proposed by Evinger and Muskat. At a given drawdown time and wellbore flowing pressure, producing GOR is used to calculate k_{rg}/k_{ro} (Eq. 27), and therefrom k_{ro}, k_{ro}/μ_oB_o and $m(p_{wf})$. Producing GOR at shut-in is assumed to apply throughout the buildup period.

Boe, et al.[15] show that after very short times the producing GOR becomes constant during transient testing. In practice this means that observed GOR is constant during a drawdown test and can be used to calculate both drawdown and buildup m(p) functions. This method was used to analyze drawdown and buildup tests given by Raghavan, resulting in estimated permeabilities of 6.19 and 6.45 md, respectively; model permeability of 6.16 md is reported by Raghavan. Producing GOR's used by the EM method in each case were 69.10 Sm^3/Sm^3 (388 scf/STB) and 333.2 Sm^3/Sm^3 (1871 scf/STB), respectively.

Boe, et al.'s drawdown and buildup tests were also analyzed using the EM method with R of 267.2 Sm^3/Sm^3 (1500 scf/STB). Estimated permeabilities were 11.8 (short DD), 12.3

(BU; short DD) and 10.6 (BU; long DD). Model permeability reported by Boe, et al. is 10 md. Although the estimated permeabilities are only approximate, they are a considerable improvement over using pressure only.

One problem with using the EM method is when producing GOR is less than R_s at a given drawdown or buildup pressure. Eq. 22 gives negative k_{rg}/k_{ro} for this situation, which also can arise using the Raghavan buildup method; Raghavan does not address the problem. Based on limited results in this study it appears that bubble-point GOR can be used instead of producing GOR if $R<R_{sb}$. In practice this situation only arises at early stages of depletion before critical gas saturation has been reached throughout the drainage radius of the well.

ANALYZING MULTIRATE TEST DATA

A general procedure is suggested for analyzing multirate test data for gas and oil reservoirs. The dimensionless log-log type curve is used to determine HVF effects and predict deliverability. If only a single-rate well test is available, then the same procedure is followed without type-curve matching; a value of D_d is assumed (e.g. zero) or estimated from a correlation.

Procedure

1. Organize and tabulate available rock and fluid data for the particular well.

2. Determine the pseudopressure function.

- For gas reservoirs m(p) is defined by PVT data - namely μ_g and Z. First plot $p/\mu_g Z$ versus pressure, then integrate using atmospheric base pressure. Numerical integration using the trapezoid rule is often simple and accurate (Table 3 gives an example of the procedure).

- For oil reservoirs the EM method can be used to estimate m(p). Assuming $R=R_{sb}$, k_{rg}/k_{ro}, k_{ro}, $k_{ro}/\mu_o B_o$, and m(p) are calculated. For undersaturated reservoirs the process is continued at $p>p_b$ holding k_{ro} at its initial (gas-free) oil value. For partially depleted reservoirs R may be considerably greater than R_{sb} and the EM procedure can be repeated. The results can then be simplified by plotting m_d versus p/p_R and fitting the data to one of the curves in Fig. 4. The best-fit value of V is then used with the generalized m_d relation (Eq. 21).

Using the straight-line pressure function for saturated oils, m(p) need only be calculated at average reservoir pressure. The necessary relations are:

$$m(p) = \left(\frac{k_{ro}}{\mu_o B_o}\right)_{p_R} \cdot \int_0^p \{x + \frac{(1-x)p}{p_R}\}dp \quad \ldots\ldots\ldots\ldots \quad (28a)$$

or

$$m(p) = \left(\frac{k_{ro}}{\mu_o B_o}\right)_{p_R} \cdot \{x \cdot p + \frac{(1-x) \cdot p^2}{2p_R}\}. \quad \ldots\ldots\ldots\ldots \quad (28b)$$

If V is assumed, then x equals V/(2-V). Based on Vogel's results, V is 0.2 and x is 1/9, resulting in

$$m(p) = \frac{1}{9}\cdot\left(\frac{k_{ro}}{\mu_o B_o}\right)_{p_R} \cdot \left(p + \frac{4}{p_R}\cdot p^2\right) \quad \ldots\ldots\ldots\ldots\ldots (29a)$$

Assuming x=0 and V=0, as suggested by Fetkovich, results in a simpler relation which is recommended for practical applications,

$$m(p) = \frac{1}{2p_R}\cdot\left(\frac{k_{ro}}{\mu_o B_o}\right)_{p_R}\cdot p^2 \quad \ldots\ldots\ldots\ldots\ldots\ldots\ldots\ldots (29b)$$

For undersaturated oils, first calculate $m(p_b)$ using Eq. 28 or 29 and $p_R=p_b$. m(p) at undersaturated pressures is calculated from

$$m(p) = m(p_b) + \frac{1}{2}\cdot(1+y)(p-p_b)\cdot\left(\frac{k_{ro}}{\mu_o B_o}\right)_{p_b}\cdot \quad \ldots\ldots\ldots\ldots (30)$$

3. Note $m(p_R)$.

4. Convert each wellbore flowing pressure to a dimensionless pseudopressure m_d.

5. Plot m_d versus rate on tracing paper, using the grid of Fig. 1.

6. Match the data with one of the D_d type curves by adjusting the tracing paper from left to right, making sure that axes are held parallel to the type curve. Only one degree of freedom is allowed in the matching process. This should ensure a unique match.

7. Note the match point: q_M, q_{dM} and D_d.

8. Calculate the theoretical maximum AOFP, $Q_{max} = q_M/q_{dM}$. True AOFP, q_{max}, is read from the matched type curve at m_d of 1.

9. Assuming permeability is known, calculate the term $\ln(r_e/r_w)-3/4+s$. For gas wells,

$$\{\ln(r_e/r_w)-3/4+s\} = \frac{\pi akhm(p_R)}{Q_{max}} \cdot \frac{T_{sc}}{T \cdot p_{sc}}, \quad \text{..........} \quad (31a)$$

and for oil wells,

$$\{\ln(r_e/r_w)-3/4+s\} = \frac{2\pi akhm(p_R)}{Q_{max}} \quad \text{.................} \quad (31b)$$

10. Calculate D from $\{\ln(r_e/r_w)-3/4+s\} \cdot D_d/Q_{max}$.

11. Determine if flow periods are stabilized - i.e., if pss has been reached. If wellbore flowing pressure versus time plots as a straight line on cartesian coordinates, then flow is probably stabilized during production. When pressure-time data are not available, Eq. 5b can be used to estimate if production time is greater than t_{pss}.

12a. If t_{pss} is reached during flow periods then the rate-m_d curve traced from the type curve is the stabilized deliverability curve. The term $\ln(r_e/r_w)-3/4$ should be estimated from drainage area, though a value near eight should usually suffice.

12b. If t_{pss} is not reached during flow periods then the term $\ln(r_e/r_w)-3/4$ should be estimated from a p_D function, e.g., Eq. 4a or 4b.

13. Calculate skin by subtracting $\ln(r_e/r_w)-3/4$ found in Step 12, from $\ln(r_e/r_w-3/4+s$, found in Step 9.

14. If a change in skin is anticipated, say from a stimulation treatment, then the test deliverability can be shifted to reflect the change in skin. This is done by calculating a new AOFP as

$$q_{max,new} = q_{max,test} \cdot \frac{\{\ln(r_e/r_w)-3/4+s\}_{test}}{\{\ln(r_e/r_w)-3/4+s\}_{new}} \quad .... \ (32)$$

The new value is located on the tracing paper at m_d of 1; this point is aligned with the type curve found from the test-data match and a new deliverability curve is drawn.

The same procedure is followed for low-permeability reservoirs having a transient rate solution. $\ln(r_e/r_w)-3/4$, or more correctly, p_D, can be calculated at several times (e.g., 1, 2, 5, and 10 years) and deliverability curves drawn for each time based on corrected q_{max} (Eq. 32).

Appendix A discusses the method suggested by Standing for correcting the rate equation in saturated-oil reservoirs which are damaged (HVF effects are neglected by Standing).

15. For saturated-oil reservoirs a similar correction must be made because of depletion. Material balance results can be used to estimate $k_{ro}/\mu_o B_o$ at several points of depletion. The procedure is to correct the true AOFP and shift the deliverability curve using the following relation:

$$q_{max,new} = q_{max,test} \cdot \frac{(k_{ro}/\mu_o B_o)_{p_{R,new}}}{(k_{ro}/\mu_o B_o)_{p_{R,test}}} \cdot \frac{p_{R,new}}{p_{R,test}} \quad (33)$$

This simplified correction for depletion is the same as proposed by Standing[7] using the Vogel pressure function. It is also suggested by Fetkovich.

An alternative method is to calculate the EM m(p) function at each new producing GOR. The engineer must decide if the extra calculations are justified for predicting future deliverability.

EXAMPLE 1: SIMULATED GASWELL MODIFIED ISOCHRONAL TEST (MIT)

The first example considers a low-permeability gas reservoir with rock and fluid properties given in Table 3. A numerical model including turbulence effects was used to simulate the test procedure given in Table 4. The model was checked against numerous published results.

Data from the 24-hour buildup are analyzed in Fig. 9. Calculated permeability (0.009 md) is about 10% lower than model permeability. Calculated skin (0.87) is about 33% lower than calculated by subtracting $p_D(t_D)$ (Eq. 4a) from calculated m_D at $p_{wf,s}$. Deviations result from the relatively short production period (12 hours); transient effets do not reach far into the reservoir, and turbulence dominates the small drainage region. Since similar errors might be expected in actual tests of low-permeability reservoirs, the calculated k and s are used to analyze MIT results.

MIT data given in Table 4 are analysed using the previously proposed procedure. Starting with step 3, results are as follow:

3. $m(p_R)$ is equal to $m(p_i)$ or $2.973 \cdot 10^7$ kPa²/Pa·s. For MIT, however, the correct $m(p_R)$ to use for calculating m_d (Step 4) is $m(p)$ corresponding to p_{ws} immediately before the drawdown begins. For rates 565.2, 1130.5, 1695.7, and 2261.0 Sm³/d, $m(p_R)$ are $2.965 \cdot 10^7$, $2.935 \cdot 10^7$, $2.889 \cdot 10^7$, and $2.834 \cdot 10^7$ kPa²/Pa·s, respectively.

4. Table 4 gives m_d for each wellbore flowing pressure.

5. Fig. 10 shows the type-curve match of q_g-m_d data using Fig. 1.

6. The D_d=2 type curve is chosen to give a best-fit.

7. The match point is chosen as q_{gM}=6218 Sm³/d at q_{DM}=1.

8. The theoretical AOFP is 6218 Sm³/d. True AOFP of 3109 Sm³/d is read from Fig. 10 at m_d of 1.

9. Using calculated permeability (0.009 md) and Eq. 29a, $\ln(r_e/r_w)-3/4+s$ is 2.833.

10. D is 2.833x2/6218 or $9.11 \cdot 10^{-4}$ 1/Sm³/d. Using the model value for HVF factor, β, D is $1.06 \cdot 10^{-3}$ 1/Sm³/d, a reasonable check. Although skin resulting from HVF effects at 3109 Sm³/d is only 3, it reduces AOFP to half its theoretical (no-HVF) value.

11. Production after 8 hours is not stabilized, as is easily shown by calculating t_D of $6.20 \cdot 10^{-5} \cdot t(hr)$, or t_D (t=8hr) of $4.96 \cdot 10^{-4}$. To reach pss after only 8 hours would require a drainage radius of 6.71 m, clearly smaller than the true drainage area.

12b. The term $\ln(r_e/r_w)-3/4$ is replaced by $p_D(t_D)$ given by Eq. 4a, and equals 3.230.

13. Steady-state skin is 2.833-3.230 or -0.4, which should be compared with zero used in the model. Practically, the

value of -0.4 would be interpreted as zero since no stimulation has been used.

14. This gas well is an obvious candidate for acid- or hydraulic-fracture treatment. Assuming a vertical fracture of 76.2 m half-length can be created, the following analysis is performed.

After stimulation, test deliverability will shift to the right in Fig. 10. Using Eq. 32, the true AOFP at 1, 2, 5, 10, and 25 years is calculated and given in Table 5. Fig. 10 shows the shifted deliverability curves; note that the original test curve is reached after 25 years.

If the well produces at constant wellhead pressure, then a tubing performance curve can be imposed on Fig. 10. This would yield rate as a function of time, the relation needed for engineering design.

EXAMPLE 2: SATURATED OILWELL ISOCHRONAL TEST

The basic data for this example are taken from Fetkovich's Well 5-C, Field D. PVT and relative permeability data were estimated from correlations (Table 6). Measured rates and pressures at the end of each 4-hour drawdown are given in Table 7. Six months separate the two four-point tests and average reservoir pressure has dropped about 690 kPa.

Pseudopressures are calculated using the EM method assuming R equal to the bubble-point solution GOR. $m(p_i)$ equals 19.63 kPa/Pa·s. After depletion of 690 kPa, $k_{ro}/\mu_o B_o$ at average reservoir pressure of 24821 kPa is 90% its initial value. Using the producing GOR calculated by a Tarner material balance (Table 6), pseudopressures are recalculated. $m(p_R)$ is 97% $m(p_i)$, considerably less change than $k_{ro}/\mu_o B_o$ experiences. This suggests a potential error using the correction procedure given by Eq. 30. The following analysis uses $m(p)$ calculated by the EM method at producing GOR.

The test data are analyzed using the multirate procedure presented earlier. Starting with Step 3, results are as follow:

3. $m(p_i)$ is 19.63 kPa/Pa·s. At p_R of 24821 kPa, $m(p_R)$ is 19.07 kPa/Pa·s.

4. Wellbore flowing pressures are converted to m_d in Table 7.

5. Fig. 11 shows the type-curve match of q_o-m_d with Fig. 1.

6. The D_d=20 type curve is chosen to give a best-fit. Flows A-3 and B-1 appear to deviate from the other data.

7. The match point is q_{oM} of 7631 Sm³/d at q_{DM} of 1.

8. Theoretical AOFP is 7631 Sm³/d. True AOFP is 1526 Sm³/d, as read from Fig. 11 at m_d of 1.

9. Using permeability reported by Fetkovich from buildup analysis and core data (2470 md), $\ln(r_e/r_w)-3/4+s$ is 20.4 using Eq. 31b. $m(p_R)$ of 28 kPa/Pa·s is assumed.

10. D is 20.4x20/7631 or 0.0535 1/Sm³/d.

11. Time to pseudosteady-state flow, t_{pss}, based on a drainage area of $2.59\cdot10^6$ m² (640 acres) is approximately six hours.

12a. The term $\ln(r_e/r_w)-3/4$ is replaced by $p_D(t_D)$. Using Eq. 4a, its value is 8.7.

13. Steady-state skin is 20.4-8.7 or 11.7.

14. If steady-state skin calculated in Step 13 is due to damage (well is fully penetrating), then an acid treatment should clean up the near-wellbore region. Assuming skin can be reduced to zero, the change in deliverability is estimated by correcting the true AOFP and shifting the deliverability curve. Also, $\ln(r_e/r_w)-3/4$ at stabilized conditions should replace $p_D(t_{D4hr})$. For 640-acre spacing, the value of $\ln(r_e/r_w)-3/4+s$ is 8.35 with $s=0$. Stabilized AOFP is 1526x20.4/8.35 or 3729 Sm^3/d. The deliverability curve is shown in Fig. 11.

The above procedure was repeated using the delta-pressure-squared procedure suggested by Fetkovich. Results are presented in Table 7 and Fig. 11 (dashed lines).

CONCLUSIONS

The purpose of this paper has been to review well-known aspects of predicting reservoir well performance and to present some new concepts which have been developed. Perhaps the most important point to be made is that gas- and oilwell tests should be conducted and analyzed in the same manner. The study gives a description of nonideal behavior of gas and oil flow; in particular, high velocity flow (turbulence) and variation in the pressure function have been described. Several conclusions are made based on the results of this study:

1. A dimensionless solution of the radial flow equation has been developed. It accounts for rate-dependent effects,

steady-state skin, and variation in the pressure function. The solution is equally applicable to gas and oil wells.

2. The Vogel inflow performance relation has been given physical meaning. It represents an expression of the radial flow equation based on the following two assumptions: (a) no high-velocity-flow effects are present (D=0), and (b) the saturated-oil pressure function, $k_{ro}/\mu_o B_o$, is a linear function with intercept at atmospheric pressure having one-nineth the value at average reservoir pressure.

3. General expressions for dimensionless pseudopressure of oil wells are developed based on the straight-line pressure functions suggested by Fetkovich. These expressions, equal to Vogel's dimensionless rate, q_o/q_{omax}, if rate-dependent effects are negligible, are applicable to undersaturated- and saturated-oil reservoirs producing at wellbore flowing pressures above and below the bubble point.

4. A good approximation of dimensionless pseudopressure for oil wells producing at saturated or undersaturated reservoir pressures is the original Vogel expression for dimensionless rate. The possible error introduced by using the Vogel relation is no larger than reported by Vogel for saturated systems having different PVT and relative permeability relations than the reservoir used to develop his general correlation.

5. The Evinger-Muskat method for predicting oilwell performance at saturated conditions is reviewed. The method is made easier-to-use by introducing generalized relative permeability curves.

6. It is shown that the Evinger-Muskat method for calculating oil pseudopressure is applicable to transient well test analysis. Saturated-oil drawdown and buildup

tests reported in the literature were used to check the validity of the method.

7. A general procedure is given for analyzing multirate tests performed on gas and oil wells. Two examples illustrate the procedure.

8. Standing's method for correcting the Vogel relation for damaged and stimulated wells is discussed. The assumptions on which it is based are given, and improvements are suggested. It appears that the original method is physically unrealistic for wells with negative skin.

NOMENCLATURE

a = units-conversion constant in flow equation
a_{HVF} = units-conversion constant in high-velocity-flow equation
a_t = units-conversion constant in dimensionless-time equations
A = area, m^2 (ft^2)
B = formation volume factor, m^3/Sm^3 (ft^3/scf or RB/STB for gas or oil, respectively)
c_{ti} = initial (or average reservoir pressure) total compressibility, kPa^{-1} (psi^{-1})
C = constant in flow equation
D = high-velocity-flow term, $1/Sm^3/d$ ($1/scf/d$)
D_d = dimensionless high-velocity-flow term
E_F = flow efficiency
$F(p)$ = pressure function (also F; $F_b = F(p_b)$, etc.), $kPa^2/Pa{\cdot}s$ or $kPa/Pa{\cdot}s$ ($psia^2/cp$ or $psia/cp$) for gas or oil, respectively
h = total formation thickness, m (ft)
h_p = perforated or producing thickness, m (ft)
k = absolute permeability, μm^2 ($md \simeq \mu m^2$)
k_{rg} = relative permeability to gas
k_{ro} = relative permeability to oil
m = semi-log slope of Horner plot, $kPa^2/Pa{\cdot}s/cycle$ or $kPa/Pa{\cdot}s/cycle$ ($psia^2/cp/cycle$ or $psia/cp/cycle$) for gas or oil, respectively
$m(p)$ = pseudopressure function, $kPa^2/Pa{\cdot}s$ or $Kpa/Pa{\cdot}s$ ($psia^2/cp$ or $psia/cp$) for gas or oil, respectively
m_d = dimensionless pseudopressure function
n = reciprocal of slope of log-log rate-pseudopressure (backpressure) curve
p = absolute pressure, kpa (psia)
p^* = specific pressure in low- or high-pressure region

of gas reservoirs, kPa (psia)

p_a = atmospheric pressure, kPa (psia)

p_b = bubble-point pressure, kPa (psia)

p_D = dimensionless pressure

p_R = average reservoir pressure, kPa (psia)

p_{sc} = pressure at standard conditions, kPa (psia)

p_{skin} = average pressure in the skin region, kPa (psia)

p_{wf} = measured wellbore flowing pressure, kPa (psia)

$p_{wf,s}$ = wellbore flowing pressure at shut-in, kPa (psia)

Δp_s = pressure drop due to skin in near-wellbore region, kPa (psia)

q_d = dimensionless rate = q/Q_{max}

q_g = surface gas rate, Sm^3/d (scf/D)

q_{HVF} = surface rate at the onset of high velocity flow (turbulence), Sm^3/d (scf/D or STB/D for gas or oil, respectively)

q_{max} = true maximum surface rate (AOFP), Sm^3/d (scf/D or STB/D for gas or oil, respectively)

Q_{max} = theoretical maximum surface rate (AOFP) if a well had no HFV effects, Sm^3/d (scf/D or STB/D for gas or oil, respectively)

r_e = external-boundary drainage radius, m (ft)

r_w = wellbore radius, m (ft)

R = producing gas-oil ratio, Sm^3/Sm^3 (scf/stb)

R_s = solution gas-oil ratio, Sm^3/Sm^3 (scf/stb)

s = steady-state skin factor

S = saturation, fraction

t = time, hours unless otherwise specified

t_D = dimensionless time

t_{pss} = time to reach pseudosteady state, hours

t_{DApss} = dimensionless time to reach pseudosteady state

T = absolute temperature, K (^{o}R)

T_{sc} = absolute temperature at standard conditions, K (^{o}R)

V = parameter in general quadratic rate equation

x = ratio of pressure function $F(p)$ at atmospheric pressure to $F(p)$ at average reservoir pressure (saturated-oil reservoirs); ratio of pressure function $F(p)$ at atmospheric pressure to $F(p)$ at bubble-point pressure (undersaturated-oil reservoirs)

x_F = vertical-fracture half-length, m (ft)

y = ratio of pressure function $F(p)$ at average reservoir pressure to $F(p)$ at bubble-point pressure for undersaturated reservoirs

Z = real-gas compressibility factor

Greek Symbols

μ = viscosity, Pa·s (cp)

ϕ = porosity, fraction

Subscripts

g = gas

new = evaluated at new reservoir conditions

o = oil

test = evaluated at test conditions

Superscripts

$E_F=1$ = value of property (q or p_{wf}) which would be measured if steady-state skin was zero (flow efficiency equal to one)

$E_F\neq 1$ = rate which would be measured if steady-state skin was nonzero (flow efficiency different than one)

REFERENCES

1. Muskat, M.: Physical Principles of Oil Production, International Human Resources Development Corporation, Boston(1981).

2. Hurst, W. "Establishment of the Skin Effect and Its Impediment to Fluid Flow Into a Wellbore," Pet.Eng. (Oct.,1953) Vol. 25,B-6.

3. van Everdingen, A.F.: "The Skin Effect and Its Influence on the Productive Capacity of a Well," Trans., AIME (1953), Vol. 198, 171-176.

4. Evinger, H.H. and Muskat, M.: "Calculation of Theoretical Productivity Factor," Trans., AIME (1942) Vol. 146, 126-139.

5. Vogel, J.V.: "Inflow Performance Relationships for Solution-Gas Drive Wells," J.Pet.Tech. (Jan., 1968) 83-92.

6. Standing, M.B.: "Inflow Performance Relationships for Damaged Wells Producing by Solution-Gas Drive," J.Pet.Tech. (Nov., 1970) 1399-1400.

7. Standing, M.B.: "Concerning the Calculation of Inflow Performance of Wells Producing from Solution Gas Drive Reservoirs," J.Pet.Tech. (Sept., 1971) 1141-1142.

8. Patton, L.D. and Goland, M.: "Generalized IPR Curves For Predicting Well Behavior," Pet.Eng. (Sept., 1980) 92-102.

9. Richardson, J.M. and Shaw, A.H.: "Two-Rate IPR Testing - A Practical Production Tool," J.Can.Pet.Tech. (March-April, 1982) 57-61.

10. Fetkovich, M.J.: "The Isochronal Testing of Oil Wells," paper SPE 4529 presented at the SPE-AIME 48th Annual Fall Meeting, Las Vegas, Nev., Sept.30-Oct.3, 1973.

11. Al-Hussainy, R., Ramey, H.J., Jr., and Crawford, P.B.: "The Flow of Real Gases Through Porous Media," J.Pet.Tech. (May, 1966) 624-636; Trans., AIME, Vol. 237.

12. Earlougher, R.C., Jr.: Advances in Well-Test Analysis, SPE Monograph Series, Vol. 5, Dallas (1977).

13. Theory and Practice of the Testing of Gas Wells, Energy Resources Conservation Board, Calgary, Alberta, Canada, Chapter 4.

14. Raghavan, R.: "Well Test Analysis: Wells Producing by Solution Gas Drive," J.Pet.Tech. (Aug., 1976) 196-208; Trans., AIME, Vol. 261.

15. Boe, A., Skjaeveland, S.M., and Whitson, C.H.: "Two-Phase Pressure Test Analysis," paper SPE 10224 presented at the SPE-AIME 56th Annual Fall Meeting, San Antonio, Tex., Oct. 5-7, 1981.

16. Dias-Couto, L.E. and Golan, M.: "General Inflow Performance Relationship for Solution-Gas Reservoir Wells," J.Pet.Tech. (Feb., 1982) 285-288.

APPENDIX A - DISCUSSION OF STANDING'S METHOD FOR CORRECTING INFLOW PERFORMANCE OF DAMAGED/STIMULATED WELLS

Standing suggests a method for using the Vogel relation to average results of multirate tests and to correct for damage or stimulation in the near-wellbore region. The averaging procedure should probably not be used since valuable data showing rate-dependent skin effects might be lost.

To ease the comparison with Standing's work it is assumed that HVF effects are neglible (D=0) and that dimensionless pseudopressure, m_d, equals the Vogel rate-ratio, q_o/q_{omax}. This assumption, as shown by Fetkovich, may result in erroneous interpretation of test data.

Instead of limiting the discussion to Vogel's relation, equations are developed in terms of the general quadratic form (Eq. 20). Following Standing's arguments, the ratio of rate to AOFP with $E_F = 1$ (no-skin) is

$$q_o/q_{omax}^{E_F=1} = 1 - V(p_{wf}^{E_F=1}/p_R) - (1-V)(p_{wf}^{E_F=1}/p_R)^2, \ \ldots \quad \text{(A-1)}$$

The no-skin wellbore flowing pressure, $p_{wf}^{E_F=1}$, is given by

$$p_{wf}^{E_F=1} = p_{wf} + \Delta p_s. \ \ldots\ldots\ldots\ldots\ldots\ldots \quad \text{(A-2)}$$

where p_{wf} is the measured wellbore flowing pressure, and Δp_s is pressure drop due to skin - positive for positive skin and negative for negative skin.

Using the definition of flow efficiency,

$$E_F = \frac{p_R - p_{wf} - \Delta p_s}{p_R - p_{wf}}, \quad \text{.........................} \quad (A\text{-}3)$$

the no-skin wellbore flowing pressure is given by

$$p_{wf}^{E_F=1} = p_{wf} \cdot E_F + (1-E_F) \cdot p_R. \quad \text{....................} \quad (A\text{-}4)$$

Standing suggests that E_F be estimated by

$$E_F \simeq \frac{\ln(r_e/r_w)-3/4}{\ln(r_e/r_w)-3/4+s}. \quad \text{.........................} \quad (A\text{-}5)$$

To arrive at this expression the oil pressure function, F(p), must be approximately the same at average pressure and in the skin zone. It also assumes that pressure drop in the reservoir is given by

$$q_o = \frac{2\pi akh}{\ln(r_e/r_w)-3/4} \cdot \frac{k_{ro}}{\mu_o B_o} \cdot (p_R - p_{wf}^{E_F=1}), \quad \text{............} \quad (A\text{-}6)$$

If $k_{ro}/\mu_o B_o$ is evaluated at the average of p_R and $p_{wf}^{E_F=1}$, then Eq. A-6 is consistent with the Vogel relation. The pressure function in the near-wellbore region is probably less than tzis value. A more correct expression for E_F is given by

$$E_F = \frac{\ln(r_e/r_w)-3/4}{\ln(r_e/r_w)-3/4 + s\cdot F(p_{avg})/F(p_{skin})} \;.\;\ldots\ldots\; \text{(A-7)}$$

The ratio $F(p_{avg})/F(p_{skin})$ can be shown to equal

$$\frac{F(p_{avg})}{F(p_{skin})} = \frac{2x + (1-x)\{2+E_F(p_{wf}/p_R-1)\}/2}{2x + (1-x)\{1-E_F+(1+E_F)p_{wf}/p_R\}/2} \;,\;\ldots\; \text{(A-8)}$$

which can be simplified by evaluating the pressure function in the near-wellbore region at the measured wellbore flowing pressure, p_{wf},

$$\frac{F(p_{avg})}{F(p_{skin})} \simeq \frac{2x + (1-x)(1+p_{wf}/p_R)/2}{2x + (1-x)\cdot p_{wf}/p_R} \;.\;\ldots\ldots\ldots\ldots\; \text{(A-9)}$$

Fig. A-1 shows the influence of the pressure-function ratio on flow efficiency for several values of positive skin; $\ln(r_e/r_w)-3/4$ equal to 7 and Vogel's pressure function ($x=1/9$) are used. The influence is greatest at large drawdowns (low p_{wf}/p_R values) and skin less than 10. The approximation given by Eq. A-9 is good at p_{wf}/p_R above 0.5 but is relatively large for large drawdowns with skin values of 3 to 5. The correction should not be applied to wells with negative skin factors.

Using the Standing procedure for stimulated wells can lead to nonphysical results. Fig. A-2 shows the case of a well with E_F of 1.5 (highly stimulated). The no-skin wellbore flowing pressure is <u>negative</u> at measured wellbore flowing pressures less than $p_R(E_F-1)/E_F$; one-third p_R for E_F of 1.5. Also, at measured wellbore flowing pressures less than

$p_R \cdot \{(E_F - 1 - x/(1-x)/E_F\}$ the rate <u>decreases</u> with increasing drawdown; at one-fourth p_R for E_F of 1.5 using Vogel's relation.

Assuming an estimate of E_F can be made, the general rate-pressure relation using Standing's arguments is

$$q_o/q_{omax}^{E_F=1} = 1 - V\{(p_{wf}/p_R)E_F + (1-E_F)\} - (1-V)\{(p_{wf}/p_R)E_F + (1-E_F)\}^2, \quad \ldots\ldots \quad \text{(A-10)}$$

or

$$q_o/q_{omax}^{E_F\neq 1} = \frac{q_o/q_{omax}^{E_F=1}}{1 - V(1-E_F) - (1-V)(1-E_F)^2}. \quad \ldots\ldots\ldots \quad \text{(A-11)}$$

The denominator in Eq. A-11 represents the ratio of AOFP with skin to AOFP without skin. Eq. A-10 reproduces Standing's Fig. 2 for V of 0.2 (x of 1/9); an equivalent expression is given by Couto and Golan[16] for V of 0.2.

TABLE 1 - UNITS CONVERSION FACTORS

Quantity	Field		SPE Preferred SI	
	Gas	Oil	Gas	Oil
a	0.006328	0.001127	$8.527 \cdot 10^{-8}$	
a_t	0.0002637		$3.553 \cdot 10^{-9}$	
a_{HVF}	$3.061 \cdot 10^6$	634.5	$9.326 \cdot 10^8$	$1.085 \cdot 10^6$
k	md		md ($\simeq \mu m^2$)	
h	ft		m	
r	ft		m	
p	psia		kPa	
c	1/psi		1/kPa	
μ	cp		Pa·s	
γ	air=1	water=1	air=1	water=1

TABLE 2 - ROCK AND FLUID PROPERTIES FOR VOGEL DATA

	Read From Vogel's Fig. 9a					Evinger-Muskat Method Using R of 102.4 Sm³/Sm³					
p (kPa)	R_s (Sm³/Sm³)	B_o (m³/Sm³)	$\mu_o \cdot 10^3$ (Pa·s)	$B_g \cdot 10^3$ (m³/Sm³)	$\mu_g \cdot 10^3$ (Pa·s)	k_{rg}/k_{ro} (Eq.22)	k_{ro} (below)	F(p) (1/Pa·s)	$\Delta m \cdot 10^{-3}$ (kP/Pa·s)	$m(p) \cdot 10^{-3}$ (kP/Pa·s)	m_d
14686	102.4	1.30	1.03	6.67	0.0195	0.0	0.444	331.6	276.8 a	2553.1	0.000
13790	98.85	1.29	1.04	7.13	0.0188	0.000356	0.384	286.1	469.8	2276.3	0.108
12066	93.51	1.28	1.12	8.08	0.0178	0.000893	0.371	259.1	419.8	1806.5	0.292
10342	85.49	1.27	1.22	9.46	0.0169	0.00174	0.353	228.0	361.8	1386.7	0.457
8618	75.70	1.26	1.38	11.4	0.0159	0.00278	0.334	191.8	306.0	1024.9	0.598
6895	66.79	1.25	1.60	14.1	0.0152	0.00382	0.326	163.3	257.6	718.9	0.718
5171	56.99	1.23	1.93	19.4	0.0142	0.00527	0.322	135.6	210.2	461.3	0.819
3447	44.53	1.18	2.47	27.7	0.0134	0.00737	0.316	108.3	161.4	251.1	0.902
1724	30.28	1.14	3.30	58.8	0.0124	0.0140	0.297	79.0	88.2	89.7	0.965
101	0.00	1.02	4.23	1000.0	0.0114	0.270	0.128	29.7	1.5	1.5	0.999

a. $276.8 \cdot 10^3 = (14686-13790)(331.6+286.1)/2$. m(p) = Δm starting at atmospheric pressure (101 kPa).

Read From Vogel's Fig. 10a		
S_o	k_{ro}	k_{rg}
0.806	0.444	0.0
0.781	0.390	0.000039
0.756	0.329	0.001
0.706	0.238	0.01
0.656	0.159	0.023
0.606	0.096	0.047
0.556	0.052	0.078
0.506	0.026	0.115

TABLE 3 - RESERVOIR ROCK AND FLUID PROPERTIES FOR GAS WELL IN EXAMPLE 1

Numerical Model:

1-Dimensional, Radial, Fully-Explicit (Fully-Implicit Check)
40 Blocks with Radii at Pressure Points $r_j=1.252\cdot r_{j-1}$ ($r_1=0.1006$ m).
Minimum:Maximum Time Step (days) = 10^{-11}:0.1 with Multiplication Factor 1.5.

General Properties:

r_w = 0.1006 m
r_e = 642.1 m (320 acre)
h = 30.48 m
k = 0.01 md ($\simeq\mu m^2$)
ϕ = 0.1
β = $3.936\cdot10^{15}$ m^{-1}

p_i = 20684 kPa
T = 79.44 °C
γ_g = 0.75 (air=1)
S_g = 1.0
c_{gi} = $4.1047\cdot10^{-8}$ kPa^{-1}
B_{gi} = $4.9240\cdot10^{-4}$ m^3/Sm^3

p	$\mu_g\cdot10^3$		$p/\mu_g Z\cdot10^{-6}$	$\Delta m\cdot10^{-12}$	$m(p)\cdot10^{-12}$
(kPa)	(Pa·s)	Z	(kPa/Pa·s)	(kPa^2/Pa·s)	
22408	0.02280	0.8347	1177	2.015 [a]	33.756
20684	0.02167	0.8229	1160	1.977	29.726
18961	0.02054	0.8149	1134	1.922	25.772
17237	0.01942	0.8091	1097	1.847	21.928
15513	0.01834	0.8084	1046	1.747	18.234
13790	0.01730	0.8127	981	1.620	14.740
12066	0.01630	0.8222	899	1.463	11.500
10342	0.01546	0.8370	799	1.279	8.574
8618	0.01469	0.8566	685	1.071	6.016
6895	0.01403	0.8805	558	0.845	3.874
5171	0.01348	0.9075	423	0.608	2.184
3447	0.01304	0.9369	282	0.364	0.968
1724	0.01271	0.9679	140	0.120	0.240
101	0.01252	0.9981	8	0.000	0.000

a. $2.015\cdot10^{12} = (22408-20684)(1177+1160)\cdot10^6/2$

TABLE 4 - TEST PROGRAM AND RESULTS FOR GAS WELL IN EXAMPLE 1

t (hr)	Δt (hr)	q_g (Sm^3/d)	p_w (kPa)	$m(p_w) \cdot 10^{-12}$ ($kPa^2/Pa \cdot s$)	m_d
-	-	-	20684	29.73	-
0- 12	12	1413	16058	22.78	-
12- 36	24	0	20484	29.27	-
36-180	144	0	20652	29.65	-
180-188	8	565	19257	26.45	0.108
188-196	8	0	20517	29.35	-
196-204	8	1130	17322	22.12	0.246
204-212	8	0	20320	28.89	-
212-220	8	1696	14715	16.62	0.425
220-228	8	0	20080	28.34	-
228-236	8	2261	10928	9.57	0.662
236-242	8	0	19797	27.70	-
242-250	8	2826	2082	0.39	0.986 [a]
250-274	24	0	20322	28.90	-

a. Highest rate not used to analyze data.

TABLE 5 - AOFP CORRECTION FOR GAS WELL IN EXAMPLE 1

t (yr)	t_D	p_D [a]	New AOFP (Sm^3/d)[b]
test	0.00050	3.23	3109
1	0.542	1.16	7593
2	1.08	1.50	5872
5	2.71	1.90	4635
10	5.40	2.22	3967
25	13.6	2.80	3145

a. Uniform-flux solution except for test point. t_{Dpss} for x_e/x_f of 15 is greater than 100.

b. $AOFP_{new} = (3.23-0.4)x3109/p_D$; -0.4 is steady-state skin estimated from test.

TABLE 6 - ROCK AND FLUID PROPERTIES FOR OILWELL TESTS IN EXAMPLE 2

General Properties:

r_w = 0.1006 m
r_e = 1284.2 m (assumed)
h = 6.096 m
k = 2470 md ($\approx \mu m^2$)
ϕ = 0.21

p_i = 25476 kPa (bubble point)
T = 93.33 ^oC
γ_{API} = 43.7 ^{o}
S_{iw} = 0.32
c_{ti} = $3.626 \cdot 10^{-6}$ kPa^{-1}

Relative Permeability:

Corey Relation (Fig. 8) with λ of 1.

$k_{ro} = S_o{*}^5$ $\quad k_{rg} = \{1-S_o*\}^2 \cdot \{1-S_o{*}^{1.5}\}$ $\quad S_o* = S_o/(1-S_{iw})$

PVT Properties:

p (kPa)	R_s (Sm^3/Sm^3)	B_o (m^3/Sm^3)	$\mu_o \cdot 10^3$ (Pa·s)	$B_g \cdot 10^3$ (m^3/Sm^3)	$\mu_g \cdot 10^3$ (Pa·s)	$m(p) \cdot 10^{-6}$ a (kPa/Pa·s)	R b (Sm^3/Sm^3)	$F\{p_R\}/F\{p_b\}$
31026	249.3	1.7116	0.2646	3.79	0.0313	32.271	249.3	0.942
29303	249.3	1.7186	0.2583	3.91	0.0301	28.427	249.3	0.961
27579	249.3	1.7265	0.2524	4.05	0.0288	24.508	249.3	0.979
25476	249.3	1.7377	0.2456	4.27	0.0273	19.631	249.3	1.000
24821	241.7	1.7175	0.2493	4.34	0.0268	18.354	241.8	0.933
24132	233.9	1.6962	0.2533	4.43	0.0263	17.335	234.6	0.838
23442	225.8	1.6751	0.2575	4.52	0.0257	16.405	229.0	0.747
22408	214.1	1.6436	0.2641	4.67	0.0249	15.113	227.4	0.624
20684	194.7	1.5918	0.2762	4.98	0.0236	13.144	264.3	0.450
17237	156.7	1.4906	0.3054	5.84	0.0208	9.685	661.0	0.241
13790	120.4	1.3931	0.3442	7.32	0.0182	6.722	1719.0	0.139
10342	85.5	1.3001	0.3993	10.1	0.0160	4.210	3526.0	0.083
6895	52.9	1.2129	0.4849	16.1	0.0143	2.182		
5171	37.6	1.1720	0.5492	22.3	0.0136	1.367		
3447	23.2	1.1337	0.6401	34.7	0.0131	0.706		
1724	10.2	1.0989	0.7778	71.9	0.0128	0.222		
101	0.4	1.0727	0.9699	124.0	0.0125	0.002		

a. m(p) calculated using the Evinger-Muskat method with R of 249.3 Sm^3/Sm^3.
b. R and F(p_R) from Tarner material balance.

TABLE 7 - 4-HOUR ISOCHRONAL TEST RESULTS FOR OIL WELL IN EXAMPLE 2.

			$m(p_R)\cdot 10^{-6}$ in kPa/Pa·s			
	p_R=25476 kPa		19.631 (Evinger-Muskat)		29.847 (Fetkovich)	
Flow ID	q_o (Sm³/d)	p_{wf} (kPa)	$m(p_{wf})\cdot 10^{-6}$ (kPa/Pa·s)	m_d	$m(p_{wf})\cdot 10^{-6}$ (kPa/Pa·s)	m_d
A-1	366.9	24401	17.733	0.0967	27.380	0.0827
A-2	230.8	24950	18.606	0.0522	28.628	0.0409
A-3	120.4	25325	19.336	0.0150	29.494	0.0118
A-4	66.6	25376	19.436	0.0099	29.614	0.0078

			$m(p_R)\cdot 10^{-6}$ in kPa/Pa·s			
	p_R=24821 kPa		19.070 (Evinger-Muskat)		27.076 (Fetkovich)	
B-1	106.4	24676	18.805	0.0139	26.761	0.0160
B-2	164.6	24475	18.435	0.0333	26.236	0.0277
B-3	224.6	24327	18.165	0.0475	26.009	0.0394
B-4	366.1	23757	17.256	0.0952	24.803	0.0839

a. Test A run 71/12/23 and Test B run 72/06/10.

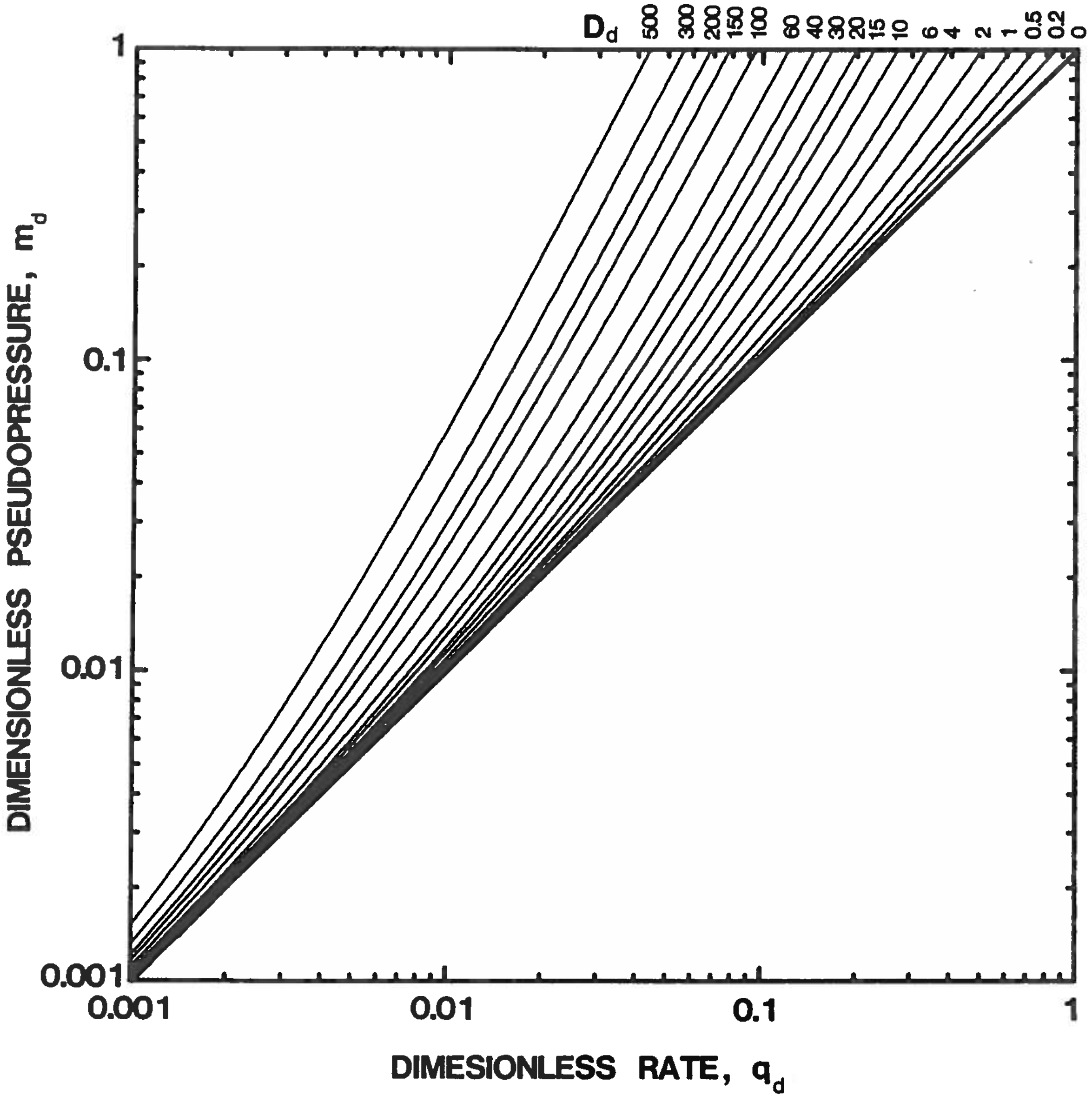

Fig. 1 - Log-log plot of dimensionless rate-pseudopressure solution including high-velocity-flow effects.

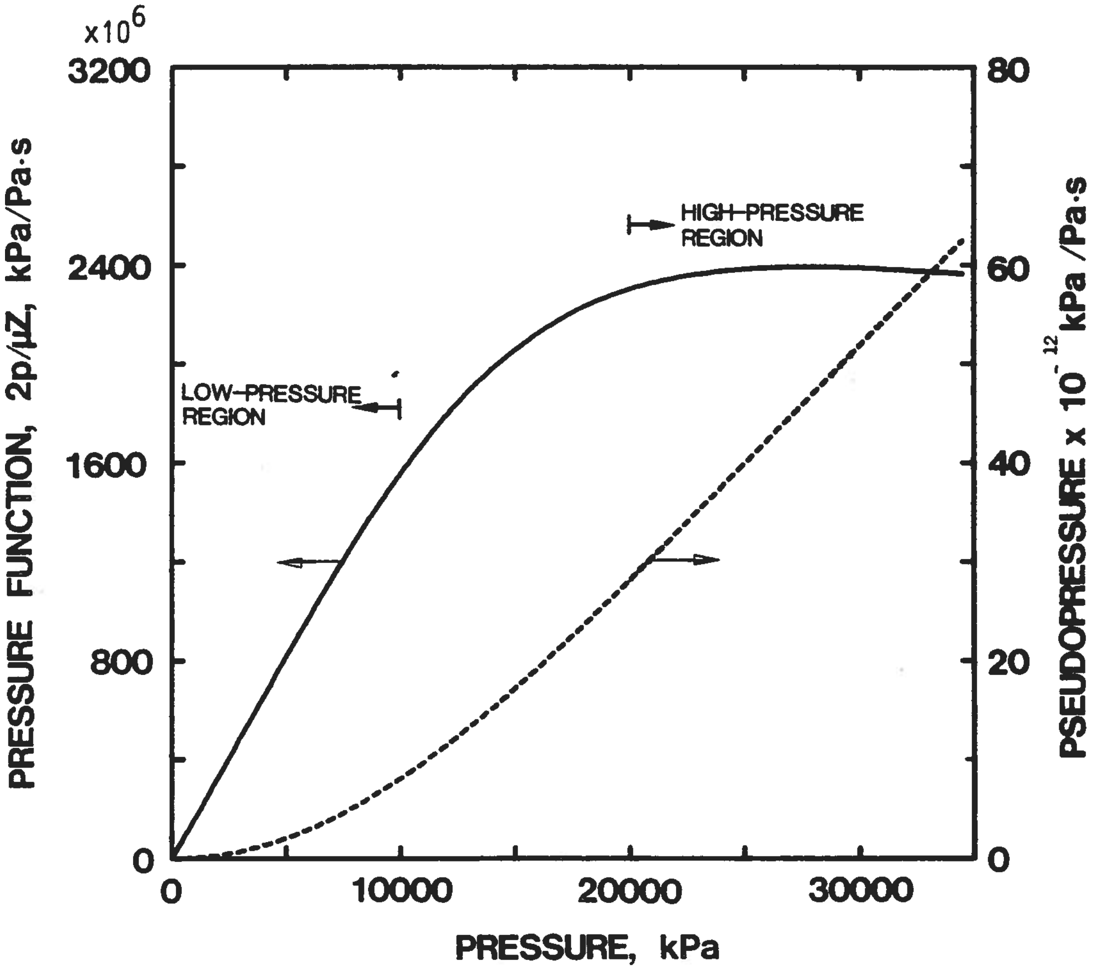

Fig. 2 - Real gas pressure and pseudopressure functions for reservoir fluid in Example 1.

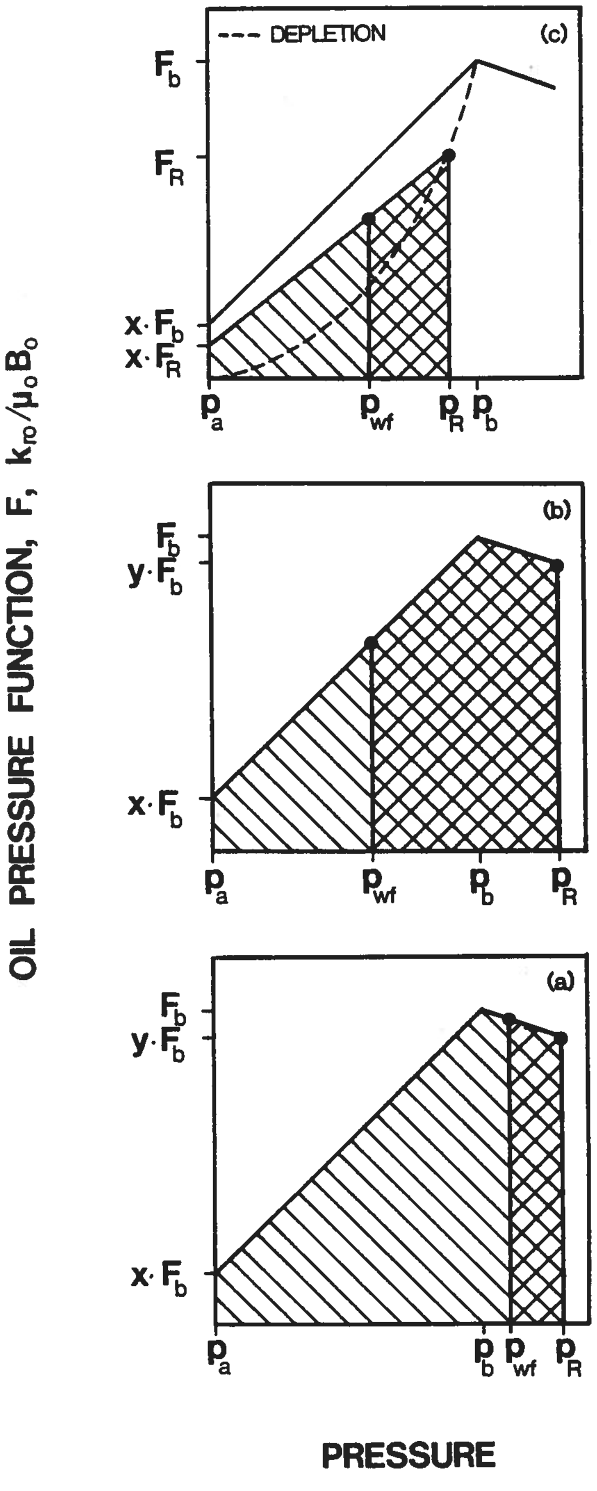

Fig. 3 - Schematic of simplified oil pressure function for three conditions of flow.

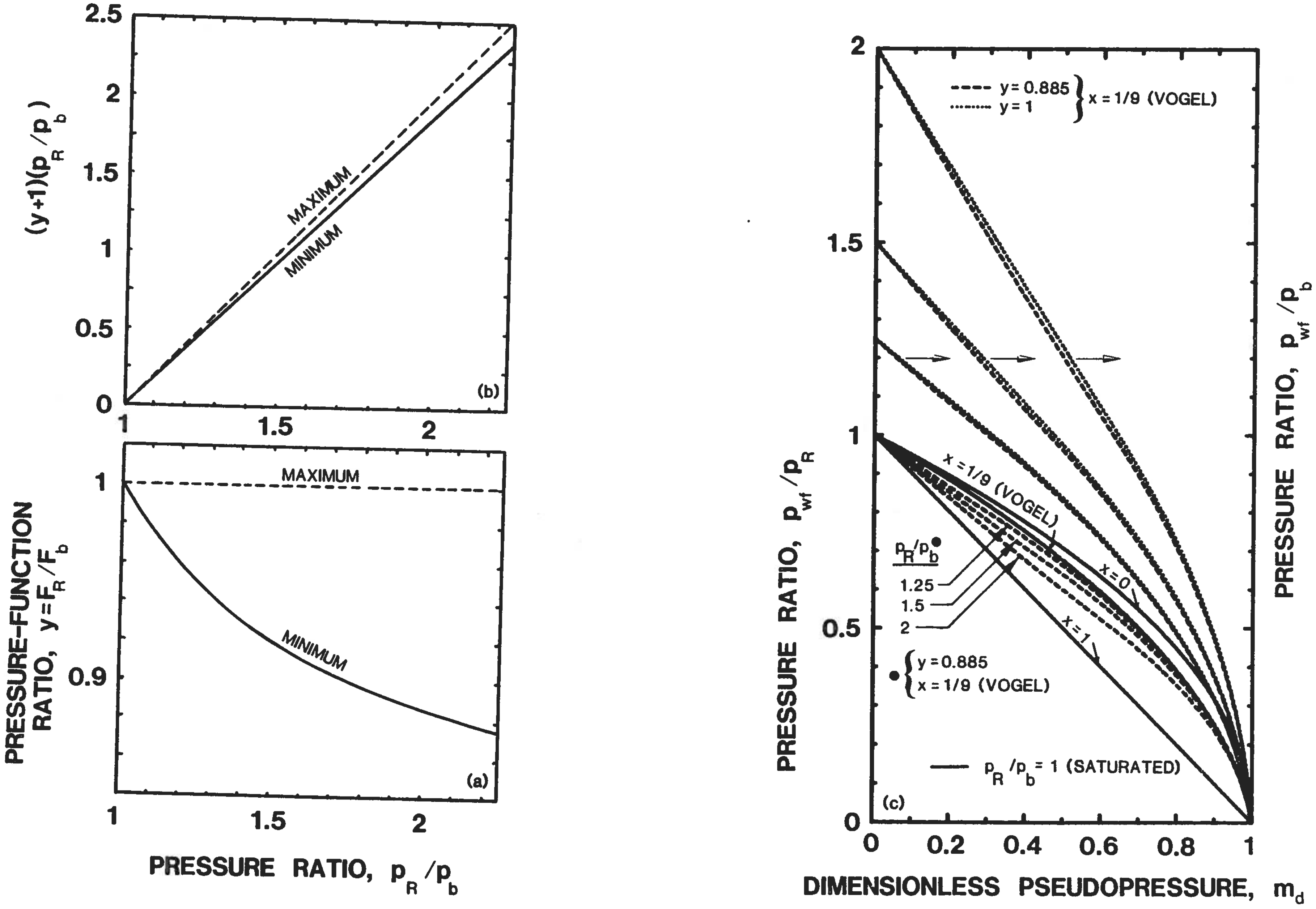

Fig. 4 - Various pressure functions illustrating the effect of undersaturated oil flow on traditional solution-gas drive (saturated) inflow performance.

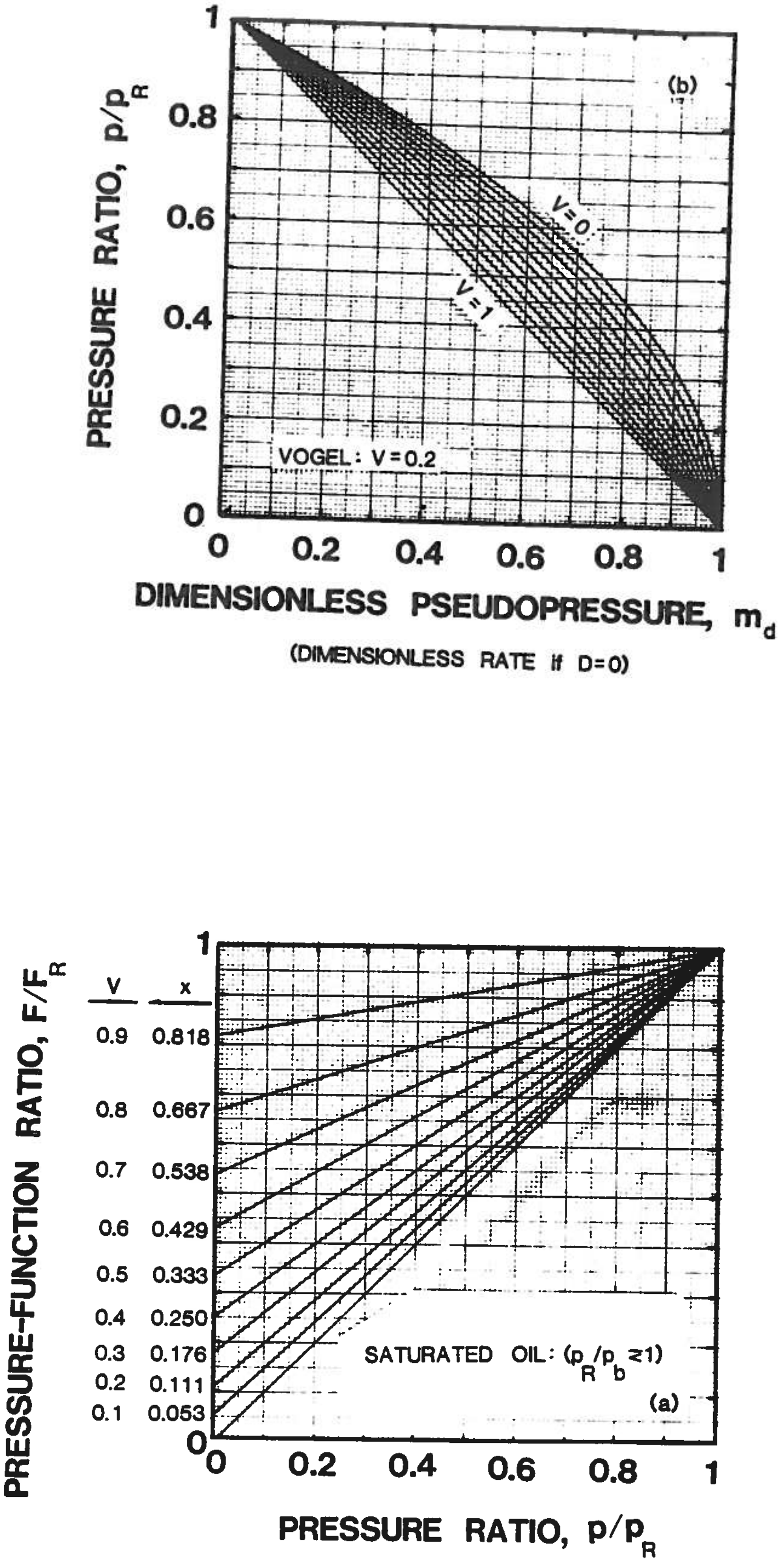

Fig. 5 - Saturated oil pressure and pseudopressure functions.

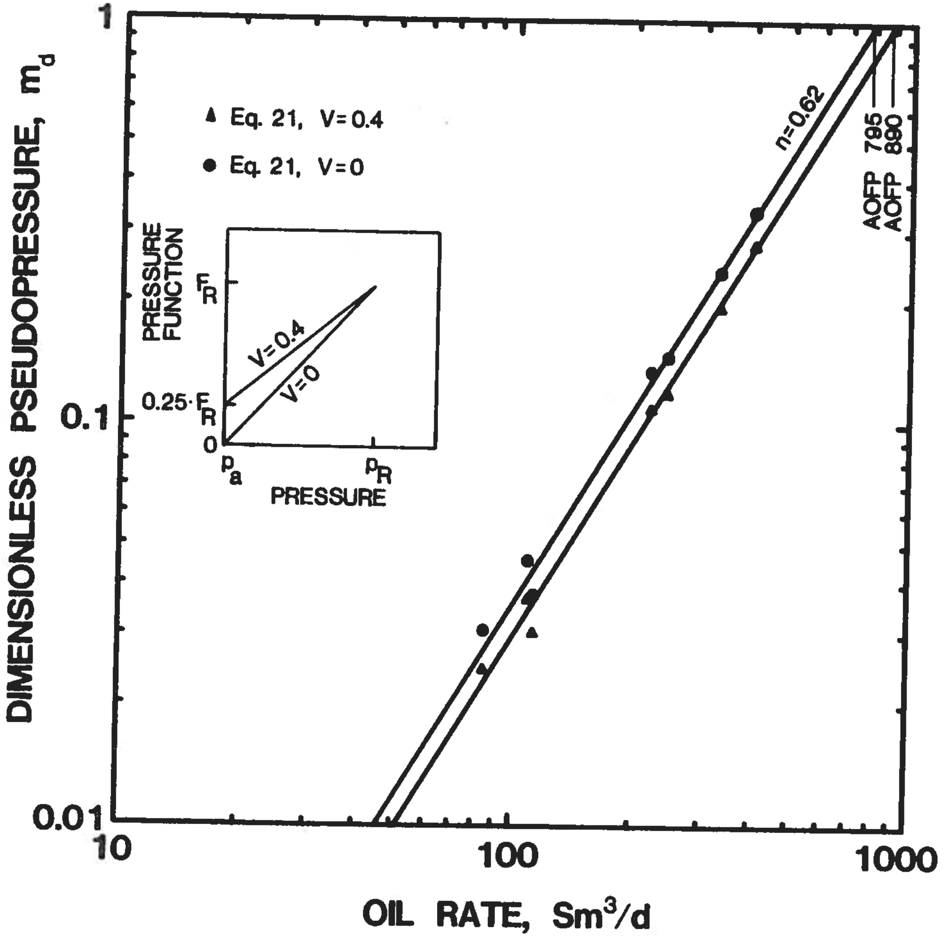

Fig. 6 - Multirate oilwell test analysed using two pseudopressure functions (Fetkovich[10] Well 3-C, Field C).

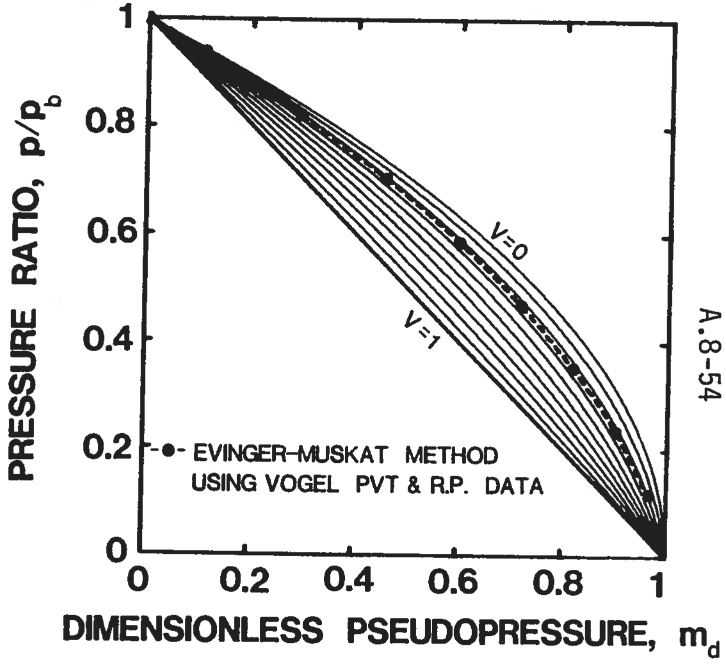

Fig. 7 - Best-fit of pseudopressure function (dimensionless Vogel rate) using the Evinger-Muskat method and Vogel's base-case reservoir rock and fluid data.

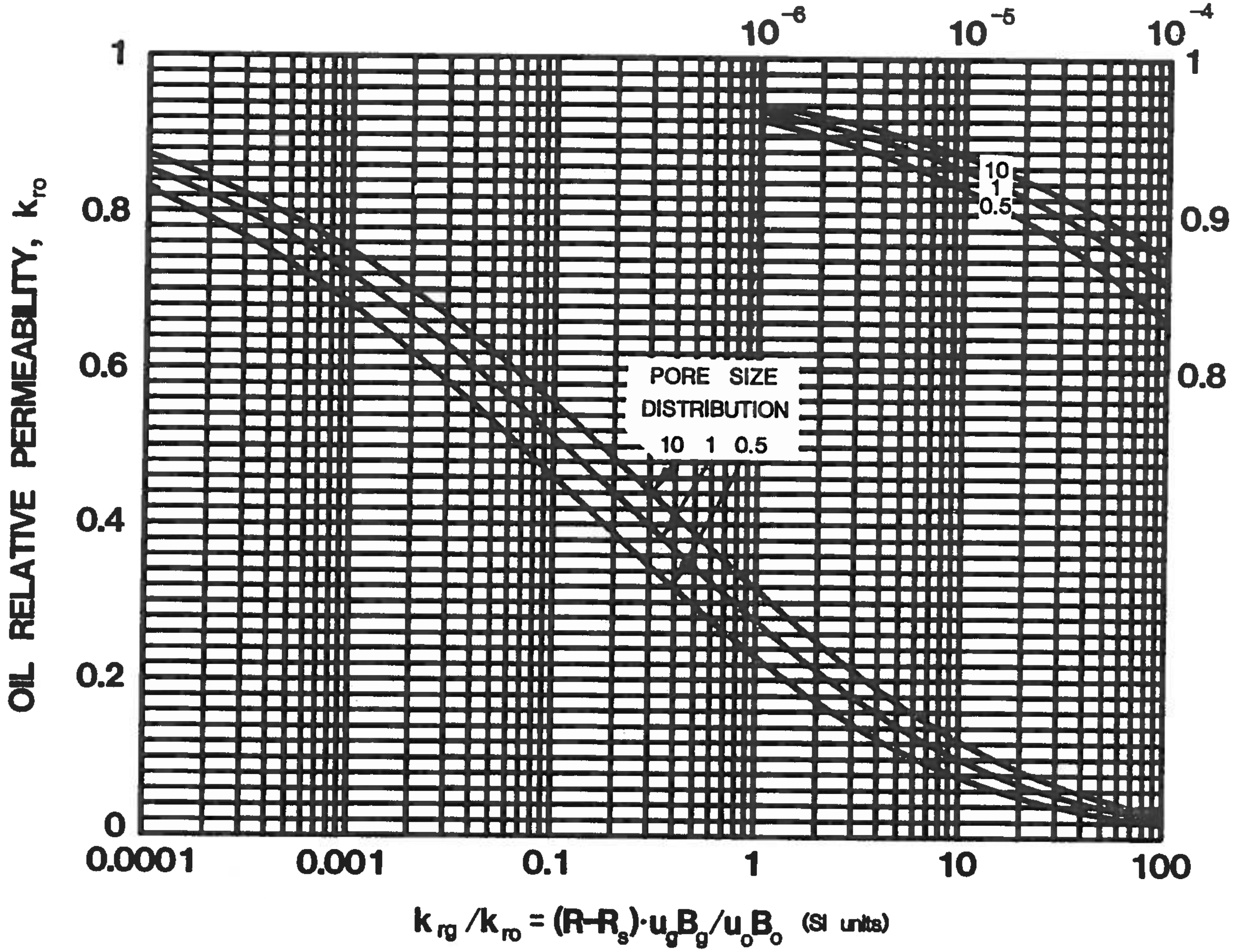

Fig. 8 - Generalized relative permeability relation for use with the Evinger-Muskat method of calculating saturated oil pseudopressure.

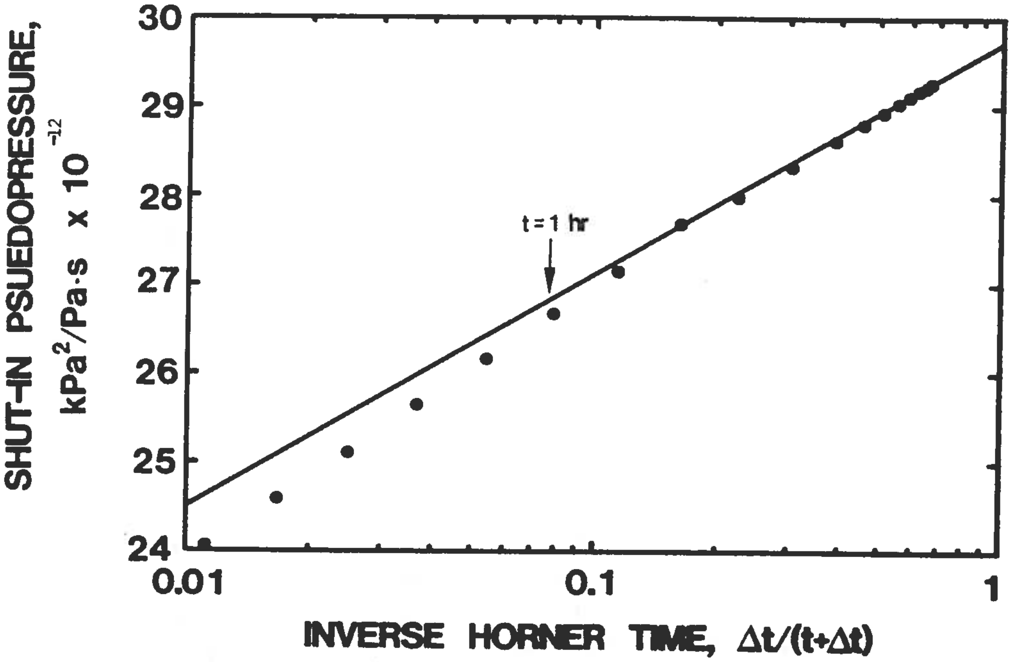

Fig. 9 - Horner analysis of simulated buildup well test in Example 1.

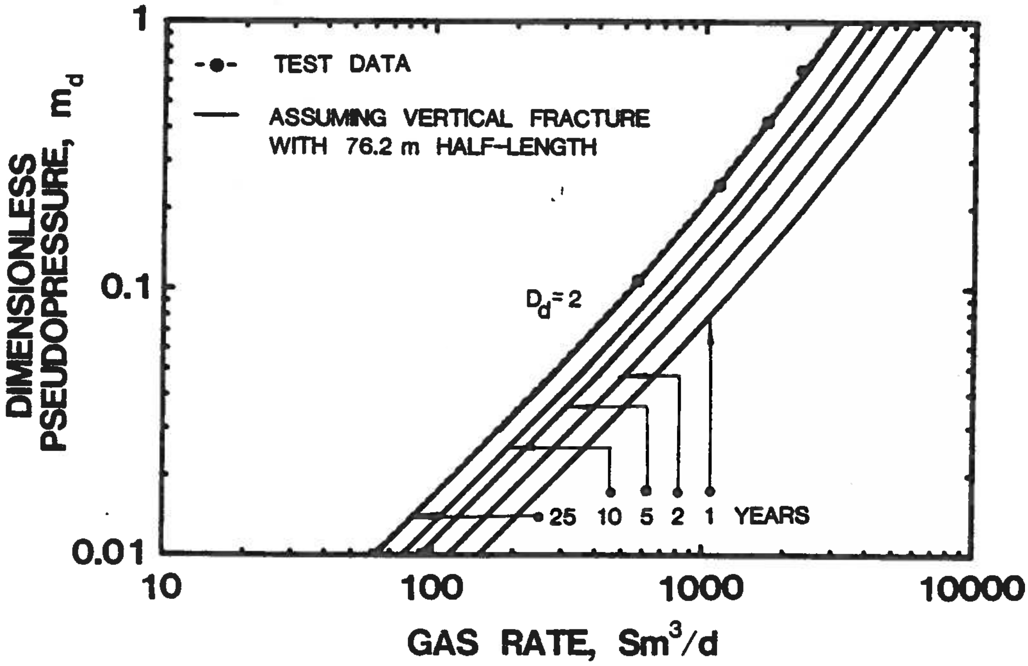

Fig. 10 - Log-log type-curve match of gaswell modified isochronal test in Example 1.

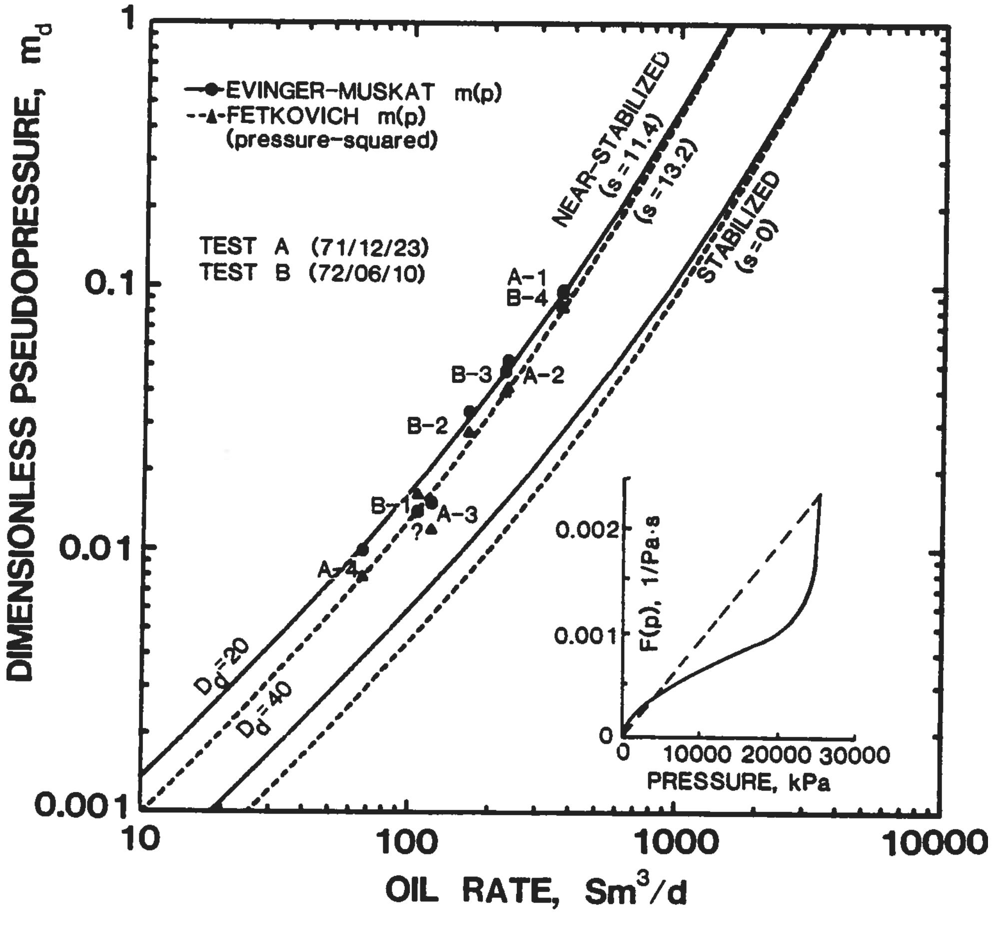

Fig. 11 - Log-log type-curve match of oilwell isochronal test in Example 2 (Fetkovich Well 5-C, Field D); insert illustrates saturated oil pressure functions corresponding to the two methods of calculating pseudopressures (Evinger-Muskat vs. Fetkovich).

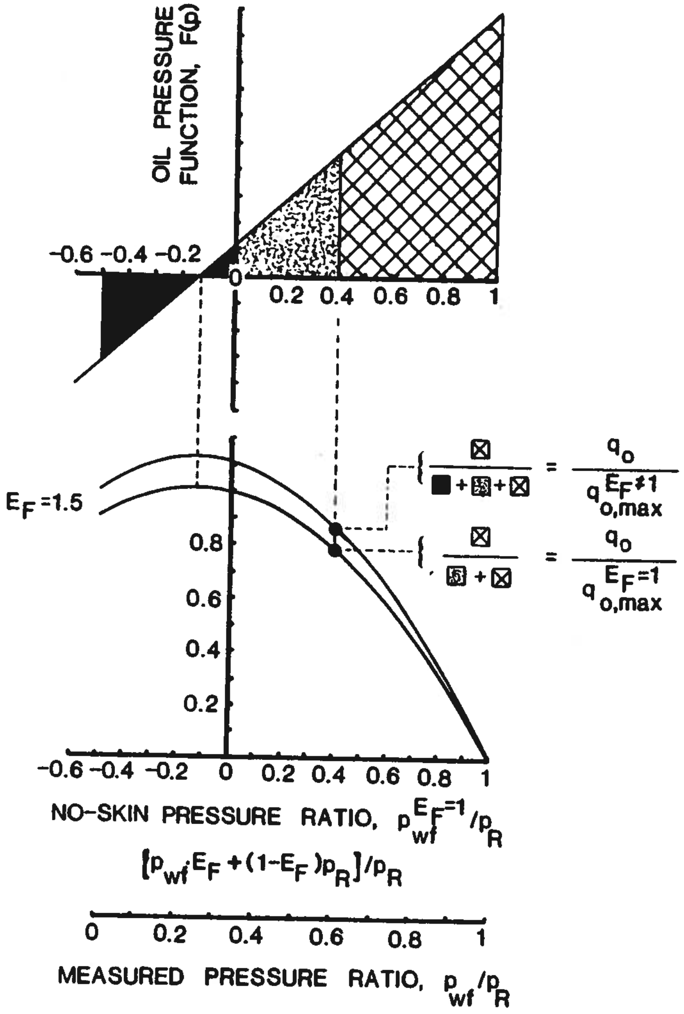

Fig. A-1 - Physical description of why the Standing method for correcting the Vogel relation for stimulated wells can lead to nonphysical rate-pressure behavior.

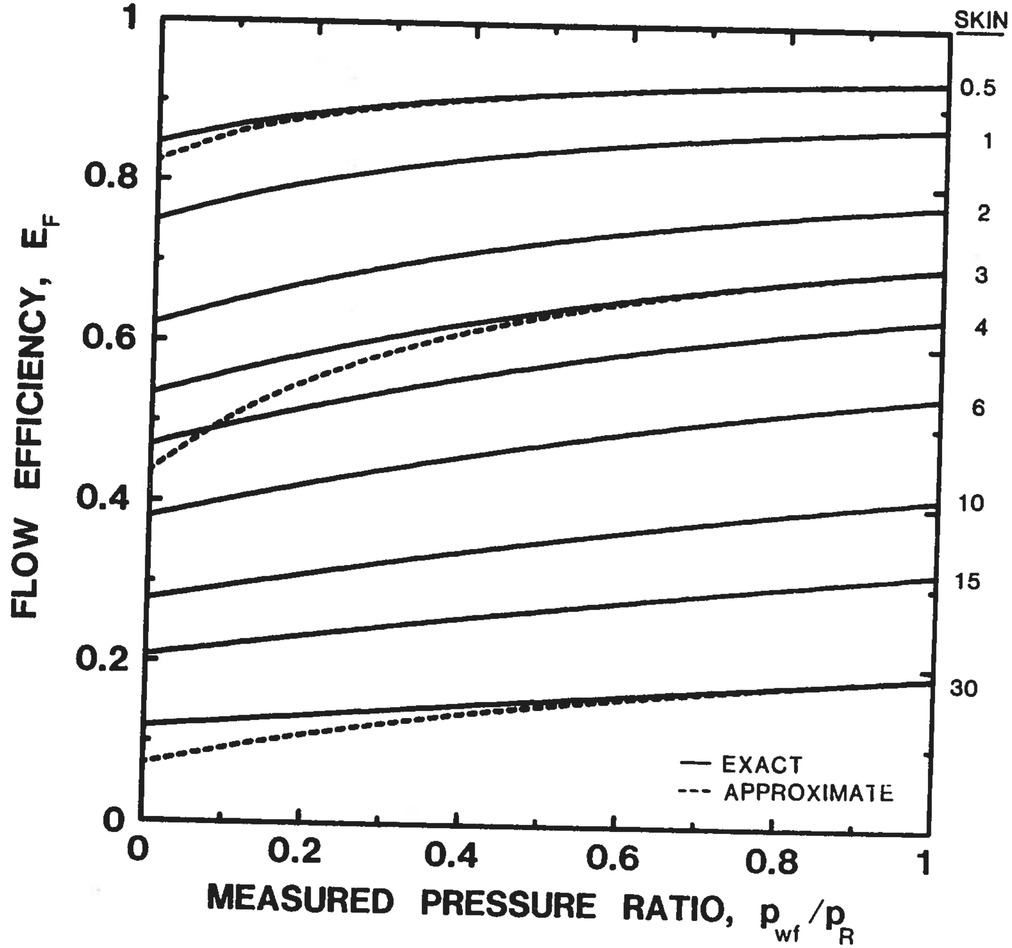

Fig. A-2 - Effect of two-phase, gas-oil flow on the relation between flow efficiency and positive skin factor; $\ln(r_e/r_w)-3/4 = 7$ and Vogel's saturated oil pressure function are assumed.

A.9-1

DISCUSSION OF CONSTANT-PRESSURE RATE DECLINE DURING DEPLETION

by

Curtis H. Whitson

1983

In 1956, Tsarevich and Kuranov[1] made the observation that a well producing at constant wellbore flowing pressure will, after sufficient time, produce at a rate which decreases exponentially. They show that the exact rate solution is an infinite sum of exponential terms. Retaining only the first term gives a surprisingly good estimate, usually within 1 or 2 percent of the exact solution. The exponential rate expression given by Tsarevich and Kuranov is,

$$q_D = c_1 \cdot \exp\{-(b_1/r_{De})^2 t_D\}, \text{ ....} \quad (1)$$

where q_D is dimensionless rate, $q(t)\mu B/kh(p_i-p_{wf})$, t_D is dimensionless time, $kt/\phi\mu c_t r_w^2$, and r_{De} is dimensionless external radius, r_e/r_w. Constant b_1 is the first and smallest root of the equation

$$Y_1(b_n)\cdot J_0(b_n/r_{De}) - J_1(b_n)\cdot Y_0(b_n/r_{De}) = 0. \text{ ....} \quad (2)$$

which results from the exact solution to the constant-pressure problem originally solved by Hurst.[2] Constant c_1 is given by

$$c_1 = \frac{2\cdot Y_1^2(b_1)}{Y_1^2(b_1/r_{De}) - Y_1^2(b_1)}, \text{ ....} \quad (3)$$

where J_0, J_1, Y_0, and Y_1, are regular Bessel functions of order zero and one. Tsarevich and Kuranov give values of b_1 and c_1 for dimensionless radii from 20 to 10^6. Table 1 reports these values, as well as those calculated by this author for r_{De} from 1.5 to 18. Dimensionless times for which Eq. 1 is within one percent accuracy are noted by an asterisk.

FETKOVICH APPROACH

Fetkovich[3] gives an empirical method for defining Eq. 1 in terms of reservoir variables for $r_{De} \geq 10$,

$$q_D = \frac{\exp\{-2t_D/[(r_{De}^2-1)(\ln(r_{De})-1/2)]\}}{\ln(r_{De})-1/2}, \quad \ldots\ldots\ldots \quad (3)$$

or, as expressed by Fetkovich,

$$q_{Dd} = e^{-t_{Dd}}, \quad \ldots\ldots\ldots\ldots\ldots\ldots\ldots\ldots \quad (4)$$

where

$$q_{Dd} = (\ln r_{De}-1/2)\cdot q_D \quad \ldots\ldots\ldots\ldots\ldots\ldots \quad (5a)$$

$$t_{Dd} = 2t_D/[(r_{De}^2-1)(\ln r_{De}-1/2)]. \quad \ldots\ldots\ldots\ldots \quad (5b)$$

Fetkovich notes that t_{Dd} of 0.3 marks the approximate start of depletion - at which time Eq. 3 becomes useful as an approximation to the analytical exponential q_D solution (Eq. 1).

It should be mentioned that Fetkovich does not use the exact analytical $q_D(t_D)$ expression to derive Eq. 3. Instead, he bases his definition on an empirical form of the exponential decline equation (Arps[4]) using common expressions for initial oil in place and maximum initial rate. His purpose is to show how the $q_D(t_D)$ depletion-stems collapse to form a single exponential curve. Within the accuracy of type curve matching field data, for which the constant-pressure solution is suggested, the expression given by Fetkovich is useful and accurate.

URAIET/RAGHAVAN AND EHLIG-ECOMOMIDES/RAMEY APPROACH

Almost simultaneously in 1980 and 1981, Uraiet and Raghavan[5] and Ehlig-Economides and Ramey[6] presented very similar results about the application of constant-pressure transient rate solutions to drawdown and buildup testing. Both sets of authors suggest the following expression for q_D during depletion,

$$q_D = \frac{\exp\{-2t_D/[r_{De}^2(\ln r_{De}-3/4)]\}}{\ln r_{De}-3/4} \text{. .... (6)}$$

Uraiet and Raghavan claim that "the times at which the closed outer boundary influences the wellbore flow rate are given (empirically) by"

$$t_D/r_{De}^2 = 0.318 + 0.040\cdot\log(r_{De}/1000). \text{ .... (7)}$$

The range of r_{De} for which Eq. 7 is applicable is not specified; from other results in their study, it appears that Eq. 8 only can be used for $500\le r_{De}\le 10^4$.

Ehlig-Economides and Ramey state that Eq. 6 is an "exact" solution for $t_D r_w^2/A>0.1$ and $r_{De}\ge 10^4$. It is probably more accurate to call Eq. 6 an approximate asymptotic solution.

Uraiet and Raghavan misleadingly attribute Eq. 6 to Fetkovich; clearly, Eqs. 4 and 6 are not equivalent. On the other hand, Ehlig-Economides and Ramey claim that Fetkovich's use of 1/2 in Eq. 4 is in error. This suggestion deserves some comment.

First, there are two differences between Eqs. 4 and 6: (1) Eq. 4 uses $\ln r_{De}-1/2$ while Eq. 6 uses $\ln r_{De}-3/4$, and (2) Eq. 4 uses r_{De}^2-1 while Eq. 6 uses r_{De}^2. Based on Ehlig-Economides and Ramey's arguements, Eq. 6 can be used for $r_{De}>10^4$ and $t_{DA}>0.1$. At such large values of dimensionless radii the difference between Eqs. 4 and 6 is quite small.

Second, it is not obvious which of the equations, 4 or 6, is more accurate at values of r_{De} less than 10^4. From a practical point of view, constant-pressure production will usually occur in stimulated, low-permeability wells. For such cases, the true wellbore radius, r_w, used to define r_{De} should be replaced by $r_w e^{-s}$, where skin, s, is negative for stimulated wells. Considering a relatively large drainage area of 900 m (≈ 640 acres) and a relatively small wellbore radius of 0.09m, r_{De} is 10000, 3700, 1350, 500, 190, and 70, for skins of 0, -1, -2, -3, -4, and -5, respectively. Clearly the value of r_{De} for most practical cases will be less than 10^4, and it may often approach values less than 100.

PAPATZACOS APPROACH

In a personal communication, Paul Papatzacos suggested the following approximation to the depletion $q_D(t_D)$ solution,

$$q_D = \frac{\exp\{-2t_D/[r_{De}^4(\ln r_{De})/(r_{De}^2-1)-(3r_{De}^2-1)/4]\}}{[r_{De}^4(\ln r_{De})/(r_{De}^2-1)-(3r_{De}^2-1)/4]/(r_{De}^2-1)}. \quad (8)$$

This expression was derived using approximations to Bessel functions found in the constant-rate pressure solution, which was then inverted using Laplace transformation. The difference between Eq. 8 and Eq. 6 arises from a more general development to better account for "small" values of dimensionless radius.

GENERAL COMMENTS

Fig. 1 was prepared to compare the various approximations to the constant-pressure q_D solution during depletion. Absolute deviation was calculated by integrating the absolute deviation in q_D given by Eqs. 4, 6, and 8 from the t_D value given in Table 1 to t_D at which q_D from Eq. 1 becomes 0.001. The basis of comparison was q_D given by Eq. 1.

It appears that Eq. 8 gives the best overall approximation, as compared with Eqs. 4 and 6. Although Eq. 4 is inferior to Eqs. 6 and 8, it still provides a good approximation for engineering/type-curve matching of field data. If high accuracy is required for $q_D(t_D)$ values, either Eq. 1 or a partial expansion of the infinite series solution should be used. Otherwise, the simplest and most accurate expression is Eq. 6. For decline type-curve matching, the exponential solution given by any of Eqs. 4, 6, or 8 can be used. Field data which are affected by rock and fluid heterogenities can hardly be expected to fit exactly the idealized model used to generate the constant-pressure rate solution.

REFERENCES

1. Tsarevich, K.A. and Kuranov, I.F.: "Calculation of the Flow Rates for the Center Well in a Circular Reservoir Under Elastic Conditions," Problems of Reservoir Hydrodynamics, Leningrad (1956) Part I, 9-34.

2. Hurst, W.: "Unsteady Flow of Fluids in Oil Reservoirs," Physics (Jan. 1934)5, 20-30.

3. Fetkovich, M.J.: "Decline Curve Analysis Using Type Curves," J.Pet.Tech. (June 1980) 1067-1077; Trans. AIME, 269.

4. Arps, J.J.: "Analysis of Decline Curves," Trans. AIME, 160, 228-247.

5. Uraiet, A.A. and Raghavan, R.: "Unsteady Flow to a Well Producing at a Constant Pressure" and "Pressure Buildup Analysis for a Well Produced at Constant Bottomhole Pressure," J.Pet.Tech. (Oct. 1980) 1803-1824; Trans. AIME, 269.

6. Ehlig-Economides, C.A. and Ramey, H.J.: "Transient Rate Decline Analysis for Wells Produced at Constant Pressure" and "Pressure Buildup for Wells Produced at a Constant Pressure," Soc.Pet.Eng.J. (Feb. 1981) 98-114; Trans. AIME, 271.

TABLE 1 - First Roots of Eq. 2 used to Define Constants in Eq. 1 For Estimating the Constant Wellbore Pressure Dimensionless Rate Solution During Depletion. Also the Dimensionless Time at which Eq. 1 deviates by 1 % from the Exact Solution.

r_{De}	b_1	c_1	t_D^*
1.5	4.33482	4.41653	5.706E-02
2.0	2.72155	2.41705	2.243E-01
2.5	2.16515	1.74659	4.972E-01
3.0	1.87679	1.40979	8.729E-01
3.5	1.69753	1.20489	1.349E+00
4.0	1.57382	1.06666	1.925E+00
5.0	1.41180	0.890488	3.371E+00
6.0	1.30843	0.781811	5.201E+00
7.0	1.23557	0.707293	7.416E+00
8.0	1.18078	0.652582	1.001E+01
10.0	1.10269	0.576811	1.631E+01
12.0	1.04869	0.526121	2.410E+01
14.0	1.00848	0.489355	3.335E+01
16.0	0.977006	0.461214	4.407E+01
18.0	0.951463	0.438822	5.622E+01
20.0	0.930177	0.420469	6.982E+01
25.0	0.889299	0.386060	1.101E+01
30.0	0.859514	0.361715	1.592E+02
40.0	0.817934	0.328786	2.837E+02
50.0	0.789445	0.306991	4.428E+02
100.0	0.716692	0.254234	1.749E+03
200.0	0.660753	0.216711	6.844E+03
500.0	0.603471	0.181181	4.130E+04
1000.0	0.568803	0.161125	1.605E+05
2000.0	0.539461	0.145044	6.237E+05
4000.0	0.514223	0.131865	2.424E+06
10000.0	0.485704	0.117711	1.458E+07
25000.0	0.461458	0.106288	8.780E+07
100000.0	0.430803	0.0926732	1.330E+08
250000.0	0.413591	0.0854380	8.024E+09
1000000.0	0.391084	0.0764036	1.219E+11

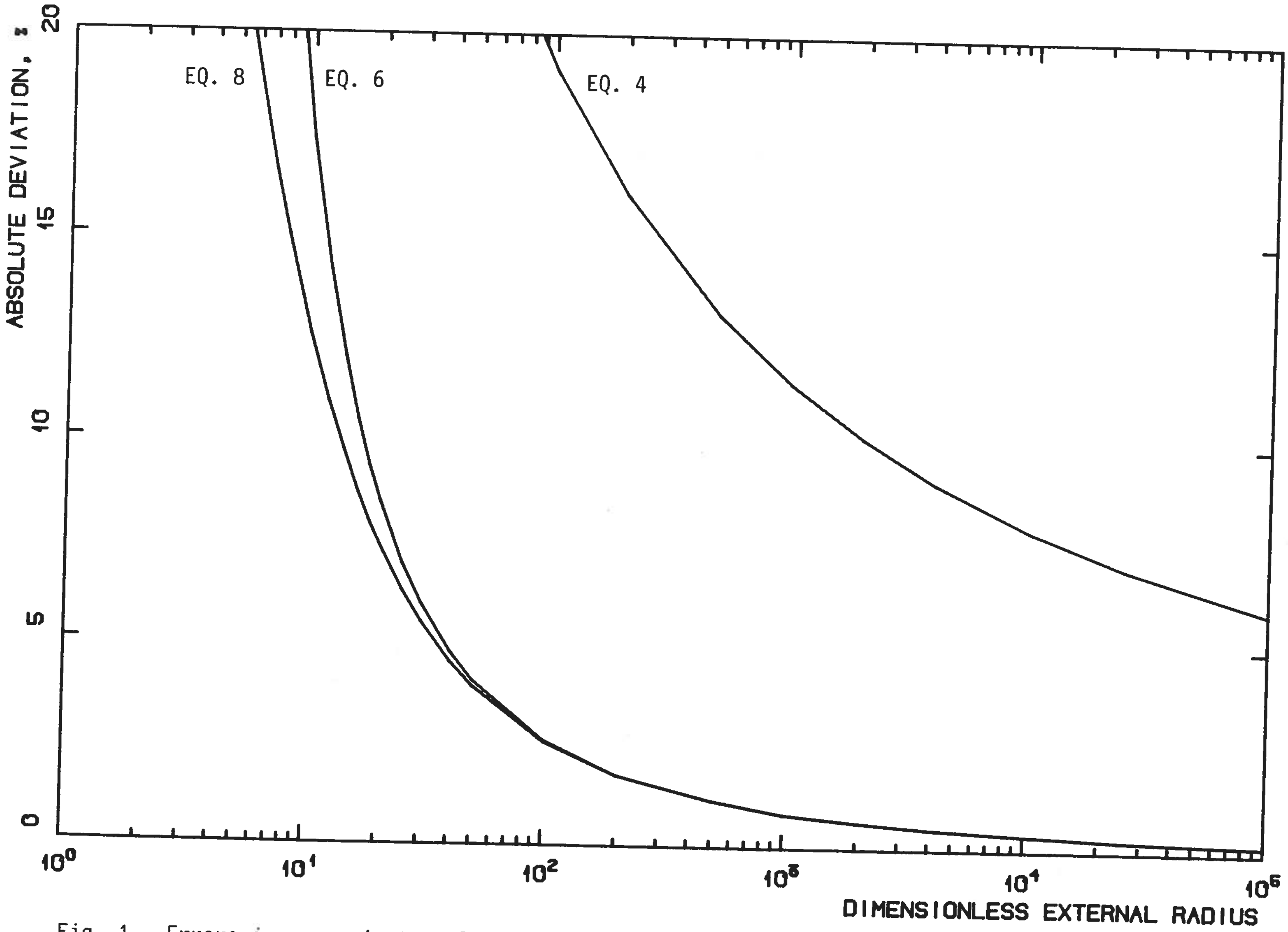

Fig. 1 - Errors in approximate solutions to the constant-pressure rate solution during depletion.

FLUID : HOFFMAN/CRUMP/HOCOTT RESERVOIR OIL

EXPERIMENTAL DISTILLATION DATA

COMP	MOLE FRACTION	MOLECULAR WEIGHT	SPECIFIC GRAVITY	BOILING POINT		WEIGHT FRACTION
				(DEG. R)	(DEG. K)	
C1	0.5200					
C2	0.0381					
C3	0.0237					
IC4	0.0076					
NC4	0.0096					
IC5	0.0069					
NC5	0.0051					
C6S	0.0206					
C7	0.0263	99.0	0.7490	668.86	371.59	0.0356
C8	0.0234	110.0	0.7580	717.89	398.83	0.0352
C9	0.0235	121.0	0.7790	763.12	423.96	0.0388
C10	0.02240	132.0	0.7860	805.11	447.28	0.0404
C11	0.02412	145.0	0.7980	844.27	469.04	0.0478
C12	0.02457	158.0	0.8120	880.99	489.44	0.0530
C13	0.02657	172.0	0.8260	915.54	508.63	0.0624
C14	0.03262	186.0	0.8460	948.15	526.75	0.0829
C15	0.03631	203.0	0.8510	979.09	543.94	0.1007
C16	0.02294	222.0	0.8520	1008.38	560.21	0.0696
C17	0.01714	238.0	0.8380	1036.30	575.72	0.0557
C18	0.01427	252.0	0.8460	1062.97	590.54	0.0491
C19	0.01303	266.0	0.8510	1088.48	604.71	0.0473
C20	0.01078	279.0	0.8710	1112.91	618.28	0.0411
C21	0.00871	290.0	0.8780	1136.30	631.28	0.0345
C22	0.00715	301.0	0.8840	1158.80	643.78	0.0294
C23	0.00575	315.0	0.8890	1171.92	651.07	0.0247
C24	0.00481	329.0	0.8930	1192.15	662.31	0.0216
C25	0.00394	343.0	0.8970	1211.87	673.26	0.0185
C26	0.00335	357.0	0.9000	1231.12	683.96	0.0163
C27	0.00280	371.0	0.9030	1249.89	694.38	0.0142
C28	0.00250	385.0	0.9060	1268.16	704.53	0.0131
C29	0.00232	399.0	0.9080	1285.88	714.38	0.0126
C30	0.00195	413.0	0.9100	1303.01	723.89	0.0110
C31	0.00170	427.0	0.9120	1319.47	733.04	0.0099
C32	0.00156	441.0	0.9140	1335.22	741.79	0.0094
C33	0.00143	455.0	0.9160	1350.19	750.11	0.0089
C34	0.00130	469.0	0.9170	1364.33	757.96	0.0083
C35	0.00118	483.0	0.9180	1377.62	765.34	0.0078
	1.00000	87.32				
C7+	0.36840	198.7	0.8409			1.0000

FLUID : HOFFMAN/CRUMP/HOCOTT RESERVOIR OIL

PENG/ROBINSON EQUATION OF STATE

		CRITICAL				
		PRESSURE		TEMPERATURE		
COMP	MOLE FRACTION	(PSIA)	(KPA)	(DEG. R)	(DEG. K)	ACENTRIC FACTOR
C7	0.02630	453.4	3126.0	995.2	552.9	0.3024
C8	0.02340	426.9	2943.0	1048.4	582.4	0.3583
C9	0.02350	412.2	2842.0	1099.4	610.8	0.4070
C10	0.02240	392.0	2703.0	1143.5	635.3	0.4570
C11	0.02412	371.5	2561.0	1183.1	657.3	0.5060
C12	0.02457	355.2	2449.0	1220.6	678.1	0.5513
C13	0.02657	339.1	2338.0	1255.0	697.2	0.5954
C14	0.03262	328.0	2262.0	1288.8	716.0	0.6351
C15	0.03631	307.2	2118.0	1315.8	731.0	0.6805
C16	0.02294	285.2	1966.0	1339.4	744.1	0.7267
C17	0.01714	265.0	1827.0	1361.4	756.3	0.7718
C18	0.01427	256.8	1771.0	1387.8	771.0	0.8064
C19	0.01303	248.4	1713.0	1412.6	784.8	0.8404
C20	0.01078	246.4	1699.0	1439.6	799.8	0.8676
C21	0.00871	242.5	1672.0	1464.2	813.4	0.8957
C22	0.00715	238.5	1644.0	1487.6	826.5	0.9231
C23	0.00575	230.5	1589.0	1497.8	832.1	0.9448
C24	0.00481	224.1	1545.0	1516.9	842.7	0.9727
C25	0.00394	218.3	1505.0	1535.6	853.1	0.9998
C26	0.00335	212.6	1466.0	1553.8	863.2	1.0265
C27	0.00280	207.3	1430.0	1571.5	873.1	1.0524
C28	0.00250	202.4	1396.0	1588.8	882.7	1.0776
C29	0.00232	197.6	1362.0	1605.4	891.9	1.1024
C30	0.00195	193.0	1331.0	1621.5	900.8	1.1265
C31	0.00170	188.7	1301.0	1636.8	909.4	1.1497
C32	0.00156	184.6	1272.0	1651.5	917.5	1.1720
C33	0.00143	180.6	1245.0	1665.3	925.1	1.1935
C34	0.00130	176.6	1218.0	1678.0	932.2	1.2143
C35	0.00118	172.8	1191.0	1689.8	938.8	1.2342

FLUID : HOFFMAN/CRUMP/HOCOTT RESERVOIR OIL

SOAVE/REDLICH/KWONG EQUATION OF STATE

		CRITICAL				
		PRESSURE		TEMPERATURE		
COMP	MOLE FRACTION	(PSIA)	(KPA)	(DEG. R)	(DEG. K)	ACENTRIC FACTOR
C7	0.02630	514.4	3547.0	1006.5	559.2	0.3024
C8	0.02340	483.9	3336.0	1059.9	588.9	0.3583
C9	0.02350	466.7	3218.0	1111.1	617.3	0.4070
C10	0.02240	443.5	3058.0	1155.2	641.8	0.4570
C11	0.02412	419.8	2895.0	1194.6	663.7	0.5060
C12	0.02457	401.1	2765.0	1232.0	684.5	0.5513
C13	0.02657	382.6	2638.0	1266.2	703.5	0.5954
C14	0.03262	369.8	2550.0	1299.8	722.1	0.6351
C15	0.03631	346.2	2387.0	1326.4	736.9	0.6805
C16	0.02294	321.1	2214.0	1349.7	749.8	0.7267
C17	0.01714	298.2	2056.0	1371.4	761.9	0.7718
C18	0.01427	288.8	1991.0	1397.5	776.4	0.8064
C19	0.01303	279.2	1925.0	1421.9	790.0	0.8404
C20	0.01078	276.8	1908.0	1448.6	804.8	0.8676
C21	0.00871	272.3	1877.0	1472.9	818.3	0.8957
C22	0.00715	267.7	1845.0	1496.1	831.1	0.9231
C23	0.00575	258.6	1783.0	1506.0	836.7	0.9448
C24	0.00481	251.4	1733.0	1524.8	847.1	0.9727
C25	0.00394	244.7	1687.0	1543.2	857.4	0.9998
C26	0.00335	238.3	1643.0	1561.1	867.3	1.0265
C27	0.00280	232.3	1601.0	1578.5	877.0	1.0524
C28	0.00250	226.7	1563.0	1595.5	886.4	1.0776
C29	0.00232	221.2	1525.0	1611.9	895.5	1.1024
C30	0.00195	216.0	1489.0	1627.6	904.2	1.1265
C31	0.00170	211.1	1455.0	1642.7	912.6	1.1497
C32	0.00156	206.4	1423.0	1657.0	920.6	1.1720
C33	0.00143	202.0	1392.0	1670.5	928.1	1.1935
C34	0.00130	197.4	1361.0	1683.0	935.0	1.2143
C35	0.00118	193.1	1331.0	1694.6	941.4	1.2342

FLUID : HOFFMAN ET AL. RESERVOIR GAS

EXPERIMENTAL DISTILLATION DATA

	MOLE	MOLECULAR	SPECIFIC	BOILING POINT		WEIGHT
COMP	FRACTION	WEIGHT	GRAVITY	(DEG. R)	(DEG. K)	FRACTION
C1	0.91350					
C2	0.04030					
C3	0.01530					
IC4	0.00390					
NC4	0.00430					
IC5	0.00150					
NC5	0.00190					
C6S	0.00390					
C7	0.36100	100.00	0.7450	668.86	371.59	0.1660
C8	0.28500	114.00	0.7530	717.89	398.83	0.1494
C9	0.22200	128.00	0.7730	763.12	423.96	0.1306
C10	0.15800	142.00	0.7790	805.11	447.28	0.1031
C11	0.12100	156.00	0.7930	844.27	469.04	0.0868
C12	0.09700	170.00	0.8040	880.99	489.44	0.0758
C13	0.08300	184.00	0.8160	915.54	508.63	0.0702
C14	0.06900	198.00	0.8360	948.15	526.75	0.0628
C15	0.05000	212.00	0.8400	979.09	543.94	0.0487
C16	0.03400	226.00	0.8390	1008.38	560.21	0.0353
C17	0.02300	240.00	0.8350	1036.30	575.72	0.0254
C18	0.01500	254.00	0.8500	1062.97	590.54	0.0175
C19	0.01000	268.00	0.8650	1088.48	604.71	0.0123
C20	0.00600	282.00	0.8730	1112.91	618.28	0.0078
C21	0.00400	296.00	0.8760	1136.30	631.28	0.0054
C22	0.00200	310.00	0.8780	1158.80	643.78	0.0029
	1.00000					
C7+	1.54000	141.25	0.7867			1.0000

FLUID : HOFFMAN ET AL. RESERVOIR GAS

PENG/ROBINSON EQUATION OF STATE

COMP	MOLE FRACTION	CRITICAL PRESSURE (PSIA)	CRITICAL PRESSURE (KPA)	CRITICAL TEMPERATURE (DEG. R)	CRITICAL TEMPERATURE (DEG. K)	ACENTRIC FACTOR
C7	0.00361	445.4	3071.0	992.7	551.5	0.3062
C8	0.00285	406.7	2804.0	1041.4	578.6	0.3687
C9	0.00222	383.2	2642.0	1088.9	604.9	0.4226
C10	0.00158	357.2	2463.0	1130.1	627.9	0.4770
C11	0.00121	339.5	2341.0	1170.2	650.1	0.5254
C12	0.00097	323.4	2230.0	1207.2	670.7	0.5717
C13	0.00083	310.0	2138.0	1242.2	690.1	0.6150
C14	0.00069	301.8	2080.0	1276.9	709.4	0.6534
C15	0.00050	288.5	1989.0	1306.8	726.0	0.6945
C16	0.00034	274.8	1895.0	1334.1	741.2	0.7351
C17	0.00023	261.5	1803.0	1359.5	755.3	0.7749
C18	0.00015	255.9	1764.0	1387.3	770.7	0.8073
C19	0.00010	250.8	1729.0	1414.0	785.5	0.8382
C20	0.00006	244.1	1683.0	1438.2	799.0	0.8698
C21	0.00004	236.5	1630.0	1460.6	811.4	0.9016
C22	0.00002	229.1	1580.0	1481.9	823.3	0.9325

SOAVE/REDLICH/KWONG EQUATION OF STATE

COMP	MOLE FRACTION	CRITICAL PRESSURE (PSIA)	CRITICAL PRESSURE (KPA)	CRITICAL TEMPERATURE (DEG. R)	CRITICAL TEMPERATURE (DEG. K)	ACENTRIC FACTOR
C7	0.00361	505.4	3484.0	1003.9	557.7	0.3062
C8	0.00285	461.0	3178.0	1052.9	585.0	0.3687
C9	0.00222	433.9	2992.0	1100.5	611.4	0.4226
C10	0.00158	404.1	2786.0	1141.7	634.3	0.4770
C11	0.00121	383.8	2646.0	1181.7	656.5	0.5254
C12	0.00097	365.2	2518.0	1218.5	676.9	0.5717
C13	0.00083	349.8	2412.0	1253.3	696.3	0.6150
C14	0.00069	340.2	2346.0	1287.7	715.4	0.6534
C15	0.00050	325.0	2241.0	1317.3	731.9	0.6945
C16	0.00034	309.4	2133.0	1344.4	746.9	0.7351
C17	0.00023	294.3	2029.0	1369.5	760.8	0.7749
C18	0.00015	287.7	1984.0	1397.0	776.1	0.8073
C19	0.00010	281.9	1944.0	1423.3	790.7	0.8382
C20	0.00006	274.2	1891.0	1447.3	804.1	0.8698
C21	0.00004	265.5	1830.0	1469.3	816.3	0.9016
C22	0.00002	257.1	1773.0	1490.3	827.9	0.9325

FLUID : STANDING/KATZ MIXTURES

REVIEW OF SURFACE MIXTURES USED TO RECOMBINE

		NATURAL GASOLINE		STOCK-TANK OIL (C7+)			"CRUDE" COMPOSITIONS (MOL)			
COMP	GAS (MOL)	NO. 1 (MOL)	NO. 2 (MOL)	(VOL)	(MOL)	(MOL)	A/B	C/F/G/H	D	E
N2	0.0043									
CO2	0.0051									
C1	0.9320									
C2	0.0425									
C3	0.0161									
IC4										
NC4		0.0813	0.1134				0.0547	0.0764	0.0700	0.0331
IC5		0.1285	0.1353				0.0865	0.0912	0.1106	0.0523
NC5		0.2695	0.2448				0.1815	0.1650	0.2320	0.1098
C6		0.2807	0.2443				0.1890	0.1647	0.2417	0.1143
F1		0.1455	0.1589	0.1250	0.0936	0.2464	0.1785	0.1874	0.1595	0.2054
F2		0.0945	0.1033	0.1250	0.0763	0.2007	0.1292	0.1351	0.1093	0.1574
F3				0.1250	0.0580	0.1526	0.0498	0.0497	0.0212	0.0904
F4				0.1250	0.0473	0.1244	0.0406	0.0406	0.0173	0.0737
F5				0.1250	0.0400	0.1052	0.0344	0.0343	0.0146	0.0624
F6				0.1250	0.0308	0.0810	0.0265	0.0264	0.0113	0.0480
F7				0.2500	0.0341	0.0897	0.0293	0.0292	0.0125	0.0532
	1.0000	1.0000	1.0000	1.0000	0.3801	1.0000	1.0000	1.0000	1.0000	1.0000
MTOT	17.28	83.40	83.07		228.5		130.7	130.5	103.5	169.4
SGTOT	0.5960	0.6536	0.6528		0.8685		0.7680	0.7681	0.7171	0.8184
API		85.00	85.20		31.40		52.75	52.72	65.82	41.39
MC7+		107.40	106.80		228.5		188.3	185.7	155.9	211.3
SPGC7+		0.690	0.690		0.8685		0.8398	0.8376	0.8084	0.8572
MOLC7+		0.2400	0.2622		1.0000		0.4883	0.5027	0.3457	0.6905
RATIO OF VOLUME NATURAL GAS TO STOCK-TANK OIL							50/50	50/50	75/25	25/75
MOLE FRACTION NATURAL GAS IN "CRUDE" MIXTURE							0.6734	0.6740	0.8609	0.4073

FLUID : STANDING/KATZ MIXTURES (STOCK-TANK OIL COMPOSITION)

EXPERIMENTAL DISTILLATION DATA

COMP	MOLE FRACTION	MOLECULAR WEIGHT	SPECIFIC GRAVITY	BOILING POINT (DEG. R)	BOILING POINT (DEG. K)	WEIGHT FRACTION
F1	0.24640	94.00	0.7035	631.00	350.56	0.1014
F2	0.20070	127.00	0.7753	780.00	433.33	0.1116
F3	0.15260	176.00	0.8173	908.00	504.44	0.1175
F4	0.12440	225.00	0.8500	1028.00	571.11	0.1225
F5	0.10520	277.00	0.8865	1128.00	626.67	0.1275
F6	0.08100	375.00	0.9232	1220.00	677.78	0.1329
F7	0.08970	730.00	0.9950	1901.39	1056.33	0.2866
	1.00000	228.49	0.8682			1.0000

FLUID : STANDING/KATZ MIXTURES

REVIEW OF RECOMBINED MIXTURE COMPOSITIONS (MOL)

COMP	A	B	C	D	E	F	G	H
N2	0.0039	0.0039	0.0035	0.0038	0.0040	0.0035	0.0036	0.0035
CO2	0.0046	0.0046	0.0042	0.0045	0.0047	0.0042	0.0042	0.0042
C1	0.8396	0.8440	0.7648	0.8274	0.8563	0.7688	0.7694	0.7686
C2	0.0383	0.0385	0.0349	0.0377	0.0391	0.0351	0.0351	0.0350
C3	0.0145	0.0146	0.0132	0.0143	0.0148	0.0133	0.0133	0.0133
NC4	0.0054	0.0052	0.0137	0.0079	0.0134	0.0134	0.0133	0.0134
IC5	0.0086	0.0082	0.0164	0.0124	0.0042	0.0160	0.0159	0.0160
NC5	0.0180	0.0171	0.0296	0.0260	0.0089	0.0289	0.0288	0.0289
C6	0.0188	0.0178	0.0295	0.0272	0.0093	0.0288	0.0287	0.0289
F1	0.0177	0.0169	0.0337	0.0179	0.0166	0.0328	0.0326	0.0330
F2	0.0128	0.0122	0.0242	0.0123	0.0128	0.0237	0.0236	0.0237
F3	0.0049	0.0047	0.0089	0.0024	0.0073	0.0087	0.0087	0.0087
F4	0.0040	0.0038	0.0073	0.0019	0.0060	0.0071	0.0071	0.0071
F5	0.0034	0.0032	0.0062	0.0016	0.0051	0.0060	0.0060	0.0060
F6	0.0026	0.0025	0.0047	0.0013	0.0039	0.0046	0.0046	0.0046
F7	0.0029	0.0028	0.0052	0.0014	0.0043	0.0051	0.0051	0.0051
	1.0000	1.0000	1.0000	1.0000	1.0000	1.0000	1.0000	1.0000
GAS MOL FRAC.	0.9009	0.9056	0.8206	0.8878	0.9189	0.8249	0.8256	0.8247

FLUID : STANDING-KATZ MIXTURES

PENG/ROBINSON EQUATION OF STATE

	CRITICAL				
	PRESSURE		TEMPERATURE		
COMP	(PSIA)	(KPA)	(DEG. R)	(DEG. K)	ACENTRIC FACTOR
F1	431.6	2976.0	939.5	521.9	0.2815
F2	394.1	2717.0	1113.6	618.7	0.4322
F3	324.4	2237.0	1239.8	688.8	0.5975
F4	284.7	1963.0	1362.0	756.7	0.7471
F5	256.2	1766.0	1462.5	812.5	0.8743
F6	205.5	1417.0	1536.2	853.5	1.0231
F7	163.8	1129.0	2270.2	1261.2	1.8258

FLUID : STANDING-KATZ MIXTURES

SOAVE/REDLICH/KWONG EQUATION OF STATE

	CRITICAL				
	PRESSURE		TEMPERATURE		
COMP	(PSIA)	(KPA)	(DEG. R)	(DEG. K)	ACENTRIC FACTOR
F1	490.1	3379.0	950.4	528.0	0.2815
F2	446.1	3076.0	1125.3	625.2	0.4322
F3	366.1	2524.0	1250.9	695.0	0.5975
F4	320.4	2209.0	1372.1	762.3	0.7471
F5	287.7	1984.0	1471.4	817.5	0.8743
F6	230.3	1588.0	1543.7	857.6	1.0231
F7	181.5	1252.0	2260.7	1256.0	1.8258

FLUID : EILERTS MIXTURES

EXPERIMENTAL DISTILLATION DATA

	AVERAGE PROPERTIES FOR ALL MIXTURES STUDIED BY EILERTS				MOLE FRACTION	
			BOILING POINT			
COMP	MOL. WEIGHT	SPEC. GR.	(R)	(K)	CO-L/ 544	CH-P/ 843
N2					0.00414	0.01375
CO2					0.00468	0.00794
C1					0.90162	0.76432
C2					0.04067	0.07923
C3					0.01616	0.04301
IC4					0.00464	0.01198
NC4					0.00390	0.01862
IC5					0.00274	0.00937
NC5					0.00123	0.00781
C6-1	86.17	0.6600	589.10	327.28	0.00175	0.00744
C6-2	86.17	0.6640	615.40	341.89	0.00243	0.00661
C7-1	100.20	0.6850	640.80	356.00	0.00097	0.00290
C7-2	100.20	0.6940	662.90	368.28	0.00068	0.00295
C8	114.22	0.7068	717.90	398.83	0.00291	0.01040
C9	128.25	0.7217	763.10	423.94	0.00207	0.00613
C10	142.28	0.7341	805.10	447.28	0.00167	0.00338
C11	156.30	0.7441	844.30	469.06	0.00122	0.00176
C12	170.33	0.7526	881.00	489.44	0.00092	0.00153
C13	184.35	0.7603	915.50	508.61	0.00096	0.00087
C14	198.38	0.7667	948.20	526.78	0.00113	
C15	212.41	0.7724	979.00	543.89	0.00093	
C16	226.43	0.7773	1008.40	560.22	0.00096	
C17	240.46	0.7818	1036.30	575.72	0.00029	
C18	254.48	0.7858	1063.00	590.56	0.00029	
C19	268.51	0.7893	1088.50	604.72	0.00021	
C20	282.54	0.7925	1112.90	618.28	0.00018	
C21	296.56	0.7955	1137.00	631.67	0.00021	
C22	310.59	0.7981	1161.00	645.00	0.00018	
C23	324.61	0.8006	1184.00	657.78	0.00017	
C24	338.64	0.8029	1207.00	670.56	0.00009	
					1.00000	1.00000

HEXANES-PLUS MOLE FRACTION	0.02022	0.04397
HEXANES-PLUS MOLECULAR WEIGHT	147.33	112.53
HEXANES-PLUS SPECIFIC GRAVITY	0.7365	0.7037

FLUID : FLUID EILERTS (GENERAL)

PENG/ROBINSON EQUATION OF STATE

	CRITICAL PRESSURE		CRITICAL TEMPERATURE		
COMP	(PSIA)	(KPA)	(DEG. R)	(DEG. K)	ACENTRIC FACTOR
C6-1	425.7	2935.0	882.7	490.4	0.2521
C6-2	439.6	3031.0	921.8	512.1	0.2649
C7-1	392.6	2707.0	938.8	521.5	0.3109
C7-2	407.2	2808.0	972.2	540.1	0.3207
C8	377.4	2602.0	1030.8	572.7	0.3851
C9	353.5	2438.0	1077.4	598.6	0.4403
C10	333.2	2297.0	1120.3	622.4	0.4925
C11	315.3	2174.0	1159.7	644.3	0.5421
C12	299.5	2065.0	1196.4	664.7	0.5890
C13	285.7	1970.0	1230.6	683.7	0.6335
C14	273.3	1884.0	1262.9	701.6	0.6761
C15	262.0	1807.0	1293.1	718.4	0.7166
C16	251.8	1736.0	1321.8	734.3	0.7555
C17	242.5	1672.0	1348.9	749.4	0.7927
C18	234.0	1613.0	1374.7	763.7	0.8284
C19	226.1	1559.0	1399.3	777.4	0.8628
C20	218.8	1509.0	1422.7	790.4	0.8959
C21	212.2	1463.0	1446.0	803.4	0.9284
C22	206.1	1421.0	1469.4	816.3	0.9605
C23	200.4	1382.0	1491.7	828.7	0.9915
C24	195.2	1346.0	1514.2	841.2	1.0221

FLUID : EILERTS (GENERAL)

PENG/ROBINSON EQUATION OF STATE

	CRITICAL PRESSURE		CRITICAL TEMPERATURE		
COMP	(PSIA)	(KPA)	(DEG. R)	(DEG. K)	ACENTRIC FACTOR
C6-1	425.7	2935.0	882.7	490.4	0.2521
C6-2	439.6	3031.0	921.8	512.1	0.2649
C7-1	392.6	2707.0	938.8	521.5	0.3109
C7-2	407.2	2808.0	972.2	540.1	0.3207
C8	377.4	2602.0	1030.8	572.7	0.3851
C9	353.5	2438.0	1077.4	598.6	0.4403
C10	333.2	2297.0	1120.3	622.4	0.4925
C11	315.3	2174.0	1159.7	644.3	0.5421
C12	299.5	2065.0	1196.4	664.7	0.5890
C13	285.7	1970.0	1230.6	683.7	0.6335
C14	273.3	1884.0	1262.9	701.6	0.6761
C15	262.0	1807.0	1293.1	718.4	0.7166
C16	251.8	1736.0	1321.8	734.3	0.7555
C17	242.5	1672.0	1348.9	749.4	0.7927
C18	234.0	1613.0	1374.7	763.7	0.8284
C19	226.1	1559.0	1399.3	777.4	0.8628
C20	218.8	1509.0	1422.7	790.4	0.8959
C21	212.2	1463.0	1446.0	803.4	0.9284
C22	206.1	1421.0	1469.4	816.3	0.9605
C23	200.4	1382.0	1491.7	828.7	0.9915
C24	195.2	1346.0	1514.2	841.2	1.0221

FLUID : EILERTS (GENERAL)

SOAVE/REDLICH/KWONG EQUATION OF STATE

	CRITICAL PRESSURE		CRITICAL TEMPERATURE		
COMP	(PSIA)	(KPA)	(DEG. R)	(DEG. K)	ACENTRIC FACTOR
C6-1	483.8	3335.0	893.2	496.2	0.2521
C6-2	499.4	3443.0	932.6	518.1	0.2649
C7-1	445.8	3074.0	949.8	527.7	0.3109
C7-2	462.2	3186.0	983.4	546.4	0.3207
C8	427.8	2950.0	1042.2	579.0	0.3851
C9	400.3	2760.0	1089.0	605.0	0.4403
C10	376.9	2599.0	1131.7	628.7	0.4925
C11	356.3	2457.0	1171.1	650.6	0.5421
C12	338.2	2332.0	1207.6	670.9	0.5890
C13	322.4	2223.0	1241.6	689.8	0.6335
C14	308.1	2124.0	1273.6	707.6	0.6761
C15	295.2	2035.0	1303.5	724.2	0.7166
C16	283.5	1955.0	1331.9	740.0	0.7555
C17	272.9	1881.0	1358.8	754.9	0.7927
C18	263.1	1814.0	1384.3	769.1	0.8284
C19	254.1	1752.0	1408.6	782.5	0.8628
C20	245.8	1695.0	1431.7	795.4	0.8959
C21	238.2	1643.0	1454.7	808.2	0.9284
C22	231.3	1595.0	1477.7	820.9	0.9605
C23	224.8	1550.0	1499.7	833.1	0.9915
C24	218.9	1509.0	1521.8	845.4	1.0221

FLUID : JACOBY SYNTHETIC MIXTURES

RECOMBINED MIXTURE COMPOSITIONS (MOL)

COMP	S-1	S-2	S-3	S-4	S-5	S-6
N2	0.0128	0.0153	0.0158	0.0166	0.0177	0.0191
CO2	0.0139	0.0156	0.0159	0.0165	0.0172	0.0182
C1	0.5634	0.6526	0.6715	0.6995	0.7401	0.7906
C2	0.0709	0.0701	0.0699	0.0697	0.0693	0.0689
C3	0.0509	0.0427	0.0410	0.0384	0.0347	0.0301
IC4	0.0164	0.0123	0.0113	0.0101	0.0082	0.0058
NC4	0.0376	0.0285	0.0266	0.0238	0.0197	0.0145
IC5	0.0208	0.0149	0.0137	0.0118	0.0092	0.0058
NC5	0.0249	0.0177	0.0162	0.0139	0.0107	0.0066
C6S	0.0365	0.0255	0.0232	0.0197	0.0147	0.0085
F1	0.0282	0.0195	0.0177	0.0150	0.0110	0.0061
F2	0.0174	0.0121	0.0109	0.0092	0.0068	0.0037
F3	0.0120	0.0083	0.0075	0.0063	0.0046	0.0025
F4	0.0201	0.0139	0.0125	0.0106	0.0077	0.0042
F5	0.0201	0.0138	0.0125	0.0105	0.0077	0.0042
F6	0.0323	0.0223	0.0202	0.0270	0.0124	0.0067
F7	0.0216	0.0149	0.0135	0.0114	0.0083	0.0045
	1.0000	1.0000	1.0000	1.0000	1.0000	1.0000

FLUID : JACOBY SYNTHETIC MIXTURES (SEPARATOR OIL COMPOSITION)

EXPERIMENTAL DISTILLATION DATA

COMP	MOLE FRACTION	MOLECULAR WEIGHT	SPECIFIC GRAVITY	BOILING POINT (DEG. R)	(DEG. K)	WEIGHT FRACTION
F1	0.19145	89.00	0.6799	610.00	338.89	0.1286
F2	0.14954	98.00	0.7181	660.00	366.67	0.1106
F3	0.09275	110.00	0.7403	710.00	394.44	0.0770
F4	0.06424	121.00	0.7542	760.00	422.22	0.0587
F5	0.10721	131.00	0.7628	810.00	450.00	0.1060
F6	0.10700	144.00	0.7749	860.00	477.78	0.1163
F7	0.17252	165.00	0.7859	910.00	505.56	0.2148
F8	0.11529	216.00	0.8140	850.00	472.22	0.1880
	1.00000	132.49	0.7585			1.0000

FLUID : JACOBY SYNTHETIC MIXTURES

PENG/ROBINSON EQUATION OF STATE

	CRITICAL				
	PRESSURE		TEMPERATURE		
COMP	(PSIA)	(KPA)	(DEG. R)	(DEG. K)	ACENTRIC FACTOR
F1	433.0	2985.0	912.6	507.0	0.2641
F2	433.3	2987.0	977.4	543.0	0.3046
F3	412.4	2843.0	1033.5	574.2	0.3587
F4	396.1	2731.0	1089.8	605.5	0.4126
F5	383.9	2647.0	1146.4	636.9	0.4661
F6	367.3	2532.0	1200.3	666.9	0.5237
F7	334.4	2305.0	1246.5	692.5	0.5929
F8	243.3	1678.0	1130.8	628.2	0.6098

FLUID : JACOBY SYNTHETIC MIXTURES

SOAVE/REDLICH/KWONG EQUATION OF STATE

	CRITICAL				
	PRESSURE		TEMPERATURE		
COMP	(PSIA)	(KPA)	(DEG. R)	(DEG. K)	ACENTRIC FACTOR
F1	491.9	3392.0	923.3	513.0	0.2641
F2	491.7	3390.0	988.6	549.2	0.3046
F3	467.5	3223.0	1045.0	580.6	0.3587
F4	448.5	3093.0	1101.4	611.9	0.4126
F5	434.3	2994.0	1158.1	643.4	0.4661
F6	414.9	2861.0	1211.8	673.2	0.5237
F7	377.3	2602.0	1257.7	698.7	0.5929
F8	274.9	1896.0	1141.8	634.3	0.6098

FLUID : OLDS/SAGE/LACEY (1945; GENERAL)

EXPERIMENTAL DISTILLATION DATA

COMP	MOL. WEIGHT	SPEC. GR.	BOILING POINT		RECOMBINED COMPOSITION AT GIVEN GOR (SCF/STB)					
			(R)	(K)	552	940	2205	5361	7393	14440
CO2					0.0020	0.0037	0.0060	0.0076	0.0081	0.0086
C1					0.2630	0.3902	0.5797	0.7148	0.7470	0.7922
C2					0.0516	0.0604	0.0733	0.0826	0.0847	0.0878
C3					0.0782	0.0710	0.0602	0.0526	0.0507	0.0482
IC4					0.0255	0.0214	0.0153	0.0110	0.0099	0.0085
NC4					0.0614	0.0504	0.0339	0.0222	0.0194	0.0155
IC5					0.0283	0.0225	0.0142	0.0081	0.0067	0.0047
NC5					0.0343	0.0304	0.0162	0.0085	0.0067	0.0041
F1	93.0	0.7212	621	345.0	0.0842	0.0652	0.0368	0.0166	0.0117	0.0050
F2	100.0	0.7451	671	372.8	0.0817	0.0641	0.0379	0.0191	0.0147	0.0084
F3	109.0	0.7665	714	396.7	0.0764	0.0591	0.0334	0.0150	0.0106	0.0045
F4	128.0	0.7892	772	428.9	0.0669	0.0518	0.0293	0.0132	0.0093	0.0039
F5	155.0	0.8170	852	473.3	0.0572	0.0443	0.0250	0.0112	0.0080	0.0034
F6	204.0	0.8433	951	528.3	0.0449	0.0347	0.0196	0.0088	0.0063	0.0026
F7	274.0	0.8822	1130	627.8	0.0444	0.0342	0.0192	0.0088	0.0062	0.0026
					1.0000	1.0000	1.0000	1.0000	1.0000	1.0000

	552	940	2205	5361	7393	14440
MIXTURE MOLECULAR WEIGHT	81.29	67.50	46.97	32.30	28.82	23.91
WEIGHT FRACTION TRAP GAS	0.0571	0.1213	0.2867	0.5335	0.6292	0.8111
MOLE FRACTION TRAP GAS	0.2285	0.4030	0.6628	0.8482	0.8936	0.9546
HEXANES-PLUS MOLE FRACTION	0.4557	0.3534	0.2012	0.0927	0.0668	0.0304
HEXANES-PLUS MOLECULAR WEIGHT	138.43		C6+ PROPERTIES SAME			
HEXANES-PLUS SPECIFIC GRAVITY	0.7981		FOR ALL MIXTURES			

FLUID : OLDS/SAGE/LACEY (1945; GENERAL)

PENG/ROBINSON EQUATION OF STATE

	CRITICAL				
	PRESSURE		TEMPERATURE		ACENTRIC FACTOR
COMP	(PSIA)	(KPA)	(DEG. R)	(DEG. K)	
F1	445.3	3070.0	930.9	517.2	0.2665
F2	446.4	3078.0	995.7	553.2	0.3076
F3	435.3	3001.0	1046.4	581.3	0.3507
F4	395.6	2728.0	1104.4	613.5	0.4239
F5	356.2	2456.0	1186.3	659.1	0.5224
F6	295.4	2037.0	1277.2	709.5	0.6610
F7	258.3	1781.0	1466.0	814.4	0.8746

FLUID : OLDS/SAGE/LACEY (1945; GENERAL)

SOAVE/REDLICH/KWONG EQUATION OF STATE

	CRITICAL				
	PRESSURE		TEMPERATURE		ACENTRIC FACTOR
COMP	(PSIA)	(KPA)	(DEG. R)	(DEG. K)	
F1	505.7	3487.0	941.8	523.2	0.2665
F2	506.5	3492.0	1007.0	559.4	0.3076
F3	493.4	3402.0	1057.9	587.7	0.3507
F4	447.9	3088.0	1116.0	620.0	0.4239
F5	402.5	2775.0	1197.8	665.5	0.5224
F6	333.0	2296.0	1288.0	715.6	0.6610
F7	290.1	2000.0	1474.9	819.4	0.8746

FLUID : OLDS/SAGE/LACEY (1949; GENERAL)

EXPERIMENTAL DISTILLATION DATA

			BOILING POINT		RECOMBINED COMPOSITION AT GIVEN GOR (SCF/STB)				
COMP	MOL. WEIGHT	SPEC. GR.	(R)	(K)	274	460	620	811	2580
CO2					0.0004	0.0009	0.0011	0.0014	0.0022
C1					0.1996	0.3151	0.3858	0.4485	0.6665
C2					0.0445	0.0494	0.0523	0.0549	0.0641
C3					0.0764	0.0728	0.0706	0.0686	0.0619
IC4					0.0205	0.0178	0.0161	0.0147	0.0096
NC4					0.0641	0.0554	0.0500	0.0452	0.0287
IC5					0.0256	0.0215	0.0191	0.0169	0.0092
NC5					0.0271	0.0228	0.0201	0.0178	0.0096
C6S					0.0564	0.0466	0.0405	0.0352	0.0166
F1	104.0	0.7451	685.0	380.6	0.0988	0.0818	0.0712	0.0617	0.0288
F2	117.0	0.7699	735.0	408.3	0.0907	0.0742	0.0642	0.0552	0.0242
F3	141.0	0.8035	814.0	452.2	0.0786	0.0643	0.0556	0.0478	0.0209
F4	194.0	0.8333	958.0	532.2	0.0592	0.0485	0.0419	0.0360	0.0158
F5	490.0	0.9365	1332.4	740.2	0.1581	0.1289	0.1115	0.0961	0.0419
					1.0000	1.0000	1.0000	1.0000	1.0000

MIXTURE MOLECULAR WEIGHT	142.5	120.4	106.8	94.7	52.9
WEIGHT FRACTION TRAP GAS	0.02066	0.05082	0.07539	0.10311	0.29778
MOLE FRACTION TRAP GAS	0.14432	0.29994	0.39469	0.47865	0.77218
HEPTANES-PLUS MOLE FRACTION	0.4854	0.3977	0.3444	0.2968	0.1316
HEPTANES-PLUS MOLECULAR WEIGHT	248.27	C7+ PROPERTIES SAME ABOUT			
HEPTANES-PLUS SPECIFIC GRAVITY	0.8767	THE SAME FOR ALL MIXTURES			

FLUID : OLDS/SAGE/LACEY (1949; GENERAL)

PENG/ROBINSON EQUATION OF STATE

	CRITICAL PRESSURE		CRITICAL TEMPERATURE		ACENTRIC FACTOR
COMP	(PSIA)	(KPA)	(DEG. R)	(DEG. K)	
F1	432.5	2982.0	1008.9	560.5	0.3264
F2	411.6	2838.0	1064.4	591.4	0.3815
F3	376.0	2592.0	1148.3	637.9	0.4743
F4	310.2	2139.0	1292.4	718.0	0.6572
F5	168.6	1162.0	1635.2	908.5	1.1923

SOAVE/REDLICH/KWONG EQUATION OF STATE

	CRITICAL PRESSURE		CRITICAL TEMPERATURE		ACENTRIC FACTOR
COMP	(PSIA)	(KPA)	(DEG. R)	(DEG. K)	
F1	490.6	3383.0	1020.3	566.8	0.3264
F2	466.3	3215.0	1076.0	597.8	0.3815
F3	425.3	2932.0	1159.9	644.4	0.4743
F4	349.7	2411.0	1303.2	724.0	0.6572
F5	188.5	1300.0	1640.9	911.6	1.1923